Non-maximum entropy polymer elasticity, viscoelasticity and the lattice Boltzmann method

Ryan Lester Benjamin

thesis presented for the degree of
DOCTOR OF PHILOSOPHY
in the department of Human Biology
UNIVERSITY OF CAPE TOWN

October 29, 2010

Mesoamerican ballgame: modified from wikimedia

http://commons.wikimedia.org/wiki/File/Tepantitla_mural_Ballplayer_B_Cropped.jpg#file

I hereby acknowledge that plagiarism is the act of using the work and ideas of another and pretending that it is one's own. I further assert that plagiarism is wrong.

I confirm that this thesis, except for the guidance of my supervisor, is the product of my own imagination and labour. The works of other contributors have been cited and referenced.

Ryan Benjamin
10/03/2010

I wish to acknowledge the patience, faith and guidance of my supervisor, Daya Reddy and previous head of department, Christopher 'Kit' Vaughn. I thank Deon Bezuidenhout and Tommy Franz at the Cardiovascular Research Unit at Groote Schuur for provided testing equipment, material and valuable support.

The document has been written in LaTeX and uses Dia and Xfig for the graphics. Programming and graphs have been performed and constructed on open source software including Open Office, R, Scilab, Octave, Geany, Gnuplot, G++ and Mayavi.

I wish to thank many not directly involved with the thesis. Many unrecognised teachers along the way are thanked but most importantly the late Mrs Louw and the late Mr "Hansie" Sauls.

The sacrifices and support of my parents Marda and Eric Benjamin, my sisters Norma and Heather and my relatives especially my cousins Keith Newton and Charmaine Pailman are appreciated.

Lastly this document is dedicated to my late cousin – Kenneth Potgieter.

Sonnet XVIII
Shall I compare thee to a summer's day?

Shall I compare thee to a summer's day?
Thou art more lovely and more temperate:
Rough winds do shake the darling buds of May,
And summer's lease hath all too short a date:
Sometime too hot the eye of heaven shines,
And often is his gold complexion dimm'd;
And every fair from fair sometime declines,
By chance, or nature's changing course untrimm'd;
But thy eternal summer shall not fade,
Nor lose possession of that fair thou ow'st,
Nor shall death brag thou wander'st in his shade,
When in eternal lines to time thou grow'st;
So long as men can breathe, or eyes can see,
So long lives this, and this gives life to thee.

William Shakespeare (1564-1616)

Abstract

Various models of viscoelasticity exist based on continuum mechanics. In this work a statistical mechanical approach is taken to derive a new isotropic, hyperelastic, viscoelastic, incompressible constitutive equation for polymers. The result has been achieved by generating a novel physics for the microscopic behaviour of polymers. A vocabulary has been created to faciliate the physics. A new differential equation describing polymer behaviour is derived based on the mathematical description of the physics. The integro-differential equation derived can either be considered to be a pair of coupled vector equivalents of the diffusion equation in Lagrangian coordinates or it can be considered to be a special case of the wave equation with non-linear damping in Eulerian coordinates. Furthermore macroscopic (and measurable) entities are derived both to facilitate testing the model and to allow the use of the Chapman-Enskog expansion (to the first order) to derive the macroscopic equations.

The first order approximation to the macroscopic equations are then derived using continuum mechanics both to provide insight and to determine stress tensors. A one dimensional spring-and-dashpot analogy is used to show that the macroscopic equations derived from the non-equilibrium behaviour of polymers is equivalent to material viscoelasticity. The relationship between the first order approximation to the macroscopc equation, linear viscoelastic models and the neo-Hookean model of hyperelasticity is demonstrated.

A finite differencing method based on the differential equation describing the microscopic behaviour of polymers is used to generate a lattice-Boltzmann type numerical method to solve the above microscopic differential equation. A Chapman-Enskog-like procedure is used directly on the numerical method to demonstrate that the first-order macroscopic equations can be derived directly from the numerical method. It should be recognised that the

above numerical method models the distribution of stretch subject to a differential equation which is independent of stress and is subject to set boundary conditions. The stress is a dependent variable which is a consequence of the distribution of stretch. This differs substantially from continuum-based constitutive equations which typically incorporate stress as a variable.

Novel experimental methods are developed and implemented in order to determine the constants of the model. Furthermore the stress relaxation experiment is used to verify the model.

The results show excellent agreement up to maximum stretch of 150% both for hyperelastic and viscoelastic behaviour. The model was never intended to be used beyond this limit and was not tested beyond this limit, beyond which it may remain valid.

Contents

List of Figures

List of Tables

Chapter 1

Introduction

This thesis presents the development of a constitutive equation for the description of the mechanical behaviour of an incompressible, viscoelastic, hyperelastic solid and the construction of a means of numerically modelling such a specimen. It derives the constitutive equation with the aid of statistical mechanics and the numerical method utilized is the Lattice Boltzmann Method (LBM).

The model uses statistical mechanics (which describes the behaviour of molecules) to derive these macroscopic, constitutive equations. Conventionally one would study the macroscopic behaviour of the specimen and develop a constitutive equation, based on the continuum mechanics, constrained by the laws of mechanics that best describe the observed phenomena. This macroscopic differential or integro-differential equation would then be solved using a numerical method. In such an approach details at the molecular level are disregarded.

1.1 Comparison of continuum and statistical mechanics

Before comparing and contrasting statistical and continuum approaches, the concepts are introduced.

1.1.1 Preliminary concepts and definitions

A specimen is constructed of a material that consists of molecules. Let it suffice that if one were to determine the properties of each individual molecule (w), one would be investigating the material at a microscopic level. Examples of the properties that would be considered at this microscopic level would be the mass of the w^{th} molecule (m_w), similarly molecular velocity ($\boldsymbol{u}_w$), molecular stretch ($\boldsymbol{\lambda}_w$) and vibration of the total chain length (f_w). An averaging procedure over all the molecules within the volume at position $\mathbf{r}$ would be required to determine the macroscopic properties of the material at that position; examples would be density ($\rho(\mathbf{r})$) , pressure (P($\mathbf{r}$)), velocity ($\mathbf{v}(\mathbf{r})$), strain ($\boldsymbol{\epsilon}(\mathbf{r})$) and temperature (T($\mathbf{r}$)). Modelling the individual molecules directly would be considered a microscopic approach. These ideas are illustrated in Figure 1.1 where the blue lines represent molecules and a property of the molecule (here velocity, $\boldsymbol{u}$) is described. The macroscopic of velocity at $\mathbf{r}$ is $\mathbf{u}(\mathbf{r})$ and is determined by averaging all of the molecular velocities $\boldsymbol{u}$.

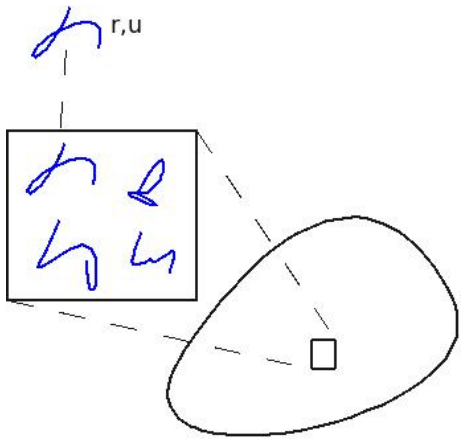

Figure 1.1: Schematic view of microscopic modelling

Alternatively, one could apply the laws of physics and thermodynamics to a kinetic theory of molecules and derive formulae describing the relationship between macroscopic (directly measurable) properties. Descriptions of the behaviour of these macroscopic properties, for example (T($\mathbf{r}$)), will be considered the macroscopic level. Modelling the interaction of these macroscopic properties directly will be considered the macroscopic approach. Although desirable to determine the macroscopic properties from the microscopic, it is not necessary for a relationship to exist.

Consider next a hybrid, intermediate situation. As for the macroscopic situation, consider an infinitesimal volume at a position $\mathbf{r}$. Within this volume, let a microscopic property, $\boldsymbol{u}$, have a statistical distribution $p(\boldsymbol{u})$, Let all the molecular properties within that volume be similar where the similarity is defined by the symmetry of $p(\boldsymbol{u})$. Conversely asymmetry of the probability distribution, excludes similarity. Let this volume be called a representative volume (RV). The dimensions of this RV are determined by the greatest distance in which similarity can occur under specified conditions. Alternatively the RV is defined by the smallest distance in which a significant change in $p(\boldsymbol{u})$ occurs under specified conditions. The RV can also be considered to be a grand canonical pressure ensemble([40] Chapter 2). As for the microscopic situation, one determines microscopic properties. However, it is not individual molecular properties that are determined. Rather, at position $\mathbf{r}$, the probability distribution ($p(\boldsymbol{u}_i)$) of molecular property $\boldsymbol{u}_i$ (where $i \in \mathbb{N}_0 \iff i = 0, 1, 2, \ldots ; i < M$ and M is the number of properties) is determined. The macroscopic properties are derived by an averaging procedure applied to the probability distribution. The consideration of the probability distribution in such a representative volume will be called the mesoscopic level. The modelling of the probability of molecular properties in a representative volume being in a given state with subsequent averaging to determine the macroscopic properties will be called the mesoscopic approach. Figure 1.2 is a representation of the mesoscopic approach in which the red square represents a representative volume, the blue lines are molecules and the green curve is the the probability distribution of the microscopic property ($\boldsymbol{u}$), $p(\boldsymbol{u})$, within the volume at position $\mathbf{r}$.

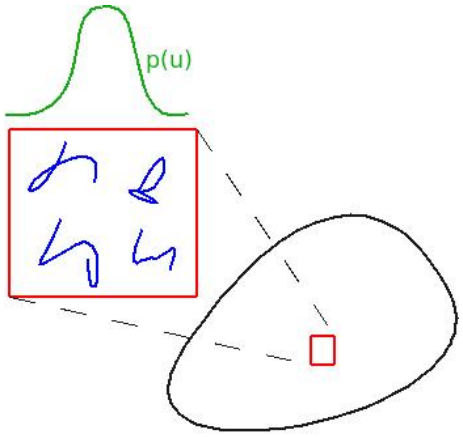

Figure 1.2: Schematic view of mesoscopic modelling

In this work, a distinction is made between the material and the specimen. The specimen properties are independent of position. Material properties (which are position dependent) will be used in and generated from the mesoscopic approach. The specimen properties will be defined as the average of material properties over the volume of the specimen. It will, however, also be shown that specimen phenomena will not necessarily be the average of material phenomena. The term specimen is never used in the mesoscopic approach. The terms viscoelasticity, stress relaxation and creep will be considered specimen phenomena and are reserved for the macroscopic approach.

The term disequilibrium will be confined to the macroscopic approach and refers to a situation in which specimen properties change with respect to time in the absence of a change in the external environment. The term steady state (for a particular property) is also reserved for the macroscopic description and refers to the situation in which a macroscopic property does not change with respect to time in the absence of a change in the external environment. The ground state is a steady state situation in which the external environment is in a default state (for example room temperature and atmospheric pressure).

Several properties have alternate interpretations microscopically and macroscopically, for example, molecular vibration translates to temperature macroscopically. However, several properties have analogues across the microscopic, mesoscopic, material and specimen range. An example of the latter situation is velocity. For this latter scenario, a mesoscopic property represents the probability that a molecule has a particular molecular property. A material property represents the average microscopic property of the population of molecules within an infinitesimal representative volume. A specimen property then represents the average material property over the volume of the specimen.

The approximation of a body as a continuum and the application of the derived mechanics or thermodynamics of these continua based on the averaged (and directly measurable) properties of that continuum, constitute continuum mechanics. In continuum mechanics the macroscopic properties are functions of position and time within the continuum.

In this work, the mesoscopic approach to physical phenomena is synony-

	Macroscopic		**Mesoscopic**
	Material	Specimen	
Model	Continuum mechanics		Statistical mechanics
State		disequilibrium steady state ground state	equilibrium non-eqilibrium maximum entropy
Phenomenon		viscoelasticity stress relaxation creep	
Property	temperature density stretch	velocity acceleration stress	molecular velocity molecular stretch vibration

Table 1.1: Macroscopic and mesoscopic terms

mous with statistical mechanics and the macroscopic approach is equivalent to continuum mechanics. In principle, it is possible to relate the mesoscopic and macroscopic descriptions but in practice this may be constrained by complexity. However, the inability to derive the macroscopic from the microscopic description generates a discontinuity between these descriptions. The derivation of the macroscopic behaviour from the microscopic behaviour has been achieved for gases but it is not necessary to be able to derive the continuum mechanics from the statistical mechanics. The Navier-Stokes equations, for example, were derived by continuum mechanics before they were derived using statistical mechanics.

The mesoscopic description will be divided into two components – equilibrium and non-equilibrium. The equilibrium behaviour refers to the situation where the averaged properties of molecules do not change with respect to time. Conversely, non-equilibrium behaviour refers to averaged properties that vary with respect to time. Implicitly, the terms equilibrium and non-equilibrium are reserved for the mesoscopic approach. The term maximum entropy state (used in Chapter 3) will also be reserved for the mesoscopic approach. The maximum entropy state refers to the least ordered distribution of microscopic properties that are compatible with a given macroscopic state. Table 1.1 categorises the terminology into macroscopic and mesoscopic groups.

1.1.2 The mesoscopic and macroscopic approaches to the derivation of constitutive equations

One is interested in the macroscopic behaviour of materials and the averaged properties. Intuitively one would anticipate that the continuum approach would be quicker and more physically relevant. Quicker because the mathematical description applies to the observed properties directly and more physically relevant because an observed property can be introduced directly into the macroscopic mathematical description even if the observed property has as yet not been derived from an averaged mesoscopic property.

In order for mesoscopic and macroscopic theory to be consistent, it is necessary to derive the latter from the former or, in principle, *vice versa* – with the proviso that the loss of information when translating the macroscopic to the microscopic may prohibit the derivation. It could, however, be argued that this simply confirms what is already known. Nevertheless, the possibility that a macroscopic phenomenon derived from the mesoscopic theory may have been neglected in derivations based directly on macroscopic theory exists. The mesoscopic approach may provide a means to derive an innovative constitutive equation.

1.2 Need for reconciliation between macroscopic and microscopic polymer theory

The study of polymers occurs on at least three levels. Briefly chemists and chemical engineers study the manufacturing process. Chemists and physicists construct theories to explain diffusion, neutron scattering, viscoelasticity and optical birefringence [115]. Structural engineers and applied mathematicians construct models to explain the mechanical behaviour of continua and to design. When considering the microscopic models of the physicists and the macroscopic models of the engineers, there is no obvious way to derive the one from the other. The macroscopic approaches are accused of being phenomenological and the microscopic approaches are not readily applicable to real-world design problems. Ensuring continuity not only provides internal consistency [40] but allows new ideas and phenomena to be transmitted from microscopic to macroscopic and *vice versa*. Thus any microscopic/mesoscopic theory that is produced should have the capacity to be extrapolated to the

macroscopic world.

The existing microscopic theories are variants of two models. Kuhn models a polymer molecule as being a collection of freely-jointed, rigid segments of equal length [115] and uses the model to construct a probability distribution function for the length of the molecule. An extension of Kuhn's model uses a partition function to separate the potential energy of the rigid link model into three contributions [40] – energy of bond interaction which is considered constant, energy due to chain link rotation and the energy of van der Waal forces. Interestingly, this approach uses several properties of a random flight model/simulation [40] and thus, unusually, extrapolates a numerical model to a physical description as apposed to extrapolating a molecular model to a physical description. The alternative to the rigid links of Kuhn is the bead-and-spring model [115]. The motion of the 'beads' in the bead-and-spring models are governed by Smulochowski's equation [28] for Brownian motion.

There is an alternate interpretation of Kuhn's model. One could consider the rigid link model as a means to determine a probability distribution for chain length. The benefit of the latter perspective is that a model already exists (Chapman-Enskog expansion [18]) for extrapolating to macroscopic behaviour. It should also be recognised that statistical mechanics acknowledges that it is not possible to predict the position of every molecule and thus one determines the probability of a molecule being at a particular position. In the bead-and-spring approach, the probability of finding a 'bead' at a particular position is being predicted. One could argue that just as it is not necessary to predict the position of every molecule to predict mechanical behaviour, it is not necessary to predict the probability distribution of the 'beads'. Rather the bead-and-spring and the rigid link models may simply be useful for predicting the probability distribution for the length of the whole molecule.

Comparing this alternate approach to the Kuhn model to the partition function [40], the latter only considers the potential energy. It is noted that the bond energy is common and that the alternate approach is at a larger scale and thus implicitly includes the van der Waal forces. The energy due to link rotation translates to molecular stretch in the alternate Kuhn model. It will become evident that the alternate approach to the Kuhn model presented in this document will also consider the effect of kinetic energy – in

contrast to the partition function approach. The latter approach will also be shown to provide an explanation for the observed macroscopic phenomenon of (specimen) stress relaxation.

1.3 Existing numerical models of mesoscopic polymer behaviour

There are existing lattice Boltzmann models of visco-elasticity which can be classified into two categories. The first group model the interaction of solid spheres (as for gases) and assume that the constitutive equation is only a function of the velocity of the solid sphere (as in a Newtonian fluid) [39,88,100]. It is not obvious that the contribution of molecular stretch can be neglected and the descriptions are acknowledged to be phenomenonological [29]. Furthermore, the variables that describe the phenomena are macroscopic and it is therefore not obvious that, in principle, they can be transposed directly to the mesoscopic scale (although a Chapman-Enskog expansion [39] or a dispersion equation analysis [88] are used to derive the macroscopic behaviour). Furthermore, it is not apparent how the numerical model relates to the idealised kinetic 'rigid-link' or 'bead-and-spring' models.

The second group provide a numerical method that is related to the 'bead-and-spring' model [8]. Essentially the Brownian motion modelled by the Smulochowski's equation [28] is circumvented by coupling the motion of the 'beads' to the motion of a surrounding fluid where the Brownian motion is provided by a fluctuating (random) term introduced into the momentum flux. Of note only one polymer chain is modelled and effectively the findings for the chain are extrapolated to the specimen. It is however not obvious when the properties of a single chain can be extrapolated to the specimen nor is a constitutive equation for stress provided – and, consequently, engineers and applied mathematicians may have difficulty using this method.

1.4 Justification for statistically derived constitutive equations

As stated, a fundamental approach (although potentially more time-consuming) may result in the derivation of constitutive equations that would not otherwise have been recognised. However, before embarking on a quest for a con-

stitutive equation, one should review the evidence and determine if a glaring omission has failed to be investigated or solved.

1.4.1 Continuous material description

The kinetic theory of gases considers gas molecules to be the equivalent of solid spheres having the properties of mass and momentum. This 'billiard ball' model can be considered the microscopic description. The mesoscopic description of the kinetic theory of gases derives the continuous Boltzmann equation (CBE) and the Boltzmann H theorem. The fundamental description spans Dalton (and the atom) in the 18^{th} century to Boltzmann (and the H-theorem) in the 19^{th} century.

The Navier-Stokes (N-S) equations for incompressible fluids were originally derived from the macroscopic description and date from 1822. They remained unrelated to the mesoscopic theory until 1916 when Chapman and Enskog [18] in 1916 and 1917 independently derived the N-S equations directly from the mesoscopic description by applying a multi-scaling expansion technique. Enskog's derivation was more mathematically precise and effectively derived the N-S equations from first principles, thus reconciling the macroscopic equations and the underlying mesoscopic theory.

Table 1.2 depicts, for fluids and viscoelastic solids, the equations and a selection of representative contributors categorised into equilibrium behaviour, non-equilibrium behaviour (both microscopic/mesoscopic), reconciliation and macroscopic equations. It will be shown that both the equilibrium and non-equilibrium microscopic theory describe material properties whereas the macroscopic behaviour is described by the distribution of material properties throughout the specimen. It should be noted that unique relationships do not exist between material distributions and specimen states. Consequently the distribution of material properties does not equate to specimen property.

The analogue of the kinetic theory of gases is the kinetic theory of polymers introduced by Guth and Mark [51] and Meyer *et al* [107]. The mesoscopic theory for the equilibrium behaviour of polymers was further advanced by Kuhn [81–83], Guth *et al* [51, 71], Flory [32, 34], Treloar [133, 134], Wall [142, 144] and others. Green and Tobolsky [47] developed a theory for the non-equilibrium behaviour of polymers that could be shown to derive two

Material	**Equi-librium behaviour**	**Non-equilibrium behaviour**	**Recon-ciliation/ expansion**	**Macroscopic behaviour**
Fluid		Boltzmann equation	Chapman-Enskog	Navier-Stokes equation
Visco-elasticity	Kuhn Flory	Green and Tobolsky		Boltzmann superposition integral Voigt model Maxwell model general spring-dashpot model Fung quasi-linear Green-Rivlin

Table 1.2: The relationship between statistical and continuum mechanics

known linear macroscopic models – the Maxwell model and the Boltzmann superposition integral. It should be noted that Green did not distinguish between material and specimen behaviour. The above theory is for Gaussian chain length distribution. Non-Gaussian chain length distribution will briefly be described in Chapter 3. Mark and Burak [103] provide a more comprehensive overview.

In parallel with the above, constitutive equations for hyperelastic and viscoelastic materials based on continuum considerations were derived by Volterra, Cosserats and Fréchet [74]. Rivlin [122] and Mooney [111] made significant contributions for isotropic materials. Ogden [113] made valuable contributions based on linear combinations of powers of prinicipal stretches in the 1970s and 1980s. Spring-and-dashpot models of viscoelasticity (time-dependent reversible elastic behaviour) exist [73,86,94]. Non-linear viscoelastic theories [43–46,93,94] have been extended to include applications to biological tissues [17,38,67,68,87].

It is thus evident that the theory of non-equilibrium behaviour of polymers is incomplete because reconciliation has not occurred. An opportunity, therefore, exists to develop a theory for the non-equilibrium behaviour of polymers that will provide additional insight and new constitutive equations. The Chapman-Enskog expansion in Table 1.2 is described under the heading of reconciliation or expansion. The original use by Enskog reconciled the CBE and N-S equations. However the expansion can also be

used as a primary method to derive macroscopic equations for fluid flow directly [18, 42, 110]. Table 1.2 deliberately omits information about the reconciliation of the macroscopic and mesoscopic theory of viscoelasticity to emphasise the absence of a Chapman-Enskog (CE) expansion for polymers.

1.4.2 Discrete material description

The distinction between analytical theory and discrete modelling can be arbitrary. In this work, discrete modelling can consist of pseudo-direct simulation, finite differencing, finite volume or the finite element method. Pseudo-direct simulation does not model individual molecules, but rather it models representatives of collections of molecules as individual molecules. Pseudo-direct simulation does not apply to an equation and can therefore be applied to mesoscopic simulations. Finite differencing, finite volume and finite element modelling apply to equations and are therefore applied to both mesoscopic and macroscopic equations. The classification is not intended to be exhaustive nor are the representatives of each category.

Consider the modelling of fluids. Lattice cell gas automata (LCGA) [36, 147] and the classical interpretation of the LBM [63, 104], which will be discussed again in Section 1.5, are pseudo-direct simulations of the kinetic theory of gases. The alternate interpretation of the LBM is a finite differencing method applied to the CBE [57, 58]. Finite volume LBMs have also been generated [20, 132, 151]. The finite volume (as presented by Patankar [114]) and finite element methods (as presented by Zienkiewicz [154]) have been applied directly to the N-S equations.

Similarly one could consider polymer simulation. Direct simulation can either be of the equilibrium scenario or the non-equilibrium scenario. Wu and van Giessen [150] provide a brief review of network theory. In network theory the behaviour of the entire network can be represented by a finite set of idealised molecules within a finite volume. James and Guth [71] have shown that, by applying the appropriate mechanics, the specimen behaviour can be reproduced from these representative molecules.

Early equilibrium contributions to polymer theory were by Kuhn and Grün [82], Wang and Guth [145], Treloar [136] and Flory and Rehner [34]. More recent contribution are by Wu and van Giessen [149, 150], Edwards and Doi [5, 27] and Boyce [3]. Micromechanical non-equilibrium polymer

elasticity has recently been explored by Chen and Cheng [19] and Bergström and Boyce [6, 7]. Because these mesoscopic models of viscoelasticity model representative molecules within a representative volume, these correspond to material viscoelasticity (time dependent stress-strain retainships observed at a position) – which differs from the observed specimen viscoelasticity (the macroscopically observed phenomena of creep and stress relation which are properties of the whole specimen). Implicitly extrapolation to the specimen requires that the specimen should be in steady state because the properties of the RVE can in general not be extrapolated to the specimen unless every RVE is in equilibrium and in exactly the same state. Furthermore the criteria for extrapolation are even more strict than just steady state – every RVE should be at the same equilibrium state. Consequently the specimen is in steady state and the whole specimen may represent an RVE – which is not generally true of the steady state. The terms equilibrium and steady state (amongst other) will be defined explicitly in Section 3.1.1. It will be shown that the non-equilibrium theory of polymer elasticity can also generate specimen viscoelasticity by applying a Chapman-Enskog-like expansion.

	Direct Simulation	**Finite Difference**	**Finite Volume**	**Finite Element**
Mesoscopic	LCGA Classical LBM *Network theory* CHEN AND CHENG BOYCE AND BERGSTRÖM	Alternate LBM	Chen Teixeira Xi *et al*	
Macroscopic			Patankar	Zienkiewicz *Hyperelastic FE* VISCOELASTIC FE

Table 1.3: Discrete models of continuum and statistical mechanics

Examples of discrete continuum modelling of hyperelastic and viscoelastic materials abound with models based on Ogden or Green-Rivlin theory (*e.g.* [9,67,121,152]) respectively or linear viscoelastic models based on spring-

dashpot assemblies (*e.g.* [73]). A summary of the discrete theory options is presented in Table 1.3. The categories are macroscopic and mesoscopic and each of these are divided into direct simulation (where the physics is modelled directly without first developing a mathematical description of the physics to which a numerical method can be applied), finite difference, finite volume and finite element. The san-serif script refers to fluids. The *italic* script is either for equilibrium or hyperelastic modelling and the SMALL CAPS script is either for non-equilibrium or viscoelastic modelling. The abbrevation FE refers to finite element discretisation. It is evident that a finite difference approach to the modelling of non-equilibrium polymer chains is absent.

The existing Lattice Boltzmann based models of Section 1.3 have been omitted either because chain stretch is not considered in their constitutive equations and their constitutive equations are not arrived directly from a microscopic model [39,88,100] or because no macroscopic constitutive equation is derived/provided [8].

1.5 Selection of a numerical method

The end result of both the mesoscopic and macroscopic description is an integro-differential equation. One is attempting to solve the equation over a domain. In general, analytical solutions are not available. A numerical solution is determined and the technique used to find this numerical solution is termed a numerical method. It has already been stated that the distinction between continuous and discrete theory can be arbitrary.

The lattice Boltzmann method (LBM) will be shown to be a finite differencing method based on the Boltzmann equation of statistical mechanics. It can also be generalised to be considered as a fully Lagrangian method for solving systems of conservation equations [2].

In Chapter 2, the lattice Boltzmann method will be reviewed. In particular, two approaches to the derivation will be described. The first will arbitrarily be called the classical derivation as reviewed by Chen and Doolen [23] and the second (also briefly presented by Chen and Doolen [23]) will be called the alternate derivation.

The classical derivation (approach/description) is the historical evolu-

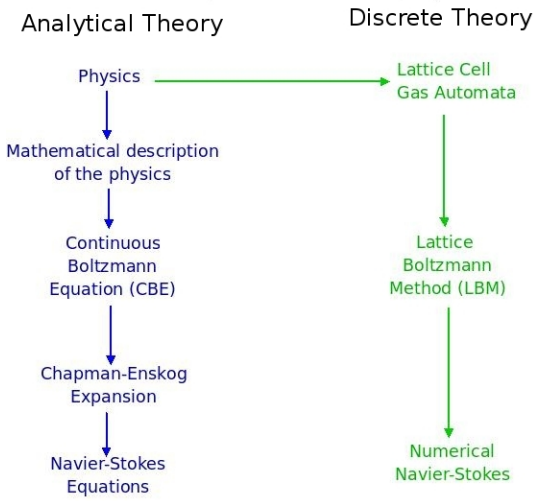

Figure 1.3: Illustration of the classical derivation of LBM

tion of the method. The LBM is a real-valued version of lattice cell gas automata (LCGA) which was an attempt to model molecular interaction directly. The method is typically divided into advection and collision (to mimic the behaviour of a molecule). This advection and collision procedure can be represented mathematically by the lattice Boltzmann equation. It can be shown that one can derive the N-S equation from the lattice Boltzmann equation [15]. In the classical description there is no clear separation of the physics, the mathematical description based on the physics and the numerical method based on the mathematical description of the physics. In the classical approach, the relationship to the conventional methods is not apparent and consequently it could be considered a separate numerical method. The classical derivation is depicted in Figure 1.3 where the blue pathway on the left is the analytical development and the green path on the right is the numerical or discrete development.

The alternate approach, as will be described, will derive the Boltzmann equation based on the kinetic theory of gases. The lattice Boltzmann equation will then be derived by applying a finite differencing method to the Boltzmann equation. As in the classical approach, the N-S equation can be derived from the lattice Boltzmann equation. The distinction between physics, mathematical description of the physics and numerical method is obvious in the alternate approach. Although the end result is the same, the alternate approach abandons the idea of advection and collision thereby allowing the application of finite differencing to any appropriate equation. A depiction of the alternate approach is presented in Figure 1.4.

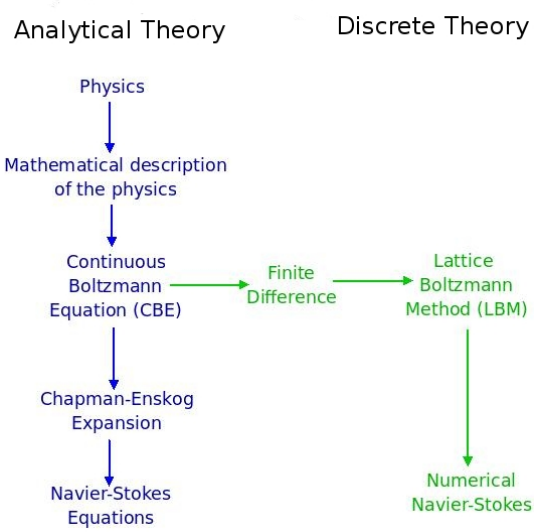

Figure 1.4: Illustration of the alternate derivation of LBM

1.6 Aims of thesis

The thesis will extend the existing statistical mechanics of polymers from the equilibrium theory to the non-equilibrium theory of polymer elasticity which will be shown to correspond to a model of viscoelasticity. The statistical theory for polymers will be used to generate a lattice Boltzmann type numerical method for polymers. This method will be Lagrangian. This thesis will achieve these aims in the following manner:

1. Polymer statistical mechanics (depicted in Figure 1.5)
    - Present the statistical mechanics for the equilibrium behaviour of a polymeric material (rubber elasticity)
    - Extend to a statistical mechanics model for the non-equilibrium behaviour of a polymeric material (viscoelasticity)
    - Apply the Chapman-Enskog expansion to derive the macroscopic equations of polymer mechanics based on the statistical model
2. Polymer continuum mechanics
    - Derive the macroscopic equations using continuum mechanics in order to determine the equivalent constitutive equations
    - Determine the equivalent spring-and-dashpot model which can either be considered a Kelvin-Voigt model with spring generalization or Boltzmann superposition integral with single viscous element.

3. Polymer discrete solution

    - Construct an LBM based on the statistical mechanics model for polymers
    - Derive the macroscopic equations for the polymer from the LBM for polymers

4. Experimentally determine the constants necessary for the model

5. Experimentally verify that utility of the numerical model

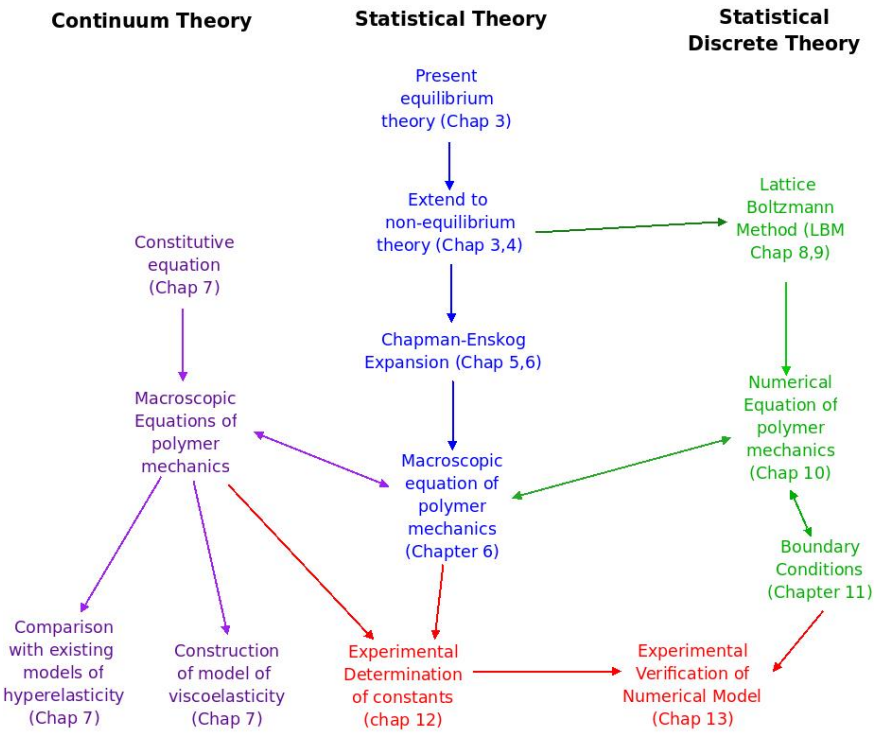

Figure 1.5: Thesis organisation and aims

1.7 The original contributions of this thesis

The original contributions will be divided into mechanics or physics, numerical methods and engineering and are:

- Mechanics

    1. Derivation of a constitutive equation for the modelling of a hyperelastic, viscoelastic specimen from statistical mechanics using the Chapman-Enskog expansion

2. Derivation of the same constitutive equation for viscoelasticity using continuum mechanics – thereby showing the equivalence of the solutions
3. Demonstration of the equivalence of a conventional spring-and-dashpot model with the 1D specialisation of the newly derived viscoelastic model

- Numerical Methods – Derivation of a LBM-type method for the modelling of an isotropic, incompressible, hyperelastic, viscoelastic solid
- Engineering – Experimental determination of constants required for the derived viscoelastic model

1.8 Thesis layout

The layout of the thesis is depicted in Figure 1.5. Chapters 3 through 6, in blue, are related to the analytical theory of statistical mechanics. Chapter 7, in purple, will incorporate all of the continuum theory and Chapters 8 through 11, in green, will construct all of the numerical theory with respect to statistical mechanics. The experimental work of Chapters 12 and 13 are depicted in red.

Chapter 2 will briefly describe the historical evolution of and justification for the lattice Boltzmann method. It will achieve this by introducing the idea of cellular automata, lattice-cell gas automata and extending these concepts to the lattice Boltzman method. References will also be provided for the derivation of the N-S equations from the LBM. This description will be called the classical derivation.

The chapter will then proceed to describe the arbitrarily termed alternate derivation. In this approach, the statistical mechanics of a fluid at equilibrium will be introduced and extended to the non-equilibrium situation. The theory will be described mathematically by the continuous Boltzmann equation (CBE). Based on the above theory, the derivation of the macroscopic equations (N-S equations) will be described.

It will then return to the CBE and derive the LBM method as a finite differencing of the continuous Boltzmann equation (CBE). The description of the derivation of the N-S equations is exactly as for the classical approach.

This, the alternate derivation, is relevant because this is the form used to develop the numerical method for polymer mechanics.

Chapter 3 will present the existing statistical mechanical theory for the equilibrium behaviour of an isotropic, incompressible, hyperelastic, viscoelastic polymeric specimen. The theory will then be extended to develop the non-equilibrium behaviour of polymer elasticity and conclude by determining the form of the mesoscopic differential equation of polymer chain interaction but will omit to determine the polymer chain interaction term – the equivalent of the collision term in the LBM.

Chapter 4 will use the geometry of molecular interaction to determine the polymer chain interaction term that was omitted in Chapter 3. Combining the result for the polymer chain interaction term with the form of the differential equation of polymer chain interaction will provide the complete description of the mesoscopic differential equation of polymer chain interaction.

Chapter 5 averages mesoscopic properties to determine and define the measurable macroscopic properties. These macroscopic properties will have to be isolated or recognised (where isolation is to group separately and recognise the group as a distinct unit) after appying the Chapman-Enskog expansion in Chapter 6.

In Chapter 6, the equations of viscoelasticity at a macroscopic level will then be derived by applying the Chapman-Enskog (CE) expansion to the mesoscopic differential equation of polymer chain interaction. The resultant equations (6.98 and 6.99) predict the propagation of stretch and stretch rate through the specimen.

Chapter 7 will derive the same macroscopic equations (6.98 and 6.99) as those derived in Chapter 6 but will do so using continuum mechanics. The continuum derivation of the macroscopic equations of Chapter 6 will rely on assumptions concerning the form of the stress tensor. Based on these assumptions, the constitutive equation (7.15, 7.16 or 7.17) for polymers will be derived. A spring-and-dashpot model of viscoelasticity will be used to derive a 1D version of the material stress. An additional spring-and-dashpot model of viscoelasticity will be used to derive a 1D version of specimen stress. The

stored energy functions of the Neo-Hookean hyperelastic model will then be compared to that derived from the statistical model.

Chapter 8 will then return to the equations describing the mesoscopic behaviour of polymers as presented in Chapter 3 and construct a LBM-type method based on these equations. The numerical method is derived based on the discretisation of the probability distribution function for polymers. Chapter 9 recovers the macroscopically measurable variables like stress from the mesoscopic distribution of stretch and stretch rate.

In Chapter 10 the equations of viscoelasticity (macroscopic equations) as described in Chapters 6 and 7 will be derived directly from the LBM-type method for polymers as constructed in Chapter 8. Chapter 11 presents novel boundary conditions for symmetry, uniaxial testing and adapts an existing boundary condition to polymers.

Chapter 12 determines the constants required for the model by determining the appropriate conditions for experimentation and using the method of least squares to calculate the constants. Chapter 13 compares the model of specimen stress relaxation and viscoelasticity to experimental results. Chapter 14 will discuss the results. The conclusion and recommendations mark the end of the thesis.

1.9 Thesis notation

The variables describing microscopic properties will be written as x if it is a scalar, $\boldsymbol{x}$ if it is a tensor. Variables describing macroscopic properties will be written as x if it is scalar and $\mathbf{x}$ for tensors. Macroscopic material properties will be in capitals letter (X or $\mathbf{X}$) and in lower case if specimen properties are being considered (x or $\mathbf{x}$). Material notation will be retained for material properties used in a macroscopic context (specimen properties) but will be qualified as X_{spec} or $\mathbf{X}_{spec}$. Greek notation will not follow the above convention. Macroscopic vectors will be underlined ($\underline{\mathbf{v}}$). The expression $\underline{\mathbf{v}}\underline{\mathbf{v}}' = \underline{\mathbf{v}} \otimes \underline{\mathbf{v}}'$, the vector product. For tensor $\mathbf{Q}$, $\underline{\mathbf{n}} \cdot \mathbf{Q} = \mathbf{Q} \cdot \underline{\mathbf{n}} = \mathbf{Q}\underline{\mathbf{n}}$.

The symbol $\boldsymbol{R}_f$ refers to the microscopic vector chain length and $\dot{\boldsymbol{R}}_f$ refers to the microscopic property chain length stretch rate. These variables are capitalised to avoid confusion with position $\mathbf{r}$. Further the microscopic

position $\boldsymbol{r}$ and the macroscopic position $\mathbf{r}$ are interchangeable. All integrals over chain length, $\boldsymbol{R}_f$, and chain length stretch rate, $\dot{\boldsymbol{R}}_f$, are from negative to positive infinity in all three directions.

1.10 Summary

At least two broad categories of approaches to the modelling of the mechanical behaviour of viscoelastic (or rubber-like) materials exist. These can be divided into macroscopic or continuum based approaches and mesoscopic or statistically based approaches. By comparing the statistical approach for polymers to the equivalent approach for gases, it has been demonstrated that a Chapman-Enskog-like expansion for polymers does not exist and represents an opportunity for exploitation.

Furthermore the opportunity exists to create a finite difference method based on the mathematical description of the polymer micromechanics and to interpret the results within the context of material and specimen properties, states and phenomena.

Chapter 2

The derivation of the lattice Boltzmann method

This chapter will review the theory behind the conventional lattice Boltzmann method as applied to fluids. It also serves as an introduction to what is referred to in this work as the alternate derivation. It is this alternate derivation which will form the basis of the LBM to be derived for polymers. The review by Chen and Doolen [23] emphasizes the conventional derivation of the LBM which this document will call the classical approach.

2.1 The classical approach

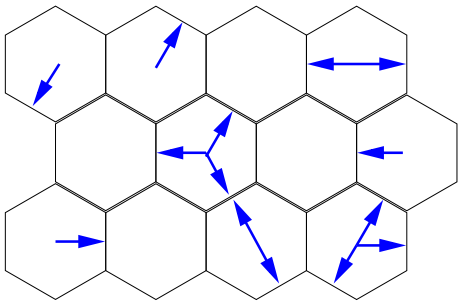

Figure 2.1: LCGA lattice: Molecular velocity is represented by the blue arrows. The presence of a blue arrow also indicates the presence of a molecule. Conversely, the absence of the arrow represents the absence of a molecule.

In the kinetic theory of gases, a molecule can be represented as a sphere (billiard ball) and these molecules are sufficiently rarefied to only have binary collisions after advection.

Lattice cell gas automata (LCGA) simulates the above directly [37, 147]. It evolved from cellular automata [148] and shares the integer nature of the latter. The simulation occurs on a regular hexagonal lattice where a molecule can either be present (1) or absent (0) and the molecule could only have one of six velocities corresponding to the midpoints of the edges of the lattice as depicted in Figure 2.1. Collision rules are created to enforce conservation of mass and momentum at the point of collision as depicted in Figure 2.2. The N-S equations can be derived from the LCGA by applying a multiscaling method [21, 36]. The classical approach to the LBM is essentially an algorithm based on the physics [89, 127].

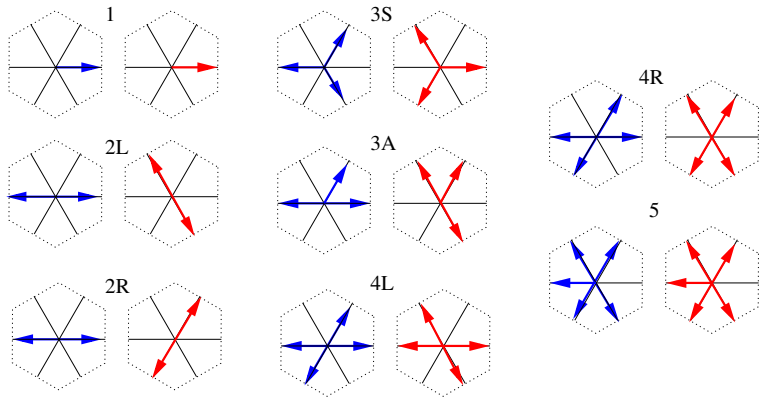

Figure 2.2: LCGA COLLISION LAWS. PRECOLLISION DISTRIBUTION IS DEPICTED IN BLUE AND THE POST-COLLISION DISTRIBUTION IS IN RED. NOTE THAT MOMENTUM AND MASS ARE CONSERVED.

The LBM is a real-valued version of the above LCGA [63,104]. The lattice Boltzmann method is constructed on a square lattice as depicted in Figure 2.3. The vertices (blue arrows) and the the mid-points of the sides (red

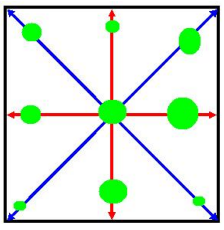

Figure 2.3: THE LBM SQUARE LATTICE. BOTH THE BLUE AND THE RED ARROWS REPRESENT CONSTANT VELOCITY VECTORS. THE BLUE VECTORS HAVE A COMMON MAGNITUDE AND THE RED VECTORS HAVE A COMMON MAGNITUDE. THE GREEN DOTS REPRESENT MASS WITH THE AREA INTENDED TO BE PROPORTIONAL TO MASS.

arrows) of the lattice represent discrete velocities, $\boldsymbol{e}_i$, where i ranges from 0 to 8. Real-valued probability density distribution values, f_i, are assigned to each of the discrete velocities. The f_i are depicted as green circles in Figure 2.3. The density of the molecules at the node is the sum of the individual f_i ($\rho = \sum_{i=0}^{8} f_i$) and the momentum at the node is the sum of products of the individual velocities and its assigned mass ($\rho \boldsymbol{U} = \sum_{i=0}^{8} f_i \boldsymbol{e}_i$). The advection and collision terminology of the kinetic theory and the lattice cell gas automata is retained [89]. Advection is represented as the movement of f_i at a given velocity to the the same velocity at the adjacent node. The mathematical description of this advection is given by

$$f_i(\boldsymbol{x}_j + \boldsymbol{e}_i \delta t, t + \delta t) = f_i(\boldsymbol{x}_j, t) \qquad 1 \leq i \leq 8$$

where $\boldsymbol{x}_j$ represents the position of the j^{th} node. The inclusion of the collision term, Ω_{ij}, redistributes $f_i(\boldsymbol{x}_j + \boldsymbol{e}_i \delta t, t + \delta t)$ such that

$$f_i(\boldsymbol{x}_j + \boldsymbol{e}_i \delta t, t + \delta t) = f_i(\boldsymbol{x}_j, t) + \Omega_{ij}$$

where Ω_{ij} represents the rate of change of f_i at the j^{th} node.

The collision rules were abandoned in favour of a collision function – the Bhatnagar-Gross-Krook approximation [10,48,80,117] – which approximates the collision as a relaxation. The relaxation occurs to an equilibrium function [75]. The collision term can thus be represented as

$$\Omega_{ij} = -\frac{f_i(\boldsymbol{x}_j) - f_i^{(eq)}(\boldsymbol{x}_j)}{\tau}$$

where $f_i^{(eq)}(\boldsymbol{x}_j)$ represents the velocity distribution of the equilibrium distribution assigned to $\boldsymbol{e}_i$ and τ is a relaxation constant. Furthermore $f_i(\boldsymbol{x}_j) - f_i^{(eq)}(\boldsymbol{x}_j)$ was selected such that momentum is conserved [75]. Consequently $\sum_{i=0}^{8} \Omega_{ij} = 0$ and $\sum_{i=0}^{8} \Omega_{ij} \boldsymbol{e}_i = 0$. Combining the advection and collision steps one obtains

$$f_i(\boldsymbol{x}_j + \boldsymbol{e}_i \delta t, t + \delta t) = f_i(\boldsymbol{x}_j, t) - \frac{f_i - f_i^{(eq)}}{\tau}$$

which is the discrete Boltzmann equation. The Navier-Stokes equations can be derived by appropriately summing over i in the above equation as shown by Hou *et al* [21,65,117]. A flow diagram depicting the classical approach is presented in Figure 1.3.

2.2 The alternate derivation of the LBM

The alternate approach views the LBM as a finite difference method applied to the continuous Boltzmann equation (CBE). The first such discretisation was by Broadwell [12, 13] who developed a one-dimensional discretisation of the CBE. Abe [1] and He and Luo [58] independently showed that the LBM is a discretisation of the CBE.

In the kinetic theory of rarefied gases the continuous Boltzmann equation

$$\left(\frac{\partial}{\partial t} + \boldsymbol{c}\cdot\nabla_{\boldsymbol{r}} + \boldsymbol{F}\cdot\nabla_{\boldsymbol{p}}\right) f(\boldsymbol{r},\boldsymbol{p},t) = \left(\frac{\partial f}{\partial t}\right)_{coll} \tag{2.1}$$

predicts the probability of finding a molecule at a given position, at a given momentum, at a given time (Huang [66], Chapter 3) where f is the probability density function, $\boldsymbol{r}$ is the position, $\boldsymbol{c}$ is the velocity and $\boldsymbol{p}$ is the momentum of the molecule. $\boldsymbol{F}$ is the applied force. The gradient with respect to position is represented as $\nabla_{\boldsymbol{r}}$ and $\nabla_{\boldsymbol{p}}$ is the gradient with respect to momentum.

Again, the collision term is approximated by the BGK relaxation [10]:

$$\left(\frac{\partial f}{\partial t}\right)_{coll} \approx -\frac{f - f^{(eq)}}{\tau\delta t}. \tag{2.2}$$

Substituting (2.2) into Equation (2.1), substituting $\frac{df}{dt} = \frac{\partial f}{\partial t} + \boldsymbol{c}\cdot\nabla_{\boldsymbol{r}} f$ and neglecting the body force $\boldsymbol{F}$,

$$\frac{df}{dt} = -\frac{1}{\tau\delta t} f + \frac{1}{\tau\delta t} f^{(eq)}. \tag{2.3}$$

The Maxwell-Boltzmann distribution (Huang [66], Chapter 4) gives the equilibrium distribution

$$f^{(eq)} = \frac{\rho}{(2\pi \mathrm{RT})^{(D/2)}} e^{-\frac{(\boldsymbol{c}-\boldsymbol{c}_0)^2}{2\mathrm{RT}}} = \frac{\rho}{(2\pi \mathrm{RT})^{(D/2)}} e^{-\frac{|\boldsymbol{c}-\boldsymbol{c}_0|^2}{2\mathrm{RT}}} \tag{2.4}$$

where R is the universal gas constant, T is the temperature in degrees Kelvin, D is the number of spatial dimensions, and $|\boldsymbol{c}-\boldsymbol{c}_0|^2 = (\boldsymbol{c}-\boldsymbol{c}_0)\cdot(\boldsymbol{c}-\boldsymbol{c}_0)$.

The above provides the theory behind the behaviour of gases at a mesoscopic level. By applying the Chapman-Enskog (CE) expansion, it is possible to derive the Navier-Stokes equations [18, 42]. The Chapman-Enskog expan-

sion is a multiscaling technique. The first order application derives the N-S equations [18] and the second order expansion derives the Burnett equations, but this and other higher order expansions, have not been shown to contribute significantly [42] for fluids.

In the conventional approach to the numerical modelling of fluids, the N-S equations would be discretised (finite difference, finite volume or finite-element method). However, when applying the LBM as a numerical method, Equation (2.3) is discretised using the finite difference method, to obtain

$$\frac{f_i(\boldsymbol{x}_j + \boldsymbol{e}_i\delta t, t+\delta t) - f_i(\boldsymbol{x}_j, t)}{\delta t} = -\frac{1}{\tau\delta t}f + \frac{1}{\tau\delta t}f^{(eq)}.$$

After multiplying by δt one gets the lattice Boltzmann equation (LBE)

$$f_i(\boldsymbol{x}_j + \boldsymbol{e}_i\delta t, t+\delta t) - f_i(\boldsymbol{x}_j, t) = -\frac{f_i - f_i^{(eq)}}{\tau} = \Omega_{ij}(\boldsymbol{r}, \boldsymbol{c}) \qquad (2.5)$$

He and Luo [58] integrated Equation (2.3) formally to derive (2.5).

A formal derivation of the discretisation of space and velocity space requires a truncated Taylor expansion of Equation (2.4) such that

$$\begin{aligned} f^{(eq)} &= \frac{\rho}{(2\pi\mathrm{RT})^{D/2}} e^{-\boldsymbol{c}^2/2\mathrm{RT}} e^{2\boldsymbol{c}\cdot\boldsymbol{c}_0/2\mathrm{RT}} e^{-c_0^2/2\mathrm{RT}} \\ &= \frac{\rho}{(2\pi\mathrm{RT})^{D/2}} e^{-c^2/2\mathrm{RT}} \left(1 + \frac{\boldsymbol{c}\cdot\boldsymbol{c}_0}{\mathrm{RT}} + \frac{(2\boldsymbol{c}\cdot\boldsymbol{c}_0)^2}{2(\mathrm{RT})^2}\right)\left(1 - \frac{\mathrm{U}^2}{2\mathrm{RT}}\right) \\ &= \frac{\rho}{(2\pi\mathrm{RT})^{D/2}} e^{-c^2/2\mathrm{RT}} \times \left(1 + \frac{\boldsymbol{c}\cdot\boldsymbol{c}_0}{\mathrm{RT}} + \frac{(2\boldsymbol{c}\cdot\boldsymbol{c}_0)^2}{2(\mathrm{RT})^2} - \frac{\mathrm{U}^2}{2\mathrm{RT}}\right). \end{aligned} \qquad (2.6)$$

Given that, at equilibrium, $\rho = \int f^{(eq)} d\boldsymbol{c}$ and $\rho\mathbf{U} = \int f^{(eq)}\boldsymbol{c} d\boldsymbol{c}$, equation (2.5) is integrated numerically with respect to $\boldsymbol{c}$ in order to satisfy conservation of mass and momentum and thus

$$\begin{aligned} \int \Omega_{ij}(\boldsymbol{r}, \boldsymbol{c})\, d\boldsymbol{c} = \quad 0 \quad &= \int -\frac{f_i(\boldsymbol{x}_j) - f_i^{(eq)}(\boldsymbol{x}_j)}{\tau}\, d\boldsymbol{c}, \\ \int \Omega_{ij}(\boldsymbol{r}, \boldsymbol{c})\boldsymbol{c}\, d\boldsymbol{c} = \quad 0 \quad &= \int -\frac{f_i(\boldsymbol{x}_j) - f_i^{(eq)}(\boldsymbol{x}_j)}{\tau}\boldsymbol{c}\, d\boldsymbol{c}. \end{aligned}$$

Integration at position $\boldsymbol{r}$ is performed approximately using Gaussian quadrature. In Section 8.2 it will be shown that various orthonormal polynomial solutions exist and that Hermite polynomials (at particular sampling veloc-

ities) generate the nine velocity square lattice [35, 58]. The N-S equations can be derived from the LBE (2.5) by using a CE-like expansion [35, 65]. A graphical depiction of the alternate derivation is given by Figure 1.4 and should be compared to the classical approach in Figure 1.3.

2.3 Success of the LBM

The LBM has modelled several standard computational fluid dynamics benchmarks [65, 97, 109, 119, 132]. In addition, the LBM algorithm is inherently parallel, making it ideal for solution on parallel computers [78, 127]. It has been used to model multiple immiscible and miscible fluids [49, 50, 55, 62, 69, 124, 129, 130] and non-ideal fluids [39, 54, 98, 116, 120, 125]. It has also been used to model porous boundary conditions [22], suspensions [84, 85], fluid-structure interaction [76, 77, 79], biomechanics [4] and solids [91, 102].

2.4 Criticism of and difficulties with the LBM

The classical approach to the LBM has been criticised for not separating physics, mathematical description of the physics and numerical solution of the mathematical description of the physics, but the alternate derivation has eliminated this criticism [1, 2, 57, 58]. Further shortcomings are the lattice is prohibitively fine for real fluids (the excessive number of nodes is a function of the velocity of the fluid). Attempts have been made to limit this restriction [20, 59, 151]. Curvilinear and non-uniform co-ordinate systems were not supported initially [56, 59]. Attempts have also been made to model higher Reynolds numbers [61]. A universally accepted approach to boundary conditions is pending [24, 60, 70, 99, 106, 112, 156].

2.5 The value of the alternate approach

This work uses the alternate approach. The value of the alternate derivation lies in the abandonment of the idea of advection and collision. This is made possible by the finite differencing of the CBE. Thus LBM-like methods can be derived for other equations without resorting to the ideas of advection and collision – which (unlike the case for gases) may not be physically relevant. In particular this thesis will construct a polymer LBM.

In Section 1.1.1 a general definition for equilibrium behaviour and non-equilibrium behaviour was presented. A specific definition can now be produced for gases. The equilibrium distribution function is the time-independent solution of the CBE (2.1) and equilibrium behaviour is the behaviour predicted by this solution (Huang [66], Chapter 4). Conversely the non-equilibrium behaviour of gases is that predicted by the general solution to equation (2.1).

2.6 Hybrid Gibbs-Boltzmann polymer formulation

Statistical descriptions of the kinetic theory of polymers have been used to formulate constitutive equations for the mechanical behaviour of polymers. Discrete models based either directly on the kinetic theory or on the constitutive equations exist and are being developed (as described in Section 1.4).

However, Edwards [30] notes that at least two approaches to statistical mechanics exist – the Boltzmann dynamic approach and the Gibbs thermodynamic approach (Huang [66], Chapter 3). Gas dynamics and the CBE (2.1) are based on the former approach, the LBE (2.5) is a discretised variant of the CBE and the LBE is the origin of the LBM for fluids as described in this chapter. Edwards notes that conventional statistical models of polymers are based on the Gibbs approach [33,34,136,142,143,145] which usually only applies at equilibrium [40]. He also shows that the Gibbs approach (unlike the Boltzmann approach) cannot derive transport phenomena. Edwards [31]

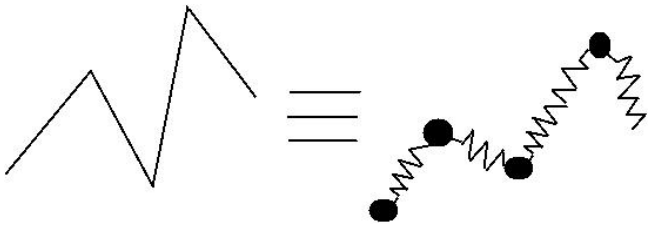

Figure 2.4: Rouse Boltzmann polymer model. Note that the individual segments of a molecular chain are modelled as ball-and-spring.

elects to formulate his dynamic approach to polymers using general, formal and robust mathematical arguments to model a molecule chain. An alternative Rouse approach [123, 140, 155] applies ball-and-spring models to the segments of a molecular chain where the segments are capable of stretch as depicted in Figure 2.4.

This thesis will formulate a Boltzmann-Gibbs hybrid approach to polymers. It will also apply mechanics to an intuitive, physically relevant ball-and-spring model. However, unlike the Rouse models, the ball-and-spring will apply to the whole molecular chain and the mechanics will be applied to the whole molecule as depicted in Figure 2.5.

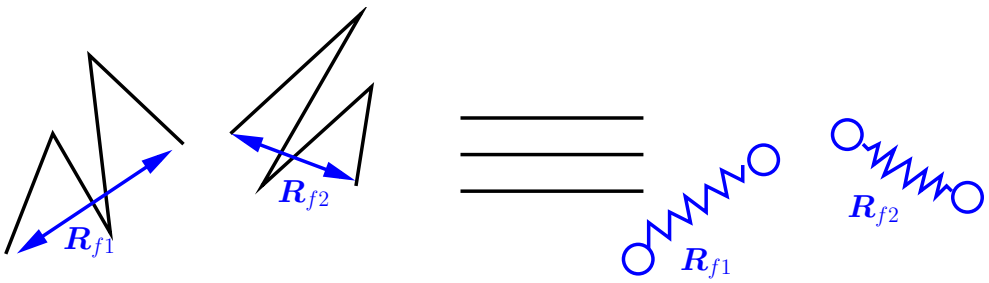

Figure 2.5: Hybrid Gibbs-Boltzmann polymer model. Note that the displacement from one end of the molecule is denoted by the vector $\boldsymbol{R}_f$ and that it is this displacement that is modelled as a ball-and-spring.

Thus the Boltzmann approach will be utilised for molecular interaction. It will be shown that this Boltzmann approach will incorporate specimen and transport phenomena. The existing Gibbs approach to the probability distribution of a polymer chain and polymer networks will be applied to individual chains and the polymer network within a representative volume, generating material properties. The Boltzmann-Gibbs hybrid approach is more closely analogous to the kinetic theory of gases. Figure 2.6 illustrates the pathways to modelling of polymers with the path taken by this thesis depicted in red.

The hybrid Gibbs-Boltzmann approach is justified by Section 2.2 in which the alternate derivation of the LBM discretises space and velocity space by applying Gaussian quadrature with Hermite polynomials. It will be shown that the form of the probability distribution function derived by the Gibbs formulation also allows discretisation by applying Gaussian quadrature with Hermite polynomials. In contrast, the formulation of the polymer interaction term in Chapter 4 and the definition of mechanical properties to be established in Chapter 5 will require a Boltzmann approach. The results of Chapters 4 and 5 will, in turn, be required for the Chapman-Enskog expansion in Chapter 6. It is the Chapman-Enskog (CE) expansion that will allow the derivation of the macroscopic description and the transport phenomena.

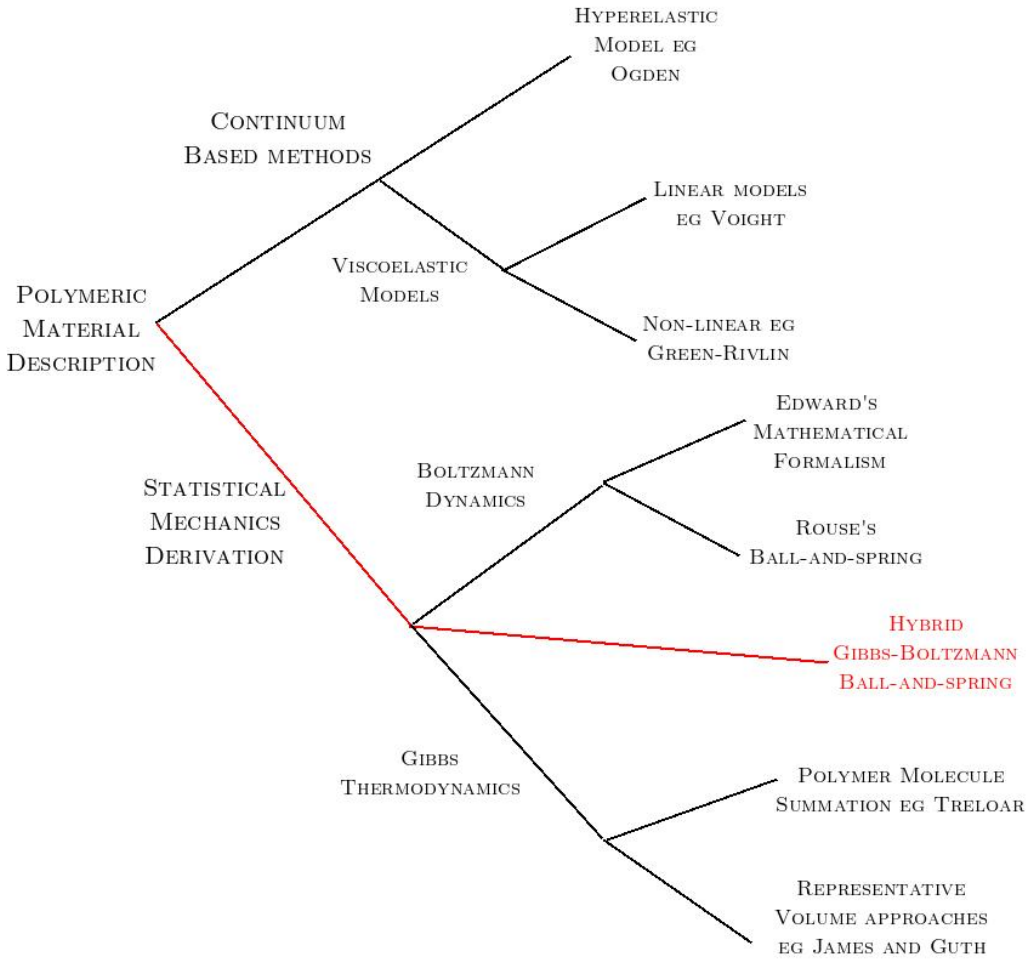

Figure 2.6: Approaches to polymer modelling. Note that the hybrid Gibbs Boltzmann approach, as represented by the RED path, is depicted in Figure 2.5 and implicitly requires interaction between molecules. The Gibbs thermodynamic approach only considers one such molecule.

Chapter 3

The differential equation of polymer chain interaction

Chapter 2 distinguishes the alternate derivation of the LBM from the classical derivation. The alternate derivation isolates/separates the mathematical description of the physics from the numerical method utilised to solve the mathematical description and it is this approach that will be adopted for polymers.

This chapter (and subsequent chapters) are structured such that the physics/assumptions/material science of polymers are stated and then followed by the mathematical description. This structure is applied to the existing theory for the statistical mechanics of polymers which corresponds to rubber elasticity. The structure will then be applied to what will be termed the non-equilibrium theory for the statistical mechanics of polymers.

The purpose of this chapter is to construct the equivalent of the continuous Boltzmann equation (2.1) for polymers. This will be termed the polymer chain interaction equation. The chapter begins by reviewing the existing theory for the elastic behaviour of polymers. The equilibrium behaviour will be that for which macroscopic properties are time-independent. As a consequence, the equilbrium behaviour will be the stretch-rate-independent solution to the polymer chain interaction equation. This equilibrium behaviour will correspond to rubber elasticity. The behaviour predicted by the general solution to the polymer chain interaction equation will be the non-equilibrium behaviour.

This chapter's relevance to the thesis will now be reiterated by present-

ing an overview. This chapter will develop a theory for the non-equilibrium behaviour of polymers and construct the mesoscopic polymer chain interaction equation to describe this theory mathematically. The chapter omits to determine the form of one of the terms in the mesoscopic polymer chain interaction equation but this term will be determined in Chapter 4. Chapter 6 will apply an averaging procedure to determine the macroscopic consequences of the mesoscopic polymer chain interaction equation and Chapter 7 will show that mathematical description of the macroscopic consequences of the polymer chain interaction equation correspond to viscoelasticity.

3.1 The preliminary requirements

Various definitions and assumptions upon which the theory is based are summarised here. These statements will be described mathematically later.

3.1.1 Polymer concepts and definitions

An equilibrium state is defined as the collection of microscopic properties under which the macroscopic properties of a material do not change with respect to time. Equilibrium states are not unique. For every given strain state, an equilibrium condition exists. By definition, a non-equilibrium state exists when the macroscopic properties change with respect to time.

A zero-stress (not zero-strain) state for a specimen is a specimen state that exists when no external forces act on the specimen. The zero-stress state (no external forces) can obviously either be in equilibrium or non-equilibrium microscopically. The former case of zero-stress with microscopic equilibrium corresponds to a zero-strain state macroscopically or ground state with respect to strain. In the latter case (zero-stress with microscopic non-equilibrium), although no external stress is being exerted on the system, the residual strain in the system is being released – and internal stress is present. Less obviously, multiple zero-strain states can exist for a given specimen. For example, as a polymer deforms plastically, new zero-strain states are continuously created.

For any given stress state, the material can be in equilibrium or non-equilibrium microscopically. Similarly, a specimen can be in steady state (if not changing in time or static) or disequilibrium (if changing in time). Vis-

coelasticity (or a time-dependent reversible stress-strain relationship) is an example of a material in non-equilibrium or a specimen in disequilibrium. Although stated as a definition here, it will be shown in Section 7.2 that the macroscopic, non-equilibrium behaviour of polymer specimens corresponds to the standard concept of viscoelasticity.

It is possible for a specimen to be in steady state with respect to a variable whilst the material is in non-equilibrium with respect to the same variable – redistributing the variable across positions within the specimen. It will be shown that stress relaxation is such a situation with respect to stretch and that creep is such a scenario with respect to stress. The converse (where the material is in equilibrium but the specimen is in disequilibrium) is not apparent.

As a consequence, some additional terminology is required. Consider the definition of equilibrium provided in the glossary. Implicitly if a material is in microscopic equilibrium it is also in material equilibrium. Similarly when considering the definition of a material in non-equilibrium, microscopic non-equilibrium must occur simultaneously. Furthermore, a microscopic maximum entropy state implies that the material has also achieved maximum entropy within the representative volume. Thus when equilibrium, non-equilibrium and maximum entropy states are used, they refer to both the microscopic and material situations unless specified. Table 3.1 categorises similar but not synonymous terms into mesoscopic, material and specimen categories.

	Mesoscopic	**Material**	**Specimen**
Default	Equilibrium	Equilibrium	Ground State
Static	Maximum Entropy	Maximum Entropy	Steady State
Transient	Non-Equilibrium	Non-Equilibrium	Disequilibrium

Table 3.1: Similar mesoscopic, material and specimen terms

3.1.2 The underlying assumptions

Consider a long chain molecule in three-dimensional space. The chain consists of multiple links that are free to rotate relative to each other. Let the position of the one end of the molecule be denoted by A (the selection of the end will be described shortly). Furthermore, let A define the position

of the molecule then the displacement of the molecule is defined to be the change in position of A. Denote the other end of the molecule by B. Let the vector from position A to position B be designated $\boldsymbol{R}_f$ and be called the molecule's vector length as depicted in Figure 3.1. When a force is ap-

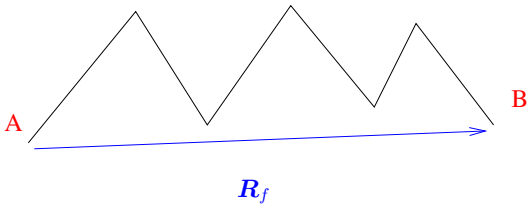

Figure 3.1: Schematic representation of an ideal polymer molecule

plied across the ends of the molecule, the links change configuration such that the vector length changes to $\boldsymbol{R}'_f$ as depicted in Figure 3.2. Upon release of the force, the molecule changes configuration and returns to the original vector length but not necessarily configuration, as depicted in Figure 3.2. Thus the analogy with a spring and the concept of non-unique equilibrium states is established. Further one can imagine a force being applied at an instant and then released. This would induce a vibration in this idealised molecule. Consider next a pair of molecules. These molecules have either

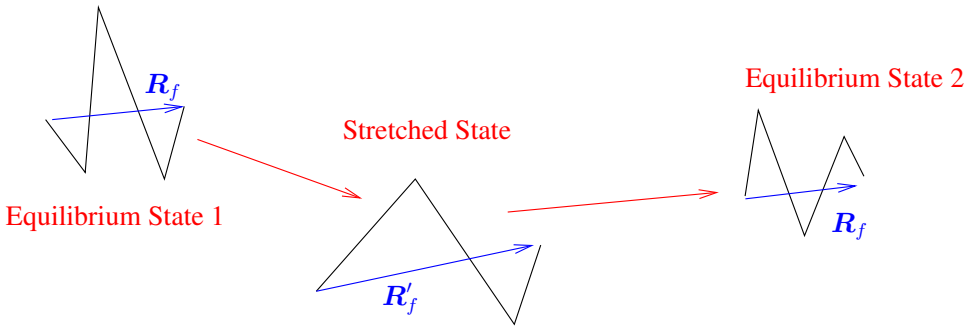

Figure 3.2: Schematic depicting the polymer molecule-spring analogy

weak, transient or strong bonds. Dependending on the type of bond, force can either be transmitted across molecules with or without delay or molecules can move relative to each other. These represent extremes of possible molecular behaviour and where along this spectrum a polymer is, is material- and condition- (*eg* temperature) specific. One should anticipate that a material in which molecules slide more easily relative to each other is more fluid-like. Materials with weaker bonds do not transmit force across the body instantaneously and consequently time-dependent behaviour would be anticipated.

Materials with stronger bonds (for example cross-linking) should not exhibit time-dependent stress-strain relationships.

In this work, only the state where weak and transient bonds dominate are considered. Furthermore, at this end of the spectrum, when the molecules interact, the molecules do not slide over each other. However, the molecules are not bound at fixed locations. Thus when a stretch (or external force) is applied at the one end of the specimen, the end where the stretch is applied experiences the force first. The stretch across the molecule is reduced as some of the stretch is transmitted to the adjacent layer of molecules. This process repeats itself as the stretch is distributed throughout the specimen. Furthermore as this stretch is relaxed between adjacent layers of molecules, vibrations are generated within the molecules (and throughout the specimen) as previously suggested for a single molecule. The above description is that of a wave and is depicted in Figure 3.3 where the blue dots represent molecular position and the spaces between the molecules represent stretch.

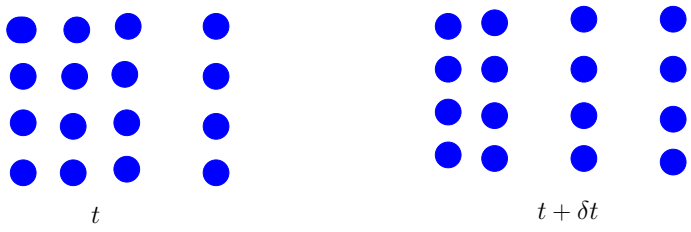

Figure 3.3: Wave model of polymer elasticity. The image on the left represents the distribution of stretch within the specimen at time t. The image on the right represents the distribution of stretch within the specimen at time $t + \delta t$ where δt is a small positive increment of time.

As an aside, it seems reasonable to assume that this vibration will experience damping due to internal molecular friction. However this would mean some of the energy transmitted into the material by the applied stretch will be dissipated as heat. This energy cannot be recovered when the force is released. Consequently hysteresis will be induced.

In much the same way as the state of a gas molecule was completely defined by the probability density distribution, f, as a function of position and momentum at any given instant in time, let the state of a long chain molecule be completely defined by a probability density distribution, p, of a finite number of variables.

From the above, for a molecule to be defined, at least the position ($\mathbf{r}$), the velocity ($\boldsymbol{c}$) of the one end of the molecule, the vector length of the molecule ($\boldsymbol{R}_f$), the amplitude of the vibration ($\boldsymbol{R}_A$) along the vector length with period T_v, the damping factor (η), a period of vibration T_a due to change in direction as the molecules interact, and the time t must be known. Figure 3.4 depicts these variables.

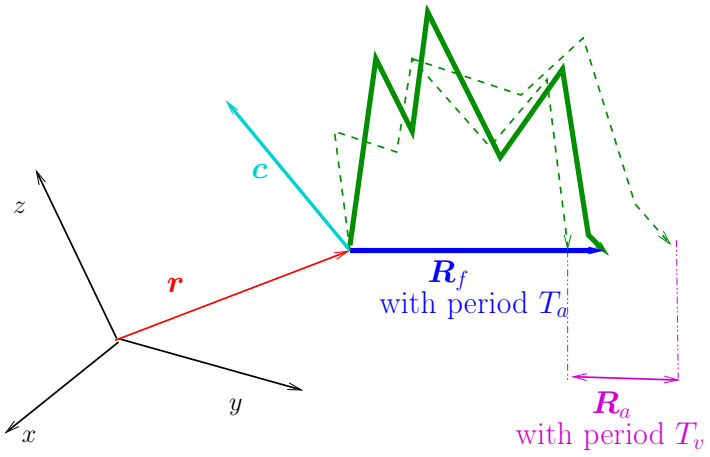

Figure 3.4: FULL MOLECULAR DESCRIPTION WHERE THE SOLID GREEN LINE REPRESENTS THE MOLECULE, THE DASHED GREEN LINES REPRESENT THE LIMITS OF THE MOLECULE DURING VIBRATION ALONG THE LENGTH AND THE BLACK ARROWS REPRESENT THE COORDINATE SYSTEM. THE RED ARROW REPRESENTS THE POSITION OF THE MOLECULE, THE CYAN ARROW REPRESENTS THE VELOCITY OF ONE END OF THE MOLECULE, THE BLUE ARROW REPRESENTS THE MOLECULE'S VECTOR LENGTH AND THE PINK ARROW REPRESENTS THE VIBRATION ALONG THE LENGTH.

Thus the probability density function p, which gives the probability of finding a molecule of predefined property per unit volume, is given by

$$p(\mathbf{r}, \boldsymbol{R}_f, \boldsymbol{c}, \boldsymbol{R}_A, T_a, T_v, \eta, t).$$

The velocity $\boldsymbol{c}$ can be divided into two components. There is a component independent of the stretch of the molecule which equates to the translation (or flow) of the molecule and will be designated $\acute{\boldsymbol{c}}$. A second component is due to the stretch rate of the molecule and will be designated $\grave{\boldsymbol{c}}$, where $\grave{\boldsymbol{c}}$ is a function of $\dot{\boldsymbol{R}}_f$. Consequently the probability density function further reduces to

$$p(\mathbf{r}, \boldsymbol{R}_f, \acute{\boldsymbol{c}}, \grave{\boldsymbol{c}}(\dot{\boldsymbol{R}}_f), \boldsymbol{R}_A, T_a, T_v, \eta, t). \tag{3.1}$$

In this model hysteresis (a consequence of η and T_v) and plastic deforma-

tion (a consequence of $\acute{\boldsymbol{c}}$) are omitted. Thus only reversible phenomena are considered.

Let the notion of vibration about a direction (with period T_a) as molecules interact also be ignored. For a body in equilibrium $\boldsymbol{R}_A = \mathbf{0}$ and $\grave{\boldsymbol{c}} = \mathbf{0}$; thus in analogy with the μ space for gases (Huang [66], Chapter 3), the state of any given molecule at equilibrium can be defined by the position of the molecule and the vector length of the molecule, reducing the probability density distribution to

$$p(\mathbf{r}, \boldsymbol{R}_f). \tag{3.2}$$

For the non-equilibrium reversible polymer situation, $\grave{\boldsymbol{c}}(\dot{\boldsymbol{R}}_f)$ cannot be neglected and the probability density distribution function at time t is

$$p(\mathbf{r}, \boldsymbol{R}_f, \grave{\boldsymbol{c}}(\dot{\boldsymbol{R}}_f), t). \tag{3.3}$$

A concept of molecular interaction is however still required. During half a

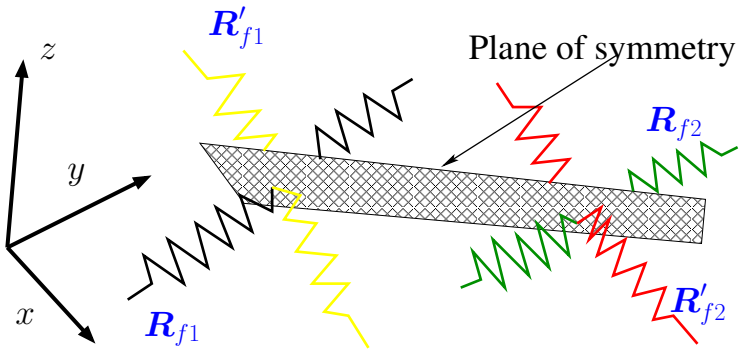

Figure 3.5: During interaction, molecules reflect in the plane of symmetry/reflection. This plane of symmetry represents the neutral position for each molecule. As depicted, the plane of reflection is common. The black molecule represents the original orientaion of molecule 1 ($\boldsymbol{R}_{f1}$). The yellow molecule is the post interaction molecule 1 ($\boldsymbol{R}'_{f1}$).

period of molecular interaction, a plane can be defined such that the vector lengths at the beginning and the end of the half-period are reflections of each other in that plane. Let this plane be called the neutral plane. Furthermore, a molecule has an orientation relative to another before and after molecular interaction. The assumption is made that the neutral planes of the two molecules are parallel. This is depicted in Figure 3.5. Although stated as an assumption here, Section 4.2 will show that this is a potential solution. Thus the microscopic discription of a molecule is established.

3.1.3 Macroscopic continuum results

In order to relate microscopic and macroscopic properties, certain continuum results are required. Consider a macroscopic body. Let $\mathbf{x}(\mathbf{X}, t)$ be the current position of particle P at time t with respect to the reference position $\mathbf{X}$. The displacement vector $\mathbf{u}$ is then $\mathbf{x}(\mathbf{X}, t) - \mathbf{X}$. The material deformation gradient tensor is defined by

$$\mathbf{F} := \mathbf{I} + \nabla\mathbf{u} = \frac{\partial \mathbf{x}}{\partial \mathbf{X}} \tag{3.4}$$

where $\nabla\mathbf{u}$ is the displacement gradient with components

$$(\nabla\mathbf{u})_{ij} = \frac{\partial u_i}{\partial X_j}.$$

The Lagrangian strain tensor $\mathbf{E}$ ([86], Chapter 3) and the infinitesimal strain tensor $\mathbf{E}^{(1)}$ are defined by

$$\mathbf{E} := \frac{1}{2}(\nabla\mathbf{u} + (\nabla\mathbf{u})^T + (\nabla\mathbf{u})^T\nabla\mathbf{u}) = \mathbf{F}^T\mathbf{F}, \tag{3.5}$$

$$\mathbf{E}^{(1)} := \frac{1}{2}(\nabla\mathbf{u} + (\nabla\mathbf{u})^T). \tag{3.6}$$

Similarly, a spatial deformation tensor, $\mathbf{P}$, can be derived and defined since $\mathbf{x}(\mathbf{X}, t)$ is invertible. Consider a spatial point Q at position $\mathbf{x}$ which has undergone a displacement $\mathbf{v}(\mathbf{x}, \mathbf{t})$ from material point P at $\mathbf{X}(\mathbf{x}, \mathbf{t})$ such that

$$\mathbf{x} = \mathbf{X}(\mathbf{x}, \mathbf{t}) + \mathbf{v}(\mathbf{x}, \mathbf{t}). \tag{3.7}$$

Then

$$\mathbf{P} := \mathbf{I} - \nabla\mathbf{v} \iff d\mathbf{X} = \mathbf{P}d\mathbf{x} \tag{3.8}$$

where the gradient of the vector field $\mathbf{v}$ is in spatial co-ordinates, with

$$(\nabla\mathbf{v})_{ji} = \frac{\partial v_j(\mathbf{x}, t)}{\partial x_i}.$$

Furthermore a spatial strain tensor (the Eulerian-Almansi strain tensor) $\boldsymbol{e}$ can be defined by

$$\begin{aligned} \mathbf{P}^T\mathbf{P} &= \mathbf{I} - \nabla\mathbf{v}^T - \nabla\mathbf{v} + (\nabla\mathbf{v})^T\nabla\mathbf{v} = \mathbf{I} - 2\boldsymbol{e} \\ &= \mathbf{I} - 2\boldsymbol{e}^{(1)} + (\nabla\mathbf{v})^T\nabla\mathbf{v} \approx \mathbf{I} - 2\boldsymbol{e}^{(1)} \end{aligned} \tag{3.9}$$

where $\boldsymbol{e}$ is the Eulerian-Almansi strain tensor and $\boldsymbol{e}^{(1)}$ is the first order approximation to the spatial strain tensor or the spatial infinitesimal strain

tensor

$$\boldsymbol{e}^{(1)} := \frac{1}{2}[(\nabla \mathbf{v})^T + \nabla \mathbf{v}]. \tag{3.10}$$

For infinitesimal deformation, ie $|\nabla \mathbf{u} \ll \mathbf{I}|$ and $|\nabla \mathbf{v} \ll \mathbf{I}|$, $\mathbf{E} \approx \mathbf{E}^{(1)}$, $\mathbf{e} \approx \mathbf{e}^{(1)}$ and

$$\mathbf{E}^{(1)} \approx \mathbf{e}^{(1)}. \tag{3.11}$$

The polar decomposition theorem states that any deformation gradient can be decomposed into a proper orthogonal matrix $\mathbf{R}$, describing rigid body rotation, and positive-definite symmetric tensors $\mathbf{U}$ and $\mathbf{V}$ describing pure stretch such that

$$\mathbf{RU} = \mathbf{F} = \mathbf{VR} \qquad \text{and} \qquad \mathbf{R}^T\mathbf{R} = \mathbf{I}. \tag{3.12}$$

3.1.4 The affine deformation assumption

An important result is the affine deformation assumption. In the continuum context, for

$$\mathbf{x} = \mathbf{FX} + \mathbf{b},$$

$\mathbf{F}$ is assumed a constant.

In the context of statistical mechanics of polymers (Treloar [138], Chapter 4), when a polymeric material is subjected to an affine deformation as described by a macroscopic deformation tensor $\mathbf{F}$, each of the individual chains rotates and stretches, with this motion described by a microscopic tensor $\mathbf{\Lambda}$ [71, 140]. This relates macroscopic to microscopic behaviour. The proof follows.

Let $\mathbf{R}_{AB}$ be a vector between points A and B in the continuum. After affine deformation, let this vector be transformed to $\mathbf{R}'_{AB}$ such that

$$\mathbf{R}'_{AB} := \mathbf{FR}_{AB}. \tag{3.13}$$

Let $\boldsymbol{R}_{fi0}$ represent the vector length of the i^{th} molecule at time $t = 0$ where $t = 0$ is a time when the molecule is in equilibrium, and $\boldsymbol{R}_{fi}$ its vector length at arbitrary time $t > 0$. Let $\boldsymbol{R}_{\mu 0}$ be the central (or averaged) measure of the collection of unstretched chains within the RVE, where the set or collection of vector lengths within the RVE is represented as $\{\boldsymbol{R}_{fi0}\}_{i=1}^{N}$. By

definition, the distribution of an RVE is the symmetric Gaussian distribution (see Section 1.1.1). Thus it is justified that the central measure is selected to be the arithmetic mean vector length of the representatitive volume element (RVE). Let $\boldsymbol{R}_\mu$ be the mean vector length of the RVE at time t. Then

$$\boldsymbol{R}_{\mu 0} = \frac{1}{N}\sum_{i=1}^{N} \boldsymbol{R}_{fi0} \qquad \text{and} \qquad \frac{1}{N}\sum_{i=1}^{N} \boldsymbol{R}_{fi} = \boldsymbol{R}_\mu.$$

Given that averaged properties are macroscopic, from Equation (3.13)

$$\begin{aligned} \frac{1}{N}\sum_{i=1}^{N} \boldsymbol{R}_{fi} = \boldsymbol{R}_\mu &= \mathbf{F}\boldsymbol{R}_{\mu 0} = \mathbf{F}\frac{1}{N}\sum_{i=1}^{N} \boldsymbol{R}_{fi0} \\ \iff \qquad \frac{1}{N}\sum_{i=1}^{N} \boldsymbol{R}_{fi} &= \mathbf{F}\frac{1}{N}\sum_{i=1}^{N} \boldsymbol{R}_{fi0} = \frac{1}{N}\sum_{i=1}^{N} \mathbf{F}\boldsymbol{R}_{fi0}. \end{aligned} \tag{3.14}$$

A *sufficient* condition to satisfy requirement (3.14) is

$$\boldsymbol{R}_{fi} = \mathbf{F}\boldsymbol{R}_{fi0}. \tag{3.15}$$

but the affine deformation assumption requires that [140]

$$\boldsymbol{R}_\mu = \frac{1}{N}\sum_{i=1}^{N} \boldsymbol{R}_{fi} \iff \boldsymbol{R}_{fi} = \mathbf{F}\boldsymbol{R}_{fi0}. \tag{3.16}$$

Thus the affine deformation assumption is a statement that (3.15) is a *necessary* condition to satisfy condition (3.14).

Furthermore, given that $\boldsymbol{R}_{fi}$ and $\boldsymbol{R}_{fi0}$ are microscopic properties, each chain ($\boldsymbol{R}_{fi}$) has an associated microscopic deformation tensor $\boldsymbol{\Lambda}_i$ such that

$$\boldsymbol{R}_{fi} = \boldsymbol{\Lambda}_i\boldsymbol{R}_{fi0} = \mathbf{F}\boldsymbol{R}_{fi0} \qquad \forall\, 1 \le i \le N.$$

Thus

$$(\boldsymbol{\Lambda}_i - \mathbf{F})\,\boldsymbol{R}_{fi0} = 0 \qquad \forall\, 1 \le i \le N$$

and since $\boldsymbol{R}_{fi0}$ is arbitrary, we find that

$$\boldsymbol{\Lambda}_i = \mathbf{F} \qquad \forall\, 1 \le i \le N. \tag{3.17}$$

The affine deformation assumption is thus established and, for an RVE, the macroscopic and microscopic deformation tensors are equal.

The polar decomposition theorem (see Section 3.1.3) implies that the macroscopic deformation tensor $\mathbf{\Lambda}$ can be decomposed such that

$$\mathbf{F} = \mathbf{RU}. \tag{3.18}$$

But as a consequence of the microscopic interpretation of the affine deformation assumption (3.17)

$$\mathbf{F} = \mathbf{\Lambda} = \mathbf{\Lambda}^{\langle R \rangle}\boldsymbol{\lambda} \iff \mathbf{U} = \boldsymbol{\lambda} \tag{3.19}$$

where the tensor $\mathbf{\Lambda}^{\langle R \rangle}$ represents rotation and the tensor $\boldsymbol{\lambda}$ represents pure stretch. The magnitude of the stretch $|\boldsymbol{\lambda}|$ is therefore given by

$$|\boldsymbol{\lambda}| = \sqrt{\frac{1}{3}\lambda_{ii}^2} = \sqrt{\frac{1}{3}\sum_{i=1}^{3}\lambda_i^2}$$

where λ_i are the eigenvalues of $\boldsymbol{\lambda}$ and $\boldsymbol{\lambda}_i$ are the eigenvectors of $\boldsymbol{\lambda}$ or the principal stretch vectors in the principal directions i.

3.2 Polymer equilibrium statistical mechanics

Although this section on the equilibrium behaviour of polymers is not novel, polymers are a significant component of this work and therefore the mathematical description will be presented in detail. Essentially the entropy of a single molecule is determined. Then the entropy of a body of molecules is summed and used to determine the work done on the body. The stresses are determined from the work.

The development of the statistical mechanics of long-chain polymers is presented by Treloar [138]. He discusses three different scenarios or situations that will be presented in this introduction to the section. Each scenario derives the statistical mechanics for a single polymer chain and then sums the results for a network of polymers. This method of derivation will be reproduced here. The results will be the same, but the derivation will be different. This difference will be that here the chains will be selected from a particular direction. Chains were selected at random in the original derivation [81]. It should be noted that these studies of the statistical mechanics of polymers were confined to the statistical mechanics of equilibrium states

as defined above.

Treloar [138] discusses three situations. The first (Treloar [138], Chapters 3 and 4) is the most trivial and is the statistical theory for a Gaussian distribution of chain length (vector length) [81, 134, 142]. The theory is only valid for modest stretches (principal stretch in the i direction, $\lambda_i \leq 1.4$) [135]. Given that hyperelasticity is a distinguishing characteristic of polymers, depending on the application, this may be a significant limitation. However, the theory is attractive because it closely resembles the theory for rarefied gases.

The second situation (Treloar [138], Chapter 6) designated non-Gaussian distribution of chain lengths) [71, 137, 145] assumes very long chains with many cross-links. This allows approximations to simplify derivation. This situation also has an elegant solution and provides better agreement with the stress-strain curve for a rubber. The solution is elegant because it defines a function called a Langevin that keeps the mathematics concise. More importantly it does not correspond to the rarefied gas analogy. Recall that the discretisation of velocity space was a consequence of Gaussian integration with Hermite polynomials [58]. The use of Hermite polynomials will not be possible for the non-Gaussian chain distribution. This implies that a new series of orthogonal polynomials will have to be generated such that the moments of the most probable distribution can be calculated.

The third situation (Treloar [138] Chapter 6) is that of representative volumes and can be used for short and long chains [34, 82]. This one will also require different orthogonal polynomials.

Not all three of these situations will be discussed further. Only the Gaussian vector length distribution will be considered because known orthogonal polynomials can be used. It should be noted that the model which will be developed in this thesis will extend the equilibrium theory to the non-equilibrium situation and consequently the probability distribution of chain stretch rate will be included. A Gaussian stretch rate is assumed (a requirement of the definition of the RVE presented in Section 1.1).

3.2.1 The polymer equilibrium distribution

A long chain molecule is considered to consist of several segments that rotate freely about each other. Each of the segments is considered to be identical. The length of a segment is l and the number of segments per molecule is n. One can define the origin of a cartesian co-ordinate system as being at the end, A, of a long polymer chain. Kuhn [81] and Guth and Mark [51] derive a

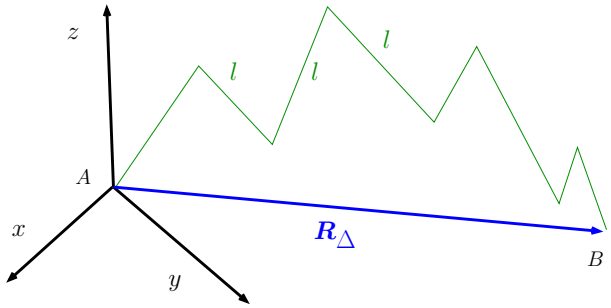

Figure 3.6: A SINGLE MOLECULE STRETCHED

formula for the probability of finding the other end, B as depicted in Figure 3.6, of the polymer chain within a volume dV about point $Q(\mathbf{r})$. Kuhn's derivation selected molecules at random. Let $\boldsymbol{R}_\Delta$ represent the vector length when molecules are selected at random. Their argument was that for every molecule of vector length $\boldsymbol{R}_\Delta$ one is equally likely to find a molecule of vector length $-\boldsymbol{R}_\Delta$. This probability is given by

$$p(\boldsymbol{R}_\Delta)d^3R_\Delta = \frac{b^3}{\pi^{3/2}}e^{-b^2|\boldsymbol{R}_\Delta|^2}d^3R_\Delta \tag{3.20}$$

where the symbol $\boldsymbol{R}_\Delta$ has been selected because by setting the origin to exist at the end A of the chain, the symbol $\boldsymbol{R}_\Delta$ represents the position of B relative to A. Note that this probability is independent of t, the chains are selected at random and that the x, y, z components can be treated independently. Equation (3.20) is analagous to the equilibrium distribution function (2.4). It is the probability density function at equilibrium where

$$p^{(eq)}(\boldsymbol{R}_\Delta) = \frac{b^3}{\pi^{3/2}}e^{-b^2|\boldsymbol{R}_\Delta|^2} \tag{3.21}$$

and

$$b^2 = \frac{3}{2nl^2}. \tag{3.22}$$

As above, n is the number of freely rotating segments and l is the length of the freely rotating segments. The above derivation is provided by Kuhn [81].

Let $\{\boldsymbol{R}_i\}_{i=1}^N$ represent the set of polymer chains in a RVE where N is large. By the definition of a RVE (Section 1.1.1), the chain lengths must be symmetrically distributed. Depending on the selection of coordinate system, $\{\boldsymbol{R}_i\}_{i=1}^N$ can be represented differently and each representation is symmetric about a unique value.

Let $\{\boldsymbol{R}_{\Delta i}\}_{i=1}^N$ be the set $\{\boldsymbol{R}_i\}_{i=1}^N$ when the chains are selected at random which is consistent with Kuhn's theory [81]. Each chain is represented by $\boldsymbol{R}_{\Delta i}$ as above and the distribution is uniquely symmetric about the origin.

Let $\{\boldsymbol{R}_{fi}\}_{i=1}^N$ be the distribution representing $\{\boldsymbol{R}_i\}_{i=1}^N$ when end A is selected from a particular direction. Then for every chain $\boldsymbol{R}_{fi}$ $\exists$ $\boldsymbol{R}_{\Delta i}$. Let $\boldsymbol{R}_\mu$ be the mean value of the distribution $\{\boldsymbol{R}_{fi}\}_{i=1}^N$ in the three directions.

Let $\{\boldsymbol{R}_i^{\langle test\rangle}\}_{i=1}^N$ be an alternate distribution where each chain i is defined by $\boldsymbol{R}_i^{\langle test\rangle} = \boldsymbol{R}_{fi} - \boldsymbol{R}_\mu$. Then $\{\boldsymbol{R}_i^{\langle test\rangle}\}_{i=1}^N$ must be symmetrically distributed about its mean value defined by

$$\frac{1}{N}\sum_{i=1}^{N} \boldsymbol{R}_i^{\langle test\rangle} = \frac{1}{N}\sum_{i=1}^{N} \left(\boldsymbol{R}_{fi} - \boldsymbol{R}_\mu\right) = \boldsymbol{0}$$

and thus $\{\boldsymbol{R}_i^{\langle test\rangle}\}_{i=1}^N$ is a distribution of $\{\boldsymbol{R}_i\}_{i=1}^N$ uniquely symmetrically distributed about the origin. Therefore the distribution $\{\boldsymbol{R}_i^{\langle test\rangle}\}_{i=1}^N$ must be the distribution $\{\boldsymbol{R}_{\Delta i}\}_{i=1}^N$ and consequently

$$\boldsymbol{R}_{\Delta i} = \boldsymbol{R}_{fi} - \boldsymbol{R}_\mu \tag{3.23}$$

where $\boldsymbol{R}_\mu$ is the mean vector length for the representative volume element defined by Equation (3.16).

Substituting (3.23) into (3.21)

$$p(\boldsymbol{R}_f)d^3R_f = \frac{b^3}{\pi^{3/2}} e^{-b^2(\boldsymbol{R}_f - \boldsymbol{R}_\mu)^2} d\boldsymbol{R}_f \qquad \text{with} \qquad \int p(\boldsymbol{R}_f)d\boldsymbol{R}_f = 1. \tag{3.24}$$

In order to attach physical relevance to the substitution (3.23) consider Equation (3.20). Equation (3.20) is symmetric about the origin. This symmetry exists because the chains are selected at random and consequently for every vector length $\boldsymbol{R}_\Delta$ there is another chain with vector length $-\boldsymbol{R}_\Delta$. Instead of

selecting chains at random, one could arbitrarily define a coordinate system and select chains from a particular direction. For example travelling in any given direction, the first end that one encounters is defined as end A and the other end is defined as B. Using this method, vector lengths are always biased in the direction in which one is travelling. $\boldsymbol{R}_f$ is defined as the vector from end A to B in the latter coordinate system. Further, let $\boldsymbol{R}_{f0}$ represent the vector length of a molecule in a material at equilibrium. For a coordinate system chosen such that one axis is always along the molecule (which corresponds to a principal direction), the affine deformation assumption (3.16) reduces to

$$\boldsymbol{R}_f = \boldsymbol{\lambda}\boldsymbol{R}_{f0}$$

where $\boldsymbol{\lambda}$ is the tensor representing stretch of the molecule. In the unstrained equilibrium state $\boldsymbol{\lambda} = \boldsymbol{I}$. The affine deformation implies that

$$\frac{1}{N}\sum_{1}^{N}\boldsymbol{R}_{fi} = \boldsymbol{\lambda}\frac{1}{N}\sum_{i=1}^{N}\boldsymbol{R}_{f0i} \quad \Longleftrightarrow \qquad \boldsymbol{R}_{\mu} = \boldsymbol{\lambda}\boldsymbol{R}_{\mu 0} \tag{3.25}$$

where $\boldsymbol{R}_{\mu 0}$ is the mean of $\boldsymbol{R}_f$ at equilibrium. Substituting (3.25) into (3.23)

$$\boldsymbol{R}_{\Delta} = \boldsymbol{R}_f - \boldsymbol{R}_{\mu} \;\; = \;\; \boldsymbol{\lambda}(\boldsymbol{R}_{f0} - \boldsymbol{R}_{\mu 0})$$

where

$$\boldsymbol{R}_{\mu 0} = \frac{1}{N}\sum_{i=1}^{N}\boldsymbol{R}_{f0i} = \boldsymbol{0}. \tag{3.26}$$

Equation (3.26) is an arithmetic mean and the use of this central measure is allowed because the N molecules are randomly and symmetrically distributed about the origin.

Consequently (3.24) can be re-expressed as

$$\begin{aligned} p(\boldsymbol{\lambda}\boldsymbol{R})d(\boldsymbol{\lambda}\boldsymbol{R}) &= \frac{b^3}{\pi^{3/2}}e^{-b^2(\boldsymbol{\lambda}(\boldsymbol{R}_{f0}-\boldsymbol{R}_{0\mu}))^2}d(\boldsymbol{\lambda}\boldsymbol{R}_{f0}) \\ &= \frac{b^3}{\pi^{3/2}}e^{-b^2(\boldsymbol{\lambda}\boldsymbol{R}_{\Delta 0})^2}d(\boldsymbol{\lambda}\boldsymbol{R}_f) \end{aligned} \tag{3.27}$$

where $\boldsymbol{R}_{\Delta 0} = \boldsymbol{R}_{f0} - \boldsymbol{R}_{0\mu}$. It should be noted that this derivation is for an RVE (where, by definition, vector lengths are symmetrically distributed). It is not obvious that the affine deformation assumption applies to the non-equilibrium state. Here it will be assumed that it does not apply to the non-equilibrium state. It does however apply to situations in which the specimen

is in disequilibrium and the material (RVE) is in equilibrium or maximum entropy – symmetric distributions apply.

3.2.2 Entropy of a single chain

The purpose of determining the entropy is to use it to calculate the work done on the system. As a preview, the derivation of the work done on the system relies on the first law of thermodynamics. The first law of thermodynamics gives

$$\mathrm{Q} - \mathrm{W} = \Delta\mathrm{E} \tag{3.28}$$

where Q is the heat entering the system, W is the work done by the system and ΔE is the change in internal energy. The internal energy is composed of molecular vibration which is a function of temperature and potential energy (PE). Thus, if no work is done by the control volume and the process is isothermal, the change in potential energy is TΔs. If this energy is released in an adiabatic process the change in potential energy is $-$TΔs. Thus, from the first law of thermodynamics, the work done by the chain equals $-$TΔs.

The entropy s (published by Plank and credited by him to Boltzmann [128]) is defined by

$$s := k \ln \Omega_n \tag{3.29}$$

where Ω_n is the number of possible configurations in a given state. In order to calculate entropy, it will prove useful to be able to separate entropy into contributions in the three orthogonal directions.

The existence of these orthogonal directions is guaranteed by $\mathbf{U}$ (3.18) (and therefore $\mathbf{\Lambda}$) being a symmetric valued tensor. Align the axes along the principal directions. Then, for a coordinate system along the principal directions, the component of the probability distribution function (3.27) due to a change in the eigenvector $\boldsymbol{\lambda}_u$ along the x-axis is given by

$$p(x) = \frac{b}{\pi^{1/2}} e^{-b^2\lambda^2(x-x_{0\mu})^2}. \tag{3.30}$$

Effectively, one has reduced the variability about $x_{0\mu}$ because of λ ($|\lambda| > 1$) in the x-direction. This can also be stated as reduction in the number of possible configurations. The result is depicted in Figure 3.7.

Thus the entropy of the chain has decreased due to the work done on the

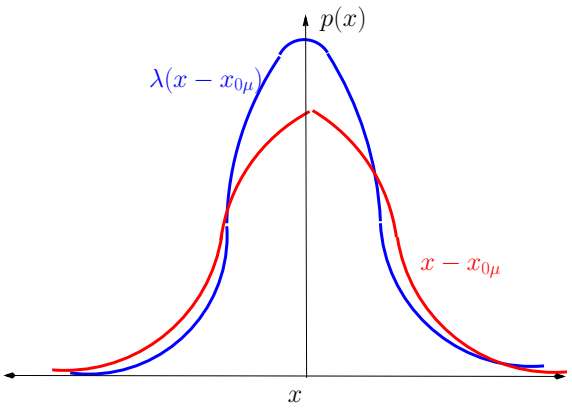

Figure 3.7: The red curve represents the Gaussian distribution from equation (3.30) for the undeformed state and the blue curve for the deformed state

chain. The proof of the latter statement requires the definition of entropy (3.29), Set

$$s_q := k \ln \Omega_t$$

where Ω_t is the total number of possible configurations. Consequently Ω_n/Ω_t represents probability p of a particular configuration.

The entropy of a chain can be quantified by using

$$s - s_q = k \ln \frac{\Omega_n}{\Omega_t} = k \ln p(\boldsymbol{R}_\Delta)$$

where k is the Boltzmann constant and Ω_n/Ω_t is the probabilty of the existence of a molecule with configuration $\boldsymbol{R}_\Delta$. Therefore in the unstrained state, the entropy of a single chain is given by

$$s_0 = k \ln \frac{b^3}{\pi^{3/2}} - kb^2 |\boldsymbol{R}_{f0} - \boldsymbol{R}_{0\mu}|^2 + s_q$$

and for the strained state

$$s = k \ln \frac{b^3}{\pi^{3/2}} - kb^2 |\boldsymbol{\lambda R}_{f0} - \boldsymbol{\lambda R}_{0\mu}|^2 + s_q.$$

The change in entropy for that single chain is

$$\begin{aligned} \Delta s &= s - s_0 = -kb^2((\lambda_{xx}^2 - 1)(R_{fx0} - R_{fx0\mu})^2 \\ &\quad +(\lambda_{yy}^2 - 1)(R_{fy0} - R_{fy0\mu})^2 + (\lambda_{zz}^2 - 1)(R_{fz0} - R_{fz0\mu})^2). \end{aligned} \quad (3.31)$$

3.2.3 Work performed by a network of chains

In order to determine the work done by the whole network, the changes in entropy for all the chains in the network at fixed stretch, has to be summed. Summing over the x components of Equation (3.31) for all N chains and denoting the change in entropy for the network as ΔS, the expression

$$\Delta S_x = -kb^2(\lambda_{xx}^2 - 1)\sum_{i=1}^{N}(R_{fx0} - R_{fx0\mu})^2 \tag{3.32}$$

is obtained. This is possible because of the affine deformation condition.

The summation $\sum_{i=1}^{N}(x_0 - x_{0\mu})^2$ is assumed to be equal for all directions because the N molecules are equally likely to be orientated in each of the three orthogonal directions. Thus summing over (3.32) in the three directions,

$$\Delta S = -kb^2(\lambda^2 - 3)\sum_{i=1}^{N}(R_{fx0} - R_{fx0\mu})^2 \tag{3.33}$$

where $\sum_{i=1}^{N}(R_{fx0} - R_{fx0\mu})^2$ is equal to $\frac{1}{3}N(R_{f0} - R_{f0\mu})_{rms}^2$ and $\lambda^2 = |\boldsymbol{\lambda}|^2$ where R_{rms} represents the mean value of the square of the length of vector $\boldsymbol{R}$. Alternatively

$$\begin{aligned}\sum_{i=1}^{N}\sum_{j\in x,y,z}(R_{fi0j} - R_{f0\mu j})^2 &= 3\sum_{i=1}^{N}(R_{fi0x} - R_{fi0\mu x})^2 \\ &= N(R_{f0} - R_{f0\mu})_{rms}^2. \end{aligned}\tag{3.34}$$

To determine the mean value of $(R_{fx0} - R_{fx0\mu})^2$ or $(R_{fx0} - R_{fx0\mu})_{rms}^2$ one has to determine the probability of finding end B within a spherical shell of radius R_D and thickness δR. $P(R)$, the probability function, is defined by

$$P(R)dr = \frac{b^3}{\pi^{3/2}}e^{-b^2(R_{fx0}-R_{fx0\mu})^2} \times 4\pi(R_{fx0} - R_{fx0\mu})^2 dR. \tag{3.35}$$

The mean value of $(R_{fx0} - R_{fx0\mu})^2 \approx (R_{fy0} - R_{fy0\mu})^2 \approx (R_{fz0} - R_{fz0\mu})^2$ is given by

$$3(R_{fx0} - R_{fx0\mu})_{rms}^2 = \frac{\int_{R_{f0\mu}}^{\infty}(R_{fx0} - R_{fx0\mu})^2 P(R)dR}{\int_{R_{f0\mu}}^{\infty}P(R)dR} = \frac{3}{2b^2} = nl^2 \tag{3.36}$$

after substitution of (3.22) and change of limits.

Therefore, summing Equation (3.36) over the N chains,

$$3\sum_{N}(R_{fx0} - R_{fx0\mu})^2 = N\frac{3}{2b^2} \tag{3.37}$$

and

$$\sum_{N}(R_{fx0} - R_{fx0\mu})^2 = N\frac{1}{2b^2}. \tag{3.38}$$

Substituting Equation (3.38) into Equation (3.33), one obtains

$$\Delta S = -\frac{1}{2}kN(\lambda^{\mathbf{2}} - 3). \tag{3.39}$$

The work done by the network is given by $W = -T\Delta S$ or substituting (3.39),

$$W = \frac{1}{2}kNT(\lambda^2 - 3). \tag{3.40}$$

3.2.4 Root mean square for mean initial chain length

The affine deformation assumption as expressed by Equation (3.16) constructs a deformation tensor $\mathbf{U}$ where, for initial vector length $\boldsymbol{R}_{f0}$, the final vector length $\boldsymbol{R}_f$ is calculated as

$$\boldsymbol{R}_f = \mathbf{U}\boldsymbol{R}_{f0}.$$

The root mean square of chain length (R_{rms}) is independent of the coordinate system. By definition, $R_{rms} = \left(\overline{|R_f|^2}\right)^{1/2}$ where the set of $\boldsymbol{R}_f := \{\boldsymbol{R}_{fi}\}_{i=1}^{N}$. The arithmetic mean of the set $\{\boldsymbol{R}_{fi}\}_{i=1}^{N}$ is a macroscopic property thus

$$\mathbf{R}_f = \overline{\boldsymbol{R}}_f := \frac{1}{N}\sum_{i=1}^{N}\boldsymbol{R}_{fi}.$$

Consider the unstrained state. In this unstrained state $R_{rms}^2 = \overline{R_{f0}^2}$. For this unstrained state, an orientation (coordinate system) exists such that chain length components are symmetrically distributed in the three orthogonal directions. Therefore

$$\overline{\boldsymbol{R}}_f = \mathbf{R}_f = \begin{pmatrix} 1 & 0 & 0 \\ 0 & 1 & 0 \\ 0 & 0 & 1 \end{pmatrix} \begin{pmatrix} \frac{1}{\sqrt{3}}R_{rms} \\ \frac{1}{\sqrt{3}}R_{rms} \\ \frac{1}{\sqrt{3}}R_{rms} \end{pmatrix} = \begin{pmatrix} \frac{1}{\sqrt{3}}R_{rms} \\ \frac{1}{\sqrt{3}}R_{rms} \\ \frac{1}{\sqrt{3}}R_{rms} \end{pmatrix} \tag{3.41}$$

Further consider the i^{th} chain length. Let the magnitude of initial vector $\boldsymbol{R}_{f0i}$ be $|\mathbf{R}_{f0i}| = R_{f0i}$. Then there exists a microscopic vector $\hat{\boldsymbol{\lambda}}$ representing the chain length stretch (or $\underline{\hat{\boldsymbol{\lambda}}}$ for the macroscopic equivalent), such that,

$$\boldsymbol{R}_{fi} = \hat{\boldsymbol{\lambda}} R_{f0i} \Longrightarrow \frac{1}{N}\sum_{i=1}^{N} \boldsymbol{R}_{fi} = \hat{\boldsymbol{\lambda}}\frac{1}{N}\sum_{i=1}^{N} R_{f0i} = \hat{\boldsymbol{\lambda}}\overline{|\mathbf{R}_{f0}|} = \hat{\boldsymbol{\lambda}} R_{\mu 0} = \underline{\hat{\boldsymbol{\lambda}}} R_{\mu 0} \tag{3.42}$$

where $R_{\mu 0} := \overline{|\boldsymbol{R}_{f0}|}$. Thus for unit vector, $\hat{\boldsymbol{\lambda}}$, a scalar, $R_{\mu 0}$, exists such that (in the coordinate system where chain length is symmetrically distributed about the orthogonal directions)

$$\mathbf{R}_f = \overline{\boldsymbol{R}}_f = \begin{pmatrix} \frac{1}{\sqrt{3}} \\ \frac{1}{\sqrt{3}} \\ \frac{1}{\sqrt{3}} \end{pmatrix} \overline{|\boldsymbol{R}_{f0}|} = \begin{pmatrix} \frac{1}{\sqrt{3}} R_{\mu 0} \\ \frac{1}{\sqrt{3}} R_{\mu 0} \\ \frac{1}{\sqrt{3}} R_{\mu 0} \end{pmatrix}. \tag{3.43}$$

Comparing Equation (3.43) to (3.41) it is evident that

$$R_{\mu 0} = R_{rms} = \sqrt{\frac{1}{N}\sum_{N} R_f^2}. \tag{3.44}$$

The latter results was a consequence of R_{rms} being independent of coordinate system.

3.2.5 Geometric mean of $\mathbf{R}_f$

In Section 3.2.1, the central measure (R_μ) was derived based on the assumption of a Gaussian chain length distribution on a coordinate system in which the first end one encounters travelling in a fixed direction is the initial position A and the other end is B. This differs from Kuhn's derivation [81] where chains were selected at random and the distribution is implicitly symmetric.

The two concepts (Gaussian chain length distribution and the biased coordinate system) are mutually exclusive because the Gaussian distribution allows for negative chain lengths but the biased coordinate system does not. This is depicted in Figure 3.8(a). Figure 3.8(b) in red is a more realistic frequency distribution for chain length. Consistent with the biased coordinate system, the minimum chain length should be greater than 0 due to the volume of the molecule. The maximum chain length is the product of the chain segment lengths (l as depicted in Figure 3.6) and the number of chain segments (n) which is nl.

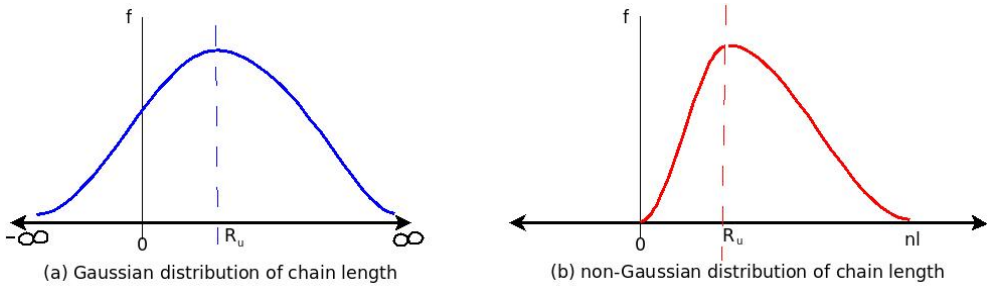

Figure 3.8: (a) is a frequency distribution for chain length based on the Gaussian chain length assumption. The chain length is distributed symmetrically about the central measure and is able to increase to infinity in either direction. (b) depicts the non-Gaussian chain length distribution. It is consistent with the coordinate system and the maximum chain length is nl.

In the unstrained state, let $|\boldsymbol{R}_f|$ be R_f such that

$$R_{fi} = \ell_i R_{\mu G0} \tag{3.45}$$

where $R_{\mu G0}$ is a central measure in the unstrained state and R_{fi} is the i^{th} chain length magnitude R_f corresponding to the i^{th} stretch $\ell_i > 0$. This set has been selected to ensure that $R_{fi} > 0 \ \forall \ i \leq N$. To calculate $R_{\mu G0}$, without loss of generality, let the set $\{\ell_i\}_{i=1}^{N}$ (where N is large) be an ordered set of stretches such that

$$\ell_i \geq \ell_k \Longleftrightarrow i \leq k \qquad \forall \, i, k \ \leq \ N \in \mathbb{N}.$$

Given that the data are asymmetrically distributed, the median is an appropriate central measure. To ensure that $R_{\mu G0}$ is a median, for every molecule with $\ell_i > 1 \ \exists \ \ell_j < 1$. Thus for large $N \ \forall \ i \ \exists \ j$ such that

$$\ell_i \ell_j = 1 \Longleftrightarrow \ell_j = \frac{1}{\ell_i} \implies \prod_{i=1}^{N} \ell_i = \prod_{i=1}^{\frac{N}{2}} \ell_i \frac{1}{\ell_i} = 1 \tag{3.46}$$

From Equation (3.45) and substituting (3.46)

$$\begin{aligned} \prod_{i=1}^{N} R_{fi} &= \prod_{i=1}^{N} \ell_i R_{\mu G0} = \prod_{i=1}^{N} \ell_i \prod_{i=1}^{N} R_{\mu 0} \\ &= 1 \times R_{\mu G0}^{N} \Longleftrightarrow R_{\mu G0} = R_{\mu G} = \sqrt[N]{\prod_{i=1}^{N} R_{fi}}. \end{aligned} \tag{3.47}$$

Thus $R_{\mu G0}$ is the geometric mean of the set of vector lengths. Furthermore, from the arithmetic-geometric mean inequality, the geometric mean is always less than the arithmetic mean: thus

$$R_{\mu G} = R_{\mu G0} < R_{\mu 0} = R_{rms} \iff \frac{R_{\mu G}}{R_{rms}} < \frac{R_{\mu 0}}{R_{rms}} = 1. \tag{3.48}$$

The last substitution $R_{\mu 0} = R_{rms}$ was established by equation (3.44). Both the geometric mean and the ratio of $R_{\mu G0}/R_{rms}$ to be determined in Section 3.2.6 will be necessary for the numerical model of Chapter 8.

3.2.6 Calculating $\frac{R_{\mu G0}}{R_{rms}}$ and $\frac{\dot{R}_{\mu G0}}{\dot{R}_{rms}}$

From Section 3.2.5, each molecule of vector length magnitude R_{fi} in the ordered set $\{R_{fi}\}_{i=1}^{N}$ can (without loss of generality) be represented by $\ell_i R_{\mu G0}$. From the idealised molecule depicted in Figure 3.6 the maximum potential length is nl and consequently the maximum possible stretch is

$$\ell_{max} = nl/R_{\mu G0}. \tag{3.49}$$

Combining this maximum potential length and stretch (3.49) and the definition of R_{fi}, the constraints on R_{fi} are

$$\ell_{min} R_{\mu G0} = \frac{1}{\ell_{max}} R_{\mu G0} \iff \frac{R_{\mu G0}^2}{nl} \leq R_{fi} \leq nl = \frac{nl}{R_{rms}} R_{\mu 0} = \frac{nl R_{\mu 0}}{R_{rms} R_{\mu G0}} R_{\mu G0} = \ell_{max} R_{\mu G0}.$$

The final substitution ($R_{\mu 0}/R_{rms} = 1$) is from (3.44). Given that the intention is to maximise

$$\frac{1}{N} \sum_{i=1}^{N} \frac{R_{fi}}{R_{rms}},$$

substitution of the arithmetic-geometric mean inequality (3.48) overestimates in the sense that

$$\frac{R_{\mu G0}}{nl} \leq \frac{R_{\mu}}{nl} = \frac{R_{rms}}{nl} \leq \frac{R_{fi}}{R_{rms}} \leq \frac{nl}{R_{rms}} \iff \frac{1}{\sqrt{n}} \leq \frac{R_{fi}}{R_{rms}} \leq \sqrt{n}$$

because, from Equation (3.36), $R_{rms} = \sqrt{n}l$. Summing over the N molecules

$$\frac{N}{\sqrt{n}} \leq \sum_{i=1}^{N} \frac{R_{fi}}{R_{rms}} \leq N\sqrt{n} \iff \frac{1}{\sqrt{n}} \leq \frac{1}{R_{rms}} \frac{1}{N} \sum_{i=1}^{N} R_{fi} \leq \sqrt{n}$$
$$\iff \frac{1}{\sqrt{n}} \leq \frac{R_{\mu 0}}{R_{rms}} \leq \sqrt{n}.$$

Given that the intention is to maximise $R_{\mu G}/R_{rms}$, from Equation (3.48),

$$\frac{1}{\sqrt{n}} \leq \frac{R_{\mu G}}{R_{rms}} \leq \frac{R_{\mu 0}}{R_{rms}} \leq 1 \tag{3.50}$$

where the lower limit is an overestimate. This data is skewed (as depicted in 3.8(b)), as each of the lengths is not equally likely. Therefore the mean for symmetrically distributed data is greater than the mean for skewed data as depicted in 3.8(b). That is,

$$\frac{R_{\mu G0}}{R_{rms}} < \frac{1}{2}\Big(1 + \frac{1}{\sqrt{n}}\Big) \Longrightarrow \lim_{n\to\infty} \frac{R_{\mu G0}}{R_{rms}} < 0.5 \tag{3.51}$$

where the right hand side of the equation is the arithmetic mean for (3.50) given a symmetric data set.

Equation (3.51) can either be interpreted physically or mathematically. Physically it is a consequence of comparing Gaussian and non-Gaussian chains. Mathematically, it is a consequence of the construction of the co-ordinate system which is not a mere displacement of Kuhn's co-ordinate system [81], it is a redefinition that does not permit a symmetric distribution of chain lengths – which has been assumed.

$R_{\mu G0}$ is a more appropriate central measure than $R_{\mu 0}$ in Equations (8.30). This is the lower limit for $R_{\mu G0}/R_{rms}$. It is recognised that the requirement that $n \to \infty$ implies infinite molecular length. An appropriate sample size (number of molecular links) will be determined based on the desired precision for the calculated mean. Let the error (E) of the estimate of the mean be $0.3 \times \sigma$ where σ is the standard deviation of the population of molecular links. The sample size (n, corresponding to the links that must be sampled for the estimate) is calculated as ([108], Chapter 7)

$$n = \Big[\frac{z_{\alpha/2} \cdot \sigma}{E}\Big]^2 = \Big[1.96 \times \frac{10}{3}\Big]^2 = 42 \tag{3.52}$$

where $z_{\alpha/2} = 1.96$ corresponds to the two-sided 95% confidence interval. Substituting this sample size into Equation (3.51),

$$\frac{R_{\mu G0}}{R_{rms}} \leq \frac{1}{2}\Big(1 + \frac{1}{\sqrt{42}}\Big) = 0.577 \approx \frac{1}{\sqrt{3}} \Longrightarrow \frac{R_{rms}^2}{3} \geq R_{\mu G0}^2. \tag{3.53}$$

From the affine deformation assumption

$$\frac{R_\mu}{R_{rms}} = \lambda \frac{R_{\mu G0}}{R_{rms}} \tag{3.54}$$

where R_μ / R_{rms} is a function of n as described by Equations (3.51) and (3.53). To assess whether $n = 42$ is appropriate, consider Figure 3.9 – an example of a typical pellethane monomer. In the figure n and n' represent the number of links where n and n' are not constant. From (3.51) and (3.53), for $n \geq 42$,

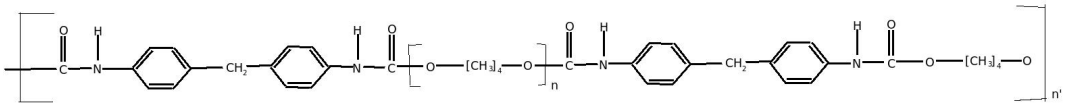

Figure 3.9: The molecular structure for pellethane reproduced from Lemm [90] where n and n' represent the number of repeats.

$$\frac{1}{2} \leq \frac{R_{\mu G0}}{R_{rms}} \leq \frac{1}{\sqrt{3}} \quad \Longrightarrow \quad \frac{\lambda}{2} \leq \frac{R_\mu}{R_{rms}} = \lambda \frac{R_{\mu G0}}{R_{rms}} \leq \frac{\lambda}{\sqrt{3}} \tag{3.55}$$

$$\frac{R_{\mu G}}{R_{rms}} = \lambda \frac{R_{\mu G0}}{R_{rms}} \quad \approx \quad \frac{\lambda}{\sqrt{3}} \tag{3.56}$$

The latter equation (3.56) will be selected to be substituted into (8.30) which is a truncated Taylor expansion of the maximum entropy function that will be used in the numerical modelling. Furthermore, given the affine deformation assumption, the deformed R_{rms} (R'_{rms}) is given by (with the appropriate substitution of (3.56))

$$R'_{rms} = \lambda R_{rms} \iff \qquad R'^2_{rms} = 3R^2_{\mu G}. \tag{3.57}$$

Lastly note that for $n \geq 42$ that the limits of the ratio $R_\mu^2 / R_{\mu G0}^2$ are $\frac{1}{3} \leq \frac{R_\mu^2}{R_{\mu G0}^2} \leq \frac{1}{4}$ where the ratio increases monotonically with n. This implies that the longer the chain (the more links) the higher the stretch that can be modelled by the numerical method to be described in Chapter 8. For $n = 42$ one would not expect the model to work for streches greater than $\sqrt{3}$ or 173%. In constrast as $n \longrightarrow \infty$, the allowable stretch increases to 2 or 200%.

3.2.7 Polymer principal stresses

This section is adapted from Treloar [138]. Consider an RVE with principal stretches $\lambda_1, \lambda_2, \lambda_3$ (the eigenvalues of $\boldsymbol{\lambda}$ from (3.19)). The generally accepted incompressibility assumption for rubber [40] requires that

$$\lambda_1\lambda_2\lambda_3 = 1.$$

This assumption is not universally accepted [140] and will be discussed in Section 3.4. Define the macroscopic property, Cauchy principal stress (σ_1) to be the force per unit deformed area and the first Piola-Kirchoff principal stress (P) as the force per unit undeformed area; then

$$\sigma_1 = \frac{P_1}{\lambda_2\lambda_3} = P_1\lambda_1$$

and

$$W = \frac{1}{2}Nk\mathrm{T}(\lambda_1^2 + \lambda_2^2 + \frac{1}{\lambda_1^2\lambda_2^2} - 3) = \frac{1}{2}\Gamma(\lambda_1^2 + \lambda_2^2 + \frac{1}{\lambda_1^2\lambda_2^2} - 3)$$

where $\Gamma = Nk\mathrm{T}$. Also,

$$\delta W = F\delta l_1 = l_2 l_3 P_1 l_1 \delta\lambda_1 = V\sigma_{n1}\delta\lambda_1$$

where δW is a small change in W. But to first order

$$\delta W = \frac{\partial W}{\partial \lambda_1}\delta\lambda_1 = \Gamma(\lambda_1 - \frac{1}{\lambda_1^3\lambda_2^2})\delta\lambda_1$$

which implies that

$$P_1 = \frac{\Gamma}{V}\left(\lambda_1 - \frac{1}{\lambda_1^3\lambda_2^2}\right) \qquad \text{and} \qquad \sigma_1 = \frac{\Gamma}{V}\left(\lambda_1^2 - \frac{1}{\lambda_1^2\lambda_2^2}\right). \tag{3.58}$$

Similarly

$$P_2 = \frac{\Gamma}{V}\left(\lambda_2 - \frac{1}{\lambda_2^3\lambda_1^2}\right) \qquad \text{and} \qquad \sigma_2 = \frac{\Gamma}{V}\left(\lambda_2^2 - \frac{1}{\lambda_1^2\lambda_2^2}\right) \tag{3.59}$$

and $\sigma_3 = 0$.

The above system cannot be solved for the general case when $\sigma_3 \neq 0$. Treloar ([138], Chapters 4 and 5) shows that the appropriate selection of stress boundary conditions makes the system fully determinate. In particular

for the uniaxial tensile test he adds a hydrostatic term (p) to (3.58), (3.59) and the free surface 3 such that

$$\sigma_1 = \frac{\Gamma}{V}\left(\lambda_1^2 - \lambda_3^2\right) + p, \qquad \sigma_2 = \frac{\Gamma}{V}\left(\lambda_2^2 - \lambda_3^2\right) + p, \qquad \sigma_3 = p$$

which can be solved for any boundary conditions.

For the case of the uniaxial tensile test ($\sigma_2 = \sigma_3 = 0$), he then subtracts σ_2 from σ_1 and sets σ_2 to zero, because it is a free surface, such that

$$\sigma_1 = \frac{\Gamma}{V}\left(\lambda_1^2 - \frac{1}{\lambda_1}\right) - \frac{\Gamma}{V}\left(\lambda_2^2 - \frac{1}{\lambda_1^2\lambda_2^2}\right) = \frac{\Gamma}{V}\left(\lambda_1^2 - \lambda_2^2\right). \tag{3.60}$$

3.3 Non-equilibrium statistical mechanics

The above equilibrium theory of rubber elasticity will now be extended to the non-equilibrium (and non-maximum entropy) situation which will later be shown to be the equivalent of viscoelasticity. It has the essential components (probability distribution function, entropy and work) used for the equilibrium statistical mechanics but applies it slightly differently – the probability distribution function will be determined from the molecule's elastic and kinetic energy.

3.3.1 Probability distribution function constraints

From Equation (3.3), the probability of finding a molecule in a given range $(\mathbf{r}, \boldsymbol{R}_f, \grave{\boldsymbol{c}})$ at time t per unit volume for the non-equilibrium situation is

$$p(\mathbf{r}, \grave{\boldsymbol{c}}(\dot{\boldsymbol{R}}_f), \boldsymbol{R}_f).$$

It is necessary to construct a differential equation to solve for $\boldsymbol{R}_f$ and $\dot{\boldsymbol{R}}_f$. From Equation (3.24), at equilibrium,

$$\int p(\mathbf{r}, \mathbf{0}, \boldsymbol{R}_f) d\boldsymbol{R}_f \, d\grave{\boldsymbol{c}} = \int \frac{b^3}{\pi^{\frac{3}{2}}} e^{-b^2(\boldsymbol{R}_f - \boldsymbol{R}_\mu)^2} \times q(\boldsymbol{R}_f, \mathbf{0}) \times Q(\mathbf{0}) d\boldsymbol{R}_f \, d\grave{\boldsymbol{c}} = 1.$$

The non-equilibrium probability density function is only a function of $\boldsymbol{R}_f$ and $\grave{\boldsymbol{c}}$ thus in general (for arbitrary functions q and Q to be determined)

$$\begin{aligned} \int p(\mathbf{r}, \grave{\boldsymbol{c}}, \boldsymbol{R}_f) d\boldsymbol{R}_f d\grave{\boldsymbol{c}} &= \int \frac{b^3}{\pi^{\frac{3}{2}}} e^{-b^2(\boldsymbol{R}_f - \boldsymbol{R}_\mu)^2} \times q(\boldsymbol{R}_f, \grave{\boldsymbol{c}}) \times Q(\grave{\boldsymbol{c}}) d\boldsymbol{R}_f d\grave{\boldsymbol{c}} \\ &= 1. \end{aligned} \tag{3.61}$$

Integrating Equation (3.61) by parts

$$\begin{aligned}
1 &= \int_{-\infty}^{\infty} q(\boldsymbol{R}_f, \grave{\boldsymbol{c}}) Q(\grave{\boldsymbol{c}}) \left(\int_{-\infty}^{\infty} \frac{b^3}{\pi^{\frac{3}{2}}} e^{-b^2 \left(\boldsymbol{R}_f - \boldsymbol{R}_\mu\right)^2} d\boldsymbol{R}_f \right) d\grave{\boldsymbol{c}} \\
&\quad - \int \left(\int_{-\infty}^{\infty} \frac{b^3}{\pi^{\frac{3}{2}}} e^{-b^2 (\boldsymbol{R}_f - \boldsymbol{R}_\mu)^2} d\boldsymbol{R}_f \right) \frac{\partial q(\boldsymbol{R}_f, \grave{\boldsymbol{c}}) Q(\grave{\boldsymbol{c}})}{\partial \boldsymbol{R}_f} d\boldsymbol{R}_f d\grave{\boldsymbol{c}} \\
&= \int_{-\infty}^{\infty} q(\boldsymbol{R}_f, \grave{\boldsymbol{c}}) Q(\grave{\boldsymbol{c}}) \big(1\big) d\grave{\boldsymbol{c}} - \int_{-\infty}^{\infty} \big(1\big) \frac{\partial q(\boldsymbol{R}_f, \grave{\boldsymbol{c}}) Q(\grave{\boldsymbol{c}})}{\partial \boldsymbol{R}_f} d\boldsymbol{R}_f d\grave{\boldsymbol{c}} \\
&= \int_{-\infty}^{\infty} q(\boldsymbol{R}_f, \grave{\boldsymbol{c}}) Q(\grave{\boldsymbol{c}}) d\grave{\boldsymbol{c}} - \int_{-\infty}^{\infty} Q(\grave{\boldsymbol{c}}) \frac{\partial q(\boldsymbol{R}_f, \grave{\boldsymbol{c}})}{\partial \boldsymbol{R}_f} d\boldsymbol{R}_f d\grave{\boldsymbol{c}}. \qquad (3.62)
\end{aligned}$$

In order to determine formulae for $q(\boldsymbol{R}_f, \grave{\boldsymbol{c}})$ and $Q(\grave{\boldsymbol{c}})$, one requires additional equations derived from a consideration of entropy and energy.

3.3.2 The polymer work constraints

The entropy(S) of a network of chains is calculated as the sum of the entropies of the individual chains. The entropy of the i^{th} chain s_i is calculated from the number of possible microscopic states and is related to the probabilty p_i of a given state for that i^{th} molecule such that

$$\mathrm{S} = \sum_{i=1}^{N} s_i \qquad \text{where} \qquad s_i = k \ln p_i \qquad (3.63)$$

and k is the Botzmann constant. Each of the s_i in Equation (3.63) represent a statistical mechanics definition of entropy. The change in entropy can also be calculated from

$$\begin{aligned}
\Delta \mathrm{S} &:= \oint \frac{1}{\mathrm{T}} d\mathrm{Q} \qquad \text{and for an isothermal process} \\
\Delta \mathrm{Q} &= \mathrm{T} \Delta \mathrm{S} \qquad (3.64)
\end{aligned}$$

where definition (3.64) is the thermodynamic definition of entropy.

It should be noted that effectively two definitions of entropy are being used – a statistical mechanics definition due to Boltzmann and a thermodynamic definition due to Clausius [25]. It is recognised that the thermodynamic definition only applies at equilibrium and is otherwise an assumption.

The thermodynamic defintion of entropy is assumed valid for systems not significantly disturbed from equilibrium. This convention will be utilised in this section.

Substituting (3.64) into Equation (3.28),

$$\mathrm{T}\Delta\mathrm{S} - \mathrm{W} = \Delta\mathrm{E} = \mathrm{f(T)} + \mathrm{KE} + \mathrm{PE}. \tag{3.65}$$

If the control volume is defined as a single chain and this chain does no work on the external environment then

$$\begin{aligned} \Delta E &= \mathrm{T}\Delta s = \mathrm{T}(s - s_0) \\ s &= k \ln p(\mathbf{r}, \dot{\boldsymbol{c}}, \boldsymbol{R}_f) + s_q = k \ln p + s_q \\ s_0 &= k \ln p(\mathbf{r}, \mathbf{0}, \boldsymbol{R}_{f0}) + s_q = k \ln p_0 + s_q \\ \Longrightarrow E - E_0 &= kT(\ln p - \ln p_0) \end{aligned}$$

where E_0 is the energy of the molecule at equilibrium. Substituting (3.61),

$$\begin{aligned} E &= -k\mathrm{T} \ln p(\mathbf{r}, \dot{\boldsymbol{c}}, \boldsymbol{R}_f) + s_q \\ &= A_1 + k\mathrm{T}b^2(R_f - R_\mu)^2 - k\mathrm{T} \ln q(\boldsymbol{R}_f, \dot{\boldsymbol{c}}) - k\mathrm{T} \ln Q(\dot{\boldsymbol{c}}) \end{aligned} \tag{3.66}$$

where $A_1 = -k\mathrm{T} \ln \frac{b^3}{\pi^{3/2}} + s_q$ is a constant. The energy of a molecule has two components – potential and kinetic. The potential energy is the stretch energy which is the same as for the equilibrium state. Thus the potential energy must be the first pair of terms

$$A_1 + k\mathrm{T}b^2(R_f - R_\mu)^2.$$

The kinetic energy is only a function of velocity and must therefore be

$$A_2 k\mathrm{T} + A_3 k\mathrm{T} + \frac{1}{2} m(\dot{c} - \dot{c}_0)^2 = -k\mathrm{T} \ln q(\boldsymbol{R}_f, \dot{\boldsymbol{c}}) - k\mathrm{T} \ln Q(\dot{\boldsymbol{c}}) \tag{3.67}$$

where A_2 and A_3 are constants, which would imply that

$$A_3 k\mathrm{T} = -k\mathrm{T} \ln q(\boldsymbol{R}_f, \dot{\boldsymbol{c}}) \Longleftrightarrow q(\boldsymbol{R}_f, \dot{\boldsymbol{c}}) = e^{-A_3/kT}.$$

Thus $q(\boldsymbol{R}_f, \dot{\boldsymbol{c}})$ is a constant. Let this constant be A: thus

$$q(\boldsymbol{R}_f, \dot{\boldsymbol{c}}) = A. \tag{3.68}$$

Furthermore, from Equation (3.67)

$$\begin{aligned} \ln Q(\grave{\boldsymbol{c}}) &= A_2 - \frac{1}{2k\mathrm{T}} m(\grave{c} - \grave{c}_0)^2 \\ \text{or} \qquad Q(\grave{\boldsymbol{c}}) &= e^{A_2} e^{-\frac{m}{2kT}(\grave{c}-\grave{c}_0)^2} = Be^{-\frac{m}{2kT}(\grave{c}-\grave{c}_0)^2} \end{aligned} \tag{3.69}$$

where $B = e^{A_2}$. It is recognised that the assumption that the thermodynamic definition of entropy (3.64) can be used in non-equilibrium states is only valid when the non-equilibrium state does not differ significantly from equilibrium.

3.3.3 The maximum entropy distribution function

Substituting Equations (3.68) and (3.69) into Equation (3.62),

$$\begin{aligned} 1 &= \int_{-\infty}^{\infty} ABe^{-\frac{m}{2k\mathrm{T}}(\grave{c}-\grave{c}_0)^2} d\grave{\boldsymbol{c}} - \int_{-\infty}^{\infty} Q(\grave{\boldsymbol{c}}) \times (0) d\boldsymbol{R}_f d\grave{\boldsymbol{c}} \\ &= \int_{-\infty}^{\infty} ABe^{-\frac{m}{2k\mathrm{T}}(\grave{c}-\grave{c}_0)^2} d\grave{\boldsymbol{c}} \end{aligned} \tag{3.70}$$

where $AB = \left(\frac{m}{2\pi k\mathrm{T}}\right)^{-\frac{3}{2}}$. Consequently

$$q(\boldsymbol{R}_f, \grave{\boldsymbol{c}}) \times Q(\grave{\boldsymbol{c}}) = \left(\frac{m}{2\pi k\mathrm{T}}\right)^{-\frac{3}{2}} e^{-\frac{m}{2k\mathrm{T}}(\grave{c}-\grave{c}_0)^2}$$

and Equation (3.61) reduces to

$$p(\mathbf{r}, \grave{\boldsymbol{c}}, \boldsymbol{R}_f) = p^{(ms)}(\mathbf{r}, \grave{\boldsymbol{c}}, \boldsymbol{R}_f) = \frac{b^3}{\pi^{\frac{3}{2}}} e^{-b^2(\boldsymbol{R}_f - \boldsymbol{R}_\mu)^2} \times \left(\frac{m}{2\pi k\mathrm{T}}\right)^{\frac{3}{2}} e^{-\frac{m}{2k\mathrm{T}}(\grave{c}-\grave{c}_0)^2}.$$

The above was derived for a single chain. The work term has to be multiplied by the number density ρ_n to determine the total work. Consequently

$$\begin{aligned} p^{(ms)}(\mathbf{r}, \grave{\boldsymbol{c}}, \boldsymbol{R}_f) &= \frac{b^3}{\pi^{\frac{3}{2}}} e^{-b^2(\boldsymbol{R}_f - \boldsymbol{R}_\mu)^2} \times \rho_n \left(\frac{m}{2\pi k\mathrm{T}}\right)^{\frac{3}{2}} e^{-\frac{m}{2k\mathrm{T}}(\grave{c}-\grave{c}_0)^2} \\ &= p_S^{(ms)} \times p_D^{(ms)} \end{aligned} \tag{3.71}$$

where

$$p_S^{(ms)} = \frac{b^3}{\pi^{\frac{3}{2}}} e^{-b^2(\boldsymbol{R}_f - \boldsymbol{R}_\mu)^2} \tag{3.72}$$

$$p_D^{(ms)} = \left(\frac{\rho}{2\pi k\mathrm{T}}\right)^{\frac{3}{2}} e^{-\frac{m}{2k\mathrm{T}}(\grave{c}-\grave{c}_0)^2}. \tag{3.73}$$

Function (3.71) requires a name. This poses a problem. It is the equivalent of the equilibrium distribution function for a material that is not at equilibrium. Consequently interpretation is required. Given that entropy always increases in a closed system, at the time at which entropy is no longer capable of increasing, the material can no longer change its macroscopic properties and the material is at equilibrium. One can thus conclude that the equilibrium state is the highest entropy state at which macroscopic properties no longer change with respect to time. Similarly, for a material which is not at equilibrium, for every given state a distribution must exist for which entropy is maximised. Furthermore the molecular distribution must 'strive', 'relax' or tend to this state. Equation (3.71) must be this maximum entropy distribution. It will therefore be referred to as the *maximum entropy distribution function.* The superscript (ms) in $p^{(ms)}$ refers to maximum entropy. One could also consider quasi-equilibrium states – if change occurs sufficiently slowly, the state at various times could be approximated as equilibrium states. Thus an alternate interpretation is that $p^{(ms)}$ represents the quasi-equilibrium probability distributions for a material at various quasi-equilibrium states.

3.3.4 Differential equation for polymer chain interaction

If the combined forces of all the adjacent molecules acting at point A on the molecule depicted in Figure 3.10 is $\boldsymbol{F}$, then for an infinitesimal time interval δt

$$\begin{aligned} m\boldsymbol{a} &= \boldsymbol{F} + K\Delta\boldsymbol{R}_f \iff m\int_t^{t+\delta t} \frac{d\dot{\boldsymbol{c}}}{dt}d\tau = \int_t^{t+\delta t} \boldsymbol{F} + K\Delta\boldsymbol{R}_f d\tau \\ \iff \dot{\boldsymbol{c}}' &= \dot{\boldsymbol{c}} + \frac{\boldsymbol{F}}{m}\delta t + \frac{K}{m}(\boldsymbol{R}'_f - \boldsymbol{R}_f)\delta t \end{aligned} \tag{3.74}$$

where the primed terms are at time $t + \delta t$. The term $\boldsymbol{R}'_f$ needs to be evaluated further.

Let the number of molecules acting on $\boldsymbol{R}'_f$ be N where N is very large. Let the mean vector length of those N molecules before the interaction be ${}^{\langle N\rangle}\boldsymbol{R}_\mu$ and after the interaction let the mean vector length be ${}^{\langle N\rangle}\boldsymbol{R}'_\mu$. If one includes molecule $\boldsymbol{R}_f$ then the mean vector length after molecular interaction

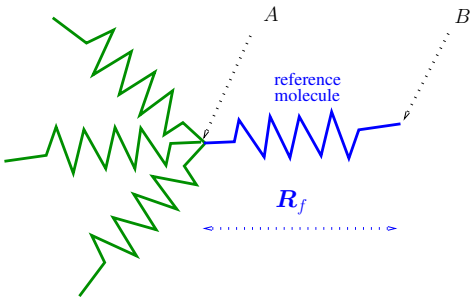

Figure 3.10: THE EFFECT OF ADJACENT MOLECULES AND REFERENCE MOLECULE STRETCH ON REFERENCE MOLECULE POSITION

(given no net force acts on the set of molecules) is given by

$$\boldsymbol{R}_\mu = \boldsymbol{R}'_\mu = \frac{(N)^{\langle N\rangle}\boldsymbol{R}'_\mu + \boldsymbol{R}'_f}{N+1}. \tag{3.75}$$

Furthermore, given that N is large, the contribution of molecule $\boldsymbol{R}_f$ to the mean is neglible and thus the approximation

$$^{\langle N\rangle}\boldsymbol{R}'_\mu \approx \boldsymbol{R}'_\mu = \boldsymbol{R}_\mu \tag{3.76}$$

may be made. Again the last substitution is because no net force acts on the set of molecules. Substituting (3.76) into (3.75)

$$(N+1)\boldsymbol{R}_\mu = N\boldsymbol{R}_\mu + \boldsymbol{R}'_f \qquad \Longleftrightarrow \qquad \boldsymbol{R}'_f = \boldsymbol{R}_\mu. \tag{3.77}$$

Substituting Equation (3.77) into (3.74),

$$\dot{\boldsymbol{c}}' \;=\; \dot{\boldsymbol{c}} + \frac{\boldsymbol{F}}{m}\delta t + \frac{K}{m}(\boldsymbol{R}_\mu - \boldsymbol{R}_f)\delta t. \tag{3.78}$$

The final position of the reference molecule is given by

$$\mathbf{r}' = \mathbf{r} + \dot{\boldsymbol{c}}\delta t \tag{3.79}$$

Next the stretch has to be considered. In order to derive an equation for vector length, one has to view the problem slightly differently. Instead of viewing the molecule as having all of the mass concentrated at point A, let half of the mass be at point A and let the other half be at point B. Let point $\acute{\boldsymbol{r}}$ be at the midpoint: thus the centre of mass is at point $\acute{\boldsymbol{r}}$. From

Newton 2, the acceleration of position $\grave{\boldsymbol{r}}$ (the centre of mass) is given by $\partial^2\grave{\boldsymbol{r}}/\partial t^2 = \boldsymbol{F}/m$. But $d\grave{\boldsymbol{r}}/dt = \grave{\boldsymbol{c}} + \dot{\boldsymbol{R}}_{\boldsymbol{f}}/2$. Re-arranging,

$$\dot{\boldsymbol{R}}_f = 2\left(\frac{d\grave{\boldsymbol{r}}}{dt} - \grave{\boldsymbol{c}}\right) = 2\left(\int_t^{t+\delta t} \frac{\boldsymbol{F}}{m} d\tau - \grave{\boldsymbol{c}}\right).$$

Integrating over an infinitesimal time interval δt from time t to $t+\delta t$,

$$\begin{aligned} \int_t^{t+\delta t} \dot{\boldsymbol{R}}_f d\tau &= 2\left(\int_t^{t+\delta t} \frac{\Delta \boldsymbol{p}}{m} d\tau - \int_t^{t+\delta t} \grave{\boldsymbol{c}} d\tau\right) \\ \text{or} \qquad \boldsymbol{R}'_f &= \boldsymbol{R}_f + 2\frac{\Delta \boldsymbol{p}}{m}\delta t - 2\grave{\boldsymbol{c}}\delta t \end{aligned} \tag{3.80}$$

where $\Delta \boldsymbol{p} = \int \boldsymbol{F} dt$.

$$\text{Consequently} \qquad \grave{\boldsymbol{c}} = \frac{\Delta \boldsymbol{p}}{m} - \frac{1}{2}\dot{\boldsymbol{R}}_f \qquad \text{and} \qquad d\grave{\boldsymbol{c}} = -\frac{1}{2} d\dot{\boldsymbol{R}}_f. \tag{3.81}$$

Furthermore, for a sufficiently small RVE and time increment (δt), the acceleration in stretch is assumed to be constant. Consequently,

$$\boldsymbol{F} + K\Delta \boldsymbol{R}_f = m\ddot{\mathbf{r}} \Longleftrightarrow \frac{\dot{\boldsymbol{F}}}{K} = -\dot{\boldsymbol{R}}_f + \frac{m}{K}\frac{\partial}{\partial t}\ddot{\mathbf{r}}. \tag{3.82}$$

Thus Equation (3.82) treats $\ddot{\mathbf{r}}$ as constant because of the small RVE and δt and

$$\frac{\partial}{\partial t}\ddot{\mathbf{r}} \approx 0 \Longleftrightarrow \frac{\dot{\boldsymbol{F}}}{K} = -\dot{\boldsymbol{R}}_f. \tag{3.83}$$

Therefore, applying Equations (3.78), (3.79) and (3.80), after an interval of time δt the change in the probability p (3.3) of finding a molecule in the range $(d\mathbf{r}, d\boldsymbol{R}_f, d\grave{\boldsymbol{c}})$ about the position $\mathbf{r}$ with vector length $\boldsymbol{R}_f$ and velocity $\grave{\boldsymbol{c}}$ is

$$p(\mathbf{r} + \grave{\boldsymbol{c}}\delta t, \boldsymbol{R}_f + 2\left(\frac{\Delta \boldsymbol{p}}{m} - \grave{\boldsymbol{c}}\right)\delta t, \grave{\boldsymbol{c}} + \frac{\boldsymbol{F}}{m}\delta t + \frac{K}{m}(\boldsymbol{R}_\mu - \boldsymbol{R}_f)\delta t, t + \delta t) d\grave{\boldsymbol{c}}\, d\boldsymbol{R}_f\, d\mathbf{r}$$
$$- p(\mathbf{r}, \boldsymbol{R}_f, d\grave{\boldsymbol{c}}, t) d\grave{\boldsymbol{c}}\, d\boldsymbol{R}_f\, d\mathbf{r}.$$

The most general solution is a function of $\mathbf{r}, t, \boldsymbol{R}_f, \dot{\boldsymbol{R}}_f$. Let the rate of change of the probability density due to molecular interaction be $\partial_e p(\mathbf{r}, \boldsymbol{R}_f, \dot{\boldsymbol{R}}_f, t)/\partial t$.

Then

$$\begin{aligned}
\dot{\boldsymbol{c}} \cdot \frac{\partial p}{\partial \mathbf{r}} d\mathbf{r} d\dot{\boldsymbol{c}} d\boldsymbol{R}_f dt &+ 2\left(\frac{\Delta \boldsymbol{p}}{m} - \dot{\boldsymbol{c}}\right) \cdot \frac{\partial p}{\partial \boldsymbol{R}_f} d\mathbf{r} d\dot{\boldsymbol{c}} d\boldsymbol{R}_f dt \\
+\frac{\boldsymbol{F}}{m} \cdot \frac{dp}{d\dot{\boldsymbol{c}}} d\mathbf{r} d\dot{\boldsymbol{c}} d\boldsymbol{R}_f dt &+ \frac{K}{m}(\boldsymbol{R}_f - \boldsymbol{R}_\mu) \cdot \frac{p}{d\dot{\boldsymbol{c}}} d\mathbf{r} d\boldsymbol{c} d\boldsymbol{R}_f dt \\
+\frac{\partial p}{\partial t} d\mathbf{r} d\dot{\boldsymbol{c}} d\boldsymbol{R}_f dt &= \frac{\partial_e p}{\partial t} d\mathbf{r} d\boldsymbol{R}_f dt \\
\text{and} \qquad \frac{\partial p}{\partial t} + 2\left(\frac{\Delta \boldsymbol{p}}{m} - \dot{\boldsymbol{c}}\right) \cdot \frac{\partial p}{\partial \boldsymbol{R}_f} &+ \dot{\boldsymbol{c}} \cdot \frac{\partial p}{\partial \mathbf{r}} \\
-\left(\frac{K}{m}\boldsymbol{R}_f - \left(\frac{\boldsymbol{F}}{m} + \frac{K}{m}\boldsymbol{R}_{\boldsymbol{\mu}}\right)\right) \cdot \frac{\partial p}{\partial \dot{\boldsymbol{c}}} &= \frac{\partial_e p}{\partial t} \qquad (3.84)
\end{aligned}$$

is the differential equation describing the mesoscopic behaviour of a polymer. Substitution of Equations (3.81), (3.81) and (3.83) into Equation (3.84) results in the revised mesoscopic equation of polymer chain interaction

$$\begin{aligned}
&\frac{\partial p}{\partial t} - \frac{\dot{\boldsymbol{F}}}{K} \cdot \frac{\partial p}{\partial \boldsymbol{R}_f} + \left(\frac{\Delta \boldsymbol{p}}{m} - \frac{1}{2}\dot{\boldsymbol{R}}_f\right) \cdot \frac{\partial p}{\partial \mathbf{r}} \\
&+2\left(\frac{K}{m}\boldsymbol{R}_f - \left(\frac{\boldsymbol{F}}{m} + \frac{K}{m}\boldsymbol{R}_\mu\right)\right) \cdot \frac{\partial p}{\partial \dot{\boldsymbol{R}}_f} = \frac{\partial_e p}{\partial t}. \qquad (3.85)
\end{aligned}$$

3.4 The incompressibility assumption

The incompressibility assumption is still accepted over a wide range of conditions [40]. Although incompressibility is only an approximation, it is a common approximation and the simplest realistic approximation. Vandoolaeghe and Terentjev [140] discuss the flaw in this approximation but the solution these authors provide is based on stress at steady state (requiring that the specimen's volume should relax after network formation). It therefore is not obvious that it applies to specimens at disequilibrium. Given the considerable increase in complexity required to implement those authors' model of rubber compressibility, incompressibility will be assumed until a disequilibrium model of rubber compressibility is available.

Chapter 4

The polymer chain interaction term – $\frac{\partial_e p}{\partial t}$

The polymer chain interaction term $\partial_e p/\partial t$ of Equation (3.84) or Equation (3.85) needs to be determined. This chapter will determine this term. Implicit in the following is that molecular interaction is binary or pairwise – a molecule can only interact with one other at a given time. In the model to follow, energy is conserved. The effect of molecular vibration is ignored and the time interval of the interaction is sufficiently long such that, at the end of the time interval, the molecules have completed one cycle or one period of what would have been their vibration. During the interaction, the internal forces between the molecules are simply redistributed.

4.1 The conservation equations

When the molecules interact, a force acts upon molecule 1 and a force acts on molecule 2. Due to the difference in these forces (the intermolecular interaction), an internal force is generated between the molecules. A 1D representation of such an interaction is depicted in Figure 4.1. In the depiction, from initial time t to final time $t + \delta t$, $\boldsymbol{F}_1$ represents the force acting on molecule 1 due to molecule 2 and $\boldsymbol{F}_2$ represents the force acting on molecule 2 due to molecule 1. $\boldsymbol{F}_1 \neq \boldsymbol{F}_2$ because the system is not in equilibrium. Prior to time t the molecules are not in contact. Note that relaxation implies a loss of energy due to internal molecular friction. Given that this model ignores this effect (and therefore hysteresis) and that the interaction is considered to result in only one cycle of vibration or periodic motion, the interaction can therefore be considered to be represented by the lower two situations (vibration) and that only one cycle is completed. Given that the self-energy of the

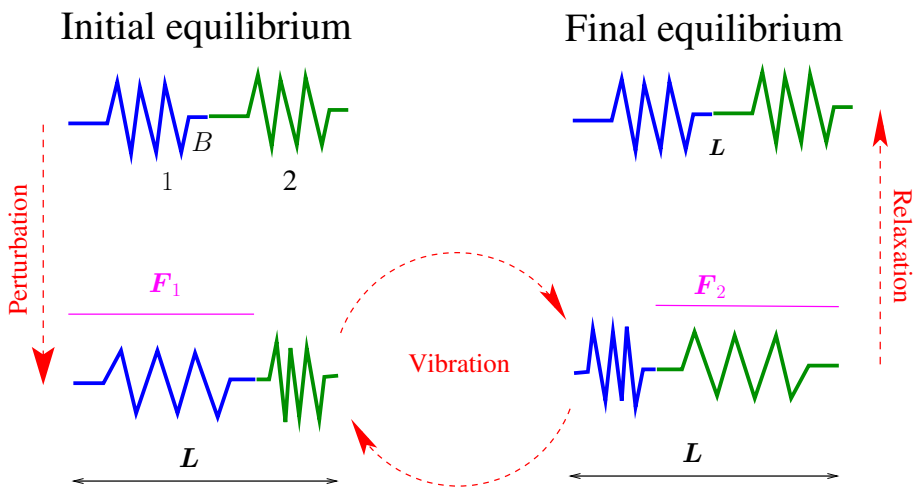

Figure 4.1: Schematic of idealised 1D binary molecule interaction. Molecule 1 is in blue and molecule 2 is in green. The diagram should be read counterclockwise from the top left corner. Note the conservation of length and that $\boldsymbol{F}_1$ represents the force on molecule 1 due to molecule 2.

individual molecules is ignored, the interaction potential between potential and kinetic can be neglected. One can therefore anticipate that the potential and kinetic energy are conserved separately but this will be shown explicitly.

Let $\grave{\boldsymbol{c}}_1$ be the velocity of the end A of molecule 1 and let $\grave{\boldsymbol{c}}_2$ be the velocity at end B as depicted in Figure 4.1. Given the manner in which these molecules are connected, the velocity at the A end of molecule 2 must be $\grave{\boldsymbol{c}}_2$. In this situation, it is only the internal forces that are being redistributed so the combined length of the molecules is the same (as represented by the length L in Figure 4.1) and more importantly the velocity at the B end of molecule 2 is $\grave{\boldsymbol{c}}_1$.

To express this mathematically, let $\boldsymbol{R}_1$ and $\boldsymbol{R}_2$ represent the initial vector length between ends A and B of molecules 1 and 2, respectively, in an arbitrary coordinate system. Furthermore let the post-interaction vector lengths be $\boldsymbol{R}'_1$ and $\boldsymbol{R}'_2$ respectively. Then, from the conservation of vector length for the molecular interaction period, δt, in the coordinate systems of Chapter 3

$$\boldsymbol{R}_{f1} + \boldsymbol{R}_{f2} = \boldsymbol{L} = \boldsymbol{R}'_{f1} + \boldsymbol{R}'_{f2} \quad , \tag{4.1}$$

$$\dot{\boldsymbol{R}}_{\Delta 1} = \dot{\boldsymbol{R}}_{f1} - \dot{\boldsymbol{R}}_{\mu} \qquad \text{where} \qquad \dot{\boldsymbol{R}}_{f1} = \grave{\boldsymbol{c}}_2 - \grave{\boldsymbol{c}}_1, \tag{4.2}$$

$$\dot{\boldsymbol{R}}_{\Delta 2} = \dot{\boldsymbol{R}}_{f2} - \dot{\boldsymbol{R}}_{\mu} \qquad \text{where} \qquad \dot{\boldsymbol{R}}_{f2} = \grave{\boldsymbol{c}}_1 - \grave{\boldsymbol{c}}_2. \tag{4.3}$$

Note that molecular interaction is being modelled using the redistribution of vector length assumption. Subtracting half of Equation (4.3) from half of Equation (4.2),

$$\frac{1}{2}\dot{\boldsymbol{R}}_{\Delta 12} = \frac{1}{2}(\dot{\boldsymbol{R}}_{\Delta 1} - \dot{\boldsymbol{R}}_{\Delta 2}) = \frac{1}{2}(\dot{\boldsymbol{R}}_{f1} - \dot{\boldsymbol{R}}_{f2}) = \dot{\boldsymbol{c}}_2 - \dot{\boldsymbol{c}}_1 = -\frac{1}{2}\dot{\boldsymbol{R}}_{\Delta 21}.$$

Similarly,

$$\begin{aligned}
\dot{\boldsymbol{R}}'_{\Delta 1} = \dot{\boldsymbol{R}}'_{f1} - \dot{\boldsymbol{R}}'_{\mu} \qquad \text{where} \qquad \dot{\boldsymbol{R}}'_{f1} &= \dot{\boldsymbol{c}}'_2 - \dot{\boldsymbol{c}}'_1, && (4.4)\\
\dot{\boldsymbol{R}}'_{\Delta 2} = \dot{\boldsymbol{R}}'_{f2} - \dot{\boldsymbol{R}}'_{\mu} \qquad \text{where} \qquad \dot{\boldsymbol{R}}'_{f2} &= \dot{\boldsymbol{c}}'_1 - \dot{\boldsymbol{c}}'_2, && (4.5)\\
\iff \frac{1}{2}\dot{\boldsymbol{R}}'_{\Delta 12} = \frac{1}{2}(\dot{\boldsymbol{R}}'_{\Delta 1} - \dot{\boldsymbol{R}}'_{\Delta 2}) = \dot{\boldsymbol{c}}'_2 - \dot{\boldsymbol{c}}'_1 &= -\frac{1}{2}\dot{\boldsymbol{R}}'_{\Delta 21}. && (4.6)
\end{aligned}$$

Substitutions of Equations (4.1), (3.81), (4.3) and (4.6) into the conservation of energy equation:

$$\begin{aligned}
& \frac{k}{2}(R_{\Delta 1}^2 + R_{\Delta 2}^2) + \frac{m}{2}(\dot{c}_2^2 + \dot{c}_1^2) = \frac{k}{2}(R_{\Delta 1}'^2 + R_{\Delta 2}'^2) + \frac{m}{2}(\dot{c}_1'^2 + \dot{c}_2'^2)\\
\iff\ & \frac{k}{4}\Big((R_{\Delta 1} + R_{\Delta 2})^2 + (R_{\Delta 1} - R_{\Delta 2})^2\Big) + \frac{m}{4}\Big((\dot{c}_1 + \dot{c}_2)^2 + (\dot{c}_1 - \dot{c}_2)^2\Big)\\
=\ & \frac{m}{4}\Big((\dot{c}'_1 + \dot{c}'_2)^2 + (\dot{c}'_1 - \dot{c}'_2)^2\Big) + \frac{k}{4}\Big((R'_{\Delta 1} + R'_{\Delta 2})^2 + (R'_{\Delta 1} - R'_{\Delta 2})^2\Big)\\
\iff\ & \frac{k}{4}\Big((L)^2 + (R_{\Delta 1} - R_{\Delta 2})^2\Big) + \frac{m}{16}\Big((2\frac{\Delta p}{m} - \dot{R}_{f1} - \dot{R}_{f2})^2 + (\dot{R}_{\Delta 1} - \dot{R}_{\Delta 2})^2\Big)\\
=\ & \frac{m}{16}\Big((2\frac{\Delta p}{m} - \dot{R}'_{f1} - \dot{R}'_{f2})^2 + (\dot{R}'_{\Delta 2} - \dot{R}'_{\Delta 1})^2\Big) + \frac{k}{4}\Big((L)^2 + (R'_{\Delta 1} - R'_{\Delta 2})^2\Big)\\
\iff\ & \frac{k}{4}(R_{\Delta 1} - R_{\Delta 2})^2 + \frac{m}{16}\Big((2\frac{\Delta p}{m} - \dot{L})^2 + (\dot{R}_{\Delta 2} - \dot{R}_{\Delta 1})^2\Big)\\
& \qquad = \frac{k}{4}(R'_{\Delta 1} - R'_{\Delta 2})^2 + \frac{m}{16}\Big((2\frac{\Delta p}{m} - \dot{L})^2 + (\dot{R}'_{\Delta 2} - \dot{R}'_{\Delta 1})^2\Big)\\
\iff\ & \frac{k}{4}(R_{\Delta 1} - R_{\Delta 2})^2 + \frac{m}{16}(\dot{R}_{\Delta 2} - \dot{R}_{\Delta 1})^2\\
& \qquad = \frac{k}{4}(R'_{\Delta 1} - R'_{\Delta 2})^2 + \frac{m}{16}(\dot{R}'_{\Delta 2} - \dot{R}'_{\Delta 1})^2. \qquad (4.7)
\end{aligned}$$

A solution (though not the only solution) of Equation (4.7) is

$$(R_{\Delta 1} - R_{\Delta 2})^2 = (R'_{\Delta 1} - R'_{\Delta 2})^2 \text{ and } (\dot{R}_{\Delta 1} - \dot{R}_{\Delta 2})^2 = (\dot{R}'_{\Delta 1} - \dot{R}'_{\Delta 2})^2.$$

This solution will be explored further because (as is being shown and will be confirmed by Equation (4.10) at the end of this section) it allows separation

of kinetic and potential energy. By definition

$$\begin{aligned}(R_{\Delta 1} - R_{\Delta 2})^2 &= |\boldsymbol{R}_{\Delta 1} - \boldsymbol{R}_{\Delta 2}|^2 = (\boldsymbol{R}_{\Delta 1} - \boldsymbol{R}_{\Delta 2}) \cdot (\boldsymbol{R}_{\Delta 1} - \boldsymbol{R}_{\Delta 2}) \\ &= (\boldsymbol{R}'_{\Delta 1} - \boldsymbol{R}'_{\Delta 2}) \cdot (\boldsymbol{R}'_{\Delta 1} - \boldsymbol{R}'_{\Delta 2}) = |\boldsymbol{R}'_{\Delta 1} - \boldsymbol{R}'_{\Delta 2}|^2 \\ &= (R'_{\Delta 1} - R'_{\Delta 2})^2. \end{aligned} \tag{4.8}$$

The trivial solution is

$$\boldsymbol{R}_{\Delta 1} - \boldsymbol{R}_{\Delta 2} = \boldsymbol{R}'_{\Delta 1} - \boldsymbol{R}'_{\Delta 2}$$

where $\boldsymbol{R}_{\Delta 1} = \boldsymbol{R}'_{\Delta 1}$. Another solution is

$$\boldsymbol{R}_{\Delta 1} - \boldsymbol{R}_{\Delta 2} = -\boldsymbol{R}'_{\Delta 1} + \boldsymbol{R}'_{\Delta 2} = \boldsymbol{R}^g_{\Delta}. \tag{4.9}$$

It is Equation (4.9) which will be adopted and considered further.

Substituting Equation (4.9) into the formula for potential energy,

$$\begin{aligned} W_p &= \frac{k}{2}(\boldsymbol{R}^2_{\Delta 1} + \boldsymbol{R}^2_{\Delta 2} - \boldsymbol{R}'^2_{\Delta 1} + -\boldsymbol{R}'^2_{\Delta 2}) \\ &= \frac{k}{4}\left((R_{\Delta 1} + R_{\Delta 2})^2 + (R_{\Delta 1} - R_{\Delta 2})^2\right) \\ &\qquad -\frac{k}{4}\left((R'_{\Delta 1} + R'_{\Delta 2})^2 + (R'_{\Delta 1} - R'_{\Delta 2})^2\right) \\ &= \frac{k}{4}\left((L)^2 + (R^g_{\Delta})^2\right) - \frac{k}{4}\left((L)^2 + (R^g_{\Delta})^2\right) = 0 \end{aligned} \tag{4.10}$$

where R^g_{Δ} is from Equation (4.9) and L is from Equation (4.1). Thus Equation (4.10) confirms that a solution exists in which potential energy is conserved. The conservation of energy equation (4.7) is a combination of kinetic and potential energy, and the implication is that a solution exists in which both kinetic energy and potential energy are conserved separately, and can be considered independently. It is this solution that will be considered further. It should be recognised that the equations for the conservation of kinetic energy and potential energy have been formulated in terms of variables $\dot{\boldsymbol{R}}_{\Delta}$ and $\boldsymbol{R}_{\Delta}$ respectively. It is desired to construct similar potential energy conservation laws in terms of $\boldsymbol{R}_f$ and similar kinetic energy conservation laws in terms of $\dot{\boldsymbol{R}}_f$. Conservation laws for $\boldsymbol{R}_f$ will be derived based on Equation (4.7) in Section 4.1.1 and similarly conservation laws in terms of $\dot{\boldsymbol{R}}_f$ will be

derived in Section 4.1.2.

The results of Section 4.1.1 and Section 4.1.2 are necessary for the geometry of Section 4.2 and Section 4.3. The geometry is necessary for the determination of the Jacobian in Section 4.4 which is used to simplify the expression for the polymer chain interaction term $\partial_e p/\partial t$ – the change in stretch and momentum due to molecular interaction.

4.1.1 Conservation of potential energy

Let $\boldsymbol{R}_{\Delta G}$ be the weighted average of a set of n vector lengths $\boldsymbol{R}_{\Delta i}$ $1 \leq i \leq n$. Let the weightings be in proportion to each vector length's contribution to the resultant force $\boldsymbol{F}_R$; that is

$$\begin{aligned} \sum_{i=1}^{n} K_i \boldsymbol{R}_{\Delta i} &= \boldsymbol{F}_R = \boldsymbol{R}_{\Delta G} \sum_{i=1}^{n} K_i \\ \iff \frac{\sum_{i=1}^{n} K_i \boldsymbol{R}_{\Delta i}}{\sum_{i=1}^{n} K_i} &= \boldsymbol{R}_{\Delta G}. \end{aligned} \tag{4.11}$$

Thus $\boldsymbol{R}_{\Delta G}$, as defined by Equation (4.11), can be called the centre of vector length.

During molecular interaction, no external forces act on the system, so that the resultant force remains constant. Consequently, during intermolecular interaction vector length is redistributed such that

$$K_1 \boldsymbol{R}_{\Delta 1} + K_2 \boldsymbol{R}_{\Delta 2} = K_1 \boldsymbol{R}'_{\Delta 1} + K_2 \boldsymbol{R}'_{\Delta 2} = K_0 \boldsymbol{R}_{\Delta G} \tag{4.12}$$

where the primed terms are post-interaction, and $K_0 = K_1 + K_2$. Let $A_1 = K_1/K_0$ and $A_2 = K_2/K_0$; then $A_1 + A_2 = 1$ and

$$\begin{aligned} \boldsymbol{R}_{\Delta 1} &= \boldsymbol{R}_{\Delta G} + \frac{K_2}{K_1}\Big(\boldsymbol{R}_{\Delta G} - \boldsymbol{R}_{\Delta 2}\Big) \\ &= \boldsymbol{R}_{\Delta G} + \frac{K_2}{K_1}\Big(A_1 \boldsymbol{R}_{\Delta 1} + A_2 \boldsymbol{R}_{\Delta 2} - \boldsymbol{R}_{\Delta 2}\Big) \\ &= \boldsymbol{R}_{\Delta G} + \frac{K_2}{K_1} A_1 \Big((\boldsymbol{R}_{\Delta 1} - \boldsymbol{R}_{\Delta 2})\Big) \\ &= \boldsymbol{R}_{\Delta G} + A_2(\boldsymbol{R}_{\Delta 1} - \boldsymbol{R}_{\Delta 2}) \\ &= \boldsymbol{R}_{\Delta G} + A_2(\boldsymbol{R}_{\Delta 12}). \end{aligned} \tag{4.13}$$

Similarly

$$\boldsymbol{R}_{\Delta 2} = \boldsymbol{R}_{\Delta G} + A_1(\boldsymbol{R}_{\Delta 21}) \tag{4.14}$$

$$\boldsymbol{R}'_{\Delta 2} = \boldsymbol{R}_{\Delta G} + A_1(\boldsymbol{R}'_{\Delta 21}) \tag{4.15}$$

$$\boldsymbol{R}'_{\Delta 1} = \boldsymbol{R}_{\Delta G} + A_2(\boldsymbol{R}'_{\Delta 12}). \tag{4.16}$$

Also note that $\boldsymbol{R}_{\Delta 12} = -\boldsymbol{R}_{\Delta 21}$ and that $\boldsymbol{R}'_{\Delta 12} = -\boldsymbol{R}'_{\Delta 21}$. Thus

$$R_{\Delta 12} = R_{\Delta 21} = R^g_\Delta \qquad \text{and} \qquad R'_{\Delta 12} = R'_{\Delta 21} = R^{g'}_\Delta.$$

The conservation of potential energy equation is

$$\frac{K_1}{2}R^2_{\Delta 1} + \frac{K_2}{2}R^2_{\Delta 2} = \frac{K_1}{2}R'^2_{\Delta 1} + \frac{K_2}{2}R'^2_{\Delta 2}.$$

After substituting Equations (4.13) to (4.16) into the above conservation of potential energy equation,

$$\frac{K_1}{2}R^2_{\Delta 1} + \frac{K_2}{2}R^2_{\Delta 2} = \frac{K_0}{2}(R^2_{\Delta G} + A_1A_2R^{g2}_\Delta)$$
$$\frac{K_1}{2}R'^2_{\Delta 1} + \frac{K_2}{2}R'^2_{\Delta 2} = \frac{K_0}{2}(R^2_{\Delta G} + A_1A_2R^{g'2}_\Delta).$$

Consequently

$$R^g_\Delta = R^{g'}_\Delta,$$

so that the relative vector length simply changes direction rather than magnitude during interaction. This is not obvious. The origin is the requirement that energy is conserved. The algebraic manipulation is tedious but not obvious. The exact derivation is not shown here but a slightly more complex variant is used in Appendix A-1. This more complex variant is necessary later. The above is for the interaction of a pair of molecules. Using exactly the same argument for the averaged property, $\boldsymbol{R}_\mu$, the conservation of energy equation becomes

$$\frac{K_1}{2}R^2_{\mu 1} + \frac{K_2}{2}R^2_{\mu 2} = \frac{K_0}{2}(R^2_{\mu G} + A_1A_2R^{g2}_\mu)$$
$$\frac{K_1}{2}R'^2_{\mu 1} + \frac{K_2}{2}R'^2_{\mu 2} = \frac{K_0}{2}(R^2_{\mu G} + A_1A_2R^{g'2}_\mu) \tag{4.17}$$

where

$$\boldsymbol{R}_{\mu 1} - \boldsymbol{R}_{\mu 2} = \boldsymbol{R}_{\mu 12} \qquad \text{and} \qquad R_{\mu 12} = R_{\mu 21} = R^g_\mu.$$

Consequently (4.17) implies that

$$R_\mu^g = R_\mu^{g\prime}.$$

Next, conservation equations are determined for $\boldsymbol{R}_f = \boldsymbol{R}_\Delta + \boldsymbol{R}_\mu$, with appropriate substitution of (4.12),

$$\begin{aligned} K_1\boldsymbol{R}_{f1} + K_2\boldsymbol{R}_{f2} &= K_1(\boldsymbol{R}_{\Delta 1} + \boldsymbol{R}_{\mu 1}) + K_2(\boldsymbol{R}_{\Delta 2} + \boldsymbol{R}_{\mu 2}) \\ &= K_1(\boldsymbol{R}_{\Delta 1}) + K_2(\boldsymbol{R}_{\Delta 2}) + K_1(\boldsymbol{R}_{\mu 1}) + K_2(\boldsymbol{R}_{\mu 2}) \\ &= K_0\boldsymbol{R}_{\Delta G} + K_0\boldsymbol{R}_{\mu G} = K_0\boldsymbol{R}_{fG} \\ &= K_0\boldsymbol{R}'_{\Delta G} + K_0\boldsymbol{R}'_{\mu G} \end{aligned}$$

$$\begin{aligned} K_1\boldsymbol{R}_{f1} + K_2\boldsymbol{R}_{f2} &= K_1(\boldsymbol{R}'_{\Delta 1}) + K_2(\boldsymbol{R}'_{\Delta 2}) + K_1(\boldsymbol{R}'_{\mu 1}) + K_2(\boldsymbol{R}'_{\mu 2}) \\ &= K_1(\boldsymbol{R}'_{\Delta 1} + \boldsymbol{R}'_{\mu 1}) + K_2(\boldsymbol{R}'_{\Delta 2} + \boldsymbol{R}'_{\mu 2}) \\ &= K_1\boldsymbol{R}'_{f1} + K_2\boldsymbol{R}'_{f2}. \end{aligned} \tag{4.18}$$

Furthermore, if molecules 1 and 2 are of the same type and in the same RVE, then for the averaged values $\boldsymbol{R}_{\mu 1} = \boldsymbol{R}_{\mu 2}$

$$\begin{aligned} \boldsymbol{R}_{\Delta 21} &= \boldsymbol{R}_{\Delta 2} - \boldsymbol{R}_{\Delta 1} = (\boldsymbol{R}_{f2} - \boldsymbol{R}_{\mu 2}) - (\boldsymbol{R}_{f1} - \boldsymbol{R}_{\mu 1}) \\ &= (\boldsymbol{R}_{f2} - \boldsymbol{R}_{f1}) - (\boldsymbol{R}_{\mu 1} - \boldsymbol{R}_{\mu 2}) = (\boldsymbol{R}_{f2} - \boldsymbol{R}_{f1}) = \boldsymbol{R}_{f21}. \end{aligned} \tag{4.19}$$

Similarly

$$\boldsymbol{R}'_{\Delta 21} = \boldsymbol{R}'_{f21} \tag{4.20}$$

and

$$R_f^{g\prime} = R'_{f21} = R'_{\Delta 21} = R_\Delta^{g\prime} = R_\Delta^g = R_{\Delta 21} = R_{f21} = R_f^g. \tag{4.21}$$

Using similar definitions to those of Equations (4.13) to (4.16),

$$K_1R_{f1}^2 + K_2R_{f2}^2 = K_0(R_{fG}^2 + A_1A_2(R_f^g)^2), \tag{4.22}$$

$$K_1R_{f1}'^2 + K_2R_{f2}'^2 = K_0(R_{fG}^2 + A_1A_2(R_f^{g\prime})^2), \tag{4.23}$$

and, given Equation (4.21),

$$\frac{1}{2}K_1R_{f1}^2 + \frac{1}{2}K_2R_{f2}^2 = \frac{1}{2}K_1R_{f1}'^2 + \frac{1}{2}K_2R_{f2}'^2. \tag{4.24}$$

4.1.2 Conservation of kinetic energy

Intuitively, the molecules can be represented or imagined to be billiard balls (as in the gas case) with an elastic component as depicted in Figure 4.2. After interaction momentum is conserved. As for the case of ideal gases

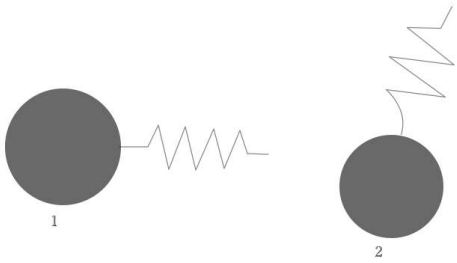

Figure 4.2: Ball-and-spring molecular schematic

Huang ([66], Chapter 3) and Chapman and Cowling [18], set

$$m_t = m_1 + m_2, \qquad M_1 = \frac{m_1}{m_0} \qquad \text{and} \qquad M_2 = \frac{m_2}{m_0}.$$

Then
$$M_1 + M_2 = 1 \tag{4.25}$$

where m_i is the mass of molecule i. Before and after the molecular interaction the centre of mass maintains the same velocity $\mathbf{G}$: thus

$$m_t \boldsymbol{G} = m_1 \grave{\boldsymbol{c}}_1 + m_2 \grave{\boldsymbol{c}}_2 = m_1 \grave{\boldsymbol{c}}'_1 + m_2 \grave{\boldsymbol{c}}'_2. \tag{4.26}$$

From Equations (4.2) to (4.5),

$$\begin{aligned}
m_1 \grave{\boldsymbol{c}}_1 &= m_1 \grave{\boldsymbol{c}}_1 \\
m_1 \grave{\boldsymbol{c}}_1 + m_2 \grave{\boldsymbol{c}}_1 &= m_1 \grave{\boldsymbol{c}}_1 + m_2 \grave{\boldsymbol{c}}_2 + m_2 (\grave{\boldsymbol{c}}_1 - \grave{\boldsymbol{c}}_2) \\
m_t \grave{\boldsymbol{c}}_1 &= m_t \boldsymbol{G} + m_2 (\grave{\boldsymbol{c}}_1 - \grave{\boldsymbol{c}}_2) \\
m_t \grave{\boldsymbol{c}}_1 &= m_t \boldsymbol{G} + m_2 (\dot{\boldsymbol{R}}_{\Delta 2}) \\
\grave{\boldsymbol{c}}_1 &= \boldsymbol{G} + M_2 (\dot{\boldsymbol{R}}_{\Delta 2}).
\end{aligned} \tag{4.27}$$

Similarly

$$\dot{\boldsymbol{c}}_2 = \boldsymbol{G} + M_1(\dot{\boldsymbol{R}}_{\Delta 1}), \tag{4.28}$$

$$\dot{\boldsymbol{c}}'_2 = \boldsymbol{G} + M_1(\dot{\boldsymbol{R}}'_{\Delta 1}), \tag{4.29}$$

and
$$\boldsymbol{c}'_1 = \boldsymbol{G} + M_2(\dot{\boldsymbol{R}}'_{\Delta 2}). \tag{4.30}$$

But $|\dot{\boldsymbol{R}}_{\Delta 1}| = |\dot{\boldsymbol{R}}_{\Delta 2}|$, $\dot{R}'^2_{\Delta 1} = \dot{R}'^2_{\Delta 2}$ by Equation (4.1)

and $\frac{1}{2}(m_1\dot{c}_1^2 + m_2\dot{c}_2^2) = \frac{1}{2}(m_1\dot{c}_1'^2 + m_2\dot{c}_2'^2)$.

Substituting Equations (4.27), (4.28), (4.29) and (4.30) into (4.26),

$$\frac{1}{2}m_t(G^2 + M_1M_2\dot{R}^2_{\Delta 1}) = \frac{1}{2}m_t(G^2 + M_1M_2\dot{R}'^2_{\Delta 1}) \tag{4.31}$$

$$\iff \dot{R}_{\Delta 1} = \dot{R}'_{\Delta 1}.$$

Similarly $\dot{R}_{\Delta 2} = \dot{R}'_{\Delta 2}$

and
$$\frac{1}{2}m_t(G^2 + M_1M_2\dot{R}^2_{\Delta 2}) = \frac{1}{2}m_t(G^2 + M_1M_2\dot{R}'^2_{\Delta 2}) \tag{4.32}$$

$$\iff M_1M_2\dot{R}^2_{\Delta 1} + M_1M_2\dot{R}^2_{\Delta 2} = M_1M_2\dot{R}'^2_{\Delta 1} + M_1M_2\dot{R}'^2_{\Delta 2} \qquad (4.31 + 4.32)$$

$$\iff \dot{R}^2_{\Delta 1} + \dot{R}^2_{\Delta 2} = \dot{R}'^2_{\Delta 1} + \dot{R}'^2_{\Delta 2}. \tag{4.33}$$

Thus during the interaction, the molecular stretch rate changes only in direction, not in magnitude. Applying Equations (4.2) through (4.5), given that during molecular interaction $\dot{R}_\mu = \dot{R}'_\mu$,

$$\dot{R}_{f2} = \dot{R}'_{f2} \qquad \text{and} \qquad \dot{R}_{f1} = \dot{R}'_{f1} \Longrightarrow \dot{R}^2_{f2} + \dot{R}^2_{f1} = \dot{R}'^2_{f2} + \dot{R}'^2_{f1}. \tag{4.34}$$

Differentiating Equation (4.1),

$$\dot{\boldsymbol{R}}_{f1} + \dot{\boldsymbol{R}}_{f2} = \dot{\boldsymbol{R}}'_{f1} + \dot{\boldsymbol{R}}'_{f1}$$

$$\iff m\dot{\boldsymbol{R}}_{f1} + m\dot{\boldsymbol{R}}_{f2} = m\dot{\boldsymbol{R}}'_{f1} + m\dot{\boldsymbol{R}}'_{f1} \tag{4.35}$$

$$\iff m(\dot{\boldsymbol{R}}_{f1} + \dot{\boldsymbol{R}}_{f2})^2 = m(\dot{\boldsymbol{R}}'_{f1} + \dot{\boldsymbol{R}}'_{f1})^2. \tag{4.36}$$

Thus (4.35) confirms the equivalent of a conservation of momentum equation for $\boldsymbol{R}_f$ for molecules that are identical.

Differentiating Equation (4.1) with respect to time,

$$\dot{\boldsymbol{R}}_{f1} + \dot{\boldsymbol{R}}_{f2} = \dot{\boldsymbol{R}}'_{f1} + \dot{\boldsymbol{R}}'_{f1} = 0 \tag{4.37}$$

$$\Longrightarrow (\dot{\boldsymbol{R}}_{f1} + \dot{\boldsymbol{R}}_{f2})^2 = (\dot{\boldsymbol{R}}'_{f1} + \dot{\boldsymbol{R}}'_{f1})^2$$

$$\iff \dot{\boldsymbol{R}}^2_{f1} + 2\dot{\boldsymbol{R}}_{f1} \cdot \dot{\boldsymbol{R}}_{f2} + \dot{\boldsymbol{R}}^2_{f2} = \dot{\boldsymbol{R}}'^2_{f1} + 2\dot{\boldsymbol{R}}'_{f1} \cdot \dot{\boldsymbol{R}}'_{f2} + \dot{\boldsymbol{R}}'^2_{f2}. \tag{4.38}$$

Subtracting (4.34) from (4.38),

$$+2\dot{\boldsymbol{R}}_{f1}\cdot\dot{\boldsymbol{R}}_{f2}=+2\dot{\boldsymbol{R}}'_{f1}\cdot\dot{\boldsymbol{R}}'_{f2} \tag{4.39}$$

and then subtracting (4.39) from (4.34),

$$\begin{aligned}
(\dot{\boldsymbol{R}}_{f1}-\dot{\boldsymbol{R}}_{f2})^2 &= (\dot{\boldsymbol{R}}'_{f1}-\dot{\boldsymbol{R}}'_{f2})^2 && (4.40)\\
\iff \qquad \dot{\boldsymbol{R}}^2_{f12} &= \dot{\boldsymbol{R}}'^2_{f12} && (4.41)\\
\iff \qquad \dot{R}_{f12}=\dot{R}^g_f &= \dot{R}^{g\prime}_f=\dot{R}'_{f12} && (4.42)\\
|\dot{\boldsymbol{R}}_{f1}-\dot{\boldsymbol{R}}_{f2}| &= |\dot{\boldsymbol{R}}'_{f1}-\dot{\boldsymbol{R}}'_{f2}|.
\end{aligned}$$

Adding Equation (4.36) to $m\times$(4.40) and dividing the result by 4 leads to

$$\frac{1}{2}m(\dot{\boldsymbol{R}}_{f1})^2+\frac{1}{2}m(\dot{\boldsymbol{R}}_{f2})^2=\frac{1}{2}m(\dot{\boldsymbol{R}}'_{f1})^2+\frac{1}{2}m(\dot{\boldsymbol{R}}'_{f2})^2, \tag{4.43}$$

the equivalent of a conservation of kinetic energy for $\dot{\boldsymbol{R}}_f$, for molecules that are identical.

4.2 Geometry of molecular interaction for stretch

After differentiating both sides of Equation (4.24) with respect to time another conservation equation,

$$K_1\boldsymbol{R}_{f1}\cdot\dot{\boldsymbol{R}}_{f1}+K_2\boldsymbol{R}_{f2}\cdot\dot{\boldsymbol{R}}_{f2}=K_1\boldsymbol{R}'_{f1}\cdot\dot{\boldsymbol{R}}'_{f1}+K_2\boldsymbol{R}'_{f2}\cdot\dot{\boldsymbol{R}}'_{f2}, \tag{4.44}$$

is established. Although Equations (4.18), (4.24) and (4.44) are not the conservation of force, energy and power respectively, they are equivalent equations for $\boldsymbol{R}_f$. Applying the result from Appendix A-1 equation (A-5)

$$\begin{aligned}
K_1\boldsymbol{R}_{f1}\cdot\dot{\boldsymbol{R}}_{f1} \;+\; & K_2\boldsymbol{R}_{f2}\cdot\dot{\boldsymbol{R}}_{f2}=K_0(\boldsymbol{R}_{fG}\cdot\dot{\boldsymbol{R}}_{fG}+A_1A_2\boldsymbol{R}_{f12}\cdot\dot{\boldsymbol{R}}_{f12})\\
&= K_0(\boldsymbol{R}_{fG}\cdot\dot{\boldsymbol{R}}_{fG}+A_1A_2R_{f12}\dot{R}_{f12}\cos\theta)\\
&= K_0(\boldsymbol{R}_{fG}\cdot\dot{\boldsymbol{R}}_{fG}+A_1A_2R^g_f\dot{R}_{f12}\cos\theta) && (4.45)
\end{aligned}$$

and

$$\begin{aligned}
K_1\boldsymbol{R}'_{f1}\cdot\dot{\boldsymbol{R}}'_{f1} \;+\; & K_2\boldsymbol{R}'_{f2}\cdot\dot{\boldsymbol{R}}'_{f2}=K_0(\boldsymbol{R}_{fG}\cdot\dot{\boldsymbol{R}}_{fG}+A_1A_2\boldsymbol{R}'_{f12}\cdot\dot{\boldsymbol{R}}'_{f12})\\
&= K_0(\boldsymbol{R}_{fG}\cdot\dot{\boldsymbol{R}}_{fG}+A_1A_2R'_{f12}\dot{R}'_{f12}\cos\phi)\\
&= K_0(\boldsymbol{R}_{fG}\cdot\dot{\boldsymbol{R}}_{fG}+A_1A_2R^{g\prime}_f\dot{R}'_{f12}\cos\phi) && (4.46)
\end{aligned}$$

where Equation (4.21) equates R_f^g and $R_f^{g\prime}$ and θ and ϕ are the angles between $\boldsymbol{R}_{f12}$ and $\dot{\boldsymbol{R}}_{f12}$ and $\boldsymbol{R}'_{f12}$ and $\dot{\boldsymbol{R}}'_{f12}$ respectively.

From Equation (4.42) $\dot{R}_{f12} = \dot{R}'_{f12}$ and therefore $\cos\theta = \cos\phi$ – confirming that the angle between the relative vector length and the relative stretch rate (or the temporal derivative of vector length) is reflected.

When molecules interact, they have an orientation relative to each other and consequently a relative vector length. The distance R_Δ^g (or R_f^g if the alternate coordinate system is used) remains constant during the interaction. Consequently the relative vector length must trace a locus that lies on the surface of a sphere. This is depicted in Figure 4.3 where the coordinate system has an origin at position A of molecule 1.

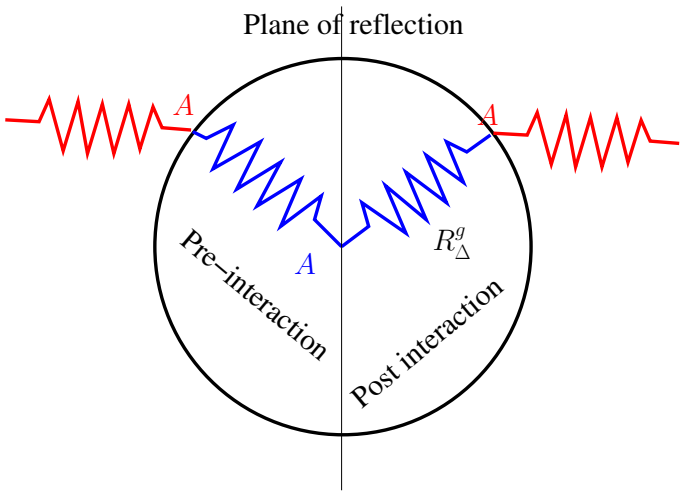

Figure 4.3: Relative vector length of molecules during interaction

In constructing this particular model, molecular vibration has been ignored. For molecule 1 with vector length $\boldsymbol{R}_{f1}(t)$ at time t, during molecular interaction, the molecule undergoes periodic motion with period T such that $\boldsymbol{R}_{f1}(t) = \boldsymbol{R}_{f1}(t+T)$. Similarly molecule 2, with which molecule 1 interacts, has motion $\boldsymbol{R}_{f2}(t)$ such that $\boldsymbol{R}_{f2}(t) = \boldsymbol{R}_{f2}(t+T)$. The molecules only undergo half a cycle of this vibration ($t = \frac{n}{2}T$) where $n \in \mathbb{N}_0$. The mean vector is $\boldsymbol{R}_i(t)$ where $t = (n+\frac{1}{4})T,\ i \in 1, 2\ )$. It is assumed that the mean vectors for the molecules are parallel and these mean vectors, therefore, lie on a plane. Thus when viewed from along molecule 1, in a plane with normal in direction of 1, molecule 2 will describe a locus as depicted in the Figure 4.4 where again the origin is at position A of molecule 1 and the axis is defined

along molecule 1. The locus traces the possible locations before and after

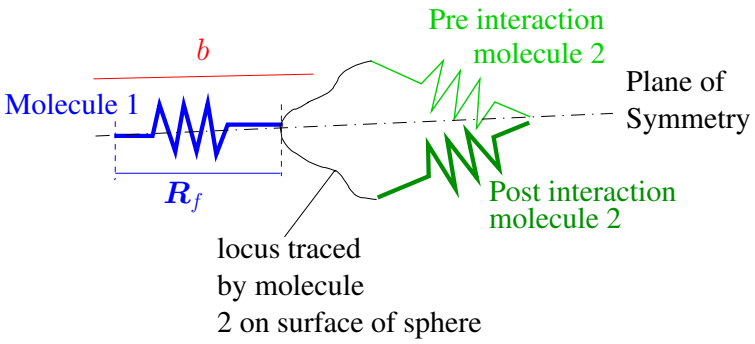

Figure 4.4: Projection of 3D vibration about molecule 1 onto 2D surface

interaction. During the interaction, the molecular stretch can vary.

Before constructing the collision term, additional geometric variables have to be defined. Referring to the Figure 4.4, let the vector $\boldsymbol{b}$ be along the shortest relative displacement between the molecules. Further let $\boldsymbol{K} = \boldsymbol{R}_{f1} \times \boldsymbol{b}$ and let the unit vector $\boldsymbol{k} = \frac{\boldsymbol{K}}{[\boldsymbol{K}]}$. Then the difference lies in the direction of $\boldsymbol{k}$ such that the difference is

$$\boldsymbol{R}_{f21} - \boldsymbol{R}'_{f21} = 2(\boldsymbol{R}_{f21} \cdot \boldsymbol{k})\boldsymbol{k}. \tag{4.47}$$

From (4.13) - (4.16), substituting Equation (4.21) and constant mean stretch,

$$\begin{aligned} \boldsymbol{R}_{f1} - \boldsymbol{R}'_{f1} &= 2A_2(\boldsymbol{R}_{f21} - \boldsymbol{R}'_{f21}) \\ \text{from (4.47)} &= 2A_2(\boldsymbol{R}'_{f21} \cdot \boldsymbol{k})\boldsymbol{k} && (4.48) \\ \text{Similarly } \boldsymbol{R}_{f2} - \boldsymbol{R}'_{f2} &= -2A_1(\boldsymbol{R}_{f21} \cdot \boldsymbol{k})\boldsymbol{k} = -2A_1(\boldsymbol{R}'_{f21} \cdot \boldsymbol{k})\boldsymbol{k} && (4.49) \end{aligned}$$

where for identical molecules $A_1 = A_2 = \frac{1}{2}$. A 3D representation of the result is provided by Figure 4.5 where A is the position of the initial end of molecule 1 and A of $\boldsymbol{R}_{f2}$ is the initial end of molecule 2. Given the construction of the model, the difference in position of A of molecule 2 and A of molecule 1 is $\boldsymbol{R}_{f1}$. Thus $\boldsymbol{R}_{f1}$ also represents the displacement between the molecules. Similarly A of $\boldsymbol{R}'_{f2}$ is the post-interaction position of molecule 2. $\boldsymbol{R}_{f21}$ is the relative vector length between molecule 1 and molecule 2. The change in displacement between the pre- and post-interaction position A of molecule 1 is $\boldsymbol{R}_{f21} - \boldsymbol{R}'_{f21}$ in Equation (4.47).

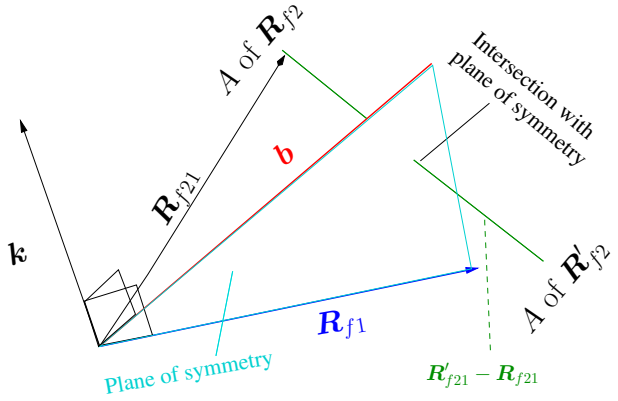

Figure 4.5: Geometry of molecular interaction in 3D

4.3 Geometry of interaction for stretch rate

Given the manner in which this model has been constructed, the stretch rate of molecule 1 would be expected to be equal and opposite to molecule 2 during one cycle of interaction. A 1D schematic representation is provided in the Figure 4.6 where the molecular stretch rates are compared over the period of an interaction. The time is normalised to the period of the interaction. A symmetric function like a sinusoidal function will result and is depicted as

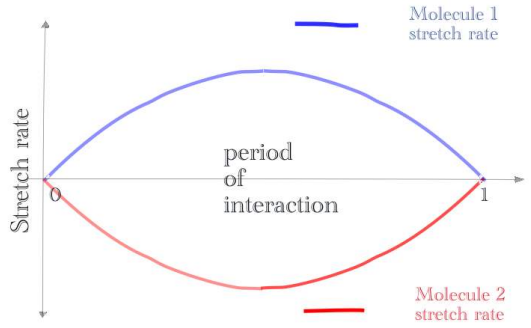

Figure 4.6: Stretch rates during the course of an interaction

such in Figure 4.6. It is not necessary for the stretch rate of each molecule to be zero before and after interaction. In this model, interaction consists of half a cycle. In the model, the stretch rates during the interaction are not considered. Only the stretch rates $\dot{\boldsymbol{R}}_i(t)$ and $\dot{\boldsymbol{R}}_i(t+T)$ before and after the interaction are considered.

Thus in a small change from the gas situation, an axis of symmetry is constructed between the pre-interaction velocity and the post-interaction ve-

locity. It is useful to visualise the problem by considering Figure 4.2 where the molecules are in contact. In exactly the same fashion as the geometry of molecular stretch, the molecular stretch rates (idealised as cylinders) can be viewed in 3D in Figure 4.7. However in Figure 4.7 the molecular stretch rates are viewed relative to molecule 1's stretch rate. The black cylinder is

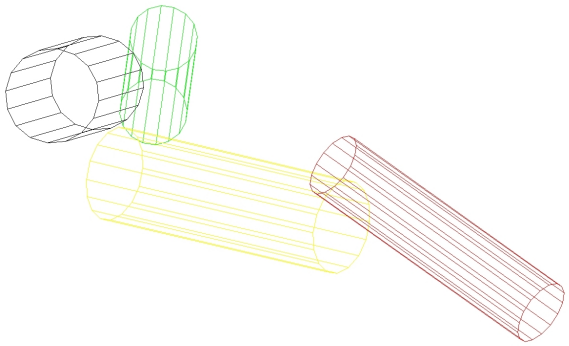

Figure 4.7: Molecular position in Eulerian co-ordinate system

the original orientation of molecule 1, the yellow cylinder is the final orientation of molecule 1, the green cylinder is the original orientation of molecule 2 and the red cylinder is the final orientation of molecule 2. Figure 4.7 is constructed in an global coordinate system.

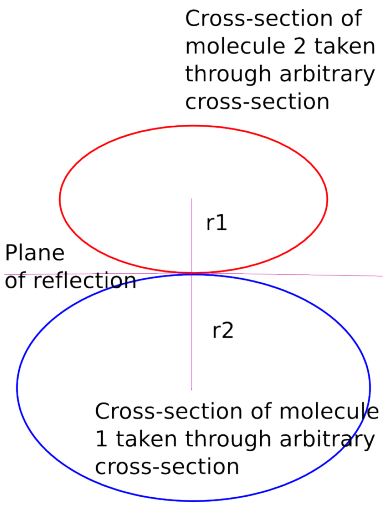

Figure 4.8: Cross-section of molecular interaction

One can take an arbitrary cross-section through molecules 1 and 2 along the axis of interaction. These cross-sections can be anticipated to be ellipses as depicted in Figure 4.8. In Figure 4.8, r_1 and r_2 represent the radii of

molecule 1 and 2 respectively. $b = r_1 + r_2$. The plane of reflection is defined as the plane with normal in direction b (which was $\boldsymbol{q}$ in the geometry of molecular stretch) where the plane passes through the tangents of the two molecule at the point at which they are in contact. In Figure 4.9 the

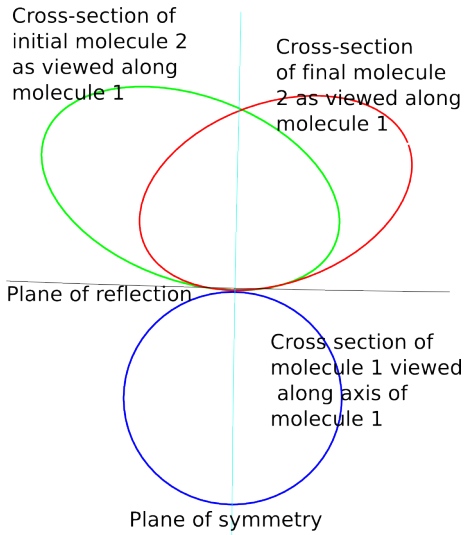

Figure 4.9: Cross-section along axis of molecule 1 (the x-axis)

red ellipse represents the post-interaction orientation of molecule 2. By constructing a coordinate system in which the xy-plane corresponds to the plane of reflection as defined above in Figure 4.8 and the x-axis is defined as the axis of molecule 1 then one can define the plane of symmetry as the plane with vectors $\boldsymbol{q}$ and the x-axis on the plane. This is depicted in Figure 4.9.

Figure 4.10 is similar to a diagram by Chapman and Cowling [18] except that only the initial ($\dot{\boldsymbol{R}}_{f12}$) and final relative stretch rates ($\dot{\boldsymbol{R}}'_{f12}$) are of relevance. $\mathbb{OP}$ represents the asymptote of initial relative stretch rate. Similarly $\mathbb{OQ}$ represents the asymptote of the final relative stretch rate. $\mathbb{OA}$ represents the axis of symmetry in the plane. In the diagram, $\boldsymbol{LMN}$ represents the potential relative stretch rate and b represents the displacement (perpendicular to the asymptote $\mathbb{OP}$) between the centers of the molecules as idealised in Figure 4.2. The angle χ represents the angle through which the stretch rate is reflected.

One can consider b to be the radius of the idealised polymer column of molecule 1 that lies perpendicular to the plane formed by $\mathbb{POQ}$. The long axis of the idealised polymer column lies at an angle into the plane defined by $\mathbb{POQ}$. Thus b represents an axis of an ellipse in the plane of $\mathbb{POQ}$. An

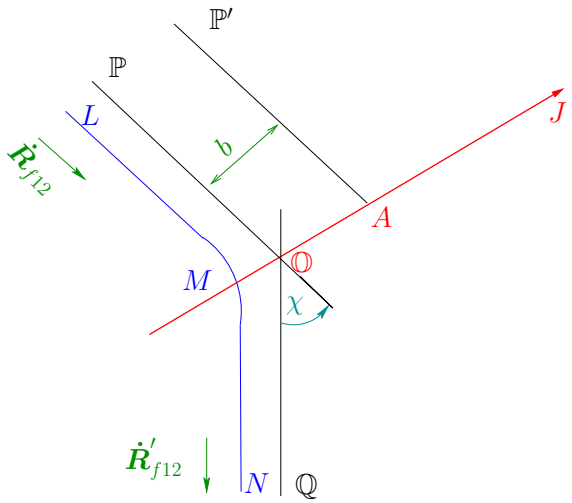

Figure 4.10: Relative stretch rate of molecule 1 relative to molecule 2

attempt is made to represent the above in Figure 4.11. In Figure 4.11 the plane $\mathbb{POQ}\boldsymbol{A}$ represents the same plane $\mathbb{POQ}\boldsymbol{A}$ in Figure 4.10 but the orientation of molecule 2 relative to the plane is also represented. The angle y in Figure 4.11 is the angle between the normal to plane $\mathbb{POQ}\boldsymbol{A}$ and the long axis of molecule 2.

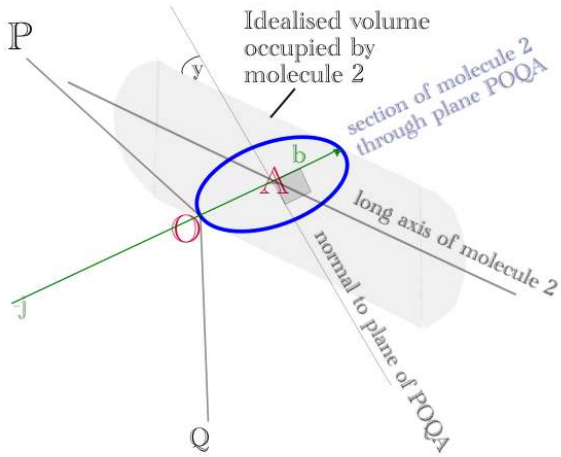

Figure 4.11: Stretch rate of molecule 1 relative to molecule 2 in 3D

A reflection of Figure 4.10 in a plane with normal OA will represent the

stretch rate of molecule 2 relative to molecule 1. Let $\boldsymbol{j} = \frac{\boldsymbol{J}}{|\boldsymbol{J}|}$; then

$$\dot{\boldsymbol{R}}_{f12} - \dot{\boldsymbol{R}}'_{f12} = 2(\dot{\boldsymbol{R}}_{f12} \cdot \boldsymbol{j})\boldsymbol{j} = -2(\dot{\boldsymbol{R}}'_{f12} \cdot \boldsymbol{j})\boldsymbol{j}, \tag{4.50}$$

$$\dot{\boldsymbol{R}}_{f21} - \dot{\boldsymbol{R}}'_{f21} = 2(\dot{\boldsymbol{R}}_{f21} \cdot \boldsymbol{j})\boldsymbol{j} = -2(\dot{\boldsymbol{R}}'_{f21} \cdot \boldsymbol{j})\boldsymbol{j}. \tag{4.51}$$

Substituting Equation (3.81) into Equations (4.27) to (4.30),

$$-\frac{\dot{\boldsymbol{R}}_{f1}}{2} = \boldsymbol{G} + M_2\dot{\boldsymbol{R}}_{\Delta 2}, \tag{4.52}$$

$$-\frac{\dot{\boldsymbol{R}}_{f2}}{2} = \boldsymbol{G} + M_1\dot{\boldsymbol{R}}_{\Delta 1}, \tag{4.53}$$

$$-\frac{\dot{\boldsymbol{R}}'_{f1}}{2} = \boldsymbol{G} + M_2\dot{\boldsymbol{R}}'_{\Delta 2}, \tag{4.54}$$

$$-\frac{\dot{\boldsymbol{R}}'_{f2}}{2} = \boldsymbol{G} + M_1\dot{\boldsymbol{R}}'_{\Delta 1}. \tag{4.55}$$

Substracting (4.54) from (4.52) then substituting $\dot{\boldsymbol{R}}_{\mu 1} \approx \dot{\boldsymbol{R}}'_{\mu 1}$ because of the infinitesimal contribution of one molecule to the average, and similarly subtracting (4.55) from (4.53),

$$\begin{aligned} -\frac{1}{2}\Big(\dot{\boldsymbol{R}}_{f1} - \dot{\boldsymbol{R}}'_{f1}\Big) &= M_2(\dot{\boldsymbol{R}}_{\Delta 2} - \dot{\boldsymbol{R}}'_{\Delta 2}) \\ &= M_2(\dot{\boldsymbol{R}}_{f2} - \dot{\boldsymbol{R}}'_{f2} + \dot{\boldsymbol{R}}_{\mu 2} - \dot{\boldsymbol{R}}'_{\mu 2}) \\ &= M_2(\dot{\boldsymbol{R}}_{f2} - \dot{\boldsymbol{R}}'_{f2}), \end{aligned} \tag{4.56}$$

$$\begin{aligned} -\frac{1}{2}\Big(\dot{\boldsymbol{R}}_{f2} - \dot{\boldsymbol{R}}'_{f2}\Big) &= M_1(\dot{\boldsymbol{R}}_{\Delta 1} - \dot{\boldsymbol{R}}'_{\Delta 1}) \\ &= M_1(\dot{\boldsymbol{R}}_{f1} - \dot{\boldsymbol{R}}'_{f1} + \dot{\boldsymbol{R}}_{\mu 1} - \dot{\boldsymbol{R}}'_{\mu 1}) \\ &= M_1(\dot{\boldsymbol{R}}_{f1} - \dot{\boldsymbol{R}}'_{f1}). \end{aligned} \tag{4.57}$$

From Equation (4.37),

$$\dot{\boldsymbol{R}}_{f1} = -\dot{\boldsymbol{R}}_{f2} \Longleftrightarrow 2\dot{\boldsymbol{R}}_{f1} = \dot{\boldsymbol{R}}_{f1} - \dot{\boldsymbol{R}}_{f2} \Longleftrightarrow \dot{\boldsymbol{R}}_{f1} = \frac{1}{2}\dot{\boldsymbol{R}}_{f12}. \tag{4.58}$$

Similarly

$$\dot{\boldsymbol{R}}_{f2} = \frac{1}{2}\dot{\boldsymbol{R}}_{f21}, \tag{4.59}$$

$$\dot{\boldsymbol{R}}'_{f1} = \frac{1}{2}\dot{\boldsymbol{R}}'_{f12}, \tag{4.60}$$

$$\dot{\boldsymbol{R}}_{f2} = \frac{1}{2}\dot{\boldsymbol{R}}'_{f21}. \tag{4.61}$$

Substituting Equations (4.58) and (4.60) into Equation (4.57) and similarly

substituting Equations (4.59) and (4.61) into Equation (4.56),

$$\dot{\boldsymbol{R}}'_{f1} - \dot{\boldsymbol{R}}_{f1} = M_2(\dot{\boldsymbol{R}}_{f21} - \dot{\boldsymbol{R}}'_{f21}), \tag{4.62}$$

$$\dot{\boldsymbol{R}}'_{f2} - \dot{\boldsymbol{R}}_{f2} = M_1(\dot{\boldsymbol{R}}_{f12} - \dot{\boldsymbol{R}}'_{f12}). \tag{4.63}$$

Finally, substituting Equation (4.62) into (4.50) and similarly substitutng (4.63) into (4.51),

$$\dot{\boldsymbol{R}}'_{f1} - \dot{\boldsymbol{R}}_{f1} = 2M_2(\dot{\boldsymbol{R}}'_{f21} \cdot \boldsymbol{j})\boldsymbol{j}, \tag{4.64}$$

$$\dot{\boldsymbol{R}}'_{f2} - \dot{\boldsymbol{R}}_{f2} = -2M_1(\dot{\boldsymbol{R}}'_{f21} \cdot \boldsymbol{j})\boldsymbol{j}. \tag{4.65}$$

4.4 The Jacobian for polymer chain interaction

The probable number of molecules of length in the range $d\boldsymbol{R}_{f1}$ about $\boldsymbol{R}_f$ and vector length stretch rate range $d\dot{\boldsymbol{R}}_f$ about $\dot{\boldsymbol{R}}_f$ (to be referred to as $(\boldsymbol{R}_f, \dot{\boldsymbol{R}}_f, d\boldsymbol{R}_{f1}, \dot{\boldsymbol{R}}_f)$) within a finite volume, δv, is equal to $p_1 d\boldsymbol{R}_{f1} d\dot{\boldsymbol{R}}_f d\boldsymbol{r}$ in a time interval dt.

In Figure 4.12, $d\varepsilon$ is an infinitesimal angle measured in radians and $\boldsymbol{b}$ is the smallest displacement from the idealised linear elastic molecule, in the radial direction, outside of which interaction can occur. This restriction can be considered to be due to a volume exclusion effect – the volume occupied by the length of the molecule in its 3D form which is not depicted in the ideal model but is in Figure 4.12. The maximum radial displacement in which molecular interaction can still occur is $b + db$. Given that in this model, the molecule is idealised as linear with end-to-end displacement of $\boldsymbol{R}_{f1}$, the volume in which molecule 2 must exist, is a cylinder as depicted in the Figure 4.12 – where only a segment of the cylinder represents the cylinder. The volume is given by the component of $\boldsymbol{R}_{f2}$ projected onto $\boldsymbol{R}_{f1}$ or $\boldsymbol{R}_{f1} \cdot \frac{\boldsymbol{R}_{f2}}{R_{f2}}$. The molecules within volume $\frac{\boldsymbol{R}_{f1} \cdot \boldsymbol{R}_{f2}}{R_{f2}} b db d\varepsilon$ have the potential to interact with molecule 1. Thus, per unit length of $\boldsymbol{R}_{f1}$, the volume in which a molecule must exist in order to interact with $\boldsymbol{R}_{f1}$ is $\frac{\boldsymbol{R}_{f1} \cdot \boldsymbol{R}_{f2}}{R_{f1} R_{f2}} b db d\varepsilon$ where $R_{f1} R_{f2}$ is the square of the geometric mean of $|\boldsymbol{R}_{f1}|$ and $|\boldsymbol{R}_{f2}|$.

The volume per unit length of this finite cylinder is given by

$$\delta V = \frac{\boldsymbol{R}_{f1} \cdot \boldsymbol{R}_{f2}}{R_{f1} R_{f2}} b \, d\varepsilon \, db.$$

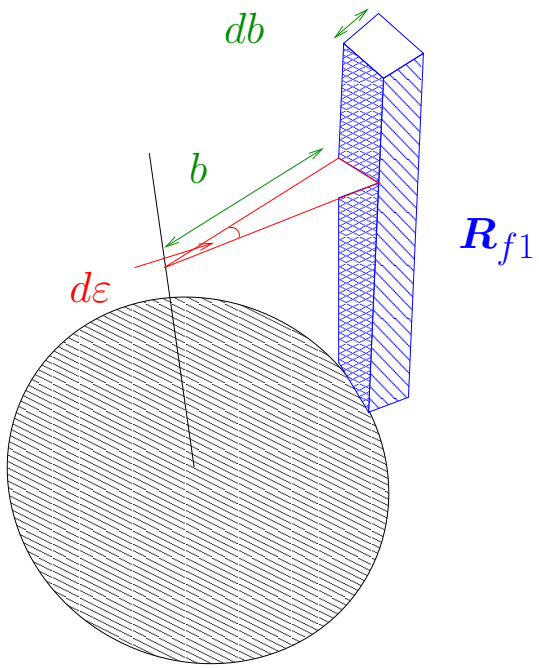

Figure 4.12: Visual representation of molecular interaction in 3D

The constant distance b can be considered the product of the constant rate at which the two molecules approach each other, a proportionality constant, a, and the constant period of interaction δt. Re-stated, b is due to the component of the rate at which the molecules approach each other in the direction of b or

$$a\dot{\boldsymbol{R}}_{f12} \cdot \frac{\boldsymbol{b}}{|\boldsymbol{b}|}\delta t = a\dot{\boldsymbol{R}}'_{f12} \cdot \frac{\boldsymbol{b}}{|\boldsymbol{b}|}dt = b$$

where δt and dt represent very small time increments. The rate at which the molecules approach each other ($\dot{\boldsymbol{R}}_{f12}$) is a constant because the molecules can only interact at the point of contact – van der Waal forces are ignored. Thus

$$b = a\dot{\boldsymbol{R}}'_{f12} \cdot \frac{\boldsymbol{b}}{|\boldsymbol{b}|}dt$$

where δt is the time interval over which the molecule can travel and still be within range of interaction. The incremental volume is

$$\delta V = a\frac{\boldsymbol{R}_{f1} \cdot \boldsymbol{R}_{f2}}{R_{f1}R_{f2}}dbd\varepsilon\dot{\boldsymbol{R}}_{f12} \cdot \frac{\boldsymbol{b}}{|\boldsymbol{b}|}dt = \boldsymbol{R}_{f1} \cdot \boldsymbol{R}_{f2}\dot{R}_{f12}a\cos(\phi)\,db\,d\varepsilon\,dt$$

where ϕ is the angle between $\dot{\boldsymbol{R}}_{f12}$ and $\boldsymbol{b}$.

If one assumes that each of the above incremental volumes, δV, consists of only one molecule of type 1 then the volume dV is the product of the

incremental volumes and the number of molecules which is

$$dV = \sum_{p_1 d\boldsymbol{R}_{f1} d\dot{\boldsymbol{R}}_{f1} d\boldsymbol{r}} \delta V = p_1 \frac{\boldsymbol{R}_{f1} \cdot \boldsymbol{R}_{f2}}{R_{f1} R_{f2}} \dot{R}_{f12} a \cos(\phi)\, db\, d\varepsilon\, d\boldsymbol{R}_{f1}\, d\dot{\boldsymbol{R}}_{f1}\, d\mathbf{r}\, dt.$$

Furthermore the number of encounters between molecules 1 and 2 is equal to $p_2 d\boldsymbol{R}_{f2}\, d\dot{\boldsymbol{R}}_{f2}\, dV$, which is equal to

$$p_1 p_2 \frac{\boldsymbol{R}_{f1} \cdot \boldsymbol{R}_{f2}}{R_{f1} R_{f2}} \dot{R}_{f12} a \cos(\phi) db\, d\varepsilon\, d\boldsymbol{R}_{f1}\, d\boldsymbol{R}_{f2}\, d\dot{\boldsymbol{R}}_{f1}\, d\dot{\boldsymbol{R}}_{f2}\, d\boldsymbol{r}\, dt.$$

As depicted in Figure 4.3, the locus of molecule 2's position (during the interaction) describes a path that lies on the surface of a sphere with radius R_f^g.

The above has all been expressed in cylindrical coordinates but could also be done in surface spherical co-ordinates. The construction of the spherical system is not obvious. Isolating the stretch components, it should be noted that the molecule is reflected in a plane with normal $\boldsymbol{k}$ passing through molecule 1. Construct a vector $\boldsymbol{q}$ such that $\boldsymbol{q}$ lies on the plane with normal $\boldsymbol{k}$ passing through molecule 1 to the point on molecule 2 with shortest $\boldsymbol{b}$. Both $\boldsymbol{R}_{f1}$ and $\boldsymbol{R}'_{f1}$ lie on the plane of reflection and b' is from the end of line b on $\boldsymbol{R}_{f2}$ to the intersection of $\boldsymbol{R}_{f1}$ and the plane of reflection. Let $\boldsymbol{k}$ be the $z-$ axis. Then the plane to which $\boldsymbol{k}$ is normal is the xy-plane. Let $\boldsymbol{R}$ be the vector from the origin of this co-ordinate system to the end of the molecule. Further let the angle between b and the xy plane be ε. Let the angle between $\boldsymbol{k}$ and $\boldsymbol{R}$ be ϖ as depicted in Figure 4.13. Figure 4.13 is an alternate representation of Figure 4.11. Then in surface spherical co-ordinates

$$d\boldsymbol{q} = \sin\varpi\, d\varpi\, d\varepsilon = \frac{\sin\varpi}{\frac{\partial b}{\partial \varpi}}\, d\varepsilon\, db. \tag{4.66}$$

But

$$a \frac{\boldsymbol{R}_{f1} \cdot \boldsymbol{R}_{f2}}{R_{f1} R_{f2}} \dot{R}_{f12}\, d\varepsilon\, d\boldsymbol{b} = q_{12} d\boldsymbol{q} \iff q_{12} = a \frac{\dot{R}_{f12} \frac{\boldsymbol{R}_{f2} \cdot \boldsymbol{R}_{f1}}{R_{f1} R_{f2}} [\frac{\partial b}{\partial \varpi}]}{\sin\varpi}.$$

Therefore the number of molecules leaving set $(\boldsymbol{r}, \boldsymbol{R}_{f1}, \boldsymbol{R}_{f2}, \dot{\boldsymbol{R}}_{f1}, \dot{\boldsymbol{R}}_{f2})$ is

$$p_1 p_2 q_{12}\, d\boldsymbol{q}\, d\boldsymbol{R}_{f1}\, d\boldsymbol{R}_{f2}\, d\dot{\boldsymbol{R}}_{f1}\, d\dot{\boldsymbol{R}}_{f2}\, d\boldsymbol{r}\, dt. \tag{4.67}$$

Equation (4.40) is used to show that $q_{21} = q_{12}$ and thereby establishes the symmetry of the interaction and the reverse interaction (where the reverse

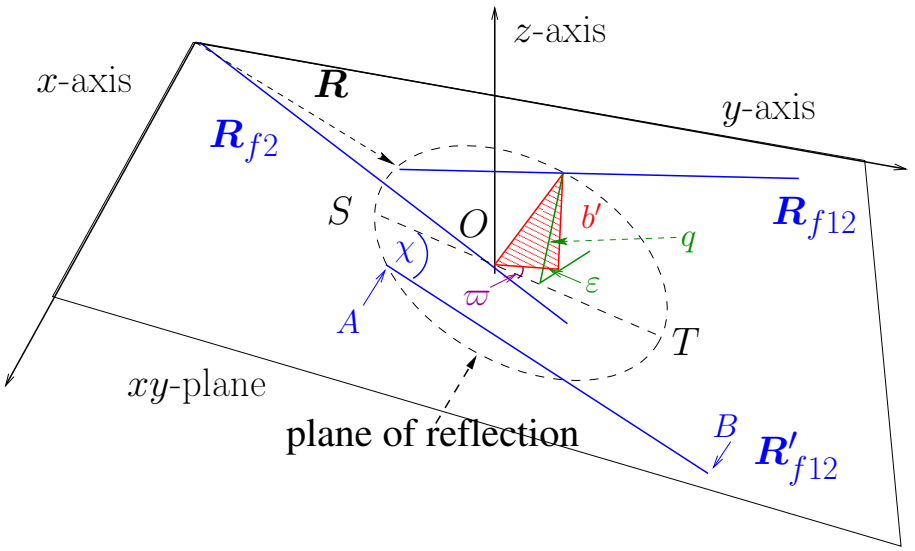

Figure 4.13: Molecular interaction in spherical co-ordinates

interaction is the interaction where molecule 1 approaches molecule 2). For the inverse molecular interaction (where the inverse molecular interaction is the interaction which would occur if the finals states returned to their initial states.) the number of molecules entering the set
$(\boldsymbol{r}, \boldsymbol{R}_{f1}, \boldsymbol{R}_{f2}, \dot{\boldsymbol{R}}_{f1}, \dot{\boldsymbol{R}}_{f2})$ is

$$\begin{aligned} & p_1' p_2' q_{21}\, d\boldsymbol{q}\, d\boldsymbol{R}'_{f1}\, d\boldsymbol{R}'_{f2}\, d\dot{\boldsymbol{R}}'_{f1}\, d\dot{\boldsymbol{R}}'_{f2}\, d\boldsymbol{r}\, dt \\ = \; & p_1' p_2' q_{12}\, d\boldsymbol{q}\, d\boldsymbol{R}'_{f1}\, d\boldsymbol{R}'_{f2}\, d\dot{\boldsymbol{R}}'_{f1}\, d\dot{\boldsymbol{R}}'_{f2}\, d\boldsymbol{r}\, dt. \end{aligned} \tag{4.68}$$

The change in the probability of finding a molecule in the given set in the time interval δt is given by the difference in the molecules entering and the molecules leaving the set.

In order to determine the above difference, the variables of integration need to be the same. It is therefore necessary to determine the Jacobian which relates $d\boldsymbol{R}'_{f1}\, d\boldsymbol{R}'_{f2}\, d\dot{\boldsymbol{R}}'_{f1}\, d\dot{\boldsymbol{R}}'_{f2}$ and $d\boldsymbol{R}_{f1}\, d\boldsymbol{R}_{f2}\, d\dot{\boldsymbol{R}}_{f1}\, d\dot{\boldsymbol{R}}_{f2}$ by

$$d\boldsymbol{R}'_{f1}\, d\boldsymbol{R}'_{f2}\, d\dot{\boldsymbol{R}}'_{f1}\, d\dot{\boldsymbol{R}}'_{f2} = [J] d\boldsymbol{R}_{f1}\, d\boldsymbol{R}_{f2}\, d\dot{\boldsymbol{R}}_{f1}\, d\dot{\boldsymbol{R}}_{f2} \tag{4.69}$$

where

$$J = \frac{\partial(\boldsymbol{R}'_{f1}, \boldsymbol{R}'_{f2}, d\dot{\boldsymbol{R}}'_{f1}, d\dot{\boldsymbol{R}}'_{f2})}{\partial(\boldsymbol{R}_{f1}, \boldsymbol{R}_{f2}, d\dot{\boldsymbol{R}}_{f1}, d\dot{\boldsymbol{R}}_{f2})}$$

which from Equations (4.48), (4.49) , (4.64) and (4.65) can only be linear

functions of K_1, K_2 , $\boldsymbol{k}$, M_1, M_2 and $\boldsymbol{j}$. However

$$J' = \frac{\partial(\boldsymbol{R}_{f1}, \boldsymbol{R}_{f2}, \dot{\boldsymbol{R}}_{f1}, \dot{\boldsymbol{R}}_{f2})}{\partial(\boldsymbol{R}'_{f1}, \boldsymbol{R}'_{f2}, \dot{\boldsymbol{R}}'_{f1}, \dot{\boldsymbol{R}}'_{f2})}$$

is the same function of K_1, K_2, $\boldsymbol{k}$, M_1, M_2 and $\boldsymbol{j}$ with only a change of sign. Since

$$JJ' = 1 \iff J = \pm 1. \tag{4.70}$$

Therefore

$$p'_1 p'_2 q_{12}\, d\boldsymbol{q}\, d\boldsymbol{R}'_{f1}\, d\boldsymbol{R}'_{f2}\, d\dot{\boldsymbol{R}}'_{f1}\, d\dot{\boldsymbol{R}}'_{f2}\, d\boldsymbol{r}\, dt$$

are the number of molecules entering the set. Consequently the molecular interaction term, which is the difference between molecules entering and leaving, is

$$\begin{aligned} \frac{\partial_e p_1}{\partial t} d\boldsymbol{R}_{f1}\, d\dot{\boldsymbol{R}}_{f1}\, d\boldsymbol{r}\, dt &= \int (p'_1 p'_2 - p_1 p_2) q_{12}\, d\boldsymbol{q}\, d\boldsymbol{R}_{f1}\, d\boldsymbol{R}_{f2}\, d\dot{\boldsymbol{R}}_{f1}\, d\dot{\boldsymbol{R}}_{f2}\, d\boldsymbol{r}\, dt \\ \frac{\partial_e p_1}{\partial t} &= \int (p'_1 p'_2 - p_1 p_2) q_{12}\, d\boldsymbol{q}\, d\boldsymbol{R}_{f2}\, d\dot{\boldsymbol{R}}_{f2} \end{aligned} \tag{4.71}$$

Thus Equation (3.85) together with Equation (4.71) describe the non-equilibrium molecular interaction at a mesoscopic level. The maximum entropy distribution for any particular molecular stretch and stretch rate is given by Equation (3.71).

4.5 Closing comments

All of the derivation may seem unnecessary given that internal forces (interaction within the molecule) are ignored and therefore kinetic and potential energy can be expected to be conserved independently during interaction. Nevertheless the mathematical approach – although complicated – is more rigorous.

It may also be argued that the selection of the time to complete half a cycle of periodic motion as a time-scale is arbitrary. However, molecular interactions are simply a series of such half cycles and thus the only rational choices are half a period or full period. Half a period is the more general selection.

Chapter 5

Macroscopic properties

This chapter defines the macroscopic properties that will be measured directly and be incorporated into the constitutive equation. It is the definition of these macroscopic properties in terms of the microscopic that associates the microscopic description with the observed macroscopic description.

5.1 The averaged mesoscopic properties

In order to recover the macroscopic equation, the macroscopic (or averaged) variables need to be defined. Consider Figure 5.1 where the surface dS rep-

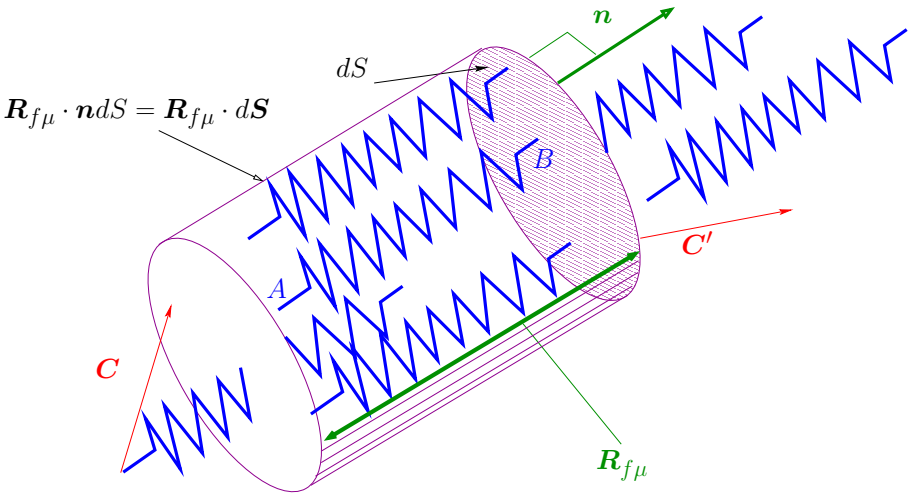

Figure 5.1: Pressure on an infinitesimal surface

resents the surface on which one wishes to determine the change in pressure. The pressure is a consequence of the force exerted by the individual molecules depicted in blue. Two components contribute to the force – a static component due to molecular stretch and a dynamic component due to stretch

rate. The force acting on the surface dS due to the static component, is the sum of the effects of the forces of all the molecules in contact with the surface. In an Eulerian coordinate system, the velocity of a molecule is the sum of the chain length rates of all the adjacent molecules in series. Thus in a short time interval dt it is assumed that the change in force due to a change in molecular stretch $\delta \boldsymbol{R}_\Delta = \dot{\boldsymbol{R}}_\Delta dt$ is neglible compared to the change in force due to the change in molecules acting on surface dS – a consequence of molecular velocity.

Consider molecules with vector length $\boldsymbol{R}_\Delta$, and range $d\boldsymbol{R}_\Delta$ – designated $\boldsymbol{R}_\Delta, d\boldsymbol{R}_\Delta$. Ignoring the effect of translation and stretch rate, at time t, for a molecule to be in contact with surface dS with normal $\boldsymbol{n}$, position A must exist within the volume $dS\boldsymbol{n} \cdot \boldsymbol{R}_\Delta \equiv (\boldsymbol{R}_f - \boldsymbol{R}_\mu) \cdot d\boldsymbol{S}$ where $\boldsymbol{n}dS = d\boldsymbol{S}$. In Figure 5.1 the large magenta cylinder represents the volume in which A must exist in order to result in a force on surface dS.

Combining translation but ignoring stretch rate; over a small time period, dt, for a molecule to be in contact with dS at $t+dt$, position A must be within the volume $d\boldsymbol{S} \cdot \boldsymbol{c}dt + d\boldsymbol{S} \cdot \boldsymbol{R}_\Delta - d\boldsymbol{S} \cdot \boldsymbol{c'}dt$, where $\boldsymbol{c'}$ is the velocity of the surface $d\boldsymbol{S}$ and $\boldsymbol{c}$ is the velocity of position A of the molecule. Incorporating stretch rate, the final position B of each molecule relative to A is given by

$$\boldsymbol{R}_\Delta(t+dt) = \boldsymbol{R}_\Delta(t) + \int_t^{t+dt} \dot{\boldsymbol{R}}_\Delta(\tau)d\tau$$

Therefore the volume, $d\grave{v}$, of molecules that will have contact with $d\boldsymbol{S}$ between time t and $t+dt$ is given by

$$\begin{aligned} d\grave{v} &= d\boldsymbol{S} \cdot (\boldsymbol{c} - \boldsymbol{c'})dt + d\boldsymbol{S} \cdot \boldsymbol{R}_\Delta + d\boldsymbol{S} \cdot (\dot{\boldsymbol{R}}_\Delta)dt \\ &= d\boldsymbol{S} \cdot (\boldsymbol{C'})dt + d\boldsymbol{S} \cdot \boldsymbol{R}_\Delta + d\boldsymbol{S} \cdot (\dot{\boldsymbol{R}}_\Delta)dt \end{aligned}$$

where $\boldsymbol{c} - \boldsymbol{c}' = \boldsymbol{C}'$. Let $\boldsymbol{c}_0$ be the mean velocity of the control volume. Let $\boldsymbol{c} - \boldsymbol{c}_0 = \boldsymbol{C}$ and $\boldsymbol{C}$ be called the perculiar velocity. Then $\boldsymbol{C}' = \boldsymbol{C} + \boldsymbol{c}_0 - \boldsymbol{c}'$. The volume containing molecules that are in contact with surface dS, at time t designated $d\acute{v}$ is given by

$$d\acute{v} = d\boldsymbol{S} \cdot \boldsymbol{R}_\Delta - d\boldsymbol{S} \cdot (\dot{\boldsymbol{R}}_\Delta)dt$$

Thus the volume of molecules not already in contact with dS that will be in

contact with dS during interval dt is given by

$$dv = d\grave{v} + d\acute{v} = d\boldsymbol{S} \cdot (\boldsymbol{C'})dt \tag{5.1}$$

As depicted in Figure 5.1, one can imagine a two-step procedure where a volume $d\boldsymbol{S} \cdot \boldsymbol{R}_\Delta$ translates a displacement $\boldsymbol{c}\delta t$ and then stretches. At the end of this translation (and stretching) the molecules span the surface dS.

Consider the particular chain length range $\boldsymbol{R}_\Delta, d\boldsymbol{R}_\Delta$. The number of molecules in the above chain length range, occupying the volume dv, is

$$N = p\, dv\, d\boldsymbol{R}_\Delta\, d\boldsymbol{C}. \tag{5.2}$$

Substituting (5.1) into (5.2), the number of molecules N that act across the surface dS is given by

$$\begin{aligned} N &= \int p\boldsymbol{C'} \cdot d\boldsymbol{S}\, d\boldsymbol{R}_\Delta\, d\boldsymbol{C}dt = \int p\boldsymbol{C'} \cdot \boldsymbol{n}dS\, d\boldsymbol{R}_\Delta\, d\boldsymbol{C}\, dt \\ &= \int pC'_n dS\, d\boldsymbol{R}_\Delta\, d\boldsymbol{C}dt \end{aligned} \tag{5.3}$$

where $C'_n = \boldsymbol{C'} \cdot \boldsymbol{n}$. The molecular density (ρ_n) or molecules per unit volume is determined from $N = \rho_n d\boldsymbol{r}$ where

$$\rho_n = \int p\, d\boldsymbol{R}_\Delta\, d\boldsymbol{C} = -\frac{1}{2}\int p\, d\boldsymbol{R}_f\, d\dot{\boldsymbol{R}}_f. \tag{5.4}$$

Equation (5.4) is due to $\boldsymbol{C} = \boldsymbol{c} - \boldsymbol{c}_0$ and the substitution of Equation (3.81),

$$\boldsymbol{C} = \frac{\Delta \boldsymbol{p}}{m} - \frac{1}{2}\dot{\boldsymbol{R}}_f - \boldsymbol{c}_0,$$

which allows the change of the variable of integration. Let m be the mass of a molecule. Then the density ρ is given by

$$\rho = \rho_n m. \tag{5.5}$$

Furthermore, if one allows the above N molecules to have a property $\phi(\boldsymbol{R}_\Delta, \boldsymbol{C})$, then the net transfer of that property across the surface dS in time interval dt is given by

$$p(\boldsymbol{R}_\Delta, \boldsymbol{C})\phi(\boldsymbol{R}_\Delta, \boldsymbol{C})C'_n\, dS\, d\boldsymbol{R}_\Delta\, d\boldsymbol{C}\, dt. \tag{5.6}$$

Let ϕ be a function of $\boldsymbol{r}, \boldsymbol{R}_\Delta, \boldsymbol{c}, t$. Then $\overline{\phi}$, at any given time t and range of

position $(\boldsymbol{r}, d\boldsymbol{r})$ can be defined as

$$\begin{aligned}\overline{\phi} &:= \frac{1}{\rho_n}\int p\phi\, d\boldsymbol{R}_\Delta\, d\boldsymbol{C} = -\frac{1}{2\rho_n}\int p\phi\, d\boldsymbol{R}_f\, d\dot{\boldsymbol{R}}_f \\ &= \frac{1}{N}\int p\phi\, d\boldsymbol{R}_\Delta\, d\boldsymbol{C}\, d\boldsymbol{r} = -\frac{1}{2N}\int p\phi\, d\boldsymbol{R}_f\, d\dot{\boldsymbol{R}}_f\, d\boldsymbol{r} \qquad (5.7)\end{aligned}$$

which can be interpreted as the average value of a function at a given location $\boldsymbol{r}, d\boldsymbol{r}$ at time t. Note that $d\boldsymbol{r}$ is in three dimensions and equates to the volume dv. Let $a^2 = \rho_n$.

Further, suppose that p like $p^{(ms)}$ in (3.71) is separable into components p_R and p_c and that likewise $\phi = \phi_R \times \phi_c$. Define

$$\overline{\phi}_R := \frac{1}{a}\int p_R\phi_R d\boldsymbol{R}_f \qquad (5.8)$$

and

$$\overline{\phi}_c := \frac{1}{a}\int p_c\phi_c d\boldsymbol{c}; \qquad (5.9)$$

then

$$\begin{aligned}\overline{\phi}_R \times \overline{\phi}_c &= \frac{1}{a}\int p_R\phi_R d\boldsymbol{R}_f \times \frac{1}{a}\int p_c\phi_c d\boldsymbol{c} \\ &= \frac{1}{a^2}\int\int p_R p_c \phi_R\phi_c d\boldsymbol{c} d\boldsymbol{R}_f = \frac{1}{\rho_n}\int p\phi d\boldsymbol{R}_f d\boldsymbol{c} = \overline{\phi}. \qquad (5.10)\end{aligned}$$

Thus (using definition (5.7)), for a fixed volume, (5.6) may be restated as

$$\rho_n dS\overline{C_n'\phi(\boldsymbol{R}_\Delta, \boldsymbol{C})}. \qquad (5.11)$$

If one defines (without new notation) $\overline{f(\boldsymbol{R}_\Delta)} = \int p_R(\boldsymbol{R}_\Delta)d\boldsymbol{R}_\Delta$ and $\overline{f(\boldsymbol{C})} = \int p_C(\boldsymbol{C})d\boldsymbol{C}$ where $p = p_R \times p_C$, then the expression (5.6) may be restated as

$$\rho_n dS\overline{C_n'\phi_C(\boldsymbol{C})} \times \overline{\phi_R(\boldsymbol{R}_\Delta)} \qquad (5.12)$$

if and only if $\phi(\boldsymbol{R}_\Delta, \boldsymbol{C}) = \phi_C(\boldsymbol{C}) \times \phi_R(\boldsymbol{R}_\Delta)$.

Under these conditions only, one can investigate two special cases. These special cases will be investigated because they correspond to the dynamic situation and the static situation respectively and simplify many results. The results of these special cases will be used in Section 5.3 to determine the conservation equations.

5.1.1 Special case of transported property $\overline{\phi_R(\boldsymbol{R}_\Delta)} = 1$

The first special case is $\overline{\phi_R(\boldsymbol{R}_\Delta)} = 1$. This case will be shown to correspond to the dynamic case. Given $C'_n = \boldsymbol{C}' \cdot \boldsymbol{n} = (\boldsymbol{C} + \boldsymbol{c}_0 - \boldsymbol{c}') \cdot \boldsymbol{n}$. For this case

$$\begin{aligned}
\rho_n dS\overline{C'_n \phi(\boldsymbol{R}_\Delta, \boldsymbol{C})} &= \rho_n dS\overline{C'_n \phi_C(\boldsymbol{C})} \times \overline{\phi_R(\boldsymbol{R}_\Delta)} = \rho_n dS\overline{C'_n \phi_C(\boldsymbol{C})} \\
&= \rho_n dS\boldsymbol{n} \cdot \overline{(\boldsymbol{C} + \boldsymbol{c}_0 - \boldsymbol{c}')\phi_C(\boldsymbol{C})} \\
&= \rho_n dS\boldsymbol{n} \cdot \overline{\boldsymbol{C}\phi_C(\boldsymbol{C})} + \rho_n dS\boldsymbol{n} \cdot \overline{(\boldsymbol{c}_0 - \boldsymbol{c}')\phi_C(\boldsymbol{C})} \\
&= \rho_n dS\boldsymbol{n} \cdot \overline{\boldsymbol{C}\phi_C(\boldsymbol{C})} + \rho_n dS\boldsymbol{n} \cdot (\boldsymbol{c}_0 - \boldsymbol{c}')\overline{\phi_C(\boldsymbol{C})} \qquad (5.13)
\end{aligned}$$

where the second term, as for the gas case, can be interpreted as the contribution to the rate of flow of ϕC due to the net relative movement of molecules across the surface dS. This is the flux vector. The first term results when the surface moves with the material. However when the surface moves with the end B of the molecule, $\boldsymbol{c}_0 - \boldsymbol{c}' = -\dot{\boldsymbol{R}}_\mu$ and

$$\rho_n dS\overline{C'_n \phi(\boldsymbol{R}_\Delta, \boldsymbol{C})} = \rho_n dS\boldsymbol{n} \cdot \overline{\boldsymbol{C}\phi_C(\boldsymbol{C})} - \rho_n dS\boldsymbol{n} \cdot (\dot{\boldsymbol{R}}_\mu)\overline{\phi_C(\boldsymbol{C})}. \qquad (5.14)$$

5.1.2 Special case of transported property $\overline{\phi_C(\boldsymbol{C})} = 1$

The second special case, is when $\overline{\phi_C(\boldsymbol{C})} = 1$ and will be shown to correspond to the static situation. For this case,

$$\begin{aligned}
\rho_n dS\overline{C'_n \phi(\boldsymbol{R}_\Delta, \boldsymbol{C})} &= \rho_n dS\overline{C'_n \phi_C(\boldsymbol{C})} \times \overline{\phi_R(\boldsymbol{R}_\Delta)} \\
&= \rho_n dS\boldsymbol{n} \cdot \overline{\boldsymbol{C} + \boldsymbol{c}_0 - \boldsymbol{c}'} \times \overline{\phi_R(\boldsymbol{R}_\Delta)} \\
&= \rho_n dS\boldsymbol{n} \cdot (\overline{\boldsymbol{c} - \boldsymbol{c}_0 + (\boldsymbol{c}_0 - \boldsymbol{c}')}) \times \overline{\phi_R(\boldsymbol{R}_\Delta)} \\
&= \rho_n dS\boldsymbol{n} \cdot \overline{(\boldsymbol{c} - \boldsymbol{c}')} \times \overline{\phi_R(\boldsymbol{R}_\Delta)} \qquad (5.15)
\end{aligned}$$

because $\boldsymbol{C} = \boldsymbol{c} - \boldsymbol{c}_0$. When the surface moves with end B of the molecule $\boldsymbol{c} + \dot{\boldsymbol{R}}_f = \boldsymbol{c}'$ and

$$\rho_n dS\overline{C'_n \phi(\boldsymbol{R}_\Delta, \boldsymbol{C})} = -\rho_n dS\boldsymbol{n} \cdot \overline{(\boldsymbol{R}_f) \times \phi_R(\boldsymbol{R}_\Delta)}. \qquad (5.16)$$

5.1.3 The dynamic pressure tensor

Consider the pressure vector $\mathbf{P}_{nD}$ (due to molecular velocity) acting normal to surface dS in Figure 5.1 and the pressure tensor (dynamic) $\mathbf{P}_D$, where $\mathbf{P}_{nD} = \mathbf{P}_D\boldsymbol{n}$. The total momentum imparted to surface element dS (recog-

nising that this is special case 1 as determined in section 5.1.1) is given by

$$\begin{aligned}\mathbf{P}_{nD}dSdt &= dSdt\Big[\int\limits_{+} C_n' m\boldsymbol{c}p(\boldsymbol{C})d\boldsymbol{C}\Big] - dSdt\Big[\int\limits_{-} -C_n' m\boldsymbol{c}p(\boldsymbol{C})d\boldsymbol{C}\Big] \\ &= dSdt\Big[\int C_n' m\boldsymbol{c}p(\boldsymbol{C})d\boldsymbol{C}\Big] \\ &= dSdt\cdot\rho_n m\overline{C_n'\boldsymbol{c}} \end{aligned} \tag{5.17}$$

where the + and − in the integral designate molecular direction. Therefore

$$\mathbf{P}_{nD} = \rho_n m\overline{C_n'\boldsymbol{c}} = \rho\overline{C_n'\boldsymbol{c}}, \tag{5.18}$$

as for gases [18].

The number of molecules impacting on the surface equals the number rebounding; thus

$$\begin{aligned} dSdt\int C_n' p(\boldsymbol{C})d\boldsymbol{C} &= dSdt\int\limits_{+} C_n' p(\boldsymbol{C})d\boldsymbol{C} \\ &- dSdt\int\limits_{-} -C_n' p(\boldsymbol{C})d\boldsymbol{C} = 0 \end{aligned} \tag{5.19}$$

which implies that $\overline{C_n'} = 0$, and consequently

$$\begin{aligned}\overline{C_n'\boldsymbol{c}} &= \overline{C_n'(\boldsymbol{c}_0+\boldsymbol{C})} = \overline{C_n'}\boldsymbol{c}_0 + \overline{C_n'\boldsymbol{C}} = \overline{(\boldsymbol{n}\cdot\boldsymbol{C}')\boldsymbol{C}} = \overline{(\boldsymbol{n}\cdot(\boldsymbol{c}-\boldsymbol{c}'))\boldsymbol{C}} \\ &= \overline{(\boldsymbol{n}\cdot(\boldsymbol{C}+\boldsymbol{c}_0-\boldsymbol{c}'))\boldsymbol{C}} = \overline{(\boldsymbol{n}\cdot\boldsymbol{C})\boldsymbol{C}} + \overline{(\boldsymbol{n}\cdot(\boldsymbol{c}_0-\boldsymbol{c}'))\boldsymbol{C}} \\ &= \boldsymbol{n}\cdot\overline{\boldsymbol{C}\boldsymbol{C}} + (\boldsymbol{n}\cdot(\boldsymbol{c}_0-\boldsymbol{c}'))\overline{\boldsymbol{C}} = \boldsymbol{n}\cdot\overline{\boldsymbol{C}\boldsymbol{C}} - (\boldsymbol{n}\cdot(\dot{\boldsymbol{R}}_f))\overline{\dot{\boldsymbol{R}}_f - \dot{\boldsymbol{R}}_\mu} \\ &= \boldsymbol{n}\cdot\overline{\boldsymbol{C}\boldsymbol{C}}. \end{aligned} \tag{5.20}$$

Substituting (5.20) into (5.18), we obtain

$$\mathbf{P}_D\boldsymbol{n} = \mathbf{P}_{nD} = \rho\boldsymbol{n}\cdot\overline{\boldsymbol{C}\boldsymbol{C}} \tag{5.21}$$

$$\Longleftrightarrow \qquad \mathbf{P}_D = \rho\overline{\boldsymbol{C}\boldsymbol{C}} \qquad \text{or} \qquad \mathbf{P}_D = -\frac{\rho}{2}\overline{\boldsymbol{C}\boldsymbol{C}} \tag{5.22}$$

after change of integration variable from $d\boldsymbol{c}$ to $-\frac{1}{2}d\dot{\boldsymbol{R}}_f$. The expression (5.22) will be called the dynamic pressure tensor and is used to calculate the change in pressure imparted to $d\boldsymbol{S}$ due to molecular stretch rate where the stretch rates are determined from the maximum entropy state.

Further, upon integration of Equation (3.81), recalling that $d\boldsymbol{r} = dv$ is an infinitesimal volume,

$$\begin{aligned}\boldsymbol{c}_0 &= \frac{1}{N}\int p\boldsymbol{c}\, d\boldsymbol{R}_f\, d\boldsymbol{c}\, d\boldsymbol{r} = \frac{1}{N}\int p\frac{\boldsymbol{\Delta p}}{m}\, d\boldsymbol{R}_f\, d\boldsymbol{c}\, d\boldsymbol{r} - \frac{1}{2N}\dot{\boldsymbol{R}}_f\, d\boldsymbol{R}_f\, d\boldsymbol{c}\, d\boldsymbol{r} \\ &= \frac{\overline{\boldsymbol{\Delta P}}}{m} - \frac{1}{2}\dot{\boldsymbol{R}}_\mu \end{aligned} \tag{5.23}$$

where $\overline{\boldsymbol{\Delta P}}/m$ is the average change in momentum per unit molecule. Substituting Equation (5.23) into Equation (5.22),

$$\begin{aligned}\mathbf{P}_D &= \overline{\rho\Big(\frac{\boldsymbol{\Delta p}}{m} - \frac{1}{2}\dot{\boldsymbol{R}}_f - \overline{\frac{\boldsymbol{\Delta p}}{m}} + \frac{1}{2}\dot{\boldsymbol{R}}_\mu\Big) \otimes \Big(\frac{\boldsymbol{\Delta p}}{m} - \frac{1}{2}\dot{\boldsymbol{R}}_f - \overline{\frac{\boldsymbol{\Delta p}}{m}} + \frac{1}{2}\dot{\boldsymbol{R}}_\mu\Big)} \\ &= \overline{\rho\Big(\frac{\boldsymbol{\Delta p}}{m} - \overline{\frac{\boldsymbol{\Delta p}}{m}} - \frac{1}{2}\dot{\boldsymbol{R}}_\Delta\Big) \otimes \Big(\frac{\boldsymbol{\Delta p}}{m} - \overline{\frac{\boldsymbol{\Delta p}}{m}} - \frac{1}{2}\dot{\boldsymbol{R}}_\Delta\Big)} = \rho\overline{\frac{1}{4}(\dot{\boldsymbol{R}}_\Delta) \otimes (\dot{\boldsymbol{R}}_\Delta)}\end{aligned}$$

is the dynamic pressure tensor which upon change of integration variable $d\boldsymbol{c}$ to $-\frac{1}{2}d\dot{\boldsymbol{R}}_f$

$$\mathbf{P}_D = -\frac{\rho}{8}\overline{\dot{\boldsymbol{R}}_\Delta \dot{\boldsymbol{R}}_\Delta} \iff \frac{\partial \mathbf{P}_D}{\partial t} = -\frac{1}{4}\overline{\ddot{\boldsymbol{R}}_\Delta \dot{\boldsymbol{R}}_\Delta} \tag{5.24}$$

and as before the dynamic pressure tensor is used to calculate the pressure acting on $d\boldsymbol{S}$ due to molecular stretch rate. The rate of change of dynamic pressure as determined above, will prove useful when determining the initial conditions for the discrete model in Chapter 11.

5.1.4 The static pressure tensor

Next, consider a second pressure vector due to the stretch of the molecules (static pressure), $\mathbf{P}_{nS}$, acting on surface dS in Figure 5.1 and the static pressure tensor, $\mathbf{P}_S$, where $\mathbf{P}_{nS} = \mathbf{P}_S\boldsymbol{n}$. Molecules acting in parallel are additive, while molecules acting in series, are more complicated. Inevitably all molecules are acting in series but at any instant only the pressure exerted by the molecule in contact with the surface is experienced. All the molecules acting on the surface act in parallel. Thus if one allows the sum of the individual elastic constants K in volume $C_n' dSdt$ to be κ where $\kappa = \rho K C_n' dSdt$, the change in force acting on the positive surface element, $d\mathbf{S}$ over dt at equilibrium (recognising that this is special case 2 of Section 5.1.2) is

$$\begin{aligned}\delta\mathbf{P}_{nS} dS_{(+)} &= -\rho dS_{(+)}\delta t\Big[\int C_n' K \boldsymbol{R}_f p(\boldsymbol{R}_\Delta) d\boldsymbol{R}_\Delta\Big] \\ &= -dS_{(+)}\delta t \cdot \rho_n K\overline{C_n'\boldsymbol{R}_f}.\end{aligned} \tag{5.25}$$

Similarly, the change in force acting on the negative surface over dt is

$$\begin{aligned}\delta\mathbf{P}_{nS}dS_{(-)} &= -\rho dS_{(-)}\delta t\Big[\int -C_n' K\boldsymbol{R}_f p(\boldsymbol{R}_\Delta)d\boldsymbol{R}_\Delta\Big] \\ &= dS_{(-)}\delta t\cdot\rho_n K\overline{C_n'\boldsymbol{R}_f} \qquad (5.26)\end{aligned}$$

and the resultant change in pressure over dt is given by

$$\begin{aligned}\delta\mathbf{P}_{nS}dS &= \Delta\mathbf{P}_{nS}dS_{(+)} - \Delta\mathbf{P}_{nS}dS_{(-)} \\ &= -dS_{(+)}\delta t\cdot\rho_n K\overline{C_n'\boldsymbol{R}_f} - dS_{(-)}\delta t\cdot\rho_n K\overline{C_n'\boldsymbol{R}_f} \\ &= -2dS\delta t\cdot\rho_n K\overline{C_n'\boldsymbol{R}_f}. \qquad (5.27)\end{aligned}$$

Therefore (given that $\kappa=\rho_n K$)

$$\begin{aligned}\lim_{\delta t\to 0}\frac{\delta\mathbf{P}_{nS}}{\delta t}=\frac{\partial\mathbf{P}_{nS}}{\partial t} &= -2\rho_n K\overline{C_n'\boldsymbol{R}_f} = -2\kappa\overline{\boldsymbol{n}\cdot(\boldsymbol{c}-\boldsymbol{c}')\boldsymbol{R}_f} \\ &= \kappa\boldsymbol{n}\cdot\overline{\dot{\boldsymbol{R}}_f\boldsymbol{R}_f} \\ \text{and}\qquad \mathbf{P}_{nS} &= \frac{1}{2}\kappa\boldsymbol{n}\cdot\overline{\boldsymbol{R}_f\boldsymbol{R}_f} = \mathbf{n}\cdot\mathbf{P}_S \qquad (5.28) \\ &= \frac{1}{2}\kappa\boldsymbol{n}\cdot\overline{(\boldsymbol{R}_\mu+\boldsymbol{R}_\Delta)(\boldsymbol{R}_\mu+\boldsymbol{R}_\Delta)} \\ &= \frac{1}{2}\kappa\boldsymbol{n}\cdot\overline{\boldsymbol{R}_\Delta\boldsymbol{R}_\Delta}+\kappa\boldsymbol{n}\cdot\overline{\boldsymbol{R}_\Delta\boldsymbol{R}_\mu}+\frac{1}{2}\kappa\boldsymbol{n}\cdot\overline{\boldsymbol{R}_\mu\boldsymbol{R}_\mu} \\ &= \frac{1}{2}\kappa\boldsymbol{n}\cdot\overline{\boldsymbol{R}_\Delta\boldsymbol{R}_\Delta}+\frac{1}{2}\kappa\boldsymbol{n}\cdot\overline{\boldsymbol{R}_\mu\boldsymbol{R}_\mu} \qquad (5.29)\end{aligned}$$

where

$$\begin{aligned}\mathbf{P}_S &= \frac{1}{2}\kappa\overline{\boldsymbol{R}_f\boldsymbol{R}_f} = \frac{1}{2}\kappa\overline{\boldsymbol{R}_\Delta\boldsymbol{R}_\Delta}+\frac{1}{2}\kappa\overline{\boldsymbol{R}_\mu\boldsymbol{R}_\mu} \qquad (5.30) \\ \text{and}\qquad \Delta\mathbf{P}_S &= \delta\mathbf{P}_S = \frac{1}{2}\kappa\overline{\boldsymbol{R}_\Delta\boldsymbol{R}_\Delta}\ \text{ or }\ -\frac{1}{4}\kappa\overline{\boldsymbol{R}_\Delta\boldsymbol{R}_\Delta}. \qquad (5.31)\end{aligned}$$

The latter result is due to $d\boldsymbol{C}=-1/2d\dot{\boldsymbol{R}}_f$ in the integration of $\overline{\phi_C(C)}$. Given that $\boldsymbol{R}_\mu$ remains constant over infinitesimal time period δt, by differentiating Equation (5.29) with respect to time one obtains

$$\frac{\partial\mathbf{P}_{nS}}{\partial t}=\kappa\boldsymbol{n}\cdot\overline{\dot{\boldsymbol{R}}_\Delta\boldsymbol{R}_\Delta}=\mathbf{n}\cdot\frac{\partial\mathbf{P}_S}{\partial t} \qquad (5.32)$$

where

$$\frac{\partial\mathbf{P}_S}{\partial t}=\kappa\overline{\dot{\boldsymbol{R}}_\Delta\boldsymbol{R}_\Delta}\qquad\text{or}\qquad-\frac{\kappa}{2}\overline{\dot{\boldsymbol{R}}_\Delta\boldsymbol{R}_\Delta},$$

depending on integration variable.

5.1.5 The measured stress

This section will define an entity designated measured or apparent stress (${}^{\langle app \rangle}\mathbf{T}$). The entity ${}^{\langle app \rangle}\mathbf{T}$ is distinct from nominal (based on initial surface configuration) and true stress (based on current surface configuration). The entity ${}^{\langle app \rangle}\mathbf{T}$ is the stress calculated by experimental testing rigs and can either be nominal or true. It is designated apparent, because it does not correspond to latent stress which will be defined in Chapter 7. Chapter 7 will also define material and specimen stress where material stress exists at a point and specimen stress is the material stress averaged over the specimen. Each of these can be either latent or apparent. Lastly, in this work, all stresses are true unless otherwise stated.

Given the definition of the dynamic pressure vector (5.17) and its formulation from the dynamic pressure tensor (5.21) and similarly the definition of the static pressure vector (5.27) with corresponding formulation from the static pressure tensor (5.30), it is apparent that the force per unit area exerted by the above molecules on surface dS is given by the sum of the static and dynamic pressure vectors. That is

$$\mathbf{P}_n = \mathbf{P}_D\mathbf{n} + \mathbf{P}_S\mathbf{n} = \mathbf{P}\mathbf{n} = \mathbf{P}_{nD} + \mathbf{P}_{nS} \tag{5.33}$$

where the tensor $\mathbf{P}$ is given by

$$\mathbf{P} = \mathbf{P}_D + \mathbf{P}_S. \tag{5.34}$$

For a surface dS at equilibrium, the pressure exerted by these molecules must be balanced by the applied force on the opposite surface – from which stress can be calculated.

Before defining the apparent (measured stress) one has to consider how stresses are determined experimentally. By convention, tensile testing instruments performing unixial tests on hyperelastic materials, calculate the stress by dividing the applied force by the current area. The current area is a consequence of the generally accepted assumption that rubbers are incompressible and that, therefore, during deformation the principal stretches satisfy

$$\lambda_1\lambda_2\lambda_3 = 1. \tag{5.35}$$

Thus the experimentally determined stress vector (${}^{\langle app \rangle}\mathbf{T} \cdot \mathbf{n}$ where ${}^{\langle app \rangle}\mathbf{T}$ is

the corresponding tensor) is defined by

$$^{\langle app\rangle}\mathbf{Tn} := \frac{\mathbf{F}}{A} = \frac{\mathbf{F}}{\lambda_2\lambda_3 A_0} = \lambda_1\frac{\mathbf{F}}{A} \tag{5.36}$$

where A_0 is the cross-sectional area of the undeformed surface upon which force $\mathbf{F}$ acts.

To emphasize, ($^{\langle app\rangle}\mathbf{T}$) will be referred to as the apparent or measured stress, it does not correspond to the latent material stress and this will be demonstrated in Chapter 7. Nevertheless at equilibrium

$$^{\langle app\rangle}\mathbf{Tn} + \mathbf{P}_n = 0 \qquad \Longleftrightarrow \qquad ^{\langle app\rangle}\mathbf{Tn} = -\mathbf{P}_n = -\mathbf{P}_{nD} - \mathbf{P}_{nS} \tag{5.37}$$

5.2 The change of transported molecular property – $\Delta\overline{\phi}$

The remainder of this chapter is concerned with the transport of the averaged molecular (microscopic) property ϕ where the description of the macroscopic (averaged) ϕ is designated $\overline{\phi}$. Consider the differential Equation (3.84) describing the change in the probability density. Let

$$\rho_n\Delta\overline{\phi} = \int \phi\frac{\partial_e p}{\partial t}\, d\boldsymbol{R}_f\, d\dot{\boldsymbol{R}}_f. \tag{5.38}$$

Then the term $\Delta\overline{\phi}$ requires interpretation. Here $\partial_e p/\partial t$ represents the rate of change of the number of molecules in the range $\boldsymbol{R}_f, d\boldsymbol{R}_f, \dot{\boldsymbol{R}}_f, d\dot{\boldsymbol{R}}_f$ due to the molecular interaction. So $\phi\,(\partial_e p/\partial t)\, d\boldsymbol{R}_f$ represents the rate of change of the $\sum_{i=1}^{N}\phi$ over all the molecules in the given range. Since $\sum_{i=1}^{N}\phi = N\overline{\phi}$, one can conclude that the rate of change of a transported property ϕ is

$$\frac{1}{\rho_n}\int \phi\frac{\partial_e p}{\partial t} d\boldsymbol{R}_f d\dot{\boldsymbol{R}}_f = \Delta\overline{\phi}. \tag{5.39}$$

From Equation (3.85) the rate of change of $\sum_{i=1}^{N}\phi$ is

$$\begin{aligned}\int \phi\frac{\partial_e p}{\partial t} d\boldsymbol{R}_f d\dot{\boldsymbol{R}}_f \;&=\; \int \phi\left[\frac{\partial p}{\partial t} - \frac{\dot{\boldsymbol{F}}}{K}\cdot\frac{\partial p}{\partial \boldsymbol{R}_f} + \left(\frac{\Delta\boldsymbol{p}}{m} - \frac{1}{2}\dot{\boldsymbol{R}}_f\right)\cdot\frac{\partial p}{\partial \boldsymbol{r}}\right] d\boldsymbol{R}_f d\dot{\boldsymbol{R}}_f \\ &+\; 2\int \phi\left[\frac{K}{m}\boldsymbol{R}_f - \left(\frac{\boldsymbol{F}}{m} + \frac{K}{m}\boldsymbol{R}_\mu\right)\right]\cdot\frac{\partial p}{\partial \dot{\boldsymbol{R}}_f} d\boldsymbol{R}_f d\dot{\boldsymbol{R}}_f. \end{aligned} \tag{5.40}$$

The terms on the right need to be evaluated further. Refer to Equation (5.40) as the transfer equation; the first term is given by

$$\begin{aligned}\int \phi\frac{\partial p}{\partial t}\,d\boldsymbol{R}_f d\dot{\boldsymbol{R}}_f &= \frac{\partial}{\partial t}\int \phi p\,d\boldsymbol{R}_f d\dot{\boldsymbol{R}}_f - \int \frac{\partial \phi}{\partial t} p\,d\boldsymbol{R}_f d\dot{\boldsymbol{R}}_f \\ &= \frac{\partial \rho_n \overline{\phi}}{\partial t} - \rho_n \overline{\frac{\partial \phi}{\partial t}}. \end{aligned} \tag{5.41}$$

In order to calculate the second term, consider the case where both ϕ and p are separable/multiplicative such that $\phi = \phi_R \times \phi_{\dot{R}}$ and $p = p_R \times p_{\dot{R}}$ respectively. Then integrating by parts and recognising that at the limits of integration ($R_{fx} = -\infty$ and $R_{fx} = \infty$) $\phi p \to 0$

$$\int \phi\frac{\partial p}{\partial \boldsymbol{R}_f} d\boldsymbol{R}_f d\dot{\boldsymbol{R}}_f = -\int p\frac{\partial \phi}{\partial R_{fx}} d\boldsymbol{R}_f d\dot{\boldsymbol{R}}_f = -\rho_n \overline{\frac{\partial \phi}{\partial \boldsymbol{R}_f}} \tag{5.42}$$

and consequently the second term reduces to

$$-\int \frac{\dot{\boldsymbol{F}}}{K}\cdot\phi\frac{\partial p}{\partial \boldsymbol{R}_f} d\boldsymbol{R}_f d\dot{\boldsymbol{R}}_f = \frac{\dot{\boldsymbol{F}}}{K}\cdot\rho_n \overline{\frac{\partial \phi}{\partial \boldsymbol{R}_f}}. \tag{5.43}$$

For the third term on the right hand side of the equation consider the x component

$$\begin{aligned}\int \phi\frac{\partial p}{\partial x}(\dot{R}_{fx}) d\boldsymbol{R}_f d\dot{\boldsymbol{R}}_f &= \frac{\partial}{\partial \boldsymbol{x}}\int \dot{R}_{fx}\phi p d\dot{R}_{fx} dR_f - \int \dot{R}_{fx} p\frac{\partial \phi}{\partial x} d\dot{R}_{fx} dR_f \\ &= +\frac{\partial \rho_n \overline{\phi \dot{R}_{fx}}}{\partial x} - \rho_n \overline{\dot{R}_{fx}\frac{\partial \phi}{\partial x}} \qquad \text{and} \end{aligned}$$

$$-\frac{1}{2}\int \phi\frac{\partial p}{\partial x}(\dot{R}_{fx}) d\boldsymbol{R}_f d\dot{\boldsymbol{R}}_f = -\frac{1}{2}\frac{\partial \rho_n \overline{\phi \dot{R}_{fx}}}{\partial x} + \frac{1}{2}\rho_n \overline{\dot{R}_{fx}\frac{\partial \phi}{\partial x}}. \tag{5.44}$$

Given that δt and the RVE are small – the latter is a consequence of the definition of the RVE requiring that properties are normally distributed – the rate of change of the change in momentum due to molecular interaction ($\Delta \boldsymbol{p}$) with respect to arbitrary variable $\boldsymbol{q}$ is negligible $\iff$ $\partial \Delta p/\partial \boldsymbol{q} = 0$ for the interval δt. The alternate interpretation is that only two scenarios exist. In the first, molecules do not interact and consequently the change in momentum is zero. The second scenario has molecular interaction which conserve momentum and thus $\Delta \boldsymbol{p} = 0$ over a collection of molecules. Consequently

$$\int \phi\frac{\Delta \boldsymbol{p}}{m}\cdot\frac{\partial p}{\partial \boldsymbol{r}} d\boldsymbol{R}_f d\dot{\boldsymbol{R}}_f = \frac{\partial}{\partial \boldsymbol{r}}\cdot\int \frac{\Delta \boldsymbol{p}}{m}\phi p d\boldsymbol{R}_f d\dot{\boldsymbol{R}}_f - \int p\frac{\Delta \boldsymbol{p}}{m}\cdot\frac{\partial \phi}{\partial \boldsymbol{r}} d\boldsymbol{R}_f d\dot{\boldsymbol{R}}_f$$

$$= \rho_n \frac{\partial}{\partial \boldsymbol{r}} \cdot \overline{\phi \frac{\Delta \boldsymbol{p}}{m}} - \rho_n \overline{\frac{\Delta \boldsymbol{p}}{m} \cdot \frac{\partial \phi}{\partial \boldsymbol{r}}}. \tag{5.45}$$

Furthermore

$$\begin{aligned} \phi(\frac{\Delta \boldsymbol{p}}{m} - \frac{1}{2}\dot{\boldsymbol{R}}_f)\frac{\partial p}{\partial \boldsymbol{r}} d\boldsymbol{R}_f d\dot{\boldsymbol{R}}_f &= \rho_n \frac{\partial}{\partial \boldsymbol{r}} \cdot (\overline{\phi \frac{\Delta \boldsymbol{p}}{m}}) - \rho_n \overline{\frac{\Delta \boldsymbol{p}}{m} \cdot \frac{\partial \phi}{\partial \boldsymbol{r}}} \\ &\quad -\frac{1}{2}\rho_n \overline{\nabla \cdot \phi \dot{\boldsymbol{R}}_f} + \frac{1}{2}\rho_n \overline{\dot{\boldsymbol{R}}_f \cdot \frac{\partial \phi}{\partial \boldsymbol{r}}}. \end{aligned} \tag{5.46}$$

Finally the fourth term will be considered in two parts: first, integrating by parts and recognising that at the limits of integration ($\dot{\boldsymbol{R}}_f = -\infty$ and $\dot{\boldsymbol{R}}_f = \infty$, $\phi p \to 0$)

$$\int \phi \frac{\partial p}{\partial \dot{\boldsymbol{R}}_f} d\boldsymbol{R}_f d\dot{\boldsymbol{R}}_f = -\int p \frac{\partial \phi}{\partial \dot{\boldsymbol{R}}_f} d\boldsymbol{R}_f d\dot{\boldsymbol{R}}_f = -\rho_n \overline{\frac{\partial \phi}{\partial \dot{\boldsymbol{R}}_f}}. \tag{5.47}$$

Therefore

$$-\int \Big(\frac{\boldsymbol{F}}{m} + \frac{K}{m}\boldsymbol{R}_\mu\Big) \cdot \phi \frac{\partial p}{\partial \dot{\boldsymbol{R}}_f} d\boldsymbol{R}_f d\dot{\boldsymbol{R}}_f = +\Big(\frac{\boldsymbol{F}}{m} + \frac{K}{m}\boldsymbol{R}_\mu\Big) \cdot \rho_n \overline{\frac{\partial \phi}{\partial \dot{\boldsymbol{R}}_f}}. \tag{5.48}$$

Secondly, considering the x-component of $\int \phi \frac{K}{m}\boldsymbol{R}_f \cdot \frac{\partial p}{\partial \dot{\boldsymbol{R}}_f} d\boldsymbol{R}_f d\dot{\boldsymbol{R}}_f$, integrating by parts

$$\begin{aligned} &\int\int \phi \frac{K}{m} R_{fx} \frac{\partial p}{\partial \dot{R}_{fx}} d\boldsymbol{R}_f d\dot{\boldsymbol{R}}_f = \frac{K}{m}\int\int \phi R_{fx} \frac{\partial p}{\partial \dot{R}_{fx}} d\boldsymbol{R}_f d\dot{\boldsymbol{R}}_f \\ &= +\frac{K}{m}\int \phi \boldsymbol{R}_f p|_{\dot{R}_{fx}=-\infty}^{\dot{R}_{fx}=\infty} d\dot{R}_{fy} d\dot{R}_{fz} d\boldsymbol{R}_f - \frac{K}{m}\int p \frac{\partial \phi}{\partial \dot{R}_{fx}} R_{fx} d\boldsymbol{R}_f d\dot{\boldsymbol{R}}_f. \end{aligned}$$

Because $\boldsymbol{R}_f$ is not a function of $\dot{\boldsymbol{R}}_f$, the first term is zero and thus combining all three directions,

$$\int\int \phi \frac{K}{m} R_{fx} \frac{\partial p}{\partial \dot{R}_{fx}} d\boldsymbol{R}_f d\dot{\boldsymbol{R}}_f = -\frac{K}{m}\rho_n \overline{\boldsymbol{R}_f \cdot \frac{\partial \phi}{\partial \dot{\boldsymbol{R}}_f}}. \tag{5.49}$$

Consequently the fourth term reduces to

$$\begin{aligned} 2\int \Big(\frac{K}{m}\boldsymbol{R}_f &- (\frac{\boldsymbol{F}}{m} + \frac{K}{m}\boldsymbol{R}_\mu)\Big) \cdot \frac{\partial p}{\partial \dot{\boldsymbol{R}}_f} d\boldsymbol{R}_f d\dot{\boldsymbol{R}}_f \\ &= -2\frac{K}{m}\rho_n \overline{\boldsymbol{R}_f \cdot \frac{\partial \phi}{\partial \dot{\boldsymbol{R}}_f}} + 2\rho_n \Big(\frac{\boldsymbol{F}}{m} + \frac{K}{m}\boldsymbol{R}_\mu\Big) \cdot \overline{\frac{\partial \phi}{\partial \dot{\boldsymbol{R}}_f}}. \end{aligned} \tag{5.50}$$

Substituting (5.41), (5.43), (5.44), 5.50) and (3.83) into (5.40), one obtains

$$\begin{aligned}\int \phi \frac{\partial_e p}{\partial t} d\boldsymbol{R}_f d\dot{\boldsymbol{R}}_f &= \frac{\partial \rho_n \overline{\phi}}{\partial t} - \sum_{q\in x,y,z} \frac{1}{2} \frac{\partial \rho_n \overline{\phi \dot{R}_{fq}}}{\partial \boldsymbol{q}} - \rho_n \Big(\overline{\frac{\partial \phi}{\partial t}} - \sum_{q\in x,y,z} \frac{1}{2} \overline{\dot{R}_{fq} \frac{\partial \phi}{\partial q}} \\ &\quad + \sum_{q\in x,y,z} \overline{-\frac{\dot{\boldsymbol{F}}}{K} \frac{\partial \phi}{\partial R_{fq}}} + \sum_{q\in x,y,z} \overline{\frac{\Delta P_q}{m} \frac{\partial \phi}{\partial r_q}} - \sum_{q\in x,y,z} \overline{\frac{\partial \phi \frac{\Delta P_q}{m}}{\partial r_q}} \\ &\quad -2 \sum_{q\in x,y,z} (\frac{F_q}{m} + \frac{K}{m} R_{\mu q}) \overline{\frac{\partial \phi}{\partial \dot{R}_{fq}}} + 2 \frac{K}{m} \sum_{q\in x,y,z} \overline{R_{fq} \frac{\partial \phi}{\partial \dot{R}_{fq}}} \Big) \\ &= \frac{\partial \rho_n \overline{\phi}}{\partial t} - \frac{1}{2} \frac{\partial}{\partial \boldsymbol{r}} \cdot \rho_n \overline{\phi \dot{\boldsymbol{R}}_f} - \rho_n \Big(\overline{\frac{\partial \phi}{\partial t}} - \frac{1}{2} \overline{\dot{\boldsymbol{R}}_f \cdot \frac{\partial \phi}{\partial \boldsymbol{r}}} \\ &\quad + \overline{\dot{\boldsymbol{R}}_f \cdot \frac{\partial \phi}{\partial \boldsymbol{R}_f}} + \overline{\frac{\Delta \boldsymbol{P}}{m} \cdot \frac{\partial \phi}{\partial \boldsymbol{r}}} - \frac{\partial}{\partial \boldsymbol{r}} \cdot \Big(\overline{\phi \frac{\Delta \boldsymbol{P}}{m}} \Big) \\ &\quad -2 (\frac{\boldsymbol{F}}{m} + \frac{K}{m} \boldsymbol{R}_\mu) \cdot \overline{\frac{\partial \phi}{\partial \dot{\boldsymbol{R}}_f}} + 2 \frac{K}{m} \overline{\boldsymbol{R}_f \cdot \frac{\partial \phi}{\partial \dot{\boldsymbol{R}}_f}} \Big). \end{aligned} \tag{5.51}$$

Instead of expressing the above in terms of the $\boldsymbol{r}, \boldsymbol{R}_f$ and t; it is expressed in terms of the perculiar vector lengths $\boldsymbol{R}_\Delta = \boldsymbol{R}_f - \boldsymbol{R}_\mu$ and the perculiar stretch rate $\dot{\boldsymbol{R}}_\Delta = \dot{\boldsymbol{R}}_f - \dot{\boldsymbol{R}}_\mu$. Given that $\boldsymbol{R}_\Delta$ is a function of $\boldsymbol{r}$ and t and that $\boldsymbol{R}_f$ and $\dot{\boldsymbol{R}}_f$ are independent variables; application of the chain rule replaces $\partial\phi/\partial \boldsymbol{R}_f$ with $\partial\phi/\partial \boldsymbol{R}_\Delta$ and $\partial\phi/\partial \dot{\boldsymbol{R}}_f$ with $\partial\phi/\partial \dot{\boldsymbol{R}}_\Delta$. Applying the chain rule to $\partial\phi/\partial t$,

$$\frac{\partial \phi}{\partial t} + \frac{\partial \phi}{\partial \boldsymbol{R}_\Delta} \cdot \frac{\partial \boldsymbol{R}_\Delta}{\partial t} + \frac{\partial \phi}{\partial \dot{\boldsymbol{R}}_\Delta} \cdot \frac{\partial \dot{\boldsymbol{R}}_\Delta}{\partial t} = \frac{\partial \phi}{\partial t} - \frac{\partial \phi}{\partial \boldsymbol{R}_\Delta} \cdot \frac{\partial \boldsymbol{R}_\mu}{\partial t} - \frac{\partial \phi}{\partial \dot{\boldsymbol{R}}_\Delta} \frac{\partial \dot{\boldsymbol{R}}_\mu}{\partial t}.$$

Similarly $\partial\phi/\partial x$ should be replaced by

$$\frac{\partial \phi}{\partial x} - \frac{\partial \phi}{\partial \boldsymbol{R}_\Delta} \cdot \frac{\partial \boldsymbol{R}_\mu}{\partial x} - \frac{\partial \phi}{\partial \dot{\boldsymbol{R}}_\Delta} \cdot \frac{\partial \dot{\boldsymbol{R}}_\mu}{\partial x}$$

and $\dot{\boldsymbol{R}}_f \cdot \partial\phi/\partial \boldsymbol{r}$ is replaced by

$$\begin{aligned} &\dot{\boldsymbol{R}}_{\boldsymbol{f}} \cdot \frac{\partial \phi}{\partial \boldsymbol{r}} - \frac{\partial \phi}{\partial \dot{\boldsymbol{R}}_\Delta} \cdot \sum_{q\in x,y,z} \dot{R}_{fq} \frac{\partial \dot{R}_{\mu q}}{\partial \boldsymbol{r}} - \frac{\partial \phi}{\partial \boldsymbol{R}_\Delta} \cdot \sum_{q\in x,y,z} \dot{R}_{fq} \frac{\partial R_{\mu x}}{\partial \boldsymbol{r}} \\ = \; &\dot{\boldsymbol{R}}_{\boldsymbol{f}} \cdot \frac{\partial \phi}{\partial \boldsymbol{r}} - \frac{\partial \phi}{\partial \dot{\boldsymbol{R}}_\Delta} \cdot \Big(\dot{\boldsymbol{R}}_f \cdot \frac{\partial}{\partial \boldsymbol{r}} \Big) \dot{\boldsymbol{R}}_\mu - \frac{\partial \phi}{\partial \boldsymbol{R}_\Delta} \cdot \Big(\dot{\boldsymbol{R}}_f \cdot \frac{\partial}{\partial \boldsymbol{r}} \Big) \boldsymbol{R}_\mu. \end{aligned}$$

Given that mean values are not affected by the change of variable,

$$\int \phi \frac{\partial_e p}{\partial t} d\boldsymbol{R}_f d\dot{\boldsymbol{R}}_f = \frac{\partial \rho_n \overline{\phi}}{\partial t} - \frac{1}{2} \frac{\partial}{\partial \boldsymbol{r}} \cdot \rho_n \overline{\phi (\dot{\boldsymbol{R}}_\mu + \dot{\boldsymbol{R}}_\Delta)}$$

$$
\begin{aligned}
&-\rho_n\Big(\overline{\frac{\partial\phi}{\partial t}}-\overline{\frac{\partial\phi}{\partial \boldsymbol{R}_\Delta}}\cdot\frac{\partial \boldsymbol{R}_\mu}{\partial t}-\overline{\frac{\partial\phi}{\partial \dot{\boldsymbol{R}}_\Delta}}\cdot\frac{\partial \dot{\boldsymbol{R}}_\mu}{\partial t}\\
&-\frac{1}{2}\overline{(\dot{\boldsymbol{R}}_\mu+\dot{\boldsymbol{R}}_\Delta)\cdot\frac{\partial\phi}{\partial \boldsymbol{r}}}+\frac{1}{2}\overline{\frac{\partial\phi}{\partial \dot{\boldsymbol{R}}_\Delta}\cdot\Big[(\dot{\boldsymbol{R}}_\Delta+\dot{\boldsymbol{R}}_\mu)\cdot\frac{\partial}{\partial \boldsymbol{r}}\Big]}\dot{\boldsymbol{R}}_\mu\\
&+\frac{1}{2}\overline{\frac{\partial\phi}{\partial \boldsymbol{R}_\Delta}\cdot\Big[(\dot{\boldsymbol{R}}_\Delta+\dot{\boldsymbol{R}}_\mu)\cdot\frac{\partial}{\partial \boldsymbol{r}}\Big]}\boldsymbol{R}_\mu\\
&-\overline{(\frac{\dot{\boldsymbol{F}}}{K})\cdot\frac{\partial\phi}{\partial \boldsymbol{R}_\Delta}}+\overline{\frac{\Delta\boldsymbol{p}}{m}\cdot\frac{\partial\phi}{\partial \boldsymbol{r}}}-\overline{\frac{\Delta\boldsymbol{p}}{m}\cdot\frac{\partial\phi}{\partial \boldsymbol{R}_\Delta}}\cdot\frac{\partial \boldsymbol{R}_\mu}{\partial \boldsymbol{r}}\\
&-\overline{\frac{\Delta\boldsymbol{p}}{m}\cdot\frac{\partial\phi}{\partial \dot{\boldsymbol{R}}_\Delta}}\cdot\frac{\partial \dot{\boldsymbol{R}}_\mu}{\partial \boldsymbol{r}}-\frac{\partial}{\partial \boldsymbol{r}}\cdot\overline{\phi\frac{\Delta\boldsymbol{p}}{m}}\\
&-2(\frac{\boldsymbol{F}}{m}+\frac{K}{m}\boldsymbol{R}_\mu)\cdot\overline{\frac{\partial\phi}{\partial \dot{\boldsymbol{R}}_\Delta}}+2\frac{K}{m}\overline{(\boldsymbol{R}_\Delta+\boldsymbol{R}_\mu)\cdot\frac{\partial\phi}{\partial \dot{\boldsymbol{R}}_\Delta}}\Big)
\end{aligned}
$$

Substituting the following definition – given that $\boldsymbol{c}_0=-\dot{\boldsymbol{R}}_\mu/2$ from (3.81) –

$$\frac{D}{Dt}:=\frac{\partial}{\partial t}+\boldsymbol{c}\cdot\frac{\partial}{\partial \boldsymbol{r}}=\frac{\partial}{\partial t}-\Big(\frac{\dot{\boldsymbol{R}}_\mu}{2}\Big)\cdot\frac{\partial}{\partial \boldsymbol{r}} \tag{5.52}$$

for the 'mobile operator' or convective derivative following motion,

$$
\begin{aligned}
\int\phi\frac{\partial_e p}{\partial t}d\boldsymbol{R}_f d\dot{\boldsymbol{R}}_f \;=\;&\frac{D\rho_n\overline{\phi}}{Dt}-\rho_n\overline{\phi}\frac{\partial}{\partial \boldsymbol{r}}\cdot\frac{\dot{\boldsymbol{R}}_\mu}{2}-\frac{1}{2}\frac{\partial}{\partial \boldsymbol{r}}\cdot\rho_n\overline{\phi\dot{\boldsymbol{R}}_\Delta}\\
&-\rho_n\Bigg(\overline{\frac{D\phi}{Dt}}-2\Big(\overline{\frac{\boldsymbol{F}}{m}-\frac{K\boldsymbol{R}_\Delta}{m}-\frac{D\frac{1}{2}\dot{\boldsymbol{R}}_\mu}{Dt}}\Big)\cdot\overline{\frac{\partial\phi}{\partial \dot{\boldsymbol{R}}_\Delta}}\\
&-\Big(\frac{D\boldsymbol{R}_\mu}{Dt}\Big)\cdot\overline{\frac{\partial\phi}{\partial \boldsymbol{R}_\Delta}}-\overline{(\frac{\dot{\boldsymbol{F}}}{K})\cdot\frac{\partial\phi}{\partial \boldsymbol{R}_\Delta}}-\nabla\cdot\overline{\frac{\phi\Delta\boldsymbol{p}}{m}}\\
&+\overline{\Big(\frac{\Delta\boldsymbol{p}}{m}-\frac{1}{2}\dot{\boldsymbol{R}}_\Delta\Big)\cdot\frac{\partial\phi}{\partial \boldsymbol{r}}}-\overline{\frac{\partial\phi}{\partial \dot{\boldsymbol{R}}_\Delta}\cdot(\frac{\Delta\boldsymbol{p}}{m}-\frac{1}{2}\dot{\boldsymbol{R}}_\Delta)\cdot\frac{\partial}{\partial \boldsymbol{r}}\dot{\boldsymbol{R}}_\mu}\\
&-\overline{\frac{\partial\phi}{\partial \boldsymbol{R}_\Delta}\cdot(\frac{\Delta\boldsymbol{p}}{m}-\frac{1}{2}\dot{\boldsymbol{R}}_\Delta)\cdot\frac{\partial}{\partial \boldsymbol{r}}\boldsymbol{R}_\mu}\Bigg)=\rho_n\Delta\overline{\phi}
\end{aligned}
$$

which further reduces to

$$
\begin{aligned}
\int\phi\frac{\partial_e p}{\partial t}d\boldsymbol{R}_f d\dot{\boldsymbol{R}}_f \;=\;&\frac{D\rho_n\overline{\phi}}{Dt}-\rho_n\overline{\phi}\frac{\partial}{\partial \boldsymbol{r}}\cdot\frac{\dot{\boldsymbol{R}}_\mu}{2}+\frac{\partial}{\partial \boldsymbol{r}}\cdot\rho_n\overline{\phi\boldsymbol{Q}}\\
-\;&\rho_n\Bigg(\overline{\frac{D\phi}{Dt}}-2\Big(\frac{\boldsymbol{F}}{m}-\frac{D\frac{\dot{\boldsymbol{R}}_\mu}{2}}{Dt}\Big)\cdot\overline{\frac{\partial\phi}{\partial \dot{\boldsymbol{R}}_\Delta}}+2\overline{\frac{K}{m}(\boldsymbol{R}_\Delta)\cdot\frac{\partial\phi}{\partial \dot{\boldsymbol{R}}_\Delta}}\\
+\;&\overline{\boldsymbol{Q}\cdot\frac{\partial\phi}{\partial \boldsymbol{r}}}-\overline{\frac{\partial\phi}{\partial \dot{\boldsymbol{R}}_\Delta}\cdot(\boldsymbol{Q}\cdot\frac{\partial}{\partial \boldsymbol{r}})\dot{\boldsymbol{R}}_\mu}-\overline{\frac{\partial\phi}{\partial \boldsymbol{R}_\Delta}\cdot(\boldsymbol{Q}\cdot\frac{\partial}{\partial \boldsymbol{r}})\boldsymbol{R}_\mu}\\
-\;&\frac{D\boldsymbol{R}_\mu}{Dt}\cdot\overline{\frac{\partial\phi}{\partial \boldsymbol{R}_\Delta}}-\overline{\frac{\dot{\boldsymbol{F}}}{K}\cdot\frac{\partial\phi}{\partial \boldsymbol{R}_\Delta}}\Bigg)=\rho_n\Delta\overline{\phi}
\end{aligned}
\tag{5.53}
$$

where $\boldsymbol{Q} = \frac{\Delta \boldsymbol{p}}{m} - \frac{1}{2}\dot{\boldsymbol{R}}_\Delta = (\frac{\Delta \boldsymbol{p}}{m} - \frac{1}{2}\dot{\boldsymbol{R}}_f) + \frac{1}{2}\dot{\boldsymbol{R}}_\mu = \boldsymbol{c} - \boldsymbol{c}_0 = \boldsymbol{C}$ and $\overline{\boldsymbol{Q}} = \overline{\frac{\Delta \boldsymbol{p}}{m}} - \frac{1}{2}\overline{\dot{\boldsymbol{R}}_\Delta}$. For non-interacting molecules, no change in $\Delta \boldsymbol{p}$ exists and for interacting molecules the effect on the one molecule is cancelled by the other. Therefore $\overline{\boldsymbol{Q}} = 0$ and

$$\begin{aligned}
\int \phi \frac{\partial_e p}{\partial t} d\boldsymbol{R}_f d\dot{\boldsymbol{R}}_f &= \frac{D\rho_n \overline{\phi}}{Dt} - \rho_n \overline{\phi} \frac{\partial}{\partial \boldsymbol{r}} \cdot \frac{\dot{\boldsymbol{R}}_\mu}{2} + \frac{\partial}{\partial \boldsymbol{r}} \cdot \rho_n \overline{\phi \boldsymbol{C}} \\
&- \rho_n \Bigg(\overline{\frac{D\phi}{Dt}} - 2\Big(\frac{\boldsymbol{F}}{m} - \frac{D\frac{\dot{\boldsymbol{R}}_\mu}{2}}{Dt}\Big) \cdot \overline{\frac{\partial \phi}{\partial \dot{\boldsymbol{R}}_\Delta}} + 2\overline{\frac{K}{m}(\boldsymbol{R}_\Delta) \cdot \frac{\partial \phi}{\partial \dot{\boldsymbol{R}}_\Delta}} \\
&+ \overline{\boldsymbol{C} \cdot \frac{\partial \phi}{\partial \boldsymbol{r}}} - \overline{\frac{\partial \phi}{\partial \dot{\boldsymbol{R}}_\Delta} \boldsymbol{C}} : \frac{\partial}{\partial \boldsymbol{r}} \dot{\boldsymbol{R}}_\mu - \overline{\frac{\partial \phi}{\partial \boldsymbol{R}_\Delta} \boldsymbol{C}} : \frac{\partial}{\partial \boldsymbol{r}} \boldsymbol{R}_\mu \\
&- \frac{D\boldsymbol{R}_\mu}{Dt} \cdot \overline{\frac{\partial \phi}{\partial \boldsymbol{R}_\Delta}} - \overline{\frac{\dot{\boldsymbol{F}}}{K} \cdot \frac{\partial \phi}{\partial \boldsymbol{R}_\Delta}} \Bigg) = \rho_n \Delta \overline{\phi} \qquad (5.54)
\end{aligned}$$

where for symmetric tensors $\boldsymbol{A}$ and $\boldsymbol{B}$, $\boldsymbol{A} : \boldsymbol{B}$ is the scalar product.

Making the same substitutions into the differential equation (3.84) allows the mathematical description of the molecular interaction to be restated as

$$\begin{aligned}
\frac{\partial_e p}{\partial t} &= \frac{Dp}{Dt} - 2\left(\frac{\boldsymbol{F}}{m} - \frac{1}{2}\frac{D\dot{\boldsymbol{R}}_\mu}{Dt}\right) \cdot \frac{\partial p}{\partial \dot{\boldsymbol{R}}_\Delta} - \frac{D\boldsymbol{R}_\mu}{Dt} \cdot \frac{\partial p}{\partial \boldsymbol{R}_\Delta} \\
&- (\frac{\dot{\boldsymbol{F}}}{K}) \cdot \frac{\partial p}{\partial \boldsymbol{R}_\Delta} + \boldsymbol{Q} \cdot \frac{\partial p}{\partial \boldsymbol{r}} + 2\frac{K}{m}\boldsymbol{R}_\Delta \cdot \frac{\partial p}{\partial \dot{\boldsymbol{R}}_\Delta} \\
&- \frac{\partial p}{\partial \dot{\boldsymbol{R}}_\Delta} \cdot (\boldsymbol{Q} \cdot \frac{\partial}{\partial \boldsymbol{r}}) \dot{\boldsymbol{R}}_\mu - \frac{\partial p}{\partial \boldsymbol{R}_\Delta} \cdot (\boldsymbol{Q} \cdot \frac{\partial}{\partial \boldsymbol{r}}) \boldsymbol{R}_\mu. \qquad (5.55)
\end{aligned}$$

5.3 Special cases of transported property – $\Delta\overline{\phi}$

The special cases are investigated next. Note that because of the fashion, in which these are constructed, kinetic and potential energy are conserved separately. The conservation of elasticity is an unconventional concept. It is simply a statement that the elastic properties of a chain are independent of the stretch state.

5.3.1 Case I: $\phi_1 = m$, conservation of mass

If $\phi = m$ then $\overline{\phi} = m$. Also $\frac{\partial \phi}{\partial \boldsymbol{R}_\Delta} = 0$, $\frac{\partial \phi}{\partial \dot{\boldsymbol{R}}_\Delta} = 0$. Furthermore $\frac{D\phi}{Dt} = 0$, $\frac{\partial \phi}{\partial \boldsymbol{r}} = 0$, $\overline{\phi \boldsymbol{Q}} = 0$ and finally $\Delta\overline{\phi} = 0$. Substituting these results into Equation (5.53),

the result obtained is

$$\int \phi_1 \frac{\partial_e p}{\partial t} d\boldsymbol{R}_f d\dot{\boldsymbol{R}}_f = \frac{D\rho_n m}{Dt} - \rho_n m \frac{\partial}{\partial \boldsymbol{r}} \cdot \left(\frac{1}{2}\dot{\boldsymbol{R}}_\mu\right) = 0 \tag{5.56}$$

or since $\rho_n m = \rho$,

$$\int \phi_1 \frac{\partial_e p}{\partial t} d\boldsymbol{R}_f d\dot{\boldsymbol{R}}_f = \frac{D\rho}{Dt} - \rho \frac{\partial}{\partial \boldsymbol{r}} \cdot \left(\frac{1}{2}\dot{\boldsymbol{R}}_\mu\right) = 0 \tag{5.57}$$

which is the conservation of mass equation.

5.3.2 Case II: $\phi_2 = K$, conservation of elasticity

If $\phi = K$ then $\overline{\phi} = K$. Also $\frac{\partial \phi}{\partial \boldsymbol{R}_\Delta} = 0$, $\frac{\partial \phi}{\partial \dot{\boldsymbol{R}}_\Delta} = 0$. Furthermore $\frac{D\phi}{Dt} = 0$, $\frac{\partial \phi}{\partial \boldsymbol{r}} = 0$, $\overline{\phi \boldsymbol{Q}} = 0$ and finally $\Delta\overline{\phi} = 0$. Substituting these results into Equation (5.53), the result obtained is

$$\int \phi_2 \frac{\partial_e p}{\partial t} d\boldsymbol{R}_f d\dot{\boldsymbol{R}}_f = \frac{D\rho_n K}{Dt} - \rho_n K \frac{\partial}{\partial \boldsymbol{r}} \cdot \left(\frac{1}{2}\dot{\boldsymbol{R}}_\mu\right) = 0 \tag{5.58}$$

or since $\rho_n K = \kappa$,

$$\int \phi_2 \frac{\partial_e p}{\partial t} d\boldsymbol{R}_f d\dot{\boldsymbol{R}}_f = \frac{D\kappa}{Dt} - \kappa \frac{\partial}{\partial \boldsymbol{r}} \cdot \left(\frac{1}{2}\dot{\boldsymbol{R}}_\mu\right) = 0 \tag{5.59}$$

which is the conservation of elastic constant equation.

Next consider the force or strain stored in each molecule. The idea is unconventional but it is simply a variant of conservation of momentum.

5.3.3 Case III: $\phi_3 = K\boldsymbol{R}_\Delta \Longleftrightarrow \phi_R \times \phi_{\dot{R}} = K\boldsymbol{R}_\Delta \times 1$, conservation of force due to stretch

This result is a consequence of the force due to molecular stretch ($K\boldsymbol{R}_\Delta$) being conserved during molecular interaction. This result was a requirement of the model in Section 4.1.

For the case, $\phi = KR_{\Delta x}$, $\overline{\phi} = 0$, $\frac{D\phi}{Dt} = 0$, $\frac{\partial \phi}{\partial \boldsymbol{R}_\Delta} = (K, 0, 0)$, $\frac{\partial \phi}{\partial \boldsymbol{r}} = 0$, $\overline{\frac{\partial \phi}{\partial \boldsymbol{R}_\Delta}\boldsymbol{Q}} = 0$, $\overline{\phi \boldsymbol{Q}} = K\overline{\boldsymbol{R}_\Delta \boldsymbol{Q}} = K\overline{\boldsymbol{R}_\Delta(\frac{\boldsymbol{\Delta p}}{m} - \frac{1}{2}\dot{\boldsymbol{R}}_\Delta)} = -\frac{1}{2}K\overline{\boldsymbol{R}_\Delta \dot{\boldsymbol{R}}_\Delta}$ which is the special case 2 of Equation (5.16) which, from Equation (5.29), equals $-\frac{1}{2}\frac{\partial_t \mathbf{P}_S}{\rho_n}$. $\frac{\partial \phi}{\partial \dot{\boldsymbol{R}}_\Delta} = 0$, $\overline{K\dot{\boldsymbol{R}}_\Delta} = 0$ and $\Delta\overline{\phi} = 0$ because of the manner in which the model

is constructed. Consequently, substituting these results into (5.53),

$$\int \phi_{3x} \frac{\partial_e p}{\partial t} d\boldsymbol{R}_f d\dot{\boldsymbol{R}}_f = -\frac{1}{2}\frac{\partial}{\partial \boldsymbol{r}} \cdot \partial_t \mathbf{P}_S + \kappa\Big(\frac{D\boldsymbol{R}_\mu}{Dt}\Big) + \frac{\kappa}{K}\dot{\boldsymbol{F}} = 0. \tag{5.60}$$

5.3.4 Case IV: $\phi_4 = m\boldsymbol{C} = m(\frac{\Delta \boldsymbol{p}}{m} - \frac{1}{2}\dot{\boldsymbol{R}}_\Delta)$, conservation of momentum due to stretch rate

For the case $\boldsymbol{\phi} = m\boldsymbol{C}$, $\overline{\phi} = 0$, $\frac{D\phi}{Dt} = 0$, $\frac{\partial \phi}{\partial \dot{\boldsymbol{R}}_\Delta} = (-\frac{1}{2}m, 0, 0)$, $\frac{\partial \phi}{\partial \boldsymbol{R}_\Delta} = 0$, $\overline{R_\Delta} = 0$, $\frac{\partial \phi}{\partial \boldsymbol{r}} = 0$, $\rho_n \overline{\boldsymbol{\phi Q}} = \rho_n m \overline{\boldsymbol{CC}} = -2\mathbf{P}_D$ and $\Delta\overline{\phi} = 0$, where $\rho_n m = \rho$ then

$$\int \phi_4 \frac{\partial_e p}{\partial t} d\boldsymbol{R}_f d\dot{\boldsymbol{R}}_f = -2\frac{\partial}{\partial \boldsymbol{r}} \cdot \mathbf{P}_D + \frac{\rho}{2}\frac{D\dot{\boldsymbol{R}}_\mu}{Dt} - \rho\frac{\boldsymbol{F}}{m} = 0 \tag{5.61}$$

The integral of case III with respect to time and case IV can be summed (in several ways) to give case V.

5.3.5 Case V $\phi_5 = \int_t^{t'} K\boldsymbol{R}_\Delta d\tau - \frac{1}{2}m\dot{\boldsymbol{R}}_\Delta$, conservation of momentum

The selection of the above means of summation is justified by noting that the change in molecular momentum due to dynamic pressure is given by Equation (5.61). The change in molecular momentum due to static pressure is given by $\int_t^{t'} \boldsymbol{F} d\tau$ where $\boldsymbol{F}$ is the force applied to the molecule. The force applied by a molecule is given by $-K\boldsymbol{R}_\Delta$. Consequently, the force ($\boldsymbol{F}$) applied to the molecule must be $\boldsymbol{F} = K\boldsymbol{R}_\Delta$ and thus the change in momentum due to the static pressure is given by $\int_t^{t'} K\boldsymbol{R}_\Delta d\tau$ and the combined momentum change is given by $\phi_5 = \int_t^{t'} K\boldsymbol{R}_\Delta d\tau - \frac{1}{2}m\dot{\boldsymbol{R}}_\Delta$. Substituting ϕ_5 into (5.53) as before,

$$\begin{aligned}\int \phi_{5x} \frac{\partial_e p}{\partial t} d\boldsymbol{R}_f d\dot{\boldsymbol{R}}_f \;=\; & -\frac{\partial}{\partial \boldsymbol{r}} \cdot (2\mathbf{P}_S|_t^{t'} + \frac{1}{2}\mathbf{P}_D|_t^{t'}) + \kappa \Delta \boldsymbol{R}_\mu|_t^{t'} - \frac{\kappa}{4}\nabla \boldsymbol{R}_\mu^2|_t^{t'} \\ & + \frac{\rho}{2}\frac{D\dot{\boldsymbol{R}}_\mu}{Dt}|_t^{t'} + \frac{\kappa}{K}\int_t^{t'} \dot{\boldsymbol{F}} d\tau - \rho\frac{\boldsymbol{F}}{m}|_t^{t'}.\end{aligned} \tag{5.62}$$

One has the choice of defining the reference time as $t = 0$ where 0 is an arbitrary time in the past at which the specimen is in ground state and t' is defined relative to 0 but in general (at time t'), a molecule's history is not known and therefore t' is not known. The alternative is to define the reference time as $t' = \infty$ where ∞ is approximated by a time in the future at which the specimen is in ground state.

An alternate summation is given by $\phi_5 = 2\int_t^{t'} K\boldsymbol{R}_\Delta d\tau - \frac{1}{4}m\dot{\boldsymbol{R}}_\Delta$

$$\begin{aligned}\int \phi_{5x}\frac{\partial_e p}{\partial t}d\boldsymbol{R}_f d\dot{\boldsymbol{R}}_f &= -\frac{\partial}{\partial \boldsymbol{r}}\cdot(\mathbf{P}_S+\mathbf{P}_D)|_t^{t'} + 2\kappa\Delta\boldsymbol{R}_\mu|_t^{t'} - \frac{\kappa}{2}\nabla\boldsymbol{R}_\mu^2|_t^{t'} \\ &\quad + \frac{\rho}{4}\frac{D\dot{\boldsymbol{R}}_\mu}{Dt}|_t^{t'} + \frac{2\kappa}{K}\int_t^{t'}\dot{\boldsymbol{F}}d\tau - \frac{\rho}{2}\frac{\boldsymbol{F}}{m}|_t^{t'}. \end{aligned} \tag{5.63}$$

The latter formulation is justified because $\mathbf{P}_S + \mathbf{P}_D$ is directly measurable and corresponds to the contribution of the hydrostatic terms $\mathbf{P}_S + \mathbf{P}_D$ to the apparent material stress tensor ${}^{\langle app\rangle}\mathbf{T}$ which was the subject of Section (5.1.5).

5.3.6 Case VI: $\phi_6 = \frac{K}{2}R_\Delta^2 \Longleftrightarrow \phi = \phi_R \times \phi_{\dot{R}_\Delta} = \frac{K}{2}R_\Delta^2 \times 1$, conservation of potential energy

For the sixth case, $\phi = \frac{K}{2}R_\Delta^2$, $\overline{\phi} = \frac{1}{2}kT(\lambda^2-3)$ per chain from Equation (3.40). $\rho_n\overline{\phi\boldsymbol{C}} = \boldsymbol{\Psi}$ is the flux of potential energy which is similar to the flux of kinetic energy to follow and should be considered in conjunction with Equation (5.13), $\frac{D\phi}{Dt} = 0$, $\frac{D\phi}{D\dot{\boldsymbol{R}}_\Delta} = 0$, $\frac{D\phi}{Dt} = K\boldsymbol{R}_\Delta \Longrightarrow \overline{\frac{D\phi}{Dt}} = 0$, $\frac{\partial\phi}{\partial\mathbf{r}} = 0$, $\frac{\partial\phi}{\partial\boldsymbol{R}_\Delta} = K\boldsymbol{R}_\Delta$ consequently $\overline{\frac{\partial\phi}{\partial\boldsymbol{R}_\Delta}} = 0$ and $\rho_n\overline{\frac{\partial\phi}{\partial\boldsymbol{R}_\Delta}\boldsymbol{C}} = -\frac{\kappa}{2}\overline{\dot{\boldsymbol{R}}_\Delta\boldsymbol{R}_\Delta} = -\frac{1}{2}\partial_t\mathbf{P}_S$. Finally $\Delta\overline{\phi} = 0$.

Substituting the above into Equation (5.53),

$$\begin{aligned}\int \phi_6\frac{\partial_e p}{\partial t}d\boldsymbol{R}_f d\dot{\boldsymbol{R}}_f &= \frac{D\left(\frac{1}{2}\rho_n k\mathrm{T}(\lambda^2-3)\right)}{Dt} - \frac{1}{2}\rho_n k\mathrm{T}(\lambda^2-3)\frac{\partial}{\partial\mathbf{r}}\cdot\frac{\dot{\boldsymbol{R}}_\mu}{2} \\ &\quad + \frac{\partial}{\partial\mathbf{r}}\cdot\boldsymbol{\Psi} + \rho_n\overline{\frac{\partial\phi}{\partial\boldsymbol{R}_\Delta}\cdot(\boldsymbol{C}\cdot\frac{\partial}{\partial\mathbf{r}})\boldsymbol{R}_\mu} \\ &= \frac{D\left(\frac{1}{2}\rho_n k\mathrm{T}(\lambda^2-3)\right)}{Dt} - \frac{1}{2}\rho_n k\mathrm{T}(\lambda^2-3)\frac{\partial}{\partial\mathbf{r}}\cdot\frac{\dot{\boldsymbol{R}}_\mu}{2} \\ &\quad + \frac{\partial}{\partial\mathbf{r}}\cdot\boldsymbol{\Psi} + \rho_n K\overline{\boldsymbol{R}_\Delta\boldsymbol{C}}:\frac{\partial}{\partial\mathbf{r}}\boldsymbol{R}_\mu \\ &= \frac{D\left(\frac{1}{2}\rho_n k\mathrm{T}(\lambda^2-3)\right)}{Dt} - \frac{1}{2}\rho_n k\mathrm{T}(\lambda^2-3)\frac{\partial}{\partial\mathbf{r}}\cdot\frac{\dot{\boldsymbol{R}}_\mu}{2} \\ &\quad + \frac{\partial}{\partial\mathbf{r}}\cdot\boldsymbol{\Psi} - \frac{1}{2}\partial_t\mathbf{P}_S:\frac{\partial}{\partial\mathbf{r}}\boldsymbol{R}_\mu \end{aligned} \tag{5.64}$$

after the substitution of Equation (5.56).

5.3.7 Case VII: $\phi_7 = \frac{m}{2}C^2$, conservation of kinetic energy

From Equation (3.78),

$$\begin{aligned} \frac{K}{m}\boldsymbol{R}_\Delta &= \frac{\boldsymbol{F}}{m} - \frac{\partial \boldsymbol{c}}{\partial t} = \frac{\boldsymbol{F}}{m} - \frac{\partial \boldsymbol{C}}{\partial t} - \frac{\partial \boldsymbol{c}_0}{\partial t} \\ \overline{\frac{K}{m}\boldsymbol{R}_\Delta \cdot \boldsymbol{C}} &= \frac{\boldsymbol{F}}{m}\cdot\overline{\boldsymbol{C}} - \overline{\frac{\partial \boldsymbol{C}}{\partial t}\cdot\boldsymbol{C}} - \frac{\partial \boldsymbol{c}_0}{\partial t}\cdot\overline{\boldsymbol{C}} \\ &= -\overline{\frac{\partial \boldsymbol{C}}{\partial t}\cdot\boldsymbol{C}} = -\frac{1}{2}\frac{\partial}{\partial t}\overline{C^2} \\ \overline{K\boldsymbol{R}_\Delta \cdot \boldsymbol{C}} &= -\frac{\partial}{\partial t}\overline{\frac{1}{2}mC^2} \end{aligned} \quad \Longleftrightarrow \quad \Longleftrightarrow \tag{5.65}$$

Equation (3.78) was used in order to introduce an independent equation. This would not have been the case had equation (3.80) been used. Before completing the calculations, $0.5\partial\overline{mC^2}/\partial t$ needs to be interpreted.

As in Section 5.3.7, (5.65) is the kinetic energy. This kinetic energy is not known. Let it be assumed that it is the same as for the gas case. Then

$$\begin{aligned} \overline{W_K} = \overline{\frac{1}{2}mC^2} &= \frac{3}{2}k\mathrm{T} = \frac{N}{2}k\mathrm{T} \\ \Longleftrightarrow \overline{K\boldsymbol{R}_\Delta \cdot \boldsymbol{C}} &= -\frac{\partial}{\partial t}\overline{\frac{1}{2}mC^2} = -\frac{\partial}{\partial t}\frac{3}{2}k\mathrm{T} = -\frac{\partial}{\partial t}\frac{3}{2}k\mathrm{T}. \end{aligned} \tag{5.66}$$

Thus the transported property in (5.53) is given by $\phi = \frac{m}{2}C^2$ and from equation (5.66), $\overline{\phi} = \frac{1}{2}Nk\mathrm{T}$, $\rho\overline{\phi\boldsymbol{C}} = \boldsymbol{q}$ the kinetic energy flux tensor as for gases. Given that ϕ is only a function of independent variables m and $\boldsymbol{C}$ only, $\frac{D\phi}{Dt} = 0$, $\frac{\partial\phi}{\partial\dot{\boldsymbol{R}}_\Delta} = \frac{\partial\phi}{\partial\boldsymbol{C}}\frac{\partial\boldsymbol{C}}{\partial\dot{\boldsymbol{R}}_\Delta} = -\frac{1}{2}m\boldsymbol{C}$ and consequently $\overline{\frac{\partial\phi}{\partial\dot{\boldsymbol{R}}_\Delta}} = 0$, $\overline{\boldsymbol{R}_\Delta} = \boldsymbol{0}$, $\frac{\partial\phi}{\partial\boldsymbol{R}_\Delta} = 0$, $\frac{\partial\phi}{\partial\boldsymbol{r}} = 0$ and $\Delta\overline{\phi} = 0$. As in Section 5.3.6, $-\rho_n 2\frac{K}{m}\overline{\frac{\partial\phi}{\partial\dot{\boldsymbol{R}}_\Delta}\cdot\boldsymbol{R}_\Delta} = -\rho_n 2\frac{K}{m}(\overline{\frac{1}{2}m\boldsymbol{C}\cdot\boldsymbol{R}_\Delta}) = \kappa\overline{\boldsymbol{C}\cdot\boldsymbol{R}_\Delta}$ has to be evaluated. Equation (3.80) or (3.81) will be used for the substitution to ensure the introduction of an independent equation.

$$\begin{aligned} \boldsymbol{c} &= +\frac{\Delta\boldsymbol{p}}{m} - \frac{1}{2}\frac{\partial\boldsymbol{R}_f}{\partial t}, \\ \boldsymbol{C} &= +\frac{\Delta\boldsymbol{p}}{m} - \frac{1}{2}\frac{\partial\boldsymbol{R}_f}{\partial t} - \boldsymbol{c}_0 \\ &= +\frac{\Delta\boldsymbol{p}}{m} - \frac{1}{2}\frac{\partial\boldsymbol{R}_\Delta}{\partial t} - \boldsymbol{c}_0 - \frac{1}{2}\frac{\partial\boldsymbol{R}_\mu}{\partial t}, \\ \boldsymbol{R}_\Delta\cdot\boldsymbol{C} &= \left(+\frac{\Delta\boldsymbol{p}}{m} - \frac{1}{2}\frac{\partial\boldsymbol{R}_\Delta}{\partial t} - \boldsymbol{c}_0 - \frac{1}{2}\frac{\partial\boldsymbol{R}_\mu}{\partial t}\right)\cdot\boldsymbol{R}_\Delta \end{aligned} \quad \Longleftrightarrow$$

$$\begin{aligned} \Longleftrightarrow \quad K\overline{\boldsymbol{R}_\Delta \cdot \boldsymbol{C}} &= -\frac{1}{2}K\overline{\frac{\partial \boldsymbol{R}_\Delta}{\partial t}\cdot \boldsymbol{R}_\Delta} \\ &= -2\frac{1}{2}K\overline{\frac{\partial}{\partial t}R_\Delta^2} = -\Big(\overline{\frac{\partial}{\partial t}KR_\Delta^2}\Big) \\ &= -2\frac{\partial}{\partial t}\overline{W_p} = -\frac{\partial}{\partial t}k\mathrm{T}(\lambda^2-3) \end{aligned} \tag{5.67}$$

from Equation (3.40).

Substituting these results into Equation (5.54),

$$\begin{aligned} \int \phi_6 \frac{\partial_e p}{\partial t} d\boldsymbol{R}_f d\dot{\boldsymbol{R}}_f &= \frac{D\rho_n \frac{1}{2}NkT}{Dt} - \rho_n \frac{1}{2}NkT\frac{\partial}{\partial \mathbf{r}}\cdot\frac{\dot{\boldsymbol{R}}_\mu}{2} + \frac{\partial}{\partial \mathbf{r}}\cdot\boldsymbol{q} \\ &\quad -\rho_n\frac{\partial}{\partial t}(kT(\lambda^2-3)) - \frac{1}{2}\rho_n m\overline{\boldsymbol{C}\boldsymbol{C}} : \frac{\partial}{\partial \mathbf{r}}\frac{\dot{\boldsymbol{R}}_\mu}{2} \\ &= \frac{D\rho_n \frac{1}{2}NkT}{Dt} - \rho_n \frac{1}{2}NkT\frac{\partial}{\partial \mathbf{r}}\cdot\frac{\dot{\boldsymbol{R}}_\mu}{2} + \frac{\partial}{\partial \mathbf{r}}\cdot\boldsymbol{q} \\ &\quad -\rho_n\frac{1}{2}\frac{\partial}{\partial t}(kT(\lambda^2-3)) + \mathbf{P}_D : \frac{\partial}{\partial \mathbf{r}}\frac{\dot{\boldsymbol{R}}_\mu}{2} \end{aligned} \tag{5.68}$$

as before, for the potential energy conservation equation.

The total energy equation is the sum of kinetic and potential energy. The above six situations account for the conservation of mass, elastic constant, force, momentum and energy have been derived for the maximum entropy or zero order state.

5.4 Closing comments

In Equation (5.66) the kinetic energy is assumed to be of the same form as for ideal gases. This may be a poor assumption because the polymer molecules have fewer degrees of freedom. This was the only assumption available and one had to be made to introduce an independent equation.

It should, however, be noted that a potential energy (5.67) is also introduced and changes the stored energy of the polymers significantly from that of gases. Thus, although the assumption of (5.66) is poor for the energy of polymers, the combined assumptions of (5.66) and (5.67) as being the energy of the polymer chains may not be.

Chapter 6

Macroscopic non-maximum entropy polymer behaviour

This chapter applies the Chapman-Enskog (CE) expansion (to first order) to derive the mathematical description of the (first order approximation to the) macroscopic behaviour of polymers from the equations that describe the mesoscopic behaviour of polymers ((3.85) and (4.71)) using the maximum entropy distribution function (3.71). The derivation of the macroscopic equations will provide a rational basis for the selection of the form of the stress tensor in Chapter 7.

It should be noted that the numerical method to be constructed in Chapter 8 will be based on the equation of polymer chain interaction (3.85) with appropriate substitution of the polymer chain interaction term (4.71) and the maximum entropy distribution function (3.71). Neither of these equations nor this chapter explicitly contain any macroscopic terms like stress. Given that the numerical method (to be constructed in Chapter 8) will be based on the equation of polymer chain interaction, this chapter is not necessary for the construction of the numerical method. However, depending on the order of the CE expansion, higher order stress tensors will be necessary, in the continuum mechanics, to reconcile the continuum mechanics and the results of the CE expansion. Of note, in the continuum based approaches, stress will be an independent variable in the solution of constitutive equations whereas, in the mesoscopic approach, stresses will be extracted post-analytically.

6.1 The Chapman-Enskog expansion applied to polymers

These sections apply the Chapman-Enskog (CE) expansion to polymers. It is a modification of the original for gases by Enskog [18]. The expansion is necessary because the derived macroscopic properties are directly measurable. A similar multiscaling method will be applied to construct the numerical method of Chapter 8. It should be recognised that the CE expansion may not be a unique method for deriving the macroscopic equations and that consequently one could potentially construct an alternate expansion.

Let p be the probability of finding a molecule within vector length range $d\boldsymbol{R}_f$ about $\boldsymbol{R}_f$, vector stretch rate $d\dot{\boldsymbol{R}}_f$ about $\dot{\boldsymbol{R}}_f$, within a volume $d\mathbf{r}$ about position $\mathbf{r}$ at time t as described in Section 3.3. Let p be expressible as an infinite series such that

$$p = p^{(0)} + p^{(1)} + p^{(2)} + \cdots \tag{6.1}$$

where each $p^{(q)}$ (where $q \in \mathbb{N}_0 \iff q = 0, 1, 2, \cdots$) will be determined. Let $\varphi(p) = 0$ represent the differential equation of polymer chain interaction (3.85). Further (as performed by Enskog) let an expansion (Chapman and Cowling [18] refer to the expansion as a division) be performed on $\varphi(p)$ such that

$$\begin{aligned} \varphi(p) &= \varphi(p^{(0)} + p^{(1)} + p^{(2)} + \cdots) \\ &= \varphi^{(0)}(p^{(0)}) + \varphi^{(1)}(p^{(0)}, p^{(1)}) + \varphi^{(2)}(p^{(0)}, p^{(1)}, p^{(2)}) + \cdots . \end{aligned} \tag{6.2}$$

One can then impose the constraints

$$\begin{aligned} \varphi^{(0)}(p^{(0)}) &= 0 \\ \varphi^{(1)}(p^{(0)}, p^{(1)}) &= 0 \\ \varphi^{(2)}(p^{(0)}, p^{(1)}, p^{(2)}) &= 0 \\ &\vdots \\ \varphi^{(r)}(p^{(0)}, p^{(1)}, \ldots, p^{(r)}) &= 0 \end{aligned} \tag{6.3}$$

in order to ensure that $\varphi(p) = 0$ as required by Equation (3.85).

Next, $\varphi(p)$ can be divided into two components. The first component

correspond to the LHS of (3.85) – the polymer flow equation. The polymer flow equation was the subject of Chapter 3 and predicts the probability distribution as a function of space and time (in the absence of inter-chain interaction). It is therefore implicitly microscopic. The second component is the polymer interaction term (4.71). The latter term was the subject of Chapter 4 and describes the contribution of molecular interaction to the polymer flow equation. Thus

$$\varphi(p) = J(pp_1) + \varrho(p) \tag{6.4}$$

where p is the probability of finding the first molecule within the above dimensions and p_1 is the probability of finding the second molecule (in the binary interaction). The function $J(FG_1)$ above is defined by

$$J(FG_1) := \int\int (FG_1 - F'G_1')q_1 d\boldsymbol{q}_1 d\boldsymbol{R}_{f1} d\dot{\boldsymbol{R}}_{f1} \tag{6.5}$$

which is recognised as the polymer chain interaction term (4.71) of the differential equation of polymer chain interaction (3.85). Also recall that the unprimed terms are before interaction and the primed terms are post interaction where the before state refers to the set of stretches and stretch rates prior to interaction and after refers to the set of stretches and stretch rates after interaction. The time increment δt of interaction is half a period of the periodic motion as described in Sections 4.2 and 4.3. Formally, an interaction between molecule 1 and molecule 2 is defined as having occurred between times t and $t+\delta t$ iff $\exists\,\{t_i\}_{i=1}^{N} \neq \emptyset$ where $\forall\, t_i$, $t \leq t_i \leq t+\delta t$, $\{t_i\}_{i=1}^{N}$ is a set of N times, $N \in \mathbb{N}$ and the time t_i is when a change in momentum or stretch occurs in at least one of the molecules due to the other. This formal definition can be compared to the intuitive description of Section 4.1.

From the definition (6.5), $J(pp_1) = -\partial_e p/\partial t$ is recognised as the right hand side of Equation (3.85). Furthermore $\varrho(p)$ is defined by

$$\begin{aligned}\varrho(p) \;:=\; & \frac{\partial p}{\partial t} - \frac{\dot{\boldsymbol{F}}}{K}\cdot\frac{\partial p}{\partial \boldsymbol{R}_f} + \Big(\frac{\boldsymbol{\Delta p}}{m} - \frac{1}{2}\dot{\boldsymbol{R}}_f\Big)\cdot\frac{\partial p}{\partial \mathbf{r}} \\ & +2\left(\frac{K}{m}\boldsymbol{R}_f - \Big(\frac{\boldsymbol{F}}{m} + \frac{K}{m}\boldsymbol{R}_\mu\Big)\right)\cdot\frac{\partial p}{\partial \dot{\boldsymbol{R}}_f},\end{aligned} \tag{6.6}$$

which is the left hand side of Equation (3.85). An expansion remains to be performed on $\varrho(p)$. The expansion will be introduced in Section 6.1.5.

Substitution of Equation (6.1) into Equation (6.4) gives $\varphi(p)$ in the form

$$\begin{aligned}\varphi(p) &= J(\sum_{r=0}^{\infty} p^{(r)} \sum_{s=0}^{\infty} p_1^{(s)}) + \varrho(\sum_{r=0}^{\infty} p^{(r)}) \\ &= \sum_{r=0}^{\infty}\sum_{s=0}^{\infty} J(p^{(r)}p_1^{(s)}) + \sum_{r=0}^{\infty} \varrho(p^{(r)}). \end{aligned} \tag{6.7}$$

6.1.1 The division of $J(pp_1)$ of the transfer equation

Let the r^{th} order approximation of $J(pp_1)$ (the r^{th} term in the expansion of $J(pp_1)$ or the r^{th} order correction may be more appropriate) be defined by

$$\begin{aligned} J^{(r)} &:= J^{(r)}(p^{(0)}, p^{(1)}, \cdots, p^{(r)}) \\ &= J(p^{(0)}p_1^{(r)}) + J(p^{(1)}p_1^{(r-1)}) + \cdots + J(p^{(r)}p_1^{(0)}). \end{aligned} \tag{6.8}$$

Note that

$$J(pp_1) = \sum_{r=0}^{\infty} J^{(r)} = \sum_{r=0}^{\infty}\sum_{s=0}^{\infty} J(p^{(r)}p_1^{(s)}).$$

Let an r^{th} order approximation exist for ϱ which is to be determined. Given that the zeroth order approximation corresponds to the maximum entropy state, molecular interaction cannot alter functions of p as this would imply a deviation from maximum entropy. Thus (consistent with Enskog) let

$$\varrho^{(0)} = 0 \tag{6.9}$$

and let

$$\varphi^{(r)} = J^{(r)} + \varrho^{(r)} \qquad \forall\ r \in \mathbb{N}_0. \tag{6.10}$$

Then, given the constraints imposed by Equation (6.3), one can conclude that

$$\varphi^{(0)} = J^{(0)}, \tag{6.11}$$

$$\varphi^{(r)} = J^{(r)} + \varrho^{(r)} = 0 \qquad \forall \qquad r > 0, \tag{6.12}$$

$$0 = J(p^{(0)}, p_1^{(0)}) = J^{(0)}$$

and for the zeroth order approximation of $J^{(0)} = J(p^{(0)}, p_1^{(0)})$, one should substitute the definition of $J(p^{(0)}, p_1^{(0)})$ from Equation (6.5),

$$0 = \int\int (p^{(0)}p_1^{(0)} - p^{(0)\prime}p_1^{(0)\prime}) q_1 d\boldsymbol{q}_1 d\boldsymbol{R}_{f1} d\dot{\boldsymbol{R}}_{f1} = \frac{\partial_e p}{\partial t}. \tag{6.13}$$

6.1.2 An H-theorem for polymers

The H-theorem can be interpreted as a restatement of the second law of thermodynamics – systems always 'tend to' or converge on a state of maximum disorder. The H-theorem guarantees that a given system in a given state will converge on a unique probability distribution p for that state. Note that the second law of thermodynamics requires convergence on the state of greatest disorder but the H-theorem only guarantees convergence on a unique solution.

The theorem achieves this by defining a functional $H(t)$ at time t, proving that $H(t)$ is monotonically decreasing and then proving that $H(t)$ decreases towards a limit. The probability distribution function is then determined at that limit. An H-theorem for polymers will be defined using the gas analogue as a template.

Huang ([66], Chapter 4) reports that for gases the functional $H(t)$ is defined by [18]

$$H(t) := \int p(\boldsymbol{c}, t) \log p(\boldsymbol{c}, t) d\boldsymbol{c}.$$

Analagously, the definition of $H(t)$ for polymers is thus

$$H(t) := \int p(\boldsymbol{R}_f, \dot{\boldsymbol{R}}_f, t) \log p(\boldsymbol{R}_f, \dot{\boldsymbol{R}}_f, t)\, d\boldsymbol{R}_f\, d\dot{\boldsymbol{R}}_f. \tag{6.14}$$

Then

$$\frac{\partial H}{\partial t} = \int\int \frac{\partial}{\partial t}(p \log p) d\boldsymbol{R}_f d\dot{\boldsymbol{R}}_f = \int\int (1 + \log p) \frac{\partial p}{\partial t}\, d\boldsymbol{R}_f\, d\dot{\boldsymbol{R}}_f.$$

Given that p is a probability, $0 \leq p \leq 1 \iff \log p \leq 0$, thus

$$\frac{\partial H}{\partial t} = 0 \qquad \iff \qquad \frac{\partial p}{\partial t} = 0 \qquad \text{or} \qquad p = 0.1$$

and the sign of $\partial H/\partial t$ is always opposite to $\partial p/\partial t$. Thus if it can be shown that $H(t)$ decreases monotonically to a limit, then p increases monotonically to a limit. The solution $p = 0.1$ is ignored because it is assumed that p is not a constant unless it is at the maximum entropy state.

Substituting the formula for the polymer chain interaction term (4.71)

into the formula for $\partial H/\partial t$,

$$\frac{\partial H}{\partial t} = \int (1+\log p)(pp_1 - p'p_1')q_1 \, d\boldsymbol{q}_1 \, d\boldsymbol{R}_{f1} \, d\boldsymbol{R}_f \, d\dot{\boldsymbol{R}}_{f1} \, d\dot{\boldsymbol{R}}_f. \tag{6.15}$$

Given the symmetry of the interaction between the molecules for both the forward interaction and the reverse (recall that the interaction model of Chapter 4 conserves momentum and energy), the variables of Equation (6.15) can be interchanged such that

$$\begin{aligned}
\frac{\partial H}{\partial t} &= \int (1+\log p_1)(pp_1 - p'p_1')q_1 \, d\boldsymbol{q}_1 \, d\boldsymbol{R}_{f1} \, d\boldsymbol{R}_f \, d\dot{\boldsymbol{R}}_f \, d\dot{\boldsymbol{R}}_{f1} \\
&= \int (1+\log p')(p'p_1' - pp_1)q_1 \, d\boldsymbol{q}_1 \, d\boldsymbol{R}'_{f1} \, d\boldsymbol{R}'_f \, d\dot{\boldsymbol{R}}'_f \, d\dot{\boldsymbol{R}}'_{f1} \\
&= \int (1+\log p')(p'p_1' - pp_1)q_1 \, d\boldsymbol{q}_1 \, d\boldsymbol{R}_{f1} \, d\boldsymbol{R}_f \, d\dot{\boldsymbol{R}}_f \, d\dot{\boldsymbol{R}}_{f1} \\
&= \int (1+\log p_1')(p'p_1' - pp_1)q_1 \, d\boldsymbol{q}_1 \boldsymbol{R}'_{f1} \, d\boldsymbol{R}'_f \, d\dot{\boldsymbol{R}}'_{f1} \, d\dot{\boldsymbol{R}}'_f \\
&= \int (1+\log p_1')(p'p_1' - pp_1)q_1 \, d\boldsymbol{q}_1 \, d\boldsymbol{R}_{f1} \, d\boldsymbol{R}_f \, d\dot{\boldsymbol{R}}_f \, d\dot{\boldsymbol{R}}_{f1}.
\end{aligned}$$

From the results for the Jacobian – (4.69) and (4.70) – the variables of integration above are equal. Summing four of the equations for $\partial H/\partial t$ above appropriately and dividing the result by four

$$\begin{aligned}
\frac{\partial H}{\partial t} &= \frac{1}{4}\int (\log p + \log p_1 - \log p' - \log p_1') \\
&\quad \times (p'p_1' - pp_1)q_1 \, d\boldsymbol{q}_1 \, d\boldsymbol{R}_{f1} \, d\boldsymbol{R}_f \, d\dot{\boldsymbol{R}}_f \, d\dot{\boldsymbol{R}}_{f1} \\
&= \frac{1}{4}\int (\log p_1 p - \log p'p_1')(p'p_1' - pp_1) \\
&\quad \times q_1 \, d\boldsymbol{q}_1 \, d\boldsymbol{R}_{f1} \, d\boldsymbol{R}_f \, d\dot{\boldsymbol{R}}_f \, d\dot{\boldsymbol{R}}_{f1}
\end{aligned} \tag{6.16}$$

and since $\log p_1 p/p_1'p'$ is always opposite in sign to $p'p_1' - pp_1$,

$$\frac{\partial H}{\partial t} \leq 0.$$

The proof that $\log \frac{p_1 p}{p_1' p'}$ is always opposite in sign to $pp_1 - p'p_1'$ relies on the fact that $p \geq 0$ because it is a probability and that therefore $p_1 p \geq 0$. Thus only two scenarios need to be considered. The first is $p_1 p \leq p_1' p' \iff \log \frac{p_1 p}{p_1' p'} \geq 0$. The converse can be shown for the second scenario. Note that if $p = 0$, no molecule exists and an interaction cannot occur. p converges on a unique solution at $\partial H/\partial t = 0$. Furthermore $\partial H/\partial t = 0 \iff J = 0$ which only occurs when the integrands of (6.15) and (6.13) are zero.

From the second law of thermodynamics [25], the functional $H(t)$ converges on a limit at the maximum entropy state. The convergence occurs when $\partial H/\partial t = 0$. For both $\partial H/\partial t = 0$ and $\partial p/\partial t = 0$ the above convergence only occurs when

$$p^{(0)\prime}p_1^{(0)\prime} - p^{(0)}p_1^{(0)} \equiv \log p^{(0)} + \log p_1^{(0)} - \log p^{(0)\prime} - \log p_1^{(0)\prime} = 0 \qquad (6.17)$$

and since this is the maximum entropy state,

$$p^{(0)} = p^{(ms)} = \frac{b^3}{\pi^{3/2}} e^{-b^2(\boldsymbol{R}_f - \boldsymbol{R}_\mu)^2} \times \Big(\frac{m}{2\pi kT}\Big)^{\frac{3}{2}} e^{-\frac{m}{2kT}(\dot{\boldsymbol{c}} - \boldsymbol{c}_0)^2}, \qquad (6.18)$$

as given by Equation (3.71). From (3.81) and (5.23),

$$\dot{\boldsymbol{c}} - \boldsymbol{c}_0 = -\frac{1}{2}\Big(\dot{\boldsymbol{R}}_f - \dot{\boldsymbol{R}}_\mu\Big). \qquad (6.19)$$

Substituting (6.19) into (6.18) with appropriate change of variable of integration and recognising that the integration limits are $-\infty, \infty$ in all directions for both vector length and velocity, it is necessary that

$$1 \;=\; \int\int p^{(ms)}(\dot{\boldsymbol{c}}, \boldsymbol{R}_f)\, d\boldsymbol{R}_f\, d\dot{\boldsymbol{c}}$$

because $p^{(ms)}$ is a probability. Changing the variable of integration to $d\dot{\boldsymbol{R}}_f$ given that $d\boldsymbol{c} = -d\dot{\boldsymbol{R}}_f/2$, integrating over limits $-\infty, \infty$ in all directions

$$1 = \int\int p^{(ms)}(\dot{\boldsymbol{c}}, \boldsymbol{R}_f) \times \Big(-\frac{1}{2}\Big)\, d\boldsymbol{R}_f\, d\dot{\boldsymbol{R}}_f$$

$$\iff \qquad p^{(ms)}(\dot{\boldsymbol{R}}_f, \boldsymbol{R}_f) = \frac{b^3}{\pi^{3/2}} e^{-b^2(\boldsymbol{R}_f - \boldsymbol{R}_\mu)^2} \times \Big(\frac{m}{8\pi kT}\Big)^{\frac{3}{2}} e^{-\frac{m}{8kT}(\dot{\boldsymbol{R}}_f - \dot{\boldsymbol{R}}_\mu)^2}. \qquad (6.20)$$

6.1.3 Defining the summational invariants and $\rho_n^2 I(\phi)$

This section will identify the summational invariants which will be shown to correspond to the conserved properties of Section 5.3. Substituting Equation (6.12) into Equation (6.8) and re-arranging

$$\begin{aligned} J(p^{(0)}p_1^{(r)}) + J(p^{(r)}p_1^{(0)}) \;&=\; -\varrho^{(r)} - J(p^{(1)}p^{(r-1)}) \\ &\quad -J(p^2p^{(r-2)}) - \cdots - J(p^{(r-1)}p^{(1)}) \end{aligned} \qquad (6.21)$$

where the RHS is known from the pre-existing results. From the definition of J (6.5), the LHS of the equation is linear in $p^{(r)}$ and corresponds to

$$\begin{aligned}\int (p^{(0)}p_1^{(r)} + p^{(r)}p_1^{(0)}) q_1 \, d\boldsymbol{q}_1 \, d\boldsymbol{R}_{f1} \, d\dot{\boldsymbol{R}}_{f1} &= p^{(0)} \int p_1^{(r)} q_1 \, d\boldsymbol{q}_1 \, d\boldsymbol{R}_{f1} \, d\dot{\boldsymbol{R}}_{f1} \\ &+ p^{(r)} \int p_1^{(0)} q_1 \, d\boldsymbol{q}_1 \, d\boldsymbol{R}_{f1} \, d\dot{\boldsymbol{R}}_{f1}.\end{aligned}$$

Given that (6.21) is linear, if $P^{(r)}$ is a solution of (6.21), then (for complementary solution $\chi^{(r)}$) $P^{(r)} + \chi^{(r)}$ is also a solution. Thus

$$J(p^{(0)}\chi^{(r)}) + J(p^{(r)}\chi^{(0)}) = 0. \tag{6.22}$$

This is a statement of the property of linear differential equations where $\chi^{(r)}$ is a complementary solution and $P^{(r)}$ is a particular solution. To determine $\chi^{(r)}$, make the substitution

$$\chi^{(r)} = p^{(0)}\phi^{(r)}. \tag{6.23}$$

Then it only remains to determine $\phi^{(r)}$. Substituting (6.23) into (6.22)

$$\begin{aligned}J(p^{(0)}p_1^{(0)}\phi_1^r) - J(p^{(0)}\phi^{(r)}p_1^{(0)}) &= \int p^{(0)}p_1^{(0)}(\phi^{(r)} + \phi_1^{(r)} - \phi^{(r)\prime} - \phi_1^{(r)\prime}) \\ &\times q_1 \, d\boldsymbol{q}_1 \, d\boldsymbol{R}_{f1} \, d\boldsymbol{R}_f \, d\boldsymbol{c} \, d\boldsymbol{c}_1 = \rho_n^2 I(\phi) = 0.\end{aligned} \tag{6.24}$$

Thus substituting (6.24) into (6.22), Equation (6.22) reduces to

$$\rho_n^2 I(\phi^{(r)}) = 0 \Longrightarrow I(\phi^{(r)}) = 0.$$

From Section 6.1.2 and the definition of H in the H-theorem, (6.24) is only true when (from (6.17)) the integrand is zero. Thus

$$\begin{aligned}0 &= p^{(0)}p_1^{(0)}(\phi^{(r)} + \phi_1^{(r)} - \phi^{(r)\prime} - \phi_1^{(r)\prime}) \\ \Longleftrightarrow \qquad 0 &= \phi^{(r)} + \phi_1^{(r)} - \phi^{(r)\prime} - \phi_1^{(r)\prime} \qquad \forall \, r, r'.\end{aligned} \tag{6.25}$$

Consequently (6.25) is a linear combination of conserved properties. These conserved properties were identified in Section 5.3 and are referred to as the summational invariants $\psi^i = m$, K, $K\boldsymbol{R}_f$, $m\boldsymbol{c}$ or $m\dot{\boldsymbol{R}}_f$, $KR_f^2 + mc^2$ or $KR_f^2 + m\dot{R}_f^2$. Finally the complementary function $\chi^{(r)}$ is given by a linear combination of the summational invariants; thus

$$\chi^{(r)} = p^{(0)}(\alpha^{(1,r)} + \alpha^{(2,r)} \cdot K(\boldsymbol{R}_f) + \alpha^{3,r} \cdot m\boldsymbol{c} + \alpha^{(4,r)}(KR_f^2 + mc^2)) \tag{6.26}$$

where the general solution is $p^{(r)} = P^{(r)} + \chi^{(r)}$ and $\alpha^{(i,r)}$ are constants.

The equation $\int p^{(r)}\psi^{(i)} d\boldsymbol{R}_f d\dot{\boldsymbol{R}}_f$ can take on any value depending on how one selects $\alpha^{(1,r)}, \alpha^{(2,r)}$, $\alpha^{(3,r)}$ and $\alpha^{(4,r)}$. In performing the Chapman-Enskog expansion, it will prove convenient to set

$$\int p^{(r)}\psi^{(i)} d\boldsymbol{R}_f d\dot{\boldsymbol{R}}_f = 0 \tag{6.27}$$

when one attempts to discretise $\varrho(p)$. Therefore $\alpha^{(1,r)}, \alpha^{(2,r)}$, $\alpha^{(3,r)}$ and $\alpha^{(4,r)}$ will be selected such that the condition (6.27) is satisfied.

6.1.4 Condition of solubility

The intention of this chapter is two-fold. The first is to find the non-maximum entropy solution of the probability density p and the second is to perform an expansion such that the macroscopic behaviour of polymers can be described. Before determing the solution of p it is wise to determine whether a solution exists. The equation to be solved is the polymer flow equation (3.85)

$$\varphi(p) = 0.$$

The constraints (6.3) combined with (6.10) impose the additional constraints

$$\varphi^{(r)}(p) = 0 = J^{(r)}(p) + \varrho^{(r)}(p) \qquad \forall\, r \in \mathbb{N} \tag{6.28}$$

where $\mathbb{N} = 1, 2, 3, \cdots$. The expansion of $\varrho^{(r)}(p)$ still needs to be defined. If (6.28) is true then

$$\int \varphi^{(r)}(p)\psi^{i}\, d\boldsymbol{R}_f\, d\dot{\boldsymbol{R}}_f = 0 \qquad \forall\, r \in \mathbb{N}_0. \tag{6.29}$$

Consider the term $\int J^{(r)}\psi^{(i)}\, d\boldsymbol{R}_f\, d\dot{\boldsymbol{R}}_f$. From (6.21),

$$\begin{aligned}\int J^{(r)}\psi^{(i)}\, d\boldsymbol{R}_f\, d\dot{\boldsymbol{R}}_f &= \int \sum_{r=0}^{\infty}\sum_{s=0}^{\infty} J(p(r), p(s))\psi^{(i)}\, d\boldsymbol{R}_f\, d\dot{\boldsymbol{R}}_f \\ &= \sum_{r=0}^{\infty}\sum_{s=0}^{\infty}\int J(p(r), p(s))\psi^{(i)}\, d\boldsymbol{R}_f\, d\dot{\boldsymbol{R}}_f.\end{aligned}$$

Given that

$$\int J(\phi F_1 F)\, d\boldsymbol{R}_f\, d\dot{\boldsymbol{R}}_f = \frac{1}{4}\int J\big((\phi + \phi_1 - \phi' - \phi_1')F_1 F\big)\, d\boldsymbol{R}_f\, d\dot{\boldsymbol{R}}_f$$

(proven in appendix A-2), it follows that, upon substitution of the definition of J (6.5),

$$\begin{aligned}\int J^{(r)}\psi^{(i)}d\boldsymbol{R}_f\,d\dot{\boldsymbol{R}}_f &= \sum_{r=0}^{\infty}\sum_{s=0}^{\infty}\int\frac{1}{4}(p(r)p(s)-p'(r)p'(s))(\psi+\psi_1\\ &\quad -\psi'-\psi'_1)\times q_1\,d\boldsymbol{q}_1\,d\boldsymbol{R}_f\,d\boldsymbol{R}_{f1}\,d\dot{\boldsymbol{R}}_f\,d\dot{\boldsymbol{R}}_{f1}\\ &= (\psi+\psi_1-\psi'-\psi'_1)\sum_{r=0}^{\infty}\sum_{s=0}^{\infty}\int\frac{1}{4}(p(r)p(s)\\ &\quad -p'(r)p'(s))\times q_1\,d\boldsymbol{q}_1\,d\boldsymbol{R}_f\,d\boldsymbol{R}_{f1}\,d\dot{\boldsymbol{R}}_f\,d\dot{\boldsymbol{R}}_{f1}\\ &= 0. \end{aligned}\tag{6.30}$$

Substituting (6.30) into (6.12) one can therefore conclude that

$$\int\varrho(p)\psi^{(i)}d\boldsymbol{R}_f d\dot{\boldsymbol{R}}_f=0\implies\int\varrho^{(r)}(p)\psi^{(i)}d\boldsymbol{R}_f d\dot{\boldsymbol{R}}_f=0\tag{6.31}$$

where $r\in\mathbb{N}$. Equation (6.31) is thus a *necessary* condition for (6.28) to be satisfied. The proof that it is a *sufficient* condition cannot be provided and has been assumed for this work. Chapman and Cowling [18] provide a proof for gases relying on the proof that

$$I(\phi^{(r)})\equiv K_0(\boldsymbol{\Gamma})+\int K(\boldsymbol{\Gamma},\boldsymbol{\Gamma}_1)\phi^{(r)}(\boldsymbol{\Gamma}_1)d\boldsymbol{\Gamma}_1$$

where (for gases) $\boldsymbol{\Gamma}=\boldsymbol{c}$ and $K(\boldsymbol{\Gamma},\boldsymbol{\Gamma}_1)$ is a symmetric function of $\boldsymbol{\Gamma}$. Consequently the gas equivalent of (6.24) is a linear orthogonal non-homogeneous integral equation with associated homogeneous linear orthogonal integral equation

$$\rho_n^2 I(\phi^{(r)})=0$$

with independent solutions $\phi^{(r)}=\psi^{(i)}$. The gas equivalent of (6.24) has a solution *if and only if*

$$\int\psi^{(r)}\Big(-\varrho^{(r)}-J(p^{(1)}p^{(r-1)})-J(p^2p^{(r-2)})-\cdots-J(p^{(r-1)}p^{(1)})\Big)d\boldsymbol{R}_f d\dot{\boldsymbol{R}}_f=0$$

which is the condition of orthogonality for the left hand side of the gas equivalent of (6.24). The above reduces to the gas equivalent of (6.29) and is therefore a *sufficient* condition for solubility of the gas equivalent of (6.28).

6.1.5 The expansion of $\varrho(p)$

Consider the conservation equations given by (5.56), (5.60), (5.61), (5.64) and (5.68). The expansion of the time derivatives are defined as follows:

$$\begin{aligned} \frac{\partial \rho_n}{\partial t} &:= \sum_{r=0}^{\infty} \frac{\partial_r \rho_n}{\partial t}, & \frac{\partial \frac{\dot{\boldsymbol{R}}_\mu}{2}}{\partial t} &:= \sum_{r=0}^{\infty} \frac{\partial_r \frac{\dot{\boldsymbol{R}}_\mu}{2}}{\partial t}, \\ \frac{\partial \boldsymbol{R}_\mu}{\partial t} &:= \sum_{r=0}^{\infty} \frac{\partial_r \boldsymbol{R}_\mu}{\partial t}, & \frac{\partial \mathrm{T}}{\partial t} &:= \sum_{r=0}^{\infty} \frac{\partial_r \mathrm{T}}{\partial t}, \\ \frac{\partial \mathrm{T}(\lambda^2-3)}{\partial t} &:= \sum_{r=0}^{\infty} \frac{\partial_r \mathrm{T}(\lambda^2-3)}{\partial t}, \end{aligned} \tag{6.32}$$

where the entities on the right are not time derivatives, need to be defined and will be defined by Equations (6.37). Similarly, let

$$\begin{aligned} \partial_t \mathbf{P}_S &= \sum_{r=0}^{\infty} \partial_t \mathbf{P}_S^{(r)}, & \mathbf{P}_D &= \sum_{r=0}^{\infty} \mathbf{P}_D^{(r)}, \\ \boldsymbol{\Psi} &= \sum_{r=0}^{\infty} \boldsymbol{\Psi}^{(r)}, & \mathbf{q} &= \sum_{r=0}^{\infty} \mathbf{q}^{(r)}. \end{aligned} \tag{6.33}$$

From the definitions (5.7), (5.24) and (5.31), the left hand side of Equations (6.33) were defined by

$$\begin{aligned} \frac{\partial \mathbf{P}_S^{(r)}}{\partial t} &= -\frac{K}{2} \int \boldsymbol{R}_\Delta p^{(r)} \boldsymbol{C} d\boldsymbol{R}_f d\dot{\boldsymbol{R}}_f, \\ \boldsymbol{\Psi}^{(r)} &= -\frac{1}{2} \int E_p p^{(r)} d\boldsymbol{R}_f d\dot{\boldsymbol{R}}_f, \\ \mathbf{P}_D^{(r)} &= -\frac{m}{2} \int \boldsymbol{C} p^{(r)} \boldsymbol{C} d\dot{\boldsymbol{R}}_f d\boldsymbol{R}_f, \\ \mathbf{q}^{(r)} &= -\frac{1}{2} \int E_k p^{(r)} d\dot{\boldsymbol{R}}_f d\boldsymbol{R}_f, \end{aligned} \tag{6.34}$$

where $E_k = \frac{1}{2} m C^2$ and $E_p = \frac{1}{2} m R_\Delta^2$. Due to the form of $p^{(0)}$,

$$\mathbf{q}^{(0)} = 0, \tag{6.35}$$

$$\boldsymbol{\Psi}^{(0)} = 0. \tag{6.36}$$

The factor $-\frac{1}{2}$ is due to the change of variable from $\boldsymbol{c}$ to $\dot{\boldsymbol{R}}_f$. The subdivisions in the expansion (6.32) require definitions. Section 5.3 calculated the zero order (or maximum entropy) transport equations for mass, elasticity, momentum, force, potential energy and kinetic energy. The results of Section

5.3 are separated using Equations (6.34) and then used to define components of the expansion of Equations (6.32) as

$$\begin{aligned}
\frac{\partial_0 \rho_n}{\partial t} &:= \frac{\partial}{\partial r} \cdot \rho_n \frac{\dot{\boldsymbol{R}}_\mu}{2}, \\
\frac{\partial_r \rho_n}{\partial t} &:= 0 \qquad\qquad \forall\, (r > 0), \\
\frac{\partial_0 \frac{\dot{\boldsymbol{R}}_\mu}{2}}{\partial t} &:= \Big(\frac{1}{2}\dot{\boldsymbol{R}}_\mu \cdot \frac{\partial}{\partial \mathbf{r}}\Big)\frac{\dot{\boldsymbol{R}}_\mu}{2} + \frac{\boldsymbol{F}}{m} + \frac{2}{\rho}\frac{\partial}{\partial \mathbf{r}} \cdot \mathbf{P}_D^{(0)} \\
&= \Big(\frac{\dot{\boldsymbol{R}}_\mu}{2} \cdot \frac{\partial}{\partial \mathbf{r}}\Big)\frac{\dot{\boldsymbol{R}}_\mu}{2} + \frac{\boldsymbol{F}}{m} + \frac{2}{\rho}\frac{\partial p_d}{\partial \mathbf{r}}, \\
\frac{\partial_r \frac{\dot{\boldsymbol{R}}_\mu}{2}}{\partial t} &:= \frac{2}{\rho}\frac{\partial}{\partial \mathbf{r}} \cdot \boldsymbol{P}^{(r)} \qquad \forall\, (r > 0), \\
\frac{\partial_0 \boldsymbol{R}_\mu}{\partial t} &:= \Big(\frac{\dot{\boldsymbol{R}}_\mu}{2} \cdot \frac{\partial}{\partial \mathbf{r}}\Big)\boldsymbol{R}_\mu - \frac{\dot{\boldsymbol{F}}}{K} + \frac{1}{2\kappa}\frac{\partial}{\partial \mathbf{r}} \cdot \partial_t \mathbf{P}_S^{(0)} \\
&= \Big(\frac{\dot{\boldsymbol{R}}_\mu}{2} \cdot \frac{\partial}{\partial \mathbf{r}}\Big)\boldsymbol{R}_\mu - \frac{\dot{\boldsymbol{F}}}{K} + \frac{1}{2\kappa}\frac{\partial^2 p_s}{\partial t \partial \mathbf{r}}, \\
\frac{\partial_r \boldsymbol{R}_\mu}{\partial t} &:= \frac{1}{2\kappa}\frac{\partial}{\partial \mathbf{r}} \cdot \partial_t \mathbf{P}_S^{(r)} \qquad \forall\, (r > 0)
\end{aligned} \tag{6.37}$$

where p_d and p_S are hydrostatic pressures. Thus, implicitly, the hydrostaic pressure assumptions that $\mathbf{P}_D = \mathbf{I}p_d$ and $\mathbf{P}_S = \mathbf{I}p_s$ have been made. These assumptions will be justified below.

Continuing with the conservation of potential energy, from Equation (5.64), the material derivative of the potential energy is

$$\begin{aligned}
\frac{D(\frac{1}{2}\rho_n k \mathrm{T}(\lambda^2 - 3))}{Dt} &- \frac{1}{2}\rho_n k \mathrm{T}(\lambda^2 - 3)\frac{\partial}{\partial \mathbf{r}} \cdot \frac{\dot{\boldsymbol{R}}_\mu}{2} + \frac{\partial}{\partial \mathbf{r}} \cdot \boldsymbol{\Psi} - \frac{1}{2}\partial_t \mathbf{P}_S : \frac{\partial}{\partial \mathbf{r}}\boldsymbol{R}_\mu \\
&= \frac{\rho_n k}{2}\frac{D\mathrm{T}(\lambda^2 - 3)}{Dt} \\
&\quad + \frac{\mathrm{T}(\lambda^2 - 3)}{2}\left(\frac{D\rho_n k}{Dt} - \rho_n k \frac{\partial}{\partial \mathbf{r}} \cdot \frac{\dot{\boldsymbol{R}}_\mu}{2}\right) \\
&\quad + \frac{\partial}{\partial \mathbf{r}} \cdot \boldsymbol{\Psi} - \frac{1}{2}\partial_t \mathbf{P}_S : \frac{\partial}{\partial \mathbf{r}}\boldsymbol{R}_\mu \\
&= \frac{\rho_n k}{2}\frac{\partial \mathrm{T}(\lambda^2 - 3)}{\partial t} - \frac{\rho_n k}{2}\frac{\dot{\boldsymbol{R}}_\mu}{2}\frac{\partial \mathrm{T}(\lambda^2 - 3)}{\partial \mathbf{r}} + \frac{\partial}{\partial \mathbf{r}} \cdot \boldsymbol{\Psi} \\
&\quad - \frac{1}{2}\partial_t \mathbf{P}_S : \frac{\partial}{\partial \mathbf{r}}\boldsymbol{R}_\mu.
\end{aligned}$$

Substituting Equation (6.36) for $\partial/\partial \mathbf{r} \cdot \boldsymbol{\Psi}$, the conservation of potential energy

further reduces to

$$\begin{aligned}
\frac{\partial_0 T(\lambda^2-3)}{\partial t} &= \frac{\dot{\boldsymbol{R}}_\mu}{2}\cdot\frac{\partial T(\lambda^2-3)}{\partial \mathbf{r}} - \frac{2}{k\rho_n}\left(\frac{\partial}{\partial \mathbf{r}}\cdot\boldsymbol{\Psi}^{(0)} - \frac{1}{2}\partial_t \mathbf{P}_S^{(0)} : \frac{\partial}{\partial \mathbf{r}}\boldsymbol{R}_\mu\right) \\
&= \frac{\dot{\boldsymbol{R}}_\mu}{2}\cdot\frac{\partial T(\lambda^2-3)}{\partial \mathbf{r}} + \frac{1}{k\rho_n}\left(\partial_t \mathbf{P}_S^{(0)} : \frac{\partial}{\partial \mathbf{r}}\boldsymbol{R}_\mu\right), \\
\frac{\partial_r T(\lambda^2-3)}{\partial t} &= -\frac{1}{k\rho_n}\left(\frac{\partial}{\partial \mathbf{r}}\cdot\boldsymbol{\Psi}^{(r)} - \partial_t \mathbf{P}_S^{(r)} : \frac{\partial}{\partial \mathbf{r}}\boldsymbol{R}_\mu\right) \qquad \forall\,(r>0). \quad (6.38)
\end{aligned}$$

Similarly (for kinetic energy), from Equation (5.68),

$$\begin{aligned}
\rho_n \frac{D\frac{1}{2}NkT}{Dt} &= -\frac{1}{2}NkT\left(\frac{D\rho_n}{Dt} - \rho_n\frac{\partial}{\partial \mathbf{r}}\cdot\frac{\dot{\boldsymbol{R}}_\mu}{2}\right) \\
&\quad +\rho_n\frac{\partial}{\partial t}kT(\lambda^2-3) - \frac{\partial}{\partial \mathbf{r}}\cdot\mathbf{q} - \mathbf{P}_D : \frac{\partial}{\partial \mathbf{r}}\frac{\dot{\boldsymbol{R}}_\mu}{2}.
\end{aligned}$$

Consequently, substituting the conservation of density equation (5.57),

$$\begin{aligned}
\frac{\partial_0 \mathrm{T}}{\partial t} &= \frac{\dot{\boldsymbol{R}}_\mu}{2}\cdot\frac{\partial \mathrm{T}}{\partial \mathbf{r}} + \frac{2}{N}\frac{\partial \mathrm{T}(\lambda^2-3)}{\partial t} - \frac{2}{Nk\rho_n}\left(\frac{\partial}{\partial \mathbf{r}}\cdot\mathbf{q}^{(0)} + \mathbf{P}_D^{(0)} : \frac{\partial}{\partial \mathbf{r}}\frac{\dot{\boldsymbol{R}}_\mu}{2}\right) \\
&= \frac{\dot{\boldsymbol{R}}_\mu}{2}\cdot\frac{\partial \mathrm{T}}{\partial \mathbf{r}} + \frac{2}{N}\frac{\partial \mathrm{T}(\lambda^2-3)}{\partial t} - \frac{2}{Nk\rho_n}\left(\mathbf{P}_D^{(0)} : \frac{\partial}{\partial \mathbf{r}}\frac{\dot{\boldsymbol{R}}_\mu}{2}\right), \\
\frac{\partial_r \mathrm{T}}{\partial t} &= -\frac{2}{Nk\rho_n}\left(\frac{\partial}{\partial \mathbf{r}}\cdot\mathbf{q}^{(r)} + \mathbf{P}_D^{(r)} : \frac{\partial}{\partial \mathbf{r}}\frac{\dot{\boldsymbol{R}}_\mu}{2}\right) \qquad \forall\,(r>0). \qquad (6.39)
\end{aligned}$$

The treatment of the pressure tensors as hydrostatic pressure requires justification. In the specimen's ground state and material's equilibrium state, the pressure is uniformly distributed throughout the body and consequently approximates a hydrostatic type pressure. Thus the assumption

$$p_d = -\rho_n kT \qquad (6.40)$$

is made where $p_d\mathbf{I}$ represents a dynamic pressure tensor change and has been selected to preserve the form of the gas scenario. The origin of the negative sign is not obvious and indicates reduction of pressure (and consequently volume) with temperature increase. Recall that in Section 3.1.2 only the molecular velocity due to stretch rate was considered. Thus the molecular velocity is not an independent variable. In the case of a gas, increasing the temperature increases the molecular velocity. In the case of a polymer, the increase in temperature is expected to increase the transverse amplitude of

vibration of the molecule which (for a molecule of fixed (scalar) length as in the rigid-link model) will reduce the molecular length in the longitudinal direction and the variability in molecular length. The reduction in variability of molecular length translates into a reduction in variability of the molecular stretch rate and therefore the root mean square molecular velocity. These arguments are represented graphically in Figure 6.1. This result is shown

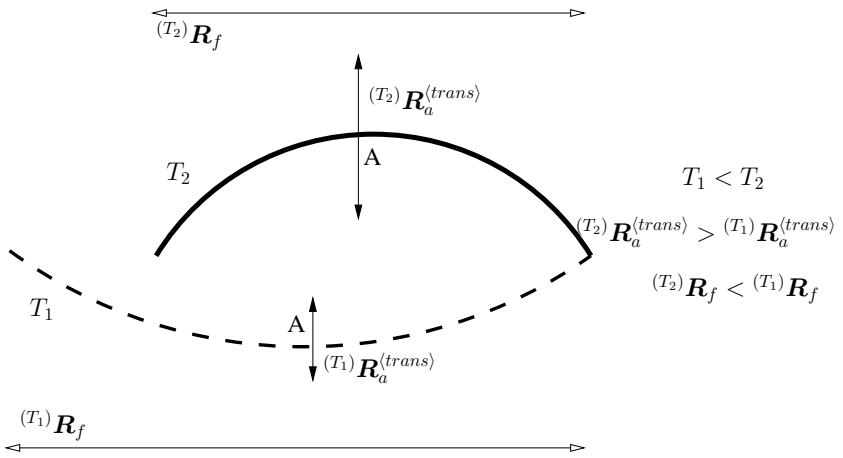

Figure 6.1: For the idealised fixed molecular (scalar) length model, the dashed and solid lines represent the same molecule at temperatures T_1 and T_2 respectively. The amplitudes of vibration of position A in the transverse direction are $^{(T_1)}\boldsymbol{R}_a^{\langle trans\rangle}$ at T_1 and $^{(T_2)}\boldsymbol{R}_a^{\langle trans\rangle}$ for T_2. The vector length at T_1 is represented by $^{(T_1)}\boldsymbol{R}_f$ and $^{(T_2)}\boldsymbol{R}_f$ at T_2. The depiction shows the reduction in molecular chain length with increasing temperature.

independently by Equations (6.57) through (6.60).

The static component, p_s, at equilibrium is calculated from Equation (3.40) as

$$\frac{\partial W}{\partial V} = p_s = \rho_n k\mathrm{T}(\lambda^2 - 3) \tag{6.41}$$

Thus the hydrostatic approximation to p_s at equilibrium is defined as $p_s = \partial W/\partial V$ where $p_s\mathbf{I}$ represents a static pressure tensor change from the unstrained or ground state. The observed volume (and pressure) change with temperature is a consequence of the net effect of p_d and p_s which can be increasing or decreasing [139] (depending on whether p_d or p_s is greater).

Given Equation (3.81) one can set the mobile operator

$$\frac{D_0}{Dt} = \frac{\partial_0}{\partial t} + \boldsymbol{c}\cdot\frac{\partial}{\partial \mathbf{r}} = \frac{\partial_0}{\partial t} - \frac{\dot{\boldsymbol{R}}_\mu}{2}\cdot\frac{\partial}{\partial \mathbf{r}}$$

so that D_0/Dt is a first approximation (or zero-order or maximum entropy approximation) to D/Dt. Then (substituting (6.40) and (6.41)) into material derivatives of the conserved entities as described by Equations (6.37), (6.38) and (6.39)

$$\begin{aligned}
\frac{D_0\rho_n}{Dt} &= \rho_n\frac{\partial}{\partial\mathbf{r}}\cdot\frac{\dot{\boldsymbol{R}}_\mu}{2},\\
\frac{D_0\frac{\dot{\boldsymbol{R}}_\mu}{2}}{Dt} &= \frac{\boldsymbol{F}}{m}+\frac{2}{\rho}\frac{\partial p_d}{\partial\mathbf{r}},\\
\frac{D_0\boldsymbol{R}_\mu}{Dt} &= -\frac{\dot{\boldsymbol{F}}}{K}+\frac{1}{2\kappa}\frac{\partial^2 p_s}{\partial t\partial\mathbf{r}},\\
\frac{D_0\mathrm{T}(\lambda^2-3)}{Dt} &= \frac{2}{k\rho_n}\partial_t(\rho_n k\mathrm{T})\frac{\partial}{\partial\mathbf{r}}\cdot\boldsymbol{R}_\mu = 2\frac{\partial\mathrm{T}}{\partial t}\frac{\partial}{\partial\mathbf{r}}\cdot\boldsymbol{R}_\mu,\\
\frac{D_0\mathrm{T}}{Dt} &= \frac{2}{N}\frac{\partial\mathrm{T}(\lambda^2-3)}{\partial t}+\frac{2}{Nk\rho_n}(\rho_n k\mathrm{T})\frac{\partial}{\partial\mathbf{r}}\cdot\frac{\dot{\boldsymbol{R}}_\mu}{2}\\
&= \frac{2}{N}\frac{\partial\mathrm{T}(\lambda^2-3)}{\partial t}+\frac{2\mathrm{T}}{N}\frac{\partial}{\partial\mathbf{r}}\cdot\frac{\dot{\boldsymbol{R}}_\mu}{2} = \frac{2\mathrm{T}}{N}\frac{\partial}{\partial\mathbf{r}}\cdot\frac{\dot{\boldsymbol{R}}_\mu}{2}
\end{aligned} \tag{6.42}$$

because the 0-strain state has $\lambda^2=3$. Consequently

$$\begin{aligned}
\frac{\mathrm{T}^{\mathrm{N}/2}}{\rho_n}\frac{D_0}{Dt}(\rho_n/\mathrm{T}^{\mathrm{N}/2}) &= \frac{D_0\ln\rho_n}{Dt}-\frac{N}{2}\frac{D_0\ln\mathrm{T}}{Dt} = \frac{1}{\rho}\frac{D_0\rho}{Dt}-\frac{N}{2T}\frac{D_0T}{Dt}\\
&= \frac{\partial}{\partial\mathbf{r}}\cdot\frac{\dot{\boldsymbol{R}}_\mu}{2}-\frac{\partial}{\partial\mathbf{r}}\cdot\frac{\dot{\boldsymbol{R}}_\mu}{2}=0.
\end{aligned} \tag{6.43}$$

If F is a function of ρ_n, $\boldsymbol{R}_\mu$, $\dot{\boldsymbol{R}}_\mu$, T where each of ρ_n, $\boldsymbol{R}_\mu$, $\dot{\boldsymbol{R}}_\mu$, T is a function of t, then

$$\begin{aligned}
\frac{\partial F}{\partial t} &= \frac{\partial F}{\partial\rho_n}\frac{\partial\rho_n}{\partial t}+\frac{\partial F}{\partial\boldsymbol{R}_\mu}\cdot\frac{\partial\boldsymbol{R}_\mu}{\partial t}+\frac{\partial F}{\partial\dot{\boldsymbol{R}}_\mu}\cdot\frac{\partial\dot{\boldsymbol{R}}_\mu}{\partial t}+\frac{\partial F}{\partial\mathrm{T}}\frac{\partial\mathrm{T}}{\partial t}\\
&= \sum_0^\infty\left(\frac{\partial F}{\partial N}\frac{\partial_r N}{\partial t}+\frac{\partial F}{\partial\boldsymbol{R}_\mu}\cdot\frac{\partial_r\boldsymbol{R}_\mu}{\partial t}+\frac{\partial F}{\partial_r\dot{\boldsymbol{R}}_\mu}\cdot\frac{\partial\dot{\boldsymbol{R}}_\mu}{\partial t}+\frac{\partial F}{\partial\mathrm{T}}\frac{\partial_r\mathrm{T}}{\partial t}\right)=\sum_0^\infty\frac{\partial_r F}{\partial t}
\end{aligned}$$

Applying all the subdivisions for the expansion (6.37) to Equation (6.6) where $\boldsymbol{U}:=\frac{\boldsymbol{\Delta p}}{m}-\frac{1}{2}\dot{\boldsymbol{R}}_f=-\frac{\dot{\boldsymbol{R}}_\mu}{2}$, $\boldsymbol{V}:=-\frac{\dot{\boldsymbol{F}}}{K}$ and $\boldsymbol{W}:=2\left(\frac{K}{m}\boldsymbol{R}_f-\left(\frac{\boldsymbol{F}}{m}+\frac{K}{m}\boldsymbol{R}_\mu\right)\right)\frac{\partial p}{\partial\dot{\boldsymbol{R}}_f}$,

$$\begin{aligned}
\varrho(p) &= \left(\sum_{r=0}^\infty\frac{\partial_r}{\partial t}+\boldsymbol{U}\cdot\frac{\partial}{\partial\mathbf{r}}+\boldsymbol{V}\cdot\frac{\partial}{\partial\boldsymbol{R}_f}+\boldsymbol{W}\cdot\frac{\partial}{\partial\dot{\boldsymbol{R}}_f}\right)\sum_{s=0}^\infty p^{(s)}\\
&= \sum_{r=0}^\infty\sum_{s=0}^\infty\frac{\partial_r p^{(s)}}{\partial t}+\sum_{s=0}^\infty\left(\boldsymbol{U}\cdot\frac{\partial p^{(s)}}{\partial\mathbf{r}}+\boldsymbol{V}\cdot\frac{\partial p^{(s)}}{\partial\boldsymbol{R}_f}+\boldsymbol{W}\cdot\frac{\partial p^{(s)}}{\partial\dot{\boldsymbol{R}}_f}\right).
\end{aligned}$$

The individual approximations (or corrections) $\varrho^{(r)}$ are calculated by applying Enskog's division of $\varrho(p)$ with $\varrho^{(0)} = 0$. These subdivisions are given by

$$\begin{aligned}\varrho^{(r)} &= \varrho^{(r)}(p^{(0)}, p^{(1)}, \cdots, p^{(r-1)}) \\ &= \frac{\partial_0 p^{(r-1)}}{\partial t} + \frac{\partial_1 p^{(r-2)}}{\partial t} + \cdots + \frac{\partial_{r-1} p^{(0)}}{\partial t} \\ &\quad + \boldsymbol{U} \cdot \frac{\partial p^{(r-1)}}{\partial \mathbf{r}} + \boldsymbol{V} \cdot \frac{\partial p^{(r-1)}}{\partial \boldsymbol{R}_f} + \boldsymbol{W} \cdot \frac{\partial p^{(r-1)}}{\partial \dot{\boldsymbol{R}}_f}. \end{aligned} \tag{6.44}$$

It remains to be shown that that the condition of solubility (6.29) determined above as

$$\int \varrho^{(r)} \psi^{(i)} d\boldsymbol{R}_f d\dot{\boldsymbol{R}}_f = 0$$

is fulfilled here. Before proving this, it should be remembered that in (6.27), $\alpha^{(1,r)}$, $\alpha^{(2,r)}$, $\alpha^{(3,r)}$ and $\alpha^{(4,r)}$ were specifically selected such that

$$\overline{\psi^{(i)}}^{(r)} = 0 \qquad (r > 0). \tag{6.45}$$

Each of the cases apply to Equation (5.53). If $\psi = m$ then $\overline{\psi}^{(0)} = m$ and, by (6.45), $\overline{\psi}^{(r)} = 0$. Also $\partial\phi/\partial \boldsymbol{R}_\Delta = 0$ and $\partial\phi/\partial \dot{\boldsymbol{R}}_\Delta = 0$. Furthermore $D\phi/Dt = 0, \partial\phi/\partial\mathbf{r} = 0$ and finally $\Delta\overline{\phi} = 0$. Substituting these results into (5.53), Equation (5.53) reduces to

$$\begin{aligned}\int \phi\varrho(p) d\boldsymbol{R}_f d\dot{\boldsymbol{R}}_f &= \sum_{r=0}^{\infty} \int \phi\varrho^{(r)} d\boldsymbol{R}_f d\dot{\boldsymbol{R}}_f = \sum_{r=0}^{\infty} \frac{\partial_r \rho_n \overline{\psi}}{\partial t} - \dot{\boldsymbol{R}}_\mu \cdot \frac{\partial \rho_n \overline{\psi}}{\partial \mathbf{r}} \\ &= \frac{D_0 \rho_n m}{Dt} - \frac{\rho}{2} \cdot \frac{\partial}{\partial \mathbf{r}} \dot{\boldsymbol{R}}_\mu + \sum_{r=1}^{\infty} \frac{\partial_r \rho_n m}{\partial t} \\ &= \int \psi^{(1)} \varrho^{(0)} \, d\boldsymbol{R}_f \, d\dot{\boldsymbol{R}}_{\boldsymbol{f}} + \sum_{r=1}^{\infty} \int \psi^{(1)} \varrho^{(r)} \, d\boldsymbol{R}_f \, d\dot{\boldsymbol{R}}_f \end{aligned}$$

where (for $r = 0$)

$$\int \psi^{(1)} \varrho^{(0)} d\boldsymbol{R}_f d\dot{\boldsymbol{R}}_f = \frac{D_0 \rho_n m}{Dt} - \frac{\dot{\boldsymbol{R}}_\mu}{2} \cdot \frac{\partial}{\partial \mathbf{r}} \rho \tag{6.46}$$

and

$$\int \psi^{(1)} \varrho^{(r)} d\boldsymbol{R}_f d\dot{\boldsymbol{R}}_f = \frac{\partial_r \rho_n m}{\partial t} \qquad (r > 0). \tag{6.47}$$

Similarly for $\psi^{(2)} = K\boldsymbol{R}_f$,

$$\int \psi^{(2)}\varrho^{(0)}d\boldsymbol{R}_f d\dot{\boldsymbol{R}}_f = -\frac{1}{2}\frac{\partial}{\partial \mathbf{r}}\cdot\partial_t \mathbf{P}_S^{(0)} + \rho_n K\frac{D_0\boldsymbol{R}_\mu}{Dt} + \rho_n K\dot{\boldsymbol{F}}, \quad (6.48)$$

$$\int \psi^{(2)}\varrho^{(r)}d\boldsymbol{R}_f d\dot{\boldsymbol{R}}_f = -\frac{1}{2}\frac{\partial}{\partial \mathbf{r}}\cdot\partial_t \mathbf{P}_S^{(r)} + \rho_n K\frac{\partial_r\boldsymbol{R}_\mu}{\partial t} \qquad (r>0). \quad (6.49)$$

For the case $\psi^{(3)} = m\mathbf{c}$,

$$\int \psi^{(3)}\varrho^{(0)}d\boldsymbol{R}_f d\dot{\boldsymbol{R}}_f = -2\frac{\partial}{\partial \mathbf{r}}\cdot\mathbf{P}_D^{(0)} - \rho\Big(\frac{\boldsymbol{F}}{m} - \frac{1}{2}\frac{D_0\dot{\boldsymbol{R}}_\mu}{Dt}\Big), \quad (6.50)$$

$$\int \psi^{(3)}\varrho^{(r)}d\boldsymbol{R}_f d\dot{\boldsymbol{R}}_f = -2\frac{\partial}{\partial \mathbf{r}}\cdot\mathbf{P}_D^{(r)} + \frac{\rho}{2}\frac{\partial_r\dot{\boldsymbol{R}}_\mu}{\partial t} \qquad (r>0). \quad (6.51)$$

For the case $\psi^{(4)} = KR_f^2/2$,

$$\begin{aligned}\int \psi^{(4)}\varrho^{(0)}d\boldsymbol{R}_f d\dot{\boldsymbol{R}}_f &= \frac{1}{2}\rho_n k\frac{D_0\mathrm{T}(\lambda^2-3)}{Dt} - \frac{1}{2}\partial_t\mathbf{P}_S^{(0)} : \frac{\partial}{\partial\mathbf{r}}\boldsymbol{R}_\mu \\ &\quad -\rho_n kT(\lambda^2-3)\frac{\partial}{\partial\mathbf{r}}\cdot\frac{\boldsymbol{R}_\mu}{2}, \quad (6.52)\\ \int \psi^{(4)}\varrho^{(r)}d\boldsymbol{R}_f d\dot{\boldsymbol{R}}_f &= \frac{1}{2}\rho_n k\frac{\partial_r\mathrm{T}(\lambda^2-3)}{\partial t} - \frac{1}{2}\partial_t\mathbf{P}_S^{(r)} : \frac{\partial}{\partial\mathbf{r}}\boldsymbol{R}_\mu \\ &\quad +\frac{\partial}{\partial\mathbf{r}}\cdot\boldsymbol{\Psi}^{(r)} \qquad (r>0), \quad (6.53)\end{aligned}$$

and finally, for the case $\psi^{(5)} = mc^2/2$,

$$\begin{aligned}\int \psi^{(5)}\varrho^{(0)}d\boldsymbol{R}_f d\dot{\boldsymbol{R}}_f &= k\rho_n\frac{N}{2}\frac{D_0\mathrm{T}}{Dt} - \frac{k\rho_n}{2}\frac{\partial\mathrm{T}(\lambda^2-3)}{\partial t} \\ &\quad -\rho_n kT\frac{N}{2}\frac{\partial}{\partial\mathbf{r}}\cdot\frac{\dot{\boldsymbol{R}}_\mu}{2} + \mathbf{P}_D^{(0)} : \frac{\partial}{\partial\mathbf{r}}\frac{\dot{\boldsymbol{R}}_\mu}{2}, \quad (6.54)\\ \int \psi^{(5)}\varrho^{(r)}d\boldsymbol{R}_f d\dot{\boldsymbol{R}}_f &= k\rho_n\frac{N}{2}\frac{\partial_r\mathrm{T}}{\partial t} + \frac{\partial}{\partial\mathbf{r}}\cdot\mathbf{q}^{(r)} \\ &\quad +\mathbf{P}_D^{(r)} : \frac{\partial}{\partial\mathbf{r}}\frac{\dot{\boldsymbol{R}}_\mu}{2} \qquad (r>0). \quad (6.55)\end{aligned}$$

Substituting Equations (6.38) through (6.42) into Equations (6.46) to (6.55), it is found that each of the integrals equals zero. Therefore the equivalent of Enskog's expansion of $\varrho(p)$ satisfies the condition of solubility (6.31) and consequently the condition of solubility, (6.29).

Further consider that R_{rms}, which can be calculated from Equation (3.37), is independent of temperature. As the internal energy of a material increases,

the volume changes. Clearly volume is a function of R_{rms} and thus

$$\frac{DR_{rms}^{3/2}}{R_{rms}^{3/2}} = \frac{D\mathrm{V}}{\mathrm{V}} \tag{6.56}$$

Let β be the isobaric thermal expansion coefficient [41]. By definition

$$\begin{aligned} \frac{1}{R_{rms}^{N/2}}\frac{DR_{rms}^{N/2}}{D\mathrm{T}} &= \frac{1}{\mathrm{V}}\frac{D\mathrm{V}}{D\mathrm{T}} = \beta = \frac{D\ln \mathrm{V}}{D\mathrm{T}} = \frac{D\ln(m/\rho)}{DT} = -\frac{D\ln\rho}{DT} \\ \iff \qquad & \frac{1}{\rho}\frac{D\rho}{Dt} = -\beta\frac{D\mathrm{T}}{Dt}. \end{aligned} \tag{6.57}$$

From Equation (6.57) and the conservation of mass equation,

$$\begin{aligned} & & \frac{D_0\mathrm{T}}{Dt} &= -\frac{1}{\beta\rho}\frac{D_0\rho}{Dt} = -\frac{1}{\beta\rho}\rho\frac{\partial}{\partial\mathbf{r}}\cdot\frac{\dot{\boldsymbol{R}}_\mu}{2} \\ \iff & \frac{D_0\ln\mathrm{T}}{Dt} = -\frac{1}{\beta\mathrm{T}}\frac{D_0\ln\rho}{Dt} & \iff \quad \frac{N}{2}\frac{D_0\ln\mathrm{T}}{Dt} &= -\frac{N}{\beta 2\mathrm{T}}\frac{D_0\ln\rho}{Dt} \\ \iff & \frac{D_0\ln\rho}{Dt} - \frac{N}{2}\frac{D_0\ln\mathrm{T}}{Dt} &= \frac{D_0\ln\rho}{Dt} + \frac{N}{\beta 2\mathrm{T}}\frac{D_0\ln\rho}{Dt} \\ \iff & \frac{D_0\ln\rho/\mathrm{T}^{(\mathrm{N}/2)}}{Dt} &= \left(1+\frac{N}{\beta 2\mathrm{T}}\right)\frac{D_0\ln\rho}{Dt} \\ \iff & \frac{\mathrm{T}^{\mathrm{N}/2}}{\rho}\frac{D_0\rho/\mathrm{T}^{N/2}}{Dt} &= \left(1+\frac{N}{\beta 2\mathrm{T}}\right)\frac{D_0\ln\rho}{Dt}. \end{aligned} \tag{6.58}$$

Substituting Equation (6.43) into (6.58), it is found that

$$\frac{\mathrm{T}^{N/2}}{\rho}\frac{D_0}{Dt}\left(\frac{\rho}{\mathrm{T}^{N/2}}\right) = 0 = \left(1+\frac{N}{\beta 2\mathrm{T}}\right)\frac{D_0\ln\rho}{Dt} \iff \left(1+\frac{N}{\beta 2\mathrm{T}}\right) = 0. \tag{6.59}$$

From the conservation of mass equation (5.56) one can conclude that

$$\beta = -\frac{N}{2\mathrm{T}} < 0 \qquad \text{and} \qquad \frac{D_0\mathrm{T}}{Dt} = \frac{2\mathrm{T}}{N}\frac{\partial}{\partial\mathbf{r}}\cdot\frac{\dot{\boldsymbol{R}}_\mu}{2}. \tag{6.60}$$

Substituting the result for β in Equation (6.60) into (6.57), it is evident that density increases and volume decreases with temperature and that, consequently, pressure increases with temperature.

Given that the condition of solubility for the CE expansion have been satisfied, Equations (5.61) and (5.60) can be re-arranged such that

$$\frac{1}{2}\frac{D\dot{\boldsymbol{R}}_\mu}{Dt} - \frac{\boldsymbol{F}}{m} = \frac{2}{\rho}\frac{\partial}{\partial\mathbf{r}}\cdot\mathbf{P}_D^{(0)} \qquad \text{and} \qquad \frac{\dot{\boldsymbol{F}}}{K} + \frac{D\boldsymbol{R}_\mu}{Dt} = \frac{1}{2\kappa}\frac{\partial}{\partial\mathbf{r}}\cdot\partial_t\mathbf{P}_S^{(0)}. \tag{6.61}$$

6.2 The first order approximation

The first order approximation to the polymer chain interaction term is given by Equation (6.44) and is

$$\varrho^{(1)} = \frac{\partial_0 p^{(0)}}{\partial t} + \boldsymbol{U} \cdot \frac{\partial p^{(0)}}{\partial \mathbf{r}} + \boldsymbol{V} \cdot \frac{\partial p^{(0)}}{\partial \boldsymbol{R}_f} + \boldsymbol{W} \cdot \frac{\partial p^{(0)}}{\partial \dot{\boldsymbol{R}}_f} \tag{6.62}$$

where from Equation (3.85),

$$\boldsymbol{U} = \frac{\Delta \boldsymbol{p}}{m} - \frac{1}{2}\dot{\boldsymbol{R}}_f, \;\; \boldsymbol{V} = -\frac{\dot{\boldsymbol{F}}}{K}, \text{ and } \boldsymbol{W} = 2\Big(\frac{\boldsymbol{K}}{m}\boldsymbol{R}_f - (\frac{\boldsymbol{F}}{m} + \frac{\boldsymbol{K}}{m}\boldsymbol{R}_\mu)\Big).$$

From (5.55) this can be re-interpreted as

$$\begin{aligned}
\varrho^{(1)} \;=\; & \frac{Dp^{(0)}}{Dt} - 2\left(\frac{\boldsymbol{F}}{m} - \frac{D\frac{\dot{\boldsymbol{R}}_\mu}{2}}{Dt}\right) \cdot \frac{\partial p^{(0)}}{\partial \dot{\boldsymbol{R}}_\Delta} - \frac{D\boldsymbol{R}_\mu}{Dt} \cdot \frac{\partial p^{(0)}}{\partial \boldsymbol{R}_\Delta} \\
& -(\frac{\dot{\boldsymbol{F}}}{K}) \cdot \frac{\partial p^{(0)}}{\partial \boldsymbol{R}_\Delta} + \boldsymbol{Q} \cdot \frac{\partial p^{(0)}}{\partial \mathbf{r}} + 2\frac{K}{m}\boldsymbol{R}_\Delta \cdot \frac{\partial p^{(0)}}{\partial \dot{\boldsymbol{R}}_\Delta} \\
& -\frac{\partial p^{(0)}}{\partial \dot{\boldsymbol{R}}_\Delta} \cdot (\boldsymbol{Q} \cdot \frac{\partial}{\partial \mathbf{r}})\dot{\boldsymbol{R}}_\mu - \frac{\partial p^{(0)}}{\partial \boldsymbol{R}_\Delta} \cdot (\boldsymbol{Q} \cdot \frac{\partial}{\partial \mathbf{r}})\boldsymbol{R}_\mu.
\end{aligned} \tag{6.63}$$

After substituting Equations (6.61) into (6.63),

$$\begin{aligned}
\varrho^{(1)} \;=\; & \frac{Dp^{(0)}}{Dt} + \frac{4}{\rho}\frac{\partial}{\partial \mathbf{r}} \cdot \mathbf{P}_D^{(0)} \cdot \frac{\partial p^{(0)}}{\partial \dot{\boldsymbol{R}}_\Delta} - \frac{1}{2\kappa}\frac{\partial}{\partial \boldsymbol{R}_\Delta} \cdot \partial_t \mathbf{P}_S^{(0)} \cdot \frac{\partial p^{(0)}}{\partial \boldsymbol{R}_\Delta} \\
& +\boldsymbol{C} \cdot \frac{\partial p^{(0)}}{\partial \mathbf{r}} + 2\frac{K}{m}\boldsymbol{R}_\Delta \cdot \frac{\partial p^{(0)}}{\partial \dot{\boldsymbol{R}}_\Delta} - \frac{\partial p^{(0)}}{\partial \dot{\boldsymbol{R}}_\Delta} \cdot (\boldsymbol{C} \cdot \frac{\partial}{\partial \mathbf{r}})\dot{\boldsymbol{R}}_\mu \\
& -\frac{\partial p^{(0)}}{\partial \boldsymbol{R}_\Delta} \cdot (\boldsymbol{C} \cdot \frac{\partial}{\partial \mathbf{r}})\boldsymbol{R}_\mu.
\end{aligned} \tag{6.64}$$

Also (6.64) can be restated as,

$$\begin{aligned}
\varrho^{(1)} \;=\; & p^{(0)}\Bigg[\frac{D\ln p^{(0)}}{Dt} + \frac{4}{\rho}\frac{\partial}{\partial \mathbf{r}} \cdot \mathbf{P}_D^{(0)} \cdot \frac{\partial \ln p^{(0)}}{\partial \dot{\boldsymbol{R}}_\Delta} - \frac{1}{2\kappa}\frac{\partial}{\partial \boldsymbol{R}_\Delta} \cdot \partial_t \mathbf{P}_S^{(0)} \cdot \frac{\partial \ln p^{(0)}}{\partial \boldsymbol{R}_\Delta} \\
& +\boldsymbol{C} \cdot \frac{\partial \ln p^{(0)}}{\partial \mathbf{r}} + 2\frac{K}{m}\boldsymbol{R}_\Delta \cdot \frac{\partial \ln p^{(0)}}{\partial \dot{\boldsymbol{R}}_\Delta} \\
& -\frac{\partial \ln p^{(0)}}{\partial \dot{\boldsymbol{R}}_\Delta} \cdot (\boldsymbol{C} \cdot \frac{\partial}{\partial \mathbf{r}})\dot{\boldsymbol{R}}_\mu - \frac{\partial \ln p^{(0)}}{\partial \boldsymbol{R}_\Delta} \cdot (\boldsymbol{C} \cdot \frac{\partial}{\partial \mathbf{r}})\boldsymbol{R}_\mu\Bigg].
\end{aligned} \tag{6.65}$$

Seven terms are present within the brackets in Equation (6.65). Considerable manipulation is required. Consequently (for ease of understanding) the terms

will be evaluated independently. Equation (3.71), that is

$$p^{(ms)} = p^{(0)} = \frac{b^3}{\pi^{\frac{3}{2}}} e^{-b^2(\boldsymbol{R}_f - \boldsymbol{R}_\mu)^2} \times \rho_n \Big(\frac{m}{2\pi k\mathrm{T}}\Big)^{\frac{3}{2}} e^{-\frac{m}{2k\mathrm{T}}(\dot{c}-\dot{c}_0)^2},$$

is substituted into the term $\ln p^{(0)}$ to give

$$\ln p^{(0)} = A - b^2(R_f - R_\mu)^2 + \ln \frac{\rho_n}{\mathrm{T}^{3/2}} - \frac{mC^2}{2k\mathrm{T}} \tag{6.66}$$

for $N = 3$. The first term is $D \ln p^{(0)}/Dt$. Given that b is assumed independent of T and using the result (6.59), the first term equates to

$$\frac{D_0 \ln p^{(0)}}{Dt} = \frac{mC^2}{2k\mathrm{T}^2} \frac{D_0\mathrm{T}}{Dt}$$

which after substitution of Equation (6.60) reduces to

$$\frac{D_0 \ln p^{(0)}}{Dt} = -\frac{mC^2}{3k\mathrm{T}} \frac{\partial}{\partial \mathbf{r}} \cdot \frac{\dot{\boldsymbol{R}}_\mu}{2}.$$

Furthermore, from Equation (6.66)

$$\frac{\partial_0 \ln p^{(0)}}{\partial \dot{\boldsymbol{R}}_\Delta} = \frac{\partial_0 \ln p^{(0)}}{\partial \mathbf{C}} \frac{\partial \boldsymbol{C}}{\partial \boldsymbol{R}_\Delta} = \frac{1}{2} \frac{m\boldsymbol{C}}{k\mathrm{T}} = -\frac{1}{4} \frac{m\dot{\boldsymbol{R}}_\Delta}{k\mathrm{T}}$$

and consequently the sixth term reduces to

$$-\frac{m}{k\mathrm{T}} \boldsymbol{C}\boldsymbol{C} : \frac{\partial}{\partial \mathbf{r}} \frac{\dot{\boldsymbol{R}}_\mu}{2}.$$

The sum of the first and sixth terms is

$$\frac{m}{k\mathrm{T}} \frac{\partial}{\partial \mathbf{r}} \frac{\dot{\boldsymbol{R}}_\mu}{2} : [\boldsymbol{C}\boldsymbol{C} - \frac{1}{3} C^2 \mathbf{I}] = 2 \frac{\partial}{\partial \mathbf{r}} \dot{\boldsymbol{R}}_\mu : [\dot{\boldsymbol{\omega}}\dot{\boldsymbol{\omega}} - \frac{1}{3} \dot{\omega}^2 \mathbf{I}] \tag{6.67}$$

where $\dot{\omega} = \Big(\frac{m}{2k\mathrm{T}}\Big)^{1/2} \boldsymbol{C} = \Big(\frac{m}{2k\mathrm{T}}\Big)^{1/2} (\frac{\Delta \boldsymbol{p}}{m} - \frac{1}{2}\dot{\boldsymbol{R}}_\Delta)$ where the volume is sufficiently small to only contain one or two molecule. For the one molecule case, $\Delta \boldsymbol{p} = 0$. For interacting molecules, 2 molecules exist in the volume and therefore $\Delta \boldsymbol{p} = 0$ for those molecules and $\dot{\omega} = -\Big(\frac{m}{2k\mathrm{T}}\Big)^{1/2} (\frac{1}{2}\dot{\boldsymbol{R}}_\Delta)$.

Next consider the seventh term. From Equation (6.66)

$$-\frac{\partial \ln p^{(0)}}{\partial \boldsymbol{R}_\Delta} = 2b^2 \boldsymbol{R}_\Delta$$

and the seventh term reduces to

$$\begin{aligned}
+2b^2\boldsymbol{R}_\Delta\boldsymbol{C}:\frac{\partial}{\partial\mathbf{r}}\boldsymbol{R}_\mu &= -\frac{1}{2}b^2\frac{\partial}{\partial t}\Big(\boldsymbol{R}_\Delta\boldsymbol{R}_\Delta\Big):\frac{\partial}{\partial\mathbf{r}}\boldsymbol{R}_\mu = -b^2\frac{\partial}{\partial t}\Big(\boldsymbol{R}_\Delta\boldsymbol{R}_\Delta\Big):\frac{\partial}{\partial\mathbf{r}}\frac{\boldsymbol{R}_\mu}{2}\\
&\quad+\frac{b^2}{3}\frac{\partial}{\partial t}\Big(R_\Delta^2\Big)\frac{\partial}{\partial\mathbf{r}}\cdot\frac{\boldsymbol{R}_\mu}{2}-\frac{b^2}{3}\frac{\partial}{\partial t}\Big(R_\Delta^2\Big)\frac{\partial}{\partial\mathbf{r}}\cdot\frac{\boldsymbol{R}_\mu}{2}\\
&= -\frac{\partial}{\partial t}\Big(b^2\boldsymbol{R}_\Delta\boldsymbol{R}_\Delta-\frac{b^2}{3}R_\Delta^2\mathbf{I}\Big):\frac{\partial}{\partial\mathbf{r}}\frac{\boldsymbol{R}_\mu}{2}\\
&\quad-\frac{b^2}{3}\frac{\partial}{\partial t}\Big(R_\Delta^2\Big)\frac{\partial}{\partial\mathbf{r}}\cdot\frac{\boldsymbol{R}_\mu}{2}\\
&= -\frac{\partial}{\partial t}(\boldsymbol{\zeta}\boldsymbol{\zeta}-\mathbf{I}\frac{\zeta^2}{3}):\frac{\partial}{\partial\mathbf{r}}\frac{\boldsymbol{R}_\mu}{2}-\frac{b^2}{3}\frac{\partial}{\partial t}\Big(R_\Delta^2\Big)\frac{\partial}{\partial\mathbf{r}}\cdot\frac{\boldsymbol{R}_\mu}{2}
\end{aligned}$$

where $\boldsymbol{\zeta}:=b\boldsymbol{R}_\Delta$. Given that at the maximum entropy state variables do not change with respect to time, $\partial\mathbf{P}_S/\partial t=\mathbf{0}$. Adding terms 3, and 5 to term 7,

$$\begin{aligned}
&-\frac{\partial}{\partial t}(\boldsymbol{\zeta}\boldsymbol{\zeta}-\mathbf{I}\frac{\zeta^2}{3}):\frac{\partial}{\partial\mathbf{r}}\boldsymbol{R}_\mu-\frac{b^2}{3}\frac{\partial}{\partial t}\Big(R_\Delta^2\Big)\frac{\partial}{\partial\mathbf{r}}\cdot\boldsymbol{R}_\mu-\frac{K}{4k\mathrm{T}}\frac{\partial}{\partial t}R_\Delta^2\\
&= -\frac{\partial}{\partial t}(\boldsymbol{\zeta}\boldsymbol{\zeta}-\mathbf{I}\frac{\zeta^2}{3}):\frac{\partial}{\partial\mathbf{r}}\boldsymbol{R}_\mu+\Big(\frac{K}{4kb^2\mathrm{T}}-\frac{1}{3}\frac{\partial}{\partial\mathbf{r}}\cdot\boldsymbol{R}_\mu\Big)\frac{\partial}{\partial t}\zeta^2. \qquad (6.68)
\end{aligned}$$

But

$$\begin{aligned}
\Big(\frac{2k\mathrm{T}}{m}\Big)^{1/2}\dot{\boldsymbol{\omega}}=-\frac{1}{2}\dot{\boldsymbol{R}}_\Delta=-\frac{\dot{\boldsymbol{\zeta}}}{2b} &\iff \Big(\frac{m}{8k\mathrm{T}b^2}\Big)^{-1/2}\dot{\boldsymbol{\omega}}=-\dot{\boldsymbol{\zeta}}\\
&\iff -\Big(\frac{m}{8k\mathrm{T}b^2}\Big)^{-1/2}\boldsymbol{\omega}=\boldsymbol{\zeta}.
\end{aligned}$$

Consequently (6.68) reduces to

$$\frac{8k\mathrm{T}b^2}{m}\Bigg(-\frac{\partial}{\partial t}(\boldsymbol{\omega}\boldsymbol{\omega}-\mathbf{I}\frac{\omega^2}{3}):\frac{\partial}{\partial\mathbf{r}}\boldsymbol{R}_\mu+\Big(\frac{K}{4kb^2\mathrm{T}}-\frac{1}{3}\frac{\partial}{\partial\mathbf{r}}\cdot\boldsymbol{R}_\mu\Big)\frac{\partial}{\partial t}\omega^2\Bigg).$$

An assumption must be made before considering terms 2 and 4. In Section 6.1.5 the assumption of hydrostatic change in dynamic pressure tensor, namely

$$\mathbf{P}_D^{(0)}=p_d\mathbf{I}$$

was made with Equation (6.40) postulating that

$$p_d=-\rho_n kT.$$

Equation (5.66) presented the assumption that the kinetic energy is given by

$$\frac{1}{\rho_n}\sum_{\rho_n}\frac{1}{2}mC^2=\frac{1}{\rho_n}\sum_{\rho_n}\frac{1}{2}m\frac{1}{4}\dot{R}_\Delta^2=\frac{1}{8\rho_n}\rho\overline{\dot{R}_\Delta^2}=\frac{1}{8\rho_n}\rho\dot{R}_{rms}^2=\frac{3}{2}kT$$

where k is the Boltzmann constant and Equation (3.36) is used to introduce the root mean square – reflecting that longitudinal (along the molecule) stretch rates are slower when the temperature is higher or conversely that reduced longitudinal vibration contributes to temperature.

Although the above appears counterintuitive, recall that the reduction in longitudinal vibration is due to an increase in transverse vibration as discussed in Section 6.1.5 and depicted in Figure 6.1. Thus a temperature increase does increase vibration – but in the transverse direction. This is a consequence of this model being a variant of Kuhn's rigid link model as discussed in Section 1.3.

Thus

$$\begin{aligned} \frac{1}{12}\rho\dot{R}_{rms}^2 &= \frac{1}{3}\Big(2\times\frac{1}{8}\Big)\rho\overline{\dot{R}_\Delta^2} = k\rho_n\mathrm{T} \Longleftrightarrow p_d = -\frac{1}{12}\rho\dot{R}_{rms}^2 \qquad (6.69)\\ \mathbf{P}_D^{(0)} &= -k\rho_n\mathrm{T}\mathbf{I} = -\frac{1}{12}\rho\dot{R}_{rms}^2\mathbf{I}. \qquad (6.70)\end{aligned}$$

Adding terms 2 and 4 and substituting Equation (6.70),

$$\begin{aligned} &\frac{1}{4}\frac{2}{\rho}\frac{\partial k\rho_n\mathrm{T}}{\partial\mathbf{r}}\cdot\frac{m}{k\mathrm{T}}\dot{\boldsymbol{R}}_\Delta + \boldsymbol{C}\cdot\frac{\partial\ln p^{(0)}}{\partial\mathbf{r}}\\ =\;& \frac{1}{\rho_n m}\frac{\partial k\rho_n\mathrm{T}}{\partial\mathbf{r}}\cdot\frac{m}{k\mathrm{T}}\frac{\dot{\boldsymbol{R}}_\Delta}{2} - \frac{1}{2}\dot{\boldsymbol{R}}_\Delta\cdot\frac{\partial\ln p^{(0)}}{\partial\mathbf{r}} = -\frac{\dot{\boldsymbol{R}}_\Delta}{2}\cdot\Big(\frac{\partial\ln(p^{(0)}/\rho_n k\mathrm{T})}{\partial\mathbf{r}}\Big)\\ =\;& -\frac{\dot{\boldsymbol{R}}_\Delta}{2}\cdot\Big(\frac{\partial\ln\mathrm{T}^{-5/2}}{\partial\mathbf{r}} + \frac{m\boldsymbol{C}^2}{2k\mathrm{T}^2}\frac{\partial\mathrm{T}}{\partial\mathbf{r}}\Big) = \frac{1}{2}\Big(\frac{5}{2} - \frac{m\frac{\dot{\boldsymbol{R}}_\Delta^2}{4}}{2k\mathrm{T}}\Big)\dot{\boldsymbol{R}}_\Delta\cdot\frac{\partial\ln\mathrm{T}}{\partial\mathbf{r}}\\ =\;& \Big(\frac{5}{4} - \frac{\dot{\omega}^2}{2}\Big)\dot{\boldsymbol{R}}_\Delta\cdot\frac{\partial\ln\mathrm{T}}{\partial\mathbf{r}}. \qquad (6.71)\end{aligned}$$

The third term requires knowledge of $\mathbf{P}_S^{(0)}$. The pressure component will be the change in force over area. The change in pressure due to a molecule for an incompressible material ($\lambda_1\lambda_2\lambda_3 = 1$) would be

$$\Delta p_s = \frac{\kappa}{4}R_{\mu 0}^2\Big(\frac{\lambda_i}{\lambda_k\lambda_j} - 3\Big) = \frac{\kappa}{4}R_{\mu 0}^2(\lambda_i^2 - 3) \qquad (6.72)$$

and

$$-\frac{\rho_0}{4\kappa}\frac{\partial}{\partial\boldsymbol{R}_\Delta}\cdot\partial_t\mathbf{P}_S^{(0)}\cdot\frac{\partial\ln p^{(0)}}{\partial\boldsymbol{R}_\Delta} = \frac{b^2}{4}\rho_0^2R_{\mu 0}\frac{\partial}{\partial t}(\lambda_1^2+\lambda_2^2+\lambda_3^2) = \rho_0\Xi \qquad (6.73)$$

where $\Xi = \frac{b^2}{4}R_{\mu 0}^2\frac{\partial}{\partial t}(\lambda_1^2+\lambda_2^2+\lambda_3^2)$.

Substituting (6.67), (6.68), (6.71) and (6.73) into Equation (6.65),

$$\begin{aligned}\varrho^{(1)} &= p^{(0)}\Bigg[\Xi+\Big(\frac{5}{2}-\dot\omega^2\Big)\frac{\dot{\boldsymbol{R}}_\Delta}{2}\cdot\frac{\partial\ln T}{\partial\mathbf{r}}+2[\dot{\boldsymbol{\omega}}\dot{\boldsymbol{\omega}}-\frac{1}{3}\dot\omega^2\mathbf{I}]:\frac{\partial}{\partial\mathbf{r}}\dot{\boldsymbol{R}}_\mu\\ &\quad-\frac{8kTb^2}{m}\frac{\partial}{\partial t}(\boldsymbol{\omega\omega}-\boldsymbol{I}\frac{\omega^2}{3}):\frac{\partial}{\partial\mathbf{r}}\boldsymbol{R}_\mu\\ &\quad+\frac{8kTb^2}{m}\Big(\frac{K}{4kb^2T}-\frac{1}{3}\frac{\partial}{\partial\mathbf{r}}\cdot\boldsymbol{R}_\mu\Big)\frac{\partial}{\partial t}\omega^2\Bigg].\end{aligned}\tag{6.74}$$

Expanding J as described by (6.8) and substituting (6.24) and (6.23),

$$\begin{aligned}J^{(1)} &= J(p^{(0)}p_1^{(1)})+J(p_1^{(0)}p^{(1)})\\ &= J(p^{(0)}p_1^{(0)}\phi_1^{(1)})+J(p_1^{(0)}p^{(0)}\phi^{(1)})=\rho_n^2I(\phi^{(1)}).\end{aligned}\tag{6.75}$$

Substituting (6.75) into Equation (6.12),

$$\begin{aligned}\rho_n^2I(\phi^{(1)}) &= p^{(0)}\Bigg[\Xi+\Big(\frac{5}{2}-\dot\omega^2\Big)\frac{\dot{\boldsymbol{R}}_\Delta}{2}\cdot\frac{\partial\ln\mathrm{T}}{\partial\mathbf{r}}+2[\dot{\boldsymbol{\omega}}\dot{\boldsymbol{\omega}}-\frac{1}{3}\dot\omega^2\boldsymbol{I}]:\frac{\partial}{\partial\mathbf{r}}\dot{\boldsymbol{R}}_\mu\\ &\quad-\frac{8k\mathrm{T}b^2}{m}\frac{\partial}{\partial t}(\boldsymbol{\omega\omega}-\boldsymbol{I}\frac{\omega^2}{3}):\frac{\partial}{\partial\mathbf{r}}\boldsymbol{R}_\mu\\ &\quad+\frac{8k\mathrm{T}b^2}{m}\Big(\frac{K}{4kb^2\mathrm{T}}-\frac{1}{3}\frac{\partial}{\partial\mathbf{r}}\cdot\boldsymbol{R}_\mu\Big)\frac{\partial}{\partial t}\omega^2\Bigg].\end{aligned}\tag{6.76}$$

In order to obtain the desired scalar solution for $\phi^{(1)}$, the form of $\phi^{(1)}$ must be

$$\begin{aligned}\phi^{(1)} &= \frac{1}{\rho_n}\Big(\frac{2k\mathrm{T}}{m}\Big)^{\frac{1}{2}}\mathbf{A}\cdot\frac{\partial\ln\mathrm{T}}{\partial\mathbf{r}}+\frac{1}{\rho_n}\mathbf{B}:\frac{\partial}{\partial\mathbf{r}}\dot{\boldsymbol{R}}_\mu\\ &\quad-\frac{1}{\rho_n}\frac{\partial}{\partial t}\mathbf{C}:\frac{\partial}{\partial\mathbf{r}}\boldsymbol{R}_\mu+\frac{D}{\rho_n}\frac{\partial}{\partial\mathbf{r}}\cdot\boldsymbol{R}_\mu+\alpha^{(1,r)}+\alpha^{(2,r)}\cdot K\boldsymbol{R}_\Delta\\ &\quad+\alpha^{3,r}\cdot m\dot{\boldsymbol{R}}_\Delta+\alpha^{(4,r)}(KR_\Delta^2+m\dot R_\Delta^2)\end{aligned}\tag{6.77}$$

where $\mathbf{A}$ is a vector, $\mathbf{B}$ is a tensor, $\mathbf{C}$ is a tensor, D is a scalar and, by (6.27), $\alpha^{(i,r)}$ have been selected such that the complementary solution equals 0. Also, the constants have been incorporated into $\alpha^{(1,r)}$. Substituting (6.77) into (6.76),

$$\begin{aligned}\rho_nI(\mathbf{A}) &= -p(\dot\omega^2-\frac{5}{2})\dot{\boldsymbol{\omega}}, & \rho_nI(\mathbf{B}) &= 2p[\dot{\boldsymbol{\omega}}\dot{\boldsymbol{\omega}}-\frac{1}{3}\dot\omega^2\mathbf{I}]\\ \rho_nI(\mathbf{C}) &= -p\frac{8k\mathrm{T}b^2}{m}\frac{\partial}{\partial t}[\boldsymbol{\omega\omega}-\frac{1}{3}\omega^2\mathbf{I}], & \rho_nI(D) &= p\frac{8k\mathrm{T}b^2}{3m}\frac{\partial}{\partial t}\omega^2\end{aligned}$$

and

$$\mathbf{B} = [\dot{\boldsymbol{\omega}}\dot{\boldsymbol{\omega}} - \frac{1}{3}\dot{\omega}^2\mathbf{I}]B(\dot{\boldsymbol{\omega}}), \qquad \mathbf{C} = \frac{\partial}{\partial t}[\boldsymbol{\omega}\boldsymbol{\omega} - \frac{1}{3}\omega^2\mathbf{I}]C(\boldsymbol{\omega})$$

where $B(\dot{\boldsymbol{\omega}})$ is a scalar function of $\rho_n, T, \dot{\boldsymbol{\omega}}$ and $C(\boldsymbol{\omega})$ is a scalar function of $\rho_n, T, b, \boldsymbol{\omega}$.

The energy components will not be considered further as they will not be used in the construction of the numerical method nor the continuum theory. The change in dynamic pressure tensor is determined to select the stress tensor in Chapter 7. Equation (6.77) has to be substituted for ϕ in (6.34) to determine the first order approximation to the dynamic pressure tensor,

$$\begin{aligned}
\mathbf{P}_D^{(1)} &= -\frac{1}{8}m\int p^{(1)}\dot{\boldsymbol{R}}_\Delta\dot{\boldsymbol{R}}_\Delta\, d\boldsymbol{R}_f\, d\dot{\boldsymbol{R}}_f = -\frac{1}{8}m\int p^{(0)}\phi^{(1)}\dot{\boldsymbol{R}}_\Delta\dot{\boldsymbol{R}}_\Delta\, d\boldsymbol{R}_f\, d\dot{\boldsymbol{R}}_f \\
&= -\frac{m}{\rho_n}\int p^{(0)}B(\dot{\boldsymbol{\omega}})\Big([\dot{\boldsymbol{\omega}}\dot{\boldsymbol{\omega}} - \frac{1}{3}\dot{\omega}^2\mathbf{I}] : \frac{\partial}{\partial\mathbf{r}}\dot{\boldsymbol{R}}_\mu\Big)\frac{\dot{\boldsymbol{R}}_\Delta}{2}\frac{\dot{\boldsymbol{R}}_\Delta}{2}\, d\boldsymbol{R}_f\, d\dot{\boldsymbol{R}}_f \\
&= -\frac{kT}{\rho_n}\int p^{(0)}B(\dot{\boldsymbol{\omega}})\Big([\dot{\boldsymbol{\omega}}\dot{\boldsymbol{\omega}} - \frac{1}{3}\dot{\omega}^2\mathbf{I}] : \frac{\partial}{\partial\mathbf{r}}\dot{\boldsymbol{R}}_{\boldsymbol{\mu}}\Big)\dot{\boldsymbol{\omega}}\dot{\boldsymbol{\omega}}\, d\boldsymbol{R}_f\, d\dot{\boldsymbol{R}}_f. \qquad (6.78)
\end{aligned}$$

Substituting the tensor integral results from Appendix A-5, with definitions provided in Appendix A-4, the above can be restated as

$$\mathbf{P}_D^{(1)} = -\frac{k\mathrm{T}}{5\rho_n}\int p^{(0)}B(\dot{\boldsymbol{\omega}})\Big([\dot{\boldsymbol{\omega}}\dot{\boldsymbol{\omega}} - \frac{1}{3}\dot{\omega}^2\mathbf{I}] : [\dot{\boldsymbol{\omega}}\dot{\boldsymbol{\omega}} - \frac{1}{3}\dot{\omega}^2\mathbf{I}]\Big)\overline{\overline{\frac{\partial}{\partial\mathbf{r}}\dot{\boldsymbol{R}}_\mu}}^{\circ}\, d\boldsymbol{R}_f\, d\dot{\boldsymbol{R}}_f.$$

Define the rate of deformation tensor by

$$\dot{D}_{ij} := -\frac{1}{4}\Big(\frac{\partial\dot{R}_{\mu i}}{\partial \mathrm{x_j}} + \frac{\partial\dot{R}_{\mu j}}{\partial \mathrm{x_i}}\Big) = \frac{1}{2}\Big(\frac{\partial \mathrm{c}_i}{\partial \mathrm{x_j}} + \frac{\partial \mathrm{c}_j}{\partial \mathrm{x_i}}\Big). \qquad (6.79)$$

Higher order approximations to (6.79) are allowed by the CE expansion but are not considered in this work. Substitution of (6.79) into (6.78) gives

$$\begin{aligned}
\mathbf{P}_D^{(1)} &= \frac{k\mathrm{T}}{5}\frac{4}{1}(\dot{\boldsymbol{D}} + \frac{1}{6}\nabla\cdot\dot{\boldsymbol{R}}_\mu\mathbf{I})\int p^{(0)}B(\dot{\boldsymbol{\omega}}) \\
&\quad \Big(\frac{1}{\rho_n}[\dot{\boldsymbol{\omega}}\dot{\boldsymbol{\omega}} - \frac{1}{3}\dot{\omega}^2\mathbf{I}]B(\dot{\boldsymbol{\omega}}) : [\dot{\boldsymbol{\omega}}\dot{\boldsymbol{\omega}} - \frac{1}{3}\dot{\omega}^2\mathbf{I}]B(\dot{\boldsymbol{\omega}})\Big)\, d\boldsymbol{R}_f\, d\dot{\boldsymbol{R}}_f \\
&= \frac{k\mathrm{T}}{5}\frac{4}{1}(\dot{\boldsymbol{D}} + \frac{1}{6}\nabla\cdot\dot{\boldsymbol{R}}_\mu\mathbf{I})\int p^{(0)}\frac{1}{\rho_n}[\dot{\boldsymbol{\omega}}\dot{\boldsymbol{\omega}} - \frac{1}{3}\dot{\omega}^2\mathbf{I}]B(\dot{\boldsymbol{\omega}}) : \mathbf{B}\, d\boldsymbol{R}_f\, d\dot{\boldsymbol{R}}_f \\
&= \frac{k\mathrm{T}}{5}\frac{4}{1}(\dot{\boldsymbol{D}} + \frac{1}{6}\nabla\cdot\dot{\boldsymbol{R}}_\mu\mathbf{I})\int I(\mathbf{B}) : \mathbf{B}\, d\boldsymbol{R}_f\, d\dot{\boldsymbol{R}}_f.
\end{aligned}$$

Define

$$\mu := -\frac{2}{5}k\mathrm{T}\int I(\mathbf{B}) : \mathbf{B}\, d\boldsymbol{R}_f\, d\dot{\boldsymbol{R}}_f, \qquad (6.80)$$

then

$$\mathbf{P}_D^{(1)} = -2\mu\Big(\dot{\boldsymbol{D}} + \frac{1}{6}\mathbf{I}(\nabla\cdot\dot{\boldsymbol{R}}_\mu)\Big). \tag{6.81}$$

Adding the zero-order hydrostatic pressure approximation (6.40)

$$\begin{aligned} 2P_{Dij} &= 2P_{Dij}^{(0)} - 4\mu\Big(\dot{D}_{ij} + \frac{1}{6}\delta_{ij}\nabla\cdot\dot{\boldsymbol{R}}_\mu\Big) \\ \text{or} \qquad 2\mathbf{P}_D &= 2p_d\mathbf{I} - 4\mu\left(\dot{\boldsymbol{D}} + \frac{1}{6}(\nabla\cdot\dot{\boldsymbol{R}}_\mu)\mathbf{I}\right) \end{aligned} \tag{6.82}$$

is the sum of the zero and first order approximation to the pressure tensor where μ is clearly the equivalent of the viscosity for a fluid.

The rate of change of static pressure tensor, $\partial\mathbf{P}_S/\partial t$, will be considered next. Equation (6.77) has to be substituted for ϕ in (6.34); this gives

$$\begin{aligned} \frac{\partial\mathbf{P}_S^{(1)}}{\partial t} &= \frac{K}{4}\int p^{(1)}\dot{\boldsymbol{R}}_\Delta\boldsymbol{R}_\Delta\,d\boldsymbol{R}_f\,d\dot{\boldsymbol{R}}_f = \frac{K}{4}\int p^{(0)}\boldsymbol{\phi^{(1)}}\dot{\boldsymbol{R}}_\Delta\boldsymbol{R}_\Delta\,d\boldsymbol{R}_f\,d\dot{\boldsymbol{R}}_f \\ &= -\frac{K}{4\rho_n}\int p^{(0)}C(\boldsymbol{\omega})\left(\frac{\partial}{\partial t}[\boldsymbol{\omega\omega} - \frac{1}{3}\omega^2\mathbf{I}] : \frac{\partial}{\partial\mathbf{r}}\boldsymbol{R}_\mu\right)\dot{\boldsymbol{R}}_\Delta\boldsymbol{R}_\Delta\,d\boldsymbol{R}_f\,d\dot{\boldsymbol{R}}_f \\ &= -\frac{K}{8\rho_n b^2}\int p^{(0)}C(\boldsymbol{\omega})\left(\frac{\partial}{\partial t}[\boldsymbol{\omega\omega} - \frac{1}{3}\omega^2\mathbf{I}] : \frac{\partial}{\partial\mathbf{r}}\boldsymbol{R}_\mu\right)\frac{\partial}{\partial t}(\boldsymbol{\zeta\zeta})\,d\boldsymbol{R}_f\,d\dot{\boldsymbol{R}}_f \\ &= -\frac{Kk\mathrm{T}}{\rho_n m}\int p^{(0)}C(\boldsymbol{\omega})\left(\frac{\partial}{\partial t}[\boldsymbol{\omega\omega} - \frac{1}{3}\omega^2\mathbf{I}] : \frac{\partial}{\partial\mathbf{r}}\boldsymbol{R}_\mu\right)\frac{\partial}{\partial t}(\boldsymbol{\omega\omega})\,d\boldsymbol{R}_f\,d\dot{\boldsymbol{R}}_f. \end{aligned}$$

Substituting the results from Appendix A-5, the above can be restated as

$$-\frac{Kk\mathrm{T}}{5\rho_n m}\int p^{(0)}C(\boldsymbol{\omega})\Big(\frac{\partial}{\partial t}[\boldsymbol{\omega\omega} - \frac{1}{3}\omega^2\boldsymbol{I}] : \frac{\partial}{\partial t}[\boldsymbol{\omega\omega} - \frac{1}{3}\omega^2\boldsymbol{I}]\Big)\overline{\overline{\frac{\partial}{\partial\mathbf{r}}\boldsymbol{R}_\mu}}^{\circ}d\boldsymbol{R}_f d\dot{\boldsymbol{R}}_f. \tag{6.83}$$

Define (where $\mathrm{v_k}(\mathbf{x})$ is the displacement vector)

$$D_{ij} := -\frac{1}{4}\Big(\frac{\partial R_{\mu i}}{\partial \mathrm{x_j}} + \frac{\partial R_{\mu j}}{\partial \mathrm{x_i}}\Big) = \frac{1}{2}\Big(\frac{\partial \mathrm{v_j}(\mathbf{x})}{\partial \mathrm{x_i}} + \frac{\partial \mathrm{v_i}(\mathbf{x})}{\partial \mathrm{x_j}}\Big) \tag{6.84}$$

which is recognised as the first-order approximation to the infinitesimal spatial strain tensor $\mathrm{e_{ij}^{(1)}}$ given by Equation (3.10). Again the qualifier 'first order' is in recognition that the CE expansion permits arbitrarily higher order approximation to be included. Furthermore Equation (3.11) allows one to recognise that

$$D_{ij} = e_{ij}^{(1)} \approx E_{ij}^{(1)}. \tag{6.85}$$

Substituting Equation (6.84) into expression (6.83),

$$\begin{aligned}\frac{\partial \mathbf{P}_S^{(1)}}{\partial t} &= \frac{4k\mathrm{T}K}{5\rho_n}\frac{1}{m}(\boldsymbol{D}+\frac{1}{6}(\nabla\cdot\boldsymbol{R}_\mu)\mathbf{I})\int p^{(0)}C(\boldsymbol{\omega})\\ &\quad\Big(\frac{\partial}{\partial t}[\boldsymbol{\omega\omega}-\frac{1}{3}\omega^2\mathbf{I}]C(\boldsymbol{\omega}):\frac{\partial}{\partial t}[\boldsymbol{\omega\omega}-\frac{1}{3}\omega^2\mathbf{I}]C(\boldsymbol{\omega})\Big)d\boldsymbol{R}_f d\dot{\boldsymbol{R}}_f\\ &= \frac{k\mathrm{T}K}{5}\frac{4}{m}(\boldsymbol{D}+\frac{1}{6}\nabla\cdot\boldsymbol{R}_\mu\mathbf{I})\\ &\quad\times\int p^{(0)}\frac{1}{\rho_n}\frac{\partial}{\partial t}[\boldsymbol{\omega\omega}-\frac{1}{3}\omega^2\mathbf{I}]C(\boldsymbol{\omega}):\frac{\partial}{\partial t}\mathbf{C}d\boldsymbol{R}_f d\dot{\boldsymbol{R}}_f\\ &= \frac{k\mathrm{T}K}{5}\frac{4}{m}(\boldsymbol{D}+\frac{1}{6}\nabla\cdot\boldsymbol{R}_\mu\mathbf{I})\int\frac{\partial}{\partial t}I(\mathbf{C}):\frac{\partial}{\partial t}\mathbf{C}d\mathbf{R}_f d\dot{\boldsymbol{R}}_f. \qquad (6.86)\end{aligned}$$

Define

$$G := -\frac{1}{10}\frac{k\mathrm{T}K}{m}\int\frac{\partial}{\partial t}I(\mathbf{C}):\frac{\partial}{\partial t}\mathbf{C}d\boldsymbol{R}_f d\dot{\boldsymbol{R}}_f; \qquad (6.87)$$

then substituting Equation (6.87) into (6.86),

$$\frac{1}{2}\frac{\partial \mathbf{P}_S^{(1)}}{\partial t} = -4G\Big(\boldsymbol{D}+\frac{1}{6}(\nabla\cdot\boldsymbol{R}_\mu)\mathbf{I}\Big) \qquad (6.88)$$

where $\boldsymbol{D}+\frac{1}{6}(\nabla\cdot\dot{\boldsymbol{R}}_\mu)\mathbf{I}$ can be interpreted as the shear strain combining the zero-order hydrostatic approximation (6.41) with the first-order approximation (6.88) to determine the approximate rate of change of static pressure tensor to first order

$$\frac{1}{2}\frac{\partial \mathrm{P}_{Sij}}{\partial t} = \frac{1}{2}\frac{\partial \mathrm{P}_{Sij}^{(0)}}{\partial t} - 4G\Big(D_{ij}+\frac{1}{6}\delta_{ij}\nabla\cdot\boldsymbol{R}_\mu\Big). \qquad (6.89)$$

Substituting Equation (6.82) into (5.61) one derives the equivalent of the Navier-Stokes equation (first order conservation of momentum) equation

$$\rho\Big(\frac{\partial}{\partial t}-\frac{\dot{\boldsymbol{R}}_{\boldsymbol{\mu}}}{2}\cdot\nabla\Big)\frac{\dot{\boldsymbol{R}}_{\boldsymbol{\mu}}}{2}-\frac{\rho}{m}\mathbf{F} = 2\nabla\cdot\mathbf{P}_D \qquad (6.90)$$

where the components of $\nabla\cdot\mathbf{P}_D$ are

$$\begin{aligned}2\frac{\partial \mathrm{P}_{Dij}}{\partial \mathrm{x_j}} &= 2\frac{\partial \mathrm{P}_{Dij}^{(0)}}{\partial \mathrm{x_i}}+\mu\Big(\nabla^2\dot{R}_{\mu i}-\frac{2}{3}\frac{\partial}{\partial \mathrm{x_j}}(\nabla\cdot\dot{\boldsymbol{R}}_\mu)\Big)\\ &\quad -4\frac{\partial\mu}{\partial \mathrm{x_j}}\Big(\dot{D}_{ij}+\frac{1}{6}\delta_{ij}\nabla\cdot\dot{\boldsymbol{R}}_\mu\Big)\\ \text{or}\qquad 2\frac{\partial \mathbf{P}_D}{\partial \mathbf{x}} &= 2\nabla\Big(p_d-\frac{\mu}{3}\nabla\cdot\dot{\boldsymbol{R}}_\mu\Big)-\mu\nabla^2\dot{\boldsymbol{R}}_\mu+\boldsymbol{\Pi}_D. \qquad (6.91)\end{aligned}$$

Substituting (6.91) into (6.90),

$$\rho\Big(\frac{\partial}{\partial t} - \frac{\dot{\boldsymbol{R}}_{\boldsymbol{\mu}}}{2}\cdot\nabla\Big)\dot{\boldsymbol{R}}_{\boldsymbol{\mu}} = \frac{\rho}{m}\mathbf{F} + 2\nabla\Big(p_d - \frac{\mu}{3}\nabla\cdot\dot{\boldsymbol{R}}_{\boldsymbol{\mu}}\Big) - \mu\nabla^2\dot{\boldsymbol{R}}_{\boldsymbol{\mu}} + \boldsymbol{\Pi}_D. \tag{6.92}$$

Let $p'_d = p_d - \frac{\mu}{3}\nabla\cdot\dot{\boldsymbol{R}}_{\boldsymbol{\mu}}$ and substitute the result into (6.92); then

$$\rho\Big(\frac{\partial}{\partial t} - \frac{\dot{\boldsymbol{R}}_{\boldsymbol{\mu}}}{2}\cdot\nabla\Big)\dot{\boldsymbol{R}}_{\boldsymbol{\mu}} = \frac{\rho}{m}\mathbf{F} + 2\nabla p'_d + 4\mu\nabla\cdot\dot{\boldsymbol{D}} + \boldsymbol{\Pi}_D \tag{6.93}$$

is recognised as being the same form as the Navier-Stokes equations.

Similarly, substituting Equation (6.89) into (5.60) one derives the conservation of force equation (conservation of momentum due to static component of stretch) to first order

$$\kappa\Big(\frac{\partial}{\partial t} - \frac{\dot{\boldsymbol{R}}_{\boldsymbol{\mu}}}{2}\cdot\nabla\Big)\boldsymbol{R}_{\boldsymbol{\mu}} + \kappa\frac{\dot{\mathbf{F}}}{K} = \frac{1}{2}\nabla\cdot\frac{\partial\mathbf{P}_S}{\partial t}$$

where the components of $\frac{1}{2}\nabla\cdot\partial\mathbf{P}_S/\partial t$ are

$$\frac{1}{2}\frac{\partial^2\mathrm{P}_{Sij}}{\partial\mathrm{x_j}\partial t} = \frac{1}{2}\frac{\partial^2\mathrm{P}_S^{(0)}}{\partial\mathrm{x_i}\partial t} + G\Big(\nabla^2 R_{\mu i} - \frac{2}{3}\frac{\partial}{\partial\mathrm{x_j}}(\nabla\cdot\boldsymbol{R}_\mu)\Big) - 4\frac{\partial G}{\partial\mathrm{x_j}}\Big(D_{ij} + \frac{1}{6}\delta_{ij}\nabla\cdot\boldsymbol{R}_\mu\Big)$$

or, in vector calculus notation,

$$\frac{1}{2}\nabla\cdot\Big(\frac{\partial\mathbf{P}_S}{\partial t}\Big) = \frac{1}{2}\nabla\cdot\Big(\frac{\partial\mathbf{P}_S^{(0)}}{\partial t}\Big) - \nabla\Big(\frac{4G}{3}\nabla\cdot\boldsymbol{R}_\mu\Big) + G\nabla^2\boldsymbol{R}_\mu + \boldsymbol{\Pi}_S \tag{6.94}$$

to first order. Given the hydrostatic approximation (6.41),

$$\kappa\Big(\frac{\partial}{\partial t} - \frac{\dot{\boldsymbol{R}}_{\mu}}{2}\cdot\nabla\Big)\boldsymbol{R}_{\mu} = -\frac{\kappa}{K}\dot{\mathbf{F}} + \frac{1}{2}\nabla\Big(\partial_t p_s - \frac{4G}{3}\nabla\cdot\boldsymbol{R}_\mu\Big) + G\nabla^2\boldsymbol{R}_\mu + \boldsymbol{\Pi}_S \tag{6.95}$$

$$= -\frac{\kappa}{K}\dot{\mathbf{F}} + \frac{1}{2}\nabla\Big(\partial_t p_s - \frac{4G}{3}\nabla\cdot\boldsymbol{R}_\mu\Big) - 4G\nabla\cdot\boldsymbol{D} + \boldsymbol{\Pi}_S. \tag{6.96}$$

Let $p'_s = p_s - \int_t^{t\prime}\frac{4}{3}\mu\nabla\cdot\boldsymbol{R}_\mu d\tau$ then (6.96) reduces to

$$\kappa\Big(\frac{\partial}{\partial t} - \frac{\dot{\boldsymbol{R}}_{\mu}}{2}\cdot\nabla\Big)\boldsymbol{R}_{\mu} = -\frac{\kappa}{K}\dot{\mathbf{F}} + \frac{1}{2}\partial_t\nabla p'_s + G\nabla^2\boldsymbol{R}_\mu + \boldsymbol{\Pi}_S \tag{6.97}$$

which is recognised as a similar form to the Navier-Stokes equations.

6.3 Combining $\boldsymbol{R}_\mu$ and $\dot{\boldsymbol{R}}_\mu$ in the polymer flow equation

Compare the second term on the RHS of (6.93) and the second term on the RHS of (6.97) to (5.37). To derive a formula for the propagation of stretch and stretch rate that is dimensionally correct, it is necessary to add a factor of (6.93) to a factor of the integral of (6.97).

Adding half of Equation (6.93) to double the integral of (6.97) with respect to time, ignoring $\boldsymbol{\Pi}_S$ and $\boldsymbol{\Pi}_D$, substituting $p' = p'_s + p'_d$ and given that $\kappa/K = \rho_n = \rho/m$, one derives a zero order pressure tensor which corresponds to the zero order apparent pressure tensor of Section 5.1.5 such that

$$\begin{aligned}
\frac{1}{2}\rho\Big(\frac{\partial}{\partial t} &- \frac{\dot{\boldsymbol{R}}_\mu}{2}\cdot\nabla\Big)\dot{\boldsymbol{R}}_\mu + 2\kappa\boldsymbol{R}_\mu - \frac{\kappa}{2}\nabla R_\mu^2 \\
&= \frac{\rho}{2m}\mathbf{F} - \frac{2\kappa}{K}\int_t^{t\prime}\dot{\mathbf{F}}d\tau + \nabla p' + \frac{1}{2}\mu\nabla^2\dot{\boldsymbol{R}}_\mu + 2\int_t^{t\prime} G\nabla^2\boldsymbol{R}_\mu d\tau \\
&= -\frac{3}{2}\rho_n\mathbf{F} + \nabla p' + \frac{1}{2}\mu\nabla^2\dot{\boldsymbol{R}}_\mu + 2\int_t^{t\prime} G\nabla^2\boldsymbol{R}_\mu d\tau \\
&= -\frac{3}{2}\rho_n\mathbf{F} + \nabla p' - 2\mu\nabla\cdot\dot{\boldsymbol{D}} - 8\int_t^{t\prime} G\nabla\cdot\boldsymbol{D}d\tau, \qquad (6.98)
\end{aligned}$$

which is the equation describing the non-equilibrium behaviour of polymers. This equation will be called the polymer flow equation. All the terms represent change in properties.

The following argument applies to both Equation (6.98) and (6.99) to follow. One can either select t or t' as a reference time because all the terms represent changes in property. It is convenient to set the reference time such that the specimen is in the ground state and the material is therefore in the equilibrium state. Intuitively one would select the reference time $t = 0$ and t' as the current time. This formulation presupposes that the full history of the specimen is known. This formulation can be used in the experimental determination of constants because the specimen's history is known. Note that in such a formulation, $t = 0$ would be an arbitrary time in the past when the specimen was in the ground state and t' would be defined relative to this zero set point.

In general, at time t', one is not aware of the complete history of the specimen and $t = 0$ cannot be set. Alternatively, set t' as the reference time, where $t' = \infty$ is a time in the future when the specimen returns to ground state and can be approximated to remain in the ground state. The latter formulation can be applied more generally and (in Section 10.3) will be shown to be the formulation being applied in the numerical method of Chapter 8.

A different formulation is derived by adding Equation (6.93) and the time integral of Equation (6.97), to give

$$\begin{aligned}\rho\Big(\frac{\partial}{\partial t} &- \frac{\dot{\boldsymbol{R}}_\mu}{2}\cdot\nabla\Big)\dot{\boldsymbol{R}}_\mu + \kappa\boldsymbol{R}_\mu - \frac{\kappa}{4}\nabla R_\mu^2 \\ &= 2\nabla p_d' + \frac{1}{2}\nabla p_s' + \mu\nabla^2\dot{\boldsymbol{R}}_\mu + \int_t^{t\prime} G\nabla^2\boldsymbol{R}_\mu d\tau \\ &= 2\nabla p_d' + \frac{1}{2}\nabla p_s' - 4\mu\nabla\cdot\dot{\boldsymbol{D}} - 4\int_t^{t\prime} G\nabla\cdot\boldsymbol{D}d\tau \qquad (6.99)\end{aligned}$$

which will be used to construct the latent stress tensor in Chapter 7.

The origin of the complete separation of the viscous term (μ) and the memory term (G) can either be interpreted mathematically or physically. Mathematically the separation is because all of the derivation for stretch is separated from that for stretch rate. This separation was justified in Section 3.3.2 and Chapter 4. Physically the separation is because intramolecular forces are ignored in this larger scale mesoscopic model.

6.4 Fully macroscopic formulation

Equation (6.98) is a macroscopic equation. The left hand side of the equation is expressed in microscopic variables. In order to make equation (6.98) fully macroscopic, use Equation (3.42) which relates microscopic principal strectch vector to macroscopic stretch vector such that $\hat{\boldsymbol{\lambda}} = \hat{\underline{\boldsymbol{\lambda}}}$. Substituting $\boldsymbol{R}_\mu = \hat{\boldsymbol{\lambda}}R_{\mu 0} = \hat{\underline{\boldsymbol{\lambda}}}R_{\mu 0}$ where $R_{\mu 0}$ is the magnitude of $\boldsymbol{R}_{\mu 0}$ and the temporal derivative

of the vector $\hat{\underline{\boldsymbol{\lambda}}}$ is $\dot{\underline{\boldsymbol{\lambda}}}$. Then

$$\begin{aligned}
\rho\Big(\frac{\partial}{\partial t} &- \frac{\dot{\boldsymbol{R}}_{\boldsymbol{\mu}}}{2}\cdot\nabla\Big)\dot{\boldsymbol{R}}_{\boldsymbol{\mu}} + \kappa\boldsymbol{R}_{\boldsymbol{\mu}} - \frac{\kappa}{4}\nabla R_\mu^2 \\
&= \rho\Big(\frac{\partial}{\partial t} - \frac{\dot{\underline{\boldsymbol{\lambda}}}R_{\mu 0}}{2}\cdot\nabla\Big)\dot{\underline{\boldsymbol{\lambda}}}R_{\mu 0} + \kappa\hat{\underline{\boldsymbol{\lambda}}}R_{\mu 0} - \frac{\kappa}{4}\nabla\hat{\underline{\lambda}}^2 R_{\mu 0}^2 \\
&= \rho R_{\mu 0}\Big(\frac{\partial}{\partial t} - \frac{\dot{\underline{\boldsymbol{\lambda}}}R_{\mu 0}}{2}\cdot\nabla\Big)\dot{\underline{\boldsymbol{\lambda}}} + R_{\mu 0}\kappa\hat{\underline{\boldsymbol{\lambda}}} - R_{\mu 0}^2\frac{\kappa}{4}\nabla\hat{\underline{\lambda}}^2 \\
&= \rho R_{\mu 0}\frac{\partial}{\partial t}\dot{\underline{\boldsymbol{\lambda}}} - \rho R_{\mu 0}^2\frac{\dot{\underline{\boldsymbol{\lambda}}}}{2}\cdot\nabla\dot{\underline{\lambda}} + R_{\mu 0}\kappa\hat{\underline{\boldsymbol{\lambda}}} - R_{\mu 0}^2\frac{\kappa}{4}\nabla\hat{\underline{\lambda}}^2 \\
&= \rho\mathrm{B}\frac{\partial}{\partial t}\dot{\underline{\boldsymbol{\lambda}}} - \rho\mathrm{B}^2\frac{\dot{\underline{\boldsymbol{\lambda}}}}{2}\cdot\nabla\dot{\underline{\boldsymbol{\lambda}}} + \mathrm{B}\kappa\hat{\underline{\boldsymbol{\lambda}}} - \mathrm{B}^2\frac{\kappa}{4}\nabla\hat{\underline{\lambda}}^2 \qquad (6.100)
\end{aligned}$$

where from equation (3.44),

$$\mathrm{B} = R_{\mu 0} = R_{rms} \qquad (6.101)$$

can be determined experimentally. Substituting Equation (6.100) and $\check{\mathbf{F}} = \rho_n\boldsymbol{F}$ (total applied force per unit volume) into Equation (6.98) gives the fully macroscopic equation

$$\begin{aligned}
\rho\mathrm{B}\frac{\partial}{\partial t}\dot{\underline{\boldsymbol{\lambda}}} &- \rho B^2\frac{\dot{\underline{\boldsymbol{\lambda}}}}{2}\cdot\nabla\dot{\underline{\boldsymbol{\lambda}}} + \mathrm{B}\kappa\hat{\underline{\boldsymbol{\lambda}}} - B^2\frac{\kappa}{4}\nabla\hat{\underline{\lambda}}^2 \\
&= -\frac{3}{2}\check{\mathbf{F}} + \nabla p' - 2\mu\nabla\cdot\dot{\boldsymbol{D}} - 8\int_t^{t\prime} G\nabla\cdot\boldsymbol{D}d\tau. \qquad (6.102)
\end{aligned}$$

6.5 The incompressible polymer flow equation

Here it will be shown that for the incompressible ($\lambda_1\lambda_2\lambda_3 = 1$) situation, generally accepted for polymers,

$$\nabla\cdot\dot{\boldsymbol{R}}_\mu = 0 \qquad \text{and} \qquad \nabla(\nabla\cdot\boldsymbol{R}_\mu) = 0$$

and that consequently $p_s = p_s'$ and $p_d = p_d'$ – thereby simplifying (6.99).

Construct a RVE within a specimen such that the axes of the RVE are in the direction of the principal stretches. Let the length of the RVE in the x-direction be

$$d\mathbf{X} = \hat{\underline{\boldsymbol{\lambda}}}R_{\mu 0} \qquad (6.103)$$

then the volume of the element is (incompressibility $\iff \lambda_1\lambda_2\lambda_3 = 1$)

$$\prod_{i=1}^{3} dX_i = \prod_{i=1}^{3} \lambda_i R_{\mu 0}^3 = R_{\mu 0}^3 \tag{6.104}$$

which is a constant. Therefore

$$\begin{aligned}
\frac{\partial}{\partial t}\prod_{i=1}^{3} dX_i = 0 &= (\dot\lambda_1\lambda_2\lambda_3 + \dot\lambda_2\lambda_1\lambda_3 + \dot\lambda_3\lambda_1\lambda_2)R_{\mu 0}^3 \\
&= (\frac{\dot\lambda_1 R_{\mu 0}}{\lambda_1 R_{\mu 0}} + \frac{\dot\lambda_2 R_{\mu 0}}{\lambda_2 R_{\mu 0}} + \frac{\dot\lambda_3 R_{\mu 0}}{\lambda_3 R_{\mu 0}})R_{\mu 0}^3 \\
&= (\frac{d\dot R_{\mu 1}}{dX_1} + \frac{d\dot R_{\mu 2}}{dX_2} + \frac{d\dot R_{\mu 3}}{dX_3})R_{\mu 0}^3 = \nabla\cdot\dot{\boldsymbol{R}}_\mu R_{\mu 0}^3 = 0 \\
\iff \qquad 0 &= \nabla\cdot\dot{\boldsymbol{R}}_\mu(\mathbf{x},t) \qquad\qquad \forall\,\mathbf{x},t. \qquad (6.105)\\
&= \nabla\cdot\frac{D\boldsymbol{R}_\mu}{Dt} = \frac{D}{Dt}\left[\nabla\cdot\boldsymbol{R}_\mu\right] \\
&= \frac{d}{dt}\left[\boldsymbol{R}_\mu(\mathbf{x}(\mathbf{X},t),t)\right] \qquad (6.106)
\end{aligned}$$

where $\boldsymbol{R}_\mu(\mathbf{x}(\mathbf{X},t),t)$ is independent of $\mathbf{x}$. Substituting Equation (6.105) into Equation (6.92), the latter reduces to

$$\rho\Big(\frac{\partial}{\partial t} - \frac{\dot{\boldsymbol{R}}_\mu}{2}\cdot\nabla\Big)\dot{\boldsymbol{R}}_\mu = \frac{\rho}{m}\mathbf{F} + 2\nabla p_d + 4\mu\nabla\cdot\dot{\boldsymbol{D}} + \boldsymbol{\Pi}_D. \tag{6.107}$$

Integrating Equation (6.105) with respect to time,

$$\int \nabla\cdot\dot{\boldsymbol{R}}_\mu dt = \Theta \qquad \iff \qquad \nabla\int\nabla\cdot\dot{\boldsymbol{R}}_{\boldsymbol{\mu}} dt = \nabla\Theta = 0 \tag{6.108}$$

where, because $\boldsymbol{R}_\mu(\mathbf{x}(\mathbf{X},t),t)$ in Equation (6.106) is independent of $\mathbf{x}$, Θ is a constant. Substituting (6.108) into (6.96)

$$\kappa\Big(\frac{\partial}{\partial t} - \frac{\dot{\boldsymbol{R}}_\mu}{2}\cdot\nabla\Big)\boldsymbol{R}_\mu = -\frac{\kappa}{K}\dot{\mathbf{F}} + \frac{1}{2}\nabla\partial_t p_s - 4G\nabla\cdot\boldsymbol{D} + \boldsymbol{\Pi}_S. \tag{6.109}$$

Adding Equation (6.107) to the integral of Equation (6.109) with respect to time reduces Equation (6.99) to

$$\begin{aligned}
\rho\Big(\frac{\partial}{\partial t} &- \frac{\dot{\boldsymbol{R}}_\mu}{2}\cdot\nabla\Big)\dot{\boldsymbol{R}}_\mu + \kappa\boldsymbol{R}_\mu - \frac{\kappa}{4}\nabla R_\mu^2 \\
&= 2\nabla p_d + \frac{1}{2}\nabla p_s - 4\mu\nabla\cdot\dot{\boldsymbol{D}} - 4\int_t^{t'} G\nabla\cdot\boldsymbol{D}d\tau. \qquad (6.110)
\end{aligned}$$

6.6 Relationship to diffusion and wave equations

Equations (6.93) and (6.97) are recognised as having the form of the Navier-Stokes equation. Expressing each component in Lagrangian co-ordinates [72], each equation is recognised as the diffusion equation ([52], Chapter 1)

$$\frac{\partial \chi}{\partial t} = k\nabla^2 \chi. \tag{6.111}$$

Equation (6.99) can be regarded as an integro-differential equation coupling two vector diffusion equations.

For arbitrary function f and vector χ, the wave equation is described by [95, 96, 101, 153]

$$\frac{\partial^2 \chi}{\partial t^2} + g(\dot{\chi})\frac{\partial \chi}{\partial t} = f(\chi, \nabla^2 \chi). \tag{6.112}$$

Comparing Equation (6.112) with Equation (6.99), the latter is recognised as an example of the non-linear wave equation of the form

$$\frac{\partial^2 \chi}{\partial t^2} + g(\dot{\chi})\frac{\partial \chi}{\partial t} = f(\chi, \chi^2, \dot{\chi}, \nabla^2 \chi, \int_t^{t'} \chi d\tau) \tag{6.113}$$

where $\chi = R_\mu$. It is recognised that the analogy is not perfect because of the additional terms. The Eulerian interpretation of Equation (6.99) is therefore as a non-linear wave equation with non-linear damping – consistent with what would be predicted intuitively given the proposed model of Figure 3.3.

The relevance of the latter result lies in establishing whether the constants G and μ, determined experimentally in Chapter 12, produce physically consistent results. The second reason for determining these equations is that Equation (6.111) will be used to estimate the initial condition in Chapter 11 that will be utilised in the numerical modelling of Chapter 13.

Chapter 7

Viscoelasticity and non-maximum entropy elasticity

Equations (6.93) and (6.97) represent the first order approximation to macroscopic equivalents of the conservation of momentum derived by statistical mechanics. In this chapter, continuum mechanics will be used to derive the same equations. This will provide an alternate interpretation of the equations and will demonstrate the equivalence of the continuum and first order statistical mechanics approaches. The stress tensor is a macroscopic concept and the continuum derivation therefore also provides a means of determining this tensor.

The purpose of this chapter is not to determine a universal theory of hyperviscoelasticity. The purpose of this chapter is to demonstrate that the result of the first order Chapman-Enskog expansion for polymers can be derived using continuum mechanics and to present an algorithm for reconciling the macroscopic expansions of mesoscopic equations with continuum based equations. Viewed in a broader context, this thesis attempts to derive a physics for polymers at a microscopic level and reconcile the result with the macroscopic observations. It should be noted that higher order CE expansions can be constructed and presumably these will account for larger strain cases. It will be shown that the first order CE expansion is for the small strain case. Finally it should be noted that the mesoscopic theory is large strain, it is the result of the first order CE expansion of the mesoscopic theory that is small strain.

It will be shown that the first-order approximation to material viscoelasticity in one dimension can be represented by a simple linear parallel spring-

and-dashpot arrangement. The observed phenomenon of viscoelasticity will be called specimen viscoelasticity and will be shown to be represented by the left-hand side of the polymer flow equation (6.98) or (6.102).

A stored energy function will be generated in order to facilitate comparison between different models. The model of hyperelastic viscoeleasticity constructed in this work will (under the appropriate special circumstances) be compared to the hyperelastic neo-Hookean model.

7.1 Continuum mechanics constitutive equations: non-maximum entropy polymer elasticity

Recall from Section 1.9 that macroscopic vectors are underlined. Then the Cauchy equation of motion ([86], Chapter 4) is given by

$$\nabla \cdot \mathbf{T} + \rho \underline{\mathbf{B}} = \rho \ddot{\underline{\mathbf{x}}} \tag{7.1}$$

where $\mathbf{T}$ is the stress tensor, $\underline{\mathbf{B}}$ is a body force (acts on the body) and $\ddot{\underline{\mathbf{x}}}$ is the acceleration. Equation (7.1) expresses conservation of linear momentum in a continuum. Conservation of angular momentum implies that $\mathbf{T}$ is symmetric. Consider a body with an arbitrary position A. When the body undergoes deformation, let the principal stretch be $\hat{\underline{\boldsymbol{\lambda}}}$. Define point B such that any line segment AB is in the direction of $\hat{\underline{\boldsymbol{\lambda}}}$. Thus the locus of AB is a line with point A and direction $\hat{\underline{\boldsymbol{\lambda}}}/\hat{\underline{\lambda}}$. Construct a coordinate system such that the origin is at A's reference position, one of the axes coincides with principal stretch $\hat{\underline{\boldsymbol{\lambda}}}$ and the system is free to rotate such that the axis is always parallel to $\hat{\underline{\boldsymbol{\lambda}}}$. The coordinate system is depicted in Figure 7.1. Thus conservation of angular momentum and elastic compatibility have been satisfied implicitly.

The polymer material can support a shear stress. It can also deform in a time-dependent fashion like a fluid. Let the stress tensor be a function of both the deformation and the deformation rate tensors. Let the stress tensor $\mathbf{T}$ consist of two components $\mathbf{T}_S$ and $\mathbf{T}_D$. Let the sum of the zero and first order approximations to the stress tensor, $\mathbf{T}_D$, be directly proportional to the deformation rate tensor such that

$$\mathbf{T}_D = -2p'_d\mathbf{I} + 4\mu\dot{\mathbf{D}} \tag{7.2}$$

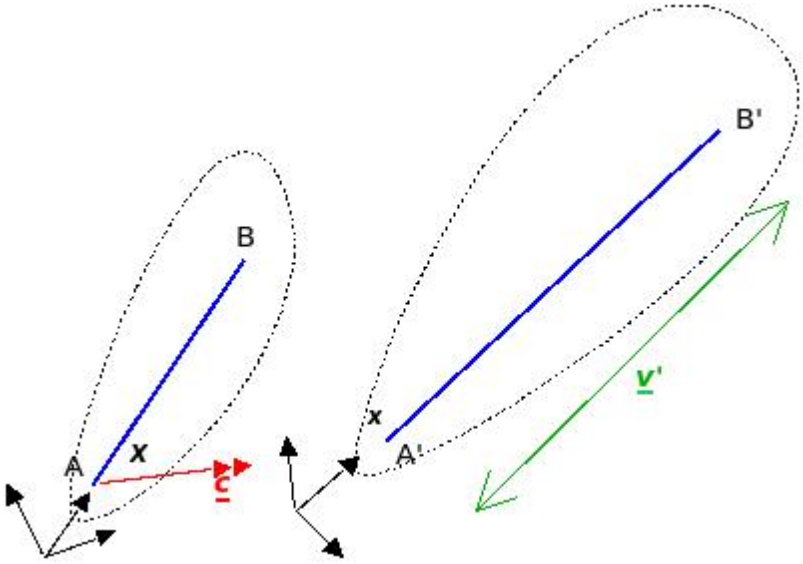

Figure 7.1: The coordinate system (in black) is aligned with the blue principal stretches as indicated. The red arrow represents the velocity of position A. The displacement ($\underline{\mathbf{v}}'$ in green) represents the displacement between points A and B. The coordinate system only rotates, it does not displace.

where, consistent with Equation (6.79),

$$\dot{\mathbf{D}} = \frac{1}{2}\left(\nabla\underline{\mathbf{c}} + (\nabla\underline{\mathbf{c}})^T\right).$$

It is recognised that this corresponds to the small strain situation. This implies that the first-order CE expansion recovers the small strain macroscopic behaviour because the non-linear terms are excluded as described in Section 3.1.3. Presumably higher order approximations will recover larger strain macroscopic behaviour. It is also noted that the macroscopic recovery does not affect the mesoscopic equations.

Let the rate of change of the sum of zero and first order approximation to the stress tensor, $\mathbf{T}_S$, be directly proportional to the deformation tensor, $\mathbf{D}$, such that

$$\partial_t \mathbf{T}_S = -p_s'\mathbf{I} + 4G\mathbf{D} \tag{7.3}$$

where; consistent with Equations (3.10), (3.11) and (6.84),

$$\mathbf{D} = \frac{1}{2}\left(\nabla\underline{\mathbf{v}} + (\nabla\underline{\mathbf{v}})^T\right) = \mathbf{e}^{(1)} \approx \mathbf{E}^{(1)}$$

and $\underline{\mathbf{v}}(\underline{\mathbf{x}})$ is the displacement vector in spatial coordinates whilst $\underline{\mathbf{x}}$ is the true

Eulerian or actual spatial coordinates. Again the theory will show that the macroscopic recovery based on the mesoscopic behaviour corresponds to the small strain situation but the underlying mesoscopic behaviour is not small strain.

Consider line segment AB in a material body as depicted in Figure 7.1. The segment is completely defined by knowing the location of point A ($\equiv \underline{\mathbf{x}}(\underline{\mathbf{X}})$) and the displacement AB ($\equiv \underline{\mathbf{v}}(\underline{\mathbf{X}})$). The segment is acted upon by forces which cause position A to be displaced to position A' and cause the displacement betweeen A and B to be transformed to $A'B'$. The objective of this section is to apply the Cauchy equation of motion to describe this schematic. This will be achieved by separating the situation into two components: the first describing the motion of point A and the second describing the displacement AB ($\equiv (\underline{\mathbf{v}}(\underline{\mathbf{X}}))$). The results will then be combined to fully describe the scenario depicted in Figure 7.1.

The first Cauchy equation to describe the motion of A is familiar and is the same for the derivation of the N-S equations. The scenario being determined is depicted in Figure 7.2. At position A an element of finite

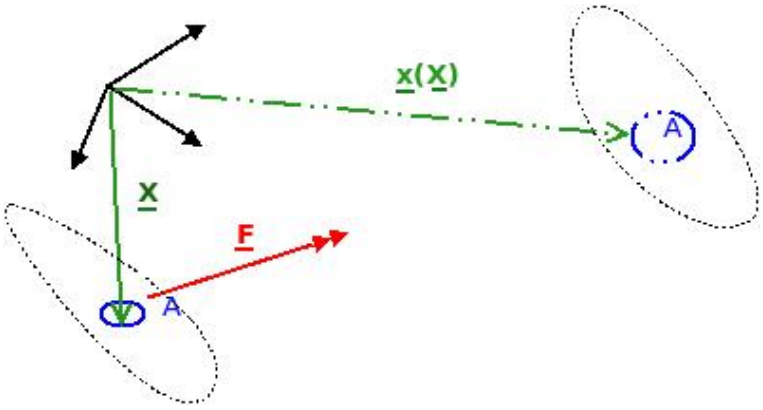

Figure 7.2: The coordinate system (in black) is aligned with the principal stretches (not depicted but corresponding to $\underline{\mathrm{v}}(\underline{\mathrm{X}})$ depicted in figure 7.1). The red arrow represents the force acting on the continuum. The green arrows indicate the position of A

volume δV unique to A is defined. Given that the continuum has density (here considered to be constant), δV has an associated mass (m). Therefore the force per unit mass is $\underline{\mathbf{F}}/m$ – corresponding to the body force acting at position A. Thus for the motion at position A, the Cauchy equation (7.1)

reduces to

$$\nabla \cdot \mathbf{T}_D - \rho \frac{\underline{\mathbf{F}}}{m} = \rho \ddot{\underline{\mathbf{x}}} = \rho \frac{D}{Dt} (\underline{\mathbf{c}}) \tag{7.4}$$

which is referred to as the dynamic component of the Cauchy equation of motion for polymers.

To determine the static component of the Cauchy equation (7.1), a preliminary result is required. The force acting on a volume δV is the product of the force per mass ($\underline{\mathbf{F}}/m$), density ρ and the volume. The limiting case for $\underline{\mathbf{F}}/m$ corresponds to the mass of one molecule. In this limiting situation the $\rho = \rho_n m$ where ρ_n is the number density and should be compared to (5.5). But from Section 5.1.4 $\kappa = \rho_n K$ where κ is the bulk modulus per unit volume and K is the elastic constant for a single molecule. From Newton 2, $\underline{\mathbf{F}}/m$ must induce an acceleration thus

$$\rho V \ddot{\underline{\mathrm{v}}} = \frac{\rho}{m} \underline{\mathbf{F}} V \iff \rho \ddot{\underline{\mathrm{v}}} = \rho_n \underline{\mathbf{F}} = \frac{\kappa}{K} \underline{\mathbf{F}} \tag{7.5}$$

Given the coordinate system depicted in Figure 7.1, The model is depicted in Figure 7.3 where the position $\mathbf{x}_B$ now indicates the displacement AB. The

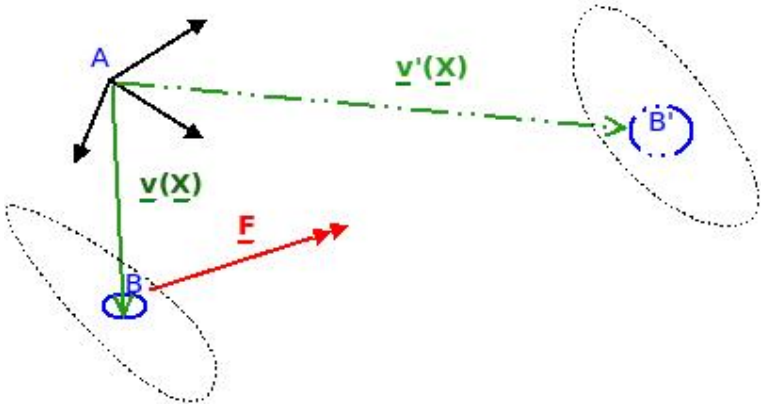

Figure 7.3: The coordinate system (in black) is aligned with the principal stretches (one of which is in direction AB). The red arrow represents the force acting on the continuum. Given that the origin of this coordinate system is A; the green arrows, indicating position B, represents the displacement AB. In the model, only half the mass is at B.

analogy with the Navier-Stokes derivation as depicted in Figure 7.2 is thus established. Let a force per unit mass, $\underline{\mathbf{Q}}/m$, be unique to line segment AB of the body in Figure 7.1. The effect of this force is to cause a change in

stretch and consequently position until equilibrium is reached at which time

$$\frac{\underline{\underline{\mathbf{Q}}}}{m} - \frac{K}{m}\underline{\mathbf{v}(\mathbf{x})} = 0 \quad \Longleftrightarrow \quad \frac{\underline{\underline{\mathbf{Q}}}}{m} = \frac{K}{m}\underline{\mathbf{v}}(\underline{\mathbf{x}}) \tag{7.6}$$

$$\Longleftrightarrow \ \rho\frac{\underline{\underline{\mathbf{Q}}}}{m} = \frac{\rho}{m}K\underline{\mathbf{v}}(\underline{\mathbf{x}}) \quad = \quad \rho_n K\underline{\mathbf{v}}(\underline{\mathbf{x}}) = \kappa\underline{\mathbf{v}}(\underline{\mathbf{x}}) \tag{7.7}$$

where $\underline{\mathbf{v}}(\underline{\mathbf{x}})$ is the displacement as a function of the spatial coordinate system and K is the scalar elastic constant. Substituting (7.6) into the Cauchy equation (7.1)

$$\nabla \cdot \mathbf{T}_S + \underline{\mathbf{Q}} = \rho\underline{\ddot{\mathbf{v}}} \qquad \Longleftrightarrow \qquad \nabla \cdot \mathbf{T}_S + \kappa\underline{\mathbf{v}}(\underline{\mathbf{X}}) = \rho\frac{D\underline{\dot{\mathbf{v}}}}{Dt}. \tag{7.8}$$

Substituting Equation (7.5) into Equation (7.8)

$$\nabla \cdot \partial\mathbf{T}_S + \kappa\underline{\mathbf{v}}(\underline{\mathbf{X}}) = \frac{\kappa}{K}\underline{\dot{\mathbf{F}}}. \tag{7.9}$$

Combining Equations (7.4) and (7.9)

$$\nabla \cdot \mathbf{T} - \rho\frac{\underline{\mathbf{F}}}{m} - \frac{\kappa}{K}\underline{\dot{\mathbf{F}}} + \kappa(\mathbf{x}_B - \mathbf{x}_A) = \rho\ddot{\mathbf{x}}_a$$

and

$$\nabla \cdot (\mathbf{T}_D + \mathrm{T}_S) - \rho\frac{\underline{\mathbf{F}}}{m} - \frac{\kappa}{K}\underline{\dot{\mathbf{F}}} + \kappa\underline{\mathbf{x}}_B = \rho\underline{\ddot{\mathbf{x}}}_A + \kappa\underline{\mathbf{x}}_A$$

is the partial differential equation to be solved for the stress tensor.

Separating the above equation into the original dynamic component (7.4) responsible for the change in position A and a static component (7.9) responsible for the change in displacement AB, the static component is given by

$$\begin{aligned} \nabla \cdot \mathbf{T}_S + \kappa\mathbf{x}_B &= \kappa\mathbf{x}_A \\ \Longleftrightarrow \qquad \frac{\partial}{\partial t}\nabla \cdot \mathbf{T}_S &= \frac{\kappa}{K}\underline{\dot{\mathbf{F}}} - \kappa\Big(\frac{\partial\underline{\mathbf{v}}}{\partial t} + \underline{\mathbf{c}} \cdot \nabla\underline{\mathbf{v}}\Big). \end{aligned} \tag{7.10}$$

Substituting Equation (7.2) into Equation (7.4)

$$\begin{aligned} \rho\Big(\frac{\partial \mathrm{c_i}}{\partial t} + \mathrm{c_j}\frac{\partial \mathrm{c_i}}{\partial \mathrm{x_j}}\Big) &= -\rho\frac{\mathrm{F_i}}{m} - 2\frac{\partial \mathrm{p'_d}}{\partial \mathrm{x_j}}\delta_{ij} + 2\mu\frac{\partial^2 \mathrm{c_i}}{\partial \mathrm{x_j}\partial \mathrm{x_j}} + 2\mu\frac{\partial^2 \mathrm{c_i}}{\partial \mathrm{x_i}\partial \mathrm{x_j}} \\ &= -\rho\frac{F_i}{m} - 2\frac{\partial \mathrm{p'_d}}{\partial \mathrm{x_j}}\delta_{ij} + 2\mu\frac{\partial^2 \mathrm{c_i}}{\partial \mathrm{x_j}\partial \mathrm{x_j}} + 2\mu\frac{\partial}{\partial \mathrm{x_i}}\Big(\frac{\partial \mathrm{c_j}}{\partial \mathrm{x_j}}\Big) \\ &= -\rho\frac{F_i}{m} - 2\frac{\partial \mathrm{p'_d}}{\partial \mathrm{x_j}}\delta_{ij} + 2\mu\frac{\partial^2 \mathrm{c_i}}{\partial \mathrm{x_j}\partial \mathrm{x_j}} \end{aligned}$$

which in vector calculus notation is

$$\rho\Big(\frac{\partial \underline{\mathbf{c}}}{\partial t} + \underline{\mathbf{c}} \cdot \nabla \underline{\mathbf{c}}\Big) = -\rho\frac{\underline{\mathbf{F}}}{m} - 2\nabla \mathrm{p}'_{\mathrm{d}} + 2\mu\nabla^2 \underline{\mathbf{c}}. \tag{7.11}$$

Substituting $\underline{\mathbf{c}} = -\dot{\mathbf{R}}_\mu/2$ into (7.11), Equation (7.11) equal Equation (6.93). Similarly, substituting Equation (7.3) into Equation (7.10),

$$\begin{aligned}
\frac{\partial^2 T_{Sij}}{\partial t \partial \mathrm{x_j}} &= -\frac{1}{2}\frac{\partial p'_s}{\partial t \partial \mathrm{x_j}}\delta_{ij} + 2G\frac{\partial^2 \mathrm{v_i}}{\partial \mathrm{x_j^2}} + 2G\frac{\partial}{\partial \mathrm{x_j}}\Big(\frac{\partial \mathrm{v_i}}{\partial \mathrm{x_i}}\Big) \\
&= \frac{\kappa}{K}\dot{F}_i - \kappa\Big(\frac{\partial \mathrm{v_i}}{\partial t} + \mathrm{c_j}\frac{\partial \mathrm{v_i}}{\partial \mathrm{x_j}}\Big) \\
&= -\frac{1}{2}\frac{\partial p'_s}{\partial t \partial \mathrm{x_j}}\delta_{ij} + 2G\frac{\partial^2 \mathrm{v_i}}{\partial \mathrm{x_j}\partial \mathrm{x_j}} = \frac{\kappa}{K}\dot{F}_i - \kappa\Big(\frac{\partial \mathrm{v_i}}{\partial t} + \mathrm{c_j}\frac{\partial \mathrm{v_i}}{\partial \mathrm{x_j}}\Big).
\end{aligned} \tag{7.12}$$

Then the vector calculus notation for Equation (7.12) is

$$\begin{aligned}
\frac{1}{2}\frac{\kappa}{K}\dot{\underline{\mathbf{F}}} - \kappa\frac{D\underline{\mathbf{v}}}{Dt} &= -\frac{1}{2}\frac{\partial}{\partial t}\nabla \mathrm{p}'_{\mathrm{s}} + 2G\nabla^2 \underline{\mathbf{v}} \\
\kappa\frac{D\underline{\mathbf{v}}}{Dt} &= \frac{\kappa}{K}\dot{\underline{\mathbf{F}}} + \frac{1}{2}\frac{\partial}{\partial t}\nabla \mathrm{p}'_{\mathrm{s}} - 2G\nabla^2 \underline{\mathbf{v}}.
\end{aligned} \tag{7.13}$$

Substituting $\Delta\underline{\mathbf{v}} = -\frac{1}{2}\mathbf{R}_\mu$ and $\underline{\mathbf{c}} = -\frac{1}{2}\dot{\mathbf{R}}_\mu$ into (7.13), Equation (7.13) is recognised as Equation (6.97) where A is a scalar constant.

Adding double the integral of (7.13) with respect to τ to half of (7.11),

$$\begin{aligned}
\frac{\rho}{2}\frac{D\underline{\mathbf{c}}}{Dt} &+ 2\kappa\Delta\underline{\mathbf{v}} + 2\kappa\Delta\underline{\mathbf{r}} \cdot \nabla\underline{\mathbf{v}} \\
&= -\rho\frac{\underline{\mathbf{F}}}{2m} + \frac{2\kappa}{K}\underline{\mathbf{F}} - \nabla \mathrm{p}' + \mu\nabla^2 \underline{\mathbf{c}} + \int_t^{t\prime} 4G\nabla^2 \underline{\mathbf{v}} d\tau \\
&= \frac{3}{2}\check{\underline{\mathbf{F}}} - \nabla \mathrm{p}' + 2\mu\nabla \cdot \dot{\mathbf{D}} + 8\int_t^{t\prime} G\nabla \cdot \mathbf{D} d\tau
\end{aligned} \tag{7.14}$$

which can also be recognised as (6.98) after the appropriate substitutions. Given $\mathbf{T} = \mathbf{T}_S + \mathbf{T}_D$, the constitutive equation for polymers is

$$\mathbf{T} = -2\mathbf{P}'_D - \frac{1}{2}\mathbf{P}'_S + 4\mu\dot{\mathbf{D}} + 4\int_t^{t\prime} G\mathbf{D} d\tau \qquad \forall\, t' > t$$

$$\mathbf{T}^{[0]} := -2\mathbf{P}'_D - \frac{1}{2}\mathbf{P}'_S + 4\mu\dot{\mathbf{D}} + 4\int_0^{t\prime} G\mathbf{D} d\tau$$

and without loss of generality

$$\mathbf{T}^{[\infty]} := -2\mathbf{P}'_D - \frac{1}{2}\mathbf{P}'_S + 4\mu\dot{\mathbf{D}} + 4\int_t^\infty G\mathbf{D}d\tau \tag{7.15}$$

where the latter two equations simply define reference times from which stresses are measured. $\mathbf{T}^{[0]}$ is measured from predefined initial time 0 and represents the sum of the zero and first order approximations to stress. $\mathbf{T}^{[\infty]}$ is measured to predefined future time where equilibrium is achieved (∞) and is the sum of the zero and first order stress. Also note that $\mathbf{T}$ is the change in stress tensor. The latter equation seems counter-intuitive until one recognises that at any time t, in general, one is not aware of the history of the molecule. Furthermore $t = 0$ is arbitrarily defined as a time when the material is in equilibrium and t is measured relative to this time. Although this is not the case numerically, it is evident that the last equation provides a superior reference point. The divergence of the tensor field (7.15) provides an alternate expression

$$\nabla\cdot\mathbf{T} = -2\nabla\mathbf{P}'_D - \frac{1}{2}\nabla\mathbf{P}'_S + 4\mu\nabla\cdot\dot{\mathbf{D}} + 4\int_t^{t'} G\nabla\cdot\mathbf{D}d\tau \qquad \forall\, t > t' \tag{7.16}$$

for the constitutive equation – recognised as the the sum of (7.13) and (7.11). Similarly, the general formulation of the sum of the zero and first order approximations to the apparent material stress defined in Section 5.1.5, ${}^{\langle app\rangle}\mathbf{T}^{[0]}$, is given by ${}^{\langle app\rangle}\mathbf{T}^{[0]} = \frac{1}{2}\mathbf{T}^{[0]}_D + 2\mathbf{T}^{[0]}_S$ and thus

$${}^{\langle app\rangle}\mathbf{T}^{[0]} = -\mathbf{P}'_D - \mathbf{P}'_S + 2\mu\dot{\mathbf{D}} + 8\int_0^t G\mathbf{D}d\tau \tag{7.17}$$

which should be compared to Equation (5.37) which only applies at equilibrium. The divergence of Equation (7.17),

$$\nabla\cdot{}^{\langle app\rangle}\mathbf{T} = -\nabla\mathbf{P}'_D - \nabla\mathbf{P}'_S + 2\mu\nabla\cdot\dot{\mathbf{D}} + 8\int_t^{t'} G\nabla\cdot\mathbf{D}d\tau \qquad \forall\, t > t', \tag{7.18}$$

can be compared to (7.16) and the right hand side of (6.102). Adding the integral of equation (7.13) with respect to time to Equation (7.11) and sub-

stituting Equation (7.15),

$$\begin{aligned}\nabla \cdot \mathbf{T} &= \rho \frac{D\underline{\mathbf{c}}}{Dt} + \kappa \Delta \underline{\mathbf{v}} + \kappa \Delta \underline{\mathbf{r}} \cdot \nabla \underline{\mathbf{v}} \\ &= \rho \mathrm{B} \frac{\partial}{\partial t} \dot{\underline{\boldsymbol{\lambda}}} - \rho B^2 \frac{\dot{\underline{\boldsymbol{\lambda}}}}{2} \cdot \nabla \dot{\underline{\boldsymbol{\lambda}}} + \mathrm{B} \kappa \Delta \hat{\underline{\boldsymbol{\lambda}}} - B^2 \frac{\kappa}{4} \nabla \hat{\underline{\lambda}}^2. \end{aligned} \tag{7.19}$$

Equation (7.19) is recognised as Equation (6.100) of Section 6.4. Also note that the principal strain vector $\boldsymbol{\epsilon}$, $\Delta \underline{\boldsymbol{\epsilon}} = \Delta(\hat{\underline{\boldsymbol{\lambda}}} - \underline{\mathbf{I}}) = \Delta \hat{\underline{\boldsymbol{\lambda}}}$ where $\hat{\underline{\boldsymbol{\lambda}}}$ is the principal stretch vectors (and can be compared to Section 6.4). Vector $\underline{\mathbf{I}} = (1, 1, 1)$.

7.2 Comparing material viscoelasticity and non-maximum entropy theory of polymer elasticity

Consider the Kelvin-Voigt model of viscoelasticity as depicted in Figure 7.4 From the parallel spring-and-dashpot formulation, the force across the struc-

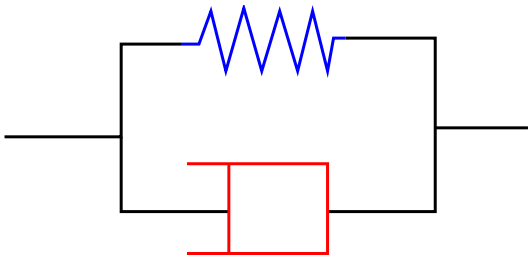

Figure 7.4: The Kelvin-Voigt model

ture is the sum of the force due to the spring (with constant K) and the force due to the dashpot (with constant J) and one can conclude that

$$\begin{aligned}\mathrm{T(t)} &= \frac{\mathrm{F}}{\mathrm{A}} = \frac{K\Delta \mathrm{x} + \mathrm{J}\partial_t \mathrm{x}}{\mathrm{A}} = \frac{\mathrm{x}}{\mathrm{A}} \frac{K\Delta \mathrm{x} + \mathrm{J}\partial_t \mathrm{x}}{\mathrm{x}} \\ &= \frac{K\mathrm{x}}{\mathrm{A}} \epsilon + \frac{\mathrm{Jx}}{\mathrm{A}} \dot{\epsilon} = 4\mathrm{E}\epsilon + 4\mu\dot{\epsilon} \\ &= 4\mathrm{E}(\lambda - 1) + 4\mu(\dot{\lambda} - \dot{1}) = -4\mathrm{E} + 4\mathrm{E}\lambda + 4\mu\dot{\lambda}\end{aligned}$$

where $4\mathrm{E} = K\mathbf{x}/\mathrm{A}$, $4\mu = \mathrm{J}\mathbf{x}/\mathrm{A}$, $-4\mathrm{E} = 2\mathrm{P}'_{\mathrm{D}}\mathrm{P}'_{\mathrm{S}}/2$ and is the 1D version of Equation (7.15). It is noted that the Kelvin-Voight model of linear viscoelasticity relaxes (in the stress relaxation experiment) instantaneously.

To derive Equation (7.15) one has to generalise the Kelvin-Voigt model to have several springs all acting at different times but subject to the same damping as depicted in Figure 7.5. These springs can be represented by the

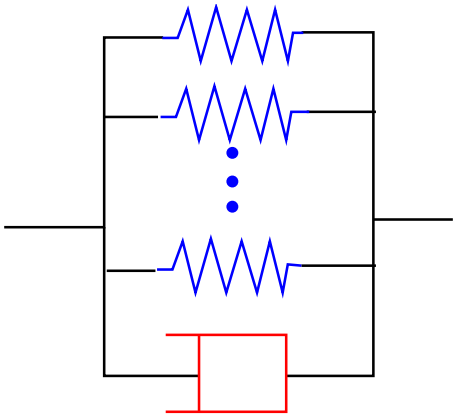

Figure 7.5: A GENERALISED SINGLE RELAXATION TIME KELVIN-VOIGT MODEL

Boltzmann superposition integral ([11], [94] Chapter 2) as

$$\mathrm{T(x,t)} = 4\mu\dot{\epsilon}\mathrm{(x,t)} + 4\int \mathrm{E(x,t)}\frac{\partial\epsilon\mathrm{(x,t)(t-\tau)}}{\partial\tau}d\tau.$$

Laplace transforming the integrand in the above integral such that

$$\mathrm{E}(s)(s\epsilon(s)) = (s\mathrm{E}(s))\epsilon(s),$$

the integral reduces to [94]

$$\begin{aligned}\int_0^t \mathrm{E}(t-\tau)\frac{\partial\epsilon(\tau)}{\partial\tau}d\tau &= \int_0^t \epsilon(t-\tau)\frac{\partial E(\tau)}{\partial\tau}d\tau \\ &= \int_0^t \epsilon(t-\tau)\mathrm{G}(\tau)d\tau\end{aligned}$$

where

$$\mathrm{G}(\tau) = \frac{\partial \mathrm{E}(\tau)}{\partial\tau}.$$

In the above $\mathrm{G}(\tau)$ and $\mathrm{E}(\tau)$ have a mathematical interpretation as variables that change with time. In order to construct a physical interpretation, $\mathrm{G}(\tau)$ and $\mathrm{E}(\tau)$ can be considered to be the average over the specimen such that

$$\mathrm{E}(t) = \frac{1}{\mathrm{V}}\oint \mathrm{E}(x,t)d\mathrm{V} \qquad \text{or} \qquad \frac{1}{\mathrm{V}}\oint \mathrm{E}(\mathbf{r},t)d\mathrm{V} \tag{7.20}$$

in three dimensions. Furthermore

$$\mathrm{G}(t) = \frac{1}{\mathrm{V}}\frac{\partial}{\partial t}\oint \mathrm{E}(x,t)d\mathrm{V} \qquad \text{or} \qquad \frac{1}{\mathrm{V}}\frac{\partial}{\partial t}\oint \mathrm{E}(\mathbf{r},t)d\mathrm{V} \tag{7.21}$$

where V is the volume.

The implication is that at any position at time t a ratio of stress(σ) to strain(ϵ), $\mathrm{E}(\mathbf{r},t)$, exists such that

$$\mathrm{E}(\mathbf{r},t) = \frac{\partial\sigma(\mathbf{r},t)}{\partial\epsilon(\mathbf{r},t)}$$

Furthermore $\mathrm{E}(t)$ is a specimen variable whereas $\mathrm{E}(\mathbf{r},t)$ is a material variable. Similarly $\mathrm{G}(t)$ is a specimen variable while $\mathrm{G}(\mathbf{r},t)$ is a material variable. The experimentally determined Young's modulus is the average of this property ($\mathrm{E}(\mathbf{r},t)$) over the volume. The origin of the change in Young's modulus with respect to time lies in the wave-like propagation of stress and strain as depicted in Figure 3.3 and explained in Section 3.1.2.

Consequently, in 1D,

$$\begin{aligned}\mathrm{T}^{[0]}(\mathrm{t}) &= 4\mu\dot{\epsilon} + 4\int_0^t \epsilon(t-\tau)\mathrm{G}(\tau)d\tau \\ &= -2\mathrm{P_D} - \frac{1}{2}\mathrm{P_S} + 4\mu\dot{\lambda} + 4\int_0^t \lambda(t-\tau)\mathrm{G}(\tau)d\tau \end{aligned} \tag{7.22}$$

is a generalised, single relaxation time Kelvin-Voigt model which is the solution to the 1D version of the polymer constitutive equation (7.15). It can also be interpreted as an alternate form of the Boltzmann superposition integral with a single relaxation time.

A constant $\mathrm{E}(\tau)$ suggests that $\mathrm{G}(\tau) = 0$ and that consequently the stress tensor of (7.22) does not reduce to the Kelvin-Voigt result of Figure 7.4. To prove the contrary, consider a set of $n \in \mathbb{N}$ elastic functions, $\{\mathrm{E}_i(t)\}_{i=1}^n$ where each $\mathrm{E}_i(t) \in \mathbb{R}$ is a function of time $t \geq 0$. Each $\mathrm{E}_i(t)$ has a unique time, τ_i, such that $\forall\, i, t < \tau_i \iff \mathrm{E}_i = 0$ and $\forall\, i, t > \tau_i \iff \mathrm{E}_i \neq 0$. Then, at any given time t,

$$\mathrm{E}(t) := \frac{1}{n}\sum_{i=1}^{n} \mathrm{E}_i(t)$$

after applying the definition (7.20). *If and only if* E_i is a constant ($\forall\, t \geq 0$), $\tau_0 := 0 = \tau_i$. Thus (7.22) reduces to

$$\begin{aligned} \mathrm{T}^{[0]}(\mathrm{t}) &= 4\mu\dot{\epsilon} + 4\int_0^t \epsilon(t-\tau_0)\mathrm{G}(\tau)d\tau \;=\; 4\mu\dot{\epsilon} + 4\int_0^t \epsilon(t)\mathrm{G}(\tau)d\tau \\ &= 4\mu\dot{\epsilon} + 4\epsilon(t)\int_0^t \mathrm{G}d\tau \;=\; 4\mu\dot{\epsilon} + 4\epsilon(t)\mathrm{E}(t) \end{aligned}$$

which is recognised as the result of the Kelvin-Voigt model.

Equation (7.22) is a constitutive equation for the material viscoelastic response. This does not correspond to the observed phenomenon of viscoelasticity. The observed viscoelasticity is designated specimen viscoelasticity.

7.3 Specimen viscoelasticity

Comparing Equations (7.15), (7.2) and (7.3) to Equations (6.102) and (7.19), it is evident that the right hand side of equation (6.99) or (7.19) is the formula for a material stress at a position $\mathbf{r}$ at time t, where the material stress is defined by Equations (7.2) and (7.3).

The left hand side of Equations (6.102) and (7.19) is the differential equation for the distribution of $\boldsymbol{\lambda}(\mathbf{r}, t)$ along the length of the specimen. The solution is given by

$$\rho\mathrm{B}\ddot{\boldsymbol{\lambda}} - \frac{\rho}{2}B^2\dot{\boldsymbol{\lambda}}\cdot\nabla\dot{\boldsymbol{\lambda}} + \mathrm{B}\kappa\Delta\boldsymbol{\lambda} - B^2\frac{\kappa}{4}\nabla\lambda^2 = \mathbf{T}(\mathbf{r}, t) \tag{7.23}$$

where $\mathbf{T}(\mathbf{r}, t)$ is the latent material stress at $\mathbf{r}, t$.

Thus the specimen (and measured) stretch $\boldsymbol{\lambda}_{sp}$ at time t can be defined as the average stretch along the length of the specimen at time t. However it should be recognised that in the co-ordinate system depicted in Figure 7.1, the stretches ($\boldsymbol{\lambda}$) are functions of position ($\mathbf{r}$), direction relative to an arbitrary global co-ordinate system ($\boldsymbol{\theta} = \theta_x, \theta_y, \theta_z$) and time ($t$). Thus before performing the averaging, all of the stretch tensors must be transformed to the global co-ordinate system by transformation matrix, $\mathbb{T}$. The eigenvectors and eigenvalues are determined on the transformed result to calculate the specimen stretch $\boldsymbol{\lambda}_{sp}(t)$. Let the function for determining eigenvalues and

eigenvectors be $\mathbb{E}$. Then

$$\boldsymbol{\lambda}_{sp}(t) := \mathbb{E}\left(\frac{\oint_{\mathrm{V}} \boldsymbol{\lambda}(\mathbf{r},\boldsymbol{\theta},t)\mathbb{T}(-\boldsymbol{\theta})dr}{\mathrm{V}}\right),$$

where V is the volume of the specimen and $\boldsymbol{\lambda}(\mathbf{r},\boldsymbol{\theta},t)$ is given by Equation (7.23). For the special case of uniaxial tension applied to a rectangular specimen one should anticipate $(\boldsymbol{\theta}) = (0,0,0)$, that consequently $\mathbb{T} = \mathbf{I}$, the identity matrix, and that $\mathbb{E}$ would be the identity function. Then the specimen stretch simplifies to

$$\boldsymbol{\lambda}_{sp}(t) := \frac{\oint_{\mathrm{V}} \boldsymbol{\lambda}(\mathbf{r},t)dr}{\mathrm{V}}. \tag{7.24}$$

Similarly the specimen stretch rate is dependent on the direction relative to a global co-ordinate system $\boldsymbol{\theta}$ and is defined as

$$\dot{\boldsymbol{\lambda}}_{sp}(t) := \mathbb{E}\left(\frac{\oint_{\mathrm{V}} \dot{\boldsymbol{\lambda}}(\mathbf{r},\boldsymbol{\theta},t)\mathbb{T}(-\boldsymbol{\theta})dr}{\mathrm{V}}\right).$$

However, for uniaxial tension on a rectangular specimen the formula for specimen stretch rate reduces to

$$\dot{\boldsymbol{\lambda}}_{sp}(t) := \frac{\oint_{\mathrm{V}} \dot{\boldsymbol{\lambda}}(\mathbf{r},t)dr}{\mathrm{V}}. \tag{7.25}$$

The zero-order (or maximum entropy) measured (apparent) stress ${}^{\langle app\rangle}\mathbf{T}$ at time t (Equation (5.36) in Section 5.1.5) is defined by the location of the sensor $\grave{\mathbf{r}}$ at time t such that

$${}^{\langle app\rangle}\mathbf{T}(t) = -\mathbf{P}(\grave{\mathbf{r}},t). \tag{7.26}$$

In Section 13.6 it will be argued that the stress that is measured is the mean of the apparent stresses applied over the area and corresponds to the pressure $(-\overline{\mathbf{P}(\grave{\mathbf{r}})} = -\overline{\mathbf{P}_S(\grave{\mathbf{r}})} - \overline{\mathbf{P}_D(\grave{r})})$. The observed phenomenon of viscoelasticity which will be called specimen viscoelasticity is defined as the response of $\boldsymbol{\lambda}_{sp}(t)$ to ${}^{\langle app\rangle}\boldsymbol{\sigma}_{sp}(t) := \overline{{}^{\langle app\rangle}\mathbf{T}(\mathbf{r})}(t)$. The term specimen viscoelasticity is used to distinguish the specimen elasticity described above from the material viscoelasticity described in Section 7.2. The creep experiment is the response of $\boldsymbol{\lambda}_{sp}(t)$ to fixed ${}^{\langle app\rangle}\boldsymbol{\sigma}_{sp}(t)$ and the stress relaxation experiment is the response of ${}^{\langle app\rangle}\boldsymbol{\sigma}_{sp}(t)$ to a fixed $\boldsymbol{\lambda}_{sp}(t)$.

By analogy, a latent specimen stress tensor may also be defined which will correspond to the average of the latent material stress tensor over the specimen and would (in the case of true stress) be described by

$$\mathbf{T}_{spec}^{(real)}(t) := \mathbb{E}\left(\frac{1}{V}\oint_{V} \mathrm{T}^{(real)}(\mathbf{r},\boldsymbol{\theta},t)\mathbb{T}(-\boldsymbol{\theta})dV\right).$$

which for the special case of uniaxial tension on a rectangular specimen reduces to

$$\mathbf{T}_{spec}^{(real)}(t) := \frac{1}{V}\oint_{V} \mathrm{T}^{(real)}(\mathbf{r},t)dV. \tag{7.27}$$

Lastly (in general) the apparent specimen stress tensor is described by

$${}^{\langle app\rangle}\mathbf{T}_{spec}^{(real)}(t) := \mathbb{E}\left(\frac{1}{V}\oint_{V} {}^{\langle app\rangle}\mathrm{T}^{(real)}(\mathbf{r},\boldsymbol{\theta},t)\mathbb{T}(-\boldsymbol{\theta})dV\right)$$

where again, $\boldsymbol{\theta}$ describes the direction relative to a global co-ordinate system and for the special case of uniaxial tension on a rectangular body the apparent specimen stress reduces to

$${}^{\langle app\rangle}\mathbf{T}_{spec}^{(real)}(t) := \frac{1}{V}\oint_{V} {}^{\langle app\rangle}\mathrm{T}^{(real)}(\mathbf{r},t)dV. \tag{7.28}$$

7.4 The stored-energy function

Existing models of hyperelasticity determine stresses based on the stored-energy function W. W is therefore constructed to compare stored-energy functions. An energy function based on latent stress (7.15) and one on apparent stress (7.17) are derived, the latter because it is measurable.

7.4.1 The latent stored-energy functions

If Equation (7.15) determines the principal Cauchy stresses, σ_{ti}, and σ_{n1} denotes the nominal principal stresses defined on the unstrained area then

$$\sigma_{ti} = \frac{\mathrm{F_i}}{\mathrm{A_t}} = \frac{\mathrm{F_i}}{\lambda_2\lambda_3 A_0} = \frac{\lambda_i \mathrm{F_i}}{\mathrm{A_0}} = \lambda_i \sigma_{ni} \tag{7.29}$$

where $\mathrm{F_i}$ is the component on force in the i direction, $\mathrm{A_0}$ is the unstrained area and $\mathrm{A_t}$ is the strained area. Then (at specimen steady state and material

maximum entropy) the latent stored energy function (nominal latent stored energy function) is

$$\mathrm{W} = \sum_{i=1}^{3} \int \sigma_{ni} d\lambda_i.$$

From Equation (7.15),

$$\begin{aligned}
\sigma_{t1} &= -2\mathrm{P}'_{\mathrm{D}} - \frac{1}{2}\mathrm{P}'_{\mathrm{S}} + 4\mu\dot{\lambda}_i + 4\int_0^t \mathrm{G}\lambda_i d\tau, \\
\sigma_{n1} &= -\frac{2\mathrm{P}'_{\mathrm{D}} + \frac{1}{2}\mathrm{P}'_{\mathrm{S}}}{\lambda_i} + 4\mu\frac{\dot{\lambda}_i}{\lambda_i} + \frac{4}{\lambda_i}\int_0^t \mathrm{G}\lambda_i d\tau, \\
\int_1^{\lambda_i} \sigma_{ni} dq &= -(2\mathrm{P}'_{\mathrm{D}} + \frac{1}{2}\mathrm{P}'_{\mathrm{S}})(\ln\lambda_i) + 4\mu\frac{\partial}{\partial t}\int_1^{\lambda_i} \ln \mathrm{q} d\mathrm{q} + 4\int_1^{\lambda_i}\int_0^t \mathrm{G} d\tau d\mathrm{q}, \\
&= -(2\mathrm{P}'_{\mathrm{D}} + \frac{1}{2}\mathrm{P}'_{\mathrm{S}})(\ln\lambda_i) + 4\mu\frac{\partial}{\partial t}(\lambda_i \ln\lambda_i - \lambda_i - 1) \\
&\quad +4\mathrm{G}\int_0^t (\lambda_i - 1) d\tau,
\end{aligned}$$

and the change in stored energy is given by $\Delta W = \sum_{i=1}^{3} \int \sigma_{ni} d\lambda_i$, or

$$\begin{aligned}
\mathrm{W} &= -(2\mathrm{P}'_{\mathrm{D}} + \frac{1}{2}\mathrm{P}'_{\mathrm{S}}) \ln(\lambda_1\lambda_2\lambda_3) + 4\mu\frac{\partial}{\partial t}(\lambda_1 \ln\lambda_1 + \lambda_2 \ln\lambda_2 + \lambda_3 \ln\lambda_3) \\
&\quad -4\mu\frac{\partial}{\partial t}(\lambda_1 + \lambda_2 + \lambda_3 + 3) + 4\mathrm{G}\int_0^t (\lambda_1 + \lambda_2 + \lambda_3 - 3) d\tau. \qquad (7.30)
\end{aligned}$$

A latent strain-energy function (true latent stored energy function) W^* is also defined such that

$$\mathrm{W}^* = \sum_{i=1}^{3} \int \sigma_{ti} d\lambda_1 \Longleftrightarrow \sigma_{ti} = \frac{\partial \mathrm{W}^*}{\partial \lambda_i} \qquad (7.31)$$

to facilitate determination of principal stresses for comparison in Section 7.5. Thus from Equation (7.15),

$$\sigma_{ti} = -2\mathrm{P}'_{\mathrm{D}} - \frac{1}{2}\mathrm{P}'_{\mathrm{S}} + 4\mu\dot{\lambda}_i + 4\int_0^t \mathrm{G}\lambda_i d\tau$$

and

$$\begin{aligned}\int_1^{\lambda_i}\sigma_{ti}d\mathrm{q} &= -(2\mathrm{P}'_\mathrm{D}+\frac{1}{2}\mathrm{P}'_\mathrm{S})(\lambda_i-1)+2\mu\frac{\partial}{\partial t}(\lambda_i^2-1)+4\int_1^{\lambda_i}\int_0^t \mathrm{G}\mathrm{q}d\tau d\mathrm{q}\\ &= -(2\mathrm{P}'_\mathrm{D}+\frac{1}{2}\mathrm{P}'_\mathrm{S})(\lambda_i-1)+2\mu\frac{\partial}{\partial t}\lambda_i^2+2\mathrm{G}\int_0^t(\lambda_i^2-1)d\tau,\\ &= -(2\mathrm{P}'_\mathrm{D}+\frac{1}{2}\mathrm{P}'_\mathrm{S})(\lambda_i-1)+2\mu\frac{\partial}{\partial t}\lambda_i^2+2\mathrm{G}\int_0^t(\lambda_i^2-1)d\tau\\ &\quad +f(\dot\lambda_i,\dot\lambda_j,\dot\lambda_k)+C, \end{aligned}\tag{7.32}$$

where $f(\dot\lambda_i,\dot\lambda_j,\dot\lambda_k)$ is an aribitrary function of $\dot\lambda_i,\dot\lambda_j,\dot\lambda_k$ and C is an arbitrary constant. In summary, let

$$\begin{aligned}A &= -2\mathrm{P}'_\mathrm{D}-\frac{1}{2}\mathrm{P}'_\mathrm{S},\\ I_1 &= \lambda_1+\lambda_2+\lambda_3,\\ I_2 &= \lambda_1^2+\lambda_2^2+\lambda_3^2,\\ I_3 &= \lambda_1\lambda_2\lambda_3,\\ I_4 &= \lambda_1\ln\lambda_1+\lambda_2\ln\lambda_2+\lambda_3\ln\lambda_3,\end{aligned}\tag{7.33}$$

then the change in the latent stored-energy function (7.30) is given by

$$\Delta\mathrm{W}=A\ln\mathrm{I}_3+4\mu\frac{\partial}{\partial t}\mathrm{I}_4-4\mu\frac{\partial}{\partial t}(\mathrm{I}_1+3)+4\mathrm{G}\int_0^t(\mathrm{I}_1-3)d\tau\tag{7.34}$$

and

$$\mathrm{W}=\mathrm{A}\ln\mathrm{I}_3+4\mu\frac{\partial}{\partial t}\mathrm{I}_4-4\mu\frac{\partial}{\partial t}\mathrm{I}_1+4\mathrm{G}\int_0^t\mathrm{I}_1d\tau.\tag{7.35}$$

Also, the change in latent strain-energy function $\Delta\mathrm{W}^*=\int\sigma_{t1}d\lambda_1+\int\sigma_{t2}d\lambda_2+\int\sigma_{t3}d\lambda_3$ is given by

$$\Delta\mathrm{W}^* = \mathrm{A}(\mathrm{I}_1-3)+2\mu\dot{\mathrm{I}}_2+2\mathrm{G}\int_0^t(\mathrm{I}_2-3)d\tau\tag{7.36}$$

$$\Longrightarrow\qquad \mathrm{W}^* = \mathrm{A}\mathrm{I}_1+2\mu\dot{\mathrm{I}}_2+2\mathrm{G}\int_0^t\mathrm{I}_2d\tau.\tag{7.37}$$

7.4.2 The apparent stored-energy function

Equation (7.17) determines the true apparent principal Cauchy stresses at equilibrium – ${}^{\langle app\rangle}\sigma_{ti}$ – at a point in a material. The nominal apparent Cauchy stress is given by ${}^{\langle app\rangle}\sigma_{ni}$ – at a point in a material. At specimen steady state and material maximum entropy, the apparent stored-energy function (nominal apparent stored energy function) is

$$ {}^{\langle app\rangle}\mathrm{W} = \sum_{i=1}^{3} \int {}^{\langle app\rangle}\sigma_{ni} d\lambda_i $$

From Equation (7.17)

$$ \begin{aligned} {}^{\langle app\rangle}\sigma_{n1} &= -\frac{\mathrm{P}}{\lambda_i} + 2\mu\frac{\dot{\lambda}_i}{\lambda_i} + \frac{8}{\lambda_i}\int_0^t \mathrm{G}\lambda_i d\tau, \\ \int_1^{\lambda_i} {}^{\langle app\rangle}\sigma_{ni} dq &= -(\mathrm{P})(\ln\lambda_i) + 2\mu\frac{\partial}{\partial t}\int_1^{\lambda_i} \ln \mathrm{q} d\mathrm{q} + 8\int_1^{\lambda_i}\int_0^t \mathrm{G} d\tau d\mathrm{q} \\ &= -(\mathrm{P})(\ln\lambda_i) + 2\mu\frac{\partial}{\partial t}(\lambda_i \ln\lambda_i - \lambda_i - 1) + 8\mathrm{G}\int_0^t (\lambda_i - 1) d\tau \end{aligned} $$

and the change in apparent stored energy is given by $\sum_{i=1}^{3}\int {}^{\langle app\rangle}\sigma_{ni} d\sigma_i$ equals

$$ \begin{aligned} {}^{\langle app\rangle}\mathrm{W} &= -(\mathrm{P})\ln(\lambda_1\lambda_2\lambda_3) + 2\mu\frac{\partial}{\partial t}(\lambda_1\ln\lambda_1 + \lambda_2\ln\lambda_2 + \lambda_3\ln\lambda_3) \\ &- 2\mu\frac{\partial}{\partial t}(\lambda_1 + \lambda_2 + \lambda_3 + 3) + 8\mathrm{G}\int_0^t (\lambda_1 + \lambda_2 + \lambda_3 - 3) d\tau. \end{aligned} \quad (7.38) $$

A strain-energy function (true apparent stored energy function) ${}^{\langle app\rangle}\mathrm{W}^*$ is also defined such that

$$ {}^{\langle app\rangle}\mathrm{W}^* = \sum_{i=1}^{3}\int \sigma_{ti} d\lambda_i \Longleftrightarrow \sigma_{ti} = \frac{\partial \mathrm{W}^*}{\partial \lambda_i} \quad (7.39) $$

to facilitate determination of principal stresses for comparison in Section 7.5. Thus from Equation (7.17),

$$ {}^{\langle app\rangle}\sigma_{ti} = -\mathrm{P} + 2\mu\dot{\lambda}_i + 8\int_0^t \mathrm{G}\lambda_i d\tau $$

and

$$\begin{aligned}\int_1^{\lambda_i} {}^{\langle app\rangle}\sigma_{ti}d\mathrm{q} &= -(\mathrm{P})(\lambda_i-1)+\mu\frac{\partial}{\partial t}\lambda_i^2+4\mathrm{G}\int_0^t(\lambda_i^2-1)d\tau \\ &\quad +f(\dot\lambda_i,\dot\lambda_j,\dot\lambda_k)+C \end{aligned} \tag{7.40}$$

where $f(\dot\lambda_i,\dot\lambda_j,\dot\lambda_k)$ is an aribitrary function of $\dot\lambda_i,\dot\lambda_j,\dot\lambda_k$ and C is an arbitrary constant. In summary, let

$$\begin{aligned} A &= -\mathrm{P} = {}^{\langle app\rangle}T^{(0)}, \\ I_1 &= \lambda_1+\lambda_2+\lambda_3, \\ I_2 &= \lambda_1^2+\lambda_2^2+\lambda_3^2, \\ I_3 &= \lambda_1\lambda_2\lambda_3, \\ I_4 &= \lambda_1\ln\lambda_1+\lambda_2\ln\lambda_2+\lambda_3\ln\lambda_3; \end{aligned} \tag{7.41}$$

then the change in the stored-energy function (7.38) is given by

$$\Delta^{\langle app\rangle}\mathrm{W} = A\ln\mathrm{I}_3+2\mu\frac{\partial}{\partial t}\mathrm{I}_4-2\mu\frac{\partial}{\partial t}(\mathrm{I}_1+3)+8\mathrm{G}\int_0^t(\mathrm{I}_1-3)d\tau \tag{7.42}$$

and

$${}^{\langle app\rangle}\mathrm{W} = \mathrm{A}\ln\mathrm{I}_3+2\mu\frac{\partial}{\partial t}\mathrm{I}_4-2\mu\frac{\partial}{\partial t}\mathrm{I}_1+8\mathrm{G}\int_0^t\mathrm{I}_1d\tau. \tag{7.43}$$

Also, the change in strain-energy function $\Delta\mathrm{W}^* = \int\sigma_{t1}d\lambda_1+\int\sigma_{t2}d\lambda_2+\int\sigma_{t3}d\lambda_3$ is given by

$${}^{\langle app\rangle}\Delta\mathrm{W}^* = \mathrm{A}(\mathrm{I}_1-3)+\mu\dot{\mathrm{I}}_2+4\mathrm{G}\int_0^t(\mathrm{I}_2-3)d\tau \tag{7.44}$$

and

$${}^{\langle app\rangle}\mathrm{W}^* = \mathrm{AI}_1+\mu\dot{\mathrm{I}}_2+4\mathrm{G}\int_0^t\mathrm{I}_2d\tau. \tag{7.45}$$

7.5 Comparison with hyperelastic models

Equation (7.15) is the constitutive equation for an isotropic, incompressible, viscoelastic material. It is thus expected that existing constitutive equations of either hyperelasticity or viscoelasticity should be able to be derived from

this model.

Three examples of models of hyperelasticity are (chronologically) by Mooney [111] and Rivlin [122] (Mooney-Rivlin), Ogden [113] and the Neo-Hookean. Only the Neo-Hookean model will be compared to the existing model. Stress relaxation and creep will be discussed in Chapters 12, 13 and 14.

7.5.1 Common postulates

Consider a uniaxial tensile test on a dumbell shaped specimen where the strain rate ($\dot{\lambda}_1$) remains constant – a typical experimental scenario. The testing assumption is that no stress is applied in the 2 and 3 directions thus for the Cauchy principal stresses σ_{ti}

$$\sigma_{t2} = \sigma_{t3} = 0 \tag{7.46}$$

The material assumption is of incompressibility, so that

$$\lambda_1\lambda_2\lambda_3 = 1. \tag{7.47}$$

The combined material and testing assumption is for an isotropic material subjected to uniaxial tension thus

$$\lambda_2 = \lambda_3. \tag{7.48}$$

Substituting (7.48) into (7.47)

$$\lambda_2^2 = \lambda_3^2 = \frac{1}{\lambda_1}. \tag{7.49}$$

For the temporal derivatives, differentiate (7.47) yielding

$$\dot{\lambda}_1\lambda_2\lambda_3 + \dot{\lambda}_2\lambda_1\lambda_3 + \dot{\lambda}_3\lambda_2\lambda_1 = 0 = \sum_{i=1}^{3}\frac{\dot{\lambda}_i}{\lambda_i}. \tag{7.50}$$

Furthermore, differentiating (7.49) with respect to time

$$\dot{\lambda}_3 = -\frac{1}{2}\frac{1}{\lambda^{3/2}}\dot{\lambda}_1 = \dot{\lambda}_2. \tag{7.51}$$

It is recognised that the hyperelastic models are independent of time. These models can however be divided into two categories – equilibrium and non-equilibrium. Equilibrium model's temporal derivatives are zero. Lastly the

stress tensors derived in this chapter were for small strain, and can therefore only be compared for the small strain special case. This may appear pointless but recall, from the introduction to this chapter, that the intention is to show that reconciliation between macroscopic expansions of mesoscopic equations and macroscopic equations can be achieved. Future work can formulate higher order CE expansions and hyperviscoelastic models.

7.5.2 Treloar's neo-Hookean theory

Treloar's theory was presented in Section 3.2.3. Treloar's stored energy function can be derived from the stored energy function (7.45). From the incompressibility condition (7.47), $\ln \lambda_1\lambda_2\lambda_3 = 0$ and given that hyperelastic models do not allow temporal derivatives, (7.45) reduces to

$$\begin{aligned} {}^{\langle app\rangle}\mathrm{W}^* &= A\mathrm{I}_1 + 4G\sum_{i=1}^{3}\frac{1}{\lambda_i}\int_1^{\lambda_i} q^2 dq = A\mathrm{I}_1 + 4G\sum_{i=1}^{3}\frac{1}{3}t_0\int_1^{\lambda_i}\frac{q^2}{q-1}dq \\ &= A\mathrm{I}_1 + \frac{4}{3}Gt_0\sum_{i=1}^{3}\left(\int_1^{\lambda_i} q + 1 + \frac{1}{q-1}dq\right). \end{aligned} \tag{7.52}$$

Given the results are being confined to $\lambda_i - 1$ small, applying a Taylor expansion, $\ln|\lambda_i - 1| \approx \lambda_i - 1$. Thus Equation (7.52) reduces to

$$\begin{aligned} {}^{\langle app\rangle}\mathrm{W}^* &= A\mathrm{I}_1 + \frac{4}{3}Gt_0\sum_{i=1}^{3}\left(\lambda_i - 1 + \ln|\lambda_i - 1|\right) + \frac{2}{3}Gt_0\sum_{i=1}^{3}\left(\lambda_i^2 - 1\right) \\ &= A\mathrm{I}_1 + \frac{8}{3}Gt_0\left(\mathrm{I}_1 - 3\right) + \frac{2}{3}Gt_0\left(\mathrm{I}_2 - 3\right) \end{aligned} \tag{7.53}$$

where t_0 is the time taken from no stretch to final stretch. Equation (7.53) can be compared to Equation (3.40):

$$W = \Gamma(\mathrm{I}_2 - 3). \tag{7.54}$$

Equation (7.53) differs from (3.40) by a constant term and a function of I_1. Differentiating the function of I_1 with respect to the principal stretches generates a hydrostatic term. It is noted that Treloar's method of making the system of equations – (3.58) and (3.59) – determinate as described in Section 3.2.7 adds a hydrostatic term. He continues to make the system of equations determinate by subtracting one of the principal stresses from the other (3.60) – which eliminates the hydrostatic term ([138], Chapter 4).

7.6 Closing comments

Reconciliation with existing continuum-based hyperelastic models was not achieved but, as stated in the introduction to this chapter, this was not the intention. An algorithm has been established to reconcile continuum based equations with the results of the Chapman-Enskog (CE) expansion of mesoscopic equations. Presumably higher order CE expansions will allow reconciliation with higher order stress tensors (not small strain) and this chapter has provided a means to achieve this reconciliation.

It should also be noted that the underlying mesoscopic theory is for large strain. It is the first order result of the CE expansion that is small strain. The discrete theory will be based on the mesoscopic theory and is therefore large strain. It is the extraction of the stress tensor (a post analytical task) which is small strain. One should recognise that the numerical method to be constructed in Chapter 8 differs from conventional continuum based approaches to discrete theory in that the model does not depend on stress.

The apparent stress was defined in Section 5.1.5 and can be either nominal (force per unit undeformed surface area) or true (force per unit deformed surface area). The stress experienced by the material is defined by Equation (7.15) and can be either nominal or true. The stress described by (7.15) will be defined as the latent stress to distinguish it from the apparent stress – the difference being in the calculation. Lastly the stresses can either be material or specimen. The material stress depends on position while the specimen stress is an averaging of the material stress over the volume of the specimen as described by Equations (7.27) and (7.28).

Chapter 8

Construction of a lattice Boltzmann method for polymers

In this chapter, the finite difference method will be applied to (3.85), the microscopic equation of polymer chain interaction, to obtain a mesoscopic lattice-Boltzmann type method for polymers. The theory is based on the work of He and Luo [57, 58].

The differential equation (3.85) will be separated into terms involving stretch-rate-space and stretch-space. The separation was justified mathematically in Sections 3.3.1 through to 3.3.3. The physical justification was provided in Section 4.1. The polymer chain interaction term given by (4.71) will be represented by the Bhatnagar-Gross-Krook (BGK) approximation [10]. The BGK approximation will then also be separated into a stretch-rate-space component and a stretch-space component.

8.1 Finite differences and uncoupling of the probability distribution function

Consider Equation (3.85) where the microscopic functional

$$p(\boldsymbol{r}, \boldsymbol{R}_f, \dot{\boldsymbol{R}}_f, t)$$

represents the probability of finding a molecule in the range $d\boldsymbol{r}$ about $\boldsymbol{r}$ and $d\boldsymbol{R}_f$ about $\boldsymbol{R}_f$ and $d\dot{\boldsymbol{R}}_f$ about $\dot{\boldsymbol{R}}_f$ at time t. Given that the discrete scheme

will model collections of molecules, define a new functional

$$\wp(\boldsymbol{r},t)=\int_{-\infty}^{\infty}\int_{-\infty}^{\infty}p(\boldsymbol{r},\boldsymbol{R}_f,\dot{\boldsymbol{R}}_f,t)d\boldsymbol{R}_f d\dot{\boldsymbol{R}}_f \tag{8.1}$$

which is clearly independent of $\boldsymbol{R}_f$ and $\dot{\boldsymbol{R}}_f$. $\wp$ represents the probability of finding a collection of molecules with mean vector length, $\overline{\boldsymbol{R}_f}$, and mean chain stretch rate, $\overline{\dot{\boldsymbol{R}}_f}$. Integration of (3.85) with respect to $\boldsymbol{R}_f$ and $\dot{\boldsymbol{R}}_f$ over $(-\infty,\infty)$ and $(-\infty,\infty)$ in all three directions gives,

$$\frac{\partial\wp}{\partial t}+\left(\frac{\Delta\boldsymbol{p}}{m}-\frac{1}{2}\dot{\boldsymbol{R}}_f\right)\cdot\frac{\partial\wp}{\partial\mathbf{r}}=\frac{\partial_e\wp}{\partial t}. \tag{8.2}$$

Given that $\frac{\Delta\boldsymbol{p}}{m}-\frac{1}{2}\dot{\boldsymbol{R}}_f=\grave{\boldsymbol{c}}$, from Equation (3.81); Equation (8.2) reduces to

$$\frac{D}{Dt}\wp(\mathbf{r},t)=\frac{\partial_e}{\partial t}\wp(\mathbf{r},t). \tag{8.3}$$

He and Luo [57] formally integrate the gas equivalent of (8.3) with respect to time between t and $t+\delta t$ and obtain

$$\wp(\mathbf{r}+\grave{\boldsymbol{c}}\delta t,t+\delta t)-\wp(\mathbf{r},t)=\Delta\wp\approx\Delta\wp_e=\wp_e(\mathbf{r},t+\delta t)-\wp_e(\mathbf{r},t).$$

Note that Chapters 3 through 6 considered the probability of finding individual molecules at the microscopic level and that Chapter 7, which dealt with the macroscopic level, did not consider molecules at all.

This chapter considers the probability of finding a collection of molecules with averaged stretch and stretch rate at a particular position and time. The probability of finding these averaged properties, as exemplified by $\wp(\mathbf{r},t)$, represents the mesoscopic level. Let $\wp$ and $\wp_e$, like $p^{(ms)}$, be multiplicative such that $\wp=\wp_R\times\wp_{\dot{R}}$ where $\wp_R$ is due to chain length and $\wp_{\dot{R}}$ is due to chain stretch rate. Thus (as in Section 3.3.)

$$\begin{aligned}\Delta\wp_R\times\Delta\wp_{\dot{R}} &= \Delta\wp_{eR}\times\Delta\wp_{e\dot{R}}\\ \iff \ln\Delta\wp_R+\ln\Delta\wp_{\dot{R}} &= \ln\Delta\wp_{eR}+\ln\Delta\wp_{e\dot{R}}.\end{aligned} \tag{8.4}$$

Investigating chain-length and chain stretch rate independently.

$$\ln\Delta\wp_R=\ln\Delta\wp_{eR}\iff\Delta\wp_R=\Delta\wp_{eR}.$$

Reversing the above process from (8.4) to (8.3), the material derivative of $\wp_R$ is given by

$$\frac{D\wp_R}{Dt} = \frac{\partial \wp_{eR}}{\partial t} \tag{8.5}$$

and can be compared to (8.3). Similarly, in stretch rate space,

$$\frac{D\wp_{\dot{R}}}{Dt} = \frac{\partial \wp_{e\dot{R}}}{\partial t}. \tag{8.6}$$

The BGK approximation can be applied to (8.5) and (8.6) independently.

The BGK approximation is based on an empiric observation that the rate of change of a property $\wp$, that tends toward an equilibrium $\wp^{(eq)}$, over a period of time δt, is directly proportional to the difference between $\wp$ and $\wp^{(eq)}$ and inversely proportional to the period δt [10]. He and Luo [58] integrate the molecular velocity based equivalent of (8.6) formally and thereby show that (8.10) is second order in δt. Applying the BGK approximation to (8.5),

$$\frac{D\wp_R}{Dt} \approx -\frac{1}{\tau_R \delta t}\Big(\wp_R - \wp_R^{(ms)}\Big) \tag{8.7}$$

$$\iff \quad \frac{\partial \wp_R}{\partial t} - \frac{\dot{\boldsymbol{R}}_\mu}{2} \cdot \nabla \wp_R \approx -\frac{1}{\tau_R \delta t}\Big(\wp_R - \wp_R^{(ms)}\Big) \tag{8.8}$$

from (5.52). The discretisation in space and time will be selected such that a lattice Boltzmann type equation is derived. A first-order time difference, first-order upwind space difference and a downwind term for the relaxation to maximum entropy are used to get

$$\begin{aligned}
&\frac{\wp_R(\mathbf{r} - \frac{\dot{\boldsymbol{R}}_\mu}{2}\delta t, t+\delta t) - \wp_R(\mathbf{r} - \frac{\dot{\boldsymbol{R}}_\mu}{2}\delta t, t)}{\delta t} \\
&\qquad \approx \frac{\boldsymbol{R}_\mu(t+\delta t) - \boldsymbol{R}_\mu(t)}{2\delta t} \cdot \frac{\wp_R(\mathbf{r} - \frac{\dot{\boldsymbol{R}}_\mu}{2}\delta t, t) - \wp_R(\mathbf{r}, t)}{\delta \mathbf{r}} \\
&\qquad\qquad - \frac{\wp_R(\mathbf{r}, t) - \wp_R^{(ms)}(\mathbf{r}, t)}{\tau_R \delta t}
\end{aligned}$$

where $\delta \boldsymbol{r} = \boldsymbol{c}\delta t = -\frac{\delta \boldsymbol{R}_\mu}{2} = \frac{\boldsymbol{R}_\mu(t+\delta t) - \boldsymbol{R}_\mu(t)}{2}$ results in

$$\begin{aligned}
&\wp_R(\mathbf{r} - \frac{\dot{\boldsymbol{R}}_\mu}{2}\delta t, t+\delta t) - \wp_R(\mathbf{r} - \frac{\dot{\boldsymbol{R}}_\mu}{2}\delta t, t) \\
&\qquad \approx -\frac{\boldsymbol{R}_\mu(t+\delta t) - \boldsymbol{R}_\mu(t)}{2} \cdot \frac{2\big(\wp_R(\mathbf{r} - \frac{\dot{\boldsymbol{R}}_\mu}{2}\delta t, t) - \wp_R(\mathbf{r}, t)\big)}{\boldsymbol{R}_\mu(t+\delta t) - \boldsymbol{R}_\mu(t)} \\
&\qquad\qquad - \frac{\wp_R(\mathbf{r}, t) - \wp_R^{(ms)}(\mathbf{r}, t)}{\tau_R}.
\end{aligned}$$

This reduces to

$$\wp_R(\mathbf{r} - \frac{\dot{\boldsymbol{R}}_\mu}{2}\delta t, t + \delta t) - \wp_R(\mathbf{r}, t) \approx -\frac{1}{\tau_R}\Big(\wp_R(\mathbf{r}, t) - \wp_R^{(ms)}(\mathbf{r}, t)\Big) \tag{8.9}$$

which is a lattice Boltzmann equation for polymer chain length. Similarly, the lattice Boltzmann equation for chain stretch rate space is

$$\wp_{\dot{R}}(\mathbf{r} - \frac{\dot{\boldsymbol{R}}_\mu}{2}\delta t, t + \delta t) - \wp_{\dot{R}}(\mathbf{r}, t) \approx -\frac{1}{\tau_{\dot{R}}}\Big(\wp_{\dot{R}} - \wp_{\dot{R}}^{(ms)}\Big). \tag{8.10}$$

8.2 Discretisation of chain-length space

In Section 8.1 it was shown that the lattice Boltzmann method is a finite difference method based on a differential equation describing mesoscopic behaviour with a time variable, three spatial variables and 3 additional variables (chain-length or chain stretch rate for polymers or velocity for fluids [57,58]). If D is the number of spatial dimensions, then from Equation (3.72),

$$p_S^{(ms)}(\boldsymbol{R}_f) = \frac{b^D}{\pi^{D/2}} e^{-b^2(\boldsymbol{R}_f - \boldsymbol{R}_\mu)^2}.$$

For $D = 2$, integrating with respect to $\boldsymbol{R}_f$ from $(-\infty, -\infty)$ to (∞, ∞),

$$\wp_S^{(ms)}(\boldsymbol{R}_f) = \int p_S^{(ms)}(\boldsymbol{R}_f)\, d\boldsymbol{R}_f = e^{-b^2|\boldsymbol{R}_f - \boldsymbol{R}_\mu|^2} = 1 \tag{8.11}$$

because p_S is a probability such that $\int p_S\, d\boldsymbol{R}_f = 1$. Performing a truncated Taylor expansion, one obtains

$$\begin{aligned}
\wp_S^{(ms)}(\boldsymbol{R}_f) &= e^{-b^2(\boldsymbol{R}_f)^2} e^{2b^2 \boldsymbol{R}_f \cdot \boldsymbol{R}_\mu} e^{-b^2 R_\mu^2} \\
&\approx e^{-b^2(\boldsymbol{R}_f)^2}\left(1 + 2b^2 \boldsymbol{R}_f \cdot \boldsymbol{R}_\mu + 2b^4(\boldsymbol{R}_f \cdot \boldsymbol{R}_\mu)^2\right)\left(1 - b^2 R_\mu^2\right) \\
&= e^{-b^2(\boldsymbol{R}_f)^2}\big(1 + 2b^2 \boldsymbol{R}_f \cdot \boldsymbol{R}_\mu + 2b^4(\boldsymbol{R}_f \cdot \boldsymbol{R}_\mu)^2 - b^2 \boldsymbol{R}_\mu^2\big).
\end{aligned} \tag{8.12}$$

Define κ (see Section 5.1.4) to be

$$\kappa := \rho_n K p.$$

Thus $\int \kappa d\boldsymbol{R}_f = \kappa_0$. Furthermore $\kappa^{(ms)} = \kappa_0 p^{(ms)}$.

To derive the equations for force, work and entropy, one has to integrate

moments of the maximum entropy function. Thus it is required to evaluate

$$I = \int \boldsymbol{R}_f^m \kappa^{(ms)} d\boldsymbol{R}_f = \int e^{-b^2 \boldsymbol{R}_f^2} \phi(\boldsymbol{R}_f) d\boldsymbol{R}_f \tag{8.13}$$

where I is the desired integral and $m = 0, 1, 2$. I can be calculated approximately by using Gaussian integration, so that

$$I \approx \sum_j W_j \phi(\boldsymbol{R}_{fj})$$

where W_j is a weighting factor and $\phi(\boldsymbol{R}_{fj})$ is the value of a property at the sampling vector $\boldsymbol{R}_{fj}$. The Hermite polynomial [26] shown in Table 8.1 is the appropriate orthogonal polynomial for the Gaussian integration of (8.13), given its weight e^{-x^2} and applicability over the interval $(-\infty, \infty)$.

Table 8.1: Orthogonal polynomials and special weights for Gaussian quadrature

Interval	Weight Function	Symbol	Name
$[-1, 1]$	1	$P_n(x)$	Legendre
$[-1, 1]$	$(1-x^2)^{-1/2}$	$T_n(x)$	Tchebyscheff 1
$[-1, 1]$	$(1-x^2)^{1/2}$	$U_n(x)$	TchebyScheff 2
$[-1, 1]$	$(1-x)^\alpha(1+x)^\beta$	$P_n^{(\alpha,\beta)})(x)$	Jacobi
$[0, \infty)$	e^{-x}	$L_n(x)$	Laguerre
$[0, \infty)$	$x^\alpha e^{-x}$	$L_n^{(\alpha)}$	Generalised Laguerre
$(-\infty, \infty)$	e^{-x^2}	$H_n(x)$	Hermite

It can be shown that the 3^{rd} order Hermite polynomial [58] reproduces the LBM, and is selected. For the third order Hermite polynomial, the 1D weights and abscissae are depicted in Table 8.2 [26]. For the two dimensional case,

Table 8.2: Weighting factors and abscissa for 1D Gaussian integration

Index (i)	Abscissa (ζ_i)	Weight (ω_i)
1	$-\sqrt{3/2}$	$\sqrt{\pi}/6$
2	0	$\frac{2}{3}\sqrt{\pi}$
3	$\sqrt{3/2}$	$\sqrt{\pi}/6$

Equation (8.13) can be separated into x and y components such that

$$I = \int e^{-b^2 R_{fx}^2} \phi(R_{fx}) dR_{fx} \int e^{-b^2 R_{fy}^2} \phi(R_{fy}) R_{fy},$$

for which the 1D sampling points for each direction are in Table 8.2.

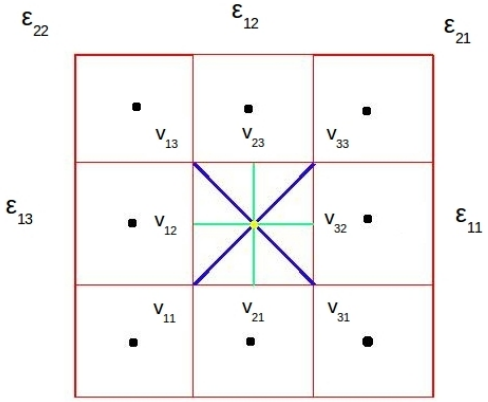

Figure 8.1: LBM DISCRETISATION OF PHYSICAL SPACE AND VECTOR SPACE

Combining the 1D results above into 2D, there are 3^2 ways of sampling two indices with replacement. The resultant two dimensional vectors derived are depicted in Figure 8.1. The results of the sampling are summarised in Table 8.3. Three dimensional schemes [58] can also be generated. The sampling vectors can either be represented in the conventional V_{ij} notation or the alternate $\boldsymbol{\epsilon}_{\sigma i}$ notation of Table 8.3. The latter is selected because it is the form used by Cao [15] and Hou [65] and will be reproduced in Chapter 10. In the alternate representation, the black dots of Figure 8.1 represent nodes, the volume occupied by the node is represented as a red square, the green chain length vector corresponds to $\sigma = 1$, blue to $\sigma = 2$ and yellow for $\sigma = 0$. The i index refers to direction – here x and y.

Table 8.3: Weighting factors and abscissae for 2D Gaussian integration

Index (i,j)	Vector Abscissa (i,j)	Weight (ω_{ij})	Alternate Vector $(\boldsymbol{\epsilon}_{\sigma i})$
11	$(-\sqrt{3/2}, -\sqrt{3/2})$	$\frac{\pi}{36}$	$\boldsymbol{\epsilon}_{23}$
12	$(-\sqrt{3/2}, 0)$	$\frac{\pi}{9}$	$\boldsymbol{\epsilon}_{13}$
13	$(-\sqrt{3/2}, \sqrt{3/2})$	$\frac{\pi}{36}$	$\boldsymbol{\epsilon}_{22}$
21	$(0, -\sqrt{3/2})$	$\frac{\pi}{9}$	$\boldsymbol{\epsilon}_{14}$
22	$(0, 0)$	$\frac{4\pi}{9}$	$\boldsymbol{\epsilon}_{00}$
23	$(0, \sqrt{3/2})$	$\frac{\pi}{9}$	$\boldsymbol{\epsilon}_{12}$
31	$(\sqrt{3/2}, -\sqrt{3/2})$	$\frac{\pi}{36}$	$\boldsymbol{\epsilon}_{24}$
32	$(\sqrt{3/2}, 0)$	$\frac{\pi}{9}$	$\boldsymbol{\epsilon}_{11}$
33	$(\sqrt{3/2}, \sqrt{3/2})$	$\frac{\pi}{36}$	$\boldsymbol{\epsilon}_{21}$

Using Gaussian quadrature at the sampling vector lengths of Table 8.3 to

evaluate Equation (8.13) approximately in 2D,

$$I = \int e^{-b^2 \boldsymbol{R}_f^2} \phi(\boldsymbol{R}_f) dR_f \approx \sum_{\sigma,i} W_{\sigma i} \phi(\mathbf{R}_{\sigma i}). \tag{8.14}$$

Thus the moments are calculated by summing the weighted results at the appropriate sampling chain length vectors.

To derive the above for the 9-chain-length 2D LBM, a Cartesian coordinate system is used. Let $\phi(\boldsymbol{R}_f) = R_x^m R_y^n$. Then from Equation (8.14),

$$I = \int e^{-b^2 \boldsymbol{R}_f^2} \phi(\boldsymbol{R}_f) d\boldsymbol{R}_f = \int e^{-b^2 R_{fx}^2} \phi(R_{fx}) dR_{fx} \int e^{-b^2 R_{fy}^2} \phi(R_{fy}) R_{fy}.$$

Setting $\zeta = bR_{fx}$ and $\eta = bR_{fy}$,

$$\begin{aligned} I &= b^{-(m+n+2)} \int_{-\infty}^{\infty} e^{-\zeta^2} \zeta^m d\zeta \int_{-\infty}^{\infty} e^{-\eta^2} \eta^n d\eta \\ &= b^{-(m+n+2)} I_m I_n \end{aligned} \tag{8.15}$$

where

$$I_m = \int_{-\infty}^{\infty} e^{-\zeta^2} \zeta^m d\zeta. \tag{8.16}$$

Third order Hermite polynomials are selected to perform the Gaussian integration. Table 8.2 provides the abscissae. From Equation (8.15) one needs to combine the 1D results above into 2D. The results are summarised in Table 8.3. The approximate integral of Equation (8.15) is

$$I = \frac{1}{b^2} \left(\omega_2^2 \phi(\mathbf{0}) + \sum_{\sigma=1,i=0}^{i=4} \omega_1 \omega_2 \phi(\mathbf{R}_{\sigma 1}) + \sum_{\sigma=2,i=0}^{i=4} \omega_1 \omega_1 \phi(\mathbf{R}_{\sigma 2}) \right) \tag{8.17}$$

where the magnitude of $\mathbf{R}_{\sigma i}$ is 0, $\sqrt{3/2}$ and $\sqrt{3}$, for $\sigma = 0$, 1 and 2 respectively. The directions $(0, \pm 1)$ and $(\pm 1, 0)$ correspond to $\sigma = 1$ and directions $(\pm\frac{1}{\sqrt{2}}, \pm\frac{1}{\sqrt{2}})$ correspond to $\sigma = 2$ as depicted in Figure 8.1. Comparing Equations (8.17) and (8.14) ,

$$W_{\sigma i} = \frac{\pi}{b^2} e^{b^2 \mathbf{R}_{\sigma i}^2} \omega_{\sigma i} \tag{8.18}$$

where

$$\omega_{0i} = \frac{4}{9}, \qquad \omega_{1i} = \frac{1}{9}, \qquad \omega_{2i} = \frac{1}{36}. \tag{8.19}$$

Finally substituting Equations (8.18) and (8.19) into Equation (8.12) one derives the polymer-LBM approximation to the maximum entropy distribution function for chain length in the form

$$\begin{aligned}\kappa_{\sigma i}^{(ms)} &= W_{\sigma i}\kappa^{(ms)}(\mathbf{r},\mathbf{R}_{\sigma i},t)\\ &= \omega_{\sigma i}\kappa_0\left(1+2b^2(\mathbf{R}_{\sigma i}\cdot\mathbf{R}_\mu)+2b^4(\mathbf{R}_{\sigma i}\cdot\mathbf{R}_\mu)^2-b^2(\mathbf{R}_\mu)^2\right).\end{aligned} \tag{8.20}$$

The above only applies for very low stretch, that is, $R^2 \ll \frac{2}{3}nl^2$.

8.3 Discretisation of chain-stretch-rate space

Similarly, chain-stretch-rate space can be discretised. From Equation (3.73) and Equation (6.20), where D is the dimension,

$$\begin{aligned} p_D^{(ms)}(\boldsymbol{c}) &= \left(\frac{\rho}{2\pi k\mathrm{T}}\right)^{\frac{D}{2}} e^{-\frac{m}{2k\mathrm{T}}(c-c_0)^2}\\ \text{and for } D=2, \qquad p_D^{(ms)}(\dot{\boldsymbol{R}}_f) &= \frac{\rho_n m}{8\pi k\mathrm{T}} e^{-\frac{m}{8k\mathrm{T}}(\dot{R}_f-\dot{R}_\mu)^2}. \end{aligned} \tag{8.21}$$

The laws of probability require that

$$\begin{aligned} \int p\, d\dot{\boldsymbol{R}}_f = 1, \qquad & \qquad \rho = \rho_n m p = \rho_0 p,\\ \int \rho\, d\dot{\boldsymbol{R}}_f = \rho_0, \qquad \text{and} \qquad & \qquad \rho^{(ms)} = \rho_0 p^{(ms)}. \end{aligned}$$

The equations for mass, and the equivalent of momentum and kinetic energy are given by the moments of the integral

$$I = \int \dot{\boldsymbol{R}}_f^m \rho^{(ms)} d\dot{\boldsymbol{R}}_f \tag{8.22}$$

for $m = 0, 1, 2$ such that

$$\begin{aligned} \rho &= \sum_{\sigma,i}\rho_{0\sigma i},\\ -\rho\frac{\dot{\boldsymbol{R}}_\mu}{2} &= \sum_{\sigma i}\mathbf{E}_{\sigma i}\rho_{0\sigma i} \qquad \Longleftrightarrow \qquad \rho\dot{\boldsymbol{R}}_\mu = \sum_{\sigma i}\dot{\mathbf{R}}_{\sigma i}\rho_{0\sigma i},\\ \rho\frac{\dot{\boldsymbol{R}}_\mu^2}{4} &= \sum_{\sigma i}\mathbf{E}_{\sigma i}^2\rho_{0\sigma i} \qquad \Longleftrightarrow \qquad \rho\dot{\boldsymbol{R}}_\mu^2 = q\sum_{\sigma i}\dot{\mathbf{R}}_{\sigma i}^2\rho_{0\sigma i}. \end{aligned} \tag{8.23}$$

Then (performing the integration as for chain length) the maximum entropy distribution function for chain-stretch rate is

$$\begin{aligned}\rho_{\sigma i}^{(ms)} &= W_{\sigma i}\rho^{(ms)}(\mathbf{r},\dot{\mathbf{R}}_{\sigma i},t) \\ &= \omega_{\sigma i}\rho_0\left(1+\frac{m}{4k\mathrm{T}}\dot{\mathbf{R}}_{\sigma i}\cdot\dot{\boldsymbol{R}}_{\mu}+\frac{m^2}{32k^2\mathrm{T}^2}(\dot{\mathbf{R}}_{\sigma i}\cdot\dot{\boldsymbol{R}}_{\mu})^2-\frac{m}{8kT}\dot{R}_{\mu}^2\right).\end{aligned} \tag{8.24}$$

Let

$$\alpha=\sqrt{\frac{m}{8kT}} \tag{8.25}$$

then, substituting Equation (8.25) into (8.24), the latter reduces to

$$\rho_{\sigma i}^{(ms)} = \omega_{\sigma i}\rho_0(1+2\alpha^2\dot{\mathbf{R}}_{\sigma i}\cdot\dot{\boldsymbol{R}}_{\mu}+2\alpha^2(\dot{\mathbf{R}}_{\sigma i}\cdot\dot{\boldsymbol{R}}_{\mu})^2-\alpha^2\dot{R}_{\mu}^2) \tag{8.26}$$

where

$$\omega_{0i}=\frac{4}{9},\qquad \omega_{1i}=\frac{1}{9},\qquad \omega_{2i}=\frac{1}{36}.$$

8.4 Recoupling of chain-length space and chain-stretch-rate space

Effectively, two independent lattices have been generated. Adding the dynamic contribution to molecule stretch rate to the static contribution establishes recoupling. This is now carried out. The result is then redistributed to the dynamic and static components.

8.4.1 Redistribution of polymer chain stretch

Re-expressing Equation (8.9) as

$$\kappa_{\sigma i}(\mathbf{r}+\delta\mathbf{r},t+\delta t)=\kappa_{\sigma i}(\mathbf{r},t)+\frac{1}{\tau_R}\Big(\kappa_{\sigma i}^{(ms)}(\mathbf{r},t)-\kappa_{\sigma i}(\mathbf{r},t)\Big), \tag{8.27}$$

substituting Equations (8.19) into Equation (8.20) and $b^2=\frac{3}{2R_{rms}^2}$ (from Equation (3.36)), the maximum entropy bulk modulus per unit volume is

$$\begin{aligned}\kappa_{01}^{(ms)} &= \frac{4}{9}\kappa_0-\frac{2}{3}\frac{\kappa_0}{R_{rms}^2}\boldsymbol{R}_{\mu}^2, \\ \kappa_{1i}^{(ms)} &= \frac{1}{9}\kappa_0+\frac{1}{3}\frac{\kappa_0}{R_{rms}^2}(\mathbf{S}_{1i}\cdot\boldsymbol{R}_{\mu})+\frac{1}{2}\frac{\kappa_0}{R_{rms}^4}(\mathbf{S}_{1i}\cdot\boldsymbol{R}_{\mu})^2-\frac{1}{6}\frac{\kappa_0}{R_{rms}^2}R_{\mu}^2, \\ \kappa_{2i}^{(ms)} &= \frac{1}{36}\kappa_0+\frac{1}{12}\frac{\kappa_0}{R_{rms}^2}(\mathbf{S}_{2i}\cdot\boldsymbol{R}_{\mu})+\frac{1}{8}\frac{\kappa_0}{R_{rms}^4}(\mathbf{S}_{2i}\cdot\boldsymbol{R}_{\mu})^2-\frac{1}{24}\frac{\kappa_0}{R_{rms}^2}R_{\mu}^2,\end{aligned} \tag{8.28}$$

where, in anticipation of Chapter 10, one may set (substituting (3.44))

$$\mathbf{S}_{\sigma i} = \mathbf{R}_{\sigma i} = R_{rms}\boldsymbol{\epsilon}_{\sigma i} = R_{\mu 0}\boldsymbol{\epsilon}_{\sigma i}. \tag{8.29}$$

In Equation(8.29), $\boldsymbol{\epsilon}_{\sigma i}$ will be defined by Equation (10.1) but is derived from Table 8.3. Substituting Equation (8.29) into (8.28),

$$\begin{aligned}
\kappa_{01}^{(ms)} &= \frac{4}{9}\kappa_0 - \frac{2}{3}\frac{\kappa_0}{R_{rms}^2}\boldsymbol{R}_\mu^2, \\
\kappa_{1i}^{(ms)} &= \frac{1}{9}\kappa_0 + \frac{1}{3}\frac{\kappa_0}{R_{rms}}(\boldsymbol{\epsilon}_{1i}\cdot\boldsymbol{R}_\mu) + \frac{1}{2}\frac{\kappa_0}{R_{rms}^2}(\boldsymbol{\epsilon}_{1i}\cdot\boldsymbol{R}_\mu)^2 - \frac{1}{6}\frac{\kappa_0}{R_{rms}^2}R_\mu^2, \\
\kappa_{2i}^{(ms)} &= \frac{1}{36}\kappa_0 + \frac{1}{12}\frac{\kappa_0}{R_{rms}}(\boldsymbol{\epsilon}_{2i}\cdot\boldsymbol{R}_\mu) + \frac{1}{8}\frac{\kappa_0}{R_{rms}^2}(\boldsymbol{\epsilon}_{2i}\cdot\boldsymbol{R}_\mu)^2 - \frac{1}{24}\frac{\kappa_0}{R_{rms}^2}R_\mu^2.
\end{aligned} \tag{8.30}$$

The $0^{th}, 1^{st}$ and 2^{nd} moments are summed at the sampling vectors to give

$$\begin{aligned}
\kappa &= \sum_{\sigma,i}\kappa_{0\sigma i}, \\
\kappa\boldsymbol{R}_\mu &= \sum_{\sigma i}\mathbf{R}_{\sigma i}\kappa_{0\sigma i} = \sum_{\sigma i}\dot{\mathbf{R}}_{\sigma i}\kappa_{0\sigma i}\delta t, \\
\kappa\boldsymbol{R}_\mu^2 &= \sum_{\sigma i}\mathbf{R}_{\sigma i}^2\kappa_{0\sigma i} \qquad \text{and} \qquad |\lambda_i^2 R_{0i}|^2 = R_i^2.
\end{aligned} \tag{8.31}$$

Substituting Equation (8.31), Equation (8.7) can be re-expressed as

$$\begin{aligned}
\frac{\partial\kappa_{\sigma i}}{\partial t} &= -\frac{1}{\delta t(\tau_R)}\Big(\kappa_{\sigma i} - \kappa_{\sigma i}^{(ms)}\Big), \\
\frac{\partial\kappa_{\sigma i}\mathbf{S}_{\sigma i}}{\partial t} &= -\frac{1}{\delta t(\tau_R)}\Big(\kappa_{\sigma i}\mathbf{S}_{\sigma i} - \kappa_{\sigma i}^{(ms)}\mathbf{S}_{\sigma i}\Big), \\
\frac{1}{\kappa}\frac{\partial\kappa_{\sigma i}\mathbf{S}_{\sigma i}}{\partial t} &= -\frac{1}{\delta t(\tau_R)\kappa}\Big(\kappa_{\sigma i}\mathbf{S}_{\sigma i} - \kappa_{\sigma i}^{(ms)}\mathbf{S}_{\sigma i}\Big), \\
\dot{\mathbf{R}}_{S\sigma i} = \frac{\partial\mathbf{R}_{S\sigma i}}{\partial t} &= -\frac{1}{\delta t(\tau_R)\kappa}\Big(\kappa_{\sigma i}\mathbf{S}_{\sigma i} - \kappa_{\sigma i}^{(ms)}\mathbf{S}_{\sigma i}\Big).
\end{aligned} \tag{8.32}$$

8.4.2 Redistribution of polymer chain stretch rate

Similarly, re-expressing Equation (8.10) as

$$\rho_{\sigma i}(\mathbf{r}+\delta\mathbf{r}, t+\delta t) = \rho_{\sigma i}(\mathbf{r}, t) + \frac{1}{\tau_{\dot{R}}}\Big(\rho_{\sigma i}^{(ms)}(\mathbf{r}, t) - \rho_{\sigma i}(\mathbf{r}, t)\Big), \tag{8.33}$$

from Equation (6.69) and (8.25)

$$\dot{R}_{rms}^2 = 12k\frac{\rho_n}{\rho}\mathrm{T} = 12\frac{k\mathrm{T}}{m} = \frac{3}{2}\frac{8k\mathrm{T}}{m} = \frac{3}{2\alpha^2}. \tag{8.34}$$

Substituting (8.19) and then (8.34) into (8.24),

$$\begin{aligned}
\rho_{01}^{(ms)} &= \frac{4}{9}\rho_0 - \frac{2}{3}\rho_0\Big(\frac{\dot{R}_\mu}{\dot{R}_{rms}}\Big)^2, \\
\rho_{1i}^{(ms)} &= \frac{1}{9}\rho_0 + \frac{1}{3}\rho_0\frac{\dot{\boldsymbol{R}}_\mu\cdot\mathbf{R}_{\sigma i}}{\dot{R}_{rms}^2} + \frac{1}{2}\rho_0\Big(\frac{\mathbf{R}_{\sigma i}\cdot\dot{\boldsymbol{R}}_\mu}{\dot{R}_{rms}^2}\Big)^2 - \frac{\rho_0}{6}\frac{\dot{R}_\mu^2}{\dot{R}_{rms}^2}, \\
\rho_{2i}^{(ms)} &= \frac{1}{36}\rho_0 + \frac{\rho_0}{12}\frac{\dot{\boldsymbol{R}}_\mu\cdot\mathbf{R}_{\sigma i}}{\dot{R}_{rms}^2} + \frac{\rho_0}{8}\frac{\big(\mathbf{R}_{\sigma i}\cdot\dot{\boldsymbol{R}}_\mu\big)^2}{\dot{R}_{rms}^4} - \frac{\rho_0}{24}\frac{\dot{R}_\mu^2}{\dot{R}_{rms}^2}.
\end{aligned} \tag{8.35}$$

Again, in anticipation of Chapter 10, one may substitute, given Equation (3.44),

$$\mathbf{E}_{\sigma i} = c\boldsymbol{\epsilon}_{\sigma i} = -\frac{\dot{\mathbf{R}}_{\sigma i}}{2} = -\frac{\dot{R}_{rms}}{2}\boldsymbol{\epsilon}_{\sigma i} = -\frac{\dot{R}_{\mu 0}}{2}\boldsymbol{\epsilon}_{\sigma i} \tag{8.36}$$

where $\boldsymbol{\epsilon}_{\sigma i}$ is derived from Table 8.3 and is defined by Equation (10.1). Then

$$\begin{aligned}
\rho_{01}^{(ms)} &= \frac{4}{9}\rho_0 - \frac{2}{3}\rho_0\Big(\frac{\dot{R}_\mu}{\dot{R}_{rms}}\Big)^2, \\
\rho_{1i}^{(ms)} &= \frac{1}{9}\rho_0 + \frac{1}{3}\rho_0\frac{\dot{\boldsymbol{R}}_\mu\cdot\boldsymbol{\epsilon}_{\sigma i}}{\dot{R}_{rms}} + \frac{1}{2}\rho_0\Big(\frac{\boldsymbol{\epsilon}_{\sigma i}\cdot\dot{\boldsymbol{R}}_\mu}{\dot{R}_{rms}}\Big)^2 - \frac{\rho_0}{6}\frac{\dot{R}_\mu^2}{\dot{R}_{rms}^2}, \\
\rho_{2i}^{(ms)} &= \frac{1}{36}\rho_0 + \frac{\rho_0}{12}\frac{\dot{\boldsymbol{R}}_\mu\cdot\boldsymbol{\epsilon}_{\sigma i}}{\dot{R}_{rms}} + \frac{\rho_0}{8}\frac{\big(\boldsymbol{\epsilon}_{\sigma i}\cdot\dot{\boldsymbol{R}}_\mu\big)^2}{\dot{R}_{rms}^2} - \frac{\rho_0}{24}\frac{\dot{R}_\mu^2}{\dot{R}_{rms}^2}.
\end{aligned} \tag{8.37}$$

Alternatively Equation (8.35) can be represented as

$$\begin{aligned}
\rho_{01}^{(ms)} &= \frac{4}{9}\rho_0 - \frac{2}{3}\rho_0\Big(\frac{\dot{R}_\mu}{\dot{R}_{rms}}\Big)^2, \\
\rho_{1i}^{(ms)} &= \frac{1}{9}\rho_0 - \frac{2}{3}\rho_0\frac{\dot{\boldsymbol{R}}_\mu\cdot\mathbf{E}_{\sigma i}}{\dot{R}_{rms}^2} + 2\rho_0\Big(\frac{\mathbf{E}_{\sigma i}\cdot\dot{\boldsymbol{R}}_\mu}{\dot{R}_{rms}^2}\Big)^2 - \frac{\rho_0}{6}\frac{\dot{R}_\mu^2}{\dot{R}_{rms}^2}, \\
\rho_{2i}^{(ms)} &= \frac{1}{36}\rho_0 - \frac{\rho_0}{6}\frac{\dot{\boldsymbol{R}}_\mu\cdot\mathbf{E}_{\sigma i}}{\dot{R}_{rms}^2} + \frac{1}{2}\rho_0\frac{\big(\mathbf{E}_{\sigma i}\cdot\dot{\boldsymbol{R}}_\mu\big)^2}{\dot{R}_{rms}^4} - \frac{\rho_0}{24}\frac{\dot{R}_\mu^2}{\dot{R}_{rms}^2}.
\end{aligned} \tag{8.38}$$

From Equations (8.23) and (8.36), the rate of change of chain length is

$$\dot{\mathbf{R}}_{D\sigma i} = \frac{\rho_{\sigma i}\dot{\mathbf{R}}_{\sigma i}}{2\rho_0} = -\frac{\rho_{\sigma i}\mathbf{E}_{\sigma i}}{\rho_0}. \tag{8.39}$$

8.4.3 Coupling $\dot{\mathbf{R}}_{D\sigma i}$ and $\dot{\mathbf{R}}_{S\sigma i}$

During interaction, density (ρ) and bulk modulus per unit volume (κ) remain constant. However, $\rho_{\sigma i}$ and $\kappa_{\sigma i}$ are redistributed to reflect a change in $\dot{\mathbf{R}}_D$ (the dynamic component given by (8.39)) and $\mathbf{R}_S$ (the static component given by (8.32)) respectively, subject to the constraints $\sum_{\sigma i}\rho_{\sigma i} = \rho$

and $\sum_{\sigma i} \kappa_{\sigma i} = \kappa$. A Kelvin-Voigt spring-dashpot-mass analogy with critical damping as depicted in Figure 7.4 is used to couple $\dot{\mathbf{R}}_D$ and $\mathbf{R}_S$. This redistribution will be referred to as polymer redistribution.

For the duration of redistribution, no external forces act on the mass-spring-damper unit. Consequently, after substituting Equation (3.81),

$$\begin{aligned} \rho_0 \frac{\partial \grave{\boldsymbol{c}}}{\partial t} + b\grave{\boldsymbol{c}} - K_0 \Delta \boldsymbol{R}_f = 0 \quad &\Longleftrightarrow \quad -\frac{\rho_0}{2}\frac{\partial^2 {}_\Delta \boldsymbol{R}}{\partial t^2} - \frac{b}{2}\frac{\partial {}_\Delta \boldsymbol{R}}{\partial t} - K_{0\Delta}\boldsymbol{R} = 0 \\ \Longleftrightarrow \qquad -\rho_0 \frac{\partial^2 {}_\Delta \boldsymbol{R}}{\partial t^2} \quad &- \quad b\frac{\partial {}_\Delta \boldsymbol{R}}{\partial t} - 2K_{0\Delta}\boldsymbol{R} = 0 \end{aligned} \tag{8.40}$$

where

$${}_\Delta \boldsymbol{R} := \boldsymbol{R}(t + k\delta t) - \boldsymbol{R}(t) \qquad \forall\, k > 0, k \in \mathbb{R}, \delta t > 0.$$

The solution to Equation (8.40) is

$${}_\Delta \boldsymbol{R}(t) = {}_\Delta \boldsymbol{R}(0) e^{-\omega t} \tag{8.41}$$

where

$$\omega = \frac{b \pm \sqrt{b^2 - 8\rho_0\kappa_0}}{2\rho_0}. \tag{8.42}$$

${}_\Delta \boldsymbol{R}$ can therefore oscillate, experience damping or critical damping. Both critical and non-critical damping are explored further. The former because the theory developed in Chapter 3 did not consider oscillation. As an aside, in Chapter 13 numerical models that include non-critical damping will be compared to those with critical damping. Given critical damping ω is determined by

$$\begin{aligned} \sqrt{b^2 - 8\rho_0\kappa_0} = 0 \qquad &\Longleftrightarrow \qquad b = \pm 2\sqrt{2\rho_0\kappa_0} \\ \text{such that} \qquad \omega = \frac{b}{2\rho_0} \quad &= \quad \frac{\pm\sqrt{2\rho_0\kappa_0}}{2\rho_0} = \pm\sqrt{\frac{\kappa_0}{2\rho_0}} \end{aligned} \tag{8.43}$$

and

$${}_\Delta \boldsymbol{R}(t) = {}_\Delta \boldsymbol{R}(0) e^{-\sqrt{\frac{\kappa_0}{2\rho_0}} t} \tag{8.44}$$

A truncated Taylor expansion is used to determine ${}_\Delta \boldsymbol{R}(t + \delta t)$ to second order. Thus

$$\begin{aligned} {}_\Delta \boldsymbol{R}(t + \delta t) &= {}_\Delta \boldsymbol{R}(0) e^{-\sqrt{\frac{\kappa_0}{2\rho_0}}(t+\delta t)} = {}_\Delta \boldsymbol{R}(t) e^{-\sqrt{\frac{\kappa_0}{2\rho_0}}\delta t} \\ &= {}_\Delta \boldsymbol{R}(t) \left(1 - \sqrt{\frac{\kappa_0}{2\rho_0}}\delta t + \frac{\kappa_0}{4\rho_0}\delta t^2\right) + O(\delta t^2). \end{aligned} \tag{8.45}$$

Furthermore differentiating Equation (8.44) in time

$$ {}_{\Delta}\dot{\boldsymbol{R}}(t) = -\omega_{\Delta}\boldsymbol{R}(t). \tag{8.46}$$

In order to account for non-critical, non-oscillatory damping, a constant $\alpha \geq 1$ is introduced such that α represents the ratio of critical damping to non-critical damping

$$ {}_{\Delta}\dot{\boldsymbol{R}}(t) = -\frac{\omega}{\alpha}{}_{\Delta}\boldsymbol{R}(t) = -\omega'{}_{\Delta}\boldsymbol{R}(t) \iff \omega' = \frac{\omega}{\alpha}. \tag{8.47}$$

It will become apparent that α relates lattice time discretisation to the real time discritisation and will relate the dynamic experiments (like stress relaxation) to dynamic numerical models. The other constants (G and μ) do not provide this information. Note that (using the nomenclature of Table 8.3 as depicted in Figure 8.1)

$$ \kappa_{\sigma i}(t) R_{rms}\boldsymbol{\epsilon}_{\sigma i} = \kappa\mathbf{R}_{\sigma i}(t) \qquad \forall\ \sigma = 0, 1, 2 \text{ and } i \in [1, 4] \tag{8.48}$$

and

$$ \kappa^{poly}_{\sigma i}(t) R_{rms}\boldsymbol{\epsilon}_{\sigma i} = \kappa\mathbf{R}^{poly}_{S\sigma i}(t) \tag{8.49}$$

where $\kappa^{poly}_{\sigma i}(t)$ is the distribution of κ at time (t) during polymer redistribution, subject to the constraint $\sum_{\sigma i}\kappa_{\sigma i} = \kappa_0$. Similarly $\mathbf{R}^{poly}_{S\sigma i}(t)$ is the distribution of ${}_{\Delta}\boldsymbol{R}$ at time t during polymer distribution. Then when considering the static vector length $\boldsymbol{R}_S$ after a period of interaction δt,

$$\begin{aligned}
\kappa\mathbf{R}^{poly}_{S\sigma i}(t+\delta t) &= \kappa\mathbf{R}_{S\sigma i}(t) + \kappa\Delta(\mathbf{R}_{S\sigma i}(t)) = \kappa(\mathbf{R}_{S\sigma i}(t+\delta t) - \mathbf{R}_{S\sigma i}(t)) \\
&= \kappa\mathbf{R}_{S\sigma i}(t) + \kappa(\mathbf{R}_{S\sigma i}(t+\delta t) - \mathbf{R}_{\mu\sigma i}) - \kappa(\mathbf{R}_{S\sigma i}(t) - \mathbf{R}_{\mu\sigma i}) \\
&= \kappa\mathbf{R}_{S\sigma i}(t) + \kappa\mathbf{R}^{poly}_{S\sigma i}(t+\delta t) - \kappa\mathbf{R}^{poly}_{S\sigma i}(t) \\
&= \kappa\mathbf{R}_{S\sigma i}(t) + \int_{t}^{t+\delta t} \kappa\dot{\mathbf{R}}^{poly}_{S\sigma i}(\tau)d\tau.
\end{aligned} \tag{8.50}$$

Let $\mathbf{g}(t) = \int \kappa\dot{\mathbf{R}}^{poly}_{S\sigma i}(\tau)d\tau$; then a trunctated Taylor expansion produces

$$ \mathbf{g}(t+\delta t) = \mathbf{g}(t) + \mathbf{g}'(t)\delta t + O(\delta t) \iff \mathbf{g}(t+\delta t) - \mathbf{g}(t) = \mathbf{g}'(t)\delta t$$

which implies that

$$\int_{t}^{t+\delta t} \kappa\dot{\mathbf{R}}^{poly}_{S\sigma i}(\tau)d\tau \;=\; \kappa\dot{\mathbf{R}}^{poly}_{S\sigma i}. \tag{8.51}$$

Assuming a BGK approximation to relaxation (where $\kappa\mathbf{R}^{(eq)}_{S\sigma i}(t)$ is the zero order stress, zero strain state), one obtains

$$\kappa_0\dot{\mathbf{R}}^{poly}_{S\sigma i}(t) = \frac{\kappa\mathbf{R}^{(eq)}_{S\sigma i}(t) - \kappa_0\mathbf{R}_{S\sigma i}(t)}{\tau'_{poly}\delta t}.$$

Integrating from t to $t+\delta t$ and substituting (8.51),

$$\iff \int_{t}^{t+\delta t} \kappa\dot{\mathbf{R}}^{poly}_{S\sigma i}(\tau)d\tau = \frac{\kappa\mathbf{R}^{(eq)}_{S\sigma i}(t) - \kappa\mathbf{R}_{S\sigma i}(t)}{\tau'_{poly}} \tag{8.52}$$

and Equation (8.52) can be substituted into Equation (8.50). Solving for τ'_{poly} in Equation (8.52) by substituting (8.47),

$$\begin{aligned} -\frac{\omega}{\alpha}\kappa\mathbf{R}_{S\sigma i}(t) = \kappa\dot{\mathbf{R}}_{S\sigma i}(t) &= \frac{\kappa\mathbf{R}^{(eq)}_{S\sigma i}(t) - \kappa\mathbf{R}_{S\sigma i}(t)}{\tau'_{poly}\delta t} \\ \iff \Big(\frac{1}{\tau'_{poly}\delta t} - \frac{\omega}{\alpha}\Big)\kappa\mathbf{R}_{S\sigma i}(t) &= \frac{\kappa\mathbf{R}^{(eq)}_{S\sigma i}(t)}{\tau'_{poly}\delta t} \end{aligned} \tag{8.53}$$

for which the homogenous solution is

$$\tau'_{poly} = \frac{\alpha}{\omega\delta t} = \frac{1}{\omega'\delta t} = \alpha\tau_{poly} \tag{8.54}$$

where $\tau_{poly} = 1/(\omega\delta t)$. Substituting (8.48) and (8.49) into (8.50), the latter reduces to

$$\begin{aligned} \kappa\mathbf{R}^{poly}_{S\sigma i}(t+\delta t) &= \kappa\mathbf{R}_{S\sigma i}(t) + \frac{\kappa\mathbf{R}^{(eq)}_{S\sigma i}(t) - \kappa\mathbf{R}_{S\sigma i}(t)}{\tau'_{poly}}, \\ R_{rms}\kappa^{poly}_{\sigma i}(t+\delta t) &= R_{rms}\kappa_{\sigma i}(t) + R_{rms}\frac{\kappa^{(eq)}_{\sigma i}(t) - \kappa_{\sigma i}(t)}{\tau'_{poly}}, \\ \kappa^{poly}_{\sigma i}(t+\delta t) &= \kappa_{\sigma i}(t) + \frac{\kappa^{(eq)}_{\sigma i}(t) - \kappa_{\sigma i}(t)}{\tau'_{poly}}. \end{aligned} \tag{8.55}$$

Given that $\mathbf{R}$ can represent $\mathbf{R}_S$ or $\mathbf{R}_D$,

$$_{\Delta}\mathbf{R}_D = \int_t^{t+\delta t} \dot{\mathbf{R}}_D(\tau)d\tau = {}_{\Delta}\mathbf{R}_S \implies \dot{\mathbf{R}}_D = \dot{\mathbf{R}}_S \text{ and } \ddot{\mathbf{R}}_S = \ddot{\mathbf{R}}_D. \quad (8.56)$$

From Equation (8.44) and upon substitution of (8.56) and (8.47)

$$\begin{aligned} \dot{\mathbf{R}}_{\sigma i}(t) &= -\frac{1}{\alpha}\sqrt{\frac{\kappa_0}{2\rho_0}}\mathbf{R}_{\sigma i}(0)e^{-\frac{1}{\alpha^2}\frac{\kappa_0}{2\rho_0}t} = -\frac{1}{\alpha}\sqrt{\frac{\kappa_0}{2\rho_0}}\mathbf{R}_{\sigma i}(t), \quad (8.57)\\ \dot{\mathbf{R}}_{S\sigma i}(t) &= -\frac{1}{\alpha}\sqrt{\frac{\kappa_0}{2\rho_0}}\mathbf{R}_{S\sigma i}(0)e^{-\frac{1}{\alpha^2}\frac{\kappa_0}{2\rho_0}t} = -\frac{1}{\alpha}\sqrt{\frac{\kappa_0}{2\rho_0}}\mathbf{R}_{S\sigma i}(t), \end{aligned}$$

For the critically damped situation

$$\dot{\mathbf{R}}_{D\sigma i}(t) = -\sqrt{\frac{\kappa_0}{2\rho_0}}\mathbf{R}_{S\sigma i}(t) \iff \frac{\dot{\mathbf{R}}_{D\sigma i}(t)}{\alpha} = -\frac{1}{\alpha}\sqrt{\frac{\kappa_0}{2\rho_0}}\mathbf{R}_{S\sigma i}(t) \quad (8.58)$$

where $\mathbf{R}_{D\sigma i}$ is the critical damped chain stretch rate. Consider (8.49) where $\kappa = \kappa_0$. Making the substitutions

$$\begin{aligned} \mathbf{R}_{S\sigma i} &= \frac{1}{\kappa_0}\kappa_{\sigma i}R_{rms}\boldsymbol{\epsilon}_{\sigma i} \quad (8.59)\\ \dot{\mathbf{R}}_{D\sigma i} &= \frac{1}{\rho_0}\rho_{\sigma i}\dot{R}_{rms}\boldsymbol{\epsilon}_{\sigma i} \iff \frac{1}{\alpha}\dot{\mathbf{R}}_{D\sigma i} = \frac{1}{\rho_0}\rho_{\sigma i}\dot{R}'_{rms}\boldsymbol{\epsilon}_{\sigma i} \quad (8.60) \end{aligned}$$

where

$$\frac{\dot{R}_{rms}}{\alpha} = \dot{R}'_{rms}. \quad (8.61)$$

Substituting (8.59),(8.60) and (8.61) into (8.58), the latter reduces to

$$\begin{aligned} \frac{1}{\rho_0}\rho_{\sigma i}(t)\dot{R}'_{rms} &= -\frac{1}{\alpha}\sqrt{\frac{\kappa_0}{2\rho_0}}\frac{1}{\kappa_0}\kappa_{\sigma i}(t)R_{rms} = \\ \text{or} \qquad \rho_{\sigma i}(t)\dot{R}'_{rms} &= -\frac{1}{2\alpha}\sqrt{\frac{2\rho_0}{\kappa_0}}\kappa_{\sigma i}(t)R_{rms} = -\frac{1}{2\alpha\omega}\kappa_{\sigma i}(t)R_{rms} \quad (8.62) \end{aligned}$$

where

$$\rho_0\dot{R}'_{rms} = \sum_{\sigma i}\rho_{\sigma i}\dot{R}'_{rms} = -\frac{1}{2\alpha\omega}\sum_{\sigma i}\kappa_{\sigma i}R_{rms} = -\frac{\kappa_0}{2\alpha\omega}R_{rms}$$

such that

$$\frac{\dot{R}'_{rms}}{R_{rms}} = -\frac{1}{\alpha\omega}\frac{\kappa_0}{2\rho_0} = -\frac{\omega}{\alpha} \iff \frac{\dot{R}_{rms}}{R_{rms}} = -\omega. \quad (8.63)$$

Substituting (8.63) into (8.62),

$$\rho_{\sigma i} = \frac{1}{2\omega^2}\kappa_{\sigma i} = \frac{\rho_0}{\kappa_0}\kappa_{\sigma i}. \tag{8.64}$$

Next the above redistribution of stretch is coupled to the redistribution of stretch rate. Given that during the redistribution/relaxation period δt the material has been idealised as a mass-spring-damper unit to 1^{st} order,

$$\rho_0\dot{\mathbf{R}}^{poly}_{D\sigma i}(t+\delta t) = \rho_0\dot{\mathbf{R}}_{D\sigma i}(t) + \int_t^{t+\delta t}\rho_0\ddot{\mathbf{R}}_{D\sigma i}(\tau)d\tau. \tag{8.65}$$

It remains to determine $\int_t^{t+\delta}\rho_0\ddot{\mathbf{R}}_{D\sigma i}(\tau)d\tau$. This can be achieved by differentiating Equation (8.52) with respect to time such that

$$\frac{\partial}{\partial t}\int_t^{t+\delta t}\kappa_0\dot{\mathbf{R}}^{poly}_{S\sigma i}(\tau)d\tau = \frac{\partial}{\partial t}\frac{\kappa_0\mathbf{R}^{(eq)}_{S\sigma i}(t) - \kappa_0\mathbf{R}_{S\sigma i}(t)}{\alpha\tau_{poly}}. \tag{8.66}$$

Then substituting (8.57) and finally (8.63) into (8.66)

$$\begin{aligned}
\int_t^{t+\delta t}\kappa_0\ddot{\mathbf{R}}_{S\sigma i}(\tau)d\tau &= \frac{\kappa_0\dot{\mathbf{R}}^{(eq)}_{S\sigma i}(t) - \kappa_0\dot{\mathbf{R}}_{S\sigma i}(t)}{\alpha\tau_{poly}} \\
\int_t^{t+\delta t}\kappa_0\ddot{\mathbf{R}}_{S\sigma i}(\tau)d\tau &= \frac{-\omega\kappa_0\mathbf{R}^{(eq)}_{S\sigma i}(t) + \omega\kappa_0\mathbf{R}_{S\sigma i}(t)}{\alpha^2\tau_{poly}}.
\end{aligned} \tag{8.67}$$

Further substituting (8.43), (8.49), (8.56) and (8.63) into (8.67)

$$\begin{aligned}
\frac{2\alpha^2\rho_0}{\kappa_0}\int_t^{t+\delta t}\kappa_0\ddot{\mathbf{R}}_{D\sigma i}(\tau)d\tau &= \frac{2\alpha^2\rho_0}{\kappa_0}\frac{\kappa^{(eq)}_{\sigma i}(t) - \kappa_{\sigma i}(t)}{\alpha^2\tau_{poly}}\Big(-\omega R_{rms}\Big)\boldsymbol{\epsilon}_{\sigma i} \\
\text{or} \qquad \int_t^{t+\delta t}\rho_0\ddot{\mathbf{R}}_{D\sigma i}(\tau)d\tau &= -\frac{R_{rms}}{2\omega}\frac{\kappa^{(eq)}_{\sigma i}(t) - \kappa_{\sigma i}(t)}{\alpha^2\tau_{poly}}\boldsymbol{\epsilon}_{\sigma i}.
\end{aligned} \tag{8.68}$$

Substituting (8.56), (8.64) and (8.67) into (8.65), the latter reduces to

$$\begin{aligned}
\rho^{poly}_{\sigma i}(t+\delta t)\dot{R}_{rms} &= \rho_{\sigma i}(t)\dot{R}_{rms} - \Big(\frac{R_{rms}}{2\omega}\Big)\Big(\frac{\kappa^{(eq)}_{\sigma i} - \kappa_{\sigma i}}{\alpha^2\tau_{poly}}\Big) \\
&= \rho_{\sigma i}(t)\dot{R}_{rms} + \Big(\frac{\dot{R}_{rms}}{2\omega^2}\Big)\Big(\frac{\kappa^{(eq)}_{\sigma i} - \kappa_{\sigma i}}{\alpha^2\tau_{poly}}\Big)
\end{aligned}$$

such that

$$\begin{aligned}\rho_{\sigma i}^{poly}(t+\delta t)\dot{R}_{rms} &= \rho_{\sigma i}(t)\dot{R}_{rms} + \Big(\rho_0\frac{\dot{R}_{rms}}{\kappa_0}\Big)\Big(\frac{\kappa_{\sigma i}^{(eq)}-\kappa_{\sigma i}}{\alpha^2\tau_{poly}}\Big)\\ \rho_{\sigma i}^{poly}(t+\delta t) &= \rho_{\sigma i}(t) + \Big(\frac{\rho_0}{\kappa_0}\Big)\Big(\frac{\kappa_{\sigma i}^{(eq)}-\kappa_{\sigma i}}{\alpha^2\tau_{poly}}\Big).\end{aligned} \tag{8.69}$$

The last term represents a redistribution and no net change in $\sum_{\sigma i}\rho_{\sigma i}$ occurs. It is also evident that the above represents one-way coupling. Two-way coupling requires that a similar procedure be applied to $\dot{\boldsymbol{R}}_D$. The relevance of the distribution of the change in $\rho_{\sigma i}$ being proportional to the change in $\kappa_{\sigma i}$ in the redistribution, as described by (8.62), will become evident in Chapter 10 where the macroscopic equations are derived from the discrete approximation. The above couples density to bulk modulus per unit volume. Now the two-way coupling will be completed by coupling bulk modulus per unit volume to density.

Differentiating Equation (8.41) in time,

$${}_{\Delta}\dot{\mathbf{R}}(t) = -\frac{1}{\alpha}\sqrt{\frac{\kappa_0}{2\rho_0}}{}_{\Delta}\mathbf{R}(0)e^{-\frac{1}{\alpha}\sqrt{\frac{\kappa_0}{2\rho_0}}t}. \tag{8.70}$$

But, from (8.47),

$${}_{\Delta}\dot{\mathbf{R}}(0) = -\frac{1}{\alpha}\sqrt{\frac{\kappa_0}{2\rho_0}}{}_{\Delta}\mathbf{R}(0) \iff {}_{\Delta}\dot{\mathbf{R}}(t) = {}_{\Delta}\dot{\mathbf{R}}(0)e^{-\frac{1}{\alpha}\sqrt{\frac{\kappa_0}{2\rho_0}}t}. \tag{8.71}$$

Allowing $\mathbf{R}$ to represent $\mathbf{R}_D$, by the definition of a definite integral

$$\rho_0\dot{\mathbf{R}}_{D\sigma i}^{poly}(t+\delta t) = \rho_0\dot{\mathbf{R}}_{D\sigma i}(t) + \int_t^{t+\delta t}\frac{\partial}{\partial t}\rho_0\dot{\mathbf{R}}_{D\sigma i}(\tau)d\tau. \tag{8.72}$$

Once again, assuming a BGK approximation to the derivative, that is

$$\frac{\partial}{\partial t}\rho_0\dot{\mathbf{R}}_{D\sigma i}(t) = \frac{\rho_0\dot{\mathbf{R}}_{D\sigma i}^{(eq)} - \rho_0\dot{\mathbf{R}}_{D\sigma i}}{\tau'_{poly2}\delta t} \tag{8.73}$$

and integrating with respect to time, one gets

$$\rho_0\dot{\mathbf{R}}_{D\sigma i}(\tau)\Big]_t^{t+\delta t} = \int_t^{t+\delta t}\frac{\rho_0\dot{\mathbf{R}}_{D\sigma i}^{(eq)} - \rho_0\dot{\mathbf{R}}_{D\sigma i}}{\tau'_{poly2}\delta t}d\tau$$

$$= \frac{\rho_0 \dot{\mathbf{R}}^{(eq)}_{D\sigma i} - \rho_0 \dot{\mathbf{R}}_{D\sigma i}}{\tau'_{poly2}} = \Delta\rho_0 \dot{\mathbf{R}}_{D\sigma i}. \tag{8.74}$$

Substituting Equation (8.74) into (8.72) and further making the substitution

$$\rho_0 \dot{\mathbf{R}}_{D\sigma i} = \rho_{\sigma i} \dot{R}_{rms} \boldsymbol{\epsilon}_{\sigma i} \iff \frac{\rho_0}{\alpha} \dot{\mathbf{R}}_{D\sigma i} = \rho_{\sigma i} \dot{R}'_{rms} \boldsymbol{\epsilon}_{\sigma i},$$

which is the equivalent of (8.49) for density, one obtains

$$\begin{aligned} \rho^{poly}_{\sigma i}(t+\delta t)\dot{R}'_{rms} &= \rho_{\sigma i}(t)\dot{R}'_{rms} + \frac{\rho^{(eq)}_{\sigma i}\dot{R}'_{rms} - \rho_{\sigma i}\dot{R}'_{rms}}{\tau'_{poly2}} \\ \text{or} \qquad \rho^{poly}_{\sigma i}(t+\delta t) &= \rho_{\sigma i}(t) + \frac{\rho^{(eq)}_{\sigma i} - \rho_{\sigma i}}{\tau'_{poly2}}. \end{aligned} \tag{8.75}$$

In order to solve for τ'_{poly2} one differentiates Equation (8.44) with respect to time to get

$$\begin{aligned} {}_{\Delta}\dot{\mathbf{R}}(t) &= -\omega_{\Delta}\dot{\mathbf{R}}(0)e^{-\omega t} = -\omega_{\Delta}\mathbf{R}(t) \\ \text{so that} \qquad {}_{\Delta}\ddot{\mathbf{R}}(t) &= -\omega_{\Delta}\dot{\mathbf{R}}(t) \\ \text{or} \qquad {}_{\Delta}\ddot{\mathbf{R}}(t) &= -\frac{\omega}{\alpha}{}_{\Delta}\dot{\mathbf{R}}(t) \end{aligned} \tag{8.76}$$

for non-critical damping. Next substitute (8.73)

$$\begin{aligned} \frac{\partial}{\partial t}\rho_{0\Delta}\dot{\mathbf{R}}(t) = \rho_{0\Delta}\ddot{\mathbf{R}}(t) &= -\frac{\omega}{\alpha}\rho_{0\Delta}\dot{\mathbf{R}}(t) = \frac{\rho_{\Delta}\dot{\mathbf{R}}^{(eq)} - \rho_{\Delta}\dot{\mathbf{R}}}{\tau_{poly2}\delta t} \\ \text{or} \qquad \Big(\frac{1}{\tau'_{poly2}\delta t} - \frac{\omega}{\alpha}\Big)\rho_0\dot{\mathbf{R}}_{\sigma i}(t) &= \frac{\rho_0\dot{\mathbf{R}}^{(eq)}_{\sigma i}}{\tau'_{poly2}\delta t}. \end{aligned} \tag{8.77}$$

The homogenous solution requires that $\dot{\mathbf{R}}_{\sigma i} = \mathbf{0}$ or

$$\tau'_{poly2} = \frac{\alpha}{\omega\delta t} = \alpha\tau_{poly}. \tag{8.78}$$

Consequently substituting (8.78) into (8.75) one obtains, that during the redistribution,

$$\rho^{poly}_{\sigma i}(t+\delta t)\dot{R}'_{rms} = \rho_{\sigma i}(t)\dot{R}'_{rms} + \dot{R}'_{rms}\frac{\rho^{(eq)}_{\sigma i} - \rho_{\sigma i}}{\alpha\tau_{poly}}. \tag{8.79}$$

From Equation (8.46)

$${}_{\Delta}\mathbf{R}(t) = -\alpha\sqrt{\frac{2\rho_0}{\kappa_0}}{}_{\Delta}\dot{\mathbf{R}}(t) = -\frac{\alpha}{\omega}{}_{\Delta}\dot{\mathbf{R}}(t). \tag{8.80}$$

Given that

$$\kappa_0 \mathbf{R}^{poly}_{D\sigma i}(t+\delta t) = \kappa_0 \mathbf{R}_{D\sigma i}(t) + \int_t^{t+\delta t} \kappa_0 \dot{\mathbf{R}}_{D\sigma i}(\tau) d\tau \quad (8.81)$$

$$\text{and} \qquad \int \kappa_0 \dot{\mathbf{R}}_{D\sigma i}(\tau) d\tau = \int \kappa_0 \Big(\int \ddot{\mathbf{R}}_{D\sigma i}(\tau_1) d\tau_1 \Big) d\tau_2, \quad (8.82)$$

substituting (8.74) into (8.82)

$$\begin{aligned} \int \kappa_0 \dot{\mathbf{R}}_{D\sigma i}(\tau) d\tau &= \int \kappa_0 \frac{\dot{\mathbf{R}}^{(eq)}_{D\sigma i}(\tau_2) - \dot{\mathbf{R}}_{D\sigma i}(\tau_2)}{\alpha \tau_{poly}} d\tau_2 \\ &= \kappa_0 \frac{\mathbf{R}^{(eq)}_{D\sigma i}(\tau_2) - \mathbf{R}_{D\sigma i}(\tau_2)}{\alpha \tau_{poly}}. \end{aligned} \quad (8.83)$$

Then substituting Equation (8.80) into (8.83)

$$\begin{aligned} \int \kappa_0 \dot{\mathbf{R}}_{D\sigma i}(\tau) d\tau &= -\frac{\alpha \kappa_0}{\omega} \frac{\dot{\mathbf{R}}^{(eq)}_{D\sigma i} - \dot{\mathbf{R}}_{D\sigma i}}{\alpha \tau_{poly}} = -\frac{\kappa_0}{\rho_0 \omega} \rho_0 \frac{\dot{\mathbf{R}}^{(eq)}_{D\sigma i} - \dot{\mathbf{R}}_{D\sigma i}}{\tau_{poly}} \quad (8.84) \\ &= -\frac{\kappa_0}{\rho_0} \frac{\dot{R}_{rms}}{\omega} \frac{\rho^{(eq)}_{\sigma i} - \rho_{\sigma i}}{\tau_{poly}} \boldsymbol{\epsilon}_{\sigma i} = \frac{\kappa_0}{\rho_0} R_{rms} \frac{\rho^{(eq)}_{\sigma i} - \rho_{\sigma i}}{\tau_{poly}} \boldsymbol{\epsilon}_{\sigma i}. \end{aligned}$$

Substituting Equation (8.84) into Equation (8.81),

$$\begin{aligned} R_{rms} \kappa^{poly}_{\sigma i}(t+\delta t) &= R_{rms} \kappa_{\sigma i}(t) + \frac{\kappa_0}{\rho_0} R_{rms} \frac{\rho^{(eq)}_{\sigma i} - \rho_{\sigma i}}{\tau_{poly}}, \\ \kappa^{poly}_{\sigma i}(t+\delta t) &= \kappa_{\sigma i}(t) + \Big(\frac{\kappa_0}{\rho_0} \Big) \frac{\rho^{(eq)}_{\sigma i} - \rho_{\sigma i}}{\tau_{poly}}. \end{aligned} \quad (8.85)$$

The combination of Equations (8.55), (8.69), (8.76) and (8.69) couples stretch and stretch rate and is given by

$$\kappa^{poly}_{\sigma i}(t+\delta t) = \kappa_{\sigma i}(t) + \frac{\kappa^{(eq)}_{\sigma i} - \kappa_{\sigma i}}{\alpha \tau_{poly}} + \Big(\frac{\kappa_0}{\rho_0} \Big) \frac{\rho^{(eq)}_{\sigma i} - \rho_{\sigma i}}{\tau_{poly}}, \quad (8.86)$$

$$\rho^{poly}_{\sigma i}(t+\delta t) = \rho_{\sigma i}(t) + \frac{\rho^{(eq)}_{\sigma i} - \rho_{\sigma i}}{\alpha \tau_{poly}} + \Big(\frac{\rho_0}{\kappa_0} \Big) \frac{\kappa^{(eq)}_{\sigma i} - \kappa_{\sigma i}}{\alpha^2 \tau_{poly}}. \quad (8.87)$$

Finally substituting Equation (8.9) into Equation (8.86) and (8.10) into

(8.87)

$$\kappa_{\sigma i}^{poly}(\mathbf{x}+\delta\mathbf{x},t+\delta t) = \kappa_{\sigma i}(\mathbf{x},t) - \frac{\kappa_{\sigma i}-\kappa_{\sigma i}^{(ms)}}{\tau_R} + \frac{\kappa_{\sigma i}^{(eq)}-\kappa_{\sigma i}}{\alpha\tau_{poly}} + \left(\frac{\kappa_0}{\rho_0}\right)\frac{\rho_{\sigma i}^{(eq)}-\rho_{\sigma i}}{\tau_{poly}}, \quad (8.88)$$

$$\rho_{\sigma i}^{poly}(\mathbf{x}+\delta\mathbf{x},t+\delta t) = \rho_{\sigma i}(\mathbf{x},t) - \frac{\rho_{\sigma i}-\rho_{\sigma i}^{(ms)}}{\tau_{\dot{R}}} + \frac{\rho_{\sigma i}^{(eq)}-\rho_{\sigma i}}{\alpha\tau_{poly}} + \left(\frac{\rho_0}{\kappa_0}\right)\frac{\kappa_{\sigma i}^{(eq)}-\kappa_{\sigma i}}{\alpha^2\tau_{poly}}. \quad (8.89)$$

In analogy with the LBM, the coupled Equations (8.88) and (8.89) can be interpreted as a three-step procedure. The first is advection, the second is redistribution to the maximum entropy state and the third is recoupling or redistribution between density and bulk modulus per unit volume.

8.5 Closing remarks on chain length and chain stretch rate recoupling and the polymer LBM

It is noted that in Section 8.4.3 a Kelvin-Voigt model of linear viscoelasticity was used to recouple stretch-space to stretch-rate-space. This model of redistribution was selected to be consistent with the material viscoelasticity of Section 7.2. The selection of this model to relate stretch to stretch rate is however arbitrary and one could select an alternate model.

Finally it should be emphasized that the numerical method constructed in this chapter is a discretisation of the mesoscopic equation of polymer interaction (3.85) which is (as the name suggests) mesoscopic, independent of macroscopic variables (like stress) and is large strain. This should be distinguished from the polymer flow equation (6.98) which is the macroscopic consequence of the Chapman-Enskog expansion performed on (3.85) to first order. It is the macroscopic polymer flow equation (6.98) which was shown to be small strain in Chapter 7.

Chapter 9

Macroscopic variable recovery

Chapter 8 effectively constructed a LBM for polymers. Of note, two interacting lattices were constructed – one for the static component of chain length, $\mathbf{R}_S$, and another for the dynamic component $\mathbf{R}_D$. These represent the same chain length and can generically be represented as $\mathbf{R}$. Chapter 8 continues with the coupling of these lattices.

In this chapter the macroscopically measurable variables are reconstructed for the discrete theory. The resultant macroscopic variables are obviously a function of the static and dynamic components. It should be noted that the macroscopic variables that are reconstructed here are not required for numerical modelling. Rather they are used in post-processing (after the numerical model has been fully implemented) to extract the macroscopic variables (e.g. stress). As previously noted, the numerical model is independent of stress.

9.1 Kinematic material variables

For a molecule with vector length AB, the rate of change of position B is due to the rate of change of vector length $\dot{\mathbf{R}}_S$ and the rate of change of position A $(-0.5\dot{\mathbf{R}}_D)$. Consider the alternate method of numbering the direction of vectors as presented in Chapter 8. The alternate numbering was compared to the conventional in Table 8.3 and was depicted Figure 8.1. At a lattice point $(\mathbf{x})$, the component of the rate of change of position B (in the direction σi) of the molecule relative to the original position A of the molecule is

$$\dot{\mathbf{R}}_{\sigma i}(\mathbf{x},t) = \dot{\mathbf{R}}_{S\sigma i}(\mathbf{x},t) + \mathbf{c}_{\sigma i}(\mathbf{x},t) = \dot{\mathbf{R}}_{S\sigma i}(\mathbf{x},t) - \frac{\dot{\mathbf{R}}_{D\sigma i}(\mathbf{x},t)}{2} \tag{9.1}$$

where $\mathbf{R}_S$ is represented by $\boldsymbol{R}_f$ of Equation (8.45) and $\mathbf{R}_D$ is represented by $\boldsymbol{R}_f$ of Equation (8.80). Note that averaged properties are macroscopic and the notation reflects this. Integrating Equation (9.1), one obtains

$$\mathbf{R}_{\sigma i} = \mathbf{R}_{S\sigma i} - \frac{1}{2}\int_0^t \dot{\mathbf{R}}_{D\sigma i} dt$$

where $\mathbf{R}_{\sigma i}$ represents the average position of the B (or distal) ends of the molecules. The contributions to these end positions are $\mathbf{R}_{S\sigma i}$ which represents the averaged molecular length and $-\frac{1}{2}\int_0^t \dot{\mathbf{R}}_{D\sigma i} dt$ which represents the average change in positions A. Thus the prinicipal lattice material or Lagrangian stretch vector $\boldsymbol{\lambda}^{(lat)} = (\lambda_1^{(lat)}, \lambda_2^{(lat)})$ is

$$\boldsymbol{\lambda}^{(lat)} = \Big(\frac{\kappa_{\sigma i}\epsilon_{\sigma ix}}{\kappa_0}, \frac{\kappa_{\sigma i}\epsilon_{\sigma iy}}{\kappa_0}\Big) \tag{9.2}$$

In Section 3.2.6 it will be shown that the real principal stretch $\boldsymbol{\lambda}^{(\boldsymbol{real})} = \sqrt{3}\boldsymbol{\lambda}^{(\boldsymbol{lat})}$. The principal strain at any given position is given by

$$\boldsymbol{\epsilon}^{(real)} = (\lambda_x^{(real)} - 1, \lambda_y^{(real)} - 1) \tag{9.3}$$

Similarly, the Lagrangian (material) lattice rate of change of length at a given position is given by Equation (8.47) where $\omega' = \omega/\alpha$ and ω corresponds to the citically damped scenario of (8.46) and α is the ratio between non-critically damped, non-oscillatory ω' and critically damped ω

$$\begin{aligned} \dot{\mathbf{R}}_{S\sigma i}^{(lat)} &= -\omega' \mathbf{R}_{S\sigma i}^{(lat)} = -\omega' \frac{\kappa_{\sigma i}\boldsymbol{\epsilon}_{\sigma i}}{\kappa_0} R_{rms} \\ \Longleftrightarrow \qquad \dot{\boldsymbol{\lambda}} &= -\omega' \boldsymbol{\lambda} = -\omega' \Big(\frac{\kappa_{\sigma i}\epsilon_{\sigma ix}}{\kappa_0}, \frac{\kappa_{\sigma i}\epsilon_{\sigma iy}}{\kappa_0}\Big) \end{aligned} \tag{9.4}$$

where $\boldsymbol{\epsilon}_{\sigma i}$ is defined in Table 8.3 and depicted in Figure 8.1. The Eulerian velocity of the sample at any given position is given, substituting (8.61), by

$$\dot{\mathbf{c}}^{(\mathbf{lat})} = -\frac{\dot{\mathbf{R}}_{D\sigma i}^{(lat)}}{2\alpha} = -\frac{\dot{R}'_{rms}}{2\rho_0}\rho_{\sigma i}\boldsymbol{\epsilon}_{\sigma i} = -\frac{\dot{R}'_{rms}}{2\rho_0}\Big(\rho_{\sigma i}\epsilon_{\sigma ix}, \rho_{\sigma i}\epsilon_{\sigma iy}\Big). \tag{9.5}$$

Finally the Eulerian velocity at the spatial limits of a control volume is given by the substitution of Equations (9.4) and (9.5) into Equation (9.1):

$$\dot{\mathbf{R}}_{\sigma i}^{(lat)} = \dot{\mathbf{R}}_{S\sigma i}^{(lat)} - \frac{1}{2}\dot{\mathbf{R}}_{D\sigma i}^{(lat)} = -\omega' \frac{\kappa_{\sigma i}\boldsymbol{\epsilon}_{\sigma i}}{\kappa_0} R_{rms} - \frac{\dot{R}'_{rms}}{2\rho_0}\rho_{\sigma i}\boldsymbol{\epsilon}_{\sigma i}. \tag{9.6}$$

The Eulerian chain stretch rate ratio ι is given by

$$\iota_j = \frac{\sqrt{3}\dot{\mathrm{R}}_{Dj}}{\dot{R}_{rms}} = \frac{\dot{\mathrm{R}}_{Dj}}{\dot{R}_{rms}/\sqrt{3}} = \frac{\dot{\mathrm{R}}_{Dj}}{\dot{\mathrm{R}}_{D\mu 0j}} \tag{9.7}$$

where the subscript j represents a principal direction. Thus ι represents the ratio of current chain stretch rate to root mean square of initial chain length stretch rate. The relationship between ι_i and $\dot{\lambda}_i$ is discussed in Section 11.7. In analogy with (9.2), the principal lattice material or Lagrangian chain stretch ratio is given by

$$\boldsymbol{\iota}^{(lat)} = \Big(\frac{\rho_{\sigma i}\epsilon_{\sigma ix}}{\rho_0}, \frac{\rho_{\sigma i}\epsilon_{\sigma iy}}{\rho_0}\Big). \tag{9.8}$$

The real version of the Lagrangian chain stretch ratio is given by

$$\boldsymbol{\iota}^{(real)} = \Big(\frac{\sqrt{3}\rho_{\sigma i}\epsilon_{\sigma ix}}{\rho_0}, \frac{\sqrt{3}\rho_{\sigma i}\epsilon_{\sigma iy}}{\rho_0}\Big). \tag{9.9}$$

9.2 Kinetic material variables

The latent material stress tensor, $\mathbf{T}$, is the combination of the 0-order approximations for the static and dynamic stress tensors $\boldsymbol{\sigma}_S^{(0)}$ and $\boldsymbol{\sigma}_D^{(0)}$ respectively and the corresponding first order approximations $\boldsymbol{\sigma}_S^{(1)}$ and $\boldsymbol{\sigma}_D^{(1)}$, such that

$$\mathbf{T} = \Big(\boldsymbol{\sigma}_S^{(0)} + \boldsymbol{\sigma}_S^{(1)}\Big) + \Big(\boldsymbol{\sigma}_D^{(0)} + \boldsymbol{\sigma}_D^{(1)}\Big) \tag{9.10}$$

which can be compared to Equations (6.88), (6.89), (6.81), (6.82), (7.15) and (6.110). Then clearly

$$\begin{aligned}
\boldsymbol{\sigma}_S^{(0)} &= -\frac{1}{2}\mathbf{P}_S, \\
\boldsymbol{\sigma}_D^{(0)} &= -2\mathbf{P}_D, \\
\boldsymbol{\sigma}_S^{(1)} &= \frac{2}{3}G\int_0^t \Big(\nabla\cdot\mathbf{R}_\mu\Big)d\tau\mathbf{I} + 4\int_0^t G\mathbf{D}d\tau, \qquad \boldsymbol{\sigma}_S^{(i1)} = \Theta + 4\int_0^t G\mathbf{D}d\tau, \\
\boldsymbol{\sigma}_D^{(1)} &= \frac{2}{3}\mu(\nabla\cdot\dot{\mathbf{R}}_\mu)\mathbf{I} + 4\mu\dot{\mathbf{D}}, \qquad \boldsymbol{\sigma}_D^{(i1)} = 4\mu\dot{\mathbf{D}}.
\end{aligned}$$

The above is for the latent material stress tensor but recall from (7.17) and the definition of the apparent material stress in Section 5.1.5 that

$${}^{\langle app\rangle}\mathbf{T} = 2\Big(\boldsymbol{\sigma}_S^{(0)} + \boldsymbol{\sigma}_S^{(1)}\Big) + \frac{1}{2}\Big(\boldsymbol{\sigma}_D^{(0)} + \boldsymbol{\sigma}_D^{(1)}\Big). \tag{9.11}$$

9.2.1 The zero order approximation

For an infinitesimal control surface, the pressure acting on a surface is equal but opposite to the stress in the direction normal to the surface. This pressure at the surface can be determined from the force applied by a tensile testing instrument. The change in force per unit volume – upon substitution of (8.46) – is

$$\begin{aligned}\frac{\mathbf{F}^{(lat)}}{V} &= \rho_0 \frac{d\dot{\mathbf{c}}^{(lat)}}{dt} = -\frac{\rho_0}{2\alpha}\sum_{\sigma i}\frac{d\dot{\mathbf{R}}^{(lat)}_{D\sigma i}(t)}{dt} \qquad \sigma = 0,1,2,\ i = 1,2,3,4 \\ &= \sum_{\sigma i}\frac{\rho_0}{2\alpha}\omega'\dot{\mathbf{R}}^{(lat)}_{D\sigma i}(t) = \sum_{\sigma i}\frac{\dot{R}'_{rms}}{2}\omega'\rho_{\sigma i}(t)\boldsymbol{\epsilon}_{\sigma i}. \end{aligned} \tag{9.12}$$

The average of the change in the force per unit volume during the time 0 to t is determined by applying the trapezoidal rule (to integrate over time). Thus

$$\begin{aligned}\overline{\frac{\Delta\mathbf{F}^{(lat)}}{V}} &= \sum_{\sigma i}\frac{1}{2}\Big(\frac{\rho_0}{2\alpha}\omega'\Big)\Big(\dot{\mathbf{R}}^{(lat)}_{D\sigma i}(t) + \dot{\mathbf{R}}^{(lat)}_{D\sigma i}(0)\Big) \\ &= \sum_{\sigma i}\frac{\dot{R}'_{rms}}{4}\omega'(\rho_{\sigma i}(t) + \rho^{(eq)}_{\sigma i})\boldsymbol{\epsilon}_{\sigma i}. \end{aligned} \tag{9.13}$$

The change in dynamic pressure acting on the surface with direction j is given by the product of the force per unit volume and the length traversed by the A end of the control volume in direction j (as determined by (5.22)). Let $\mathrm{P}_{Djj} = \mathrm{P}_{Djk}\delta_{jk}$ where δ_{ij} is the Kronecker delta and the result is not summed, then

$$\begin{aligned}\Delta\mathrm{P}^{(0)(lat)}_{Djj} &= \overline{\frac{F^{(lat)}_j}{V}}L_j = -\overline{\frac{\rho_0}{2\alpha}\ddot{\mathrm{R}}^{(lat)}_{D\sigma ij}(t)}\cdot\int_0^t \dot{c}^{(lat)}_j d\tau \\ &= -\overline{\frac{\rho_0}{2\alpha}\ddot{\mathrm{R}}^{(lat)}_{D\sigma ij}(t)}\cdot\int_0^t \frac{\dot{\mathrm{R}}^{(lat)}_{D\sigma ij}}{-2}d\tau \\ &= -\frac{\dot{R}'_{rms}}{4}\omega'(\rho_{\sigma i}(t) + \rho_{\sigma i}(0))\epsilon_{\sigma ij}\frac{\dot{\mathrm{R}}_{D\sigma ij}(t)|^t_0}{2\omega'} \\ &= -\frac{\dot{R}'^2_{rms}}{8\rho_0}(\rho_{\sigma i}(t) + \rho_{\sigma i}(0))\epsilon_{\sigma ij}(\rho_{\sigma i}(t) - \rho_{\sigma i}(0))\epsilon_{\sigma ij} \end{aligned} \tag{9.14}$$

$$\Longrightarrow \Delta\mathrm{P}^{(0)(lat)}_{Djj}|^t_0 = -\frac{\dot{R}'^2_{rms}}{8\rho_0}\Big(\sum_{\sigma i}\rho^2_{\sigma i}\epsilon_{\sigma ij}\epsilon_{\sigma ik}\delta_{jk} - \sum_{\sigma i}\rho^{(eq)2}_{\sigma i}\epsilon_{\sigma ij}\epsilon_{\sigma ik}\delta_{jk}\Big) \tag{9.15}$$

and can be compared to (5.24). Alternatively, one can set a time in the future when the material is at equilibrium as a reference time, and then

$$\begin{aligned}\Delta \mathrm{P}_{Djj}^{(0)(lat)}|_t^\infty &= -\overline{\frac{\rho_0}{2}\ddot{\mathrm{R}}_{\sigma ijD}(t)} \cdot \int_t^\infty \grave{c}_j d\tau \\ &= -\frac{\dot{R}'^2_{rms}}{8\rho_0}\sum_{\sigma i}(\rho_{\sigma i}(t)+\rho_{\sigma i}^{(eq)})\epsilon_{\sigma ij}\sum_{\sigma i}(\rho_{\sigma i}^{(eq)}-\rho_{\sigma i}(t))\epsilon_{\sigma ij} \\ &= -\frac{\dot{R}'^2_{rms}}{8\rho_0}\Big(\sum_{\sigma i}\rho_{\sigma i}^{(eq)2}\epsilon_{\sigma ij}\epsilon_{\sigma ik}\delta_{jk}-\sum_{\sigma i}\rho_{\sigma i}^{2}\epsilon_{\sigma ij}\epsilon_{\sigma ik}\delta_{jk}\Big). \quad (9.16)\end{aligned}$$

Given that the lattice dynamic pressure is the product of two lattice properties, the real dynamic pressures are given by

$$\mathrm{P}_{Djj}^{(0)(real)}|_0^t = 3\times \mathrm{P}_{Djj}^{(0)(lat)}|_0^t, \qquad \mathrm{P}_{Djj}^{(0)(real)}|_t^\infty = 3\times \mathrm{P}_{Djj}^{(0)(lat)}|_t^\infty. \quad (9.17)$$

The apparent zero order dynamic stress tensor (with axes aligned in principal directions and with non-diagonal terms equalling zero) is (again without summing)

$$-\Delta^{\langle app\rangle}\sigma_{Djj}^{(0)(lat)}|_0^t = \mathrm{P}_{Djj}^{(0)(lat)} = -\frac{\dot{R}'^2_{rms}}{8\rho_0}\sum_{\sigma i}\Big(\rho_{\sigma i}^2\epsilon_{\sigma ij}-\rho_{\sigma i}^{(eq)2}\epsilon_{\sigma ij}\Big)\epsilon_{\sigma ik}\delta_{jk}. \quad (9.18)$$

Next consider the latent stress. Given that $\boldsymbol{\sigma}_D^{(0)} = -2\mathbf{P}_D$,

$$\Delta\sigma_{Djj}^{(0)(lat)}|_0^t = \frac{\dot{R}'^2_{rms}}{4\rho_0}\sum_{\sigma i}\Big(\rho_{\sigma i}^2\epsilon_{\sigma ij}-\rho_{\sigma i}^{(eq)2}\epsilon_{\sigma ij}\Big)\epsilon_{\sigma ik}\delta_{jk} \quad (9.19)$$

or, setting the reference time in the future, when steady state is reached,

$$\Delta\sigma_{Djj}^{(0)(lat)}|_t^\infty = -\frac{\dot{R}'^2_{rms}}{4\rho_0}\Big(\sum_{\sigma i}\rho_{\sigma i}^{(eq)2}\epsilon_{\sigma ij}\epsilon_{\sigma ik}\delta_{jk}-\sum_{\sigma i}\rho_{\sigma i}^{2}\epsilon_{\sigma ij}\epsilon_{\sigma ik}\delta_{jk}\Big). \quad (9.20)$$

The real versions are

$$\Delta\sigma_{Djj}^{(0)(real)}|_0^t = 3\Delta\sigma_{Djj}^{(0)(lat)}|_0^t, \qquad \Delta\sigma_{Djj}^{(0)(real)}|_t^\infty = 3\Delta\sigma_{Djj}^{(0)(lat)}|_t^\infty. \quad (9.21)$$

Equations (9.14) and (9.15) should be compared to Equation (5.24). The change in sign is because the pressure exerted by the control volume is opposite to the pressure acting across the control volume.

The static pressure acting on a surface induces a force **F** opposite in

direction to the pressure and this force produces a molecular stretch directly proportional to molecular length: that is

$$\frac{\mathbf{F}}{\mathrm{V}} = \kappa \mathbf{R}_S. \tag{9.22}$$

Applying the trapezoidal rule for integration from time $\tau = 0$ or $\tau = \infty$ (depending on reference time) to $\tau = t$, the approximate average force per unit volume is

$$\frac{\overline{\mathbf{F}}}{\mathrm{V}} = \frac{1}{2}\kappa\big(\mathbf{R}_S + \mathbf{R}_{S0}\big). \tag{9.23}$$

The pressure is given by the product of the force per unit volume and the length of the control volume as derived from

$$\frac{\mathbf{F}}{\mathrm{A}} = \frac{\mathbf{F}}{\Delta \mathrm{y}\Delta \mathrm{z}} = \frac{\mathbf{F}}{\Delta \mathrm{x}\Delta \mathrm{y}\Delta \mathrm{z}}\Delta \mathrm{x} = \frac{\mathbf{F}}{\mathrm{V}}\Delta \mathrm{x}$$

where the cross-sectional area on which the force acts is A. For a rectangular specimen, the area is given by the product of the edges $\Delta \mathrm{x} \times \Delta \mathrm{y}$, the length of the specimen along the direction of applied force is $\Delta \mathrm{z}$ and thus the volume $\mathrm{V} = \Delta \mathrm{x}\Delta \mathrm{y}\Delta \mathrm{z}$. The length ($\mathrm{L}_j$ from Equation (5.31)) is given by

$$\begin{aligned} \mathrm{L}_j &= \int_0^t \dot{\mathrm{R}}_{\sigma ij} - \grave{c}_{\sigma ij} d\tau = \int_0^t \Big(\dot{\mathrm{R}}_{\sigma ij} + \frac{1}{2}\dot{\mathrm{R}}_{D\sigma ij}\Big) d\tau = \int_0^t \dot{\mathrm{R}}_{S\sigma ij} d\tau = \mathrm{R}_{S\sigma ij}|_0^t \\ &= \mathrm{R}_{S\sigma ij}(t) - \mathrm{R}_{S\sigma i0j} \iff \mathrm{L}_j^{(lat)} = \frac{R_{rms}}{\kappa_0}\sum_{\sigma i}(\kappa_{\sigma i} - \kappa_{\sigma i0})\epsilon_{\sigma ij}. \end{aligned} \tag{9.24}$$

Consequently the change in pressure is given by

$$\begin{aligned} \Delta \mathrm{P}_{Sjj}^{(0)}|_0^t &= \frac{\overline{\mathrm{F}_j}}{\mathrm{V}}\mathrm{L}_j = \frac{\kappa_0}{2}(\mathrm{R}_{S\sigma ij} + \mathrm{R}_{S\sigma i0j})(\mathrm{R}_{S\sigma ij}(t) - \mathrm{R}_{S\sigma i0j}) \\ &= \frac{\kappa_0}{2}\frac{R_{rms}^2}{\kappa_0^2}\sum_{\sigma i}(\kappa_{\sigma i} + \kappa_{\sigma i0})\epsilon_{\sigma ij}\sum_{\sigma i}(\kappa_{\sigma i} - \kappa_{\sigma i0})\epsilon_{\sigma ij} \\ \Delta \mathrm{P}_{Sjj}^{(0)(lat)}|_0^t &= \frac{R_{rms}^2}{2\kappa_0}\sum_{\sigma i}\left(\kappa_{\sigma i}^2\epsilon_{\sigma ij}\epsilon_{\sigma ik}\delta_{jk} - \kappa_{\sigma i}^{(eq)2}\epsilon_{\sigma ij}\epsilon_{\sigma ik}\delta_{jk}\right). \end{aligned} \tag{9.25}$$

Setting the reference time as ∞ (defined by a future specimen ground state),

$$\Delta \mathrm{P}_{Sjj}^{(0)(lat)}|_t^\infty = \frac{R_{rms}^2}{2\kappa_0}\sum_{\sigma i}\left(\kappa_{\sigma i}^{(eq)2}\epsilon_{\sigma ij}\epsilon_{\sigma ik}\delta_{jk} - \kappa_{\sigma i}^2\epsilon_{\sigma ij}\epsilon_{\sigma ik}\delta_{jk}\right).$$

The changes in the latent zero order stress tensors are thus

$$\Delta\sigma_{Sjj}^{(0)(lat)}|_0^t = -\frac{R_{rms}^2}{4\kappa_0}\sum_{\sigma i}\left(\kappa_{\sigma i}^2\epsilon_{\sigma ij}\epsilon_{\sigma ik}\delta_{jk} - \kappa_{\sigma i}^{(eq)2}\epsilon_{\sigma ij}\epsilon_{\sigma ik}\delta_{jk}\right) \quad (9.26)$$

$$\Delta\sigma_{Sjj}^{(0)(lat)}|_t^\infty = -\frac{R_{rms}^2}{4\kappa_0}\sum_{\sigma i}\left(\kappa_{\sigma i}^{(eq)2}\epsilon_{\sigma ij}\epsilon_{\sigma ik}\delta_{jk} - \kappa_{\sigma i}^2\epsilon_{\sigma ij}\epsilon_{\sigma ik}\delta_{jk}\right). \quad (9.27)$$

Furthermore the apparent stress tensor is

$$\Delta^{\langle app\rangle}\sigma_{Sjj}^{(0)(lat)} = -\frac{R_{rms}^2}{2\kappa_0}\sum_{\sigma i}\left(\kappa_{\sigma i}^2 - \kappa_{\sigma i}^{(eq)2}\right)\epsilon_{\sigma ij}\epsilon_{\sigma ij}.$$

The real stress tensor is the product of two lattice vectors where the ratio of true vector to lattice vector is $\sqrt{3}$. Thus

$$\Delta\sigma_{Sjj}^{(0)(real)}|_0^t = 3\Delta\sigma_{Sjj}^{(0)(lat)}|_0^t, \qquad \Delta\sigma_{Sjj}^{(0)(real)}|_t^\infty = 3\Delta\sigma_{Sjj}^{(0)(lat)}|_t^\infty. \quad (9.28)$$

9.2.2 The first order approximation

The first order approximation to the static pressure tensor is $\int_t^\infty 4G\mathrm{D}_{jk}$ where

$$\mathrm{D}_{kj} = -\frac{1}{4}\Big(\frac{\partial \mathrm{R}_{S\mu k}}{\partial x_j} + \frac{\partial \mathrm{R}_{S\mu j}}{\partial x_k}\Big). \quad (9.29)$$

The limits of integration are justified in Section 10.3. Furthermore, for the discrete theory, let the central difference approximation to the partial derivative of the k component of $\mathbf{R}_{S\mu}$ in the x-direction at node x_j be defined as

$$\frac{\partial \mathrm{R}_{S\mu k}}{\partial x_j} := \frac{\mathrm{R}_{S\mu k}(x_{j+1},t) - \mathrm{R}_{S\mu k}(x_{j-1},t)}{x_{j+1} - x_{j-1}}\,. \quad (9.30)$$

Equation (9.30) can either be calculated in the conventional manner or using the LBM discretisation. An alternate classification would be that the derivative can either be calculated directly or indirectly. Two indirect methods (corresponding to the conventional approach of calculating $\mathbf{R}_S$ at fixed locations and applying a differencing procedure) will be mentioned generating a second order tensor – for the 2D scenario. The third option is direct calculation of the temporal derivative of static stretch – 9 components corresponding to the nine vectors (numbered σi) generated by the LBM discretisation.

Indirect static chain length stretch rate

The first indirect method calculates the stretch in either the x or y direction for the adjacent nodes. A parabolic approximation is used to calculate the gradient in each of the two directions. Thus the calculation of the first order stress requires the derivative at position x_j (depicted as a green point in Figure 9.1) be determined. The two (one for each direction), one-dimensional second order accurate solutions are depicted in Figure 9.1(a). The second

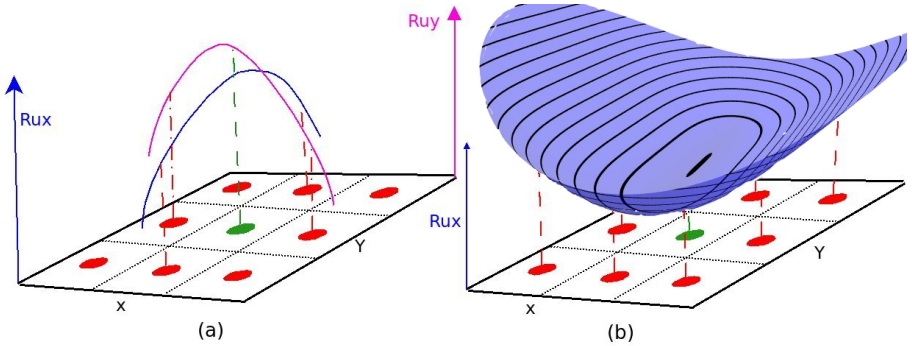

Figure 9.1: (a) APPROXIMATION OF STRETCH BY TWO 1D PARABOLAE (b) APPROXIMATION OF STRETCH BY BIPARABOLIC SURFACE

indirect method will fit a paraboloid surface in nine unknowns to the nine points (equations) as depicted in Figure 9.1(b). The form of the equation is

$$z(x,y) = A_j \sum_{n=0}^{4} \sum_{i=0}^{n} x^i y^{n-i}$$

where $0 < j \leq 9$ $j, n \in \mathbb{N}_0$ and $0 \leq i \leq 2, i \leq n \; \forall \; n, \; i \in \mathbb{N}_0$. The partial derivatives in the x and y directions are used to calculate the gradient. The latter option is more computationally expensive because matrices have to be solved. This need not necessarily be a limitation because the calculation of stress is not used directly in the numerical modelling. The stress can and is calculated post-analytically (post-processing).

Direct static chain length stretch rate

Geometrically, the nine components of the stretch gradients are given by the difference between the weighting (or bulk modulus $\kappa_{\sigma i}$) and the corresponding 'advected' weighting divided by the distance as depicted in Figure 9.2. In Figure 9.2 the nine black squares represent nine LBM cells. The central cell represents position x with the coloured arrows representing stretches. The

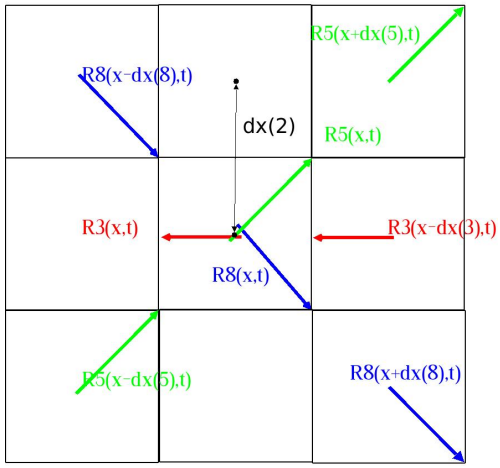

Figure 9.2: THE DISCRETISATION OF PHYSICAL SPACE FOR STRETCH GRADIENTS

colours are defined by direction. Recall that

$$\begin{aligned} \frac{\mathbf{S}_{\sigma i}}{\mathbf{E}_{\sigma i}} &= -2\frac{R_{rms}}{\dot{R}_{rms}} \\ \iff \quad \frac{\mathbf{S}_{\sigma i}}{\mathbf{E}_{\sigma i}\delta t} &= -2\frac{R_{rms}}{\dot{R}_{rms}\delta t} = \frac{R_{rms}\boldsymbol{\epsilon}_{\sigma i}}{\delta x \boldsymbol{\epsilon}_{\sigma i}} = \frac{\mathbf{S}_{\sigma i}}{\Delta \mathbf{x}_{\sigma i}} \end{aligned} \tag{9.31}$$

because $\mathbf{E}_{\sigma i}\delta t$ is always selected to equal $\Delta \mathbf{x}_{\sigma i}$. The gradient of stretch in a given direction is given by the upwind difference divided by the distance in the given direction. Upon substitution of (9.31) into the formula for finite difference

$$\begin{aligned} \frac{\partial \mathrm{R}_{S\sigma ik}(t)}{\partial x_j} &= \frac{\mathrm{R}_{S\sigma ik}(x+\delta x_{\sigma j},t) - \mathrm{R}_{S\sigma ik}(x-\delta x_{\sigma j},t)}{2\delta x_{\sigma j}} + O(\delta x^2) \\ &= \frac{\kappa_{\sigma i}(x+\delta x_{\sigma j},t)\mathrm{S}_{\sigma ik} - \kappa_{\sigma i}(x-\delta x_{\sigma j},t)\mathrm{S}_{\sigma ik}}{2\kappa_0 \delta x_{\sigma j}} \\ &= \Big(\kappa_{\sigma i}(x+\delta x_{\sigma j},t) - \kappa_{\sigma i}(x-\delta x_{\sigma j},t)\Big)\frac{\mathrm{S}_{\sigma ik}}{2\kappa_0 \delta x_{\sigma j}} + O(\delta x^2) \\ \frac{\partial \mathrm{R}^{(lat)}_{S\sigma ik}(t)}{\partial x_j} &= R_{rms}\frac{\kappa_{\sigma i}(x+\delta x_{\sigma j},t) - \kappa_{\sigma i}(x-\delta x_{\sigma j},t)}{2\kappa_0 \delta x_j}\epsilon_{\sigma ik} \qquad (9.32) \\ &= -\frac{R_{rms}}{\dot{R}_{rms}}\frac{\kappa_{\sigma i}(x+\delta x_{\sigma j},t) - \kappa_{\sigma i}(x-\delta x_{\sigma j},t)}{\kappa_0 \delta t}\epsilon_{\sigma ik} \qquad (9.33) \end{aligned}$$

where the directions of (9.32) are unit directions (which differs from the LBM). The temporal formulation (9.33) makes the unit directions more obvious. Note that central differencing has been utilised for second order accu-

racy ([52], Chapter 13). Substituting Equation (9.32) into Equation (9.29)

$$\begin{aligned}
\mathrm{D}_{jk}^{(lat)} = \mathrm{D}_{jk}^{(real)} &= -\frac{R_{rms}}{8\kappa_0\delta x_j}\Big(\kappa_{\sigma i}(x+\delta x_{\sigma k},t)\epsilon_{\sigma ij} - \kappa_{\sigma i}(x-\delta x_{\sigma k},t)\epsilon_{\sigma ij} \\
&\quad +\kappa_{\sigma i}(x+\delta x_{\sigma j},t)\epsilon_{\sigma ik} - \kappa_{\sigma i}(x-\delta x_{\sigma j},t)\epsilon_{\sigma ik}\Big) \qquad (9.34) \\
&= \frac{R_{rms}}{4\dot{R}_{rms}\kappa_0\delta t}\Big(\kappa_{\sigma i}(x+\delta x_{\sigma k},t)\epsilon_{\sigma ij} - \kappa_{\sigma i}(x-\delta x_{\sigma k},t)\epsilon_{\sigma ij} \\
&\quad +\kappa_{\sigma i}(x+\delta x_{\sigma j},t)\epsilon_{\sigma ik} - \kappa_{\sigma i}(x-\delta x_{\sigma j},t)\epsilon_{\sigma ik}\Big). \qquad (9.35)
\end{aligned}$$

The first order approximation (proven in Section 10.4) to the latent first order stress tensor is

$$\begin{aligned}
\Delta\boldsymbol{\sigma}_S^{(1)(real)}(\tau)|_0^t &= 4G^{(real)}\int_0^t \mathbf{D}^{(real)}(\tau)d\tau = -4G^{(real)}\int_t^\infty \mathbf{D}^{(real)}(\tau)d\tau \\
&= -\frac{4G}{\omega'}\big(\mathbf{D}^{(real)}(t) - \mathbf{D}^{(real)}(0)\big) = 3\Delta\boldsymbol{\sigma}_S^{(1)(lat)}(\tau)|_0^t \qquad (9.36)
\end{aligned}$$

depending on the reference point. $G^{(real)} = G$. Note that $G\int \mathbf{D}dt \approx G\mathbf{D}/\omega'$ only applies during polymer redistribution and is an approximation here. To determine $4G\int_t^\infty \mathbf{D}d\tau$ consider – with appropriate substitution of (8.46) –

$$\begin{aligned}
\int_t^\infty \frac{\partial \mathrm{R}_{S\sigma ij}(\tau)}{\partial x_k}d\tau &= \frac{\partial}{\partial x_k}\int_t^\infty \mathrm{R}_{S\sigma ij}(\tau)d\tau = \frac{\partial}{\partial x_k}\frac{\mathrm{R}_{S\sigma ij(\tau)}|_t^\infty}{-\omega'} \\
&= -\frac{1}{\omega'}\frac{\partial}{\partial x_k}\Big(\mathrm{R}_{S\sigma i\infty j} - \mathrm{R}_{S\sigma ij}\Big) = \frac{1}{\omega'}\frac{\partial \mathrm{R}_{S\sigma ij}}{\partial x_k}. \qquad (9.37)
\end{aligned}$$

Substituting Equation (9.34) into Equation (9.36)

$$\Delta\boldsymbol{\sigma}_S^{(1)(lat)}(\tau)|_0^t = -\frac{4G^{(lat)}}{\omega'}\mathbf{D}^{(lat)}(t) = \frac{1}{3}\Delta\boldsymbol{\sigma}_S^{(1)(real)}(\tau)|_0^t.$$

Alternatively,

$$\begin{aligned}
\Delta\sigma_{Sjk}^{(1)(lat)}(\tau)|_0^t &= \frac{G^{(lat)}R_{rms}}{2\omega'\kappa_0\delta x}\Big(\kappa_{\sigma i}(x+\delta x_{\sigma k},t)\epsilon_{\sigma ij} - \kappa_{\sigma i}(x-\delta x_{\sigma k},t)\epsilon_{\sigma ij} \\
&\quad +\kappa_{\sigma i}(x+\delta x_{\sigma j},t)\epsilon_{\sigma ik} - \kappa_{\sigma i}(x-\delta x_{\sigma j},t)\epsilon_{\sigma ik}\Big) \qquad (9.38) \\
&= -\frac{G^{(lat)}R_{rms}}{\omega'\kappa_0\dot{R}_{rms}\delta t}\Big(\kappa_{\sigma i}(x+\delta x_{\sigma k},t)\epsilon_{\sigma ij} - \kappa_{\sigma i}(x-\delta x_{\sigma k},t)\epsilon_{\sigma ij} \\
&\quad +\kappa_{\sigma i}(x+\delta x_{\sigma j},t)\epsilon_{\sigma ik} - \kappa_{\sigma i}(x-\delta x_{\sigma j},t)\epsilon_{\sigma ik}\Big). \qquad (9.39)
\end{aligned}$$

The first order approximation to the dynamic pressure tensor is given by $4\mu\dot{\mathrm{D}}_{jk}$ where

$$\dot{\mathrm{D}}_{jk} = -\frac{1}{4\alpha}\Big(\frac{\partial\dot{\mathrm{R}}_{D\mu k}}{\partial x_j} + \frac{\partial\dot{\mathrm{R}}_{D\mu j}}{\partial x_k}\Big) \tag{9.40}$$

and

$$\frac{\partial\dot{\mathrm{R}}_{D\mu k}}{\partial x_j} = \frac{\dot{\mathrm{R}}_{D\mu k}(x_{j+1},t) - \dot{\mathrm{R}}_{D\mu k}(x_{j-1},t)}{x_{j+1} - x_{j-1}}.$$

The principles depicted in Figure 9.2 are used – as for chain length.

$$\begin{aligned}
\Delta\sigma^{(1)}_{Djk}(t) &= 4\mu\dot{\mathrm{D}}_{jk} = -4\frac{\mu}{\alpha}\left(\frac{\partial\dot{\mathrm{R}}_{D\sigma ij}}{\partial x_k} + \frac{\partial\dot{\mathrm{R}}_{D\sigma ik}}{\partial x_j}\right)\frac{1}{4} \\
&= -\frac{\mu}{2\alpha}\left(\frac{\dot{\mathrm{R}}_{D\sigma ij}(x+\delta x_{\sigma k},t) - \dot{\mathrm{R}}_{D\sigma ij}(x-\delta x_{\sigma k},t)}{\delta x_{\sigma k}}\right. \\
&\quad \left. + \frac{\dot{\mathrm{R}}_{D\sigma ik}(x+\delta x_{\sigma j},t) - \dot{\mathrm{R}}_{D\sigma ik}(x-\delta x_{\sigma j},t)}{\delta x_{\sigma j}}\right) \\
\Delta\sigma^{(1)(lat)}_{Djk}(t) &= \frac{\mu^{(lat)}}{\alpha\rho_0}\left(\rho_{\sigma i}(x+\delta x_{\sigma k},t) - \rho_{\sigma i}(x-\delta x_{\sigma k},t)\frac{\mathrm{E}_{\sigma ik}}{\delta x_j}\right. \\
&\quad \left. + \rho_{\sigma i}(x+\delta x_{\sigma j},t) - \rho_{\sigma i}(x-\delta x_{\sigma j},t)\frac{\mathrm{E}_{\sigma ij}}{\delta x_k}\right)
\end{aligned}$$

where the omission of the factor 2 is because $-\mathbf{R}_{\sigma i}/2 = -\boldsymbol{\epsilon}_{\sigma i}\dot{R}_{rms}/2 = \mathbf{E}_{\sigma i}$. Finally the first order approximation to the change in dynamic stress is

$$\begin{aligned}
\Delta\sigma^{(1)(real)}_{Djk}(t) &= -\frac{\mu\dot{R}'_{rms}}{2\rho_0}\Big(\frac{\rho_{\sigma i}(x+\delta x_{\sigma k},t)\epsilon_{\sigma ij} - \rho_{\sigma i}(x-\delta x_{\sigma k},t)\epsilon_{\sigma ij}}{\delta x_k} \\
&\quad + \frac{\rho_{\sigma i}(x+\delta x_{\sigma j},t)\epsilon_{\sigma ik} - \rho_{\sigma i}(x-\delta x_{\sigma j},t)\epsilon_{\sigma ik}}{\delta x_j}\Big) \qquad (9.41) \\
&= \frac{\mu}{\alpha\rho_0\delta t}\Big(\rho_{\sigma i}(x+\delta x_{\sigma k},t)\epsilon_{\sigma ij} - \rho_{\sigma i}(x-\delta x_{\sigma k},t)\epsilon_{\sigma ij} \\
&\quad + \rho_{\sigma i}(x+\delta x_{\sigma j},t)\epsilon_{\sigma ik} - \rho_{\sigma i}(x-\delta x_{\sigma j},t)\epsilon_{\sigma ik}\Big) \qquad (9.42)
\end{aligned}$$

The first order approximation to the dynamic stress tensor represents a direct method for the calculation of the gradient of stretch rate. The alternative would be to use one of the indirect methods for dynamic stretch rate as depicted and described for static stretch in Figure 9.1.

9.2.3 The resultant discrete stress tensor

Having completed the numerical simulation, the stress tensor can be determined from the resultant vector length distributions. In order to determine

the stress tensor to first order, substitute Equations (9.27), (9.20), (9.38) and (9.41) into Equation (9.10)

$$\begin{aligned}
\mathrm{T}_{jk}^{(lat)}|_0^t &= \frac{\dot{R}_{rms}'^2}{4\rho_0}\Big(\sum_{\sigma i}\rho_{\sigma i}^2\epsilon_{\sigma ij}\epsilon_{\sigma ik}\delta_{jk} - \sum_{\sigma i}\rho_{\sigma i}^{(eq)2}\epsilon_{\sigma ij}\epsilon_{\sigma ik}\delta_{jk}\Big) \\
&\quad -\frac{R_{rms}^2}{4\kappa_0}\sum_{\sigma i}\Big(\kappa_{\sigma i}^2\epsilon_{\sigma ij}\epsilon_{\sigma ik}\delta_{jk} - \kappa_{\sigma i}^{(eq)2}\epsilon_{\sigma ij}\epsilon_{\sigma ik}\delta_{jk}\Big) \\
&\quad +\frac{G^{(lat)}R_{rms}}{2\omega\kappa_0\delta x}\Big(\kappa_{\sigma i}(x+\delta x_{\sigma k},t)\epsilon_{\sigma ij} - \kappa_{\sigma i}(x-\delta x_{\sigma k},t)\epsilon_{\sigma ij} \\
&\quad +\kappa_{\sigma i}(x+\delta x_{\sigma j},t)\epsilon_{\sigma ik} - \kappa_{\sigma i}(x-\delta x_{\sigma j},t)\epsilon_{\sigma ik}\Big) \\
&\quad -\frac{\mu^{(lat)}\dot{R}_{rms}'}{2\rho_0}\Big(\frac{\rho_{\sigma i}(x+\delta x_{\sigma k},t)\epsilon_{\sigma ij} - \rho_{\sigma i}(x-\delta x_{\sigma k},t)\epsilon_{\sigma ij}}{\delta x_k} \\
&\quad +\frac{\rho_{\sigma i}(x+\delta x_{\sigma j},t)\epsilon_{\sigma ik} - \rho_{\sigma i}(x-\delta x_{\sigma j},t)\epsilon_{\sigma ik}}{\delta x_j}\Big) \qquad (9.43)
\end{aligned}$$

which is local in time and local in space. It is recognised that $|\epsilon_{\sigma ik}| = 1$. The real stress tensor (given by half the static component of the apparent stress tensor and double the dynamic component of the apparent stress tensor) is

$$\begin{aligned}
\mathrm{T}_{jk}^{(real)}|_0^t &= \frac{3\dot{R}_{rms}'^2}{4\rho_0}\Big(\sum_{\sigma i}\rho_{\sigma i}^2\epsilon_{\sigma ij}\epsilon_{\sigma ik}\delta_{jk} - \sum_{\sigma i}\rho_{\sigma i}^{(eq)2}\epsilon_{\sigma ij}\epsilon_{\sigma ik}\delta_{jk}\Big) \\
&\quad -\frac{3R_{rms}^2}{4\kappa_0}\sum_{\sigma i}\Big(\kappa_{\sigma i}^2\epsilon_{\sigma ij}\epsilon_{\sigma ik}\delta_{jk} - \kappa_{\sigma i}^{(eq)2}\epsilon_{\sigma ij}\epsilon_{\sigma ik}\delta_{jk}\Big) \\
&\quad -\frac{3G^{(lat)}}{\omega'\kappa_0\delta t}\frac{R_{rms}}{\dot{R}_{rms}}\Big(\kappa_{\sigma i}(x+\delta x_{\sigma k},t)\epsilon_{\sigma ij} - \kappa_{\sigma i}(x-\delta x_{\sigma k},t)\epsilon_{\sigma ij} \\
&\quad +\kappa_{\sigma i}(x+\delta x_{\sigma j},t)\epsilon_{\sigma ik} - \kappa_{\sigma i}(x-\delta x_{\sigma j},t)\epsilon_{\sigma ik}\Big) \\
&= \frac{3\mu^{(lat)}}{\alpha\rho_0}\Big(\frac{\rho_{\sigma i}(x+\delta x_{\sigma k},t)\epsilon_{\sigma ij} - \rho_{\sigma i}(x-\delta x_{\sigma k},t)\epsilon_{\sigma ij}}{\delta t} \\
&\quad +\frac{\rho_{\sigma i}(x+\delta x_{\sigma j},t)\epsilon_{\sigma ik} - \rho_{\sigma i}(x-\delta x_{\sigma j},t)\epsilon_{\sigma ik}}{\delta t}\Big) \qquad (9.44)
\end{aligned}$$

where in Section 10.1.3 it is shown that $G^{(real)} = 3G^{(lat)}$ and in Section 10.2.3 that $\mu^{(real)} = 3\mu^{(lat)}$.

9.3 Kinematic specimen variables

The approximate method presented in this work is based on uniformly distributed nodes. These nodes can either be defined based on the specimen dimensions at time (t) (disequilibrium state), constant specimen dimensions

originally defined at time (t) (steady-state) or reference (ground-state) dimensions.

A disequilibrium state would imply an adaptive specimen size. This is not allowed in the current method. Steady-state does not exclude material non-equilibrium. Furthermore, stress relaxation (and creep) as presented in this document is a consequence of the latter phenomenon. If stretches calculated on such a method assume constant material dimensions, a weighting (proprtional to the stretch) will be required to calculate specimen properties. Calculations of specimen properties based on ground state dimensions will also require weighting. The latter option is the simplest to implement and will therefore be the approach in this work. Although in principle it can be applied to a non-equilibrium steady-state, the weightings will have to be relative to the stretch state at the time when the node grid is uniformly distributed.

The material stretches as defined by Equation (9.2) are specified at particular positions and times. The specimen length in the x-direction at time t ($\mathrm{L}_x(t)$) is the product of the specimen stretch at time t ($\lambda_{spx}(t)$) and the initial specimen length (L_0). Thus $\mathrm{L}_x(t) = \mathrm{L}_0 \times \lambda_{spx}(t)$. The specimen stretch is defined by Equation (7.24). Let the initial (ground state) be discretised to a grid of $n_l \times n_w = n$ square of dimensions $\Delta\mathrm{L}$ by $\Delta\mathrm{L}$. At time t, the material stretch in the x direction at point $\mathbf{x}$ is $\lambda_{matx}(\mathbf{x}, t)$. Furthermore from the incompressibility condition $\lambda_{maty}(\mathbf{x}, t) = \frac{1}{\lambda_{matx}(\mathbf{x},t)}$. Discretising (7.24) ,

$$\begin{aligned}
\lambda_{spx}^{(lat)} &= \frac{\sum_{j=1}^{n_w}\sum_{i=1}^{n_l}\lambda_{matx}^{(lat)}(\mathbf{x},t)\lambda_{matx}^{(lat)}(\mathbf{x},t)\Delta\mathrm{L}\times\frac{1}{\lambda_{matx}^{(lat)}(\mathbf{x},t)}\Delta\mathrm{L}}{\sum_{j=1}^{n_w}\sum_{i=1}^{n_l}\Delta\mathrm{L}\times\Delta\mathrm{L}} \\
\boldsymbol{\lambda}_{sp}^{(lat)} &= \frac{\sum_{i=1}^{n}\boldsymbol{\lambda}_{mat}^{(lat)}(\mathbf{x},t)\Delta\mathrm{L}\times\Delta\mathrm{L}}{\sum_{i=1}^{n}\Delta\mathrm{L}\times\Delta\mathrm{L}} = \frac{\sum_{i=1}^{n}\boldsymbol{\lambda}_{mat}^{(lat)}(\mathbf{x},t)}{n}.
\end{aligned}$$

The specimen stretch is defined by

$$\begin{aligned}
\boldsymbol{\lambda}_{sp}^{(lat)} &:= \frac{1}{n}\sum_{i=1}^{n}\boldsymbol{\lambda}_i^{(lat)} = \overline{\boldsymbol{\lambda}_i^{(lat)}} \iff \boldsymbol{\lambda}_i^{(real)} = \sqrt{3}\boldsymbol{\lambda}_i^{(lat)}, \qquad (9.45)\\
\boldsymbol{\lambda}_{sp}^{(real)} &:= \frac{\sqrt{3}}{n}\sum_{i=1}^{n}\boldsymbol{\lambda}_i^{(lat)} = \sqrt{3}\overline{\boldsymbol{\lambda}_i^{(lat)}} = \frac{1}{n}\sum_{i=1}^{n}\boldsymbol{\lambda}_i^{(real)} = \overline{\boldsymbol{\lambda}_i^{(real)}},
\end{aligned}$$

where $\boldsymbol{\lambda}_i$ is defined by Equation (9.2) and the resemblance to Equation (7.24) is apparent. Thus the strain, as measured by a tensile measuring instrument,

is the arithmetic mean of the material stretches. Note that this stress is defined on the initial specimen dimensions. Similarly

$$\begin{aligned}
\mathrm{L}_{sp}\int_0^t \dot{\boldsymbol{\lambda}}_{sp}^{(lat)}d\tau &= \Delta\mathrm{L}\sum_{i=1}^{n}\int_0^t \dot{\boldsymbol{\lambda}}_i^{(lat)}d\tau \iff \int_0^t \dot{\boldsymbol{\lambda}}_{sp}^{(lat)}d\tau = \frac{1}{n}\sum_{i=1}^{n}\int_0^t \dot{\boldsymbol{\lambda}}_i^{(lat)}d\tau \\
\iff \quad 0 &= \int_0^t \Big(\dot{\boldsymbol{\lambda}}_{sp}^{(lat)} - \frac{1}{n}\sum_{i=1}^{n}\dot{\boldsymbol{\lambda}}_i^{(lat)}\Big)d\tau \qquad \forall\, t \\
\iff \quad 0 &= \dot{\boldsymbol{\lambda}}_{sp}^{(lat)} - \frac{1}{n}\sum_{i=1}^{n}\dot{\lambda}_i^{(lat)} \iff \dot{\boldsymbol{\lambda}}_{sp}^{(lat)} := \frac{1}{n}\sum_{i=1}^{n}\dot{\boldsymbol{\lambda}}_i^{(lat)} = \overline{\dot{\boldsymbol{\lambda}}_i^{(lat)}} \\
\dot{\boldsymbol{\lambda}}_{sp}^{(real)} &:= \frac{1}{n}\sum_{i=1}^{n}\dot{\boldsymbol{\lambda}}_i^{(real)} = \overline{\dot{\boldsymbol{\lambda}}_i^{(real)}} = \frac{\sqrt{3}}{n}\sum_{i=1}^{n}\dot{\boldsymbol{\lambda}}_i^{(lat)} = \sqrt{3}\overline{\dot{\boldsymbol{\lambda}}_i^{(lat)}}.
\end{aligned}$$

Thus the measured stretch rate (corresponding to the specimen stretch rate) is the arithmetic mean of LBM cell stretch rates.

9.4 Kinetic specimen variables

Given that the objective is to demonstrate viscoelasticity as measured by the testing rig, the kinetic variables must correspond to these variables. The latent specimen stress in the direction of stretch (T_{sp}) cannot be measured by the testing rig because the instrument measures the apparent specimen stress as discussed in Section 5.1.5. Nevertheless, the concept can be derived from the assumption that the specimen potential energy is the sum of the individual potential energies. Thus (for principal directions i)

$$\frac{1}{2}\mathrm{T}_{sp}\lambda_{sp}^2 = \frac{1}{2}\sum_{=1}^{n}\mathrm{T}_i\lambda_i^2 \iff \mathrm{T}_{sp}\overline{\lambda_i^2} = \sum_{i=1}^{n}\mathrm{T}_i\lambda_i^2 \iff \mathrm{T}_{sp} = \frac{\sum_{i=1}^{n}\mathrm{T}_i\lambda_i^2}{\overline{\lambda_i^2}}$$

and is the weighted average of the material stresses with respect to the square of the stretch. The result applies both for real and lattice energy. Similarly the specimen stress rate ($\dot{\mathrm{T}}_{sp}$) in the direction of stretch can be derived by the assumption that the averaged kinetic energy of the specimen is the sum of the individual kinetic energies and thus the specimen stress rate is the weighted average of the individual material stresses with respect to the square of the stretch rate: that is

$$\dot{\mathrm{T}}_{sp} = \frac{\sum_{=1}^{n}\dot{\mathrm{T}}_i\dot{\lambda}_i^2}{\overline{\dot{\lambda}_i^2}}.$$

The above discrete approximations to the stress tensor should be compared to the continuous definitions of Equations (7.27) and (7.28) in Section 7.3. The difference is in in the manner in which the averaging is applied. The reason (7.27) is unweighted is because it is measured on the deformed specimen whereas in the numerical approximation the measurements are being made on the undeformed specimen. To account for the deformation, the weighted average is required

9.5 Measured stress

At least three interpretations of measured stress can be proposed. The first is that the measured stress corresponds to the material stress at a particular position $\mathbf{r}$ where $\mathbf{r}$ corresponds to the location of the sensor. Consider a uniaxial tensile test testing rig with one mobile arm. One may propose that the sensor is at the point where the mobile arm grips. The theory predicts that this location will experience maximum stretch before the next layer of molecules are stretched. Thus one should anticipate that the specimen should achieve maximum measured stress and then remain constant as the specimen increases in length. This does not occur and the proposal is rejected.

The alternative is to propose that the measured stress represents an average of the stresses experienced throughout the specimen as described by Equations (7.27) and (7.28) in Section 7.3. Then two additional possibililties exist. The first is that measured stress is the average of the stress tensor in a principal direction. The second option is that the measured stress is the average of the zero order approximation to the apparent stress tensor as suggested by Sections 5.1.3 and 5.1.4.

The stress measured by the tensile testing rig is the force and consequently the pressure required to increase a specimen from length L to length $\mathrm{L} + \delta\mathrm{L}$ whilst the area decreases from A to $\mathrm{A} + \delta\mathrm{A}$. Thus the testing rig measures the pressure required to move a surface as described in Section 5.1. Section 5.1 does not consider the macroscopic entity of stress. It is therefore proposed that the stress measured by the tensile testing rig is the pressure required to move a surface and that this pressure corresponds to the zero order approximation to the apparent stress tensor.

Thus at maximum entropy, the change in measured, or apparent specimen

stress at time t ($\Delta^{\langle app\rangle}_{spec}\mathrm{T}^{(0)(lat)}_{jk}|^t_0$) , is defined by the average over the specimen of $-\Delta\mathbf{P}^{(0)}_D$ in Equation (9.15) and $-\Delta\mathbf{P}^{(0)}_S$ of Equation (9.25) at time t.

$$\begin{aligned}\Delta^{\langle app\rangle}_{spec}\mathrm{T}^{(0)(lat)}_{jk}|^t_0 &= \frac{1}{\mathrm{v}}\oint -\Delta P^{(0)}_{jk}\,d\mathrm{V} = \oint\Big(\frac{\dot{R}'^2_{rms}}{8\rho_0}\sum_{\sigma i}\Big(\rho^2_{\sigma i}-\rho^{(eq)2}_{\sigma i}\Big)\epsilon_{\sigma ij}\epsilon_{\sigma ik}\delta_{jk}\\ &\quad -\frac{R^2_{rms}}{2\kappa_0}\sum_{\sigma i}\Big(\kappa^2_{\sigma i}-\kappa^{(eq)2}_{\sigma i}\Big)\epsilon_{\sigma ij}\epsilon_{\sigma ik}\delta_{jk}\Big)\,d\mathrm{V}\times\frac{1}{\mathrm{V}} \qquad (9.46)\end{aligned}$$

and given the ratio between real and lattice vectors is $\sqrt{3}$ – Section 3.2.6 –

$$\begin{aligned}\Delta^{\langle app\rangle}_{spec}T^{(0)(real)}_{jj}|^t_0 &= 3\times\Delta^{\langle app\rangle}_{spec}T^{(0)(lat)}|^t_0\\ &= \oint\left(\frac{3\dot{R}'^2_{rms}}{8\rho_0}\sum_{\sigma i}\Big(\rho^2_{\sigma i}(\mathbf{x})-\rho^{(eq)2}_{\sigma i}(\mathbf{x})\Big)\epsilon_{\sigma ij}\epsilon_{\sigma ik}\delta_{jk}\right.\\ &\quad\left.-\frac{3R^2_{rms}}{2\kappa_0}\sum_{\sigma i}\Big(\kappa^2_{\sigma i}(\mathbf{x})-\kappa^{(eq)2}_{\sigma i}(\mathbf{x})\Big)\epsilon_{\sigma ij}\epsilon_{\sigma ik}\delta_{jk}\right)d\mathrm{V}. \qquad (9.47)\end{aligned}$$

9.6 Discrete stress calculation

In Section 3.2.7 the derivation of the principal stresses as presented by Treloar was reproduced. Two problems were identified: in general, the system of equations is indeterminate (Treloar [138], Chapter 4) and it was required that the specimen had to be in steady state. The system is indeterminate because principal stresses in directions not corresponding to the direction of applied stretch cannot be solved for arbitrary applied stresses as discussed in Section 3.2.7. However, for the uniaxial tensile test where, the principal stress at the free surfaces should be zero, Treloar demonstrated how to make the system determinate.

Regarding the latter problem of the specimen not being in steady state, by selecting a time at which the specimen is in steady state and every point in the specimen is at maximum entropy, the steady state of the specimen is equivalent to the maximum entropy state of the material at any location in the specimen. This relationship permits the determination of material constants. Reversing the argument, by selecting a region of the specimen that is at maximum entropy even though the whole specimen is not at steady state, one should be able to use Treloar's method, as decribed in Section 3.2.7, on the region of maximum entropy. Furthermore a specimen that is not at steady state can be approximated by a collection of regions of maximum entropy.

Treloar solved the problem of non-zero principal stress by determining or specifying the principal stress at an edge for a particular experiment. Treloar ([138], Chapter 4) made the system determinate by subtracting the unknown principal stress at one surface from the known principal stress at another and relating these to the principal stretches as demonstrated in Section 3.2.7 and Equation (3.60). This same procedure will be used in Section 12.2.4 (Equations (12.16) and (12.22)).

When considering a discrete model, principal stresses have to be determined for an indeterminate system of equations when the specimen is in disequilibrium and assumptions can therefore not be made about the material based on the specimen. However, it should be recognised that the

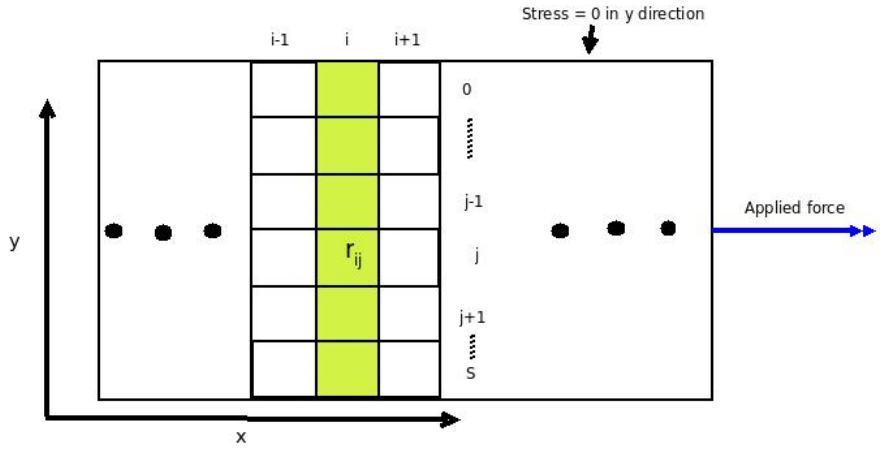

Figure 9.3: RVEs selected (as depicted in yellow) such that the stress at one edge of the collection is known. The position of the RVE in the x-direction is denoted by i and the position in the y-direction is denoted by j.

discrete system has been constructed such that the size of the RVE is defined by the ability to apply a Gaussian distribution approximation to the molecular properties and this distribution has been constructed for the maximum entropy state for the material at that point as described in Section 13.3.5. Thus, for the RVE, the principles used by Treloar ([138], Chapter 4) can be utilised. These principles cannot be used directly because the stress at one surface of the RVE is not known for all RVEs. However a set of RVEs can be selected such that the one surface (or edge in 2D) of the collection is known. The collection of RVEs is selected such that they form a column of width one RVE such that the long axis of the column is perpendicular to the applied force as depicted in yellow in Figure 9.3.

For the column of RVEs at x-location i, let the principal Cauchy stress in the x-direction be $\sigma_1^{\{i\}}$. From Section 7.3, Section 13.6 and (9.46)

$$\sigma_1^{\{i\}} := \frac{1}{s+1}\sum_{j=0}^{s}\sigma_1^{\{i,j\}} \tag{9.48}$$

for both latent and apparent stress and real and lattice stress. Furthermore the principal stress at the free surface in the y direction at horizontal location i is given by

$$\sigma_2^{\{i,0\}} = 0 \tag{9.49}$$

where the constraint $\sigma_2^{\{i\}} = 0$ is imposed by the BC for the uniaxial stretch experiment. From (9.48) - (9.49)

$$\begin{aligned}\sigma_1^{\{i\}} - \sigma_2^{\{i,0\}} = \sigma_1^{\{i\}} &= \left(\frac{1}{s+1}\sum_{j=0}^{s}\sigma_1^{\{i,j\}}\right) - \sigma_2^{\{i,0\}} \\ &= \frac{1}{s+1}\sum_{j=0}^{s}\left(\sigma_1^{\{i,j\}} - \sigma_2^{\{i,0\}}\right) \ \forall\, j \in \mathbb{N}_0,\ j \le s\end{aligned} \tag{9.50}$$

is the prinicipal stress in the x-direction for the uniaxial stretch experiment and applies to both real and apparent components. Similarly in the y-direction

$$\begin{aligned}\sigma_2^{\{i\}} - \sigma_2^{\{i,0\}} = \sigma_2^{\{i\}} &= \left(\frac{1}{s+1}\sum_{j=0}^{s}\sigma_2^{\{i,j\}}\right) - \sigma_2^{\{i,0\}} \\ &= \frac{1}{s+1}\sum_{j=0}^{s}\left(\sigma_2^{\{i,j\}} - \sigma_2^{\{i,0\}}\right) \ \forall\, j \in \mathbb{N}_0,\ j \le s.\end{aligned} \tag{9.51}$$

9.7 Closing remarks on the recovery of the macroscopic variables

The majority of the variables discussed in this chapter are not directly involved in the modelling. The only derived variables used in the numerical modelling are the lattice Lagrangian stretch $\boldsymbol{\lambda}^{(lat)}$ as described by (9.2) and the lattice Lagrangian chain stretch rate ratio $\boldsymbol{\iota}^{(lat)}$ as described by (9.8). The remaining variables discussed in this chapter are used post-analytically and are based on the distribution of chain length $\mathbf{R}_S$ and chain length stretch rate $\dot{\mathbf{R}}_D$. Section 11.7 will relate $\boldsymbol{\iota}$ to $\dot{\boldsymbol{\lambda}}$.

Chapter 10

Derivation of specimen viscoelasticity from polymer LBM

Chapter 3 derives the physics for the non-maximum entropy polymer interaction. Chapter 6 determines the first order macroscopic description for the non-maximum entropy theory of polymer elasticity which was shown to be equivalent to viscoelasticity in Chapter 7. Similarly, in this chapter, an expansion is performed on the polymer LBM (approximate theory derived in Chapter 8) to show that the discrete equivalent of the macroscopic equations derived in Chapter 6 can be derived directly from the discrete method (LBM). The derivation is only for the 2D case because only a 2D model will be constructed.

The method is based on the discretisation of both stretch and stretch rate. The discretisation was determined in Table 8.3, is depicted in Figure 8.1 and can be re-expressed in terms of directions $\boldsymbol{\epsilon}_{\sigma i}$ where

$$\begin{aligned} \boldsymbol{\epsilon}_{0i} &= (0,0) \\ \boldsymbol{\epsilon}_{1i} &= \left(\cos\frac{i-1}{2}\pi, \sin\frac{i-1}{2}\pi\right) \\ \boldsymbol{\epsilon}_{2i} &= \sqrt{2}\left(\cos\left(\frac{i-1}{2}\pi+\frac{\pi}{4}\right), \sin\left(\frac{i-1}{2}\pi+\frac{\pi}{4}\right)\right) \\ i &= 1,2,3,4 \end{aligned} \tag{10.1}$$

and where $|\boldsymbol{\epsilon}_{1i}| = 1$ and $|\boldsymbol{\epsilon}_{2i}| = \sqrt{2}$. From (8.29) and (3.44) the stretch discretisation is given by constant vectors

$$\mathbf{S}_{\sigma i} = \boldsymbol{\epsilon}_{\sigma i} R_{rms} = \boldsymbol{\epsilon}_{\sigma i} R_{\mu 0} \tag{10.2}$$

and from (8.36) and (3.44) the stretch rate vector discretisation is

$$\mathbf{E}_{\sigma i} = \boldsymbol{\epsilon}_{\sigma i} c = \boldsymbol{\epsilon}_{\sigma i} \frac{\delta x}{\delta t} = -\boldsymbol{\epsilon}_{\sigma i} \frac{\dot{R}_{rms}}{2} = -\boldsymbol{\epsilon}_{\sigma i} \frac{\dot{R}_{\mu 0}}{2}. \tag{10.3}$$

When considering the case of non-critical damping from Section 8.4.3, the ratio of critical damping to non-critical damping is α from Equation (8.47). From Equation (8.61)

$$\frac{\dot{R}_{rms}}{\alpha} = \dot{R}'_{rms} \tag{10.4}$$

Thus for non-critical damping (10.3) reduces to

$$\mathbf{E}_{\sigma i} = \boldsymbol{\epsilon}_{\sigma i} c = \boldsymbol{\epsilon}_{\sigma i} \frac{\delta x}{\delta t} = -\boldsymbol{\epsilon}_{\sigma i} \frac{\dot{R}'_{rms}}{2} = -\boldsymbol{\epsilon}_{\sigma i} \frac{\dot{R}'_{\mu 0}}{2}. \tag{10.5}$$

where $\dot{R}'_{\mu 0} = \dot{R}_{\mu 0}/\alpha$. Hou *et al*'s [65] multi-scaling method will be applied to (8.88) and (8.89). Equation (8.88) can be separated into (8.9) and (8.87). Similarly (8.89) can be separated into (8.10) and (8.86). The multiscaling method will be applied to (8.9) in Section 10.1 and (8.10) in Section 10.2. The omission of (8.86) and (8.87) in Section 10.2 and Section 10.1 respectively is justified in Section 10.3 where it is shown that

$$\rho^{poly}_{\sigma i}(\mathbf{x}, t)\dot{R}_{rms} + \int_t^\infty \kappa^{poly}_{\sigma i} R_{rms}(\mathbf{x}, \eta) d\eta = 0.$$

The relevance of the above operation is that this corresponds to the operation performed to derive the polymer flow equation (6.99). The lattice constants derived (as described above), will be related to real constants.

In the derivation of the Navier-Stokes (N-S) type equations, an unexpected factor 2/3 will be produced. The chapter will conclude by showing that the factor is due to the use of a 2D lattice as opposed to the 3D lattice and by introducing Buick's general formulation [14].

10.1 Expansion of stretch

The vector products of (10.3) (also called the tensor sums) required for the expansion are determined from the spatial discretisation (10.1), the consequent stretch discretisation (10.2) and stretch rate discretisation (10.3) by substituting (10.1) into (10.2) and into (10.3) [14, 147]. Summing over σi

where $\sigma = 0, 1, 2$ and $i = 1, 2, 3, 4$ for free spatial indices α, β, γ and θ

$$\begin{aligned}
\sum_i \mathrm{E}_{\sigma i\alpha} &= 0 \qquad (10.6)\\
\sum_i \mathrm{E}_{\sigma i\alpha}\mathrm{S}_{\sigma i\alpha} &= -\epsilon_\sigma^2 \dot{R}'_{rms} R_{rms}\delta_{\alpha\beta}\\
\sum_i \mathrm{E}_{\sigma i\alpha}\mathrm{S}_{\sigma i\alpha}\mathrm{S}_{\sigma i\beta} &= 0\\
\sum_i \mathrm{E}_{\sigma i\alpha}\mathrm{S}_{\sigma i\beta}\mathrm{S}_{\sigma i\gamma}\mathrm{S}_{\sigma i\theta} &= -\dot{R}'_{rms} R^3_{rms}\delta_{\alpha\beta\gamma\theta} \qquad \sigma = 1\\
\sum_i \mathrm{E}_{\sigma i\alpha}\mathrm{S}_{\sigma i\beta}\mathrm{S}_{\sigma i\gamma}\mathrm{S}_{\sigma i\theta} &= -2\dot{R}_{rms} R^3_{rms}\Delta_{\alpha\beta\gamma\theta} + 4\dot{R}'_{rms} R^3_{rms}\delta_{\alpha\beta\gamma\theta} \qquad \sigma = 2\\
\sum_i \mathrm{E}_{\sigma i\alpha}\mathrm{E}_{\sigma i\beta}\mathrm{S}_{\sigma i\gamma}\mathrm{S}_{\sigma i\theta} &= \frac{1}{2}\dot{R}'^2_{rms} R^2_{rms}\delta_{\alpha\beta\gamma\theta} \qquad \sigma = 1\\
\sum_i \mathrm{E}_{\sigma i\alpha}\mathrm{E}_{\sigma i\beta}\mathrm{S}_{\sigma i\gamma}\mathrm{S}_{\sigma i\theta} &= \dot{R}'^2_{rms} R^2_{rms}\Delta_{\alpha\beta\gamma\theta} - 2\dot{R}'^2_{rms} R^2_{rms}\delta_{\alpha\beta\gamma\theta} \qquad \sigma = 2\\
\text{where} \qquad \delta_{\alpha\beta\gamma\theta} &= 1 \Leftrightarrow \alpha = \beta = \gamma = \theta\\
\text{and} \qquad \Delta_{\alpha\beta\gamma\theta} &= \delta_{\alpha\beta}\delta_{\gamma\theta} + \delta_{\alpha\gamma}\delta_{\beta\theta} + \delta_{\alpha\theta}\delta_{\beta\gamma}
\end{aligned}$$

where both $\mathbf{E}_{\sigma i}$ and $\mathbf{S}_{\sigma i}$ are constant vectors. Note that the results are inversely proportional to the dimension – here dimension is 2 [14] – and that for vectors $\mathbf{A}, \mathbf{B}$ the vector product $\mathbf{AB} = \mathbf{A} \otimes \mathbf{B}$. Using Equation (3.81) and substituting $\delta\mathbf{r} = \boldsymbol{c}\delta t = -\dot{\boldsymbol{R}}_f \delta t/2 = \mathbf{E}_{\sigma i}\delta t$ into (8.27), one obtains

$$\kappa_{\sigma i}(\mathbf{x} + \delta_t \mathbf{E}_{\sigma i}, t + \delta_t) - \kappa_{\sigma i}(\mathbf{x}, t) = -\frac{1}{\tau_R}\left(\kappa_{\sigma i}(\mathbf{x}, t) - \kappa^{(ms)}_{\sigma i}(\mathbf{x}, t)\right) \qquad (10.7)$$

where $\kappa^{(ms)}_{\sigma i}$ is given by Equations (8.28). A truncated Taylor expansion to order $O(\delta_t^2)$ of Equation (10.7) gives

$$\begin{aligned}
\delta\left(\frac{\partial}{\partial t} + (\mathbf{E}_{\sigma i}\cdot\nabla)\right)\kappa_{\sigma i} + \frac{\delta_t^2}{2}\left(\frac{\partial}{\partial t} + (\mathbf{E}_{\sigma i}\cdot\nabla)\right)^2 \kappa_{\sigma i} + O(\delta_t^3)&\\
= -\frac{1}{\tau_R}\left(\kappa_{\sigma i}(\mathbf{x}, t) - \kappa^{(ms)}_{\sigma i}(\mathbf{x}, t)\right). \qquad (10.8)&
\end{aligned}$$

Next a Chapman-Enskog-like expansion is performed as described by Hou *et al* [65] and Cao *et al* [15] for gases. Let – by analogy with Equation (6.1) –

$$\kappa_{\sigma i} = \kappa^{(0)}_{\sigma i} + \delta_t \kappa^{(1)}_{\sigma i} + \delta_t^2 \kappa^{(2)}_{\sigma i} + O(\delta_t^3). \qquad (10.9)$$

The conservation laws

$$\sum_{\sigma,i} \kappa_{\sigma i} = \kappa, \qquad \sum_{\sigma,i} \kappa_{\sigma i}\mathbf{S}_{\sigma i} = \kappa\mathbf{R}_\mu \tag{10.10}$$

$$\sum_{\sigma,i} \rho_{\sigma i} = \rho, \qquad \sum_{\sigma,i} \rho_{\sigma i}\mathbf{E}_{\sigma i} = -\rho\frac{\dot{\mathbf{R}}_\mu^{'}}{2} \tag{10.11}$$

must apply for progressively higher order approximations of $\kappa_{\sigma i}$ and $\rho_{\sigma i}$ as described by (10.9) and $\dot{\mathbf{R}}_\mu^{'}/2 = \dot{\mathbf{R}}_\mu/2\alpha$. By induction (see Appendix (A-6)),

$$\begin{aligned}
\sum_\sigma\sum_i \kappa_{\sigma i}^{(0)} &= \kappa, & \sum_\sigma\sum_i \kappa_{\sigma i}^{(n)} &= 0 \Leftrightarrow n \neq 0,\\
\sum_\sigma\sum_i \kappa_{\sigma i}^{(0)}\mathbf{S}_{\sigma i} &= \kappa\mathbf{R}_\mu, & \sum_\sigma\sum_i \kappa_{\sigma i}^{(n)}\mathbf{S}_{\sigma i} &= 0 \Leftrightarrow n \neq 0,\\
\sum_\sigma\sum_i \rho_{\sigma i}^{(0)} &= \rho, & \sum_\sigma\sum_i \rho_{\sigma i}^{(n)} &= 0 \Leftrightarrow n \neq 0,\\
\sum_\sigma\sum_i \rho_{\sigma i}^{(0)}\mathbf{E}_{\sigma i} &= -\rho\frac{\dot{\mathbf{R}}_\mu^{'}}{2}, & \sum_\sigma\sum_i \rho_{\sigma i}^{(n)}\mathbf{E}_{\sigma\mathbf{i}} &= 0 \Leftrightarrow n \neq 0.
\end{aligned} \tag{10.12}$$

For constants κ and ρ an additional conservation equation is

$$\kappa = a \times \rho \iff \sum \kappa_{\sigma i} = a \times \sum \rho_{\sigma i} \tag{10.13}$$

where a is a scalar constant relating κ to ρ. But from (10.10) and (10.11),

$$\begin{aligned}
\sum \kappa_{\sigma i}\boldsymbol{\epsilon}_{\sigma i}R_{rms} &= 2b\frac{R_{rms}}{\dot{R}'_{rms}} \times \sum \rho_{\sigma i}\boldsymbol{\epsilon}_{\sigma i}\frac{\dot{R}'_{rms}}{2},\\
\sum \kappa_{\sigma i}\boldsymbol{\epsilon}_{\sigma i}\frac{R_{rms}}{R_{rms}} &= b \times \sum \rho_{\sigma i}\boldsymbol{\epsilon}_{\sigma i}\frac{\dot{R}'_{rms}}{\dot{R}'_{rms}},\\
\sum \kappa_{\sigma i}\boldsymbol{\epsilon}_{\sigma i} &= b \times \sum \rho_{\sigma i}\boldsymbol{\epsilon}_{\sigma i}
\end{aligned} \tag{10.14}$$

where constant b relates these conserved quantities. Multiplying (10.13) by $\boldsymbol{\epsilon}_{\sigma i}$,

$$\sum \kappa_{\sigma i}\boldsymbol{\epsilon}_{\sigma i} = a \times \sum \rho_{\sigma i}\boldsymbol{\epsilon}_{\sigma i}. \tag{10.15}$$

Therefore $a = b$ and consequently, summing over (10.14),

$$\frac{\kappa\mathbf{R}_\mu}{R_{rms}} = a \times 2\frac{\rho\frac{\dot{\mathbf{R}}_\mu^{'}}{2}}{\dot{R}'_{rms}} \tag{10.16}$$

Dividing (10.16) by (10.13)

$$\frac{\mathbf{R}_\mu}{R_{rms}} = \frac{\dot{\mathbf{R}}_\mu^{'}}{\dot{R}'_{rms}}. \tag{10.17}$$

10.1.1 The zero order approximation for stretch

In order to account for different time scales, substitute

$$\frac{\partial}{\partial t} = \frac{\partial}{\partial t_0} + \delta_t \frac{\partial}{\partial t_1}. \tag{10.18}$$

Substitution of (10.9) and (10.18) into (10.8) gives, to order δ,

$$\left(\frac{\partial}{\partial t_0} + \mathbf{E}_{\sigma i} \cdot \nabla\right) \kappa_{\sigma i}^{(0)} = \frac{\partial}{\partial t_0}\kappa_{\sigma i}^{(0)} + \nabla\cdot(\mathbf{E}_{\sigma i}\kappa_{\sigma i}^{(0)}) - \kappa_{\sigma i}^{(0)}\nabla\cdot\mathbf{E}_{\sigma i} = -\frac{1}{\tau}\kappa_{\sigma i}^{(1)}. \tag{10.19}$$

Since $\mathbf{E}_{\sigma i}$ is a constant, $\nabla \cdot \mathbf{E}_{\sigma i} = 0$. Summing over σ and i for Equation (10.19) and using Equations (10.12) and (10.17), one obtains

$$\begin{aligned}
\frac{\partial}{\partial t_0}\kappa_{\sigma i}^{(0)} + \nabla \cdot \left(\mathbf{E}_{\sigma i}\kappa_{\sigma i}^{(0)}\right) &= \frac{\partial}{\partial t_0}\kappa_{\sigma i}^{(0)} + \nabla \cdot \left(a \times \mathbf{E}_{\sigma i}\rho_{\sigma i}^{(0)}\right) \\
&= \frac{\partial \kappa_0}{\partial t_0} - \nabla \cdot \left(a \times \rho_0 \frac{\dot{\mathbf{R}}_\mu'}{2}\right).
\end{aligned}$$

The zero-order approximation of the bulk modulus per unit volume continuity equation is then given by

$$\frac{\partial}{\partial t_0}\kappa_{\sigma i}^{(0)} + \nabla \cdot \left(\mathbf{E}_{\sigma i}\kappa_{\sigma i}^{(0)}\right) = \frac{\partial \kappa_0}{\partial t_0} - \nabla \cdot \left(\kappa_0 \frac{\dot{\mathbf{R}}_\mu'}{2}\right) = 0. \tag{10.20}$$

Next, consider the first moment about $\mathbf{S}_{\sigma i}$ which will generate the zero order approximation to the conservation of force/momentum due to stretch. Multiplying (10.19) by constant vector $\mathbf{S}_{\sigma i}$ – using the tensor sums (10.12),

$$\begin{aligned}
& \mathbf{S}_{\sigma i}\frac{\partial \kappa_{\sigma i}^{(0)}}{\partial t_0} + \mathbf{S}_{\sigma i}\nabla \cdot \left(\mathbf{E}_{\sigma i}\kappa_{\sigma i}^{(0)}\right) &&= -\frac{1}{\tau_R}\kappa_{\sigma i}^{(1)}\mathbf{S}_{\sigma i} \\
\iff \quad & \mathbf{S}_{\sigma i}\frac{\partial \kappa_{\sigma i}^{(0)}}{\partial t_0} + \mathbf{S}_{\sigma i}\nabla \cdot \left(\mathbf{E}_{\sigma i}\kappa_{\sigma i}^{(0)}\right) + \mathbf{E}_{\sigma i}\kappa_{\sigma i}\nabla \cdot \mathbf{S}_{\sigma i} &&= -\frac{1}{\tau_R}\kappa_{\sigma i}^{(1)}\mathbf{S}_{\sigma i} \\
\iff \quad & \frac{\partial \kappa_{\sigma i}^{(0)}\mathbf{S}_{\sigma i}}{\partial t_0} + \nabla \cdot \left(\mathbf{E}_{\sigma i}\kappa_{\sigma i}^{(0)}\mathbf{S}_{\sigma i}\right) &&= 0 \\
\iff \quad & \frac{\partial \kappa \mathbf{R}_\mu}{\partial t_0} + \nabla \cdot \left(\mathbf{E}_{\sigma i}\kappa_{\sigma i}^{(0)}\mathbf{S}_{\sigma i}\right) &&= 0 \\
\iff \quad & \frac{\partial \kappa \mathbf{R}_\mu}{\partial t_0} + \nabla \cdot \Pi^{(0)} &&= 0
\end{aligned} \tag{10.21}$$

where $\mathbf{\Pi}^{(0)} = \sum\sum(\mathbf{S}_{\sigma i} \otimes \mathbf{E}_{\sigma i}\kappa_{\sigma i}^{(0)})$. Given that the maximum entropy bulk modulus per unit volume is approximated by the zero order bulk modulus per unit volume ($\kappa^{(ms)} \approx \kappa^{(0)}$), the approximation to $\kappa^{(0)}$ given by (8.28) is

substituted in $\mathbf{\Pi}^{(0)}$. The tensor sum results of (10.6) are used to evaluate the resultant $\mathbf{\Pi}^{(0)}$ and the results are

$$\begin{aligned}
\sum\sum S_{0i}E_{0i}\kappa_{0i}^{(0)} &= 0,\\
\sum\sum S_{1i}E_{1i}\kappa_{1i}^{(0)} &= -\frac{1}{9}\kappa_0\dot{R}'_{rms}R_{rms}\delta_{\alpha\beta} + 0 - \frac{1}{2}\kappa_0\frac{R_{rms}^3\dot{R}'_{rms}}{R_{rms}^4}\mathrm{R}_{\mu\alpha}\mathrm{R}_{\mu\beta}\delta_{\alpha\beta}\\
&\quad +\frac{1}{6}\kappa_0\frac{R_{rms}\dot{R}'_{rms}}{R_{rms}^2}\mathrm{R}_{\mu}^2\delta_{\alpha\beta}\\
&= -\frac{1}{9}\kappa_0\dot{R}'_{rms}R_{rms}\delta_{\alpha\beta} - \frac{1}{2}\kappa_0\frac{\dot{R}'_{rms}}{R_{rms}}R_{\mu\alpha}\mathrm{R}_{\mu\beta}\delta_{\alpha\beta}\\
&\quad +\frac{1}{6}\kappa_0\frac{\dot{R}'_{rms}}{R_{rms}}\mathrm{R}_{\mu}^2\delta_{\alpha\beta},\\
\sum\sum S_{2i}E_{2i}\kappa_{2i}^{(0)} &= -2\times\frac{1}{36}\kappa_0\dot{R}'_{rms}R_{rms}\delta_{\alpha\beta} + 0\\
&\quad -2\times\frac{1}{8}\kappa_0\frac{\dot{R}'_{rms}R_{rms}^3}{R_{rms}^4}\mathrm{R}_{\mu}^2\delta_{\alpha\beta} - 4\times\frac{1}{8}\kappa_0\frac{R_{rms}^3\dot{R}'_{rms}}{R_{rms}^4}\mathrm{R}_{\mu\alpha}\mathrm{R}_{\mu\beta}\\
&\quad +4\times\frac{1}{8}\kappa_0\frac{\dot{R}'_{rms}R_{rms}^3}{R_{rms}^4}\mathrm{R}_{\mu\alpha}\mathrm{R}_{\mu\beta}\delta_{\alpha\beta} + 2\times\frac{1}{24}\kappa_0\frac{\dot{R}'_{rms}R_{rms}}{R_{rms}^2}\mathrm{R}_{\mu}^2\delta_{\alpha\beta}\\
&= -\frac{1}{18}\kappa_0\dot{R}'_{rms}R_{rms}\delta_{\alpha\beta} - \frac{1}{4}\kappa_0\frac{\dot{R}'_{rms}}{R_{rms}}\mathrm{R}_{\mu}^2\delta_{\alpha\beta} - \frac{1}{2}\kappa_0\frac{\dot{R}'_{rms}}{R_{rms}}\mathrm{R}_{\mu\alpha}\mathrm{R}_{\mu\beta}\\
&\quad +\frac{1}{2}\kappa_0\frac{\dot{R}'_{rms}}{R_{rms}}\mathrm{R}_{\mu\alpha}\mathrm{R}_{\mu\beta}\delta_{\alpha\beta} + \frac{1}{12}\kappa_0\frac{\dot{R}'_{rms}}{R_{rms}}\mathrm{R}_{\mu}^2\delta_{\alpha\beta}.
\end{aligned}$$

Consequently (where α and β are free spatial indices)

$$\begin{aligned}
\Pi_{\alpha\beta}^{(0)} &= -\frac{1}{2}\Big((\frac{2}{9}\kappa_0+\frac{1}{9}\kappa_0)\dot{R}'_{rms}R_{rms} + (\frac{1}{2}\kappa_0-\frac{1}{3}\kappa_0-\frac{1}{6}\kappa_0)\frac{\dot{R}'_{rms}}{R_{rms}}\mathrm{R}_{\mu}^2\Big)\delta_{\alpha\beta}\\
&\quad -\frac{1}{2}\kappa_0\frac{\dot{R}'_{rms}}{R_{rms}}\mathrm{R}_{\mu\alpha}\mathrm{R}_{\mu\beta} - \frac{1}{2}(\kappa_0\frac{\dot{R}'_{rms}}{R_{rms}} - \kappa_0\frac{\dot{R}'_{rms}}{R_{rms}})\mathrm{R}_{\mu\alpha}\mathrm{R}_{\mu\beta}\delta_{\alpha\beta}
\end{aligned}$$

and therefore, upon substitution of Equation (10.17),

$$\Pi_{\alpha\beta}^{(0)} = -\frac{1}{6}\kappa_0\dot{R}'_{rms}R_{rms}\delta_{\alpha\beta} - \kappa_0\frac{\dot{\mathrm{R}}'_{\mu\alpha}\mathrm{R}_{\mu\beta}}{2}.$$

Substitution of this expression into (10.21) yields

$$\begin{aligned}
\frac{\partial\kappa\mathbf{R}_\mu}{\partial t_0} &= \nabla\cdot(\kappa\frac{\mathbf{R}_\mu\otimes\dot{\mathbf{R}}'_\mu}{2}) + \nabla(\frac{1}{6}\dot{R}'_{rms}R_{rms}\kappa)\\
\text{or}\qquad \frac{\partial\kappa\mathbf{R}_\mu}{\partial t_0} &= \frac{1}{4}\frac{\partial}{\partial t}\nabla\cdot(\kappa\mathbf{R}_\mu\otimes\mathbf{R}_\mu) + \frac{\partial}{\partial t}\nabla(\frac{1}{12}R_{rms}^2\kappa). \qquad (10.22)
\end{aligned}$$

10.1.2 The first order approximation for stretch

The derivation of the first order approximation requires the substitution of (10.9), (10.18) and (10.19) into (10.8) to order δ^2. The result is

$$\partial_{t_1}\kappa_{\sigma i}^{(0)} + (\partial_{t_0} + \mathbf{E}_{\sigma i}\cdot\nabla)\left[\left(1 - \frac{1}{2(\tau_R)}\right)\kappa_{\sigma i}^{(1)}\right] = -\frac{1}{\tau_R}\kappa_{\sigma i}^{(2)}; \tag{10.23}$$

the derivation is presented in Appendix A-3. Summing over σ and i for (10.23), using (10.12) and the fact that $\nabla\cdot\mathbf{E}_{\sigma i} = 0$ and $\nabla\mathbf{E}_{\sigma i} = 0$, one gets

$$\begin{aligned}
\partial_{t_1}\kappa_{\sigma i}^{(0)} + \Big(1 - \frac{1}{2\tau_R}\Big)\partial_{t_0}\kappa_{\sigma i}^{(1)} + \Big(1 - \frac{1}{2\tau_R}\Big)\nabla\cdot\Big(\mathbf{E}_{\sigma i}\kappa_{\sigma i}^{(1)}\Big) &= -\frac{1}{\tau_R}\kappa_{\sigma i}^{(2)} \\
\text{or } \partial_{t_1}(\kappa_0) + \Big(1 - \frac{1}{2\tau_R}\Big)\partial_{t_0}(0) + \Big(1 - \frac{1}{2\tau_R}\Big)\frac{\dot{R}'_{rms}}{2R_{rms}}\nabla\cdot\Big(\mathbf{S}_{\sigma i}\kappa_{\sigma i}^{(1)}\Big) &= -\frac{1}{\tau_R}(0). \\
\text{That is,} \qquad \partial_{t_1}(\kappa_0) &= 0 \qquad (10.24)
\end{aligned}$$

is recognised as the first order approximation to the bulk modulus per unit volume continuity equation.

In order to get the first order approximation to the conservation of momentum due to stretch, one uses the same approach by multiplying (10.23) by constant vector $\mathbf{S}_{\sigma i}$. The tensor sums (10.12) are substituted into the result to obtain

$$\partial_{t_1}\left(\mathbf{S}_{\sigma i}\kappa_{\sigma i}^{(0)}\right) + (\partial_{t_0} + \mathbf{E}_{\sigma i}\cdot\nabla)\left[\left(1 - \frac{1}{2\tau_R}\right)\mathbf{S}_{\sigma i}\kappa_{\sigma i}^{(1)}\right] = -\frac{1}{\tau_R}\mathbf{S}_{\sigma i}\kappa_{\sigma i}^{(2)}.$$

Note that $\nabla\cdot\mathbf{E}_{\sigma i}\otimes\mathbf{S}_{\sigma i}\kappa_{\sigma i} = \mathbf{E}_{\sigma i}\cdot\nabla\mathbf{S}_{\sigma i}\kappa_{\sigma i} + \mathbf{S}_{\sigma i}\kappa_{\sigma i}\cdot\nabla\mathbf{E}_{\sigma i}$ where $\mathbf{E}_{\sigma i}$ are constants. Therefore

$$\begin{aligned}
\partial_{t_1}\left(\mathbf{S}_{\sigma i}\kappa_{\sigma i}^{(0)}\right) + \left(1 - \frac{1}{2\tau_R}\right)\partial_{t_0}\left(\mathbf{S}_{\sigma i}\kappa_{\sigma i}^{(1)}\right) & \\
+ \left(1 - \frac{1}{2\tau_R}\right)\nabla\cdot\left(\mathbf{E}_{\sigma i}\mathbf{S}_{\sigma i}\kappa_{\sigma i}^{(1)}\right) &= -\frac{1}{\tau_R}\mathbf{S}_{\sigma i}\kappa_{\sigma i}^{(2)}, \\
\partial_{t_1}(\kappa\mathbf{R}_\mu) + \left(1 - \frac{1}{2\tau_R}\right)\partial_{t_0}(0) + \left(1 - \frac{1}{2\tau_R}\right)\nabla\cdot\mathbf{\Pi}^{(1)} &= -\frac{1}{\tau_R}(0), \\
\partial_{t_1}(\kappa_0\mathbf{R}_\mu) + \left(1 - \frac{1}{2\tau_R}\right)\nabla\cdot\mathbf{\Pi}^{(1)} &= 0, \qquad (10.25)
\end{aligned}$$

where $\mathbf{\Pi}^{(1)} = \sum_\sigma\sum_i \mathbf{E}_{\sigma i}\mathbf{S}_{\sigma i}\kappa_{\sigma i}^{(1)}$. But, from Equation (10.19),

$$\kappa_{\sigma i}^{(1)} = -\tau_R\left(\partial_{t_0}\kappa_{\sigma i}^{(0)} + \big(\nabla\cdot\mathbf{E}_{\sigma i}\big)\kappa_{\sigma i}^{(0)}\right);$$

solving for $\mathbf{\Pi}^{(1)}$ and then substituting the definition of $\mathbf{\Pi}^{(0)}$, one finds that for constant vectors $\mathbf{S}_{\sigma i}$ and $\mathbf{E}_{\sigma i}$

$$\begin{aligned}
\mathbf{\Pi}^{(1)} &= -\tau_R \mathbf{S}_{\sigma i}\mathbf{E}_{\sigma i}\left(\partial_{t0}\kappa^{(0)}_{\sigma i}\right) - \tau_R \nabla\cdot\left(\mathbf{E}_{\sigma i}\mathbf{E}_{\sigma i}\mathbf{s}_{\sigma i}\kappa^{(0)}_{\sigma i}\right) \\
\mathbf{\Pi}^{(1)} &= -\tau_R \left(\mathbf{S}_{\sigma i}\mathbf{E}_{\sigma i}\partial_{t0}\kappa^{(0)}_{\sigma i}\right) - \tau_R \nabla\cdot\left(\mathbf{E}_{\sigma i}\mathbf{E}_{\sigma i}\mathbf{s}_{\sigma i}\kappa^{(0)}_{\sigma i}\right) \\
&= -\tau_R \partial_{t_0}\mathbf{\Pi}^{(0)} - \tau_R \nabla\cdot\left(\mathbf{\Pi}^{(3)}\right) \qquad (10.26)
\end{aligned}$$

where $\mathbf{\Pi}^{(3)} = \mathbf{E}_{\sigma i}\mathbf{E}_{\sigma i}\mathbf{S}_{\sigma i}\kappa^{(0)}_{\sigma i}$ is a third order tensor and $\nabla\cdot\mathbf{\Pi}^{(3)}$ is a second order tensor with terms $\Pi^{(3)}_{ijk,k}$. After substituting (8.28) into $\mathbf{\Pi}^{(3)}$ one obtains

$$\mathbf{\Pi}^{(3)} = (\mathbf{E}_{1i}\mathbf{E}_{1i}\mathbf{S}_{1i}\mathbf{S}_{1i}\cdot\mathbf{R}_\mu)\times\frac{1}{3}\frac{\kappa_0}{R^2_{rms}} + (\mathbf{E}_{2i}\mathbf{E}_{2i}\mathbf{S}_{2i}\mathbf{S}_{2i}\cdot\mathbf{R}_\mu)\times\frac{1}{12}\frac{\kappa_0}{R^2_{rms}}.$$

Substituting the results for the tensor sum (10.6) into $\mathbf{\Pi}^{(3)}$,

$$\begin{aligned}
\Pi^{(3)}_{\alpha\beta} &= \left(\dot{R}'^2_{rms}R^2_{rms}\delta_{\alpha\beta}\mathrm{R}_{\mu\beta}\right)\times\frac{1}{6}\frac{\kappa_0}{R^2_{rms}} \\
&\quad + \left(\dot{R}'^2_{rms}R^2_{rms}\Delta_{\alpha\beta\gamma\theta} - 2\dot{R}'^2_{rms}R^2_{rms}\delta_{\alpha\beta\gamma\theta}\right)\mathrm{R}_\mu\frac{1}{12}\frac{\kappa_0}{R^2_{rms}} \qquad (10.27)
\end{aligned}$$

and thus

$$\begin{aligned}
(\nabla\cdot\mathbf{\Pi}^{(3)})_\alpha &= \dot{R}'^2_{rms}\kappa_0\partial_\alpha\left(\frac{1}{6}-\frac{2}{12}\right)\delta_{\alpha\beta}\mathrm{R}_{\mu\beta} \\
&\quad + \left(\partial_\gamma\mathrm{R}_{\mu\gamma}\delta_{\alpha\beta} + \partial_\alpha\mathrm{R}_{\mu\beta} + \partial_\beta\mathrm{R}_{\mu\alpha}\right)\frac{1}{12}\kappa_0\dot{R}'^2_{rms}. \qquad (10.28)
\end{aligned}$$

Substituting Equation (10.27) and $\mathbf{\Pi}^{(0)}$ into Equation (10.26),

$$\begin{aligned}
\Pi^{(1)}_{\alpha\beta} &= \tau_R\left(\frac{1}{6}\dot{R}'_{rms}R_{rms}\delta_{\alpha\beta}\partial_{t0}\kappa_0 + \partial_{t0}\kappa_0\mathrm{R}_{\mu\alpha}\frac{\dot{\mathrm{R}}'_{\mu\beta}}{2}\right) \\
&\quad -\tau_R\frac{1}{12}\Bigg(\partial_\gamma\mathrm{R}_{\mu\gamma}\delta_{\alpha\beta}\kappa_0\dot{R}'^2_{rms} + \partial_\alpha\mathrm{R}_{\mu\beta}\kappa_0\dot{R}'^2_{rms} \\
&\qquad +\partial_\beta\mathrm{R}_{\mu\alpha}\kappa_0\dot{R}'^2_{rms}\Bigg). \qquad (10.29)
\end{aligned}$$

Substituting the result $\partial_{t_0}\kappa = \partial_\gamma\kappa\dot{R}'_{\mu\gamma}/2$, from (10.20), into (10.29)

$$\begin{aligned}
\Pi^{(1)}_{\alpha\beta} &= \tau_R\left(\frac{1}{6}\dot{R}'_{rms}R_{rms}\delta_{\alpha\beta}\partial_\gamma(\kappa_0\frac{\dot{\mathrm{R}}'_{\mu\gamma}}{2}) + \partial_{t0}\kappa_0\mathrm{R}_{\mu\alpha}\frac{\dot{\mathrm{R}}'_{\mu\beta}}{2}\right) \\
&\quad -\tau_R\frac{1}{12}\left(\partial_\gamma\mathrm{R}_{\mu\gamma}\delta_{\alpha\beta}\kappa_0\dot{R}'^2_{rms} + \partial_\alpha\mathrm{R}_{\mu\beta}\kappa_0\dot{R}'^2_{rms} + \partial_\beta\mathrm{R}_{\mu\alpha}\kappa_0\dot{R}'^2_{rms}\right).
\end{aligned}$$

Further, substituting (10.17) into the above result,

$$\begin{aligned}
\Pi^{(1)}_{\alpha\beta} &= \tau_R\left(\frac{1}{12}\dot{R}'^2_{rms}R_{rms}\delta_{\alpha\beta}\partial_\gamma(\kappa_0\frac{\mathrm{R}_{\mu\gamma}}{R_{rms}})+\frac{1}{2}\partial_{t0}\kappa_0\mathrm{R}_{\mu\alpha}\dot{\mathrm{R}}'_{\mu\beta}\right)\\
&\quad -\tau_R\frac{1}{12}\left(\partial_\gamma\mathrm{R}_{\mu\gamma}\kappa_0\dot{R}'^2_{rms}\delta_{\alpha\beta}+\partial_\alpha\mathrm{R}_{\mu\beta}\kappa_0\dot{R}'^2_{rms}+\partial_\beta\mathrm{R}_{\mu\alpha}\kappa_0\dot{R}'^2_{rms}\right)\\
&= \tau_R\left(\frac{1}{12}\dot{R}'^2_{rms}\delta_{\alpha\beta}\partial_\gamma(\kappa_0\mathrm{R}_{\mu\gamma})+\frac{1}{2}\partial_{t0}\kappa_0\mathrm{R}_{\mu\alpha}\dot{\mathrm{R}}'_{\mu\beta}\right)\\
&\quad -\tau_R\frac{1}{12}\left(\partial_\gamma\mathrm{R}_{\mu\gamma}\kappa_0\dot{R}'^2_{rms}\delta_{\alpha\beta}+\partial_\alpha\mathrm{R}_{\mu\beta}\kappa_0\dot{R}'^2_{rms}+\partial_\beta\mathrm{R}_{\mu\alpha}\kappa_0\dot{R}'^2_{rms}\right)\\
&= -\tau_R\frac{1}{4}\left(\partial_\alpha\mathrm{R}_{\mu\beta}\frac{1}{3}\kappa_0\dot{R}'^2_{rms}+\partial_\beta\mathrm{R}_{\mu\alpha}\frac{1}{3}\kappa_0\dot{R}'^2_{rms}\right)\\
&\quad +\tau_R\frac{1}{4}\left(2(\kappa_0\dot{\mathrm{R}}'_{\mu\alpha}\dot{\mathrm{R}}'_{\mu\beta})+2\mathrm{R}_{\mu\alpha}\ddot{\mathrm{R}}_{\mu\beta}\right). \qquad (10.30)
\end{aligned}$$

Consider the last term in (10.30). From Equations (10.22) and (10.12) and ignoring second derivatives, the tensor

$$\begin{aligned}
2\kappa\dot{\mathrm{R}}'_{\mu\alpha}\dot{\mathrm{R}}'_{\mu\beta} &= 2\dot{\mathrm{R}}'_{\mu\alpha}\partial_{t0}\kappa\mathrm{R}_{\mu\beta}+2\dot{\mathrm{R}}'_{\mu\beta}\partial_{t0}\kappa\mathrm{R}_{\mu\alpha}\\
&= 2\dot{\mathrm{R}}'_{\mu\alpha}\partial_\beta\partial_{t0}\left(\frac{1}{12}R^2_{rms}\kappa\right)+2\dot{\mathrm{R}}'_{\mu\beta}\partial_\alpha\partial_{t0}\left(\frac{1}{12}R^2_{rms}\kappa\right)\\
&\quad +2\times\frac{1}{4}\dot{\mathrm{R}}'_{\mu\alpha}\partial_\beta\partial_{t0}\kappa\mathrm{R}_{\mu\beta}\mathrm{R}_{\mu\gamma}+2\times\frac{1}{4}\dot{\mathrm{R}}'_{\mu\beta}\partial_\alpha\partial_{t0}\kappa\mathrm{R}_{\mu\alpha}\mathrm{R}_{\mu\gamma}\\
&= 4\dot{\mathrm{R}}'_{\mu\alpha}\partial_\beta\dot{R}'_{rms}\partial_{t0}\left(\frac{1}{12}R_{rms}\kappa\right)+4\dot{\mathrm{R}}'_{\mu\beta}\partial_\alpha\dot{R}'_{rms}\partial_{t0}\left(\frac{1}{12}R_{rms}\kappa\right)\\
&\quad +\frac{1}{2}\dot{\mathrm{R}}'_{\mu\alpha}\partial_\beta\partial_{t0}\kappa\mathrm{R}_{\mu\beta}\mathrm{R}_{\mu\gamma}+\frac{1}{2}\dot{\mathrm{R}}'_{\mu\beta}\partial_\alpha\partial_{t0}\kappa\mathrm{R}_{\mu\alpha}\mathrm{R}_{\mu\gamma}\\
&= \dot{\mathrm{R}}'_{\mu\beta}\partial_\beta\left(\frac{1}{3}\dot{R}'^2_{rms}\kappa\right)+\dot{\mathrm{R}}'_{\mu\beta}\partial_\alpha\left(\frac{1}{3}\dot{R}'^2_{rms}\kappa\right)\\
&\quad +\partial_\gamma\kappa\mathrm{R}_{\mu\gamma}\dot{\mathrm{R}}'_{\mu\alpha}\dot{\mathrm{R}}'_{\mu\beta} \qquad (10.31)
\end{aligned}$$

and therefore for free spatial indices α,β

$$\Pi^{(1)}_{\alpha\beta}=-\tau_R\left(\frac{1}{12}\dot{R}^2_{rms}\kappa\partial_\alpha\mathrm{R}_{\mu\beta}+\frac{1}{12}\dot{R}^2_{rms}\kappa\partial_\beta\mathrm{R}_{\mu\alpha}-\frac{1}{4}\partial_\gamma\kappa\mathrm{R}_{\mu\gamma}\dot{\mathrm{R}}_{\mu\beta}\dot{\mathrm{R}}_{\mu\alpha}\right). \qquad (10.32)$$

Next, Equation (10.32) is substituted into Equation (10.25) yielding

$$\begin{aligned}
\partial_{t_1}\kappa\mathrm{R}_{\mu\alpha} &= \tau_R\left(1-\frac{1}{2\tau_R}\right)\partial_\beta\left(\frac{1}{12}\kappa\dot{R}^2_{rms}(\partial_\alpha\mathrm{R}_{\mu\beta}+\partial_\beta\mathrm{R}_{\mu\alpha})\right)\\
&\quad - \tau_R\left(1-\frac{1}{2\tau_R}\right)\frac{1}{4}\partial_\beta\partial_\gamma(\kappa\mathrm{R}_{\mu\gamma}\dot{\mathrm{R}}_{\mu\beta}\dot{\mathrm{R}}_{\mu\alpha})=\mathbf{0}. \qquad (10.33)
\end{aligned}$$

10.1.3 Sum of 0^{th} and 1^{st} order approximations for stretch

Summing Equations (10.20) and (10.24) the result is

$$\frac{\partial \kappa}{\partial t} - \nabla \cdot (\kappa \frac{\dot{\mathbf{R}}'_{\mu}}{2}) = 0. \tag{10.34}$$

Similarly, summing Equations (10.22) and (10.33),

$$\begin{aligned}
\partial_t \kappa \mathrm{R}_{\mu\alpha} - \frac{1}{4}\partial_t\partial_\beta \kappa \mathrm{R}_{\mu\alpha}\mathrm{R}_{\mu\beta} &= \partial_t\partial_\alpha\left(\frac{1}{12}R^2_{rms}\kappa\right) \\
&\quad +\delta_t\partial_\alpha\left(\tau_R - \frac{1}{2}\right)\left(\frac{1}{12}\dot{R}'^2_{rms}\kappa(\partial_\alpha \mathrm{R}_{\mu\beta} + \partial_\beta \mathrm{R}_{\mu\alpha})\right) \\
&\quad -\left(\tau_R - \frac{1}{2}\right)\frac{1}{4}\delta_t\partial_\beta\partial_\gamma(\kappa \mathrm{R}_{\mu\alpha}\dot{\mathrm{R}}'_{\mu\beta}\dot{\mathrm{R}}'_{\mu\gamma}) + O(\delta_t^2) \\
&= \frac{1}{2}\partial_t\partial_\alpha\left(\frac{1}{6}R^2_{rms}\kappa\right) \\
&\quad +\delta_t\partial_\beta\left(\tau_R - \frac{1}{2}\right)\left(\frac{1}{12}\dot{R}'^2_{rms}\kappa(\partial_\alpha \mathrm{R}_{\mu\beta} + \partial_\beta \mathrm{R}_{\mu\alpha})\right) \\
&\quad -\left(\tau_R - \frac{1}{2}\right)\frac{1}{4}\delta_t\partial_\beta\partial_\gamma(\kappa \mathrm{R}_{\mu\alpha}\dot{\mathrm{R}}'_{\mu\beta}\dot{\mathrm{R}}'_{\mu\gamma}) + O(\delta_t^2) \\
&= \frac{1}{2}\partial_t\partial_\alpha\left(\frac{2}{3}\times\frac{1}{4}R^2_{rms}\kappa\right) - 4\partial_\beta(G^{(lat)}\mathrm{D}^{(lat)}_{\alpha\beta}) \\
&\quad -\left(\tau_R - \frac{1}{2}\right)\frac{1}{4}\delta_t\partial_\beta\partial_\gamma(\kappa \mathrm{R}_{\mu\alpha}\dot{\mathrm{R}}'_{\mu\beta}\dot{\mathrm{R}}'_{\mu\gamma}) \\
&\quad +O(\delta_t^2)
\end{aligned} \tag{10.35}$$

where $\mathrm{D}^{(lat)}_{\alpha\beta} = -\frac{1}{4}(\partial_\alpha \mathrm{R}_{\mu\beta} + \partial_\beta \mathrm{R}_{\mu\alpha}) = \mathrm{D}^{(real)}_{\alpha\beta}$, $p_s^{(lat)} = \frac{1}{6}\kappa R^2_{rms} = \frac{1}{3}p_s^{(real)}$, $\frac{\partial p_s^{(lat)}}{\partial t} = -\frac{\omega}{3}\kappa R_{rms}R_{rms} = \frac{1}{3}\frac{\partial p_s^{(real)}}{\partial t}$ and

$$G^{(lat)} = \frac{2\tau_R - 1}{24}\dot{R}'^2_{rms}\delta_t\kappa \qquad = \qquad \frac{2\tau_R - 1}{24}\dot{\mathrm{R}}'^2_{\mu 0}\delta_t\kappa = \frac{1}{3}G^{(real)}. \tag{10.36}$$

Equation (10.35) can be recognised as the incompressible stretch flow equation (6.109). The third term has been identified as the non-linear deviation term [118]. Given (10.4) and given that G is a constant and independent of damping,

$$G^{(real)} = \frac{2\tau_R - 1}{24}\frac{\dot{R}^2_{rms}}{\alpha^2}\alpha^2\delta'_t\kappa \tag{10.37}$$

where $\alpha^2\delta'_t = \delta_t$, δ'_t is the time increment for critical damping and δ_t is the time increment for non-critical damping. Then (10.37) reduces to

$$G^{(real)} = \frac{2\tau_R - 1}{24}\frac{\dot{R}^2_{rms}}{\alpha^2}\delta_t\kappa \tag{10.38}$$

where $\dot{R}_{rms}/\alpha$ is the chain-length stretch-rate for the non-critically damped scenario. This result will allow the numerical model to be scaled between the non-critically damped model and the critically damped model. This means that the time results obtained from the critically damped model can be multiplied by α^2 to get the non-critically damped time and the critically damped stretch rate result can be divided by α to calculate the chain stretch rate for non-critical damping. Section 10.3 will show why this indirect method of applying non-critical damping is necessary.

10.2 Expansion of stretch rate

The tensor sums for $\mathbf{E}_{\sigma i}$ resemble the gas analogy more closely. Once again they are determined by substituting (10.1) into (10.3) and summing moments 1 through 4 of $\mathbf{E}_{\sigma i}$. Thus the tensor sums for stretch rate are [65]

$$\begin{aligned}
\sum_i \mathrm{E}_{\sigma i\alpha} &= 0 \\
\sum_i \mathrm{E}_{\sigma i\alpha}\mathrm{E}_{\sigma i\beta} &= \frac{1}{2}e_\sigma^2 \dot{R}'^2_{rms}\delta_{\alpha\beta} \\
\sum_i \mathrm{E}_{\sigma i\alpha}\mathrm{E}_{\sigma i\beta}\mathrm{E}_{\sigma i\gamma} &= 0 \\
\sum_i \mathrm{E}_{\sigma i\alpha}\mathrm{E}_{\sigma i\beta}\mathrm{E}_{\sigma i\gamma}\mathrm{E}_{\sigma i\theta} &= \frac{1}{8}\dot{R}'^4_{rms}\delta_{\alpha\beta\gamma\theta} \qquad \sigma = 1 \\
\sum_i \mathrm{E}_{\sigma i\alpha}\mathrm{E}_{\sigma i\beta}\mathrm{E}_{\sigma i\gamma}\mathrm{E}_{\sigma i\theta} &= \frac{1}{4}\dot{R}'^4_{rms}\Delta_{\alpha\beta\gamma\theta} - \frac{1}{2}\dot{R}'^4_{rms}\delta_{\alpha\beta\gamma\theta} \qquad \sigma = 2
\end{aligned} \tag{10.39}$$

where, as before,

$$\delta_{\alpha\beta\gamma\theta} = 1 \Leftrightarrow \alpha = \beta = \gamma = \theta$$

and

$$\Delta_{\alpha\beta\gamma\theta} = \delta_{\alpha\beta}\delta_{\gamma\theta} + \delta_{\alpha\gamma}\delta_{\beta\theta} + \delta_{\alpha\theta}\delta_{\beta\gamma}.$$

Note that the same calculations that were performed for chain length, in Section 10.1, will be duplicated in this section for chain stretch rate. The only difference being the tensor sums (10.39) above. The derivation of the N-S type equations is more closely analagous to Hou *et al*'s [65] for fluids.

Substituting $\delta\mathbf{r} = \mathbf{E}_{\sigma i}\delta t$ into equation (8.33)

$$\rho_{\sigma i}(\mathbf{x} + \delta_t\mathbf{E}_{\sigma i}, t + \delta_t) - \rho_{\sigma i}(\mathbf{x}, t) = -\frac{1}{\tau_R}\left(\rho_{\sigma i}(\mathbf{x}, t) - \rho_{\sigma i}^{(ms)}(\mathbf{x}, t)\right) \tag{10.40}$$

where $\rho_{\sigma i}^{(ms)}$ is given by (8.35). Performing a truncated Taylor expansion to order $O(\delta_t^2)$ of Equation (10.40) one obtains

$$\delta\left(\frac{\partial}{\partial t}+(\mathbf{E}_{\sigma i}\cdot\nabla)\right)\rho_{\sigma i}+\frac{\delta_t^2}{2}\left(\frac{\partial}{\partial t}+(\mathbf{E}_{\sigma i}\cdot\nabla)\right)^2\rho_{\sigma i}+O(\delta_t^3) = -\frac{1}{\tau_{\dot{R}}}\left(\rho_{\sigma i}(\mathbf{x},t)-\rho_{\sigma i}^{(ms)}(\mathbf{x},t)\right). \quad (10.41)$$

The Chapman-Enskog-like expansion,

$$\rho_{\sigma i}=\rho_{\sigma i}^{(0)}+\delta_t\rho_{\sigma i}^{(1)}+\delta_t^2\rho_{\sigma i}^{(2)}+O(\delta_t^3), \quad (10.42)$$

which resembles Hou et al's [65] description for gases, is used. The conservation laws (10.12), (10.17) and time scales (10.18) are used.

10.2.1 The zero order approximation for stretch rate

Substituting Equations (10.42) and (10.18) into Equation (10.41) to order δ

$$\begin{aligned}\left(\frac{\partial}{\partial t_0}+\mathbf{E}_{\sigma i}\cdot\nabla\right)\rho_{\sigma i}^{(0)} &= \frac{\partial}{\partial t_0}\rho_{\sigma i}^{(0)}+\nabla\cdot(\mathbf{E}_{\sigma i}\rho_{\sigma i}^{(0)})-\rho_{\sigma i}^{(0)}\nabla\cdot\mathbf{E}_{\sigma i}\\ &= -\frac{1}{\tau_{\dot{R}}}\rho_{\sigma i}^{(1)} \quad (10.43)\end{aligned}$$

where $\mathbf{E}_{\sigma i}$ is constant and consequently $\nabla\cdot\mathbf{E}_{\sigma i}=0$. Summing (10.43) over σ and i using (10.12) one obtains

$$\Big(\frac{\partial}{\partial t_0}+\mathbf{E}_{\sigma i}\cdot\nabla\Big)\rho_{\sigma i}^{(0)}=\frac{\partial\rho_0}{\partial t_0}-\nabla\cdot(\rho_0\frac{\dot{\mathbf{R}}_\mu}{2})=0. \quad (10.44)$$

Next the first moment given by the product of (10.43) and $\mathbf{E}_{\sigma i}$ is determined. The product is summed and the conservation equations (10.12) substituted to yield

$$\frac{1}{2}\frac{\partial\rho\dot{\mathbf{R}}_\mu'}{\partial t_0}=\frac{1}{4}\nabla\cdot(\rho\dot{\mathbf{R}}_\mu'\otimes\dot{\mathbf{R}}_\mu')+\nabla\left(\frac{1}{12}\dot{R}_{rms}'^2\rho\right). \quad (10.45)$$

10.2.2 The first order approximation for stretch rate

Substituting Equations (10.42), (10.18) and (10.43) into Equation (10.41),

$$\partial_{t_1}\rho_{\sigma i}^{(0)}+(\partial_{t_0}+\mathbf{E}_{\sigma i}\cdot\nabla)\left(1-\frac{1}{2\tau_{\dot{R}}}\right)\rho_{\sigma i}^{(1)}=-\frac{1}{\tau_{\dot{R}}}\rho_{\sigma i}^{(2)}. \quad (10.46)$$

Summing (10.46) using Equations (10.12) and the fact that $\nabla \cdot \mathbf{E}_{\sigma i} = 0$,

$$\partial_{t_1}(\rho_0) = 0. \tag{10.47}$$

Similarly, for the first moment, the product of (10.46) and $\mathbf{E}_{\sigma i}$ is required. Substitution of Equation (10.12) into the result yields

$$\partial_{t_1}\left(\rho_0 \frac{\dot{\mathbf{R}}'_\mu}{2}\right) - \left(1 - \frac{1}{2\tau_{\dot{R}}}\right)\nabla \cdot \mathbf{\Pi}^{(1)} = 0 \tag{10.48}$$

where $\mathbf{\Pi}^{(1)} = \sum_\sigma \sum_i \mathbf{E}_{\sigma i}\mathbf{E}_{\sigma i}\rho^{(1)}_{\sigma i}$. From Equation (10.43),

$$\rho^{(1)}_{\sigma i} = -\tau_{\dot{R}}\left(\partial_{t_0}\rho^{(0)}_{\sigma i} + \nabla \cdot \left(\mathbf{E}_{\sigma i}\rho^{(0)}_{\sigma i}\right)\right).$$

Substituting $\rho^{(1)}_{\sigma i}$ and $\mathbf{\Pi}^{(0)}$ into $\mathbf{\Pi}^{(1)}$ one obtains

$$\begin{aligned}\mathbf{\Pi}^{(1)} &= -\tau_{\dot{R}}\mathbf{E}_{\sigma i}\mathbf{E}_{\sigma i}\partial_{t_0}\left(\rho^{(0)}_{\sigma i}\right) - \tau_{\dot{R}}\nabla \cdot \left(\mathbf{E}_{\sigma i}\mathbf{E}_{\sigma i}\mathbf{E}_{\sigma i}\rho^{(0)}_{\sigma i}\right) \\ &= -\tau_{\dot{R}}\partial_{t_0}\mathbf{\Pi}^{(0)} - \tau_{\dot{R}}\nabla \cdot \mathbf{\Pi}^{(3)}\end{aligned} \tag{10.49}$$

where $\mathbf{\Pi}^{(3)} = \mathbf{E}_{\sigma i}\mathbf{E}_{\sigma i}\mathbf{E}_{\sigma i}\rho^{(0)}_{\sigma i}$ is a third order tensor. Substituting (8.38) into $\mathbf{\Pi}^{(3)}$ and then using (10.39) to perform the summation,

$$-\tau_{\dot{R}}\partial_\beta \Pi^{(3)}_{\alpha\beta} = \tau_{\dot{R}}\left(\partial_\gamma \dot{\mathrm{R}}'_{\mu\gamma}\delta_{\alpha\beta} + \partial_\alpha \dot{\mathrm{R}}'_{\mu\beta} + \partial_\beta \dot{\mathrm{R}}'_{\mu\alpha}\right)\frac{1}{24}\rho_0 \dot{R}'^2_{rms}. \tag{10.50}$$

Substituting $\mathbf{\Pi}^{(0)}$, (10.50) and (10.43) into (10.49) one obtains

$$\Pi^{(1)}_{\alpha\beta} = \frac{\tau_{\dot{R}}}{24}\left(\partial_\alpha \dot{\mathrm{R}}'_{\mu\beta}\rho_0 \dot{R}'^2_{rms} + \partial_\beta \dot{\mathrm{R}}'_{\mu\alpha}\rho_0 \dot{R}'^2_{rms}\right) - \frac{\tau_{\dot{R}}}{4}\partial_{t_0}\rho_0 \dot{\mathrm{R}}'_{\mu\alpha}\dot{\mathrm{R}}_{\mu\beta}{}'. \tag{10.51}$$

Given that (10.45) can be re-expressed as

$$\frac{1}{2}\partial_{t_0}\rho \dot{\mathrm{R}}'_{\mu\alpha}\dot{\mathrm{R}}'_{\mu\beta} = \dot{\mathrm{R}}'_{\mu\alpha}\partial_\beta\left(\frac{1}{12}\rho \dot{R}'^2_{rms}\right) + \dot{\mathrm{R}}'_{\mu\beta}\partial_\alpha\left(\frac{1}{12}\rho \dot{R}'^2_{rms}\right)\frac{1}{4}\partial_\gamma \rho \dot{\mathrm{R}}'_{\mu\alpha}\dot{\mathrm{R}}'_{\mu\beta}\dot{\mathrm{R}}'_{\mu\gamma},$$

substitution of this result into (10.51) gives $\mathbf{\Pi}^{(1)}$ as

$$\Pi^{(1)}_{\alpha\beta} = \frac{\tau_{\dot{R}}}{24}\rho \dot{R}'^2_{rms}(\partial_\alpha \dot{\mathrm{R}}'_{\mu\beta} - \partial_\beta \dot{\mathrm{R}}'_{\mu\alpha}) - \frac{1}{8}\partial_\gamma \rho \dot{\mathrm{R}}'_{\mu\alpha}\dot{\mathrm{R}}'_{\mu\beta}\dot{\mathrm{R}}'_{\mu\gamma}. \tag{10.52}$$

Finally substitution of (10.52) into (10.48) yields

$$\begin{aligned}\frac{1}{2}\partial_{t_1}\rho\dot{\mathrm{R}}'_{\mu} &= \tau_{\dot{R}}\left(1-\frac{1}{2\tau_{\dot{R}}}\right)\partial_{\beta}\left(\frac{1}{24}\rho\dot{R}'^{2}_{rms}(\partial_{\beta}\dot{\mathrm{R}}'_{\mu\alpha}+\partial_{\alpha}\dot{\mathrm{R}}'_{\mu\beta})\right)\\ &\quad -\tau_{\dot{R}}\left(1-\frac{1}{2\tau_{\dot{R}}}\right)\partial_{\beta}\frac{1}{8}\partial_{\gamma}\rho\dot{\mathrm{R}}'_{\mu\alpha}\dot{\mathrm{R}}'_{\mu\beta}\dot{\mathrm{R}}'_{\mu\gamma} \qquad (10.53)\end{aligned}$$

10.2.3 Sum of 0^{th} and 1^{st} order approximations for stretch rate

Summing Equation (10.44) and Equation (10.47)

$$\frac{\partial\rho}{\partial t}-\nabla\cdot\left(\rho\frac{\dot{\mathbf{R}}'_{\mu}}{2}\right)=0$$

Summing Equations (10.45) and (10.53) and doubling the result,

$$\begin{aligned}\frac{\partial\rho\dot{\mathrm{R}}'_{\mu\alpha}}{\partial t}-\frac{1}{2}\partial_{\beta}\rho\dot{\mathrm{R}}'_{\mu\alpha}\dot{\mathrm{R}}'_{\mu\beta} &= 2\partial_{\alpha}\left(\frac{2}{3}\times\frac{1}{8}\rho\dot{R}'^{2}_{rms}\right)+4\partial_{\alpha}\delta_t\frac{1-2\tau_{\dot{R}}}{24}\\ &\quad\times\Big(-\frac{1}{4}\rho\dot{R}'^{2}_{rms}(\partial_{\alpha}\dot{\mathrm{R}}'_{\mu\beta}+\partial_{\beta}\dot{\mathrm{R}}'_{\mu\alpha})\Big)\\ &\quad-\frac{1}{8}\delta_t\left(2\tau_{\dot{R}}-1\right)\partial_{\beta}\partial_{\gamma}\dot{\mathrm{R}}'_{\mu\alpha}\dot{\mathrm{R}}'_{\mu\beta}\dot{\mathrm{R}}'_{\mu\gamma}+O(\delta_t^2)\\ &= 2\partial_{\alpha}p_d+4\partial_{\beta}\mu\dot{\mathrm{D}}_{\alpha\beta}-\frac{1}{8}\delta_t\left(2\tau_{\dot{R}}-1\right)\times\\ &\quad\partial_{\beta}\partial_{\gamma}\dot{\mathrm{R}}'_{\mu\alpha}\dot{\mathrm{R}}'_{\mu\beta}\dot{\mathrm{R}}'_{\mu\gamma}+O(\delta_t^2) \qquad (10.54)\end{aligned}$$

where $\dot{\mathrm{D}}^{(lat)}=-\frac{1}{4}\left(\partial_{\beta}\dot{\mathrm{R}}'_{\mu\alpha}+\partial_{\beta}\dot{\mathrm{R}}'_{\mu\alpha}\right)=\dot{\mathrm{D}}^{(real)}$, $p_d^{(lat)}=\frac{2}{3}\times\frac{1}{8}\rho\dot{R}'^{2}_{rms}=\frac{1}{3}p_d^{(real)}$.

$$\mu^{(lat)}=\frac{1-2\tau_{\dot{R}}}{24}\dot{R}'^{2}_{rms}\rho\delta_t \;=\; \frac{1-2\tau_{\dot{R}}}{24}\dot{R}'^{2}_{\mu 0}\rho\delta_t=\frac{1}{3}\mu^{(real)}. \qquad (10.55)$$

Equation (10.54) is the incompressible stretch rate flow equation (6.107). The third term is the non-linear deviation term [118]. Given that the constant μ does not depend on critical damping, substituting (10.4) into (10.55)

$$\mu^{(real)}=\frac{1-2\tau_{\dot{R}}}{24}\frac{\dot{R}^2_{rms}}{\alpha^2}\rho\alpha^2\delta'_t$$

where $\delta_t=\alpha^2\delta'_t$. The term δ'_t is the time increment for the critically damped scenario. For non-critical damping, the time increment is $\delta_t=\alpha^2\delta'_t$.

10.3 Polymer equation truncation justification

Adding Equation (10.54) to the integral of Equation (10.35) with respect to time, and recognising the corresponding terms in Equation (7.16),

$$\begin{aligned} -\left(\nabla\cdot\mathbf{T}\right)_\alpha &= \kappa \mathrm{R}_{\mu\alpha} - \frac{1}{4}\partial_\beta \kappa \mathrm{R}_{\mu\alpha}\mathrm{R}_{\mu\beta} + \frac{\partial \rho \dot{\mathrm{R}}_{\mu\alpha}}{\partial t} - \frac{1}{2}\partial_\beta \rho \dot{\mathrm{R}}_{\mu\alpha}\dot{\mathrm{R}}_{\mu\beta} \\ &= \frac{1}{2}\partial_\alpha \mathrm{P}'_S + 2\partial_\alpha \mathrm{P}'_D - 4\partial_\beta \mu \dot{\mathrm{D}}_{\alpha\beta} - 4\int_t^{t'} \partial_\beta G \mathrm{D}_{\alpha\beta} dt \quad (10.56) \end{aligned}$$

for $t' > t$. Equation (10.56) is recognised as (6.99) – the equation of polymer flow. The constitutive equation (7.16) can also be identified. This represents the multiscaling method applied to

$$\begin{aligned} \int_t^{t'} \kappa_{\sigma i}^{poly} \mathbf{S}_{\sigma i} d\tau + 2\rho_{\sigma i}^{poly} \mathbf{E}_{\sigma i} &= \int_t^{t\prime} \kappa_{\sigma i}^{poly} R_{rms} \boldsymbol{\epsilon}_{\sigma i} d\tau + 2\rho_{\sigma i}^{poly} \frac{\dot{R}'_{rms}}{2} \boldsymbol{\epsilon}_{\sigma i} \\ &= \boldsymbol{\epsilon}_{\sigma i}\Big(\int_t^{t'} \kappa_{\sigma i}^{poly} R_{rms} d\tau + \rho_{\sigma i}^{poly} \dot{R}'_{rms} \Big) \end{aligned}$$

where $\rho_{\sigma i}^{poly}$ and $\kappa_{\sigma i}^{poly}$ are from Equations (8.88) and (8.89) respectively. In Equation (8.87), let

$$\begin{aligned} \rho_{\sigma i}^{poly}(t+\delta t) &= \rho_{\sigma i}(t) + \rho_{\sigma i}^{poly1} + \rho_{\sigma i}^{poly2} \\ &= \rho_{\sigma i}(t+\delta t) + \frac{\rho_{\sigma i}^{(eq)} - \rho_{\sigma i}}{\alpha \tau_{poly}} + \frac{\rho_0}{\kappa_0}\frac{\kappa_{\sigma i}^{(eq)} - \kappa_{\sigma i}}{\alpha^2 \tau_{poly}} \quad (10.57) \end{aligned}$$

$$\text{where} \qquad \rho_{\sigma i}^{poly1} = \frac{\rho_{\sigma i}^{(eq)} - \rho_{\sigma i}}{\alpha \tau_{poly}} \quad (10.58)$$

$$\text{and} \qquad \rho_{\sigma i}^{poly2} = \frac{\rho_0}{\kappa_0}\frac{\kappa_{\sigma i}^{(eq)} - \kappa_{\sigma i}}{\alpha^2 \tau_{poly}}.$$

Similarly, in Equation (8.86), let

$$\begin{aligned} \kappa_{\sigma i}^{poly}(t+\delta t) &= \kappa_{\sigma i}(t) + \kappa_{\sigma i}^{poly1} + \kappa_{\sigma i}^{poly2} \\ &= \kappa_{\sigma i}(t+\delta t) + \frac{\kappa_{\sigma i}^{(eq)} - \kappa_{\sigma i}}{\alpha \tau_{poly}} + \frac{\kappa_0}{\rho_0}\frac{\rho_{\sigma i}^{(eq)} - \rho_{\sigma i}}{\tau_{poly}} \quad (10.59) \end{aligned}$$

$$\text{where} \qquad \kappa_{\sigma i}^{poly1} = \frac{\kappa_{\sigma i}^{(eq)} - \kappa_{\sigma i}}{\alpha \tau_{poly}}$$

$$\text{and} \qquad \kappa_{\sigma i}^{poly2} = \frac{\kappa_0}{\rho_0}\frac{\rho_{\sigma i}^{(eq)} - \rho_{\sigma i}}{\tau_{poly}}. \quad (10.60)$$

Equation (8.87) identifies the component of $\rho_{\sigma i}^{poly}$ due to recoupling as $\rho_{\sigma i}^{poly2}$. Consequently,

$$\begin{aligned}
\rho_{\sigma i}^{poly2}\dot{R}'_{rms} &= \frac{\rho_0}{\kappa_0}\frac{\kappa_{\sigma i}^{(eq)}-\kappa_{\sigma i}}{\alpha^2\tau_{poly}}\dot{R}'_{rms} = \frac{1}{2}\frac{2\rho_0}{\kappa_0}\frac{\kappa_{\sigma i}^{(eq)}-\kappa_{\sigma i}}{\alpha^2\tau_{poly}}\dot{R}'_{rms} \\
&= \frac{1}{2\omega^2}\frac{\kappa_{\sigma i}^{(eq)}-\kappa_{\sigma i}}{\alpha^2\tau_{poly}}\dot{R}'_{rms}. \qquad (10.61) \\
\Longleftrightarrow\ \rho_{\sigma i}^{poly2}\dot{R}_{rms} &= \frac{1}{2\omega^2}\frac{\kappa_{\sigma i}^{(eq)}-\kappa_{\sigma i}}{\alpha^2\tau_{poly}}\dot{R}_{rms}. \qquad (10.62)
\end{aligned}$$

It remains to determine the form of $\int_t^{t'}\kappa_{\sigma i}^{poly1}R_{rms}d\tau$ and to show that

$$2\rho_{\sigma i}^{poly2}\frac{\dot{R}'_{rms}}{2}+\int_t^{t'}\kappa_{\sigma i}^{poly1}R_{rms}d\tau = 0.$$

First, the contribution of κ to the recoupling of $\dot{\mathbf{R}}_{D\sigma i}$ to $\mathbf{R}_{S\sigma i}$ is given by the last two terms in (10.59). The change in the first of the terms in (10.59) is $\kappa_{\sigma i}^{poly1}R_{rms}$. The change in $\kappa_{\sigma i}^{poly1}R_{rms}$ from time t to t' when recoupling occurs is given by the integral of $\kappa_{\sigma i}^{poly1}$ with respect to time. Thus

$$\begin{aligned}
\int_t^{t'}\kappa_{\sigma i}^{poly1}R_{rms}d\tau &= \int_t^{t'}\frac{\kappa_{\sigma i}^{(eq)}-\kappa_{\sigma i}}{\alpha\tau_{poly}}R_{rms}d\tau = -\frac{\alpha}{\omega}\int_t^{t'}\frac{\kappa_{\sigma i}^{(eq)}-\kappa_{\sigma i}}{\alpha\tau_{poly}}\dot{R}'_{rms}d\tau \\
&= -\frac{1}{\omega}\dot{R}_{rms}\int_t^{t'}\frac{\kappa_{\sigma i}^{(eq)}-\kappa_{\sigma i}}{\alpha\tau_{poly}}d\tau \\
&= -\frac{1}{\omega}\dot{R}'_{rms}\int_t^{t'}\frac{\kappa_{\sigma i}^{(eq)}-\kappa_{\sigma i}}{\tau_{poly}}d\tau. \qquad (10.63)
\end{aligned}$$

Let the arbitrary reference $t'\to\infty$ because $t'=\infty$ is defined by $\boldsymbol{R}_\Delta=\mathbf{0}$ permanently in the future. Then

$$\begin{aligned}
-2\int_t^{\infty}\kappa_0 R_{\Delta i}d\tau &= -2\int_t^{\infty}\kappa_0\frac{R_{\Delta i}}{\dot{R}_{\Delta i}}dR_{\Delta i} = -\kappa_0\frac{R^2}{\dot{R}}\Big]_{R_{\Delta i}}^{0} \\
&= \frac{\alpha}{\omega}\kappa_0 R\Big]_{R_{\Delta i}}^{0} = -\frac{\alpha\kappa_0}{\omega}R_{\Delta i} \\
\Longleftrightarrow -2\int\kappa_{\sigma i}R_{rms}dt &= -\frac{\alpha\kappa_{\sigma i}}{\omega}R_{rms}.
\end{aligned}$$

Consequently

$$\int_t^\infty \kappa_{\sigma i} d\tau = \frac{1}{2}\frac{\alpha}{\omega}\kappa_{\sigma i}. \tag{10.64}$$

Substituting Equation (10.64) into Equation (10.63) and recognising (10.62),

$$\begin{aligned} \int_t^\infty \kappa_{\sigma i}^{poly1} R_{rms} d\tau &= -\frac{\alpha}{2\omega^2}\frac{\kappa_{\sigma i}^{(eq)} - \kappa_{\sigma i}}{\tau_{poly}}\dot{R}'_{rms} = -\alpha^2 \rho_{\sigma i}^{poly2}\dot{R}'_{rms} \\ \iff \quad 0 &= \int_t^\infty \kappa_{\sigma i}^{poly1} R_{rms} d\tau + \alpha^2 \rho_{\sigma i}^{poly2}\dot{R}'_{rms} \qquad \forall\, \sigma, i. \end{aligned} \tag{10.65}$$

Similarly, when considering the contribution of the second term in (10.57) to polymer recoupling (which is (10.58)),

$$\rho_{\sigma i}^{poly1}\dot{R}'_{rms} = \frac{\rho_{\sigma i}^{(eq)} - \rho_{\sigma i}}{\tau_{poly}}\dot{R}'_{rms} = -\omega\frac{\rho_{\sigma i}^{(eq)} - \rho_{\sigma i}}{\alpha\tau_{poly}}R_{rms}. \tag{10.66}$$

Next the contribution of the second term in Equation (10.59) is considered. From Equation (10.60) (with appropriate substitution of $\omega = \kappa/(2\rho)$ from Equation (8.43))

$$\begin{aligned} \kappa_{\sigma i}^{poly2} R_{rms} &= \frac{\kappa_0}{\rho_0}\frac{\rho_{\sigma i}^{(eq)} - \rho_{\sigma i}}{\tau_{poly}}R_{rms} = 2\frac{\kappa_0}{2\rho_0}\frac{\rho_{\sigma i}^{(eq)} - \rho_{\sigma i}}{\tau_{poly}}R_{rms} \\ &= 2\omega^2\frac{\rho_{\sigma i}^{(eq)} - \rho_{\sigma i}}{\tau_{poly}}R_{rms}. \end{aligned} \tag{10.67}$$

Integrating Equation (10.67) with respect to time, from current time to reference time $t = \infty$, and substituting Equation (10.66); one obtains (by recognising (10.58)) that

$$\begin{aligned} \int_t^\infty \kappa_{\sigma i}^{poly2} R_{rms} d\tau &= \int_t^\infty 2\omega^2\frac{\rho_{\sigma i}^{(eq)} - \rho_{\sigma i}}{\tau_{poly}}R_{rms} d\tau = \alpha\omega\frac{\rho_{\sigma i}^{(eq)} - \rho_{\sigma i}}{\tau_{poly}}R_{rms} \\ &= -\alpha^2\rho_{\sigma i}^{poly1}\dot{R}'_{rms} \\ \iff 0 &= \int_t^\infty \kappa_{\sigma i}^{poly2} R_{rms} d\tau + \alpha^2\rho_{\sigma i}^{poly1}\dot{R}'_{rms} \qquad \forall\, \sigma, i. \end{aligned} \tag{10.68}$$

Combining Equations (10.65) and (10.68),

$$\begin{aligned} 0 &= \int_t^\infty \kappa_{\sigma i}^{poly2} R_{rms} d\tau + \alpha^2 \rho_{\sigma i}^{poly1} \dot{R}'_{rms} + \int_t^\infty \kappa_{\sigma i}^{poly1} R_{rms} d\tau + \alpha^2 \rho_{\sigma i}^{poly2} \dot{R}'_{rms} \\ &= \int_t^\infty \kappa_{\sigma i}^{poly} R_{rms} d\tau + \alpha^2 \rho_{\sigma i}^{poly} \dot{R}'_{rms} \qquad \forall\, \sigma, i. \end{aligned} \tag{10.69}$$

Thus the omission of Equations (8.86) and (8.87) in Section 10.1 and Section 10.2 is only justified for $\alpha = 1$ which (given the definition of α from Section 8.4.3 Equation (8.47)) corresponds to critical damping. Thus, when constructing the numerical model, only the case of critical damping can be used. However, in Chapter 13 non-critically damped polymer recoupling results will be presented to determine the effect.

10.4 The first order LBM stress tensor

Lastly, taking the reference time as $t' \to \infty$ effectively defines the stress tensor in the LBM as

$$-\mathbf{T}|_t^\infty := \frac{1}{2}\mathbf{P}'_S + 2\mathbf{P}'_D - 4\mu\dot{\mathbf{D}}(t) - 4G \lim_{t'\to\infty} \int_t^{t'} \mathbf{D}(\tau) d\tau. \tag{10.70}$$

Let the first order approximation to the static stress tensor (given incompressibility) be

$$\mathbf{T}_S^{(1)}|_t^\infty = 4G \int_t^\infty \mathbf{D}(\tau) d\tau \tag{10.71}$$

then the change in the first order approximation to the static stress tensor is

$$\begin{aligned} \Delta\mathbf{T}_S^{(1)}(\tau)|_0^t &= \mathbf{T}_S^{(1)}|_t^\infty - \mathbf{T}_S^{(1)}|_0^\infty = (4G \int_t^\infty \mathbf{D}(\tau) d\tau) - (4G \int_0^\infty \mathbf{D}(\tau) d\tau) \\ &= -4G \int_0^\infty \mathbf{D}(\tau) d\tau - 4G \int_\infty^t \mathbf{D}(\tau) d\tau \\ &= -4G \int_0^t \mathbf{D}(\tau) d\tau. \end{aligned} \tag{10.72}$$

10.5 Relationship between 2D and 3D models

It is noted that although Equations (10.35) and (10.54) provide the correct form (Navier-Stokes type equation) for the equation of polymer flow, the additional factor 2/3 is present. Buick [14] documents the following relations for the tensor sums in arbitrary dimension D with constants c and b for gases

$$\begin{aligned}
\sum_{\sigma i} \epsilon_{\sigma i\alpha} &= 0 \\
\sum_{\sigma i} \epsilon_{\sigma i\alpha}\epsilon_{\sigma i\beta} &= \frac{c^2 b}{D}\delta_{\alpha\beta} \\
\sum_{\sigma i} \epsilon_{\sigma i\alpha}\epsilon_{\sigma i\beta}\epsilon_{\sigma i\gamma} &= 0 \\
\sum_{\sigma i} \epsilon_{\sigma i\alpha}\epsilon_{\sigma i\beta}\epsilon_{\sigma i\gamma}\epsilon_{\sigma i\delta} &= \frac{c^2 b}{D(D+2)}\left(\delta_{\alpha\beta}\delta_{\gamma\delta} + \delta_{\alpha\gamma}\delta_{\beta\delta} + \delta_{\alpha\gamma}\delta_{\beta\delta}\right).
\end{aligned}$$

Thus the tensor sums (10.6) and (10.39) are inversely proportional to dimension as previously noted. He further derives the pressure term and shows it to be

$$\frac{\rho(1-d_0)}{D}c^2\delta_{\alpha\beta}$$

where ρ and d_0 are constants. Thus for gases, the ratio of the 2D pressure term to the 3D pressure term would be 3/2. Thus to determine the 3D pressure term from the 2D term one would have to multiply by 2/3.

The origin of the 2/3 factor has not been determined explicitly for polymers. This formulation has, however, been constructed on a two dimensional lattice where the theory for this work (prior to this chapter) is in three dimensions. Applying the more general formulation for the tensor sums (which include the dimension D as a variable) as provided by Buick [14] should predict the factor 2/3.

The alternate interpretation, is that $\frac{2}{3}R^2_{rms}$ is the sum of the projections of the 3D molecules of (3.44) onto a 2D surface. Similarly, the projection onto a 1D problem would require the factor 1/3.

10.6 The application of non-critical damping in polymer recoupling

In Section 8.4.3 the LBM constructed for chain length, as determined in Section 8.2, was coupled to the LBM for chain stretch rate constructed in Section 8.3. This recoupling was achieved by idealising the interaction between chain length and chain stretch rate as an example of a Kelvin-Voigt spring-dashpot model of viscoelasticity as depicted in Figure 7.4. It has already been emphasized that one need not necessarily have selected this model (see Section 8.5).

It is also noted that Section 8.4.3 uses both critical damping where $\omega^2 = \kappa/(2\rho)$ from Equation (8.43) and non-critical, non-oscillatory damping where $\omega' = \omega/\alpha$ from Equation (8.47). Section 10.3, Equation (10.69) shows that the Navier-Stokes type behaviour predicted by the analytical theory of Chapter 6 is only reproduced by the discrete theory of Chapters 8 and 10 when $\alpha = 1$ which corresponds to critical damping. Section 10.1.3, Equations (10.37) and (10.38) however provide a means of applying damping indirectly by scaling the critically damped result. The net effect being that the critically damped time increment δ_t' is related to the non-critically damped time increment δ_t by $\delta_t = \alpha^2\delta_t'$ and the critically damped chain-stretch rate $\dot{\mathbf{R}}_D$ is related to the non-critically damped chain-stretch rate $\dot{\mathbf{R}}_D'$ by $\dot{\mathbf{R}}_D' = \dot{\mathbf{R}}_D/\alpha$.

Thus one may conclude that two means of applying non-critical, non-oscillatory damping have been introduced. The first is the direct application of non-critical damping to chain-length and chain-stretch-rate recoupling (as described in Section 8.4.3) and the second is the indirect application of non-critical damping to polymer recoupling (as described in Section 10.1.3). The latter effectively uses the critically damped solution to Equation (6.110) and the factor α as a scaling factor to relate the critically-damped and non-critically damped solutions.

Chapter 11

Polymer initial and boundary conditions

The numerical method of Chapter 8 will be used to model the stress relaxation experiment of Chapter 12. The stress relaxation experiment can be divided into two stages as depicted in Figure 11.1 – ramping and isometry. Since the LBM cannot be used to model moving boundaries, only the iso-

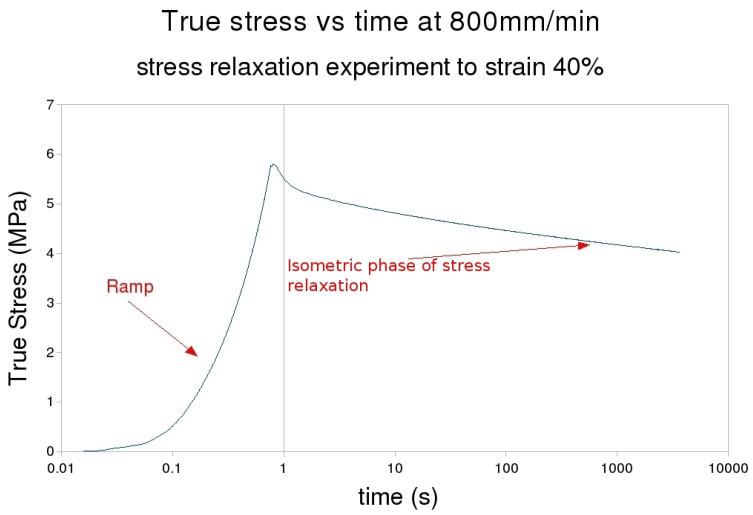

Figure 11.1: The stress relaxation experiment

metric stage will be modelled. Thus the initial state (for the purposes of the numerical model) will be defined as the end of ramping or the beginning of isometry.

The theory predicts that two variants of viscoelasticity exist. The first is designated material viscoelasticity – due to the stretch and stretch rate of

the molecules as discussed in Section 7.2. The second variant is specimen viscoelasticity – due to the distribution of stretch and stretch rate throughout the specimen (see Section 7.3). As a consequence, the initial (end of ramping) distribution of stretch and stretch rate is fundamentally important to the numerical model. This chapter will present the initial conditions (IC) to be used for modelling the isometric phase of the stress relaxation experiment of Chapter 13.

The boundary conditions (BCs) which are known to be problematic (see Section 2.4) for the LBM will also be presented. The application of these BCs will be considerably different from the traditional approaches. Recognising that the length of a specimen at any time is the integral of the stretch with respect to position at that time over the specimen (see Equation (7.24)), the boundary conditions adapt to ensure fixed length as required by the stress relaxation experiment. These are designated adaptive BCs. The BCs that are not constructed to conserve specimen length will be designated non-adaptive BCs. The non-adaptive BCs can be divided into two types: symmetry, and fixed BCs. The symmetry BC is designed to impose symmetry conditions. The fixed BC is analagous to the traditional method of applying BCs – specifies fixed material stretches at the boundaries that equal the known specimen stretch.

The details of the stress relaxation experiment will be presented first. It should be recognised that the numerical method has separated the equation of polymer flow (6.98) into a stretch component (6.97) and a stretch rate component (6.93) – each resembling a Navier-Stokes (N-S) type equation. Approximate analytical solutions to (6.93) and (6.97) will be determined independently by providing solutions to the diffusion equation (6.111) for stretch and stretch rate (in Section 6.6 it was shown that, in a Lagrangian coordinate system, the 1D N-S type equation reduces to a diffusion equation). These approximate analytical solutions will provide the IC for the isometric phase of the relaxation experiment.

The stretch IC will be determined subject to a known specimen stress and specimen stretch. The stretch rate IC will be determined based on specimen stretch rate and stress rate. It will be shown that the above provide a system of 4 equations in 5 unknowns. The fifth equation will be provided by the geometry (or predicted profile) of the stretch distribution.

The approximate solutions to the polymer flow equation are deemed acceptable because a physically appropriate solution is assumed sufficient as an IC. The resultant analytical solutions will be solved for $G > 0$ and $\mu < 0$. The justification for the selection of these values of G and μ will be apparent in Chapter 12 where their values are determined based on experimental data.

The remainder of the chapter considers four types of BCs. The symmetry BC will be presented first. This will be common to the remaining BCs to be presented – adaptive and fixed. An adaptive BC in the direction parallel to the direction of the applied force will then be presented and the adaptive BCs perpendicular to the applied force next. The final boundary condition will be that of fixed stretch at the edges.

11.1 The stress relaxation experiment

The stress relaxation experiment consists of a dumbell-shaped specimen held in position by two grips. One grip is stationary and the second is mobile, as depicted in Figure 11.2. The specimen is stretched and then held at fixed (specimen) stretch. The BCs are constructed to ensure fixed specimen stretch. The stress relaxation experiment can be divided into two phases

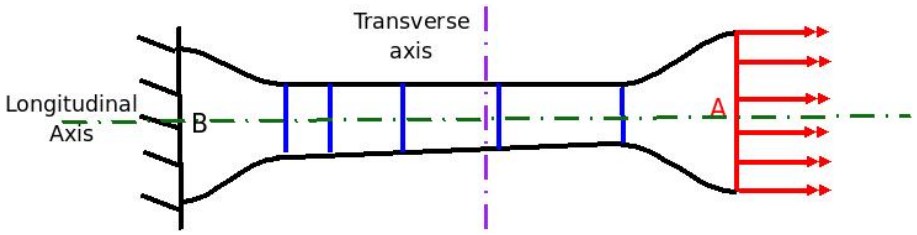

Figure 11.2: The tensile testing rig has a fixed grip and a mobile grip. The mobile grip is attached to edge A of the dumbell specimen and the applied force is depicted in red. The fixed grip is at the apposing end B in black. The blue lines are intended to depict the non-uniform distribution of stretch. At material maximum entropy (either strained or unstrained) the blue lines are intended to be equidistant. During the isometric phase of stress relaxation, the blue lines are not necessarily equidistant except when the specimen is in steady state and the material at maximum entropy.

– ramping and isometric phase – as depicted in Figure 11.1. The ramping phase corresponds to the displacement of the mobile grip and the consequent stretching of the specimen. The subsequent isometric phase corresponds to

the absence of change in length of the specimen.

Given the known limitations of the LBM with respect to boundary conditions, it is to be expected that the isometric phase is suited to the LBM but that the moving boundary or ramping phase will not be possible. Thus the effect of the ramping has to be estimated and imposed as the IC at time $t = 0$ of the isometric phase of the stress relaxation experiment.

11.1.1 Solution of the diffusion equation

Ideally an analytical solution to (6.98) should be used to determine the IC. Failing this, analytical solutions to (6.93) and (6.97) should suffice. Equations (6.93) and (6.97) are vector equations but, in one direction in a Lagrangian coordinate system, they reduce to the diffusion equation. The two Lagrangian linear partial differential equations (PDE) to be solved are thus

$$\frac{\partial \mathrm{R}_{\mu x}}{\partial t} = G\frac{\partial^2 \mathrm{R}_{\mu x}}{\partial x^2} + \Pi_R \quad \Longleftrightarrow \quad \frac{\partial \mathrm{R}_{S\mu x}}{\partial t} = G\frac{\partial^2 \mathrm{R}_{S\mu x}}{\partial x^2} + \Pi_{R_S}, \tag{11.1}$$

$$\frac{\partial \dot{\mathrm{R}}_{\mu x}}{\partial t} = \mu\frac{\partial^2 \dot{\mathrm{R}}_{\mu x}}{\partial x^2} + \Pi_{\dot{R}} \quad \Longleftrightarrow \quad \frac{\partial \dot{\mathrm{R}}_{D\mu x}}{\partial t} = \mu\frac{\partial^2 \dot{\mathrm{R}}_{D\mu x}}{\partial x^2} + \Pi_{\dot{R}_D} \tag{11.2}$$

with the macroscopic variables reflecting that these are proxy measures for stretch and stretch rate.

The stretch constraints on the stretch diffusion equation

The stretch component (11.1) will be considered first. The IC is the solution to (11.1) at the end of the ramping phase of the stress relaxation experiment. Eventually the PDE will only be evaluated at $t = 0$, thereby reducing to an ordinary differential equation (ODE) in x subject to the constraint that the mean stretch corresponds to the specimen stretch. This is simply a statement of the definition of specimen stretch (7.24). The theory predicts a non-uniform distribution of stretch. One of two scenarios are anticipated and depicted in Figure 11.3

It is recognised that, at $t = 0$ and throughout isometry, the specimen length is constant and equals the specimen stretch multiplied by the unstrained specimen length. Restated, on the domain $x \in [0, \mathrm{L}_0]$ (where L_0 is

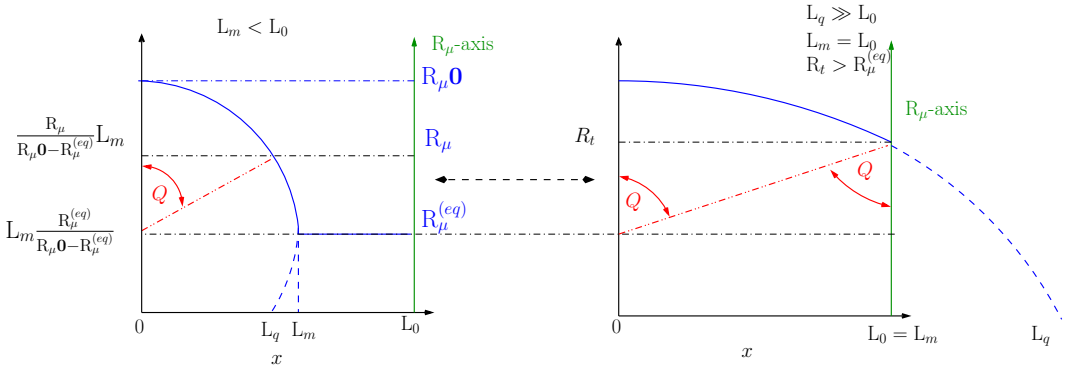

Figure 11.3: EXPECTED INITIAL MOLECULAR STRETCH DISTRIBUTIONS. $\mathrm{R}_\mu^{(eq)}$ IS THE MEAN MOLECULAR STRETCH AT EQUILIBRIUM AND $\mathrm{R}_\mu\mathbf{0}$ IS THE MEAN MOLECULAR STRETCH AT $x = 0$ AND $t = 0$. L_0 IS HALF THE UNDEFORMED LENGTH, L_m IS THE VALUE OF x AT WHICH THE MEAN MOLECULAR STRETCH AT $t = 0$ IS THE EQUILIBRIUM MOLECULAR STRETCH AND L_q IS THE PREDICTED x-INTERCEPT FOR THE CURVE.

the undeformed length in the x direction)

$$\int_0^{\mathrm{L}_m} \frac{\mathrm{R}_{\mu x}(x,0)}{\mathrm{R}_\mu^{(eq)}} dx + \mathrm{L}_0 - \mathrm{L}_m = \lambda_{spec}\mathrm{L}_0. \tag{11.3}$$

where λ_{spec} is the specimen stretch in the x-direction, $\mathrm{R}_\mu(x,0)$ molecular stretch at position x at the end of ramping and $\mathrm{R}_\mu^{(eq)}$ is the molecular stretch at equilibrium. The origin of the form of (11.3) is the anticipated discontinuous distribution of $\mathrm{R}_{S\mu x}$ depicted in Figure 11.3 where the two images represent extremes of possible distribution.

Let L_m be the location on the undeformed specimen corresponding to zero strain as depicted in Figure 11.3. Then the constraint (11.3) can further be refined to

$$\mathrm{R}_{S\mu x}(\mathrm{L}_m, 0) = \mathrm{R}_\mu^{(eq)}, \tag{11.4}$$

$$\mathrm{R}_{S\mu x}(0,0) = \mathrm{R}_\mu\mathbf{0}, \tag{11.5}$$

$$\frac{\partial \mathrm{R}_{S\mu x}}{\partial t}(0,0) = 0 \qquad \text{and} \tag{11.6}$$

$$\frac{\partial \mathrm{R}_{S\mu x}}{\partial t}(x,0) = 0 \qquad \forall\, \mathrm{L}_M < x \le \mathrm{L}_0 \tag{11.7}$$

where $\mathrm{R}_\mu\mathbf{0}$ is $\mathrm{R}_{S\mu}(x,t)$ at $x = 0$ and $t = 0$. Thus $0 \le L_m \le L_0$ and (11.3) through (11.7) represent the constraints on the stretch IC PDE (11.1) at $t = 0$ (end of ramping). The solution to the PDE is given by (C-11). At

$t = 0$ the PDE solution (C-11) reduces to (C-10) or (11.8), that is

$$\mathrm{R}_{\mu x}(x,0) = \begin{cases} \left(\mathrm{R}_\mu \mathbf{0} - \mathrm{R}_\mu^{(eq)}\right)\cos(\sqrt{|\eta_R|}x) + \mathrm{R}_\mu^{(eq)} & \forall\ 0 \le x \le \mathrm{L}_m \le \mathrm{L}_0 \\ \mathrm{R}_\mu^{(eq)} & \forall\ \mathrm{L}_m \le x \le \mathrm{L}_0 \end{cases} \tag{11.8}$$

where $\mathrm{R}_\mu\mathbf{0}$, η_R and L_m are to be determined. Furthermore (11.3) is an equation in three unknowns ($\mathrm{L}_m, \mathrm{R}_\mu\mathbf{0}$ and η_R) and, as described in Appendix C-1 and Equation (C-13), reduces to

$$(\lambda_{spec} - 1)\mathrm{R}_\mu^{(eq)}\mathrm{L}_0 = \frac{\mathrm{R}_\mu\mathbf{0} - \mathrm{R}_\mu^{(eq)}}{\sqrt{\eta_R}}\sin(\sqrt{\eta_R}\mathrm{L}_m). \tag{11.9}$$

At least two additional equations are required. The first is provided by the geometry (of the stretch profile) for Figure 11.3, that is,

$$\sqrt{\eta_R}\mathrm{L}_m = \frac{\pi}{2} \qquad \Longleftrightarrow \qquad \eta_R = \left(\frac{\pi}{2\mathrm{L}_m}\right)^2 \tag{11.10}$$

which reduces Equation (11.9), as described by (C-14), to

$$(\lambda_{spec} - 1)\mathrm{R}_\mu^{(eq)}\mathrm{L}_0 = 2\mathrm{L}_m\frac{\mathrm{R}_\mu\mathbf{0} - \mathrm{R}_\mu^{(eq)}}{\pi}\sin\frac{\pi}{2} = 2\mathrm{L}_m\frac{\mathrm{R}_\mu\mathbf{0} - \mathrm{R}_\mu^{(eq)}}{\pi}. \tag{11.11}$$

The stretch rate constraint on the stretch rate diffusion equation

The constraints applied to $\dot{\mathrm{R}}_{D\mu x}(x,0)$ to solve the stretch rate diffusion equation (11.2) are apparent from the discontinuous stretch distribution depicted in Figure 11.3 and are

$$\dot{\mathrm{R}}_{D\mu x}(0,0) = 0 \tag{11.12}$$

$$\dot{\mathrm{R}}_{D\mu x}(x,0) = 0 \qquad \forall\ \mathrm{L}_m < x \le \mathrm{L}_0. \tag{11.13}$$

An alternate physical interpretation is that the molecules at the application point are fully stretched and consequently at $x = 0$ the stretch rate is zero. Thus the constraint (11.12) is established. The stretch rate is maximum at the 'wave front' ($x = \mathrm{L}_M$) and zero for $\mathrm{L}_m < x \le \mathrm{L}_0$. The specimen stretch rate is calculated from Equation (7.25) and is

$$\int_0^{\mathrm{L}_m} \dot{\lambda}(x,0)dx = \int_0^{\mathrm{L}_m} \frac{\dot{\mathrm{R}}_{D\mu x}(x,0)}{\mathrm{R}_\mu^{(eq)}}dx = \dot{\lambda}_{spec}\mathrm{L}_0. \tag{11.14}$$

Let $\dot{\mathrm{L}}$ be the rate of change of the specimen length; then

$$\dot{\lambda}_{spec}\mathrm{L}_0 = \frac{\dot{\mathrm{L}}}{\mathrm{L}_0}\mathrm{L}_0 = \dot{\mathrm{L}}$$

which can be substituted into (11.14). The solution to the stretch rate diffusion equation (11.2) is provided in Appendix C-2 as (C-23). Evaluating PDE (C-23) at $t = 0$ reduces the solution to the ODE (see (C-22)) to

$$\dot{\mathrm{R}}_{\mu x}(x,0) = \begin{cases} c_4 \sinh(\sqrt{|\eta_{\dot{R}}|}x) & \forall\ 0 \le x \le \mathrm{L}_m \le \mathrm{L}_0, \\ 0 & \forall\ \mathrm{L}_m \le x \le \mathrm{L}_0. \end{cases} \tag{11.15}$$

Substitution of (11.15) into (11.14), as described in Appendix C-2 and by Equation (C-25), yields

$$\dot{\mathrm{L}} = \frac{1}{\mathrm{R}_\mu^{(eq)}} \int_0^{\mathrm{L}_m} c_4 \sinh\sqrt{|\eta_{\dot{R}}|}x dx = \frac{c_4}{\sqrt{|\eta_{\dot{R}}|}\mathrm{R}_\mu^{(eq)}} \left(\cosh\left(\sqrt{|\eta_{\dot{R}}|\mathrm{L}_m}\right) - 1 \right), \tag{11.16}$$

an equation in three unknowns, and (11.16) is independent of (11.9). Thus Equations (11.9) and (11.16) form a system of two equations in five unknowns $(c_4, \eta_{\dot{R}}, \eta_R, \mathrm{L}_m, \mathrm{R}_\mu\mathbf{0})$. Two of the remaining equations will be determined from the principal stress and stress rate constraints. The third equation was derived from the geometry of Figure 11.3 and is given by Equation (11.10).

Kinetic and geometric constraints

The apparent specimen principal stress as determined experimentally by the tensile testing instrument at time $t = 0$ is known. The apparent principal stress based on the distribution of stretch and stretch rate should equal the experimentally determined value and can be calculated as (see (C-30))

$$\begin{aligned} {}^{\langle app \rangle}\sigma_{sp1}(0) \;=\; & -\frac{1}{\mathrm{L}_0}\int_0^{\mathrm{L}_0} p'_{dxx} - p'_{dyy} dx - \frac{1}{\mathrm{L}_0}\int_0^{\mathrm{L}_0} p'_{sxx} - p'_{syy} dx \\ & -\frac{\mu}{2\mathrm{L}_0}\int_0^{\mathrm{L}_0} 2\frac{\partial \dot{\mathrm{R}}_{D\mu x}}{\partial x} dx + \frac{4G}{\omega \mathrm{L}_0}\int_0^{\mathrm{L}_0} \frac{\partial \mathrm{R}_{S\mu x}}{\partial x} dx \end{aligned} \tag{11.17}$$

as described in Appendix C-3. Appendix C-3 provides the apparent principal stress rate which, although not provided directly by the tensile test, can be

calculated from the experimental results. Thus the second equation is

$$
\begin{aligned}
{}^{\langle app \rangle}\dot{\sigma}_{sp1}(0) &= \frac{2\omega}{\mathrm{L}_0}\frac{\partial}{\partial t}\int_0^{\mathrm{L}_0} p_{dxx} - p_{dyy}dx + \frac{2\omega}{\mathrm{L}_0}\frac{\partial}{\partial t}\int_0^{\mathrm{L}_0} p_{sxx} - p_{syy}dx \\
&\quad + \frac{\omega\mu}{\mathrm{L}_0}\dot{\mathrm{R}}_{D\mu}(x)|_0^{\mathrm{L}_m} - \frac{4G}{\mathrm{L}_0}\mathrm{R}_{S\mu}(x)|_0^{\mathrm{L}_m}. \qquad (11.18)
\end{aligned}
$$

Thus (11.9), (11.16), (11.17), (11.18) and (11.10) form a system of five equations in five unknowns. It will prove difficult to solve for all five unknowns because the equations are non-linear and some of the functions are periodic. A special case will be used in Chapter 13 where initial stretch rate is equal to zero, all the apparent principal stress is due to stretch and $\mathrm{L}_m = \mathrm{L}_0$. This special proves to set the appropriate conditions for the experiment being modelled and will be referred to as the curved stretch, zero stretch rate IC – the proof that the above IC is appropriate is provided in Appendix C. This initial special case (curved stretch, zero stretch rate) will be used in the numerical model which is constructed based on the equation of polymer flow (6.98). The results of the numerical model based on curved stretch, zero stretch rate will be presented in Section 13.6.

11.1.2 Modelling symmetry

In Figure 11.2 the longitudinal axis is depicted in green along the direction of the tensile load. It is apparent that this is an axis of symmetry. A transverse axis is depicted in purple. The transverse axis is not an axis of symmetry due to the non-uniform and asymmetric distribution of stretch as depicted by the blue lines in Figure 11.2. There would, however, be an advantage to treating the short axis as an axis of symmetry as, effectively, it would reduce the domain to be modelled by a factor of four. Macroscopically there will be no effect – the effect is mesoscopic. Thus, despite not being physically correct, both axes of symmetry are used. The symmetry boundary condition will be applied to two surfaces as depicted in Figure 11.4. The remaining two surfaces will either have adaptive or fixed BCs applied. When applying the adaptive BC option, one surface has the adaptive BC parallel to the applied force whilst the remaining surface will have the adaptive BC perpendicular to the applied force as depicted in Figure 11.4. The alternative to the adaptive BC is the fixed BC where the stretches applied at the edges correspond to

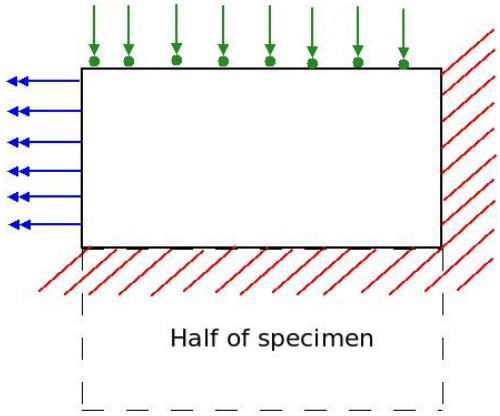

Figure 11.4: THE RED HATCHED AREA REPRESENTS THE SYMMETRY CONDITION. THE BLUE ARROWS INDICATE THE ADAPTIVE BOUNDARY CONDITION PARALLEL TO THE APPLIED FORCE AND THE GREEN ARROWS REPRESENT THE ADAPTIVE BOUNDARY CONDITIONS PERPENDICULAR TO THE APPLIED FORCE

the specimen stretch – analogous to the conventional way of applying BCs.

11.2 Symmetry boundary condition

Potential existing solutions are the bounceback boundary condition or the non-slip boundary condition already used in the fluid LBM and depicted in Figure 11.5. However, these BCs were developed to ensure zero velocity at

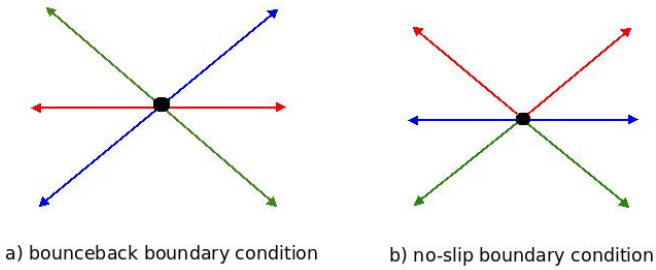

Figure 11.5: (a) THE BOUNCEBACK BOUNDARY CONDITION REVERSES THE DIRECTION OF THE VECTOR. (b)NON-SLIP BOUNDARY CONDITION REFLECTS IN THE PLANE OF THE INTERFACE

walls – thereby remaining physically consistent for fluids. The equivalent for the polymer LBM would be zero strain and zero strain rate at the walls – but these are physically inconsistent. Thus these BCs are rejected. The obvious alternative is simple reflection of the adjacent node. This also produces physically inconsistent results – shown here using proof by contradiction. Consider a perfectly uniform distribution at the boundary as depicted in Figure 11.6.

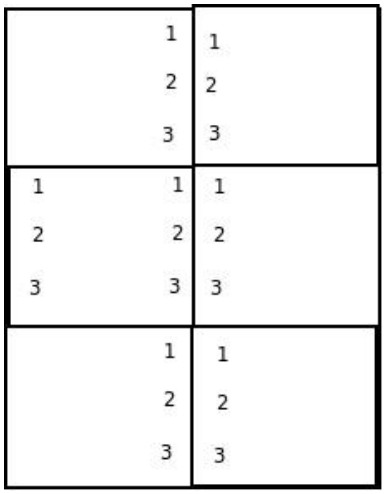

Figure 11.6: Each number represents a magnitude of a vector

Under these conditions, the BC reduces to the non-slip BC which is known to be physically inconsistent. Thus simple reflection is physically inconsistent.

Duplication of the adjacent reference node will be used at the wall. This

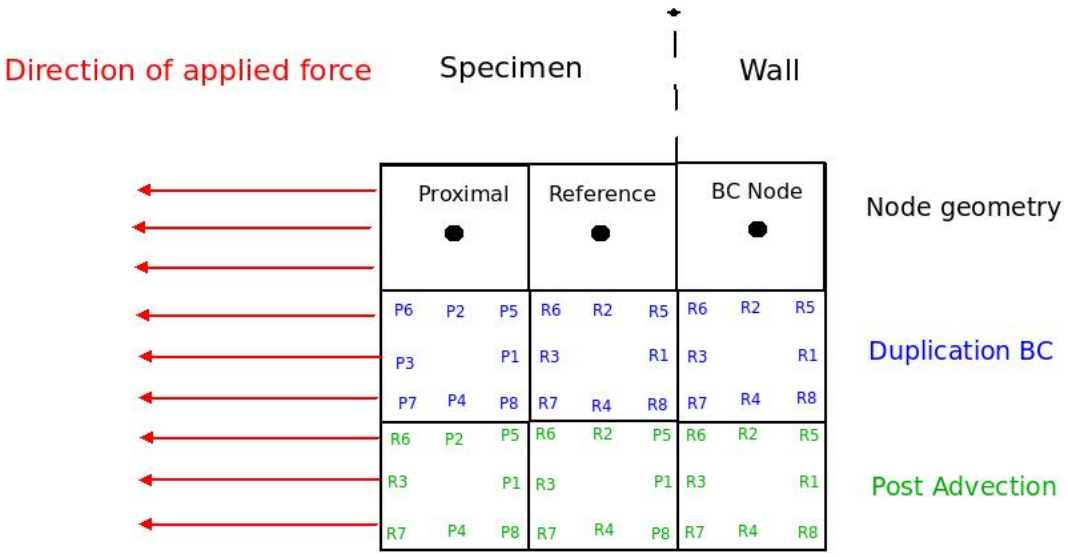

Figure 11.7: The advection, as depicted, resembles translation to the adjacent node. This is unintentional and should resemble advection as for fluids.

does not produce the non-physical zero-stretch and zero-stretch rate result. Only the nodes proximal to the reference nodes (relative to the applied force) can affect the reference nodes. The 'advection' step does not necessarily conserve mass or elasticity but the redistribution can be selected to do so.

The geometry and advection is depicted in Figure 11.7. This duplication BC produces several physically consistent results – only the proximal nodes alter the reference nodes, at steady state the stretches and stretch rates are uniformly distributed through the specimen and, at the symmetry interfaces, stretches and stretch rates are non-zero.

11.3 Non-adaptive boundary condition

Note that Equations (11.1) and (11.2) cannot apply length and velocity BCs directly. These have to be calculated and boundary stretches have to be set such that length and velocity BCs are achieved. These adaptive boundary conditions are presented in Sections 11.4 and 11.5. This section presents non-adaptive BCs which resemble the conventional method of applying BCs more closely. In particular, the non-adaptive BCs are of the form

$$\mathrm{R}_{S\mu x}(x_0, y_0, t) = c_1 \qquad \text{and} \qquad \dot{\mathrm{R}}_{D\mu x}(x_0, y_0, t) = c_2$$

where x_0 and y_0 denote the edges of the specimen and c_1 and c_2 are constants.

Figure 11.4 depicts the adaptive BC with the symmetry BC applied at two edges. The non-symmetric BC uses the maximum entropy functions (8.30) and (8.37) to determine the density and bulk modulus per unit volume distribution at the walls of these non-symmetric BCs. The actual stretch and stretch rates at these walls are determined from the calculated and expected stretches. The alternate boundary condition is that of pure symmetry. In

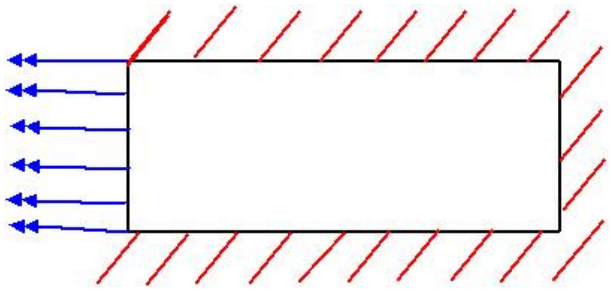

Figure 11.8: The red lines represent the duplication, symmetry condition and the blue arrows represent the fixed specimen stretch.

this scenario, three of the edges will be the symmetry (duplication) boundary condition as presented in Section 11.2. The remaining edge (applied force edge depicted in blue in Figure 11.8) also represents a symmetry BC but

the BC is constant and corresponds to the expected specimen stretch. The symmetry only becomes apparent at steady state. The latter scenario is presented in Figure 11.8.

Note that this represents a section of a very large specimen. The justification lies in the recognition that when the LBM for gases was first formulated, the application of BCs had as yet not been determined. The early researchers compromised by reflecting the results at the edges to avoid BCs [141]. The sample of an infinite specimen scenario, depicted in Figure 11.8, represents an attempt to apply the same compromise as that of the early gas LBM researchers.

11.4 Adaptive boundary condition parallel to applied force

The underlying principle being applied for the adaptive BC is that, for the isometric phase of the stress relaxation experiment, the specimen length remains constant. For this to occur, the specimen stretch must remain constant. Given that specimen stretch is the arithmetic mean of stretch over the specimen length (7.24), the applied stretch at the edges must be selected (updated) to ensure constant specimen stretch.

Equation (9.45) calculates the magnitude of λ_1 at time t. Let a rectangular specimen be discretised into a rectangular lattice consisting of q horizontal RVEs and s vertical RVEs. Without loss of generality, the first row and the first column of these RVEs represent the BC application RVEs. The position of an RVE is designated by coordinate (i, j), its location in a Cartesian coordinate system, where horizontal RVE location $i \in \mathbb{N}_0$ such that $1 \leq i \leq q$ and vertical RVE location $j \in \mathbb{N}_0$ such that $1 \leq j \leq s$.

Consider a BC being applied on the first column of RVEs. Let the total number of RVEs be designated $N_{-0} = qs$. Let the sum of the non-wall RVEs and the BC application RVEs be $N_{-1} = (q)(s-1)$. Let the non-wall RVEs be designated $N_{-2} = (q-1)(s-1)$. Then the actual (or calculated from

numerical model) stretch is due to the non-wall RVEs such that

$$\begin{aligned} {}_{(actual)}\lambda_{spx}^{(real)}(t) &= \frac{1}{N_{-2}}\sum_{i=2}^{q}\sum_{j=2}^{s}\lambda_x^{\{ij\},(real)}(t) \\ = \sqrt{3}\ {}_{(actual)}\lambda_{spx}^{(lat)}(t) &= \frac{\sqrt{3}}{N_{-2}}\sum_{i=2}^{q}\sum_{j=2}^{s}\lambda_x^{\{ij\},(lat)}(t). \end{aligned} \tag{11.19}$$

From (7.24) and given the expected (or predicted from analytical theory) stretch $\left({}_{(expected)}\lambda_{spx}\right)$ (for both real and lattice) in the x-direction is calculated over the sum of non-wall RVEs and BC application RVEs,

$$\begin{aligned} (s-1)\lambda_x^{\{ij\}}(t) &= N_{-1\ (expected)}\lambda_{spx}(t) - \sum_{i=2}^{q}\sum_{j=2}^{s}\lambda_x^{\{ij\}}(t) \\ &= N_{-1\ (expected)}\lambda_{spx}(t) - (N_{-2})\ {}_{(actual)}\lambda_x^{\{ij\}}(t) \end{aligned} \tag{11.20}$$

where $\lambda_x^{\{1j\}}$ are the horizontal material stretches at the application points. Also, for the isometric phase of the stress relaxation experiment, ${}_{(expected)}\lambda_{spx}(t)$ is a constant. Given the incompressibility condition, for the plane strain situation

$$\begin{aligned} \lambda_x^{\{1j\},(real)}\lambda_y^{\{1j\},(real)} = \pm 1 \quad &\Longleftrightarrow \quad \lambda_x^{\{1j\},(real)} = \pm\frac{1}{\lambda_y^{\{1j\},(real)}} \\ \lambda_x^{\{1j\},(lat)}\lambda_y^{\{1j\},(lat)} = \pm\frac{1}{3} \quad &\Longleftrightarrow \quad \lambda_x^{\{1j\},(lat)} = \pm\frac{1}{3\lambda_y^{\{1j\},(lat)}} \end{aligned} \tag{11.21}$$

where the product is positive or negative depending on the initial representative molecule orientation. Similarly the specimen stretch rate is 0 and therefore for both real and lattice components,

$$\begin{aligned} {}_{(expected)}\dot{\lambda}_{spx}(t) &= 0 = \frac{1}{N_{-1}}\sum_{i=1}^{q}\sum_{j=2}^{s}\dot{\lambda}_x^{\{ij\}}(t) \\ \text{and} \qquad {}_{(actual)}\dot{\lambda}_{spx}(t) &= \frac{1}{N_{-2}}\sum_{i=2}^{q}\sum_{j=2}^{s}\dot{\lambda}_x^{\{ij\}}(t). \end{aligned}$$

From the definition of the specimen stretch rate,

$$\begin{aligned} (s-1)\dot{\lambda}_x^{\{1j\}}(t) &= N_{-1\ (expected)}\dot{\lambda}_{spx}(t) - \sum_{i=2}^{q}\sum_{j=2}^{s}\dot{\lambda}_x^{\{ij\}}(t) \\ &= -(N_{-2})\ {}_{(actual)}\dot{\lambda}_x^{\{ij\}}(t). \end{aligned} \tag{11.22}$$

Again given incompressibility, differentiating Equation (11.21), the relation

$$\lambda_x^{\{1j\}}\dot{\lambda}_y^{\{1j\}} + \dot{\lambda}_x^{\{1j\}}\lambda_y^{\{1j\}} = 0 \qquad \Longleftrightarrow \qquad -\frac{\lambda_x^{\{1j\}}}{\lambda_y^{\{1j\}}} = \frac{\dot{\lambda}_x^{\{1j\}}}{\dot{\lambda}_y^{\{1j\}}} \tag{11.23}$$

is obtained for both real and lattice components. Alternatively, from incompressibility and for uniaxial tension with two free surfaces,

$$\begin{aligned} \lambda_x^{\{1j\},(real)}\lambda_y^{\{1j\},(real)2} = \pm 1 \quad &\Longleftrightarrow \quad \lambda_x^{\{1j\},(real)} = \pm\frac{1}{\lambda_y^{\{1j\},(real)2}} \\ \lambda_x^{\{1j\},(lat)}\lambda_y^{\{1j\},(lat)2} = \pm\frac{1}{3} \quad &\Longleftrightarrow \quad \lambda_x^{\{1j\},(lat)} = \pm\frac{1}{3\lambda_y^{\{1j\},(lat)2}} \end{aligned} \tag{11.24}$$

where the product is positive or negative depending on the initial representative molecule orientation. Differentiating Equation (11.24), both in real and lattice components, for uniaxial tension

$$2\lambda_x^{\{1j\}}\dot{\lambda}_y^{\{1j\}} + \dot{\lambda}_x^{\{1j\}}\lambda_y^{\{1j\}} = 0 \qquad \Longleftrightarrow \qquad -2\frac{\lambda_x^{\{1j\}}}{\lambda_y^{\{1j\}}} = \frac{\dot{\lambda}_x^{\{1j\}}}{\dot{\lambda}_y^{\{1j\}}} \tag{11.25}$$

11.5 Adaptive boundary condition perpendicular to applied force

The additional complexity of the boundary condition perpendicular to the applied force is that the stretch propagates, and is therefore not uniform, along the length of the specimen. Nevertheless, the principle is the same as for the parallel adaptive BC. Two examples of BCs perpendicular to the applied stress are considered. The first is plane strain. This is counterintuitive because unixial tension is not plane strain. The reason for using a plane strain BC is that the 2D model is implicitly plane strain. The second BC perpendicular to the applied force is intended to model the real situation more closely because the 3D incompressibility condition ($\Pi_{i=1}^{3}\lambda_i = 1$ where λ_i is a principal stretch, $\lambda_2 = \lambda_3 = 1/\sqrt{\lambda_1}$ and λ_1 is the stretch parallel to the applied load) is used. Although the latter BC is a closer approximation to reality, it is not obvious that it is of relevance because the underlying 2D method only allows for plane strain.

11.5.1 Plane strain adaptive boundary conditions

The plane strain situation fixes the principal stretch in one of the three directions as one. Given horizontal RVE location $i \in \mathbb{N}_0$ where $1 \leq i \leq q$

and vertical RVE location $j \in \mathbb{N}_0$ where $1 \leq j \leq s$ and the incompressibility condition, the specimen stretch in the vertical direction at every horizontal location i ($\lambda_{spy}^{\{i\}}$) is calculated as

$$\lambda_x^{\{ji\},(real)} \lambda_y^{\{ji\},(real)} = \pm 1 \qquad \forall\, 1 \leq j \leq s \text{ and } 1 \leq i \leq q \quad (11.26)$$

which would imply that

$$\begin{aligned} {}_{(expected)}\lambda_{spy}^{\{i\},(real)} &:= \frac{1}{{}_{(expected)}\lambda_{spx}^{\{i\}}} = \pm \frac{1}{\frac{1}{s}\sum_{j=1}^{s} \lambda_x^{\{ji\},(real)}} \\ &\approx \pm \frac{1}{\frac{1}{s-1}\sum_{j=2}^{s} \lambda_x^{\{ji\},(real)}} = \pm \frac{1}{\lambda_{x\mu}^{\{i\},(real)}} \end{aligned}$$

where $\lambda_x^{\{ji\},(real)}$ is the material stretch in the x-direction of the ji^{th} node. Thus the specimen stretch in the y-direction is the inverse of the arithmetic mean of the horizontal stretches at the i position The actual specimen stretch in the y-direction is given by

$${}_{(actual)}\lambda_{spy}^{\{i\},(real)} = \frac{1}{s-1} \sum_{j=2}^{s} \lambda_y^{\{ji\},(real)}. \quad (11.27)$$

Clearly the sum of the material stretches in the vertical direction must equal the specimen stretches for each horizontal location i, so that

$$\begin{aligned} s\ {}_{(expected)}\lambda_{spy}^{\{i\},(real)} &= \lambda_y^{\{1i\},(real)} + \sum_{j=2}^{s} \lambda_y^{\{ji\},(real)} \\ \text{(substituting (11.27))} \qquad &= \lambda_y^{\{1i\},(real)} + (s-1)\ {}_{(actual)}\lambda_{spy}^{\{i\},(real)} \end{aligned}$$

where $\lambda_y^{\{ji\},(real)}$ is the stretch in the y-direction at horizontal location i and vertical location j. Consequently the BC is given by

$$\lambda_y^{\{1i\},(real)} = s\ {}_{(expected)}\lambda_{spy}^{\{i\},(real)} - (s-1)\ {}_{(actual)}\lambda_{spy}^{\{i\},(real)} \quad (11.28)$$

and the x-component is given by the incompressibity condition (11.21)

$$\lambda_x^{\{1i\},(real)} = \pm \frac{1}{\lambda_y^{\{1i\},(real)}}. \quad (11.29)$$

The lattice version of the above is derived as above subject to the constraint

$$\begin{aligned}
\lambda_x^{\{ij\},)(lat)}\lambda_y^{\{ij\},(lat)} &= \pm\frac{1}{3} \qquad \forall\, 1 \le j \le s \text{ and } 1 \le i \le q \\
\Longrightarrow {}_{(expected)}\lambda_{spy}^{\{i\},(lat)} &\approx \pm\frac{1}{3}\frac{1}{\frac{1}{(s-1)}\sum_{j=2}^{s}\lambda_x^{\{ji\},(lat)}} = \pm\frac{1}{3\lambda_{x\mu}^{\{i\},(lat)}} \\
{}_{(actual)}\lambda_{spy}^{\{i\},(lat)} &= \frac{1}{3(s-1)}\sum_{j=2}^{s}\lambda_y^{\{ji\},(lat)} \\
\lambda_y^{\{1i\},(lat)} &= s\ {}_{(expected)}\lambda_{spy}^{\{i\},(lat)} - (s-1)\ {}_{(actual)}\lambda_{spy}^{\{i\},(lat)}.
\end{aligned}$$

With regard to stretch rate, by differentiating Equation (11.21),

$$\begin{aligned}
& \lambda_x^{\{ji\},(real)}\lambda_y^{\{ji\},(real)} = \pm 1 \\
\Longrightarrow \quad & \dot{\lambda}_x^{\{ji\},(real)}\lambda_y^{\{ji\},(real)} + \lambda_x^{\{ji\},(real)}\dot{\lambda}_y^{\{ji\},(real)} = 0 \\
\Longleftrightarrow \quad & \dot{\lambda}_y^{\{ji\},(real)} = -\frac{\lambda_y^{\{ji\},(real)}}{\lambda_x^{\{ji\},(real)}}\dot{\lambda}_x^{\{ji\},(real)}.
\end{aligned} \tag{11.30}$$

Substituting Equation (11.21) into Equation(11.30)

$$\dot{\lambda}_y^{(ji,real)} = \mp\frac{1}{\lambda_x^{(ji,real)2}}\dot{\lambda}_x^{(ji,real)}$$

then, given that specimen properties are the arithmetic mean of material properties, the expected specimen stretch in the y direction is

$${}_{(expected)}\dot{\lambda}_y^{\{i\},(real)} = \mp\frac{\frac{1}{s-1}\sum_{j=2}^{s}\dot{\lambda}_x^{\{ij\},(real)}}{\left(\frac{1}{s-1}\sum_{j=2}^{s}\lambda_x^{\{ij\},(real)}\right)^2} = \mp\frac{\dot{\lambda}_{\mu x}}{\lambda_{\mu x}^2}. \tag{11.31}$$

The actual stretch rate in the y direction is given by

$${}_{(actual)}\dot{\lambda}_y^{\{i\},(real)} = \frac{1}{s-1}\sum_{j=2}^{s}\dot{\lambda}_y^{\{ij\},(real)}. \tag{11.32}$$

Given that, in principle, the expected stretch rate in the y-direction is the arithmetic mean of the material stretches,

$$s\ {}_{(expected)}\dot{\lambda}_y^{(\{i\},(real)} = \dot{\lambda}_y^{\{i1\},(real)} + \sum_{j=2}^{s}\dot{\lambda}_y^{\{i1\},(real)}. \tag{11.33}$$

Substituting Equation (11.32)) into Equation (11.33)

$$\begin{aligned} s\ {}_{(expected)}\dot{\lambda}_y^{(\{i\},(real)} &= \dot{\lambda}_y^{\{i1\},(real)} + (s-1)\ {}_{(actual)}\dot{\lambda}_y^{\{i\},(real)} \\ \iff \dot{\lambda}_y^{\{i1\},(real)} &= s\ {}_{(expected)}\dot{\lambda}_y^{\{i\},(real)} - (s-1)\ {}_{(actual)}\dot{\lambda}_y^{\{i\},(real)}. \end{aligned} \tag{11.34}$$

Non-zero specimen stretch rates imply moving boundaries but the model does not permit this phenomenon. Nevertheless, moving boundaries are physically consistent. The x-component of stretch rate is determined by substituting (11.28), (11.29) and (11.34) into Equation (11.30) or (11.23) such that

$$\dot{\lambda}_x^{\{1i\},(real)} = -\frac{\lambda_x^{\{1i\},(real)}}{\lambda_y^{\{1i\},(real)}}\dot{\lambda}_y^{\{1i\},(real)}. \tag{11.35}$$

The results above, that were derived for real components, can also be shown to apply to lattice components.

11.5.2 Adaptive boundary conditions parallel to the applied force for two free surfaces

The underlying principle being applied is conservation of specimen length – as for the plane strain situation. The second principle is conservation of volume (incompressibility) as summarised by

$$\prod_{i=1}^{3}\lambda_i = 1. \tag{11.36}$$

Further, given that two surfaces are free, $\lambda_2 = \lambda_3$ and consequently

$$\lambda_1\lambda_2^2 = 1 \qquad \lambda_2 = \frac{1}{\sqrt{\lambda_1}}.$$

Given that (11.36) applies to specimen stretches,

$$\lambda_x^{\{ji\},(real)}\lambda_y^{\{ji\},(real)2} = \pm 1 \qquad \forall\ 1 \le j \le s \text{ and } 1 \le i \le q \tag{11.37}$$

which implies that

$${}_{(expected)}\lambda_{spy}^{\{i\},(real)} := \frac{1}{\sqrt{{}_{(expected)}\lambda_{spx}^{\{i\},(real)}}} = \pm\frac{1}{\sqrt{\frac{1}{s}\sum_{j=1}^{s}\lambda_x^{\{ji\},(real)}}}$$

$$\approx \pm\frac{1}{\sqrt{\frac{1}{s-1}\sum_{j=2}^{s}\lambda_x^{\{ji\},(real)}}} = \pm\frac{1}{\sqrt{\lambda_{x\mu}^{\{i\},(real)}}}$$

where $\lambda_x^{\{ji\},(real)}$ is the material stretch in the x-direction of the ji^{th} node. Thus the specimen stretch in the y-direction is the inverse of the square root of the arithmetic mean ($\lambda_{x\mu}^{\{i\},(real)}$) of the horizontal stretches at the i position. The actual specimen stretch in the y-direction is

$$_{(actual)}\lambda_{spy}^{\{i\},(real)} = \frac{1}{s-1}\sum_{j=2}^{s}\lambda_y^{\{ji\},(real)}. \tag{11.38}$$

The sum of the material stretches in the vertical direction must equal the specimen stretches for each horizontal location i, so that

$$\begin{aligned} s\ _{(expected)}\lambda_{spy}^{\{i\},(real)} &= \lambda_y^{\{1i\},(real)} + \sum_{j=2}^{s}\lambda_y^{\{ji\},(real)} \\ \text{(substituting (11.38))} \qquad &= \lambda_y^{\{1i\},(real)} + (s-1)\ _{(actual)}\lambda_{spy}^{\{i\},(real)} \end{aligned}$$

where $\lambda_y^{\{ji\},(real)}$ is the stretch in the y-direction at horizontal location i and vertical location j. Consequently the BC is

$$\lambda_y^{\{1i\},(real)} = s\ _{(expected)}\lambda_{spy}^{\{i\},(real)} - (s-1)\ _{(actual)}\lambda_{spy}^{\{i\},(real)} \tag{11.39}$$

and the x-component is given by the incompressibity condition (11.24) as

$$\lambda_x^{\{1i\},(real)} = \pm\frac{1}{\lambda_y^{\{1i\},(real)2}}. \tag{11.40}$$

The lattice version of the above is derived as above subject to the constraint

$$\begin{aligned} \lambda_x^{\{ij\},)(lat)}\lambda_y^{\{ij\},(lat)2} &= \pm\frac{1}{3} \qquad \forall\ 1 \le j \le s \text{ and } 1 \le i \le q \\ \Longrightarrow\ _{(expected)}\lambda_{spy}^{\{i\},(lat)} &\approx \pm\frac{1}{3}\frac{1}{\sqrt{\frac{1}{(s-1)}\sum_{j=2}^{s}\lambda_x^{\{ji\},(lat)}}} = \pm\frac{1}{3}\frac{1}{\sqrt{\lambda_{x\mu}^{\{i\},(lat)}}} \\ _{(actual)}\lambda_{spy}^{\{i\},(lat)} &= \frac{1}{3}\frac{1}{\sqrt{\frac{1}{(s-1)}\sum_{j=2}^{s}\lambda_y^{\{ji\},(lat)}}} \\ \lambda_y^{\{1i\},(lat)} &= s\ _{(expected)}\lambda_{spy}^{\{i\},(lat)} - (s-1)\ _{(actual)}\lambda_{spy}^{\{i\},(lat)}. \end{aligned}$$

With regard to stretch rate, differentiating (11.24),

$$\begin{aligned} & \lambda_x^{\{ji\},(real)}\lambda_y^{\{ji\},(real)2} = \pm 1 \\ \Longrightarrow \quad & \dot{\lambda}_x^{\{ji\},(real)}\lambda_y^{\{ji\},(real)} + 2\lambda_x^{\{ji\},(real)}\dot{\lambda}_y^{\{ji\},(real)} = 0 \\ \Longleftrightarrow \quad & \dot{\lambda}_y^{\{ji\},(real)} = -\frac{\lambda_y^{\{ji\},(real)}}{2\lambda_x^{\{ji\},(real)}}\dot{\lambda}_x^{\{ji\},(real)}. \end{aligned} \tag{11.41}$$

Substituting (11.24) into (11.41),

$$\dot{\lambda}_y^{(ji,real)} = \mp\frac{1}{2\lambda_x^{(ji,real)1.5}}\dot{\lambda}_x^{(ji,real)}.$$

Then, given that specimen properties are the arithmetic mean of material properties, the expected specimen stretch in the y direction is

$${}_{(expected)}\dot{\lambda}_y^{\{i\},(real)} = \mp\frac{\frac{1}{s-1}\sum_{j=2}^{s}\dot{\lambda}_x^{\{i,j\}}}{2\left(\frac{1}{s-1}\sum_{j=2}^{s}\lambda_x^{\{i,j\}}\right)^{1.5}} = \mp\frac{\dot{\lambda}_{\mu x}^{\{i\}}}{2(\lambda_{\mu x}^{\{i\}})^{1.5}}. \tag{11.42}$$

The actual stretch rate in the y direction is given by

$${}_{(actual)}\dot{\lambda}_y^{\{i\},(real)} = \frac{1}{s-1}\sum_{j=2}^{s}\dot{\lambda}_y^{\{ij\},(real)}. \tag{11.43}$$

Given that, in principle, the expected stretch rate in the y-direction is the arithmetic mean of the material stretches,

$$s\ {}_{(expected)}\dot{\lambda}_y^{(\{i\},(real)} = \dot{\lambda}_y^{\{i1\},(real)} + \sum_{j=2}^{s}\dot{\lambda}_y^{\{i1\},(real)}. \tag{11.44}$$

Substituting (11.43) into (11.44)

$$\begin{aligned} s\ {}_{(expected)}\dot{\lambda}_y^{(\{i\},(real)} &= \dot{\lambda}_y^{\{i1\},(real)} + (s-1)\ {}_{(actual)}\dot{\lambda}_y^{\{i\},(real)} \\ \Longleftrightarrow \quad \dot{\lambda}_y^{\{i1\},(real)} &= s\ {}_{(expected)}\dot{\lambda}_y^{\{i\},(real)} - (s-1)\ {}_{(actual)}\dot{\lambda}_y^{\{i\},(real)}. \\ &. \end{aligned} \tag{11.45}$$

Again, non-zero specimen stretch rates imply moving boundaries (not allowed by the model) but these are physically consistent. The x-component of stretch rate is calculated by substituting (11.39), (11.40) and (11.45) into

Equation (11.41) or (11.25) such that

$$\dot{\lambda}_x^{\{1i\},(real)} = -2\frac{\lambda_x^{\{1i\},(real)}}{\lambda_y^{\{1i\},(real)}}\dot{\lambda}_y^{\{1i\},(real)}. \tag{11.46}$$

11.6 The corner node boundary conditions

The theory predicts that every RVE should be incompressible. Thus

$$\lambda_{lx}\lambda_{ly} = 1 = \lambda_{tx}\lambda_{ty} = \lambda_{ltx}\lambda_{lty}$$

where the l subscript designates the left RVE, the t is top and lt is the left-top corner node. The geometric mean satifies the above conditions as shown by

$$\begin{aligned} \lambda_{ltx} &= \sqrt{\lambda_{lx}\lambda_{tx}} \qquad \text{and} \qquad \lambda_{lty} = \sqrt{\lambda_{ly}\lambda_{ty}} \\ \Longrightarrow \lambda_{ltx}\lambda_{lty} &= \sqrt{\lambda_{lx}\lambda_{tx}}\sqrt{\lambda_{ly}\lambda_{ty}} = \sqrt{\lambda_{lx}\lambda_{ly}}\sqrt{\lambda_{tx}\lambda_{ty}} = 1. \end{aligned} \tag{11.47}$$

The stretch rates will be the geometric mean of the stretch rates of the adjacent nodes to ensure that Equation (11.23) is satisfied. The proof relies on Section 11.4. The nodes adjacent to the corner nodes satisfy (11.23). Thus

$$\begin{aligned} & \frac{\lambda_x^{(l)}}{\lambda_y^{(l)}} = \pm\frac{\dot{\lambda}_x^{(l)}}{\dot{\lambda}_y^{(l)}} \qquad \text{and} \qquad \frac{\lambda_x^{(t)}}{\lambda_y^{(t)}} = \pm\frac{\dot{\lambda}_x^{(t)}}{\dot{\lambda}_y^{(t)}} \\ \Longrightarrow \quad & \frac{\lambda_x^{(l)}}{\lambda_y^{(l)}}\frac{\lambda_x^{(t)}}{\lambda_y^{(t)}} = \frac{\dot{\lambda}_x^{(l)}}{\dot{\lambda}_y^{(l)}}\frac{\dot{\lambda}_x^{(t)}}{\dot{\lambda}_y^{(t)}} \\ \Longleftrightarrow \quad & \sqrt{\frac{\lambda_x^{(l)}}{\lambda_y^{(l)}}\frac{\lambda_x^{(t)}}{\lambda_y^{(t)}}} = \sqrt{\frac{\dot{\lambda}_x^{(l)}}{\dot{\lambda}_y^{(l)}}\frac{\dot{\lambda}_x^{(t)}}{\dot{\lambda}_y^{(t)}}} \qquad \Longleftrightarrow \qquad \frac{\lambda_x^{(lt)}}{\lambda_y^{(lt)}} = \sqrt{\frac{\dot{\lambda}_x^{(l)}}{\dot{\lambda}_y^{(l)}}\frac{\dot{\lambda}_x^{(t)}}{\dot{\lambda}_y^{(t)}}}. \end{aligned}$$

Thus setting the stretch rates of the corner nodes to be the geometric means of those for the adjacent nodes,

$$\dot{\lambda}_x^{(lt)} := \sqrt{\dot{\lambda}_x^{(l)}\dot{\lambda}_x^{(t)}} \text{ and } \dot{\lambda}_y^{(lt)} := \sqrt{\dot{\lambda}_y^{(l)}\dot{\lambda}_y^{(t)}} \qquad \Longrightarrow \frac{\lambda_x^{(lt)}}{\lambda_y^{(lt)}} = \frac{\dot{\lambda}_x^{(lt)}}{\dot{\lambda}_y^{(lt)}} \tag{11.48}$$

and thereby satisfies Equation (11.23).

11.7 Relating chain rate ratio to stretch rate

The stretch rate $\dot{\lambda}$, as used in this text, refers to the ratio of chain stretch rate to initial chain length. Thus the stretch rate is defined by

$$\dot{\lambda}_i := \frac{\dot{\mathrm{R}}_{fi}}{\mathrm{R}_{\mu 0 i}}. \tag{11.49}$$

The computer program used to model the behaviour of the material, as described in Chapters 8 through 10, uses the chain rate ratio defined by

$$\iota_i = \frac{\dot{\mathrm{R}}_{fi}}{\dot{\mathrm{R}}_{\mu 0 i}}. \tag{11.50}$$

These results are related by recognising that by multiplying (11.49) by

$$1 = \frac{R_{\mu 0 i}}{\dot{\mathrm{R}}_{\mu 0 i}} \frac{\dot{\mathrm{R}}_{\mu 0 i}}{\mathrm{R}_{\mu 0 i}},$$

one determines the relationship

$$\dot{\lambda}_i = \frac{\dot{\mathrm{R}}_{fi}}{\mathrm{R}_{\mu 0 i}} = \frac{\dot{\mathrm{R}}_{fi}}{\mathrm{R}_{\mu 0 i}} \times \frac{\mathrm{R}_{\mu 0 i}}{\dot{\mathrm{R}}_{\mu 0 i}} \frac{\dot{\mathrm{R}}_{\mu 0 i}}{\mathrm{R}_{\mu 0 i}} = \iota_i \frac{\dot{\mathrm{R}}_{\mu 0 i}}{\mathrm{R}_{\mu 0 i}}. \tag{11.51}$$

Furthermore, substituting these result into the boundary conditions of Sections 11.4 through 11.6, it is evident that the result of the above sections are still valid.

Chapter 12

Theory validation

The theory for polymer viscoelasticity, as presented in this thesis, has been based on the assumption of a Gaussian chain length (vector length) distribution in an isotropic material. Although this theory is not valid for the full range of polymer elasticity, Treloar ([138], Chapter 5) shows that it is valid to a strain of 40% [135]. One should therefore conclude that this theory applies to certain incompressible, isotropic, viscoelastic, hyperelastic materials (like polymers), but only upto stretches of the order of 1.4, and not subject to creep or plastic deformation.

The constitutive equation (7.15) is a relatively simple equation in only two unknowns – μ and G. The complexity in experimentation is due to the appropriate selection of material, the derivation of the constitutive equation on the deformed state and material hyperelasticity.

Here, experimentation has four functions – material selection, constant determination, prediction, and experimental verification of the numerical model. In Section 3.1.2 the velocity of the molecule ($\boldsymbol{c}$) was separated into a component due to molecular stretch rate or vibration ($\grave{\boldsymbol{c}}$) and a component due to molecular translation or flow ($\acute{\boldsymbol{c}}$). The velocity $\grave{\boldsymbol{c}}$ is therefore associated with completely reversible time-dependent behaviour, that is viscoelasticity. In contrast, $\acute{\boldsymbol{c}}$ is associated with either incompletely reversible time-dependent elastic behaviour which will be called creep, or irreversible time-dependent or time-independent behaviour which will be called plastic deformation.

The model considered here is constructed only for viscoelastic materials. Thus material selection includes establishing the conditions under which the

material behaves as an isotropic, viscoelastic, hyperelastic material without creep or plastic deformation.

It is a known property of polymers that the stress-strain curve of a previously strained specimen will be different from that of the original stress-strain curve for that specimen. The present model predicts that this is a consequence of molecular flow or slippage as represented by $\boldsymbol{\acute{c}}$ in this model. One would therefore also expect that under the appropriate conditions ($\boldsymbol{\acute{c}} = 0$) stress-strain curves for a particular specimen will be reproducible.

In this chapter the first set of experiments will establish the conditions (at room temperature) under which this polymer will behave as an isotropic, viscoelastic, hyperelastic material without creep or yield. The second set of experiments will determine the unknowns μ and G. The third set of experiments will verify the reproducibility of the stress-strain curve on the same specimen. Verification of the model is the subject of Chapter 13.

12.1 Material selection

The material used in these experiments is pellethane 2363 AE with density $1150kg/m^3$. The material was donated by the Cardiovascular Research Unit (CVRU) at the University of Cape Town. The uniaxial tests were performed on an Instron 5544 (described in Appendix B-5) – also belonging to CVRU.

Specimen	**Depth(D)** mm	**W** mm	**L** mm	**S** mm	**T** mm
S1	1.02	4.00	25	45	74.97
S2	1.02	4.02	25	46	74.98
S3	1.01	3.94	25	46	74.98
S4	1.01	3.96	25	46	74.96
S8T1	0.90	3.98	25	46	74.63
S9T2	0.90	3.99	25	46	74.80
S10T3	0.99	4.02	25	46	74.87
S11T4	0.93	4.02	25	47	74.77
S12V1	0.90	3.94	25	46	75

Table 12.1: Test specimen dimensions

Nine standard dumbell specimens were used for this series of experiments. Four of these specimens (designated S1,S2,S3,S4) were used to determine the conditions under which the specimens would not exhibit creep, stress

relaxation or plastic deformation. An additional four specimens (designated S8T1, S9T2, S10T3, S11T3) were used to determine the material constants μ and G and also to illustrate the reproducibility of the stress strain curve under the established conditions. The remaining specimen (S12V1) will be used for the numerical model verification in Chapter 13. The dimensions of the nine specimens are summarised in Table 12.1. The specimen depth was

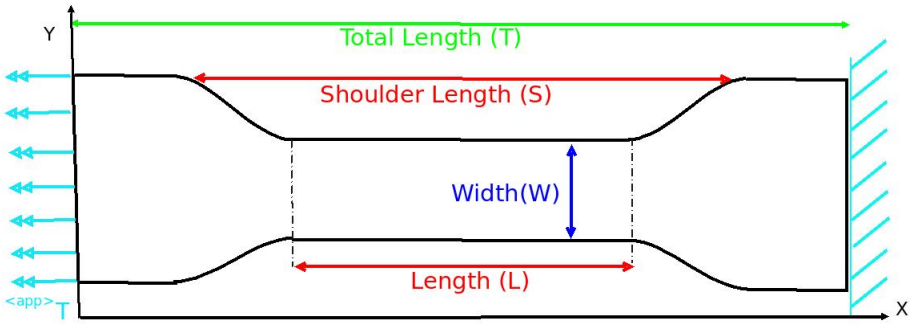

Figure 12.1: Dumbell with measured dimensions designated

measured with a micrometer (precision 0.01 mm) and the length, shoulder length and total length were measured with a caliper (precision 0.02 mm). The dimensions in Table 12.1 are depicted in Figure 12.1.

12.1.1 Criteria for exclusion of creep and plasticity

For practical reasons, the conditions for which there is no creep or plasticity are assumed to exist if the material returns to the original total length (T) within 30 minutes. The presence of a change in total length (T) is defined by a statistically significant difference in the measured value as determined in Appendix B-4. For T, this significant change is 0.11 mm. Conversely, a change of measurement of less than 0.11 mm is assumed to signify the absence of a significant difference. If no significant difference can be detected in 30 minutes, creep and plasticity are deemed to be absent or neglible.

12.1.2 Stretch and stretch-rates that do not allow creep

All specimens were tested at room temperature. Specimen S1 was strained to a maximum of 10%, S2 to 20%, S3 to 30% and S4 to 40%. Each specimen was strained at 2, 5, 10, 20, 50, 100, 150, 200, 300 and 600 mm/min. The changes in total length immediately after straining and relaxation are given in Table 12.2.

	Specimen	**S1**	**S2**	**S3**	**S4**
Stretch Rate mm/min	**Maximum Strain**	**10%**	**20%**	**30%**	**40%**
2		75.40	75.40	75.70	75.60
5		75.20	75.30	75.68	75.40
10		75.13	75.13	75.29	75.33
20		75.05	75.33	75.20	75.20
50		74.98	75.13	75.24	75.23
100		74.99	75.13	75.14	75.13
150		75.00	75.06	75.11	75.09
200		74.96	75.11	75.14	75.15
400		74.98	75.14	75.14	75.15
600		75.00	75.18	75.19	75.26
900		74.97	75.13	75.13	75.10

Table 12.2: Immediate post strain total lengths

The difference in length (T) 30 minutes after the start of the strain experiments are shown in Figure 12.2 as a function of stretch rate. The y-axis indicates the change in total length, the red line is the smallest significant difference and the curves represent the maximum strains as indicated in the legend. Based on these results, the maximum allowable strain is 40% and

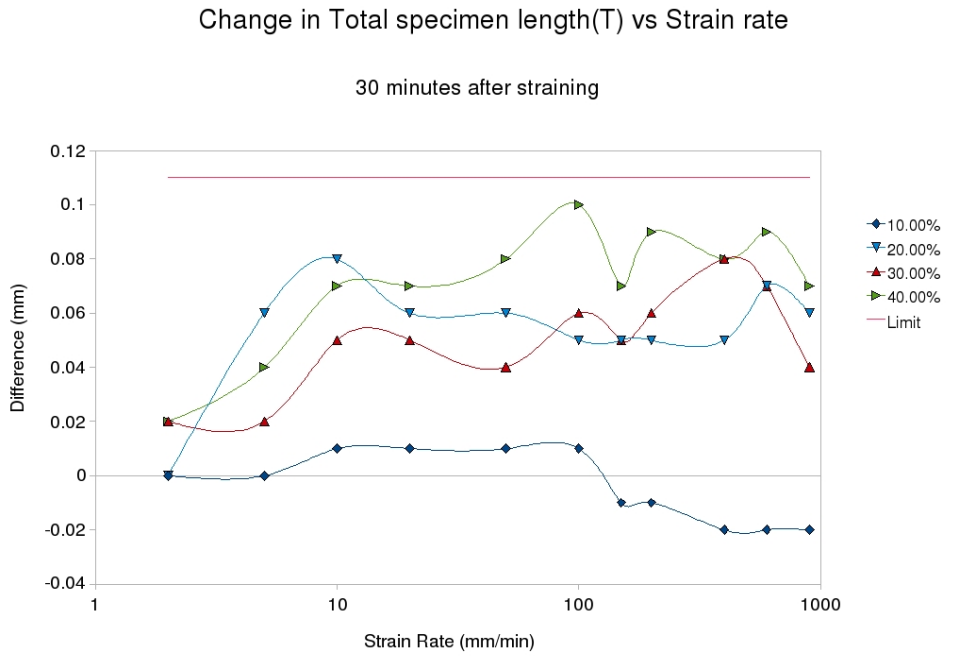

Figure 12.2: Change in length by strain rate and maximum strain

the maximum allowable strain rate is $900\,mm/min$ – to avoid creep in this material.

12.1.3 Criteria to exclude stress relaxation

Stress relaxation is a known feature of polymers. In the theory constructed in this document, stress is a function of stretch and stretch rate. Equation (7.15) cannot derive a form consistent with experimentally observed stress relaxation because, in 1D, (7.15) reduces to a generalisation of the Kelvin-Voigt model of viscoelasticity as demonstrated in Section 7.2. The Kelvin-Voigt model is known to predict instantaneous stress relaxation [16]. The theory for specimen viscoelasticity does, however, predict stress relaxation.

Consider Equation (6.102). This equation describes a wave-like propagation of stretch and stretch rate through a material specimen and is an example of a non-linear wave equation as described in Section 6.6. The right hand side is the divergence of the stress tensor as given by Equation (7.18). The theory predicts that stress relaxation is a consequence of this stretch and stretch rate propagation and redistribution within the specimen – specimen viscoelasticity. Thus the measured (which for the instron is true apparent specimen) stress is a function of the measured stretch and stretch-rate and the propagation and distribution of stretch and stretch-rate through the specimen. In order to negate the latter effect, the appropriate conditions have to be established. The absence of inappropriate conditions will be informed by recognising the absence of the consequences of these inappropriate conditions – stress relaxation.

It is predicted that, for smaller specimens at lower stretch rates, stress relaxation under isometric conditions will be less significant because the specimen is able to be in quasi-equilibrium. Thus, in the stress relaxation experiment, at the loading transition from displacement ramp to isometric stretch; the specimen stretch and length are constant. Stress relaxation is predicted to be a consequence of the specimen's approach to steady state (and each RVE material's approach to maximum entropy with respect to stretch). The ramp and isometric stretch are depicted in Figure 12.3.

The absence of stress relaxation will be determined in terms of the accuracy of the load measuring instrument. A significant load difference is 4.5% as determined in Appendix B-5. A significant true apparent specimen stress

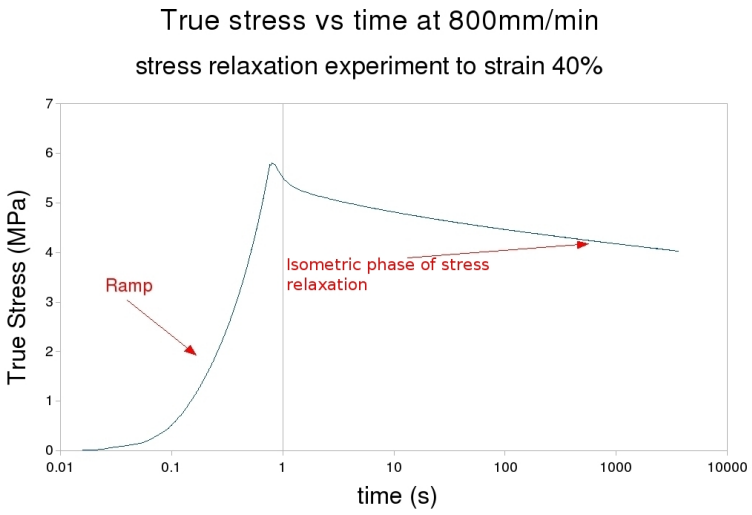

Figure 12.3: The stress relaxation experiment

difference, as measured by the instron, is $0.48\,MPa$ (see Equation (B-4)). If the maximum difference between the measured stresses at the end of ramping and 30 minutes into the isometric phase is less than $0.48\,MPa$ of the measured stress at end of ramping, stress relaxation is considered to be absent.

12.1.4 Stretch rates that exclude stress relaxation

Specimens S8 through S11 were strained to 40% at various stretch rates as indicated in Table 12.3 where the lower limit of $0.05\,mm/min$ and upper limit of $800\,mm/min$ are constrained by the limits of the testing instrument. The results of the stress relaxation experiment are provided in Table 12.4.

	Stretch Rate (mm/min)			
S8T1	0.2	2	40	500
S9T2	0.1	1	10	100
S10T3	0.4	4	20	400
S11T4	0.05	0.5	5	800

Table 12.3: Stretch rates to maximum strain 40%

The results are colour-coded to correspond to the stretch rates in Table 12.3. The **bold** results, on the left, are the stresses at the end of ramping to maximum strain and the *italic* results, on the right, correspond to the stress at 30 minutes after the maximum strain is attained and maintained. Figure 12.4 charts the changes in measured stress (true apparent specimen), from

	Measured Stress (MPa) – 3 significant figures							
S8T1	**4.61**	*4.25*	**4.87**	*4.25*	**5.22**	*4.20*	**5.84**	*4.19*
S9T2	**4.34**	*4.07*	**4.57**	*4.08*	**4.79**	*4.08*	**5.75**	*4.07*
S10T3	**4.58**	*4.14*	**4.64**	*4.00*	**4.95**	*4.08*	**5.70**	*4.10*
S11T4	**4.23**	*4.04*	**4.57**	*4.14*	**4.73**	*4.10*	**5.81**	*4.03*

Table 12.4: End of ramp and 30 minute stress (stress relaxation)

Figure 12.4: Absolute change with stress relaxation

Table 12.4, vs strain rate. The limit for the absence of a significant change is $0.233\,MPa$ and is depicted as a red line. The absence of a significant change signifies that specimen properties approximate material properties. The strain rate that avoids stress relaxation is $0.05\,mm/min$. This stretch rate will be used to determine the material constants.

12.2 Theory validation

At least three predictions can be made based upon the theory and Equation (7.19). Given that the left hand side of (7.19) depends on only two material constants (G and μ), one should anticipate that, at steady state in a stress relaxation experiment, the steady state stress is independent of the initial ramp stretch rate.

One would further predict that the steady state stress in a stress relax-

ation experiment is directly proportional to the stretch. Lastly, the appropriate manipulation of Equation (7.15) – the equation for material stress – can determine pellethane's material constants at a stretch rate of $0.05\,mm/min$ (refer to Sections 12.1.3 and 12.1.4) because, under these conditions, the material properties of pellethane correspond to the specimen properties.

12.2.1 Strain-rate-independent steady state stress

The LHS of Equation (7.19) is written in terms of gradients of the square of stretch, stretch rate and temporal derivatives of stretch rate. The theory predicts that disequilibrium is due to redistribution of macroscopic properties through the specimen. Conversely, at steady state, macroscopic properties are uniformly distributed throughout the specimen. By definition, at steady state temporal derivatives are zero. Thus at steady state (in one dimension where end $x = \mathrm{L}(t)$ is fixed and end $x = 0$ is the point of tensile load application, $\mathbf{x}$ is in the opposite direction to the applied tensile load as depicted in Figure 12.1. In Figure 12.1 x is in black and the apparent principal stress, ${}^{\langle app\rangle}\mathrm{T}$, is in cyan).

Let the principal strain $\boldsymbol{\epsilon}$ be defined as $\boldsymbol{\epsilon} := \Delta\boldsymbol{\lambda}$, then Equation (7.19) reduces to

$$
\begin{aligned}
\kappa\Delta\mathbf{v} + \kappa\Delta\mathbf{r}\cdot\nabla\mathbf{v} &= -\frac{\partial}{\partial x}\mathbf{T} = \kappa B\boldsymbol{\epsilon} - \frac{B^2\kappa}{4}\frac{\partial\lambda^2}{\partial x} = \frac{1}{2}\frac{\partial\mathbf{P}_S}{\partial x} = -\frac{1}{2}\frac{\partial}{\partial x}{}^{\langle app\rangle}\mathbf{T} \\
\iff \quad -\Delta{}^{\langle app\rangle}\mathrm{T}_1 &= 2\kappa B\Delta x_1\epsilon_1 - \frac{B^2\kappa}{2}\Delta\lambda_1^2 \\
&= 2\kappa\mathrm{R}_{\mu 0x}r_0(\epsilon)\epsilon_1 - \frac{\mathrm{R}_{\mu 0x}^2\kappa}{2}(\epsilon_1+2)(\epsilon_1) = -a\epsilon_1^2 - b\epsilon_1 \\
&= \left(2\kappa\mathrm{R}_{\mu 0x}r_0 - \frac{\mathrm{R}_{\mu 0x}^2\kappa}{2}\right)\epsilon_1^2 - \mathrm{R}_{\mu 0x}^2\kappa\epsilon_1 = -2\Delta\mathrm{T} \\
\iff \quad \Delta{}^{\langle app\rangle}\mathrm{T}_1 &= \left(\frac{\mathrm{R}_{\mu 0x}^2\kappa}{2} - 2\kappa\mathrm{R}_{\mu 0x}r_0\right)\epsilon_1^2 + \mathrm{R}_{\mu 0x}^2\kappa\epsilon_1 \qquad (12.1)
\end{aligned}
$$

where the penultimate substitution is from (6.101) and ϵ_1 is the principal strain parallel to the applied force. The change in the length of a line segment Δx (where the direction of x is parallel to the applied force) can either be interpreted as the change in position of an RVE or the change in RVE length. Further, $\Delta\delta x = \Delta\lambda\delta x_0 = \epsilon\delta x_0$ where the specimen RVE length is $\delta x = \lambda\delta x_0$. The initial length $r_0 = \delta x_0$ is therefore the initial specimen RVE length. Thus the steady state stress of a specimen strained to a fixed stretch is constant independent of stretch rate.

Figure 12.5 charts the apparent stresses at steady state (30 minutes) for each stretch rate. The experiments were performed for each of the stretch rates described in Table 12.3 and to strains of 10%, 20%, 30% and 40%. Figure 12.5(a) illustrates that for the strains tested, the steady state stresses

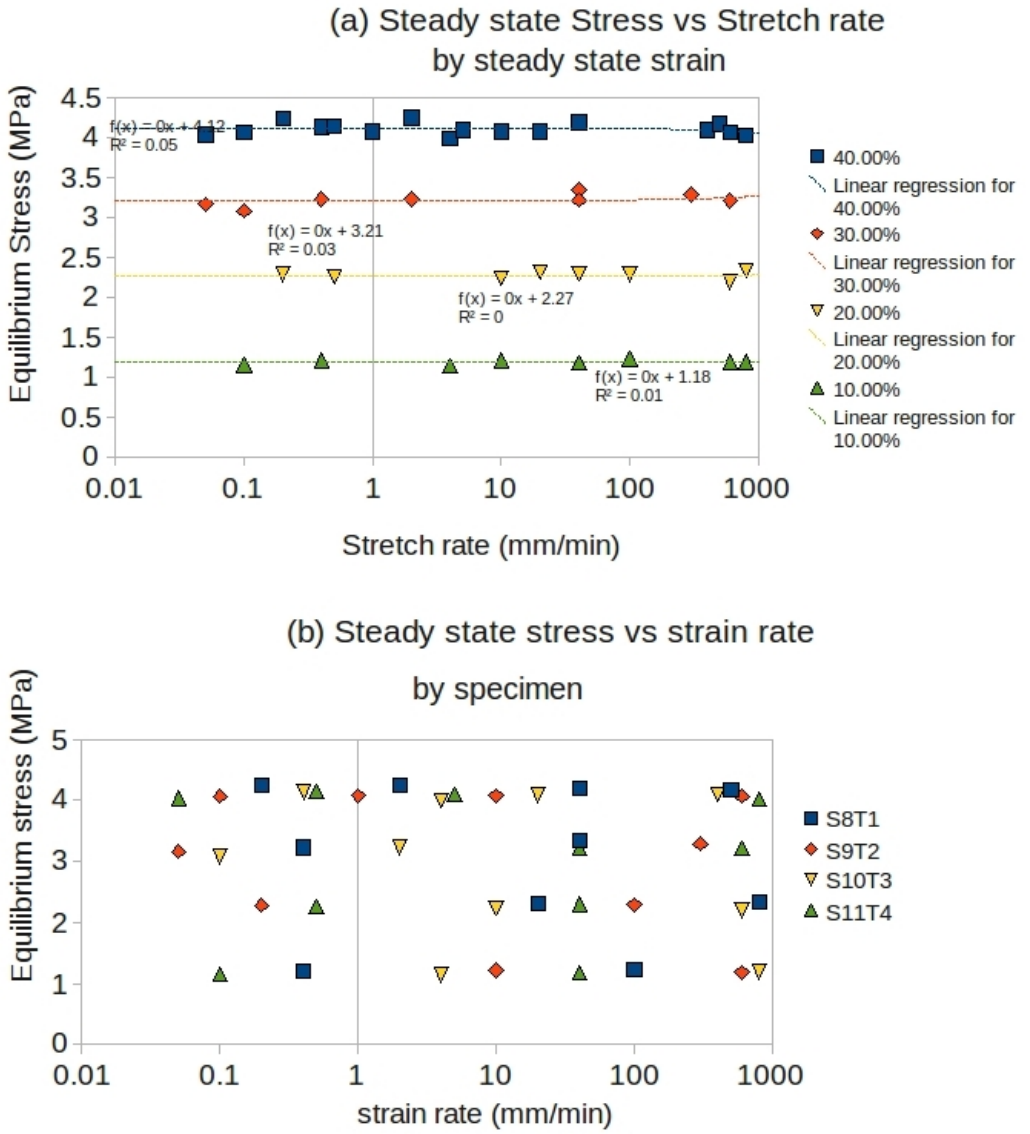

Figure 12.5: Strain rate independent steady state stress

remain constant. The linear regression [64] results depicted in Figure 12.5(a) confirm this observation. The R value is the Pearson correlation coefficient which here approximates zero, indicating a poor correlation between stretch rate and steady state stress at best. Figure 12.5(b) depicts the same result but emphasizes the specimen tested, thereby confirming the specimen independence of the result.

12.2.2 Material maximum entropy stress-strain relationship

Equation (12.1) predicts that, at steady state, a parabolic relationship exists between principal stress and principal strain. To negate hydrostatic effects, ${}^{\langle app \rangle}\mathrm{T}_2$ needs to be subtracted subject to the constraint $\prod_{i=1}^{3} \lambda_i = 1 \iff \lambda_1 = \frac{1}{\lambda_2^2} = \frac{1}{\lambda_3^2}$ and ${}^{\langle app \rangle}\mathrm{T}_2 = 0$ in the uniaxial test. Therefore

$$\begin{aligned} \Delta^{\langle app \rangle}\mathrm{T}_1 &= \Big(\frac{\mathrm{R}_{\mu 0x}^2 \kappa}{2} - 2\kappa \mathrm{R}_{\mu 0x} \mathrm{r}_0\Big)\Big(\epsilon_1^2 - \frac{1}{\epsilon_1 + 1} + \frac{2}{\sqrt{\epsilon_1 + 1}} - 1\Big) \\ &\quad + \mathrm{R}_{\mu 0x}^2 \kappa \Big(\epsilon_1 - \frac{1}{\sqrt{\epsilon_1 + 1}} + 1\Big) \end{aligned} \tag{12.2}$$

is the non-parabolic equation for the apparent specimen and material principal stress (specimen and material properties are equal at steady state). Figure 12.6(a) uses a box-and-whisker plot to display the relationship between stress and strain. This particular plot is intended to display the low variability at each strain. The n values correspond to the number of measurements made. Figure 12.6(b) performs linear regression to provide a visual depiction of the linearity.

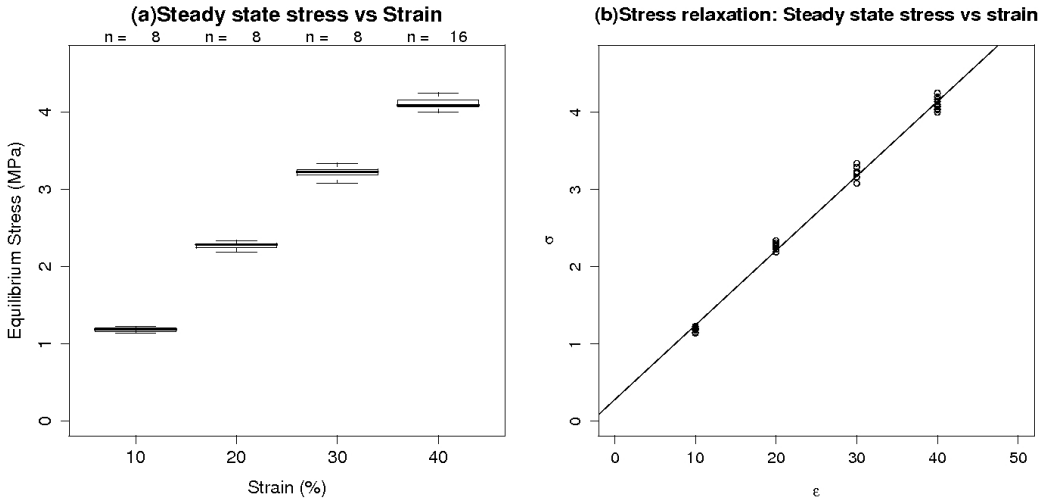

Figure 12.6: Linear regression of specimen steady state true apparent stress for stress relaxation. Strain, ϵ, is reported as a percentage.

The difference between the median and whiskers is $1.53 \times IQR$ where IQR is the interquartile range ($75^{th}centile - 25^{th}centile$). The box is defined by the $75^{th}centile$ and $25^{th}centile$ ([108], Chapter 2). The gradient of the least squares line in Figure 12.6(b) is 9.65 MPa with an intercept of 0.278 MPa.

The Pearson correlation coefficient is 0.9952 [64]. ($P < 2e^{-16}$ for the gradient and $P < 1.89e^{-10}$ for the intercept where P is the probability that such an event can occur at random). Of note, the higher number of measurements at the 40% strain effectively increases the weighting of the 40% strain.

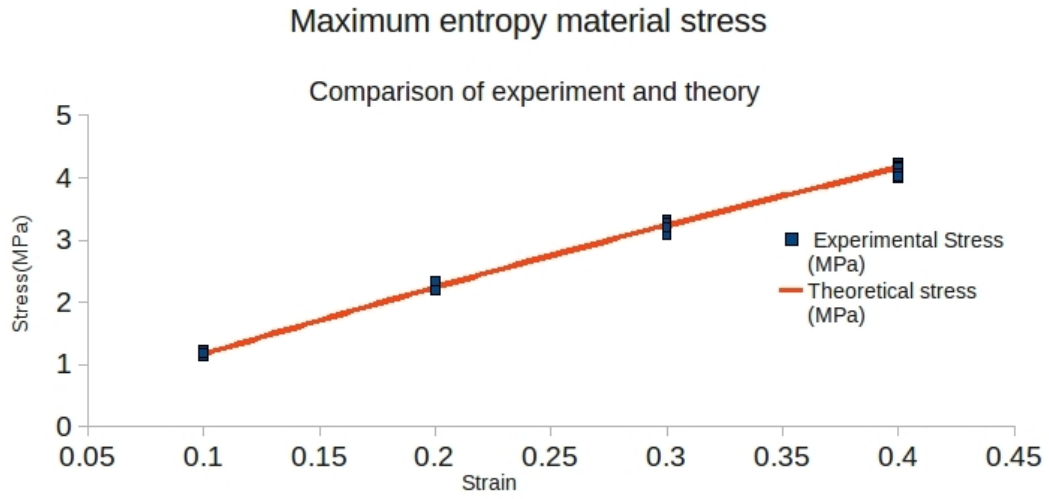

Figure 12.7: The parabolic principal material maximum entropy stress-strain relationship

A least squares fit has been conducted to determine the constants for Equation (12.2). The constant $a = -2.3015\,MPa$ and $b = 8.0618\,MPa$ where $a = \mathrm{R}_{\mu 0x}^2\kappa/2 - 2\kappa\mathrm{R}_{\mu 0x}\mathrm{r}_0$ and $b = \mathrm{R}_{\mu 0x}^2\kappa$. Figure 12.7 compares the predicted material maximum entropy principal stress in red to the experimental material maximum entropy principal stresses in blue.

12.2.3 Uniaxial test theory: specimen steady state model

This section will determine the constant κ. Recall that Equation (7.19) is a macroscopic differential equation. However the left hand side of the equation is a specimen description and the right hand side is a material description. At steady state two implicit conditions are satisfied. The first (by definition) is that temporal derivatives are zero. The second is that the specimen description is the same as the material description. This result is implicit in the model of specimen viscoelasticity presented in this work. An alternate interpretation is that, at steady state, the whole specimen can be approximated as an RVE. This is consistent with the definition of the RVE (Section 1.1) because the theory predicts that, at steady state, there is homogeneity with respect to molecular distribution. Thus, from the left

hand side of Equation (7.19), for displacement $\mathbf{v}$

$$\nabla \cdot \mathbf{T} = \kappa\Delta\mathbf{v} + \kappa\Delta\mathbf{r} \cdot \nabla\mathbf{v} = \kappa\Delta\mathbf{v} - \kappa\mathbf{v} \cdot \nabla\mathbf{v} = \kappa\Delta\mathbf{v} - \frac{\kappa}{2}\nabla \mathrm{v}^2$$

where the direction of $\mathbf{v}$ is opposite to the direction of $\mathbf{r}$ as depicted in Figure 12.1, and consequently $\mathbf{v} = -\Delta\mathbf{r}$. Then the one-dimensional solution is

$$-\frac{\partial \mathrm{T}_1}{\partial x} = \kappa \mathrm{v}_1\epsilon_1 - \frac{\kappa}{2}\frac{\partial \lambda_1^2 \mathrm{v}_1^2}{\partial x} \iff -\Delta \mathrm{T}_1 = \kappa(\Delta x)(\mathrm{v}_1\epsilon_1) - \frac{\kappa}{2}(\lambda_1^2 - 1)\mathrm{v}_1^2,$$

where the subscript 1 refers to the relevant principal vector component – parallel to the applied force. After integrating with respect to x,

$$\begin{aligned} \Delta \mathrm{T}_1 &= -\kappa \mathrm{v}_1^2\epsilon_1^2 + \frac{\kappa \mathrm{v}_1^2}{2}\epsilon_1(\epsilon_1 + 2) = -\frac{\kappa \mathrm{v}_1^2}{2}(\lambda_1 - 1)^2 + \kappa \mathrm{v}_1^2(\lambda_1 - 1) \\ &= -\frac{1}{2}\kappa \mathrm{v}_1^2\lambda_1^2 + 2\kappa \mathrm{v}_1^2\lambda_1 - \frac{3}{2}\kappa \mathrm{v}_1^2 \end{aligned} \tag{12.3}$$

where v_1 is the initial specimen length and $\Delta x = \mathrm{v}_1\epsilon_1$ is the change in specimen length.

The same result can be derived for the remaining two directions. Subtracting half the sum of the stresses in the 2 and 3 directions from that in the 1 direction,

$$\begin{aligned} \Delta \mathrm{T}_1 - \frac{\Delta \mathrm{T}_2 + \Delta \mathrm{T}_3}{2} &= -\frac{1}{2}\kappa \mathrm{v}_1^2\lambda_1^2 + \frac{1}{4}\kappa \mathrm{v}_2^2\lambda_2^2 + \frac{1}{4}\kappa \mathrm{v}_3^2\lambda_3^2 \\ &\quad + 2\kappa \mathrm{v}_1^2\lambda_1 - \kappa \mathrm{v}_2^2\lambda_2 - \kappa \mathrm{v}_3^2\lambda_3 - \frac{3}{2}\kappa \mathrm{v}_1^2 + \frac{3}{4}\kappa \mathrm{v}_2^2 + \frac{3}{4}\kappa \mathrm{v}_3^2. \end{aligned} \tag{12.4}$$

Given $\lambda_1\lambda_2\lambda_3 = 1$, the isotropic material and the uniaxial tensile test,

$$\lambda_1 = \frac{1}{\lambda_2^2} = \frac{1}{\lambda_3^2} \iff \lambda_2 = \lambda_3 = \frac{1}{\sqrt{\lambda_1}} \iff \lambda_2^2 = \lambda_3^2 = \frac{1}{\lambda_1},$$
$$\Delta \mathrm{T}_2 = \Delta \mathrm{T}_3 = 0$$

and Equation (12.4) reduces to

$$\begin{aligned} \Delta \mathrm{T}_1 &= -\frac{\kappa \mathrm{v}_1^2}{2}\lambda_1^2 + 2\kappa \mathrm{v}_1^2\lambda_1 - \frac{3}{2}\kappa \mathrm{v}_1^2, \\ &\quad + \kappa\frac{\mathrm{v}_2^2 + \mathrm{v}_3^2}{4\lambda_1} - \kappa\frac{\mathrm{v}_2^2 + \mathrm{v}_3^2}{\sqrt{\lambda_1}} + \frac{3}{4}\kappa(\mathrm{v}_2^2 + \mathrm{v}_3^2). \end{aligned} \tag{12.5}$$

$$\begin{aligned} \text{Similarly, } \Delta^{\langle app \rangle}\mathrm{T}_1 &= -\kappa \mathrm{v}_1^2\lambda_1^2 + 4\kappa \mathrm{v}_1^2\lambda_1 - 3\kappa \mathrm{v}_1^2 \\ &\quad + \kappa\frac{\mathrm{v}_2^2 + \mathrm{v}_3^2}{2\lambda_1} - 2\kappa\frac{\mathrm{v}_2^2 + \mathrm{v}_3^2}{\sqrt{\lambda_1}} + \frac{3}{2}\kappa(\mathrm{v}_2^2 + \mathrm{v}_3^2). \end{aligned} \tag{12.6}$$

A least squares fit was conducted to show that $\kappa = 10.55GPa.m^{-2}$ which cannot be compared to Young's modulus. Figure 12.8 displays the curve fit to the data and differs from Figure 12.7 by substituting κ as an unknown.

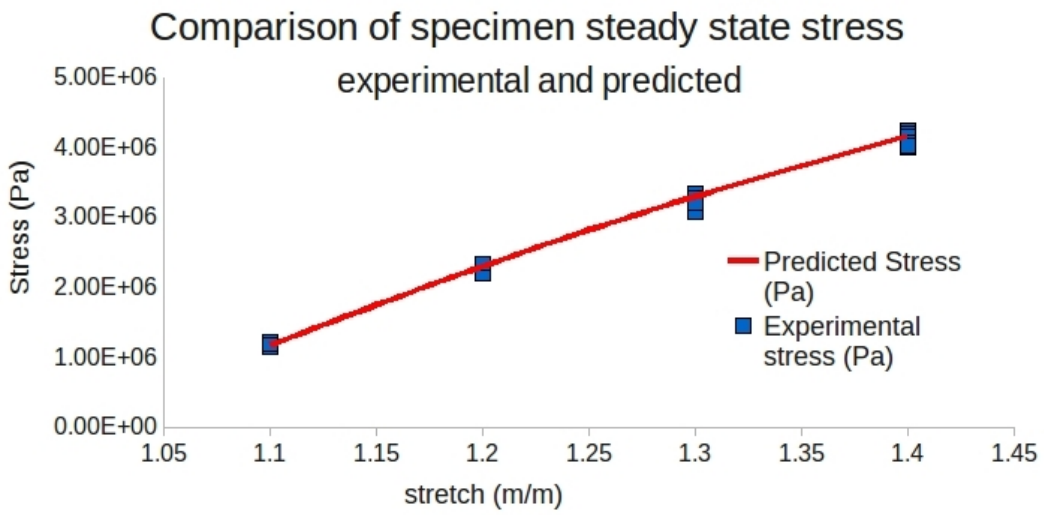

Figure 12.8: The parabolic specimen steady state stress-stretch relationship

12.2.4 Uniaxial test theory: fixed strain-rate model

It should be noted that the following derivation is for a material – the right hand side of Equation (7.19). However, the tensile test is performed on a specimen. In order for specimen properties to approximate material properties, the specimen has to be in steady state. It should be noted that (7.17) is less correct than the unmeasurable formulation based on Equation (7.15). Equation (7.15) is more correct because it corresponds to the specimen stress whereas (7.17) is the measured stress as discussed in Section 5.1.5. A formulation based on (7.17) is measurable and is thus presented.

True fixed strain-rate model

A uniaxial tensile test is typically performed at a fixed stretch rate. Thus the specimen is never in steady state. Consequently the test has to be conducted at quasi-equilibrium – where quasi-equilibrium is defined as a macroscopic specimen phenomenon which describes a state of disequilibrium sufficiently close to steady state such that a steady state approximation can be made. In Section 12.1.3 it has been determined that the stretch rate $0.05\,mm/min$ is compatible with quasi-equilibrium.

Under fixed stretch rate conditions, a material behaves as follows:

$$\delta\lambda_1 = \dot{\lambda}_1\delta t \qquad \Longleftrightarrow \qquad \lambda(t) = \int_0^t \dot{\lambda}_1 d\tau = 1 + \dot{\lambda}_1 t \tag{12.7}$$

$$\Longleftrightarrow \qquad \frac{\lambda_1 - 1}{\dot{\lambda}_1} = t \tag{12.8}$$

$$\Longleftrightarrow \qquad \dot{\lambda}_1 t^2 = \frac{(\lambda_1 - 1)^2}{\dot{\lambda}_1}. \tag{12.9}$$

From Equation (7.37)) and the incompressibility condition (7.47) ($\lambda_1\lambda_2\lambda_3 = 1$), the true latent strain energy function is

$$\begin{aligned} W^* &= A(\lambda_1 + \lambda_2 + \frac{1}{\lambda_1\lambda_2}) + 2\mu\frac{\partial}{\partial t}(\lambda_1^2 + \lambda_2^2) + 2\mu\frac{\partial}{\partial t}\frac{1}{\lambda_1^2\lambda_2^2} \\ &\quad +2G\int_0^t (\lambda_1^2 + \lambda_2^2)d\tau + 2G\int_0^t \frac{1}{\lambda_1^2\lambda_2^2}d\tau. \end{aligned} \tag{12.10}$$

W^* is used because the data reported by the tensile testing instrument is corrected for current area. The stress results reported by the instrument are thus true stress (σ_t). However, true latent specimen stress which, for quasi-equilibrium, corresponds to true latent material stress is being determined here. The latent stress cannot be measured. Differentiating Equation (12.10) with respect to λ_1,

$$\begin{aligned} \sigma_{t1} = \frac{\partial W^*}{\partial \lambda_1} &= A - \frac{A}{\lambda_1^2\lambda_2} + 4\mu\dot{\lambda}_1 - 4\mu\frac{\partial}{\partial t}\frac{1}{\lambda_1^3\lambda_2^2} \\ &\quad +4G\int_0^t \lambda_1 d\tau - 4G\int_0^t \frac{1}{\lambda_1^3\lambda_2^2}d\tau. \end{aligned} \tag{12.11}$$

Then using the relation $\lambda_3^2 = \lambda_2^2 = \frac{1}{\lambda_1}$ from (7.49) in (12.11),

$$\begin{aligned} \sigma_{t1} &= A - \frac{A}{\lambda_1^{3/2}} + 4\mu\dot{\lambda}_1 - 4\mu\frac{\partial}{\partial t}\frac{1}{\lambda_1^2} + 4G\int_0^t \lambda_1 d\tau - 4G\int_0^t \frac{1}{\lambda_1^2}d\tau \\ &= A - \frac{A}{\lambda_1^{3/2}} + 4\mu\dot{\lambda}_1 + 8\mu\lambda_1^{-3}\dot{\lambda}_1 + 4G\int_0^t \lambda_1 d\tau - 4G\int_0^t \frac{1}{\lambda_1^2}d\tau. \end{aligned}$$

Substituting (12.7) and using (12.8) and (12.9),

$$\begin{aligned}
\sigma_{t1} &= A - \frac{A}{\lambda_1^{3/2}} + 4\mu\dot{\lambda}_1 + 8\mu\lambda_1^{-3}\dot{\lambda}_1 \\
&\quad +4\int_0^t G(1+\dot{\lambda}_1\tau)d\tau - 4\int_0^t G\frac{1}{(1+\dot{\lambda}_1\tau)^2}d\tau \\
&= A - \frac{A}{\lambda_1^{3/2}} + 4\mu\dot{\lambda}_1 + 8\mu\lambda_1^{-3}\dot{\lambda}_1 + 2G\frac{(1+\dot{\lambda}_1\tau)^2}{\dot{\lambda}_1}\Big|_0^t + \frac{G}{(1+\dot{\lambda}_1\tau)}\frac{4}{\dot{\lambda}_1}\Big|_0^t \\
&= A - \frac{A}{\lambda_1^{3/2}} + 4\mu\dot{\lambda}_1 + 8\mu\lambda_1^{-3}\dot{\lambda}_1 \\
&\quad +2G\frac{(1+\dot{\lambda}_1 t)^2 - 1}{\dot{\lambda}_1} + \frac{G}{(1+\dot{\lambda}_1 t)}\frac{4}{\dot{\lambda}_1} - \frac{4G}{\dot{\lambda}_1}.
\end{aligned}$$

Consequently

$$\sigma_{t1} = A - \frac{A}{\lambda_1^{3/2}} + 4\mu\dot{\lambda}_1 + 8\mu\lambda_1^{-3}\dot{\lambda}_1 + 2G\frac{\lambda_1^2 - 1}{\dot{\lambda}_1} + \frac{4G}{\lambda_1\dot{\lambda}_1} - \frac{4G}{\dot{\lambda}_1} \quad (12.12)$$

Given that under these conditions $\dot{\lambda}_i$ is not constant for $i = 2, 3$, it follows that σ_{t2} and σ_{t3} are not of the same form as Equation (12.12). From Equation (12.11) with appropriate change of variable,

$$\begin{aligned}
\sigma_{t3} = \frac{\partial W^*}{\partial \lambda_3} &= A - \frac{A}{\lambda_3^2\lambda_2} + 4\mu\dot{\lambda}_3 - 4\mu\frac{\partial}{\partial t}\frac{1}{\lambda_3^3\lambda_2^2} \\
&\quad +4G\int_0^t \lambda_3 d\tau - 4G\int_0^t \frac{1}{\lambda_3^3\lambda_2^2}d\tau. \qquad (12.13)
\end{aligned}$$

Substituting Equation (7.49) into (12.13),

$$\begin{aligned}
\sigma_{t3} &= A - A\lambda_1^{3/2} + 4\mu\left(\dot{\lambda}_3 - \frac{\partial}{\partial t}\lambda_1^{5/2}\right) + 4G\int_0^t \left(\frac{1}{\sqrt{\lambda_1}} - \lambda_1^{5/2}\right)d\tau \\
&= A(1-\lambda_1^{3/2}) + 4\mu\left(\dot{\lambda}_3 - \frac{5}{2}\lambda_1^{3/2}\dot{\lambda}_1\right) + 4G\int_0^t \left(\frac{1}{\sqrt{\lambda_1}}d\tau - \lambda_1^{5/2}\right)d\tau.
\end{aligned}$$

Further, upon substitution of Equations (7.51) and (12.7),

$$\begin{aligned}
\sigma_{t3} &= A - A\lambda_1^{3/2} + 2\mu\frac{\dot{\lambda}_1}{\lambda_1^{3/2}} - 10\mu\lambda_1^{3/2}\dot{\lambda}_1 \\
&\quad +4G\int_0^t \frac{1}{\sqrt{1+\dot{\lambda}_1\tau}}d\tau - 4G\int_0^t (1+\dot{\lambda}_1\tau)^{5/2}d\tau \\
&= A - A\lambda_1^{3/2} + 2\mu\frac{\dot{\lambda}_1}{\lambda_1^{3/2}} - 10\mu\lambda_1^{3/2}\dot{\lambda}_1 \\
&\quad +8G\frac{\sqrt{1+\dot{\lambda}_1\tau}}{\dot{\lambda}_1}\Big|_0^t - \frac{8}{7}G\frac{(1+\dot{\lambda}_1\tau)^{7/2}}{\dot{\lambda}_1}\Big|_0^t. \qquad (12.14)
\end{aligned}$$

Then substituting Equation (12.8),

$$\begin{aligned}
\sigma_{t3} &= A - A\lambda_1^{3/2} + 2\mu\frac{\dot{\lambda}_1}{\lambda_1^{3/2}} - 10\mu\lambda_1^{3/2}\dot{\lambda}_1 \\
&\quad +8G\frac{\sqrt{1+\dot{\lambda}_1 t}-1}{\dot{\lambda}_1} - \frac{8}{7}\frac{G}{\dot{\lambda}_1}(1+\dot{\lambda}_1 t)^{7/2} + \frac{8}{7}\frac{G}{\dot{\lambda}_1} \\
\sigma_{t3} &= A - A\lambda_1^{3/2} + 2\mu\frac{\dot{\lambda}_1}{\lambda_1^{3/2}} - 10\mu\lambda_1^{3/2}\dot{\lambda}_1 \\
&\quad +8G\frac{\sqrt{\lambda_1}-1}{\dot{\lambda}_1} - \frac{8}{7}\frac{G}{\dot{\lambda}_1}(\lambda_1)^{7/2} + \frac{8}{7}\frac{G}{\dot{\lambda}_1}. \qquad (12.15)
\end{aligned}$$

Subtracting (12.15) from (12.12) and using (7.46),

$$\begin{aligned}
\sigma_{t1} - \sigma_{t3} &= -A\lambda_1^{-3/2} + 4\mu\dot{\lambda}_1 + 8\mu\lambda_1^{-3}\dot{\lambda}_1 + G\frac{\lambda_1^2-1}{\dot{\lambda}_1} \\
&\quad +\frac{4G}{\lambda_1\dot{\lambda}_1} - \frac{4G}{\dot{\lambda}_1} + A\lambda_1^{3/2} - 2\mu\frac{\dot{\lambda}_1}{\lambda_1^{3/2}} + 10\mu\lambda_1^{3/2}\dot{\lambda}_1 \\
&\quad -8G\frac{\sqrt{\lambda_1}-1}{\dot{\lambda}_1} + \frac{8}{7}\frac{G}{\dot{\lambda}_1}(\lambda_1)^{7/2} - \frac{8}{7}\frac{G}{\dot{\lambda}_1} \\
\sigma_{t1} &= 8\mu\lambda_1^{-3}\dot{\lambda}_1 - A\lambda_1^{-3/2} - 2\mu\lambda_1^{-3/2}\dot{\lambda}_1 + \frac{4G\lambda_1^{-1}}{\dot{\lambda}_1} + \frac{6}{7}\frac{G}{\dot{\lambda}_1} + 4\mu\dot{\lambda}_1 \\
&\quad -\frac{8G}{\dot{\lambda}_1}\lambda_1^{1/2} + A\lambda_1^{3/2} + 10\mu\lambda_1^{3/2}\dot{\lambda}_1 + \frac{2G}{\dot{\lambda}_1}\lambda_1^2 + \frac{8}{7}\frac{G}{\dot{\lambda}_1}\lambda_1^{7/2}, \\
&= A(\lambda_1^{-3/2} + \lambda_1^{3/2}) + \mu\dot{\lambda}_1\Big(\frac{8}{\lambda_1^3} - \frac{2}{\lambda_1^{3/2}} + 4 + 10\lambda_1^{3/2}\Big) \\
&\quad +\frac{2G}{\dot{\lambda}_1}\Big(\frac{2}{\lambda_1} + \frac{3}{7} - 4\lambda_1^{1/2} + \lambda_1^2 + \frac{4}{7}\lambda_1^{7/2}\Big) \qquad (12.16)
\end{aligned}$$

for the fixed stretch-rate uniaxial tensile test on an isotropic, incompressible, viscoelastic specimen. It should be noted that $\dot{\lambda}$ is true stretch rate or (for

current length $s(t)$)

$$\dot{\lambda} = \frac{\partial}{\partial t}\Big(\frac{d\mathrm{s}}{\mathrm{s}}\Big) = \frac{\dot{\mathrm{s}}}{\mathrm{s}}. \tag{12.17}$$

The true stretch rate $\dot{\lambda}$ has to be distinguished from the nominal stretch rate which will be designated $\dot{\lambda}_0$. The nominal stretch rate will be defined by Equation (12.23) and is the stretch rate reported by the tensile testing instrument. The nominal stretch rate corresponds to the conventional definition of stretch rate and differs from the true stretch rate by being the ratio of the rate of change of length relative to the undeformed length or s_0.

Apparent fixed strain-rate model

The true fixed strain-rate model above determines the Cauchy true maximum entropy latent stress. However, the latent stress is not directly measurable (discussed in Section 5.1.5). The apparent stress ${}^{\langle app\rangle}\mathbf{T}$ is measurable and can be determined from the apparent stored energy functions.

Substituting Equation (7.47) into Equation (7.45),

$$\begin{aligned} {}^{\langle app\rangle}W^* &= A(\lambda_1+\lambda_2+\frac{1}{\lambda_1\lambda_2}) + \mu\frac{\partial}{\partial t}(\lambda_1^2+\lambda_2^2) + \mu\frac{\partial}{\partial t}\frac{1}{\lambda_1^2\lambda_2^2} \\ &\quad +4G\int_0^t(\lambda_1^2+\lambda_2^2)d\tau + 4G\int_0^t\frac{1}{\lambda_1^2\lambda_2^2}d\tau. \end{aligned} \tag{12.18}$$

Differentiating Equation (12.18) with respect to λ_1 and substituting $\lambda_3^2 = \lambda_2^2 = \frac{1}{\lambda_1}$, from (7.49), into Equation (12.19),

$$\begin{aligned} {}^{\langle app\rangle}\sigma_{t1} &= \frac{\partial {}^{\langle app\rangle}W^*}{\partial\lambda_1} \\ &= A - \frac{A}{\lambda_1^2\lambda_2} + 2\mu\left(\dot{\lambda}_1 - \frac{\partial}{\partial t}\frac{1}{\lambda_1^3\lambda_2^2}\right) + 8G\int_0^t\left(\lambda_1 d\tau - \frac{1}{\lambda_1^3\lambda_2^2}\right)d\tau \\ &= A - \frac{A}{\lambda_1^{3/2}} + 2\mu\dot{\lambda}_1 + 4\mu\lambda_1^{-3}\dot{\lambda}_1 + 8G\int_0^t\left(\lambda_1 - \frac{1}{\lambda_1^2}\right)d\tau. \end{aligned} \tag{12.19}$$

Substituting (12.7)–(12.9) into Equation (12.19),

$$\begin{aligned} {}^{\langle app\rangle}\sigma_{t1} &= A - \frac{A}{\lambda_1^{3/2}} + 2\mu\dot{\lambda}_1 + 4\mu\lambda_1^{-3}\dot{\lambda}_1 \\ &\quad +4G\frac{(1+\dot{\lambda}_1 t)^2-1}{\dot{\lambda}_1} + \frac{G}{(1+\dot{\lambda}_1 t)}\frac{8}{\dot{\lambda}_1} - \frac{8G}{\dot{\lambda}_1} \end{aligned}$$

$$
\begin{aligned}
&= A - \frac{A}{\lambda_1^{3/2}} + 2\mu\dot{\lambda}_1 + 4\mu\lambda_1^{-3}\dot{\lambda}_1 + 4G\frac{\lambda_1^2 - 1}{\dot{\lambda}_1} \\
&\quad + \frac{8G}{\lambda_1\dot{\lambda}_1} - \frac{8G}{\dot{\lambda}_1}. \qquad (12.20)
\end{aligned}
$$

Next, from Equation (12.19) with appropriate change of variable, and using Equations (7.49), (7.51), (12.7) and (12.8)

$$
\begin{aligned}
{}^{\langle app\rangle}\sigma_{t3} &= \frac{\partial^{\langle app\rangle}W^*}{\partial\lambda_3} \\
&= A - \frac{A}{\lambda_3^2\lambda_2} + 2\mu\dot{\lambda}_3 - 2\mu\frac{\partial}{\partial t}\frac{1}{\lambda_3^3\lambda_2^2} + 8G\int_0^t \left(\lambda_3 - \frac{1}{\lambda_3^3\lambda_2^2}\right) d\tau \\
&= A(1 - \lambda_1^{3/2}) + 2\mu\dot{\lambda}_3 - 5\mu\lambda_1^{3/2}\dot{\lambda}_1 + 8G\int_0^t \left(\frac{1}{\sqrt{\lambda_1}} - \lambda_1^{5/2}\right) d\tau.
\end{aligned}
$$

The resultant principal stress is

$$
\begin{aligned}
{}^{\langle app\rangle}\sigma_{t3} &= A(1 - \lambda_1^{3/2}) + \mu\frac{\dot{\lambda}_1}{\lambda_1^{3/2}} - 5\mu\lambda_1^{3/2}\dot{\lambda}_1 \\
&\quad + 16G\frac{\sqrt{1 + \dot{\lambda}_1\tau}}{\dot{\lambda}_1}\Big|_0^t - \frac{16}{7}G\frac{(1 + \dot{\lambda}_1\tau)^{7/2}}{\dot{\lambda}_1}\Big|_0^t \\
&= A - A\lambda_1^{3/2} + \mu\frac{\dot{\lambda}_1}{\lambda_1^{3/2}} - 5\mu\lambda_1^{3/2}\dot{\lambda}_1 \\
&\quad + 16G\frac{\sqrt{\lambda_1} - 1}{\dot{\lambda}_1} - \frac{16}{7}\frac{G}{\dot{\lambda}_1}(\lambda_1)^{7/2} + \frac{16}{7}\frac{G}{\dot{\lambda}_1}. \qquad (12.21)
\end{aligned}
$$

The elimination of hydrostatic components in Equation (12.20) is achieved by subtracting Equation (12.21) from Equation (12.20) which yields

$$
\begin{aligned}
{}^{\langle app\rangle}\sigma_{t1} - {}^{\langle app\rangle}\sigma_{t3} &= -A\lambda_1^{-3/2} + 2\mu\dot{\lambda}_1 + 4\mu\lambda_1^{-3}\dot{\lambda}_1 \\
&\quad + 2G\frac{\lambda_1^2 - 1}{\dot{\lambda}_1} + \frac{8G}{\lambda_1\dot{\lambda}_1} - \frac{8G}{\dot{\lambda}_1} \\
&\quad + A\lambda_1^{3/2} - \mu\frac{\dot{\lambda}_1}{\lambda_1^{3/2}} + 5\mu\lambda_1^{3/2}\dot{\lambda}_1 \\
&\quad - 16G\frac{\sqrt{\lambda_1} - 1}{\dot{\lambda}_1} + \frac{16}{7}\frac{G}{\dot{\lambda}_1}(\lambda_1)^{7/2} - \frac{16}{7}\frac{G}{\dot{\lambda}_1}.
\end{aligned}
$$

Finally, given Equation (7.46),

$$\begin{aligned} {}^{\langle app\rangle}\sigma_{t1} &= A(\lambda_1^{-3/2}+\lambda_1^{3/2})+\mu\dot{\lambda}_1\Big(\frac{4}{\lambda_1^3}-\frac{1}{\lambda_1^{3/2}}+2+5\lambda_1^{3/2}\Big) \\ &\quad +\frac{4G}{\dot{\lambda}_1}\Big(\frac{2}{\lambda_1}+\frac{3}{7}-4\lambda_1^{1/2}+\lambda_1^2+\frac{4}{7}\lambda_1^{7/2}\Big) \end{aligned} \tag{12.22}$$

for the apparent fixed stretch-rate uniaxial tensile test on an isotropic, incompressible, viscoelastic specimen where, as for the true latent stress, $\dot{\lambda}$ is true stretch rate or $\dot{s}/s$. Note that because (12.22) is directly measurable, it will be used for experimental purposes.

12.2.5 Experimental description and results

The uniaxial tensile tests described in Section 12.2.4 are described for materials in quasi-equilibrium. Section 12.1.4 determines that the stretch rate compatible with quasi-equilibrium is 0.05 mm/min (quasi-equilibrium stretch rate). The experimental data from the ramp components of the stress relaxation experiments conducted in Section 12.2.4 and described in Section 12.1.3 are used to determine the material constants in Equation (12.22). The constants will be numerically equal to those of Equation (12.16)

It has been noted that in Section 12.2.4 the true strain rate $\dot{\lambda}$ is used in Equation (12.22). The tensile testing instrument is only capable of a fixed nominal stretch rate $\dot{\lambda}_0$ where $\dot{\lambda}_0 = \dot{s}/s_0$, s is the current specimen length and s_0 is the initial specimen length. From (12.17) and substituting the above

$$\dot{\lambda} = \frac{\dot{s}}{s} = \frac{\dot{s}}{\lambda s_0} = \frac{\dot{\lambda}_0}{\lambda}. \tag{12.23}$$

Substituting Equation (12.23) into Equation (12.22),

$$\begin{aligned} {}^{\langle app\rangle}\sigma_{t1} &= A(\lambda_1^{-3/2}+\lambda_1^{3/2})+\frac{1}{2}\mu\dot{\lambda}_{01}\Big(\frac{8}{\lambda_1^4}-\frac{2}{\lambda_1^{5/2}}+\frac{4}{\lambda_1}+10\lambda_1^{1/2}\Big) \\ &\quad +4\frac{G}{\dot{\lambda}_{01}}\Big(2+\frac{3\lambda_1}{7}-4\lambda_1^{3/2}+\lambda_1^3+\frac{4}{7}\lambda_1^{9/2}\Big) \end{aligned} \tag{12.24}$$

where $\dot{\lambda}_{01}$ is $3.333\times10^{-5}s^{-1}$.

Multiple linear regression ([108], Chapter 11) is used to determine the constants A, G and μ. These are found to be $A = 6.213\,MPa$, $G = 0.971\times10^{-6}\,MPa.s^{-1}$ and $\mu = -3.748\times10^{4}\,MPa.s$.

12.2.6 Comparing experiment and theory

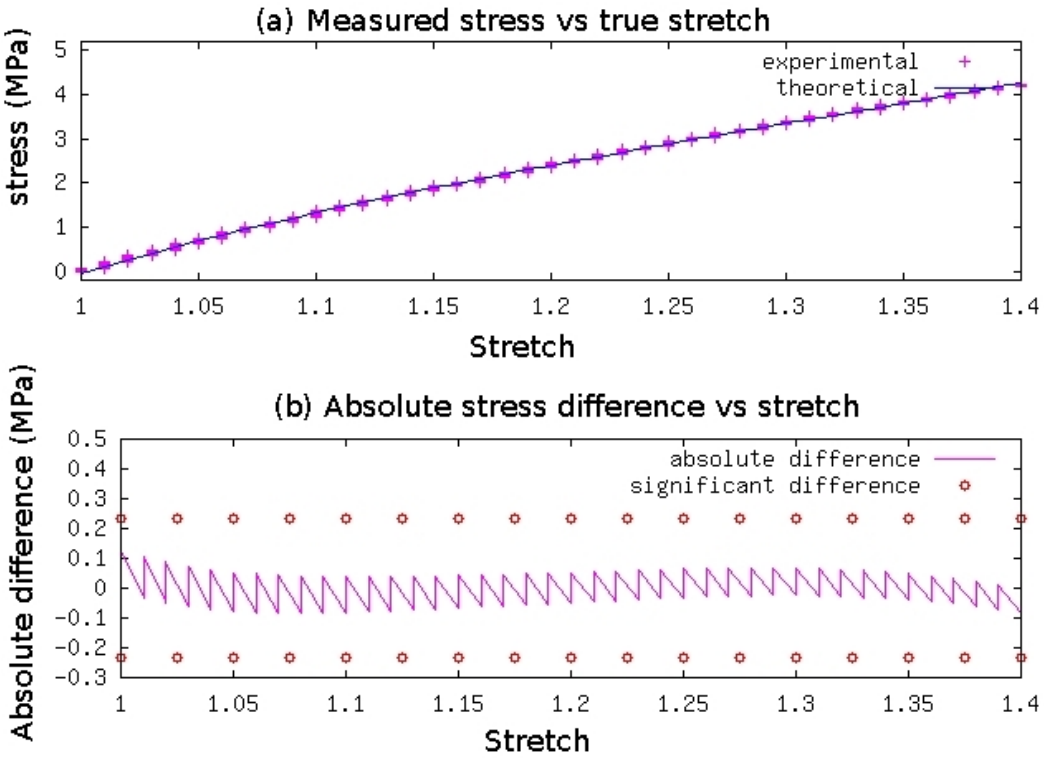

Figure 12.9: Multilinear regression fit of experimental data

The experimental results for the quasi-equilibrium stretch rates are compared to those predicted by Equation (12.22), and are charted in Figure 12.9. Figure 12.9(a) is a plot of the experimental and theoretical stress across the range of stretch. The discrete nature of the experimental results is due to rounding error during data storage. Figure 12.9(b) is a plot of the difference between experimental and theoretical results across the range of stretch. The red circles indicate the smallest significant difference – which Equation (B-4) calculats to be 0.233 MPa. There is clearly close agreement between theoretical and experimental results.

The results for the disequilibrium stretch rates (the complementary set to the quasi-equilibrium stretch rates) cannot be calculated directly and are the subject of Chapter 13. The methods described above can be applied to the disequilibrium stretch rates but the values determined would be specimen variables rather than the intended material constants.

Chapter 13

Model experimental verification

This chapter will present several results that are distinguished from those of Chapter 12 by being based either on discrete theory or on approximate special cases. Although Chapter 12 determined the material constants and reproduced the uniaxial stretch data, it did not demonstrate viscoelastic behaviour. There are three components to the demonstration of viscoelastic behaviour. The first is to show that for a fixed tensile load, the theory reproduces creep. Thus it must be demonstrated that a specimen with a constant specimen principal stress, will deform to a state in which the stretch is greater than the initial stretch. Secondly, a specimen at fixed stretch will achieve a steady state where the principal stress is less than the initial. The third component requires that between the initial and steady state the model must reproduce the time-dependent behaviour.

The polymer flow equation (6.98) could not be solved analytically. However in Appendices C-1 and C-2, (6.98) is separated into stretch and stretch rate components. Approximations to the stretch component (6.97) and stretch rate component (6.93) were solved analytically. The initial stretch distribution was calculated and shown to be related to stretch rate. For each specimen the steady state stretch and principal stress are calculated to demonstrate stress relaxation and creep. These experiments do not however reproduce time-dependent behaviour, nor are they based directly on the constitutive equation.

Time-dependent behaviour will be demonstrated using the discrete theory – the polymer lattice Boltzmann method. This will also serve to verify that the polymer LBM is a valid numerical method. One should be aware that at present the LBM has limitations with respect to boundary conditions.

In particular, actual displacement is not modelled, only strain at a specified position. Thus a displacement boundary condition is not currently possible, though a strain boundary condition is possible.

The creep experiment is isotonic and monitors the specimen stretch ($\boldsymbol{\lambda}_{sp}$) against time. For this experiment either ${}^{\langle app\rangle}\boldsymbol{\sigma}_{sp}(t)$ and ${}^{\langle app\rangle}\dot{\boldsymbol{\sigma}}_{sp}$ remain constant or ${}^{\langle app\rangle}\mathbf{T}$ and ${}^{\langle app\rangle}\dot{\mathbf{T}}$ remain constant as boundary conditions – depending on how the measured stress is defined (briefly discussed in Section 7.3). The specimen stretch is determined from Equation (9.45). The stress relaxation experiment is isometric. Isometry is defined by a constant specimen stretch $\boldsymbol{\lambda}_{sp}$ in the direction parallel to the applied force and stretch rate $\dot{\boldsymbol{\lambda}}_{sp} = 0$ in the direction parallel to the applied load. The apparent specimen stress, ${}^{\langle app\rangle}\boldsymbol{\sigma}_{sp}$, is monitored against time.

Given the limitations of the LBM, it is the stress relaxation experiment that will be modelled. The polymer LBM will thus be used to model the time required for a viscoelastic specimen to reach steady state under a predefined stress. The results of the numerical model are compared to the experimentally determined results. In addition, Section 12.2.1 does not document the stress as a function of time. This chapter will compare the numerically determined stress, as a function of time, to the stress relaxation stress versus time data determine in Section 12.2.1 but omitted there.

13.1 The stress relaxation prediction

Several stress relaxation experiments were conducted at various stretch rates and specimen stretches. At steady state all spatial derivatives of the principal stress are zero, stretch is uniformly distributed throughout the specimen and thus spatial derivatives of stretch and stretch rate are zero. Thus the specimen principal stress, based on Equation (7.17), reduces to

$$
\begin{aligned}
{}^{\langle app\rangle}\sigma_{sp1}(0) &= \nabla\cdot\mathbf{P}_D + \nabla\cdot\mathbf{P}_S && (13.1)\\
&= -\frac{\int_0^{L_0} p'_{dxx}dx}{L_0} - \frac{\int_0^{L_0} p'_{sxx}dx}{L_0}\\
&= \frac{\kappa R_{rms}^2}{6}\left({}^{(spec)}\lambda_x^2 - 1\right) - \frac{\kappa R_{rms}^2}{6}\left({}^{(spec)}\lambda_y^2 - 1\right)\\
&= \frac{\kappa R_{rms}^2}{6}\left({}^{(spec)}\lambda_x^2 - \frac{1}{{}^{(spec)}\lambda_x}\right) && (13.2)
\end{aligned}
$$

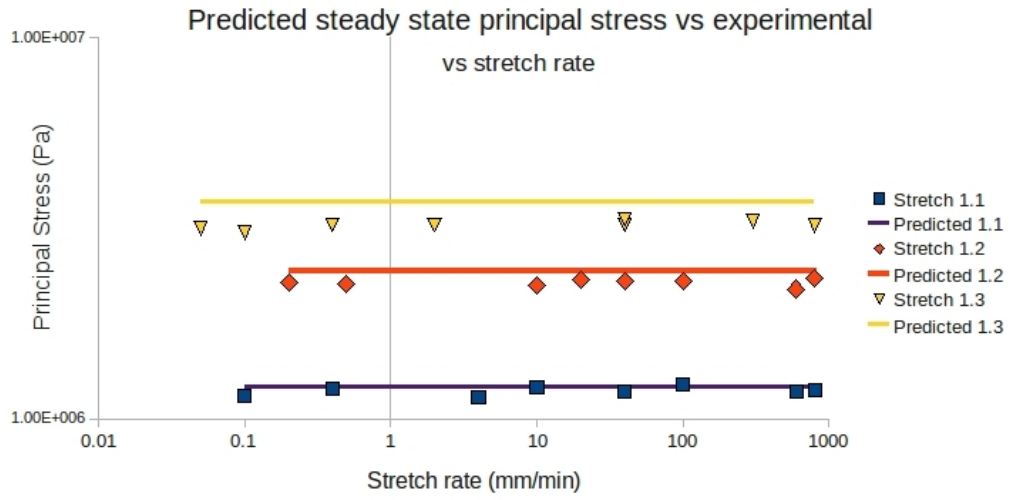

Figure 13.1: The solid lines are the steady state stresses predicted by the model while the icons represent the experimental results. Data has been stratified by specimen stretch.

where ${}^{(spec)}\lambda_x$ is the specimen principal stretch. Equation (13.2) was previously determined by Treloar ([138], Chapter 4) and reproduced by Equation (3.58) in Section 3.2.7. The predicted steady state stress versus stretch rate is depicted in Figure 13.1. The figure should be compared to Figure 12.3. It is noted that the theoretical prediction is greater than the experimental results. This can be explained in part by having stopped the experiment after half an hour. At half an hour, the change in stress was very low but not zero.

Appendix C (Equation (C-47)) provides a means of determining the initial material stretch distribution for various experimental (true latent specimen) principal stresses – where the potential material stretch distribution was described in Chapter 11. The effect of stretch rate on stretch distribution is depicted in Table 13.1. All the stretches and stretch rates in Table 13.1 that are not depicted in red could be determined using Equation (C-52) which corresponds to the distribution depicted in Figure 11.3(b). Although only the red stretch/stretch rate combinations had to be determined using (C-52), the stretch/stretch rate distributions depicted in blue were also determined using (C-52). All of the remaining stretch/stretch rate combinations could be determined either using (C-52) or (C-47) – where the latter corresponds to the distribution depicted in Figure 11.3(a). All the stretch/stretch rates in black were however determined using (C-47) – the results were more plau-

Stretch rate	**Specimen stretch**						
	1.1		**1.2**		**1.3**		
mm/min	$\eta_R(m^{-2})$	λ_m	$\eta_R(m^{-2})$	λ_m	$\eta_R(m^{-2})$	λ_m	$L_m\, ratio(\%)$
0.05					13148	0.86	55
0.1	280	0.103			11953	0.82	57
0.2			234	0.21			
0.4	2593	0.137			22300	1.12	40
0.5			711	0.22			
2					30976	1.32	36
10	4237	0.179	2567	0.27			
20			3543	0.32			
40	4296	0.181			51377	1.7	28
40			3764	0.33	72540	2.02	23
100	5352	0.26	4192	0.36			
300					81415	2.14	22
600	5729	0.25	4574	0.38			
800	5850	0.256	5389	0.46	82944	2.16	22

Table 13.1: NOTE THAT INITIAL REFERS TO THE TIME AT THE END OF THE RAMPING PHASE OF THE STRESS RELAXATION EXPERIMENT. EQUATION (11.8) DEFINES η_R, $\lambda_M = \frac{R_\mu \mathbf{0} - R_\mu^{(eq)}}{R_\mu^{(eq)}}$ WHERE $R_\mu^{(eq)}$ IS THE CHAIN LENGTH IN THE GROUND STATE AND $R_\mu \mathbf{0}$ IS THE MAXIMUM POSSIBLE STRETCH AS DEPICTED IN FIGURE 11.3(A). THE DOMAIN OVER WHICH THE CHAIN LENGTH IS NOT THE EQUILIBRIUM CHAIN LENGTH IS $[0, L_m]$ IS – AS DEPICTED IN FIGURE 11.3(A).

sible because the distribution of Figure 11.3(a) is anticipated with the higher stretch rates.

It must be recognised that the results of Table 13.1 were derived based on a diffusion equation approximation to the initial conditions defined by the end of ramping in the stress relaxation experiment. The actual differential equation is an example of the wave equation not the diffusion equation. An analytical solution to the wave equation could not be found. Similarly, the results of Section 13.2 are based on the diffusion equation approximation. As discussed in Section 11.1.2, the traditional symmetry about the short axis is assumed for pragmatic reasons. Under these conditions the $0.4\, mm/min$ stretch rate at 10% stretch gives $\eta_R = 12840$ and $\lambda_M = 0.15$.

13.2 Prediction of creep

Creep experiments were not conducted. However, the theory predicts that every principal stress has a unique steady state principal stretch given by

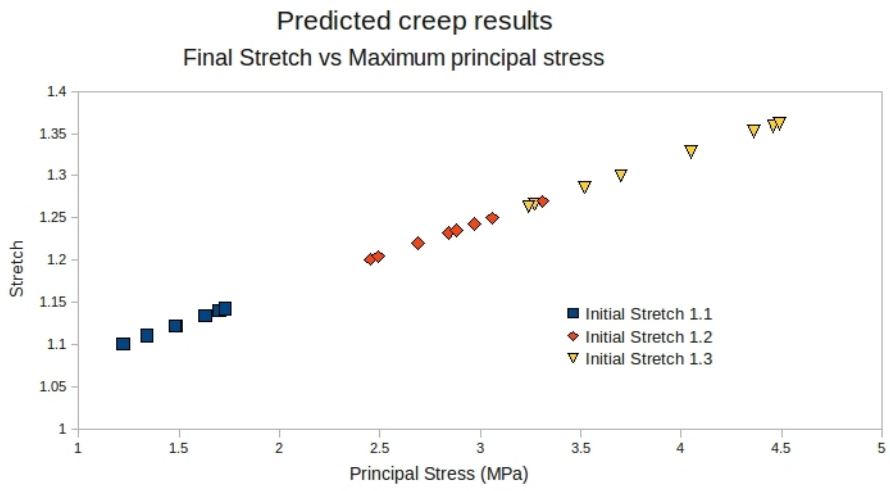

Figure 13.2: The predicted final stretch for a creep experiment conducted on pelethane. Results are stratified by initial stretch (end of ramping)

Equation (13.2). Thus, in a creep experiment, the steady state stretch can be predicted. The initial (end of ramping) stresses from the stress relaxation experiments are used to predict the final stretch. Thus a calculation of the final stretch was performed. The relationship between steady state stretch and initial principal stress is a consequence of Equation (13.2). The predicted relationship with stretch rate is depicted in Figure 13.3 and reflects the relationship between stretch rate and initial (end of ramping) principal stress. It is noteworthy that there appears to be a logarithmic relationship between change in stretch and stretch rate in the creep experiment. This may be because Equation (11.15) predicts a hyperbolic relationship between stretch rate and position for the diffusion equation approximation (11.2).

13.3 Common model requirements

The remainder of the chapter is devoted to modelling a real material where the specimen is in disequilibrium. A numerical model is required because an analytical solution could not be found to the polymer flow equation (6.98)

13.3.1 Macroscopic material constants

The material density is documented and in this case is $1150\,kg/m^3$. The value of κ was determined in Section 12.2.3 and equals $10.55\,GPa.m^{-2}$. Sec-

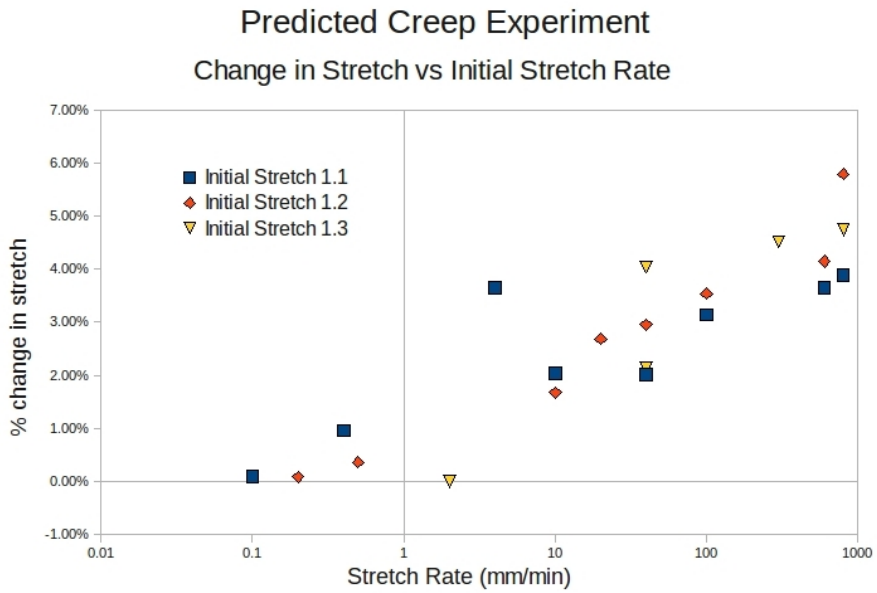

Figure 13.3: The predicted percentage change in stretch for a creep experiment conducted on pelethane depicting an apparent logarithmic relationship between stretch rate and steady state stretch. Results are stratified by initial stretch (end of ramping).

tion 12.2.5 determined that $G = 0.971 \times 10^{-6}\, MPa.s^{-1}$ and $\mu = -3.748 \times 10^{4}\, MPa.s$. The results are summarised in Table 13.2.

Material constant	**Value**	**Unit**
ρ	1150	kg/m^3
κ	10.55×10^9	$Pa.m^{-2}$
G	0.971	$Pa.s^{-1}$
μ	-3.748×10^{10}	$Pa.s$

Table 13.2: Material constants

The values of τ_R and $\tau_{\dot{R}}$ are obtained by solving for the 4 unknowns τ_R, $\tau_{\dot{R}}$, δt and δx in the three equations (10.3), (10.55) and (10.36) subject to the constraints $\tau_R > 0.5$ and $\tau_{\dot{R}} > 0.5$ where $\dot{R}_{rms}$ is given by (13.7).

13.3.2 Maximum entropy mesoscopic material constants

The constants in (12.1) have (in Section 12.2.2) been calculated to be

$$\begin{aligned} a = \frac{\mathrm{R}_{\mu 0x}^2 \kappa}{2} - 2\kappa \mathrm{R}_{\mu 0x} r_0 &= -2.30\, MPa \\ b = \mathrm{R}_{\mu 0x}^2 \kappa &= 8.06\, MPa. \end{aligned}$$

Then

$$\begin{aligned} -2\kappa \mathrm{R}_{\mu 0x}\mathrm{r}_0 = a - \frac{b}{2} \quad &\Longleftrightarrow \quad -\frac{2\mathrm{r}_0}{R_{rms}} = \frac{a-b/2}{b} \\ \Longleftrightarrow \quad \mathrm{R}_{\mu 0x} = -\frac{2b r_0}{a-b/2} \quad &\Longleftrightarrow \quad \mathrm{r}_0^2 = \frac{b(a-b/2)^2}{4b^2\kappa} \end{aligned} \tag{13.3}$$

where κ was calculated in Section 13.3.1. Therefore

$$\begin{aligned} \mathrm{r}_0 &= 1.09 \times 10^{-2}\, m = 10.9\, mm, \\ \mathrm{R}_{\mu 0x} &= 2.76 \times 10^{-2}\, m = 27.6\, mm, \end{aligned} \tag{13.4}$$

thereby establishing that the maximum possible length of the RVE is $10.9\, mm$ and the longest $R_{\mu 0x} = R_{rms}/\sqrt{3}$ is $27.6\, mm$, at steady state.

Physically, the results of (13.4) are absurd and it appears that stress is dependent on specimen size. The true latent material stress is defined by one of the constitutive Equations (7.15) or (7.16). Here, it is the LHS of the polymer flow equation (6.98) (that predicts the propagation of stretch and stretch rate) which is being equated to the true latent specimen stress under the very special condition of quasi-equilibrium – a surrogate for steady state. These experiments are being performed at steady state (and more importantly quasi-equilibrium) to ensure that material properties and specimen properties are equivalent. Given that, by the definition proposed in Section 1.1.1, the RVE is at a maximum at steady state and potentially is the size of the specimen; effectively one is determining the maximum possible size of the RVE and the longest possible $\mathbf{R}_{\mu 0}$.

The physical explanation for the large $\mathbf{R}_{\mu 0}$ is that the model was designed such that information/force is transmitted across the molecule instantaneously while the origin of time dependent behaviour is the delay in the interaction between molecules. In a quasi-equilibrium experiment the delays are negligible and consequently, from the perspective of the model, all the molecules act as one long molecule. This is the origin of the large calculated $\mathbf{R}_{\mu 0}$.

These maximum limits are necessary because the LBM is only valid for calculated $R_f \ll R_{rms}$. Finally it should be noted that the purpose of Section 13.3.2 is not to determine the mean molecular length but to determine parameters required in numerical modelling.

Given that Equations (8.43), (8.63), (13.3) and (13.4) relate R_{rms} and $\dot{R}_{rms}$,

$$\dot{\mathrm{R}}_{\mu 0x} = -\mathrm{R}_{\mu 0x}\sqrt{\frac{\kappa_0}{2\rho_0}} = -59.1\, m/s \tag{13.5}$$

where the negative sign indicates the molecular stretch rate is opposite in direction to molecular stretch. It is recognised that root mean square values are non-negative scalars and that $\dot{R}_{rms} = \sqrt{3\dot{\mathrm{R}}^2_{\mu 0x}}$. Also note that the numerical method is on a 2D projection of the 3D model and consequently for the purposes of the model, ${}^{[model]}R^2_{rms} = \frac{2}{3}R^2_{rms}$.

13.3.3 Non-maximum entropy mesoscopic material constants

For the non-maximum entropy state, the value of R_{rms} is transformed to R^*_{rms} by the affine deformation assumption and is given by (3.57). Therefore

$$R^*_{rms} = \lambda R_{rms} \qquad \text{and} \qquad \mathrm{R}^*_{\mu G} = \frac{R^*_{rms}}{\sqrt{3}} \tag{13.6}$$

where $\mathbf{R}^*_{\mu G}$ is the central measure in the non-maximum entropy state (see Section 3.2.5). Again the relationship between $\dot{R}^*_{rms}$ and R^*_{rms} is given by (8.63) such that

$$\dot{R}^*_{rms} = -\omega R^*_{rms} \tag{13.7}$$

for critical damping.

Non-critical damping can be introduced in two ways. The first is direct (see Section 8.4.3). The direct introduction of non-critical damping reduces (13.7) to

$$\dot{R}^{*\prime}_{rms} = -\omega' R^*_{rms} = -\frac{\omega}{\alpha}R^*_{rms}. \tag{13.8}$$

In Section 10.3 it was however shown that the direct method for non-critical damping does not reproduce Navier-Stokes-like numerical modelling. The alternative is indirect and is analogous to scaling the critical solution. In Section 10.1.3, Equation (10.38), it is shown how the latter implementation of non-critical damping is achieved. In short, stretch is not affected, the non-critically damped stretch rate is given by the critically damped stretch rate divided by α (see Section 8.4.3 and (10.38)) whilst the non-critically damped

time is α^2 multiplied by the critically damped time as summarised by

$$\dot{\mathbf{R}}_D' = \frac{\dot{\mathbf{R}}_D}{\alpha} \qquad \text{and} \qquad \delta t = \alpha^2 \delta t'$$

where the $\dot{\mathbf{R}}_D'$ is the non-critically damped chain stretch rate, $\dot{\mathbf{R}}_D$ is the critically damped chain stretch rate, $\delta t'$ is the critically damped time increment and δt is the non-critically damped time increment.

13.3.4 Initial chain length orientation

In Section 3.2.1, the coordinate system was constructed such that molecules were always biased in the direction of the applied force and the coordinate system for each molecule was force dependent. In the idealised representation that is the numerical model (the polymer LBM), it is noted that the coordinate system is invariant or fixed. In order to remain consistent with the theory, the idealised averaged representatives of the unstrained molecules are orientated such that they are aligned with the applied force.

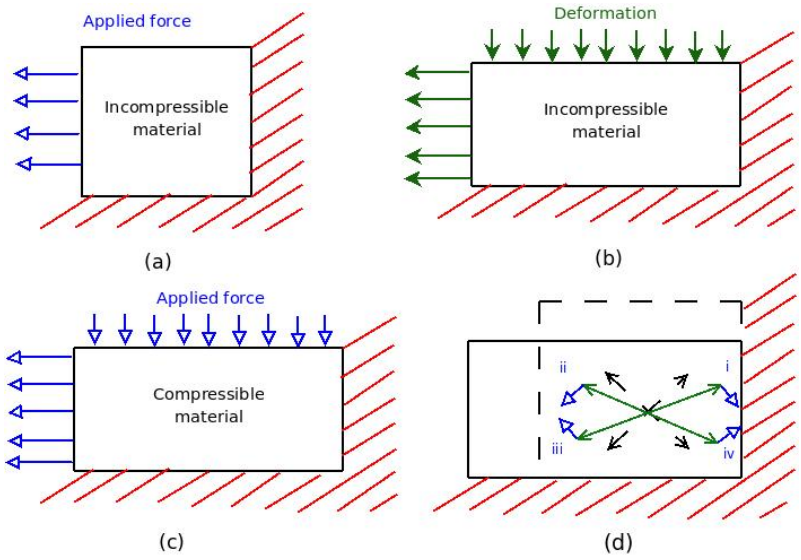

Figure 13.4: (A) Undeformed idealised incompressible RVE. (B) Deformation due to force applied to incompressible RVE. (C) Equivalent forces to generate the same deformation in a compressible material, (D) Deformation of molecules and the molecular forces required to induce the deformation. The RED hatched area represents symmetry.

Figure 13.4(a) depicts an idealised RVE in the undeformed state with the applied force. Figure 13.4(b) depicts the same incompressible RVE deformed

with the direction of the deformation indicated. Figure 13.4(c) depicts the forces that would have to be applied to produce the same deformation as in 13.4(b) for a compressible material. In Figure 13.4(d) the dashed lines represent the undeformed specimen and the solid lines represent the deformed specimen. The dashed arrows represent averaged molecules. The corresponding green arrows represent deformed molecules. Figure 13.4(d) depicts the deformation of potential representatives of the averaged molecules and the forces that would induce such changes. When comparing the forces that would induce the desired changes in the molecules to the forces that would induce the equivalent deformation in a compressible material (Figure 13.4(c)), it is apparent that in Figure 13.4(d) molecular orientation (ii) has the force that corresponds Figure 13.4(c). It is therefore molecular orientation (ii) that is selected to represent the average of the collection of unstrained idealised molecules in the RVE.

13.3.5 The maximum entropy function formulation

Equations (8.30) represent the maximum entropy function for stretch. Two formulations exist: compressible and incompressible. Both will be presented. Given that Equations (10.12) and (10.2) require that

$$\kappa_0 \mathbf{R}_\mu = \sum_{\sigma i} \kappa_{\sigma i} R_{rms} \boldsymbol{\epsilon}_{\sigma i} = \sum_{\sigma i} \hat{\boldsymbol{\kappa}}_{\sigma i} R_{rms} \tag{13.9}$$

where $\hat{\boldsymbol{\kappa}}_{\sigma i} = \kappa_{\sigma i} \boldsymbol{\epsilon}_{\sigma i}$, the incompressible formulation of (8.30) is obtained by substitution of (13.9) to obtain

$$\begin{aligned}
\kappa_{01}^{(ms)} &= \frac{4}{9}\kappa_0 - \frac{2}{3}\kappa_0 \Big(\frac{\kappa}{\kappa_0}\Big)^2 \\
\kappa_{1i}^{(ms)} &= \frac{1}{9}\kappa_0 + \frac{1}{3}\kappa_0 (\frac{\hat{\boldsymbol{\kappa}}_{\sigma i}}{\kappa_0} \cdot \boldsymbol{\epsilon}_{1i}) + \frac{1}{2}\kappa_0 (\frac{\hat{\boldsymbol{\kappa}}_{\sigma i}}{\kappa_0} \cdot \boldsymbol{\epsilon}_{1i})^2 - \frac{1}{6}\kappa_0 \Big(\frac{\kappa}{\kappa_0}\Big)^2 \\
\kappa_{2i}^{(ms)} &= \frac{1}{36}\kappa_0 + \frac{1}{12}\kappa_0 (\frac{\hat{\boldsymbol{\kappa}}_{\sigma i}}{\kappa_0} \cdot \boldsymbol{\epsilon}_{2i}) + \frac{1}{8}\kappa_0 (\frac{\hat{\boldsymbol{\kappa}}_{\sigma i}}{\kappa_0} \cdot \boldsymbol{\epsilon}_{2i})^2 - \frac{1}{24}\kappa_0 \Big(\frac{\kappa}{\kappa_0}\Big)^2
\end{aligned} \tag{13.10}$$

where

$$\kappa^2 = \Big(\sum_{\sigma i} \hat{\kappa}_{\sigma i x}\Big)^2 + \Big(\sum_{\sigma i} \hat{\kappa}_{\sigma i y}\Big)^2.$$

The compressible formulation uses (13.9) but is based on instantaneous κ:

$$\begin{aligned}
\kappa_{01}^{(ms)} &= \frac{4}{9}\kappa - \frac{2}{3}\kappa\Big(\frac{\kappa}{\kappa}\Big)^2 \\
\kappa_{1i}^{(ms)} &= \frac{1}{9}\kappa + \frac{1}{3}\kappa(\frac{\hat{\boldsymbol{\kappa}}_{\sigma i}}{\kappa}\cdot\boldsymbol{\epsilon}_{1i}) + \frac{1}{2}\kappa(\frac{\hat{\boldsymbol{\kappa}}_{\sigma i}}{\kappa}\cdot\boldsymbol{\epsilon}_{1i})^2 - \frac{1}{6}\kappa\Big(\frac{\kappa}{\kappa}\Big)^2 \\
\kappa_{2i}^{(ms)} &= \frac{1}{36}\kappa + \frac{1}{12}\kappa(\frac{\hat{\boldsymbol{\kappa}}_{\sigma i}}{\kappa}\cdot\boldsymbol{\epsilon}_{2i}) + \frac{1}{8}\kappa(\frac{\hat{\boldsymbol{\kappa}}_{\sigma i}}{\kappa}\cdot\boldsymbol{\epsilon}_{2i})^2 - \frac{1}{24}\kappa\Big(\frac{\kappa}{\kappa}\Big)^2
\end{aligned} \tag{13.11}$$

where

$$\kappa = \sum_{\sigma i}\kappa_{\sigma i}.$$

Similarly, for stretch rates, from (10.12) and (10.3)

$$\begin{aligned}
\rho_0\frac{\dot{\mathbf{R}}_\mu}{2} &= \sum_{\sigma i}\rho_{\sigma i}\frac{\dot{R}_{rms}}{2}\boldsymbol{\epsilon}_{\sigma i} = \hat{\boldsymbol{\rho}}_{\sigma i}\frac{\dot{R}_{rms}}{2} \\
\iff \rho_0\dot{\mathbf{R}}_\mu &= \sum_{\sigma i}\hat{\boldsymbol{\rho}}_{\sigma i}\dot{R}_{rms}.
\end{aligned} \tag{13.12}$$

Therefore the incompressible formulation of the stretch rate maximum entropy function (8.37) reduces to

$$\begin{aligned}
\rho_{01}^{(ms)} &= \frac{4}{9}\rho_0 - \frac{2}{3}\rho_0\Big(\frac{\rho}{\rho_0}\Big)^2 \\
\rho_{1i}^{(ms)} &= \frac{1}{9}\rho_0 + \frac{1}{3}\rho_0\Big(\frac{\hat{\boldsymbol{\rho}}_{\sigma i}}{\rho_0}\cdot\boldsymbol{\epsilon}_{\sigma i}\Big) + \frac{1}{2}\rho_0\Big(\frac{\hat{\boldsymbol{\rho}}_{\sigma i}}{\rho_0}\cdot\boldsymbol{\epsilon}_{\sigma i}\Big)^2 - \frac{\rho_0}{6}\Big(\frac{\rho}{\rho_0}\Big)^2 \\
\rho_{2i}^{(ms)} &= \frac{1}{36}\rho_0 + \frac{\rho_0}{12}\Big(\frac{\hat{\boldsymbol{\rho}}_{\sigma i}}{\rho_0}\cdot\boldsymbol{\epsilon}_{\sigma i}\Big) + \frac{\rho_0}{8}\Big(\boldsymbol{\epsilon}_{\sigma i}\cdot\frac{\hat{\boldsymbol{\rho}}}{\rho_0}\Big)^2 - \frac{\rho_0}{24}\Big(\frac{\rho}{\rho_0}\Big)^2
\end{aligned} \tag{13.13}$$

where

$$\rho = \sum_{\sigma i}\rho_{\sigma i}$$

and the compressible formulation is

$$\begin{aligned}
\rho_{01}^{(ms)} &= \frac{4}{9}\rho - \frac{2}{3}\rho\Big(\frac{\rho}{\rho}\Big)^2 \\
\rho_{1i}^{(ms)} &= \frac{1}{9}\rho + \frac{1}{3}\rho\Big(\frac{\hat{\boldsymbol{\rho}}_{\sigma i}}{\rho}\cdot\boldsymbol{\epsilon}_{\sigma i}\Big) + \frac{1}{2}\rho\Big(\frac{\hat{\boldsymbol{\rho}}_{\sigma i}}{\rho}\cdot\boldsymbol{\epsilon}_{\sigma i}\Big)^2 - \frac{\rho}{6}\Big(\frac{\rho}{\rho}\Big)^2 \\
\rho_{2i}^{(ms)} &= \frac{1}{36}\rho + \frac{\rho}{12}\Big(\frac{\hat{\boldsymbol{\rho}}_{\sigma i}}{\rho}\cdot\boldsymbol{\epsilon}_{\sigma i}\Big) + \frac{\rho}{8}\Big(\boldsymbol{\epsilon}_{\sigma i}\cdot\frac{\hat{\boldsymbol{\rho}}_{\sigma i}}{\rho}\Big)^2 - \frac{\rho}{24}\Big(\frac{\rho}{\rho}\Big)^2.
\end{aligned} \tag{13.14}$$

Given the focus of this work, only the incompressible formulation will be used in the models.

13.4 Evaluating the numerical method

Before modelling a real material, a fictitious material is constructed to test whether the numerical method works. The evaluation is based on two criteria: (a) at steady state, it is anticipated that the stretch is uniformly distributed and the stretch rate is zero. The second is that the time to steady state should be physically appropriate.

13.4.1 Prediction of time-dependent viscoelastic behaviour

The fictitious material has $\mu = -3.748 \times 10^{10}\, Pa.s$, $\kappa = 10.55e \times 10^{9}\, Pa/m^2$ and $\rho = 1150\, kg/m^3$. Figure 13.5 shows the specimen pressure (zero-order stress) versus run number for an example of the above material with $G = 9.71 \times 10^{6}\, Pa.s^{-1}$ and $\tau_R = 1.2$. The initial condition had a curved vector length profile along the length of the specimen with zero stretch rate. Of

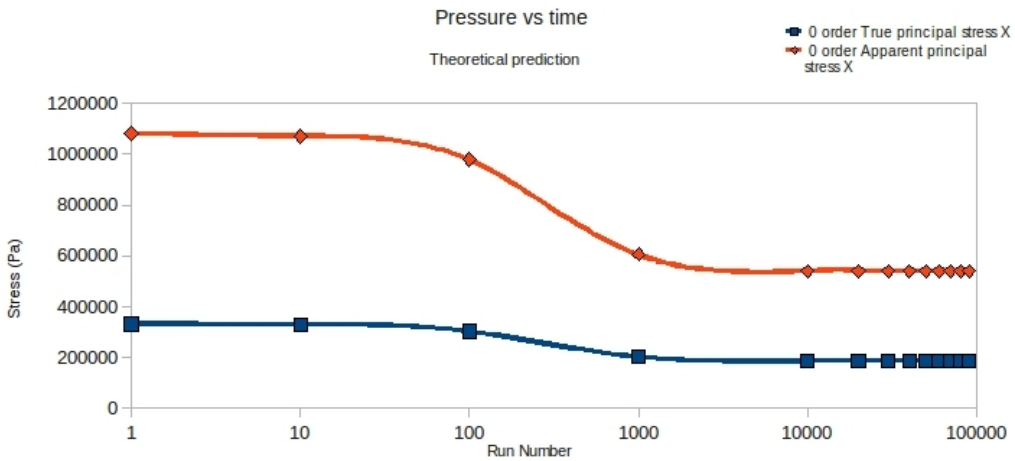

Figure 13.5: This specimen has material properties $\mu = -3.748 \times 10^{10}\, Pa.s$, $\kappa = 10.55 \times 10^{9}\, Pa/m^2$, $\rho = 1150\, kg/m^3$ and $G = 9.71 \times 10^{6}\, Pa.s^{-1}$. The relaxation constant $\tau_R = 1.2$. The time increment $\delta t = 4.92 \times 10^{-7}\, s$ corresponds to critial damping. The logarithm of the x-axis is used.

note, the model appears to provide the correct form for the stress relaxation experiment. Two result are, however, of concern. The first is that the specimen stress at steady state appears too low relative to the original and the second is the time increment. For the above material, the initial distribution of stress throughout the specimen is depicted in Figure 13.6 where the BCs applied are three surfaces duplicated and one with fixed stretch – here 1.1.

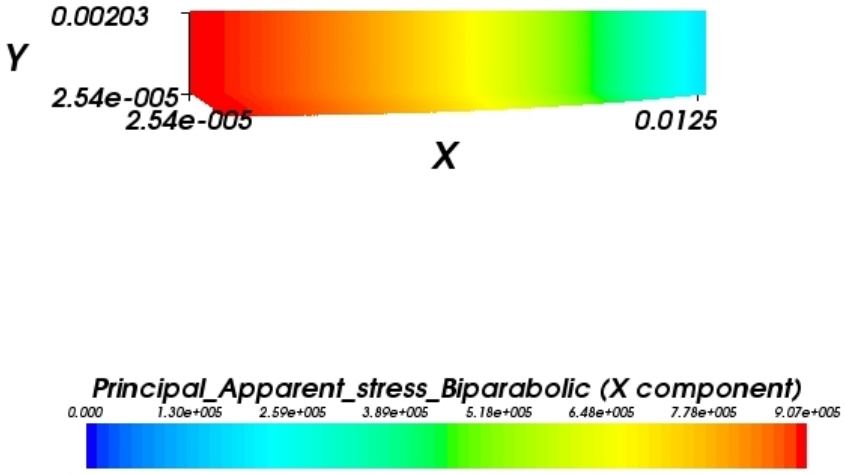

Figure 13.6: The vector direction is such that the x-component is positive and y-component is negative – indicating tension in the x-direction and compression in the y-direction.

The distribution of stretch over the length of the specimen for various times is depicted in Figure 13.7. Of note the stretch distribution is becoming

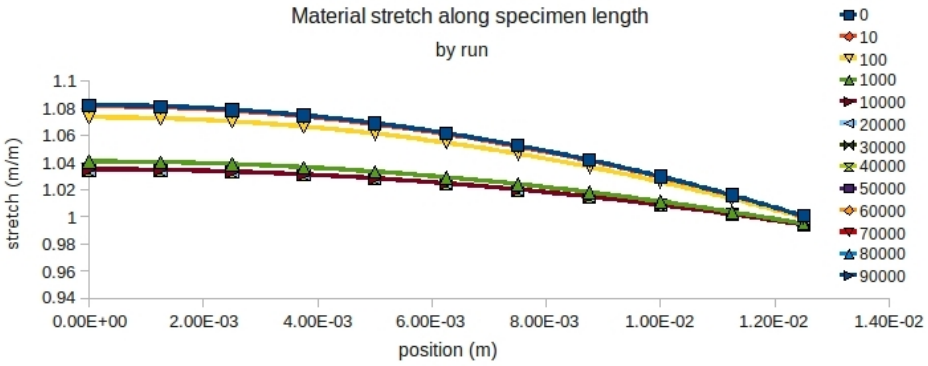

Figure 13.7: The x-axis is the position along the length of the undeformed specimen. The position $x = 0$ corresponds to the mobile edge of the specimen. The y-axis is the stretch in the x-direction.

more uniform as predicted. However, it was predicted that the stretch would become uniformly distributed about 1.1. Furthermore the area under the curve should remain constant – representing constant specimen length.

13.4.2 The effect of relaxation constant

Figure 13.8 depicts the effect of critical damping on the stress relaxation experiment for a material with $G = 9.71 \times 10^6\, Pa.s^{-1}$. Note that the time to

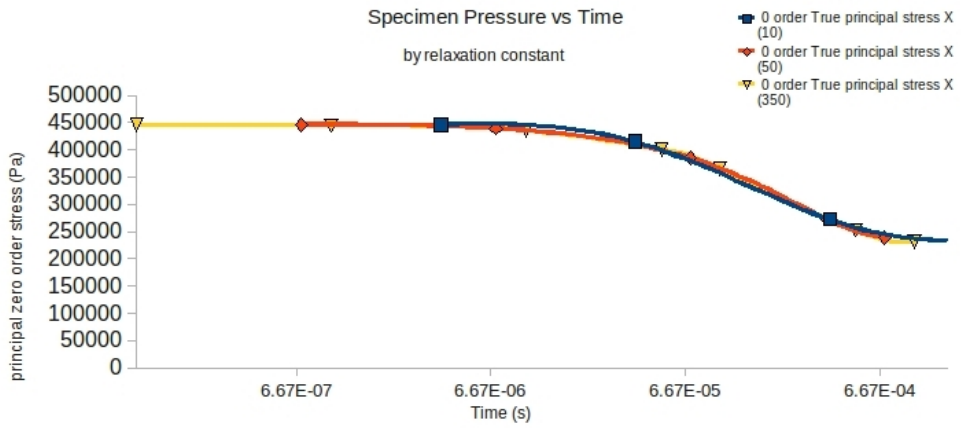

Figure 13.8: The model is for critical damping. The x-axis is time with zero order stress charted on the y-axis. The relaxation constant τ_R is in brackets in the legend.

steady state remains constant.

13.4.3 The effect of non-critical damping

Two forms of non-critical damping can be applied. The first is direct damping as described in Section 8.4.3. The second is indirect damping as described in Section 10.1.3. This section explores the effect of the direct application

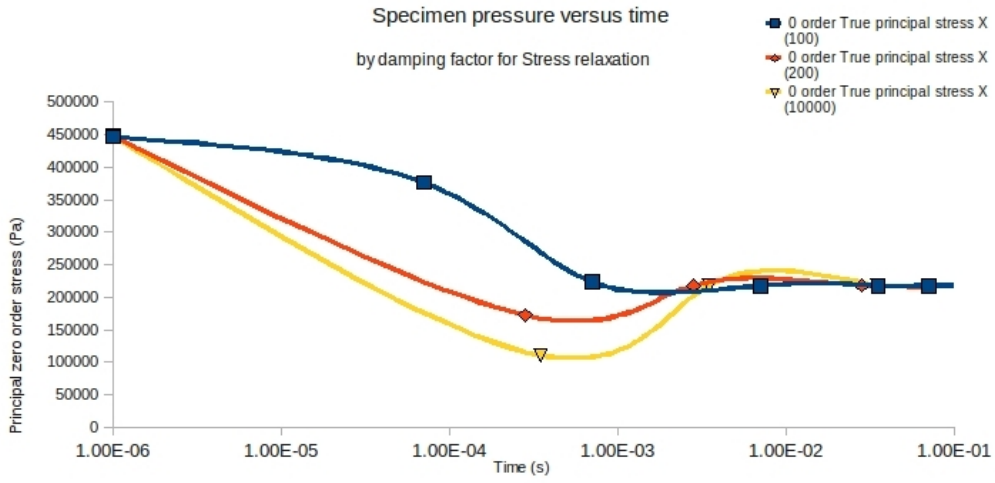

Figure 13.9: The x-axis is time from the onset of stress relaxation and the y-axis is the zero order principal stress in the x-direction. The damping constant α of Section 8.4.3 is in brackets in the legend.

of non-critical damping. It is noted that Section 10.3 shows that the appli-

cation of direct non-critical damping does not reproduce Navier-Stokes-like equations. Figure 13.9 depicts the effect of damping on zero-order stress over time and also the effect of direct damping to the time required to reach steady state for the above fictitious material with $G = 971 \times 10^6\, Pa.s^{-1}$ and $\tau_R = 50$. Note that the time to steady state is independent of direct damping.

13.4.4 Boundary condition evaluation

The effect of the BC on the zero-order stress, for critical damping, is depicted in Figure 13.10 for a material with $G = 9.71 \times 10^6\, Pa.s^{-1}$. The BC has a

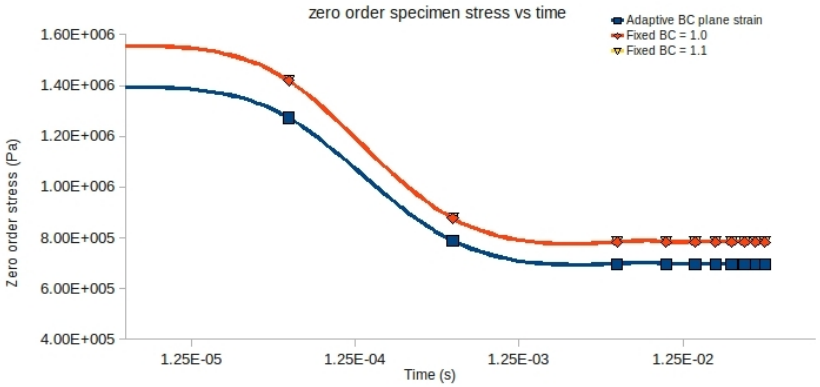

Figure 13.10: The x-axis is the logarithmic scale for time from the onset of the isometric phase in the stress relaxation. The fixed BC is either $\lambda_x = 1.0$ or $\lambda_x = 1.1$. The adaptive BC is full adapt.

negligible effect on the stress. The difference in measured stress is due to the initial stress. The absence of an effect of the BC is because the effect is not propagating through the specimen. To confirm that the stretch is not propagating through the specimen, a model was created with half of the specimen at stretch 1.0 and the remainder at stretch 1.2. The stretch along the specimen is depicted in Figure 13.11. Note that the stretch does not propagate through the specimen as is required by the theory.

13.5 Computational constraints

It is desirable to have as large a value for τ_R and $\tau_{\dot{R}}$ as is possible. Given equations (10.36) and (10.55) it is an absolute requirement that $\tau_R > 0.5$ and $\tau_{\dot{R}} > 0.5$. It is also evident, from (10.36) and (10.55), that the discretisation of the physical space (δx) and the discretisation of time (δt) is dependent on

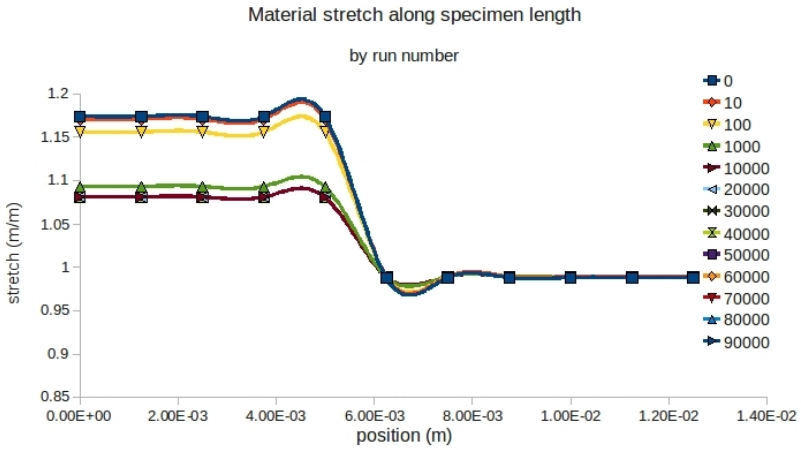

Figure 13.11: This specimen has half the specimen unstrained and the other half strained. In theory the stretch should propagate along the specimen length over time.

the material constants G and μ. The discritisation is related to the number of nodes which can be modelled which is limited by the programming language. In C++ the maximum size of long integer is 2147483647. This represents the theoretical maximum number of nodes. This may or may not further be inhibited by the memory constraints of the hardware. 64 bit integer types have as yet not been standardised in C++.

For the specimen modelled here, the ratio of length to height is 6 and thus the maximum number of nodes along the length is 113511, $\delta x \geq 1.1 \times 10^{-7}\, m$ and $\tau_R \leq 0.500044$. This is sub-optimal [89, 126] – leading to instability. It should be noted that the physical memory may or may not permit this number of nodes. The results presented will be for $\tau_R = 0.500002$ and $\tau_R = 0.500005$. The latter corresponds to the memory limit.

13.6 Specimen stress vs time

This section compares the indirect application of non-critical damping model results to an experiment. Three models are compared to the experimental result. The difference is in the initial and boundary conditions. One model uses an adapive BC with plane strain at the boundaries. A second model uses an adaptive BC subject to the constraint $\lambda_1\lambda_2^2 = 1$. The third model uses fixed BC with stretch at boundaries equal to 1.1. The results are depicted in Figure 13.12(a) where the time axis is not logarithmic while Figure 13.12(b)

is on a logarithmic time scale. This experiment is for a real specimen with $G = 0.971\,Pa.s^{-1}$ and damping factor $\alpha = 2000$.

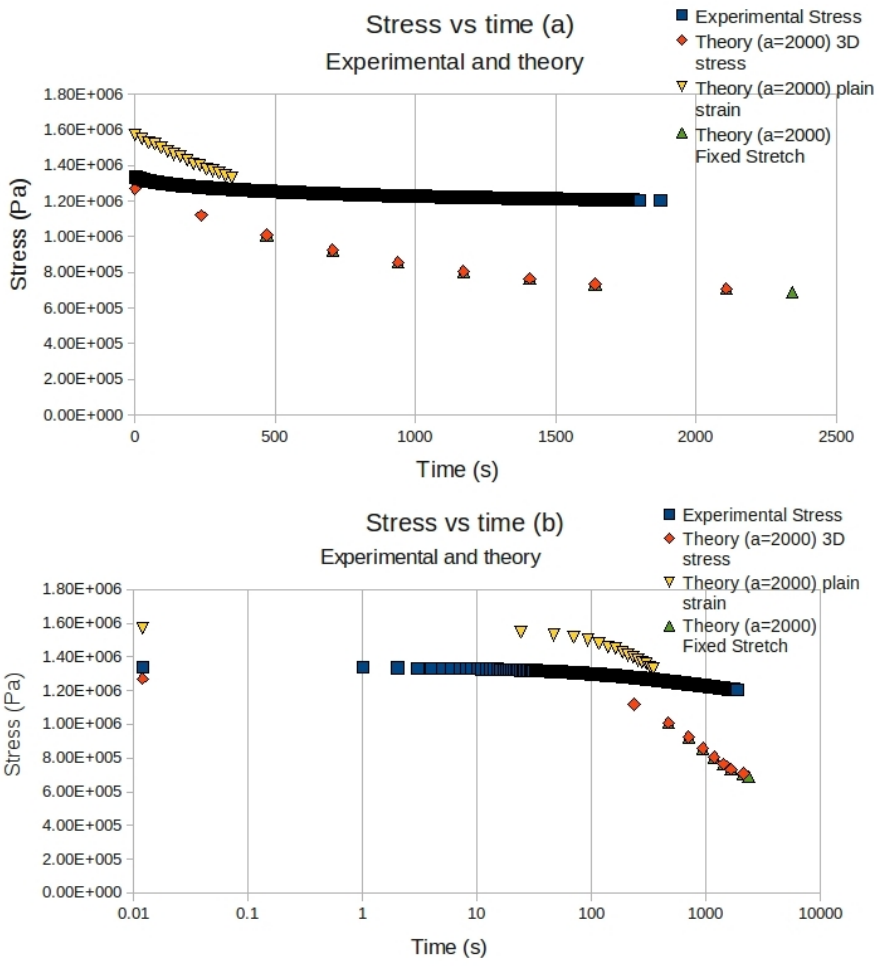

Figure 13.12: Indirect non-critical damping: (a)Comparison of model and experimental stress versus time. (b)Comparison of model and experimental stress on a logarithmic time scale.

It is evident that the predicted stresses decay much faster than is compatible with experiment. A small part of this is because the experiment has as yet not reached steady state. Superficially, the results can become more compatible by increasing the factor α. The bulk of the discrepancy is because of failure to maintain specimen length because the stretch does not propagate through the specimen.

Chapter 14

Discussion

Several observations are noted with respect to experimentation. These can be explained by the wave-like propagation of stretch (presented in Section 3.1.2 and depicted by Figure 3.3). This wave-like propagation of vector length and the Gaussian distribution of vector length form the basis of this thesis.

14.1 Reconciliation of mathematical description and physical interpretation

Vocabulary has been introduced to facilitate physical interpretation. This thesis switches between purely mathematical descriptions and physically relevant descriptions. This is most evident in Chapter 6 where the zero-order approximation is alternatively described as the maximum entropy approximation and the first order approximation is described as the non-maximum entropy approximation. These terms should not be used interchangeably.

The zero-order and first-order approximations are purely mathematical consequences of the Chapman-Enskog expansion. The maximum entropy approximation is a physical term consistent with the zero-order mathematical approximation and thus provides physical interpretation to the mathematical approximation. Similarly, the concept of non-maximum entropy approximation provides physical interpretation to the higher-order approximations.

It may thus seem arbitrary and superfluous to have generated the distinction between the macroscopic material description and the mesoscopic description in Chapter 3 and in particular in Table 3.1, given the uniformity of the mathematical description. However, this distinction and isolation im-

proves physical interpretation.

14.2 Viscoelasticity

A distinction has to be generated between specimen viscoelasticity (which is measured) and material viscoelasticity. The latter is defined by a volume sufficiently small such that in a specified period of time the properties of all the constitutive molecules are common. Molecular viscoelasticity is not measured.

This document's theory predicts that the phenomenon of viscoelasticity is a consequence of the redistribution of stretch and stretch rate towards steady state in a specimen – described by the LHS of Equation (6.98). Given the analogy between the polymer flow equation (6.98) and the Navier-Stokes equation, it is predicted that an analytical solution does not, as yet, exist.

Stretch and stretch rate redistribute towards steady state at a rate. If this rate of redistribution is greater than the rate of change of the applied force, one would predict that macroscopically the specimen is observed to be in quasi-equilibrium. Conversely, if the rate at which the specimen approaches steady state is significantly less than the rate of change of the applied force, the specimen will always be in a state of disequilibrium. When the rate of change of the applied force is zero – the isotonic creep experiment – specimen elongation will be observed as the specimen approaches steady state. The isometric stress relaxation experiment also applies a force to reach the fixed stress. The measured specimen stretch is initially the consequence of the cumulative stretches of the proximal layers of molecules as given by Equation (7.24). The observed stress relaxation is a consequence of the redistribution of stretch such that the vector length is common throughout the specimen. The measured (true apparent specimen) stress is a function of the stretch and stretch rate of the most proximal layer of molecules as given by (7.26).

Section 7.2 presents a modified Kelvin-Voigt model of viscoelasticity as being the one-dimensional representation of Equation (7.15). This represents the viscoelastic response of a collection of molecules in a volume sufficiently small for properties to be common to all the molecules – a representative volume. This is material viscoelasticity.

The above description may be considered to be either a mesoscopic phenomenon or a macroscopic phenomenon. In this work, viscoelasticity is considered to be a macroscopic phenomenon – although Table 3.1 demonstrates that analogues between the material and mesoscopic descriptions often exist. The reason is that one can argue that the mesoscopic description is a compromise – because one cannot predict the behaviour of one molecule. Thus the mesoscopic description is a proxy representation of one molecule. Viscoelasticity, however, is not a property of a molecule – it is a phenomenon due to the interaction between molecules. Thus one should conclude that (in this model) viscoelasticity is not a mesoscopic phenomenon. One could counter-argue that, considering interacting molecular pairs as a unit, the mesoscopic description could be a proxy for the description of two molecules and that then the mesoscopic description could include viscoelastic phenomena. It is noted that the former description (mesoscopic description of one molecule) generates a paradox because a macroscopic phenomenon cannot be represented mesoscopically – there is loss of information translating from macroscopic to mesoscopic which usually only occurs in the opposite direction.

A specimen is a collection of such molecules or representative volumes. The viscoelastic response of a specimen is the consequence of several of the modified Kelvin-Voigt idealisations as represented by Figure 7.5 in series. The specimen viscoelasticity is predicted by Equation (6.98).

Viscoelasticity is a phenomenon and differs from a property because specimen phenomena are not necessarily averages of material phenomena – as demonstrated in this work. For viscoelasticity, the specimen viscoelasticity is due to the redistribution of stretch along the specimen to the maximum entropy stretch distribution.

14.3 Prediction and theory validation

The experiments that were conducted in Section 12.1.1 to confirm that creep and plasticity do not occur in those specimen under those particular stretches and stretch rates (exclusion of creep experiments) would indicate that the rate of relaxation towards ground state is proportional to the stretch rate and inversely proportional to maximum specimen stretch. This result is tabulated in Table 12.2. The sample size is insufficient to confirm the above observation. The relationship to strain is intuitively correct. The relation-

ship to stretch rate can be predicted by the wave-like stretch propagation assumption. At lower stretch rates, during the course of the experiment, there is more time for the specimen to approach steady state. Alternatively, a greater proportion of the specimen is stretched. Consequentl,y in the relaxation towards ground state, a greater proportion of the specimen has to relax and this takes longer.

The experiments conducted in Section 12.1.3 to confirm that stress relaxation does not occur in those specimens under particular loading conditions (exclusion of stress relaxation experiments) indicate that the time to ground state is proportional to the stretch rate. This would be predicted by the theory. More data is required to confirm the observation.

14.4 Continuum hyper- and viscoelasticity

The Ogden theory of hyperelasticity and the Rivlin-Green theory of viscoelasticty are mathematical theories that form the supersets of mathematical theories of hyperelasticity and viscoelasticity respectively. Furthermore, Ogden theory is a subset of Rivlin-Green theory. The strength of these theories lies in their excellent agreement with experiment. The agreement with experiment is due to their mathematical generality. The strength of these theories is also their weakness. Their generality is a consequence of their purely mathematical nature but it is their purely mathematical nature that detaches them from simple physical principles.

Given their mathematical generality, these continuum theories can be constructed such that, under the appropriate constraints, they can produce the same results as the more trivial statistical models of Treloar and of this work. However, the mesoscopic theory does not detach from the underlying physics. As a consequence, it has been possible to recognise the distinction between material viscoelasticity and specimen viscoelasticity and to relate these to the microscopic and mesoscopic architecture. Furthermore, a rational basis to the experimental determination of the material constants has been formulated and these constants necessarily have a physical interpretation.

It must be recognised that this theory is not designed to predict the full range of hyperelasticity. This requires a consideration of molecular

flow/slippage/plastic deformation. Thus the full range of hyperelasticity cannot negate the effect of $\acute{\boldsymbol{c}}$ in the probabilty distribution function (3.1). However the limits to which the theory can be applied both with respect to stretch rate and stretch have not been established.

A comparison of Ogden's hyperelastic theory and Rivlin-Green viscoelastic theory with the mesoscopic maximum entropy theory presented in this document needs to be made. It has been demonstrated that the Ogden and Rivlin-Green theories represent supersets in their respective categories and that, given that these are supersets, they contain the maximum entropy theory contained in this document. It has, however, not been shown that the maximum entropy theory contains Ogden and Rivlin-Green theory. This may be possible. The maximum entropy theory presented in this document was only expanded to zero and first order. It is plausible that when expressed to n^{th} order where $n \rightarrow \infty$, it can be shown to contain both Ogden and Rivlin-Green where Ogden is a subset of Rivlin-Green. This would establish the equivalence of Rivlin-Green and the n^{th} order Chapman-Enskog expansion of the maximum entropy theory.

It should be recognised that the mesoscopic theory produces a finite strain equation for chain length. It is the Chapman-Enskog expansion applied to first order which reduces the finite strain mesoscopic theory to the infinitesimal strain macroscopic theory. The numerical method is based directly on the finite strain mesoscopic theory. The value of determining higher order Chapman-Enskog expansions lies in determining the experimental constants and in extracting more accurate macroscopic entities like stress. It should however be recognised that the numerical method does not use stress directly.

14.5 Experimental principles

This document distinguishes between specimen viscoelasticity and material viscoelasticity. In order to determine material properties, it is necessary to negate specimen phenomena. Specimen phenomena approximate material phenomena when the specimen is in quasi-equilibrium. Quasi-equilibrium can only be achieved at very slow stretch rates – effectively allowing the specimen time to reach steady state.

Given that the observed phenomenon of viscoelasticity is assumed to be

specimen viscoelasticity, the material constants can only be determined when viscoelasticity is negligible.

Although the stretch rate of 0.5 mm/min still produced stress relaxation, this was only marginally beyond the limit of statistically significant difference. It is believed that a slower stretch rate would negate viscoelasticity. The experiment was limited by the lower limit for stretch rate of the testing rig.

14.6 Material constants

The material constants can be divided into two categories. The first is physical material constants and the second is numerical model material constants. The former has the conventional meaning of material constant – a property which is independent of the state of the material or its environment. Oddly the same concept may not have the value in the physical space as it does in the modelling space – the numerical model is an abstract representation of the physical model which is also a representation of the real world. Some properties retain their values between the spaces.

14.6.1 Numerical model material constants

In Section 13.3.2, the RVE size (r_0), the mean value of the chain length ($R_{\mu 0x}$) and consequently the mean value of the chain stretch rate were calculated at quasi-equilibrium. This resulted in physically improbable $R_{\mu 0x} = 27.6\,mm$ and $r_0 = 10.9\,mm$. The origin of these improbable values is that, for the numerical model, the size of a molecule is not determined by its physical length, but by the delay in the interaction between the molecules. Since these experiments are being performed at quasi-equilibrium conditions, no delay in interaction is apparent and thus all the (physical) molecules behave (collectively) as one large molecule or magniectomer. Thus the magniectomer will be defined as the representative molecule that is predicted in quasi-equilibrium experiments and is due to all the molecules behaving (or responding) to external forces in unison because delays are negligible. Similarly (by the RVE definition proposed in Section 1.1.1) all the physical molecules are similar and thus the RVE approximates the whole specimen – or half a specimen in this case. These parameters represent the maximum limits on the RVE size and the R_{rms}, respectively, to be used in numerical modelling.

14.6.2 Physical constants

The most alarming of the physical constants is the viscous term – μ – which is negative. To explain this result, and the paradoxes it will generate, one should recognise that there are at least two interpretations of the uniaxial tensile test. These interpretations are a consequence of the model used to construct this thesis.

One should recognise that the (physical) model that that has been constructed in this thesis is for a pair of interacting molecules (described in Section 4.1 where the molecules are represented as a mass-and-spring unit and are depicted in Figure 4.2). As discussed in Sections 13.3.2 and 14.6.1, in the quasi-equilibrium uniaxial tensile test (which has also been used to calculate μ) the molecular length is the size of the whole specimen because no delay in molecular interaction exists along the length of the specimen. Given that model is for pairwise interaction, there must be a second (virtual) magniectomer subject to the constraints depicted in Figure 4.1.

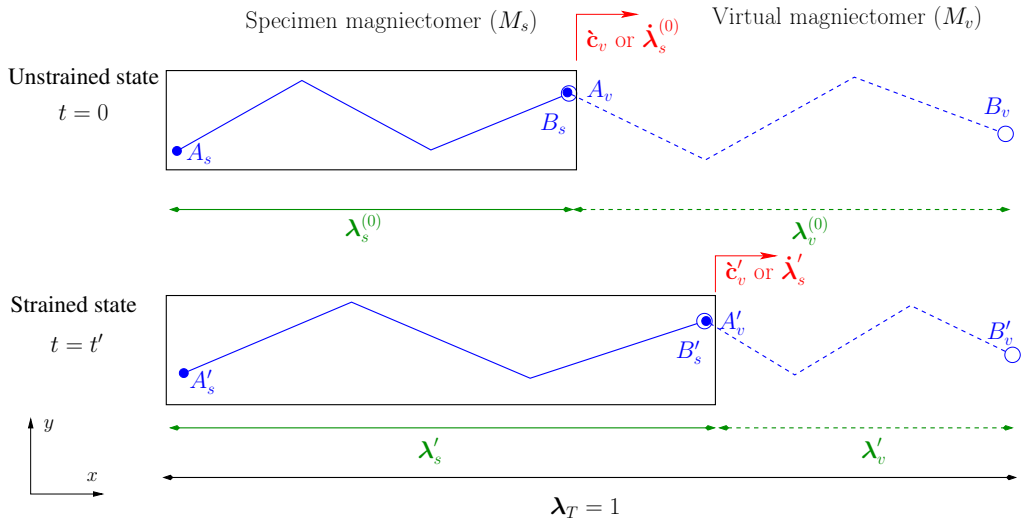

Figure 14.1: An initial unstrained state at $t = 0$ and a strained state at $t = t'$ are depicted in this idealisation of the uniaxial tensile test. Representative magniectomers are depicted in BLUE with the virtual magniectomer dashed. The mass is at position A for the respective magniectomers. The stretches are represented in GREEN and the velocities and stretch rates in RED. The specimen is in BLACK.

Figure 14.1 depicts the specimen magniectomer and the corresponding virtual magniectomer required for the uniaxial tensile test. Implicitly, all of the variables are functions of time. The viscous constant μ was calculated

from Equation (12.22) where the variables $\dot{\boldsymbol{\lambda}}_s(t)$ and $\boldsymbol{\lambda}_s(t)$, from Figure 14.1, were substituted into $\dot{\boldsymbol{\lambda}}$ and $\boldsymbol{\lambda}$, respectively, in Equation (12.22). This substitution resulted in a negative μ.

The negative μ may or may not generate paradoxes. The first paradox is that the material stress decreases with increasing stretch rate. At quasi-equilibrium, the material stress reduces to the measured specimen stress which is known to increase with stretch rate. However, the greater the stretch rate, the less appropriate the quasi-equilibrium approximation becomes and, consequently, the material stress cannot reduce to specimen stress. The greater the stretch rate, the less homogenous the stretch distribution and, consequently, the measured specimen stress increases.

The second paradox is that, in the absence of an elastic component, the Kelvin-Voigt model should reduce to a Newtonian fluid. Such a Newtonian fluid should have a positive viscous coefficient – μ. The potential paradox is due to the definition of μ. The viscous coefficient of the fluid (which is relative to velocity) is the negative of the viscous coefficient of the polymer (which is relative to stretch rate). The origin of the change in sign is Equation (3.81).

Should either of these paradoxes exist, the origin may be that the instrument is actually measuring the velocity $\grave{\mathbf{c}}_v$ at position A_v (the location of the mass of the virtual magniectomer based on this work's model) which corresponds to position B_s.

The alternative interpretation is counterintuitive. Basically the positions of the virtual magniectomer and the specimen magniectomer should be reversed such that the velocity measured by the instrument corresponds to the velocity of the specimen's magniectomer. Thus the velocity $\grave{\mathbf{c}}_s$ measured by the testing instrument applies to the specimen magniectomer. The specimen stretch rate is in the opposite direction to the stretch and is thus negative. The stretch remains positive because it is measured from position A_s. This alternate representation is depicted in Figure 14.2. It should also be noted that Figure 12.1, which was used used to justify the displacement $\mathbf{v}$ being in the opposite direction to the position vector $\mathbf{r}$ in the derivation of Equation (12.6), corresponds to the orientation of Figure 14.2 and would have interpreted the stretch rate of (12.22) as negative and μ would have been positive.

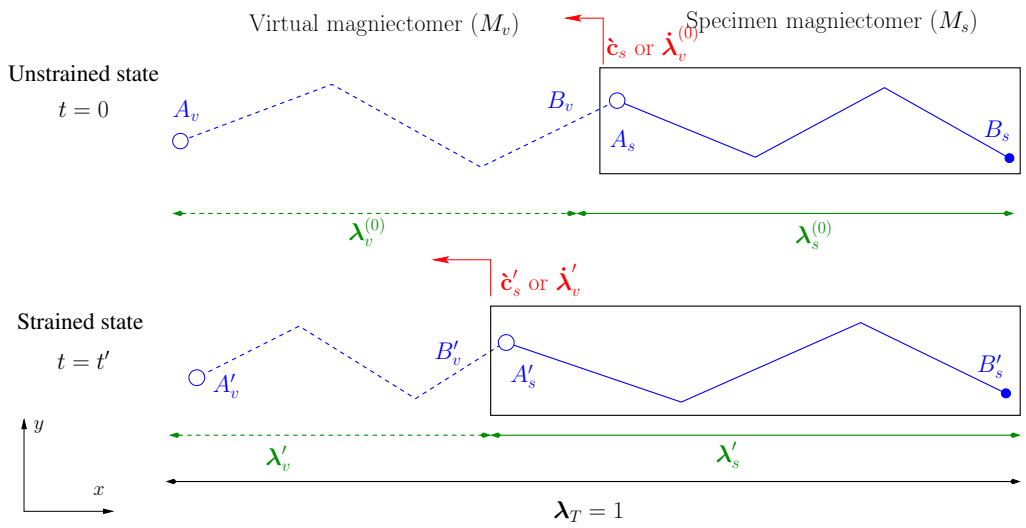

Figure 14.2: An initial unstrained state at $t = 0$ and a strained state at $t = t'$ are depicted in this idealisation of the uniaxial tensile test. Representative magniectomers are depicted in BLUE with the virtual magniectomer dashed. The mass is at position A for the respective magniectomers. The stretches are represented in GREEN and the velocities and stretch rates in RED. The black rectangle is the specimen.

14.7 Model verification

In Section 13.6, the stress calculated by the tensile testing rig is described as being equivalent of the true, apparent, zero-order specimen stress in the $x-$direction (direction of applied load). The justification for the use of the zero order stress is provided in Section 9.5 and the analogy with the measurement of pressure (not stress) in a fluid is apparent.

Figure 13.5 clearly shows relaxation to material maximum entropy and specimen steady state. It has, however, been noted that the time to steady state is too short to achieve steady state. Furthermore, Figure 13.11 depicts a physically implausible scenario – the stretch is not propagating through the specimen. The absence of the propagation of stretch is especially important because the theory for specimen viscoelasticity requires the propagation of stretch through the specimen. In the absence of the propagation of stretch, the numerical model reduces to the modelling of material viscoelasticty. In Section 7.2 it had been established that material viscoelasticity is a variant of the Kelvin-Voigt model of linear viscoelasticity which relaxes to steady state instantaneously as discussed in Section 12.1.3. Supportive evidence that it is material viscoelasticity that is being modelled is provided by Figure 13.9

where the effect of the direct application of non-critical damping is applied.

An attempt was made to establish the origin of the failure of stretch to propagate. Figure 13.8 was an attempt to determine the effect of relaxation constant. No effect was detected. However, it should be recognised that to achieve higher relaxation constants the material constant G had to be increased by a factor of 1×10^9. Thus, to determine the effect of increasing the relaxation constant by a factor of 700, the material stiffnesss had to increase by a factor of 1×10^9. It is therefore proposed that the origin of this problem is the very small relaxation parameter τ_R – imposed by the physical limitations of the computational hardware. This low τ_R induces very fast relaxation. The theory predicts that the propagation of stretch through the specimen counteracts the relaxation due to material viscoelasticity. It is proposed that because of the magnitude of τ_R, the material relaxes towards maximum entropy faster than the wave propagates through the specimen.

The lattice Boltzmann method is typically performed on massively parallel machines. For this work, the algorithm was written for a uni-core processor. Performing the modelling using a parallel algorithm would have had three advantages. Firstly, the calculations would have occurred faster and, secondly, massively parallel machines typically have more memory and would therefore have allowed higher relaxation constants and, as a consequence, a finer mesh (more RVEs) would have been allowed. Lastly the higher relaxation constants would have allowed a slower rate of stretch decay. However, as discussed in Section 13.5 there may still be limitations to the programming language.

Although Figure 13.12 shows more appropriate stress relaxation results, it is recognised that this was achieved with indirect non-critical damping. Indirect non-critical damping simply represents a scaling of the critically damped case – subject to the constraint that the material constants as calculated from the discrete theory remain constant (see Section 10.1.3). This scaling has not negated the problem of not retaining specimen length as depicted in Figure 13.7.

Analytical solutions to the polymer flow equations could not be generated. It was possible to find an analytical solution to an approximation to the polymer flow equations.

It has been demonstrated that both creep and stress relaxation phenomena can be generated by this model/theory.

14.8 Polymer boundary conditions

Novel symmetry boundary conditions have been defined for polymers in this document. The wall BCs for the fluid LBM have the advantage of being local in time and space. The symmetry BC is no longer local in space but remains local in time. The absence of a local solution to the BC adds to the computational expense.

The adaptive BC parallel to the applied force is less complex than the equivalent perpendicular BC because the BC is applied uniformly. The adaptive BC perpendicular to the applied force is more complex because the stretch propagates through the specimen and consequently the BC is not applied uniformly.

Furthermore, the walls perpendicular to the applied force move as the stretch propagates through the specimen. The numerical model does not allow for moving boundaries. Therefore the approximation that the walls are stationary was made – this is not consistent with the proposed theory.

14.9 Numerical method

It is apparent that the numerical method constructed here has limitations. These limitations can broadly be grouped as shared with the fluid and polymer LBM specific.

The two major criticisms of the fluid LBM (see Section 2.4) are the constraints concerning boundary conditions and the prohibitively fine mesh at higher Reynolds numbers. The BC problem is illustrated in this document. A new BC type has also been introduced that, although local in time, is not local in space – in contrast to the fluid lattice Boltzmann method boundary conditions. The equivalent of higher Reynolds numbers is a high κ and low G. Thus the combination of high κ, low G and the non-local calculation of the boundary condition, required by the fixed specimen length, effectively doubles the computational expense of just the high κ and G.

The constraints perculiar to the polymer LBM are a direct consequence of the Gaussian chain-length distribution. Equations (3.55) and (3.56) constrain R_μ/R_{rms} such that chains with less than 42 links (n) are modelled with reduced accuracy. For chains with 42 links or more ($n \geq 42$)

$$\frac{R_\mu}{R_{rms}} \leq \frac{\lambda}{\sqrt{3}} \ll 1,$$

and for chains where $n \to \infty$,

$$\frac{R_\mu}{R_{rms}} \geq \frac{\lambda}{2} \ll 1.$$

Thus the finite strain, mesoscopic theory is constrained to the modelling of shorter molecules to stretches much less than 1.7 and the longer molecules to stretches much less than 2.

Furthermore the plastic region cannot be modelled because of the omission of $\acute{\mathbf{c}}$ in the probability distribution functional (3.1) used in the derivation of the theory. It is noted that the mesh generated by this method is prohibitively fine. This is a known limitation of the lattice Boltzmann method.

The LBM constructed in this document was confined to 2D. As for gases, one could construct a 3D LBM. However, depending on the number of vector lengths selected for the 3D LBM (15 vector length, 21 vector length, 27 vector length) the memory requirements may increase substantially.

The stresses extracted from the numerical model are based on the small strain assumption. The underlying model (which is based on the propagation of stretch throughout the specimen) does not have this restriction. However, to acquire more accurate predictions of stress (particularly for larger strain), higher order stress tensors will have to be formulated. It should be recognised that exactly the same simulation is conducted whether one runs small strain or large strain. The stresses are determined in post-processing and are a consequence of the distribution of stretch and the form of the stress tensor. The underlying simulation does not consider stress.

Chapter 15

Conclusion

This thesis has used an idealised model of a rigid billiard ball molecule with an elastic component to model polymers. Thus a specialised gas model has been shown to model polymers. The limitation of this model is easily recognised if one models matter occupying only a portion of a lattice space. This matter will rapidly occupy the whole space like a gas.

An alternate interpretation is that a Gaussian chain length distribution model for polymer molecules has been modified to include velocity (time-dependent) effects. A Chapman-Enskog type expansion is then applied to the resultant partial differential equation. The elastic component is due to the vibration of the chain as a whole – and not the individual segments.

The most general description would be that this is a theory of the transmission of properties (both information and responses to information) between molecules (or individuals) of a material (with the same innate characteristics) that possess non-adaptive memory (or instinct) and the prediction of the resultant response (or behaviour) of the whole specimen (or group) that is made of the above material – when the properties cannot be transmitted instantaneously and simultaneously (or efficiently) between molecules.

15.1 Summary of results

A unique model of the microscopic behaviour of polymers has been constructed and has been extended into the macroscopic domain. Considerable analogy with the Navier-Stokes equations have been demonstrated. The theory is based on a wave-like propagation of stretch within a specimen. The observed viscoelastic phenomena are not material properties but specimen

properties – a consequence of the initial and steady state distributions of stretch within the specimen. The concept of material and specimen viscoelasticity has been introduced as a consequence.

A new means of generating constitutive equations for polymers has been established based on statistical mechanics. The mesoscopic theory based on a Gaussian chain length distribution can be used to generate progressively higher order macroscopic constitutive equations by applying the Chapman-Enskog expansion to the mesoscopic theory for polymers to progressively higher order. The underlying mesoscopic theory can also be adapted in two ways. The first is by extending the underlying theory to variants of non-Gaussian chain length and the second is to include more variables in the underlying probability distribution function. In particular, adding a velocity component that is independent of stretch should introduce the 'slippage' of plastic deformation and vibration should introduce hysteresis. Progressively higher order Chapman-Enskog expansions can be applied to these mesoscopic models to generate more macroscopic constitutive equations. This method of deriving constitutive equations cannot be accused of being phenomenological.

New and physically justified experimental methods have been developed to determine the material constants. These results show excellent agreement. Although a numerical method has been developed to model the stress relaxation experiment, this has not proven as successful as anticipated. The limitations are those already known to the pre-existing LBM – boundary conditions and the excessive number of representative volume elements required.

15.2 Recommendations and future work

Future work will be divided into four components – theory, experimentation, numerical method and application.

This theory was based on the Gaussian chain-length distribution. Treloar has shown that use of the functional (Langevin) provides better results. The theory may well be improved if one uses the Langevin. The theory as presented was only developed with respect to mass, elasticity, momentum and force. Internal energy and therefore temperature was not developed. An opportunity therefore exists to extend this theory to include thermal effects.

The effect of molecular translation/flow/slippage as represented by $\acute{\mathbf{c}}$ was negated in the curent model. Incorporating this variable should account for plastic deformation, yield and anisotropy. The incorporation of damping should allow for hysteresis.

The theory was developed only for incompressible materials. It is acknowledged that this is only an approximation. The theory should therefore be extended to include compressible materials.

It has been shown that Rivlin-Green theory is the superset of viscoelastic constitutive equations and that the maximum entropy theory to first order is contained in Rivlin-Green. It remains to be shown that the n^{th} order statistical theory where $n \rightarrow \infty$ contains Rivlin-Green theory.

In Section 6.1.4 it was shown that $\int \rho(p)\psi^{(i)} = 0$ is a *necessary* condition for $\rho^{(r)} + J^{(r)} = 0$ to have a solution. It remains to be shown that this is a *sufficient* condition.

Experimentally only a finite set of strains and strain-rates were tested to determine when this one material would behave as a pure hyperelastic, viscoelastic, isotropic material without creep. These experiments should be repeated with larger sample volumes, on more materials at different temperatures. The constants μ and G also need to be determined for more materials at more temperatures, strains and strain-rates. Once a more comprehensive theory has been constructed these experiments may be extended to plastic deformation and anisotropy. The observation that the relaxation towards ground state is proportional to the stretch rate towards maximum stretch during the ramping phase of the stress relaxation experiment needs to be confirmed.

The numerical method has to be extended into 3D and implemented on a massively parallel machine. The time modelled will then be able to be increased. Massively parallel machines will allow for larger relaxation constants and consequently smaller time increments.

As for gases, the internal energy has yet to be incorporated into the numerical method. The numerical method at present does not model displacement. To make this modelling method more physically relevant, boundary

conditions (and the method itself) would have to be modified such that displacement can be incorporated. Modelling of displacement would also facilitate tensile, compression and shear testing. In Chapter 10, a factor 2/3 appears in Equations (10.35) and (10.54). Although it has been suggested that it is a consequence of the 2D lattice when the theory was developed for 3D, this remains to be shown explicitly.

Chapter 9 used a direct finite differencing procedure to calculate the derivatives of stretch and stretch rate – used to determine the stress. An indirect method (comparable to the conventional) would be to use either a paraboloid or biparabolic curves (the one can be shown to reduce to the other) to approximate the stretch and then to differentiate over that function. The results of these three forms for the calculation of stress remain to be compared.

In the calculation of intergrals, the approximation $\int_0^t \mathbf{R}_S d\tau = -\mathbf{R}_S/\omega$ is used. The alternative would be to add the $\mathbf{R}_S \delta t$ for small increment in time δt from 0 to t. Similarly, $\ddot{\mathbf{R}}_D$ was approximated by $-\omega\dot{\mathbf{R}}_D$. The alternative would be the more conventional $(\dot{\mathbf{R}}_D(t+\delta t) - \dot{\mathbf{R}}_D(t))/\delta t$ for small time increment δt. The advantage of the method used in this thesis is that it is local in time.

It should be noted that the stress calculation presented in Chapter 9 was for nominal stress (relative to original surface area). A formulation for true stress should also be constructed (relative to current surface area) and the results should be compared.

Chapter 13 has shown that this numerical method can be used to model viscoelasticity but this does not prove the theory correct. Chapter 13 does, however, provide supportive evidence for the theory. Additional validation would be provided by showing directly that stretch and stress are propagated in a wave-like manner. The wave propagation of stretch may be able to be demonstrated with high frame-rate cameras and markings on the test specimen. The wave-like propagation of stress may also be demonstrated qualitatively using non-destructive real time optical birefringence. It may also be possible to quantify using polarisation sensitive optical coherence tomography [146].

The theory predicts that increased polymer cross-linking should not affect the constant G. The constant $|\mu|$ should however increase. The microstructure therefore should be correlated with the macroscopic properties.

In Chapter 11, two boundary condition options were presented – adaptive and non-adaptive. Chapter 13 briefly compared these BCs. The effect was neglible. This may be a consequence of the low relaxation constants or the mesh discretisation. The origin of the absence of effects due to BCs remain to be investigated.

The obvious application is polymeric material. Of note biological tissue has similar behaviour and the model could be applied to a range of biological tissues.

The numerical method is unusual in that it is a Lagrangian description of a solid. Fluids are typically modelled using a Lagrangian description. This numerical method may therefore facilitate the modelling of fluid-structure interaction.

Finally it is suggested that Table 3.1 should be refined to incorporate the findings in this theory. The microscopic and material categories remain the same but the specimen terms are refined. Thus the specimen can either be homogenous or not. Four homogenous specimen terms are defined – ground state corresponds to $\mathbf{R}_\mu = \mathbf{R}_{\mu 0}, \dot{\mathbf{R}}_\mu = 0$, steady state refers to $\mathbf{R}_\mu \neq \mathbf{R}_{\mu 0}, \dot{\mathbf{R}}_\mu = 0$, quasi-equilibrium implies that $\dot{\mathbf{R}}_\mu \approx 0$ and isolibrium is defined by $\mathbf{R}_\mu \neq \mathbf{R}_{\mu 0}, \|\dot{\mathbf{R}}_\mu\| \gg 0$. The inhomogenous states remain the same. Table 15.1 summarises the results with homogenous terms in *italics* and **bold** inhomogenous terms. Note that the static states have changed

	Mesoscopic	**Material**	**Specimen**
Default	Equilibrium	Equilibrium	*Ground State*
Static	Equilibrium	Equilibrium	*Steady State*
Transient	Maximum Entropy	Maximum Entropy	*Quasi-equilibrium*
	Maximum Entropy	Maximum Entropy	*isolibrium*
	Non-Equilibrium	Non-Equilibrium	**Disequilibrium**

Table 15.1: Refined mesoscopic, material and specimen terms

mesoscopically when compared to Table 3.1.

References

[1] T. Abe. Derivation of the lattice Boltzmann method by means of the discrete ordinate method for the Boltzmann equation. *J. Comp. Phy.*, 131:241–246, 1997.

[2] M.G. Ancona. Fully-Lagrangian and lattice Boltzmann methods for solving systems of conservation equations. *J. Comp. Phy.*, 115:107–120, 1994.

[3] E.M. Arruda and M.C. Boyce. A three-dimensional constitutive model for large stretch behaviour of rubber materials. *J. Mech. Phys. Solids*, 41:389–412, 1993.

[4] A.M. Artoli, A.G. Hoekstra, and P.M.A. Sloot. Simulation of a systolic cycle in a realistic artery with the lattice Boltzmann BGK method. *Int. J. Mod. Phys. B*, 17:95–98, 2003.

[5] R.C. Ball, M. Doi, S.F. Edwards, and M. Warner. Elasticity of tangled network. *Polymer*, 10:1010–1018, 1981.

[6] J.S. Bergström. *Large strain time-dependent behaviour of elastomeric materials*. PhD thesis, Massachussets Institute of Technology, 1999.

[7] J.S. Bergström and M.C. Boyce. Constitutive modelling of large-strain time-dependent behaviour of elastomers. *J. Mech. Phys. Solids*, 46:931–954, 1998.

[8] O. Berk Usta, A.J.C. Ladd, and J.E. Butler. Lattice-Boltzmann simulations of the dynamics of polymer solutions in periodic and confined geometries. *J. Chem. Phys.*, 122:094902, 2005.

[9] B. Bernstein, E.A. Kearsley, and L.J. Zapas. A study of stress relaxation with finite strain. *Trans. Soc. Rheol.*, 7:391–410, 1963.

[10] P.L. Bhatnagar, E.P. Gross, and M. Krook. A model for collision processes in charged and neutral one-component systems. *Phys. Rev*, 94:511–525, 1954.

[11] L. Boltzmann. Zur Theorie der elastischen Nachwirkung. *Ann. Phys. Chem*, 7(Ergänzungsband):624–654, 1876.

[12] J. Broadwell. Shock structure in a simple discrete velocity gas. *Phys. Fluids*, 7(8):1243–1247, 1964.

[13] J.E. Broadwell. Study of rarefied shear flow by the discrete velocity method. *J. Fluid Mech.*, 19:401–414, 1964.

[14] J. Buick. *Lattice Boltzmann Methods in Interfacial Wave Modelling*. PhD thesis, University of Edinburgh, 1997.

[15] N. Cao, S. Chen, S. Jin, and D. Martinez. Physical symmetry and lattice symmetry in the Lattice Boltzmann method. *Phys. Rev. E.*, 55:21–24, 1997.

[16] G. Casula and J.M. Carcione. Generalised mechanical model analogues of linear viscoelastic behaviour. *Bollettino di Geofisica Teorica ed Applicata*, 34(136):235–256, 1992.

[17] W.V. Chang, R. Bloch, and N.W. Tschoegl. Interrelation of creep and relaxation: a modeling approach for ligaments. *J. Biomech. Eng.*, 121:612–615, 1999.

[18] S. Chapman and T.G. Cowling. *The Mathematical Theory of Non-Uniform Gases*. Cambridge University Press, Cambridge, 2^{nd} edition, 1952.

[19] C.H. Chen and C.H. Cheng. Micromechanical modelling of creep behaviour in particle-reinforced silicon rubber composites. *J. Appl. Mech.*, 64:781–786, 1997.

[20] H. Chen. Volumetric formulation of the lattice Boltzmann method for fluid dynamics: Basic concept. *Phys. Rev. E*, pages 3955–3963, 1998.

[21] H. Chen, S. Chen, and W.H. Matthaeus. Recovery of the Navier-Stokes equations using a lattice-gas Boltzmann method. *Phys. Rev. A.*, 67:3776–79, 1992.

[22] S. Chen, K. Diemer, G.D. Doolen, K. Eggert, C. Fu, S. Gutman, and B.J. Travis. Lattice gas automata for flow through porous media. *Physica D*, 47:72–84, 1991.

[23] S. Chen and G.D. Doolen. Lattice Boltzmann method for fluid flows. *Annu. Rev. Fluid Mech.*, 30:329–364, 1998.

[24] S. Chen, D. Martinez, and R. Mei. On boundary conditions in lattice Boltzmann methods. *Phys. Fluids*, 8(9):2527–2536, 1996.

[25] R Clausius. *The mechanical theory of heat, with its applications to the steam engine and the physical properties of bodies*. London: John van Voorst, 1 Paternoster Row, 1^{st} edition, 1867.

[26] P.J. Davis and P. Rabinowitz. *Methods of Numerical Integration*. Academic Press, New York, 2^{nd} edition, 1975.

[27] R.T. Deam and S.F. Edwards. The theory of rubber elasticity. *Phil. Trans. R. Soc. London A*, 280:317–353, 1976.

[28] M. Doi and S.F. Edwards. *The theory of polymer dynamics*. Clarendon Press, 1^{st} edition, 1986.

[29] M. Doi and T. Ohta. Dynamics and rheology of complex interfaces. I. *J. Chem. Phys.*, 95(2):1242–1248, 1991.

[30] S. Edwards. The theory of rubber elasticity. *Proc. Royal. Soc. Lond. A.*, 351:397–406, 1976.

[31] S.F. Edwards. The dynamics of polymer networks. *J. Phys. A*, 7(2):318–331, 1974.

[32] P.J. Flory. Network structure and the elastic properties of vulcanised rubber. *Chem. Rev.*, 35:51–75, 1944.

[33] P.J. Flory. Statistical thermodynamics of random networks. *Proc. Roy Soc. Lond. A.*, 351:351–380, 1976.

[34] P.J. Flory and J. Rehner. Statistical mechanics of cross-linked polymer networks I: Rubberlike elasticity. *J. Chem. Phys*, 11:512–520, 1943.

[35] U. Frisch. Relation between the Lattice Boltzmann Equation and the Navier-Stokes Equation. *Phys. D*, 47:231–232, 1991.

[36] U. Frisch, D. d' Humières, B. Hasslacher, P. Lallemand, and Y. Pomeau. Lattice Gas Hydrodynamics in two and three dimensions. *Comp. Sys*, 1:649–707, 1987.

[37] U. Frisch, B. Hasslacher, and Y. Pormeau. Lattice-gas automata for the Navier-Stokes equations. *Phys Rev. Lett.*, 56:1505–8, 1988.

[38] Y.C. Fung, N. Perrone, and M. Anliker, editors. *Biomechanics, its Foundations and Objectives*. Prentice Hall, Englewood Cliffs, NJ, 1972.

[39] L Giraud, D. d'Humières, and P. Lallemand. A lattice Boltzmann model for Jeffreys viscoelastic fluid. *Europhys. lett.*, 42(6):625–630, June 1998.

[40] L.A. Girifalco. *Statistical Mechanics of Solids*. Oxford University Press, 1^{st} edition, 2000.

[41] L.A. Girifalco. *Statistical Mechanics of Solids*, chapter 1, pages 28–30. Oxford University Press, 1^{st} edition, 2000.

[42] H. Grad. Asymptotic theory of the Boltzmann equation. *Phys. Fluids*, 6(2):147–181, 1963.

[43] A.E. Green and R.S. Rivlin. The mechanics of non-linear materials with memory. part III. *Arch. Rat. Mech. Anal.*, 4:387–404, 1960.

[44] A.E. Green and R.S. Rivlin. Multipolar continuum mechanics. *Arch. Rat. Mech. Anal.*, 17(2):113–147, 1964.

[45] A.E. Green and R.S. Rivlin. Multipolar continuum mechanics: functional theory I. *Proc. Roy. Soc. Lond. A*, 284:303–324, 1965.

[46] A.E. Green, R.S. Rivlin, and A.J.M. Spencer. The mechanics of non-linear materials with memory. part II. *Arch. Rat. Mech. Anal.*, 3:82–90, 1959.

[47] M.S. Green and A.V. Tobolsky. A new approach to the theory of relaxing polymeric media. *J. Chem. Phy.*, 14(2):80–92, 1946.

[48] E.P. Gross. Recent investigations of the Boltzmann equation. In F.M Devienne, editor, *Proceedings of first International Symposium on Rarefied Gas Dynamics*, pages 139–150. Pergamon Press Inc, New York, 1960.

[49] D. Grunau, S. Chen, and K. Eggert. A lattice Boltzmann model for multiphase fluid flows. *Phys. Fluids A*, 5:2557–62, 1993.

[50] A.K. Gunstensen, D.H. Rothman, S. Zaleski, and G. Zanetti. Lattice Boltzmann model of immiscible fluids. *Phys. Rev. A.*, 43:4320–4327, 1991.

[51] E. Guth and H. Mark. Zur innermoleckularen Statistik, insbesondere bei Kettenmolekulen. *Monats. Chem.*, 65:93–121, 1934.

[52] R. Haberman. *Elementary Applied Partial Differential Equations*. Prentice-Hall Inc, 2^{nd} edition, 1987.

[53] E.K. Harris. Some theory of reference values II. comparison of some statistical models of intraindividual variation in blood constituents. *Clin. Chem.*, 22(8):1343–1350, 1976.

[54] X. He, R. Chen, and A. Zhang. A discrete Boltzmann model for non-ideal gases. *J. Comp. Phys.*, 152:642–, 1999.

[55] X. He, S. Chen, and R. Zhang. A lattice Boltzmann scheme for the incompressible multiphase flow and it's applications in simulation of Rayleigh-Taylor instability. *J. Comp. Phy.*, 152:642–663, 1999.

[56] X. He and G. Doolen. Lattice Boltzmann method on curvilinear coordinate system: Flow around a circular cylinder. *J. Comp. Phys.*, 134:306–315, 1997.

[57] X. He and L-S. Luo. A priori derivation of the lattice Boltzmann equation. *Phys. Rev. E.*, 55:6333–36, 1997.

[58] X. He and L-S Luo. Theory of the lattice Boltzmann method: From the Boltzmann equation to the lattice Boltzmann equation. *Phys. Rev. E*, 56:6811–6817, 1997.

[59] X. He, L-S. Luo, and M. Dembo. Some progress in lattice Boltzmann method. part I. nonuniform mesh grids. *J. Comp Phys.*, 129:357–363, 1996.

[60] X. He, L-S. Luo, and M. Dembo. Analytical solutions of simple flows and analysis of nonslip boundary conditions for the lattice Boltzmann BGK model. *J. Stat. Phy.*, 87:115–136, 1997.

[61] X. He, L-S. Luo, and M. Dembo. Some progress in the lattice Boltzmann method: Reynolds number enhancement in simulation. *Physica A*, 239:276–285, 1997.

[62] X. He, X. Shan, and G.D. Doolen. A lattice Boltzmann scheme for incompressible multiphase flow and its application in simulation of Rayleigh-Taylor instability. *Phys. Rev. E*, 57:R13–R16, 1998.

[63] F.J. Higuera and J. Jiménez. Boltzmann approach to lattice gas simulations. *Europhys. Lett.*, 9:663–8, 1989.

[64] J.P. Holman. *Experimental Methods for Engineers*, chapter 3. McGraw-Hill Inc, 6^{th} edition, 1994.

[65] S. Hou, Q. Zou, S. Chen, G. Doolen, and AC. Cogley. Simulation of cavity flow by the lattice Boltzmann method. *J. Comp. Phy*, 118:329–347, 1995.

[66] K. Huang. *Statistical Mechanics*. John Wiley and Sons, 2^{nd} edition, 1987.

[67] J.D. Humphrey, R.K. Strumpf, and F.C.P. Yin. Determination of a constitutive relation for passive myocardium: I. a new functional form. *J. Biomech. Eng.*, 112(3):333–339, 1999.

[68] J.D. Humphrey, R.K. Strumpf, and F.C.P. Yin. Determination of a constitutive relation for passive myocardium: II. parameter estimation. *J. Biomech. Eng.*, 112(3):340–349, 1999.

[69] T. Inamuro, N. Konishi, and F. Ogino. A Galilean invariant model of the lattice Boltzmann method for multiphase fluid flows using free-energy approach. *Comp. Phys. Comm.*, 129:32–45, 2000.

[70] T. Inamuro, M. Yoshino, and F. Ogino. A non-slip boundary condition for lattice Boltzmann simulations. *Phys. Fluids*, 7(12):2928–2930, 1995.

[71] H.M. James and E. Guth. Theory of the elastic properties of rubber. *J. Chem. Phys.*, 11:455–481, 1943.

[72] S. Jiang, Z.P. Xin, and P. Zhang. Global weak solutions to 1D compressible isentropic Navier-Stokes equations with density dependent viscocity. *Methods and Applications of Analysis*, 12(3):239–252, 2005.

[73] S.J. Kim, K.S. Kim, and J.Y. Cho. Viscoelastic model of finitely deforming rubber and its finite element analysis. *J. Appl. Mech.*, 64(4):835–841, 1997.

[74] K.A. Kline and C.N. DeSilva. A Nonlinear theory of thermoviscoelasticity for materials with memory. In M.F. Kanninen, W.F. Adler, A.R. Rosenfield, and R.I. Jaffee, editors, *Inelastic Behaviour of Solids*, pages 327–348. McGraw-Hill, 1970.

[75] J.M.V.A Koelman. A simple lattice Boltzmann scheme for the Navier-Stokes fluid flow. *Europhys. Lett.*, 15(6):603–607, 1991.

[76] S. Kollmannsberger, S. Geller, A. Düster, J. Tölke, C. Sorger, M. Krafczyk, and E. Rank. Fixed-grid fluid-structure interaction in two dimensions based on a partitioned lattice Boltzmann and p-FEM approach. *Int. J. Numer. Meth. Engng*, 79:817–845, 2009.

[77] M. Krafczyk, M. Cerroloza, M. Schultz, and E. Rank. Analysis of 3D transient blood flow passing through an artificial aortic valve by lattice-Boltzmann methods. *J. Biomech.*, 31:453–462, 1998.

[78] M. Krafczyk and E. Rank. A parallelized lattice-gas solver for the transient Navier-Stokes flow: Implementation and simulation results. *Int. J. Num. Meth. Eng.*, 38:1243–1258, 1995.

[79] M. Krafczyk, J. Tölke, E. Rank, and M. Schultz. Two-dimensional simulation of fluid-structure interaction using lattice-Boltzmann methods. *Comp. Struct.*, 79:2031–2037, 2001.

[80] M. Krook. On the solutions of the equations of transfer I. *Astrophys. J*, 122:488–497, 1955.

[81] W. Kuhn. Über die Gestalt fadenförmiger Moleküle in Lösungen. *Koll. Z*, 68:2–15, 1934.

[82] W. Kuhn and F. Grün. Beziehungen zwischen elastischen Konstanten und Dehnungsdoppelbrechung hochelastischer stoffe. *Koll. Z*, 101:248–271, 1942.

[83] W. Kuhn and H. Kuhn. Statistische und energieelastische Rückstellkraft bei stark auf Dehnung beansprucken Fadenmolekeln. *Helv. Chim. Acta*, 29:1095–1115, 1946.

[84] A.J.C. Ladd. Numerical simulations of particulate suspensions via a discretized Boltzmann equation. part 1. Theoretical foundation. *J. Fluid Mech.*, 271:285–309, 1994.

[85] A.J.C Ladd. Numerical simulations of particulate suspensions via a discretized Boltzmann equation. part 2. Numerical results. *J. Fluid Mech.*, 271:311–339, 1994.

[86] W.M. Lai, D. Rubin, and E. Krempl. *Introduction to Continuum Mechanics*. Pergamon Press, 1^{st} edition, 1993.

[87] R.S. Lakes and R. Vanderby. Interrelation of creep and relaxation: a modelling approach for ligaments. *J. Biomech. Eng.*, 121:612–615, 1999.

[88] P. Lallemand, D. d'Humières, L-S. Luo, and R. Rubinstein. Theory of the lattice Boltzmann method: Three-dimensional model for linear viscoelastic fluids. *Phys. Rev. E*, 67:021203, 2003.

[89] P. Lallemand and L-S. Luo. Theory of lattice Boltzmann method: Dispersion, dissipation, isotropy, galilean invariance and stability. *Phys. Rev. E*, 61:6546–6562, 2000.

[90] W. Lemm, editor. *The Reference Materials of the European Communities (results of haemocompatibility tests)*. Kluwer Academic Publishing, 1992.

[91] H. Li, H. Frang, and Z. Lin. Lattice Boltzmann simulation of deformable membrane in fluid. *Int. J. Mod. Phy. B*, 17, 2003.

[92] K. Linnet and M. Kondratovich. Partly non-parametric approach for determining the limit of detection. *Clin. Chem.*, 50(4):732–740, 2004.

[93] F.J. Lockett. Creep and stress-relaxation experiments for non-linear materials. *Int. J. Eng. Sci.*, 3:59–75, 1965.

[94] F.J. Lockett. *Nonlinear Viscoelastic Solids*. Academic Press London, 1972.

[95] N.T. Long. On the non-linear wave equation $u_{tt} - b(t, u^2, u_x^2)u_{xx} = f(x, t, u, u_x, u_t, u^2, u_x^2)$ associated with mixed homogenous conditions. *Journal of Mathematical Analysis and Applications*, 306:243–268, 2005.

[96] J. López-Gómez. On the linear damped wave equation. *J. Differential Equations*, 134:26–45, 1997.

[97] L-S. Luo. Symmetry breaking of flow in 2-D symmetric channels: simulations by lattice Boltzmann method. *Int. J. Mod. Phy. C*, 1997.

[98] L-S. Luo. Unified theory of lattice Boltzmann models for nonideal gases. *Phys. Rev. Lett*, 81:1618–1621, 1998.

[99] R.S. Maier, R.S. Bernard, and D.W. Grunau. Boundary conditions for the lattice Boltzmann method. *Phys. Fluids*, 8(7):1788–1801, 1996.

[100] A. Malevalents and J.M. Yeomans. Lattice Boltzmann simulations of complex fluids : viscoelastic effects under oscillatory shear. *Faraday Discuss*, 112:237–248, 1999.

[101] P. Marcati and K. Nishihara. The $l^p - l^q$ estimates of solutions to one-dimensional damped wave equations and their application to compressible flow through porous media. *J. Differential Equations*, 191:445–469, 2003.

[102] S. Marconi and B. Chopard. A lattice Boltzmann model for a solid body. *Int. J. Mod. Phy. B*, 17, 2003.

[103] J.E. Mark and B Erman. *Rubberlike elasticity: A molecular primer*. Cambridge University Press, 2^{nd} edition, 2007.

[104] G.R. McNamara and G. Zanetti. Use of the Boltzmann equation to simulate lattice-gas automata. *Phys. Rev. Lett.*, 61:2332–35, 1988.

[105] Q. McNemar. *Psychological Statistics*, chapter 6, pages 80–109. John Wiley and Sons Inc, 4^{th} edition, 1969.

[106] R. Mei, W. Shyy, D. Yu, and L-S. Luo. Lattice Boltzmann method for 3-D flows with curved boundary. *J. Comp. Phys.*, 161:680–699, 2000.

[107] K.H. Meyer, G. v. Susich, and E. Valkó. Die elastischen Eigenschaften der organischen Hochpolymeren und ihre kinetische Deutung. *Koll. Z*, 59(2):208–216, 1939.

[108] I. Miller, J.E. Freund, and R.A. Johnson. *Probability and Statistics for Engineers*. Prentice-Hall Int. Inc., 4^{th} edition, 1990.

[109] W. Miller. Flow in the driven cavity calculated by the lattice Boltzmann method. *Phys. Rev. E*, pages 3659–3669, 1995.

[110] J.S. Montanero, A. Santos, and V. Garzó. First-order Chapman-Enskog velocity distribution function in a granular gas. *Physica A*, 376:75–93, 2007.

[111] M. Mooney. A theory of large elastic deformation. *J. App. Phys.*, 11:582–593, 1940.

[112] D.R. Noble, S. Chen, J.G. Georgiadis, and R.O. Buckius. A consistent hydrodynamic boundary condition for the lattice Boltzmann method. *Phys. Fluids*, 7(1):203–209, 1995.

[113] R.W. Ogden. Large deformation isotropic elasticity – the correlation of theory and experiment for incompressible rubberlike solids. *Proc. Roy. Soc. Lond. A*, 326:565–584, 1972.

[114] S.V. Patankar. *Numerical Heat Transfer and Fluid Flow*. Hemisphere Publishing Corporation, New York, 1980.

[115] V.N. Pokrovskii. *The mesoscopic theory of polymer dynamics*. Springer, 2^{nd} edition, 2010.

[116] Y-H. Qian and Y-H. Deng. A lattice BGK model for viscoelastic media. *Phys. Rev. Lett.*, 79(14):2742–2745, 1997.

[117] Y.H. Qian, D. d'Humières, and P. Lallemand. Lattice BGK models for the Navier-Stokes equation. *Europhys. Lett.*, 17:479–84, 1992.

[118] Y.H. Qian and S.A. Orszag. Lattice BGK models for the Navier-Stokes equations: Nonlinear deviation in compressible regimes. *Europhysics letters*, 21(3):255–259, 1993.

[119] Y.H. Qian, S. Succi, F. Massaioli, and Orszag S.A. A benchmark for lattice BGK model flow over a backward-facing step. *Fields Inst. Comm*, 1996.

[120] Y.H. Qian, S. Succi, and S.A. Orszag. Recent advances in lattice Boltzmann computing. *Annu. Rev. Comp. phys.*, 3:295–242, 1995.

[121] M. Renardy. Mathematical analysis of viscoelastic flows. In *Annual Review of Fluid Mechanics*, volume 21, pages 21–36. Annual Reviews Inc., 1989.

[122] R.S. Rivlin. Large elastic deformations of isotropic materials. I. fundamental concepts. *Phil. Trans. Roy. Soc*, 240:459–490, 1948.

[123] P.E. Rouse. A theory of the linear viscoelastic properties of dilute solutions of coiling polymers. *J. Chem. Phys.*, 21(7):1272–1280, 1953.

[124] X. Shan and H. Chen. Lattice Boltzmann model for simulating flows with multiple phases and components. *Phys. Rev. E*, 47:1815–19, 1993.

[125] X. Shan and H. Chen. Simulation of non-ideal gases and liquid-gas phase transitions by the lattice Boltzmann equation. *Phys. Rev. E*, 49(4):2941–2948, 1994.

[126] J.D. Sterling and S. Chen. Stability analysis of lattice Boltzmann methods. *J. Comp. Phys*, 123:196–206, 1996.

[127] S. Succi, R. Benzi, and F. Higuera. The lattice Boltzmann equation. *Physica D*, 47:219–230, 1991.

[128] R.H. Swendson. Gibbs' paradox and the definition of entropy. *Entropy*, 10:15–18, 2008.

[129] M.R. Swift, E. Orlandini, W.R. Osborn, and J.M. Yeomans. Lattice Boltzmann simulation of liquid-gas and binary fluid systems. *Phys. Rev. E*, 54(5):5041–5052, 1996.

[130] M.R. Swift, W.R. Osborn, and J.M. Yeomans. Lattice Boltzmann simulation of nonideal fluids. *Phys. Rev. Lett*, 75(5):830–833, 1995.

[131] E.W. Swokowski. *Calculus with Analytical Geometry*, chapter 3, pages 156–158. PWS-Kent Publishing Company, 2^{nd} edition, 1988.

[132] C.M. Teixeira. Digital physics simulation of lid-driven cavity flow. *Int. J. Mod. Phy. C.*, 8(4):675–691, 1997.

[133] L.R.G. Treloar. The elasticity of a network of long-chain molecules I. *Trans. Faraday Soc.*, 39:36–41, 1943.

[134] L.R.G. Treloar. The elasticity of a network of long-chain molecules II. *Trans. Faraday Soc.*, 39:241–246, 1943.

[135] L.R.G. Treloar. Stress-strain data for vulcanised rubber under various types of deformation. *Trans. Faraday Soc.*, 40:59–70, 1944.

[136] L.R.G. Treloar. The elasticity of a network of long-chain molecules III. *Trans. Faraday Soc.*, 42:83–94, 1946.

[137] L.R.G. Treloar. The statistical length of long-chain molecules. *Trans. Faraday Soc.*, 42:77–81, 1946.

[138] L.R.G. Treloar. *The Physics of Rubber Elasticity.* Clarendon Press, 3^{rd} edition, 1975.

[139] L.R.G. Treloar. *The Physics of Rubber Elasticity*, chapter 13. Clarendon Press, 3^{rd} edition, 1975.

[140] W.L. Vandoolaeghe and E.M. Terentjev. Constrained rouse model of rubber viscoelasticity. *J. Chem. Phys.*, 123:034902–034902.13, 2005.

[141] R. Wagner and F. Hayot. Lattice Boltzmann simulations of flow past a cylindrical obstacle. *J. Stat. Phys.*, 81:63–70, 1995.

[142] F.T. Wall. Statistical thermodynamics of rubber. *J. Chem. Phys*, 10:132–134, 1942.

[143] F.T. Wall. Statistical thermodynamics of rubber II. *J. Chem. Phys.*, 10:485–488, 1942.

[144] F.T. Wall. Statistical thermodynamics of rubber III. *J. Chem. Phys*, 11:527–530, 1943.

[145] M.C. Wang and E Guth. Statistical theory of networks of non-Gaussian flexible chains. *J. Chem. Phy*, 20(7):1144–1157, 1952.

[146] K. Wiesauer, A.D. Sanchiz Dufau, S. Gotzinger, M. Pircher, C.K. Hitzenberger, and D. Stifter. Non-destructive quantification of internal stress in polymer materials by polarisation sensitive optical coherence tomography. *Acta Mat.*, 53(9):2785–2791, 2005.

[147] S. Wolfram. Cellular Automaton Fluids. *J. Stat. Phys.*, 45:471–526, 1986.

[148] S. Wolfram. *Theory and Applications of Cellular Automata.* World Scientific, 1986.

[149] P.D. Wu, K.W. Neale, and E. Van der Giessen. Large strain torsion of axially constrained solid rubber bars. *ACTA Mech. Sin.*, 10(2):136–149, 1994.

[150] P.D. Wu and E. Van der Giessen. On improved network models for rubber elasticity and their applications to orientation hardening in glassy polymers. *J. Mech. Phys. Polymers*, 41:427–456, 1993.

[151] H. Xi, G. Peng, and S-H. Chou. Finite-volume lattice Boltzmann method. *Phys. Rev. E.*, 59(5):6202–6205, 1999.

[152] L.J. Zapas. Viscoelastic behaviour under large deformation. *J. Research of the N.B.S – A. Physics and Chemistry*, 70A:525–532, 1966.

[153] Y. Zhijian. Viscous solutions on some non-linear wave equations. *Nonlinear Analysis*, 63:e2607–e2619, 2005.

[154] O.C. Zienkiewicz and R.L. Taylor. *The Finite Element Method*, volume 3:Fluid Dynamics. Butterworth Heinemann, Boston, 5^{th} edition, 2000.

[155] B.H. Zimm. Dynamics of polymer molecules in dilute solution: viscoelasticity, flow birefringence and dielectric loss. *J. Chem. Phys.*, 24(2):269–278, 1956.

[156] Q. Zou and X. He. On pressure and velocity boundary conditions for the lattice Boltzmann BGK model. *Phys. Fluids*, 9(6):1591–1598, 1997.

Glossary

affine	The affine deformation assumption in statistical mechanics states that for a body at steady state stretched by a fixed stretch tensor $\boldsymbol{\lambda}$ each molecule in the body is also stretched by $\boldsymbol{\lambda}$.
Cauchy	Cauchy stress tensor is a stress tensor defined on the deformed area – the true stress.
chain length	Vector from one end of a molecule to the other end of a molecule representing the displacement from end-to-end for the molecule. The entity is the same as vector length. Chain length is the terminology used by Treloar [138]. Vector length is the preferred term because the measured entity is a vector.
continuum	Continuum mechanics is the branch of mechanics in which bodies are considered to be continua in which the macroscopic properties are functions of position
creep	Phenomenologically defined as incompletely reversible time-dependent elastic specimen behaviour of a specimen at fixed stress. An example of disequilibrium.
disequilibrium	A macroscopic phenomenologically defined term in which macroscopic properties change with respect to time
ensemble	Collection of systems (all of which are replicas of the system being investigated) that are separated by artificial boundaries and are grouped together (as an ensemble) by virtue of being able to form a single mass in space because the artificial borders are shared between the systems.
equilibrium	The collection of microscopic states of a material for which the macroscopic properties of the material do not vary with respect to time.
ground state	Steady state of a specimen where the external environment is in a default state

inverse	in a binary or pairwise interaction, the inverse interactions are the interactions which would occur if the final states returned to their initial states.
isolates	To group separately and recognise as a distinct unit.
isolibrium	Homogenous specimen state where the common mean vector length is not the equilibrium or ground state mean vector length and the common mean vector length stretch rate is not zero. Derived from Latin (iso and libra).
macroscopic	Properties of a continuous body are a function of position in the continuum.
magniectomer	The representative molecule that is predicted in quasi-equilibrium experiments. The collection of molecules that behave (or respond to external forces) in unison because delays are negligible and thus act as a single molecule. Derived from Latin (magna and coniecto) and Greek (meros).
material	Let the superset be matter. Let any contiguous (or simply connected) region of the superset of matter be a subset of matter. The collection of contiguous subsets of matter that have common macroscopic properties that are independent of spatial dimension (like density, temperature and magnetism) constitute a material. Thus a material is defined by matter with common spatially-independent properties. Given that the subsets are contiguous, each has an associated position. Thus the material description is united by common position-dependent but spatially-independent properties. Material descriptions can be either microscopic or macroscopic.
maximum entropy	The maximum entropy state is the collection of microscopic states for which, under conditions where the material macroscopic properties are varying, the entropy is maximised at any instant in time. Therefore, under these varying conditions, properties change until the above microscopic states are achieved.
measured stress	On the instron uniaxial testing rig, this corresponds to the true apparent specimen stress. The instron corrects for current surface area by using the incompressibility assumption.
mesoscopic	Description of the probability of a collection of molecules having a set of properties.
microscopic	The complete description of the properties of an individual molecule.

non-equilibrium	The microscopic states of a material for which macroscopic properties of the material vary with respect to time.
phenomena	Observed relationship between one macroscopic property and another macroscopic property
plastic	Plastic deformation will be defined phenomenologically as irreversible non-elastic time-dependent or time-independent specimen behaviour.
pressure tensor	Pressure exerted by a system on a surface due to the x component where $x = D$ refers to dynamic and $x = S$ refers to static
quasi-equilibrium	A state of disequilibrium sufficiently close to steady state such that a steady state approximation can be made
representative	The representative volume with respect to statistical mechanics will be the largest volume within a material in which the microscopic properties can be represented by a narrowly distributed symmetric probability distribution
reverse	In a binary or pairwise interaction, the effect of molecule 1 on molecule 2 is the forward interaction, the reverse interactions would be the effect of molecule 2 on molecule 1.
specimen	A well defined geometric shape composed of a material. A specimen has all the macroscopic properties of a material as well as properties that are due to the space occupied by the geometric shape
statistical	Statistical mechanics is the physics of deriving the macroscopic properties of a material from the microscopic properties of the material under specified conditions. The microscopic properties of individual molecules are not utilised, rather the probability distribution of microscopic properties is used
steady state	State of a specimen in which the macroscopic properties do not change with respect to time in the absence of a changing external environment
stress relaxation	Phenomenologically defined as time dependent stress behaviour of a specimen at a fixed stretch. An example of disequilibrium.

stress tensor	Nine component second order tensor with the components representing axial and tangential components of stress on the faces of an idealised cube. The cube represents a portion of the material
stretch	Material stretch is the length of a representative volume divided by the length of the original representative volume. Specimen stretch is the average material stretch over the volume of the specimen. Can also be represented as a tensor.
stretch rate	The temporal derivative of vector length when interpreted microscopically. The temporal derivative of stretch when interpreted macroscopically.
vector length	Vector from one end of a molecule to the other end of a molecule representing the displacement from end-to-end for the molecule. There are two variants in the document. The first end of $\mathbf{R}_f$ is selected from a particular direction. The first end of $\mathbf{R}_\Delta$ is selected at random.
viscoelasticity	Phenomenologically defined as completely reversible time-dependent elastic specimen behaviour. An example of disequilibrium.

List of Symbols

$\acute{\boldsymbol{c}}$	velocity independent of stretch rate
$\dot{\boldsymbol{R}}_f$	chain/vector length stretch rate
$\grave{\boldsymbol{c}}$	velocity due to stretch rate of adjacent molecules
$\boldsymbol{\lambda}$	microscopic stretch tensor
$\boldsymbol{\lambda}_{sp}$	specimen stretch – the average of material stretches over the specimen
$\boldsymbol{C}$	the perculiar velocity – $\boldsymbol{c} - \boldsymbol{c}_0$
$\boldsymbol{c}$	velocity of position A – due to a stretch rate component $\grave{\boldsymbol{c}}$ and an independent component $\acute{\boldsymbol{c}}$
$\boldsymbol{c}_0$	mean velocity of the control volume
$\boldsymbol{F}$	force acting on a molecule
$\boldsymbol{p}$	momentum of a molecule
$\boldsymbol{r}$	microscopic position
$\boldsymbol{R}_f$	chain/vector length selected from a fixed direction
$\boldsymbol{R}_\Delta$	vector/chain length of randomly selected chain
$\boldsymbol{R}_{\mu 0}$	mean vector/chain length for a RVE at equilibrium
$\boldsymbol{R}_\mu$	mean of non-randomly selected vector lengths within an RVE
$\boldsymbol{R}_{f0}$	vector length of a non-randomly selected molecule at equilibrium
$\frac{\partial_e p}{\partial t}$	Polymer chain interaction term. change in stretch and momentum due to molecular interaction
$\hat{\boldsymbol{\lambda}}$	microscopic chain length stretch vector
ι	the ratio of current chain stretch rate to root mean square initial chain length stretch rate
κ	elastic constant per unit volume
$\mathbf{P}_D$	dynamic pressure tensor
$\mathbf{P}_S$	static pressure tensor
$\mathbf{P}_{nD}$	dynamic pressure vector
$\mathbf{P}_{nS}$	static pressure vector
$\mathbf{r}$	macroscopic position
$\mathbf{T}$	the latent material stress tensor
$\mathrm{R}_\mu\mathbf{0}$	$\mathrm{R}_\mu(x,t)$ at $x = 0$ and $t = 0$ where $x = 0$ is the point at which the force is applied and $t = 0$ is the end of ramping in the stress relaxation experiment
S	Entropy of a network (of chains)
ρ	demsity or mass per unit volume
ρ_n	molecular density or moleculesper unit volume
$\underline{\hat{\boldsymbol{\lambda}}}$	macroscopic chain length stretch vector
f	gas probability distribution function
K	elastic constant for an individual molecule
m	mass of a molecule
p	polymer probability distribution function
$p^{(ms)}$	maximum entropy distribution function
$R_{\mu G0}$	magnitude of geometric mean of non-random vector lengths within an RVE at equilibrium
s_i	Entropy of the $i^{th} chain$
${}^{\langle app\rangle}\mathbf{T}$	the apparent material stress which (to zero order) is $-\mathbf{P}_S - \mathbf{P}_D$
${}^{\langle app\rangle}\boldsymbol{\sigma}_{sp}(t)$	specimen stress is the average of the apparent stress over the volume of the specimen

Appendix A: Statistical Mechanics Specific results

A-1 Proof that $K_1\boldsymbol{R}_{\Delta 1}\cdot\dot{\boldsymbol{R}}_{\Delta 1}+K_2\boldsymbol{R}_{\Delta 2}\cdot\dot{\boldsymbol{R}}_{\Delta 2}=K_0(\boldsymbol{R}_{\Delta G}\cdot\dot{\boldsymbol{R}}_{\Delta G}+A_1A_2\boldsymbol{R}_{\Delta 12}\cdot\dot{\boldsymbol{R}}_{\Delta 12})$

Let

$$\boldsymbol{R}_{\Delta 1}=\boldsymbol{R}_{\Delta G}+A_2\boldsymbol{R}_{12}$$

where $\boldsymbol{R}_{12}=\boldsymbol{R}_1-\boldsymbol{R}_2$, $A_2=\frac{K_2}{K_0}$, $K_0=K_1+K_2$ and $K_0\boldsymbol{R}_{\Delta G}=K_1\boldsymbol{R}_1+K_2\boldsymbol{R}_2$. Thus

$$K_1A_2=K_1\frac{K_2}{K_0}=K_2\frac{K_1}{K_0}=K_2A_1. \tag{A-1}$$

Similarly, let $\boldsymbol{R}_{\Delta 2}=\boldsymbol{R}_{\Delta G}+A_1\boldsymbol{R}_{21}$, $\dot{\boldsymbol{R}}_{\Delta 1}=\dot{\boldsymbol{R}}_{\Delta G}+A_2\dot{\boldsymbol{R}}_{12}$ and $\dot{\boldsymbol{R}}_{\Delta 2}=\dot{\boldsymbol{R}}_{\Delta G}+A_1\dot{\boldsymbol{R}}_{21}$. Consider

$$\begin{aligned}
K_1\boldsymbol{R}_1\cdot\dot{\boldsymbol{R}}_1 &= K_1(\boldsymbol{R}_{\Delta G}+A_2\boldsymbol{R}_{12})\cdot(\dot{\boldsymbol{R}}_{\Delta G}+A_2\dot{\boldsymbol{R}}_{12})\\
&= K_1(\boldsymbol{R}_{\Delta G}\cdot\dot{\boldsymbol{R}}_{\Delta G}+A_2^2\boldsymbol{R}_{12}\cdot\dot{\boldsymbol{R}}_{12}\\
&\qquad +A_2\dot{\boldsymbol{R}}_{12}\cdot\boldsymbol{R}_{\Delta G}+\dot{\boldsymbol{R}}_{\Delta G}\cdot A_2\boldsymbol{R}_{12})\\
&= K_1(\boldsymbol{R}_{\Delta G}\cdot\dot{\boldsymbol{R}}_{\Delta G}+A_2^2(\boldsymbol{R}_1-\boldsymbol{R}_2)\cdot(\dot{\boldsymbol{R}}_1-\dot{\boldsymbol{R}}_2)\\
&\qquad +A_2(\dot{\boldsymbol{R}}_1-\dot{\boldsymbol{R}}_2)\cdot(A_1\boldsymbol{R}_1+A_2\boldsymbol{R}_2)\\
&\qquad +A_2(A_1\dot{\boldsymbol{R}}_1+A_2\dot{\boldsymbol{R}}_2)\cdot(\boldsymbol{R}_1-\boldsymbol{R}_2)\\
&= K_1(\boldsymbol{R}_{\Delta G}\cdot\dot{\boldsymbol{R}}_{\Delta G}+A_2^2\boldsymbol{R}_1\cdot\dot{\boldsymbol{R}}_1-\dot{\boldsymbol{R}}_1\cdot\boldsymbol{R}_2-\dot{\boldsymbol{R}}_2\cdot\boldsymbol{R}_1\\
&\qquad +\boldsymbol{R}_2\cdot\dot{\boldsymbol{R}}_2+A_2A_1\dot{\boldsymbol{R}}_1\cdot\boldsymbol{R}_1-A_2A_1\boldsymbol{R}_1\cdot\dot{\boldsymbol{R}}_2\\
&\qquad +A_2^2\dot{\boldsymbol{R}}_1\cdot\boldsymbol{R}_2-A_2^2\boldsymbol{R}_2\cdot\dot{\boldsymbol{R}}_2+A_2A_1\dot{\boldsymbol{R}}_1\cdot\boldsymbol{R}_1\\
&\qquad -A_2A_1\dot{\boldsymbol{R}}_1\cdot\boldsymbol{R}_2+A_2^2\boldsymbol{R}_1\cdot\dot{\boldsymbol{R}}_2-A_2^2\boldsymbol{R}_2\cdot\dot{\boldsymbol{R}}_2)\\
&= K_1(\boldsymbol{R}_{\Delta G}\cdot\dot{\boldsymbol{R}}_{\Delta G}+(A_2^2+2A_2A_1)\boldsymbol{R}_1\cdot\dot{\boldsymbol{R}}_1\\
&\qquad -A_1A_2\dot{\boldsymbol{R}}_1\cdot\boldsymbol{R}_2-A_2A_1\boldsymbol{R}_1\cdot\dot{\boldsymbol{R}}_2-A_2^2\boldsymbol{R}_2\cdot\dot{\boldsymbol{R}}_2).
\end{aligned}\tag{A-2}$$

Similarly

$$\begin{aligned}
K_2\boldsymbol{R}_2\cdot\dot{\boldsymbol{R}}_2 &= K_1(\boldsymbol{R}_{\Delta G}\cdot\dot{\boldsymbol{R}}_{\Delta G}+(A_1^2+2A_1A_2)\boldsymbol{R}_2\cdot\dot{\boldsymbol{R}}_2\\
&\qquad -A_1A_2\dot{\boldsymbol{R}}_1\cdot\boldsymbol{R}_2-A_1A_2\boldsymbol{R}_1\cdot\dot{\boldsymbol{R}}_2-A_2^2\boldsymbol{R}_1\cdot\dot{\boldsymbol{R}}_1).
\end{aligned}\tag{A-3}$$

Summing Equations (A-2) and (A-3)

$$\begin{aligned} K_1\boldsymbol{R}_1\cdot\dot{\boldsymbol{R}}_1 \;+\; & K_2\boldsymbol{R}_2\cdot\dot{\boldsymbol{R}}_2 = K_0\boldsymbol{R}_{\Delta G}\cdot\dot{\boldsymbol{R}}_{\Delta G} \\ & +(K_2A_1A_2+2K_1A_1A_2-K_1A_1A_2)\boldsymbol{R}_1\cdot\dot{\boldsymbol{R}}_1 \\ & -K_0A_1A_2\dot{\boldsymbol{R}}_1\cdot\boldsymbol{R}_2-K_0A_1A_2\boldsymbol{R}_1\cdot\dot{\boldsymbol{R}}_2 \\ & +(K_1A_1A_2+2K_2A_1A_2-K_2A_1A_2)\boldsymbol{R}_2\cdot\dot{\boldsymbol{R}}_2 \end{aligned} \quad \text{(A-4)}$$

and applying Equation (A-1) to Equation (A-4)

$$\begin{aligned} K_1\boldsymbol{R}_1\cdot\dot{\boldsymbol{R}}_1 \;+\; & K_2\boldsymbol{R}_2\cdot\dot{\boldsymbol{R}}_2 = K_0\boldsymbol{R}_{\Delta G}\cdot\dot{\boldsymbol{R}}_{\Delta G}+K_0A_1A_2\boldsymbol{R}_1\cdot\dot{\boldsymbol{R}}_1 \\ & -K_0A_1A_2\dot{\boldsymbol{R}}_1\cdot\boldsymbol{R}_2-K_0A_1A_2\boldsymbol{R}_1\dot{\boldsymbol{R}}_2+K_0A_1A_2\boldsymbol{R}_2\cdot\dot{\boldsymbol{R}}_2 \\ = \;& K_0(\boldsymbol{R}_{\Delta G}\cdot\dot{\boldsymbol{R}}_{\Delta G}+A_1A_2(\boldsymbol{R}_1-\boldsymbol{R}_2)\cdot(\dot{\boldsymbol{R}}_1-\dot{\boldsymbol{R}}_2)) \\ = \;& K_0(\boldsymbol{R}_{\Delta G}\cdot\dot{\boldsymbol{R}}_{\Delta G}+A_1A_2\boldsymbol{R}_{12}\cdot\dot{\boldsymbol{R}}_{12}). \end{aligned} \quad \text{(A-5)}$$

A-2 $\int\phi_1(FF_1-F'F_1')q_1\,d\boldsymbol{q}\,d\boldsymbol{R}_f\,d\boldsymbol{R}_{f1}\,d\dot{\boldsymbol{R}}_f\,d\dot{\boldsymbol{R}}_{f1}=\frac{1}{4}\int(\phi+\phi_1-\phi'-\phi_1')(FF_1-F'F_1')q_1\,d\boldsymbol{q}\,d\boldsymbol{R}_f\,d\boldsymbol{r}_{f1}\,d\dot{\boldsymbol{R}}_f\,d\dot{\boldsymbol{R}}_{f1}$

If the function q is symmetric (ie $q_{12}=q_{21}$) and F, G and ϕ are functions of position, time, $\boldsymbol{R}_f$ and $\dot{\boldsymbol{R}}_f$ such that

$$\int\phi_1F_1'G_2'q_{12}d\boldsymbol{q}d\boldsymbol{R}_{f1}d\boldsymbol{R}_{f2}d\dot{\boldsymbol{R}}_{f1}d\dot{\boldsymbol{R}}_{f2}=\int\phi_1'F_1G_2q_{12}d\boldsymbol{q}d\boldsymbol{R}_{f1}d\boldsymbol{R}_{f2}d\dot{\boldsymbol{R}}_{f1}d\dot{\boldsymbol{R}}_{f2}.$$

If ϕ_1 is replaced by 1 and F_1 by ϕ_1F_1, on either side of the above; then

$$\int\phi_1'F_1'G_2'q_{12}d\boldsymbol{q}d\boldsymbol{R}_{f1}d\boldsymbol{R}_{f2}d\dot{\boldsymbol{R}}_{f1}d\dot{\boldsymbol{R}}_{f2}=\int\phi_1F_1G_2q_{12}d\boldsymbol{q}d\boldsymbol{R}_{f1}d\boldsymbol{R}_{f2}d\dot{\boldsymbol{R}}_{f1}d\dot{\boldsymbol{R}}_{f2}.$$

Therefore

$$\begin{aligned} & \int\phi_1(F_1G_2-F_1'G_2')q_{12}\,d\boldsymbol{q}\,d\boldsymbol{R}_{f1}\,d\boldsymbol{R}_{f2}\,d\dot{\boldsymbol{R}}_{f1}\,d\dot{\boldsymbol{R}}_{f2} \\ = \;& \int\phi_1'(F_1G_2-F_1'G_2')q_{12}\,d\boldsymbol{q}\,d\boldsymbol{R}_{f1}\,d\boldsymbol{R}_{f2}\,d\dot{\boldsymbol{R}}_{f1}\,d\dot{\boldsymbol{R}}_{f2} \\ = \;& \frac{1}{2}\int(\phi-\phi_1')(F_1G_2-F_1'G_2')q_{12}\,d\boldsymbol{q}\,d\boldsymbol{R}_{f1}\,d\boldsymbol{R}_{f2}\,d\dot{\boldsymbol{R}}_{f1}\,d\dot{\boldsymbol{R}}_{f2}. \end{aligned}$$

If the molecules are both of the same type, suffix 2 can be omitted such that

$$\begin{aligned} & \int\phi_1(F_1G-F_1'G')q_1\,d\boldsymbol{q}\,d\boldsymbol{R}_{f1}\,d\boldsymbol{R}_f\,d\dot{\boldsymbol{R}}_{f1}\,d\dot{\boldsymbol{R}}_f \\ = \;& \frac{1}{2}\int(\phi_1-\phi_1')(F_1G-F_1'G')q_1\,d\boldsymbol{q}\,d\boldsymbol{R}_{f1}\,d\boldsymbol{R}_f\,d\dot{\boldsymbol{R}}_{f1}\,d\dot{\boldsymbol{R}}_f. \end{aligned} \quad \text{(A-6)}$$

Since $\boldsymbol{R}_{f1}$, $\boldsymbol{R}_f$, $\dot{\boldsymbol{R}}_f$ and $\dot{\boldsymbol{R}}_{f1}$ all refer to either m_1 or K_1; interchanging $\boldsymbol{R}_{f1}$, $\boldsymbol{R}_f$, $\dot{\boldsymbol{R}}_f$ and $\dot{\boldsymbol{R}}_{f1}$ on the right does not alter the integral (A-6). Therefore

$$\begin{aligned} & \int \phi_1(F_1G - F_1'G')q_1\, d\boldsymbol{q}\, d\boldsymbol{R}_{f1}\, d\boldsymbol{R}_f\, d\dot{\boldsymbol{R}}_{f1}\, d\dot{\boldsymbol{R}}_f \\ = \; & \frac{1}{2}\int (\phi - \phi')(FG_1 - F'G_1')q_1\, d\boldsymbol{q} d\boldsymbol{R}_{f1}\, d\boldsymbol{R}_f\, d\dot{\boldsymbol{R}}_{f1}\, d\dot{\boldsymbol{R}}_f. \end{aligned} \tag{A-7}$$

Similarly, by interchanging $F_1G - F_1'G'$ with $FG_1 - F'G_1'$

$$\begin{aligned} & \int \phi_1(FG_1 - F'G_1')q_1\, d\boldsymbol{q}\, d\boldsymbol{R}_{f1}\, d\boldsymbol{R}_f\, d\dot{\boldsymbol{R}}_f\, d\dot{\boldsymbol{R}}_{f1} \\ = \; & \frac{1}{2}\int (\phi_1 - \phi_1')(FG_1 - F'G_1')q_1\, d\boldsymbol{q}\, d\boldsymbol{R}_{f1}\, d\boldsymbol{R}_f\, d\dot{\boldsymbol{R}}_{f1}\, d\dot{\boldsymbol{R}}_f \end{aligned} \tag{A-8}$$

and

$$\begin{aligned} & \int \phi_1(FG_1 - F'G_1')q_1\, d\boldsymbol{q}\, d\boldsymbol{R}_{f1}\, d\boldsymbol{R}_f\, d\dot{\boldsymbol{R}}_{f1}\, d\dot{\boldsymbol{R}}_f \\ = \; & \frac{1}{2}\int (\phi - \phi')(F_1G - F_1'G')q_1\, d\boldsymbol{q} d\boldsymbol{R}_{f1}\, d\boldsymbol{R}_f\, d\dot{\boldsymbol{R}}_{f1}\, d\dot{\boldsymbol{R}}_f. \end{aligned} \tag{A-9}$$

Adding one quarter of Equations (A-6), (A-7), (A-8) and (A-9), the result is

$$\begin{aligned} & \frac{1}{2}\int \phi_1(F_1G + FG_1 - F_1'G' - F'G_1')q_1\, d\boldsymbol{q}\, d\boldsymbol{R}_{f1}\, d\boldsymbol{R}_f\, d\dot{\boldsymbol{R}}_{f1}\, d\dot{\boldsymbol{R}}_f \\ = \; & \frac{1}{4}\int (\phi + \phi_1 - \phi' - \phi_1')(F_1G + FG_1 - F_1'G' - F'G_1') \\ & \times q_1\, d\boldsymbol{q}\, d\boldsymbol{R}_{f1}\, d\boldsymbol{R}_f\, d\dot{\boldsymbol{R}}_{f1}\, d\dot{\boldsymbol{R}}_f \end{aligned}$$

and, if $F = G$, then

$$\begin{aligned} & \int \phi_1(F_1F - F_1'F')q_1\, d\boldsymbol{q}\, d\boldsymbol{R}_{f1}\, d\boldsymbol{R}_f\, d\dot{\boldsymbol{R}}_{f1}\, d\dot{\boldsymbol{R}}_f \\ = \; & \frac{1}{4}\int (\phi + \phi_1 - \phi' - \phi_1')(FF_1 - F'F_1')q_1\, d\boldsymbol{q}\, d\boldsymbol{R}_{f1}\, d\boldsymbol{R}_f\, d\dot{\boldsymbol{R}}_{f1}\, d\dot{\boldsymbol{R}}_f. \end{aligned}$$

A-3 Lattice Boltzmann equation 1^{st} order expansion

$$\begin{aligned} n(x+\delta x, t+\delta t) \; - \; & n(x,t) = \delta\left(\frac{\partial n}{\partial x}\cdot\mathbf{m} + \frac{\partial n}{\partial t}\right) + \frac{(\delta)^2}{2!}\left(\frac{\partial^2 n}{\partial x^2}m^2\right. \\ & \left. +2\frac{\partial^2 n}{\partial x \partial t}\cdot\mathbf{m} + \frac{\partial^2 n}{\partial t^2}\right) = -\frac{1}{\gamma}(n - n^{(eq)}) \end{aligned} \tag{A-10}$$

where

$$n(x,t) := n_0 + \delta n_1 + \delta^2 n_2 + \ldots, \tag{A-11}$$

$$\frac{\partial}{\partial t} := \frac{\partial}{\partial t_0} + \delta\frac{\partial}{\partial t_1} + \delta^2\frac{\partial}{\partial t_2} \quad \text{and} \tag{A-12}$$

$$-\frac{1}{\gamma}n^{(1)} := \Big(\frac{\partial}{\partial t_0} + \mathbf{m}\cdot\nabla\Big)n^{(0)} \tag{A-13}$$

Substituting definitions (A-11) and (A-12) into Equation (A-10) to order δ^2,

$$\begin{aligned}
-\frac{1}{\gamma}(n - n^{(eq)}) &= \delta\left(\frac{\partial}{\partial x}\cdot\mathbf{m} + \frac{\partial}{\partial t_0} + \delta\frac{\partial}{\partial t_1}\right)n \\
&\quad + \frac{(\delta)^2}{2!}\left(\frac{\partial}{\partial x}\cdot\mathbf{m} + + \frac{\partial}{\partial t_0} + \delta\frac{\partial}{\partial t_1}\right)^2 n \\
&= -\frac{1}{\gamma}(n_0 + \delta n_1 + \delta^2 n_2 - n_0) \\
&= \delta\left(\frac{\partial}{\partial x}\cdot\mathbf{m} + \frac{\partial}{\partial t_0} + \delta\frac{\partial}{\partial t_1}\right)(n_0 + \delta n_1 + \delta^2 n_2) \\
&\quad + \frac{\delta^2}{2!}\left(\frac{\partial}{\partial x}\cdot\mathbf{m} + \frac{\partial}{\partial t_0} + \delta\frac{\partial}{\partial t_1}\right)^2 (n_0 + \delta n_1 + \delta^2 n_2) \\
-\frac{1}{\gamma}(\delta n_1 + \delta^2 n_2) &= \delta\left(\frac{\partial}{\partial x}\cdot\mathbf{m} + \frac{\partial}{\partial t_0}\right)(n_0) + \delta^2\frac{\partial}{\partial t_1}n_0 + \delta^2\left(\frac{\partial}{\partial x}\cdot\mathbf{m}\right. \\
&\qquad \left. + \frac{\partial}{\partial t_0}\right)(n_1) + \frac{\delta^2}{2!}\left(\frac{\partial}{\partial x}\cdot\mathbf{m} + \frac{\partial}{\partial t_0}\right)^2 (n_0).
\end{aligned}$$

Substituting definition (A-13) into the result and re-arranging,

$$\begin{aligned}
-\frac{1}{\gamma}(\delta n_1 + \delta^2 n_2) &= \delta\left(-\frac{\delta}{\gamma}\right)(n_1) + \delta^2\frac{\partial}{\partial t_1}n_0 + \delta^2\left(\frac{\partial}{\partial x}\cdot\mathbf{m}\right. \\
&\qquad \left. + \frac{\partial}{\partial t_0}\right)(n_1) - \delta^2\left(\frac{\partial}{\partial x}\cdot\mathbf{m} + \frac{\partial}{\partial t_0}\right)\frac{1}{\gamma}\frac{n_1}{2} \\
-\frac{\delta^2}{\gamma}(n_2) &= \delta^2\frac{\partial}{\partial t_1}n_0 + \left(\frac{\partial}{\partial t_0} + \mathbf{m}\cdot\frac{\partial}{\partial x}\right)\left(1 - \frac{1}{2\gamma}\right)n_1.
\end{aligned}$$

A-4 Tensor definitions

Let $\mathbf{w}$ be a tensor with componentes w_{ij}. Let $\overline{\mathbf{w}}$ be a tensor called the conjugate such that $w_{ij} = \overline{w}_{ji}$. *If and only if* $\mathbf{w} = \overline{\mathbf{w}}$ is the tensor $\mathbf{w}$

symmetric. A symmetric tensor $\overline{\overline{\mathbf{w}}}$ can be formed from $\mathbf{w}$ by

$$\overline{\overline{\mathbf{w}}} = \frac{1}{2}(\mathbf{w} + \overline{\mathbf{w}}). \tag{A-14}$$

The divergence of tensor $\mathbf{w} = w_{xx}+w_{yy}+w_{zz}$. Next, non-divergent (the trace is zero) tensors are constructed. For any tensor $\mathbf{w}$ a non-divergent tensor $\mathring{\mathbf{w}}$ can be formed by

$$\begin{aligned} \mathring{\mathbf{w}} &= \mathbf{w} - \frac{1}{3}(w_{xx} + w_{yy} + w_{zz})\mathbf{I} && \text{(A-15)} \\ &= \mathbf{w} - \frac{1}{3}(\mathbf{w} : \mathbf{I})\mathbf{I}. && \text{(A-16)} \end{aligned}$$

Consequently

$$\begin{aligned} \mathring{\overline{\overline{\mathbf{w}}}} &= \overline{\overline{\mathbf{w}}} - \frac{1}{3}(\overline{\overline{\mathbf{w}}} : \mathbf{I})\mathbf{I} && \text{(A-17)} \\ &= \overline{\overline{\mathbf{w}}} - \frac{1}{3}(\mathbf{w} : \mathbf{I})\mathbf{I} && \text{(A-18)} \\ &= \overline{\overline{\mathbf{w}}} - \frac{1}{3}(w_{xx} + w_{yy} + w_{zz})\mathbf{I}. && \text{(A-19)} \end{aligned}$$

A-5 A tensor integral results

Let $\mathbf{w}$ be any tensor independent of $\mathbf{\Gamma}$. then the following five integral are equal provided they converge.

1. $\int F(\Gamma)\mathbf{\Gamma}\mathbf{\Gamma}(\mathring{\mathbf{\Gamma}\mathbf{\Gamma}} : \mathbf{w})d\mathbf{\Gamma}$
2. $\int F(\Gamma)\mathring{\mathbf{\Gamma}\mathbf{\Gamma}}(\mathring{\mathbf{\Gamma}\mathbf{\Gamma}} : \mathbf{w})d\mathbf{\Gamma}$
3. $\int F(\Gamma)\mathring{\mathbf{\Gamma}\mathbf{\Gamma}}(\mathbf{\Gamma}\mathbf{\Gamma} : \mathbf{w})d\mathbf{\Gamma}$
4. $\frac{1}{5}\mathring{\overline{\overline{\mathbf{w}}}}\int F(\Gamma)(\mathring{\mathbf{\Gamma}\mathbf{\Gamma}} : \mathring{\mathbf{\Gamma}\mathbf{\Gamma}})d\mathbf{\Gamma}$
5. $\frac{2}{15}\mathring{\overline{\overline{\mathbf{w}}}}\int F(\Gamma)\Gamma^4 d\mathbf{\Gamma}$

Equivalence of the above equations is documented by Chapman and Cowling [18].

A-6 Inductive proof of the conservation laws

Let

$$\kappa_{\sigma i}^{\langle r \rangle} := \begin{cases} \kappa_{\sigma i}^{(0)} & r = 0 \\ \kappa_{\sigma i}^{(0)} + \sum_{j=1}^{r} \delta_t^r \kappa_{\sigma i}^{(j)} & r > 0 \end{cases} + O(\delta_t^{r+1}).$$

Then

$$\kappa_{\sigma i}^{\langle r+1\rangle} = \kappa_{\sigma i}^{\langle r\rangle} + \delta_t^{r+1}\kappa_{\sigma i}^{(r+1)}. \tag{A-20}$$

Given that the conservation laws (10.10) must apply to progressively higher order approximations of $\kappa_{\sigma i}$,

$$\kappa_{\sigma i}^{\langle 0\rangle} = \kappa \tag{A-21}$$

and

$$\kappa_{\sigma i}^{\langle r\rangle} = \kappa \qquad \forall\, r \in \mathbb{N}_0. \tag{A-22}$$

But, from (A-20),

$$\kappa = \kappa_{\sigma i}^{\langle r+1\rangle} = \kappa_{\sigma i}^{\langle r\rangle} + \delta_t^{r+1}\kappa_{\sigma i}^{(r+1)}. \tag{A-23}$$

Substituting (A-22) into (A-23)

$$\begin{aligned} \kappa &= \kappa_{\sigma i}^{\langle r+1\rangle} = \kappa_{\sigma i}^{\langle r\rangle} + \delta_t^{r+1}\kappa_{\sigma i}^{(r+1)} = \kappa + \delta_t^{r+1}\kappa_{\sigma i}^{(r+1)} \qquad \forall\, \delta_t \\ \Longrightarrow 0 &= +\delta_t^{r+1}\kappa_{\sigma i}^{(r+1)} \qquad \forall\, \delta_t \iff \kappa_{\sigma i}^{(r+1)} = 0 \qquad \forall\, r \in \mathbb{N}_0. \end{aligned} \tag{A-24}$$

Similarly for $\kappa_{\sigma i}\mathbf{S}_{\sigma i}$ it can be shown that

$$\begin{aligned} \sum_{\sigma,i} \kappa_{\sigma i}^{(0)}\mathbf{S}_{\sigma i} &= \kappa\mathbf{R}_\mu, \\ \sum_{\sigma,i} \kappa_{\sigma i}^{(r)}\mathbf{S}_{\sigma i} &= 0 \qquad \forall\, r \in \mathbb{N}, \end{aligned} \tag{A-25}$$

and

$$\begin{aligned} \sum_{\sigma,i} \rho_{\sigma i}^{(0)} &= \rho, \\ \sum_{\sigma,i} \rho_{\sigma i}^{(r)} &= 0 \qquad \forall\, r \in \mathbb{N}, \\ \sum_{\sigma,i} \rho_{\sigma i}^{(0)}\mathbf{E}_{\sigma i} &= \rho\frac{\dot{\mathbf{R}}_\mu}{2}, \\ \sum_{\sigma,i} \rho_{\sigma i}^{(r)}\mathbf{E}_{\sigma i} &= 0 \qquad \forall\, r \in \mathbb{N}. \end{aligned} \tag{A-26}$$

Appendix B: Statistics and instruments of measure

B-1 The concept of significant change

Repeated measurements of a measurand are rarely the same. One would anticipate a probability distribution and typically the distribution is Gaussian about the true measurement. Although not necessarily the case, in this document it will be assumed that the data is parametrically distributed – a Gaussian distribution.

A significant change from a value x is defined by a value y which can be distinguished from x with greater than 95% probability. At least two approaches exist. The first focusses on the analytical variability or the variability of the analyser. This concept is encapsulated by the limit of detection (LoD). The second approach factors in a 'natural' variation in the measurement that may occur over time (eg. length that may vary with ambient temperature). This latter concept is based on the analysis of time-series and is represented by the concept of reference change values (RCV).

B-2 The limit of detection

Linnet and Kondratovitch [92] document the derivation of the concept of LoD. By definition, LoD is the smallest value that can be distinguished from zero. Linnet and Kondratovitch [92] recognise that at zero the inevitable negative values are approximated to zero. Thus the distribution about zero is not considered Gaussian and non-parametric analysis is conducted.

A schematic representation of the LoD is given in Figure B-1. In the model, the most distal 5% is considered a type I error (α in Figure B-1) – detection of measurand in the absence of measurand. The most proximal 5% of measurements of a measurand just greater than zero, is considered a type II error (β in Figure B-1) – failure to detect measurand in the presence thereof. Let the 95^{th} centile of the zero measurement be P_{95} (thus excluding α). For a one-sided significance level of 95% on a Gaussian distribution

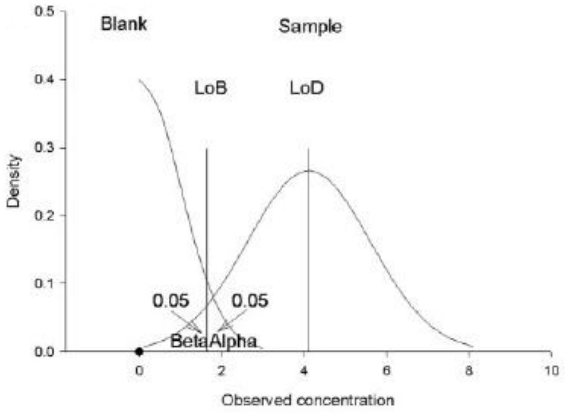

Figure B-1: Limit of detection

$z = 1.65$ (thus excluding β). Consequently

$$LoD = P_{95} + 1.65\sigma_s \tag{B-1}$$

where σ_s is the standard deviation of a measurement very close to zero. The LoD is thus the smallest significant value that can be distinguished from zero.

Of note the theory is non-parametric and assumes that a significant difference can only be greater than zero. P_{95} is determined on measurements performed on one sample on the same day and σ_s is performed on one sample on consecutive days. Also note that the theory only considers analyser variability.

B-3 Reference change values

Reference change values (RCV) also consider a significant change. This theory focusses on measurand variability. Thus if a measurand varies naturally over time (for example length in response to different ambient temperatures), then the RCV is the smallest difference between a measurement taken at time t_1 and time t_2 that can be considered significant.

The theory relies on the analysis of time series [105] and various models can be generated [53]. The simplest of which is

$$RCV = z\sqrt{\sigma_a^2 + \sigma_g^2}$$

where σ_a is the analytical standard deviation and σ_g is the standard deviation

over time. For a two-sided 95% Gaussian significance level $z = 1.96$. One would anticipate that $\sigma_a \leq \sigma_g$ thus a conservative significant change would be given by

$$RCV = 2.77\sigma_a \tag{B-2}$$

This concept is applicable in scenarios where the experiment is conducted over several days to weeks.

B-4 Arbitrary non-time-series significant change

Although the concept of *LoD* is more appropriate to the experimental analysis conducted over a few hours it should be recognised that in Equation (B-1) the significance level is one-sided whereas in Equation (B-2) the significance level is two-sided.

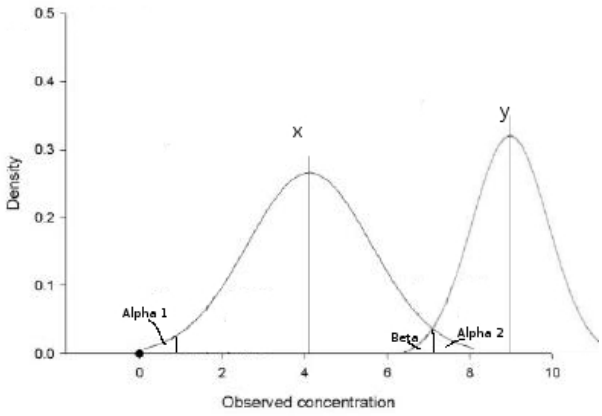

Figure B-2: A significant difference

The origin of the one-sided 95% significance level (P_{95}) is the observation that the measurements about zero are asymmetric. When determining a significant change about an arbitrary value x, a two-sided 95% significance level is required because in general the measurements will be normally distributed about x. The type I error (α_1 and α_2 in Figure B-2 each contributing 2.5%) is symmetrical about x. The smallest significant value greater than x is then y where the type II error is one-sided and equates to 5% (β in Figure B-2). The smallest significant difference (SSD) is then $y - x$ such that

$$y - x = z_1\sigma_1 + z_2\sigma_2$$

where z_1 is for the two-sided significance level, σ_1 is the standard deviation of

measurements about x, z_2 is for the one-sided significance level and σ_2 is the standard deviation for a value close to x. For 95% significance level, where $\sigma_1 \approx \sigma_2$, the smallest significant difference (SSD) is given by

$$y - x = SSD = 1.96\sigma_1 + 1.65\sigma_2 \approx 3.61\sigma_1. \tag{B-3}$$

Equation (B-3) can be applied to a significant change less than or greater than a measured value provided the data is normally distributed and that the 'natural variation with time' is limited.

B-5 Instruments

The specimen depth was measured with a micrometer with precision $0.01mm$. It is assumed that repeated measurements of the same length will be normally distributed about the true length with 95% of readings being within $0.03\,mm$ (three times precision) of the true length. The standard deviation when measuring using the micrometer is therefore $0.015\,mm$. A significant difference for the micrometer is given by Equation (B-3) as $0.05\,mm$.

The remaining spatial dimensions were measured with a caliper with precision $0.02\,mm$. It is assumed that 95% of repeated measurements of the same length will lie within $0.06\,mm$ of the true length. The standard deviation is thus $0.03\,mm$. Equation (B-3) therefore predicts that smallest significant difference is $0.11\,mm$.

The uniaxial testing rig was an Instron 5544 with load capacity of $2\,kN$, maximum travel range of $1067\,mm$, load range of $8\,N$ to $2\,kN$, load precision of 0.5% and speed range $0.05\,mm/min$ to $1000\,mm/min$. It is assumed tht 95% of results will be within 1.5% of true value, the standard deviation (SD) is thus 0.75% and a significant difference in load is therefore 2.7%. The precision of extension is $0.01\,mm$. Again the anticipated standard deviation is $0.015\,mm$.

The measured stress (σ_t), however, is derived from force ($\mathbf{F}$) and area (A) where (given an incompressible material with initial dimensions x_0, y_0, z_0)

$$\begin{aligned} x_0 y_0 z_0 &= \mathrm{V} = x\mathrm{A} \\ \sigma_t = \frac{\mathbf{F}}{\mathrm{A}} &= \frac{\mathbf{F}}{x_0 y_0 z_0} x = \frac{\mathbf{F}}{\mathrm{V}} x \end{aligned}$$

where x is the final length in the direction of tension and A is the true area. The standard deviation of σ_t is given by [64]

$$\sqrt{\left(\frac{\partial\sigma_t}{\partial\mathbf{F}}SD_F\right)^2+\left(\frac{\partial\sigma_t}{\partial x}SD_x\right)^2+\left(\frac{\partial\sigma_t}{\partial x_0}SD_{x_0}\right)^2+\left(\frac{\partial\sigma_t}{\partial y_0}SD_{y_0}\right)^2+\left(\frac{\partial\sigma_t}{\partial z_0}SD_{z_0}\right)^2}$$
$$=\sqrt{\left(\frac{x}{\mathrm{V}}SD_F\right)^2+\left(\frac{\mathbf{F}}{\mathrm{V}}SD_x\right)^2+\left(\frac{\mathbf{F}}{x_0\mathrm{V}}SD_{x_0}\right)^2+\left(\frac{\mathbf{F}}{y_0\mathrm{V}}SD_{y_0}\right)^2\left(\frac{\mathbf{F}}{z_0\mathrm{V}}SD_{z_0}\right)^2}$$

This result is used in Section 12.1.4 where the steady state force is always greater than $10\,N$. At $10\,N$ the standard deviation would then be $0.075\,N$. The extension x is $35\,mm$ with $SD_x = 0.015\,mm$, $\mathrm{V} \approx 100\,mm^3$ thus SD_{σ_t} is

$$\sqrt{\left(\frac{35}{100}0.075\right)^2+\left(\frac{10}{100}0.015\right)^2+\left(\frac{350}{100}\frac{0.03}{25}\right)^2+\left(\frac{350}{100}\frac{0.03}{4}\right)^2+\left(\frac{350}{100}\frac{0.015}{1}\right)^2}$$

and the smallest significant difference in σ_t is given by

$$\begin{aligned} & SD_{\sigma_t} &=& \ 6.45e^{-2}\,MPa \\ \Longleftrightarrow \qquad & SSD_{\sigma_t} &=& \ 3.61\times 6.45e^{-2}\,MPa = 0.233\,MPa. \end{aligned} \qquad \text{(B-4)}$$

Appendix C: Diffusion equation solutions

C-1 Solution of stretch diffusion equation

The diffusion equation is for a scalar. Here (for the surrogate of the macroscopic stretch being modelled) the homogenous solution to the partial differential equation

$$\frac{\partial \mathrm{R}_{S\mu x}}{\partial t} = G\frac{\partial^2 \mathrm{R}_{S\mu x}}{\partial x^2} \tag{C-1}$$

(for $G > 0$) will be determined in order to establish the initial value problem for the numerical modelling based on predefined boundary conditions. Separation of variables (Haberman [52], Chapter 1) will be used. Let

$$\begin{aligned} \mathrm{R}_{S\mu x}(x,t) &= \mathrm{R}_{Sx}(x) \times \mathrm{R}_{St}(t) && \text{(C-2)} \\ \iff \mathrm{R}_{Sx}(x)\dot{\mathrm{R}}_{St}(t) &= G\mathrm{R}_{St}(t)\frac{\partial^2 \mathrm{R}_{Sx}}{\partial x^2} \\ \iff \frac{1}{G}\frac{\dot{\mathrm{R}}_{St}(t)}{\mathrm{R}_{St}(t)} &= \frac{1}{\mathrm{R}_{Sx}(x)}\frac{\partial^2 \mathrm{R}_{Sx}(x)}{\partial x^2} = -\eta_R. && \text{(C-3)} \end{aligned}$$

Consider the temporal component (LHS) of Equation (C-3).

$$\begin{aligned} \dot{\mathrm{R}}_{St}(t) &= -\eta_R G\mathrm{R}_{St}(t) \\ \iff \mathrm{R}_{St}(t) &= A_0 e^{-\eta_R G t}. && \text{(C-4)} \end{aligned}$$

Given that the molecular length must relax to the unstrained state, this function must be monotonically decreasing. Given that $G > 0$, for this function to decrease, $\eta_R > 0$. Thus, for molecular stretch,

$$\eta_R > 0. \tag{C-5}$$

Consider the spatial component (RHS) of Equation (C-3).

$$\begin{aligned} \frac{\partial^2 \mathrm{R}_{Sx}(x)}{\partial x^2} &= -\eta_R \mathrm{R}_{Sx}(x) \\ \iff \quad AB^2 e^{Bx} &= -A\eta_R e^{Bx} \iff B^2 + \eta_R = 0 && \text{(C-6)} \end{aligned}$$

subject to (C-5). The solution is therefore $B = \pm\sqrt{|\eta_R|}i$ where $i = \sqrt{-1}$ and thus (without loss of generality), the homeogenous solution is

$$\begin{aligned} \mathrm{R}_{Sx}(x) &= e^{\sqrt{|\eta_R|}xi} + e^{-\sqrt{|\eta_R|}xi} \\ &= c_1 \cos(\sqrt{|\eta_R|}x) + c_2 \sin(\sqrt{|\eta_R|}x). \end{aligned} \tag{C-7}$$

Combining (C-4) and (C-7) as described by (C-2)

$$\begin{aligned} \mathrm{R}_{S\mu x}(x,t) &= e^{-\eta_R G t}\big(A_1 \cos(\sqrt{|\eta_R|}x) + A_2 \sin(\sqrt{|\eta_R|}x)\big), \\ \mathrm{R}_{S\mu x}(x,0) &= A_1 \cos(\sqrt{|\eta_R|}x) + A_2 \sin(\sqrt{|\eta_R|}x) \end{aligned} \tag{C-8}$$

where $A_1 = A_0 c_1$ and $A_2 = A_0 c_2$. The boundary conditions are as for Section 11.1.1. As is suggested by (11.4) through (11.7), the predicted molecular stretch distribution is as depicted in Figure 11.3. From Equation (11.5)

$$\mathrm{R}_{S\mu x}(x,0) = \left(\mathrm{R}_\mu \mathbf{0} - \mathrm{R}_{S\mu x}^{(eq)}\right) \cos(\sqrt{|\eta_R|}x) + A_2 \sin(\sqrt{|\eta_R|}x) + \mathrm{R}_{S\mu x}^{(eq)}. \tag{C-9}$$

Stretch distribution for special case $\mathrm{L}_m \leq \mathrm{L}_0$

Referring to Figure 11.3, two situations or cases are identified. The first, in Figure 11.3(a), is for $\mathrm{L}_m < \mathrm{L}_0$. Substituting IC constraint (11.6) into (C-9) yields

$$\mathrm{R}_{S\mu x}(x,0) = \begin{cases} \left(\mathrm{R}_\mu \mathbf{0} - \mathrm{R}_\mu^{(eq)}\right) \cos(\sqrt{|\eta_R|}x) + \mathrm{R}_\mu^{(eq)} & \forall\ 0 \leq x \leq \mathrm{L}_m \leq \mathrm{L}_0 \\ \mathrm{R}_\mu^{(eq)} & \forall\ \mathrm{L}_m \leq x \leq \mathrm{L}_0 \end{cases} \tag{C-10}$$

and the solution to (C-1) is

$$\mathrm{R}_{S\mu x}(x,t) = \begin{cases} \left(\mathrm{R}_\mu \mathbf{0} - \mathrm{R}_\mu^{(eq)}\right) e^{-\eta_R G t} \cos(\sqrt{|\eta_R|}x) + \mathrm{R}_\mu^{(eq)} & \forall\ 0 \leq x \leq \mathrm{L}_q \\ \mathrm{R}_\mu^{(eq)} & \forall\ \mathrm{L}_m \leq x \leq \mathrm{L}_0 \end{cases}. \tag{C-11}$$

As an aside, differentiating Equation (C-11),

$$\dot{\mathrm{R}}_{S\mu x} = -\eta_R G \mathrm{R}_{S\mu x} \text{ or integrating } -\frac{\mathrm{R}_{S\mu x}}{\eta_R G} = -\frac{\mathrm{R}_{S\mu x}}{\omega_{IC}^{\langle R \rangle}} = \int_0^t \mathrm{R}_{S\mu x} d\tau \tag{C-12}$$

which (when compared to (8.41), (8.46) and (8.63)) provides an alternate interpretation of ω that only applies for the Lagrangian approximation. It

should however be recognised that (8.46) is also an approximation.

Substitution of the stretch diffusion equation solution (C-10) into IC constraint (11.3) yields

$$(\lambda_{spec}-1)\mathrm{R}_{\mu}^{(eq)}\mathrm{L}_0 = \frac{\mathrm{R}_{\mu}\mathbf{0}-\mathrm{R}_{\mu}^{(eq)}}{\sqrt{|\eta_R|}}\sin\left(\sqrt{|\eta_R|}\mathrm{L}_m\right)+\mathrm{R}_{\mu}^{(eq)}\mathrm{L}_m-\mathrm{R}_{\mu}^{(eq)}\mathrm{L}_m \quad \text{(C-13)}$$

as the specimen stretch solution which is an equation in three unknowns. The geometry of Figure 11.3 introduces the additional constraint (11.10) and consequently Equation (C-13) reduces to

$$(\lambda_{spec}-1)\mathrm{R}_{\mu}^{(eq)}\mathrm{L}_0 = 2\mathrm{L}_m\frac{\mathrm{R}_{\mu}\mathbf{0}-\mathrm{R}_{\mu}^{(eq)}}{\pi}. \quad \text{(C-14)}$$

Stretch distribution for special case $\mathrm{L}_m = \mathrm{L}_0$

For special case $\mathrm{L}_m = \mathrm{L}_0$, as depicted in Figure 11.3(b), IC constraints (11.4) and (11.7) do not apply. Thus

$$\begin{aligned}
\mathrm{R}_{S\mu x}(x,0) &= \left(\mathrm{R}_{\mu}\mathbf{0}-\mathrm{R}_{S\mu}^{(eq)}\right)\cos(\sqrt{|\eta_R|}x)+\mathrm{R}_{S\mu}^{(eq)} \quad \forall\, 0\le x\le \mathrm{L}_m=\mathrm{L}_0,\\
\mathrm{R}_{S\mu x}(x,t) &= \left(\mathrm{R}_{\mu}\mathbf{0}-\mathrm{R}_{S\mu}^{(eq)}\right)e^{-\eta_R G t}\cos(\sqrt{|\eta_R|}x)+\mathrm{R}_{S\mu}^{(eq)}\\
&\qquad\qquad \forall\, 0\le x\le \mathrm{L}_m=\mathrm{L}_0 \qquad \text{(C-15)}
\end{aligned}$$

and $(\mathrm{R}_{\mu}\mathbf{0}-\mathrm{R}_{\mu}^{(eq)})\cos(\sqrt{|\eta_R|}\mathrm{L}_m) = (\mathrm{R}_{\mu}\mathbf{0}-\mathrm{R}_{\mu}^{(eq)})\cos(\sqrt{|\eta_R|}\mathrm{L}_0) \neq \mathrm{R}_{\mu}^{(eq)}$. For $\mathrm{L}_m = \mathrm{L}_0$, IC constraint (11.3) reduces to

$$\frac{1}{\mathrm{L}_0}\int_0^{\mathrm{L}_0}\frac{\mathrm{R}_{S\mu x}}{\mathrm{R}_{S\mu x}^{(eq)}}dx = \dot{\lambda}_{spec} \quad \text{(C-16)}$$

and substitution of (C-10) into (C-16) yields

$$(\lambda_{spec})\mathrm{R}_{S\mu x}^{(eq)}\mathrm{L}_0 = \frac{\mathrm{R}_{\mu}\mathbf{0}-\mathrm{R}_{S\mu}^{(eq)}}{\sqrt{|\eta_R|}}\sin(\sqrt{|\eta_R|}\mathrm{L}_0)+\mathrm{R}_{S\mu}^{(eq)}\mathrm{L}_0. \quad \text{(C-17)}$$

C-2 Solution of stretch rate diffusion equation

The homogenous solution to the partial differential equation

$$\frac{\partial\dot{\mathrm{R}}_{D\mu x}}{\partial t} = \mu\frac{\partial^2\dot{\mathrm{R}}_{D\mu x}}{\partial x^2} \quad \text{(C-18)}$$

(for $\mu < 0$) will be determined in order to establish the initial value problem for the numerical modelling based on the boundary conditions of Section 11.1.1. Applying the same arguments as in Section C-1,

$$\dot{\mathrm{R}}_{Dt}(t) = A_0 e^{-\eta_{\dot{R}}\mu t} \tag{C-19}$$

where, given $\mu < 0 \Longrightarrow \eta_{\dot{R}} < 0$,

$$\frac{\partial^2 \dot{\mathrm{R}}_{Dx}}{\partial x^2} = -\eta_{\dot{R}} \dot{\mathrm{R}}_{Dx}$$

for which the characteristic equation is

$$B^2 + \eta_{\dot{R}} = 0 \tag{C-20}$$

where $\eta_{\dot{R}} < 0$. Therefore

$$\begin{aligned} \dot{\mathrm{R}}_{Dx}(x) &= c_1 e^{-\sqrt{|\eta_{\dot{R}}|}x} + c_2 e^{\sqrt{|\eta_{\dot{R}}|}x} \\ &= C_3 \cosh\sqrt{|\eta_{\dot{R}}|}x + C_4 \sinh\sqrt{|\eta_{\dot{R}}|}x \end{aligned} \tag{C-21}$$

where $\cosh q = (e^{-q} + e^{q})/2$ and $\sinh q = (e^{-q} - e^{q})/2$. Substituting BC (11.12)

$$\dot{\mathrm{R}}_{Dx}(x) = c_4 \sinh\sqrt{|\eta_{\dot{R}}|}x \tag{C-22}$$

and consequently

$$\dot{\mathrm{R}}_{D\mu x} = c_4 e^{-\eta_{\dot{R}}\mu t} \sinh\sqrt{|\eta_{\dot{R}}|}x \Longrightarrow \ddot{\mathrm{R}}_{D\mu x} = -\eta_{\dot{R}}\mu \dot{\mathrm{R}}_{D\mu x}. \tag{C-23}$$

Alternatively,

$$\mathrm{R}_{D\mu x} = -\frac{1}{\eta_{\dot{R}}\mu}\int \dot{\mathrm{R}}_{D\mu x} = -\frac{1}{\omega_{IC}^{\langle \dot{R} \rangle}}\int \dot{\mathrm{R}}_{D\mu x} \tag{C-24}$$

only applies for the Lagrangian approximation to the stretch rate diffusion equation utilised exclusively as an approximation to the IC. Returning to Equation (C-23), two unknowns are recognised. From Equation (11.14)

$$\dot{\mathrm{L}} = \frac{1}{\mathrm{R}_{\mu}^{(eq)}}\int_0^{\mathrm{L}_m} c_4 \sinh\sqrt{|\eta_{\dot{R}}|}x dx = \frac{c_4}{\sqrt{|\eta_{\dot{R}}|}\mathrm{R}_{\mu}^{(eq)}}\left(\cosh\left(\sqrt{|\eta_{\dot{R}}|}\mathrm{L}_m\right) - 1\right) \tag{C-25}$$

can be solved for $\eta_{\dot{R}}$ and c_4 and applies to both $\mathrm{L}_m < \mathrm{L}_0$ and $\mathrm{L}_m = \mathrm{L}_0$.

Relating the stretch and stretch rate initial conditions

It is recognised that in principle $\mathrm{R}_{S\mu}$ and $\mathrm{R}_{D\mu}$ refer to the same variable R_{μ}. R_{μ} has been separated into $\mathrm{R}_{S\mu}$ and $\mathrm{R}_{D\mu}$ components both to facilitate numerical modelling and to generate an analytical solution to the IC approximation to Equations (11.1) and (11.2). Equations (C-24) and (C-12) provide an opportunity to recouple the stretch and stretch rate solutions to the Lagrangian diffusion equation approximation to the polymer flow equation (6.98). Comparing (C-24) to (C-12), which also only applies for the IC approximation, it is apparent that

$$\eta_R G = \omega_{IC}^{\langle R \rangle} = \omega_{IC}^{\langle \dot{R} \rangle} = \eta_{\dot{R}}\mu \implies \sqrt{|\eta_{\dot{R}}|} = \sqrt{|\eta_R|}\sqrt{\left|\frac{G}{\mu}\right|}. \tag{C-26}$$

Equation (C-26) is used in Section 13.2 to show that diffusion equation approximations to the polymer flow equation predict both creep and stress relaxation.

C-3 The stress and stress rate constraints on the diffusion equations

By the definition of the measured principal apparent specimen stress tensor provided by (7.28),

$$\begin{aligned} {}^{\langle app \rangle}\boldsymbol{\sigma}_{sp}(0) &= \int_0^{\mathrm{L}_0} \frac{{}^{\langle app \rangle}\mathbf{T}(\mathbf{r},0)dx}{\mathrm{L}_0} = -\frac{\int_0^{\mathrm{L}_0} p'_d dx}{\mathrm{L}_0}\mathbf{I} - \frac{\int_0^{\mathrm{L}_0} p'_s dx}{\mathrm{L}_0}\mathbf{I} \\ &\quad +2\frac{\mu}{\mathrm{L}_0}\int_0^{\mathrm{L}_0} 2\frac{d\dot{\mathbf{R}}_{D\mu}}{dx}dx + 8\frac{G}{\mathrm{L}_0}\int_0^{\mathrm{L}_0}\int_0^{t} 2\frac{d\mathbf{R}_{S\mu}}{dx}d\tau dx \end{aligned} \tag{C-27}$$

where the components are not independent. Equation (C-28) should also be compared to the alternative for discrete theory provided in Section 9.4. The principal stress in the x-direction is then given by

$$\begin{aligned} {}^{\langle app \rangle}\sigma_{spx}(0) &= \int_0^{\mathrm{L}_0} \frac{{}^{\langle app \rangle}\mathrm{T}(x,0)dx}{\mathrm{L}_0} = -\frac{\int_0^{\mathrm{L}_0} p'_d dx}{\mathrm{L}_0} - \frac{\int_0^{\mathrm{L}_0} p'_s dx}{\mathrm{L}_0} \\ &\quad +2\frac{\mu}{\mathrm{L}_0}\int_0^{\mathrm{L}_0} 2\frac{d\dot{\mathrm{R}}_{Dx\mu}}{dx}dx + 8\frac{G}{\mathrm{L}_0}\int_0^{\mathrm{L}_0}\int_0^{t} 2\frac{d\mathrm{R}_{Sx\mu}}{dx}d\tau dx. \end{aligned}$$

As noted, the y-component is not independent of x. The substitution (C-12) could be used but the approximation $\int \mathrm{R}_{Sx} dx = -\mathrm{R}_{Sx}/\omega$ is made as in Section 9.2.2 and therefore (C-28) expands to

$$\begin{aligned}
{}^{\langle app \rangle}\sigma_{sp1}(0) &= -\frac{\int_0^{\mathrm{L}_0} p'_{dxx} dx}{\mathrm{L}_0} - \frac{\int_0^{\mathrm{L}_0} p'_{sxx} dx}{\mathrm{L}_0} + 2\frac{\mu}{\mathrm{L}_0} \int_0^{\mathrm{L}_0} \dot{\mathrm{D}}_{xx} + \dot{\mathrm{D}}_{yx} dx \\
&\quad -\frac{8G}{\omega \mathrm{L}_0} \int_0^{\mathrm{L}_0} (\mathrm{D}_{xx} + \mathrm{D}_{yx}) dx \\
&= -\frac{\int_0^{\mathrm{L}_0} p'_{dxx} dx}{\mathrm{L}_0} - \frac{\int_0^{\mathrm{L}_0} p'_{sxx} dx}{\mathrm{L}_0} - \frac{2}{4}\frac{\mu}{\mathrm{L}_0} \int_0^{\mathrm{L}_0} 2\frac{\partial \dot{\mathrm{R}}_{D\mu x}}{\partial x} + \frac{\partial \dot{\mathrm{R}}_{D\mu y}}{\partial x} dx \\
&\quad + \frac{8G}{4\omega \mathrm{L}_0} \int_0^{\mathrm{L}_0} 2\frac{\partial \mathrm{R}_{S\mu x}}{\partial x} + \frac{\partial \mathrm{R}_{S\mu y}}{\partial x} dx, \qquad \text{(C-28)}
\end{aligned}$$

upon substititution of the definition of $\mathbf{D}$ (6.84) and $\dot{\mathbf{D}}$ (6.79). As in Chapter 12, the principal stress is indeterminate but is possible to calculate by the appropriate selection of constraints, as determined by the experimetal conditions, as previously described in Section 3.2.7 for the equilibrium situation and Section 9.6 for discrete, disequilibrium theory.

The principles to be applied are briefly described here. Thus for the stress relaxation experiment in 1D being conducted here, the second principal stress (perpendicular to the applied load) is zero. Thus subtracting the second principal stress from the first principal stress will yield the first principal stress as in Section 3.2.7.

Based on the above principles, in analogy with the case for the first principal stress (parallel to the applied load) above, the second principal stress is thus

$$\begin{aligned}
{}^{\langle app \rangle}\sigma_{sp2}(0) &= -\frac{\int_0^{\mathrm{L}_0} p'_{dyy} dx}{\mathrm{L}_0} - \frac{\int_0^{\mathrm{L}_0} p'_{syy} dx}{\mathrm{L}_0} - \frac{2}{4}\frac{\mu}{\mathrm{L}_0} \int_0^{\mathrm{L}_0} 2\frac{\partial \dot{\mathrm{R}}_{D\mu y}}{\partial y} + \frac{\partial \dot{\mathrm{R}}_{D\mu y}}{\partial x} dx \\
&\quad + \frac{8G}{4\omega \mathrm{L}_0} \int_0^{\mathrm{L}_0} 2\frac{\partial \mathrm{R}_{S\mu y}}{\partial y} + \frac{\partial \mathrm{R}_{S\mu y}}{\partial x} dx \qquad \text{(C-29)}
\end{aligned}$$

where all functions are uniform in the y-direction. Thus subtracting (C-29)

from (C-28) one gets

$$\begin{aligned}
{}^{\langle app\rangle}\sigma_{sp1}(0) \;-\; {}^{\langle app\rangle}\sigma_{sp2}(0) &= -\frac{\int_0^{\mathrm{L}_0} p'_{dxx}dx}{\mathrm{L}_0} - \frac{\int_0^{\mathrm{L}_0} p'_{sxx}dx}{\mathrm{L}_0} + \frac{\int_0^{\mathrm{L}_0} p'_{dyy}dx}{\mathrm{L}_0} \\
&\quad + \frac{\int_0^{\mathrm{L}_0} p'_{syy}dx}{\mathrm{L}_0} - \frac{\mu}{2\mathrm{L}_0}\int_0^{\mathrm{L}_0} 2\frac{\partial \dot{\mathrm{R}}_{D\mu x}}{\partial x}dx + \frac{4G}{\omega \mathrm{L}_0}\int_0^{\mathrm{L}_0}\frac{\partial \mathrm{R}_{S\mu x}}{\partial x}dx \\
\Longrightarrow {}^{\langle app\rangle}\sigma_{sp1}(0) &= -\frac{\int_0^{\mathrm{L}_0} p'_{dxx} - p'_{dyy}dx}{\mathrm{L}_0} - \frac{\int_0^{\mathrm{L}_0} p'_{sxx} - p'_{syy}dx}{\mathrm{L}_0} \\
&\quad - \frac{\mu}{\mathrm{L}_0}\dot{\mathrm{R}}_{D\mu}(x)|_0^{\mathrm{L}_m} + \frac{4G}{\omega \mathrm{L}_0}\mathrm{R}_{S\mu}(x)|_0^{\mathrm{L}_m}. \qquad \text{(C-30)}
\end{aligned}$$

From the 2D correction factor provided by Section 10.1.3, (3.44), $\lambda_2 = \lambda_3$ and $\prod \lambda_i = 1 \Longrightarrow \lambda_y^2 = 1/\lambda_x$,

$$\begin{aligned}
-p_{sxx} &= \frac{2}{3}\times\frac{\kappa}{4}\left(\mathrm{R}_{\mu x}^2 - \mathrm{R}_{\mu x}^{(eq)2}\right) = \frac{\kappa}{6}\mathrm{R}_{\mu 0x}^2\left(\lambda_x^2 - 1\right) = \frac{\kappa}{6}\frac{R_{rms}^2}{3}\left(\lambda_x^2 - 1\right) \\
p_{syy} &= -\frac{\kappa}{6}\mathrm{R}_{\mu 0y}^2\left(\frac{1}{\lambda_x} - 1\right) = -\frac{\kappa}{6}\frac{R_{rms}^2}{3}\left(\frac{1}{\lambda_x} - 1\right) \qquad \text{(C-31)} \\
&= -\frac{\kappa}{6}R_{rms}'^2\left(\frac{1}{\lambda_x} - 1\right) \qquad \text{where} \qquad R_{rms}'^2 = \frac{R_{rms}^2}{3}.
\end{aligned}$$

Let

$$\frac{\mathrm{R}_\mu \mathbf{0} - \mathrm{R}_\mu^{(eq)}}{\mathrm{R}_\mu^{(eq)}} = \lambda_M \qquad \text{(C-32)}$$

be designated maximum change in principal stretch. Then substituting (C-10)

$$\begin{aligned}
-p_{sxx} &= \frac{\kappa}{6}R_{rms}'^2\left(\lambda_M^2\cos^2\sqrt{|\eta_R|}x\right) + \frac{\kappa}{6}R_{rms}'^2\left(2\lambda_M\cos\sqrt{|\eta_R|}x\right) \qquad \text{(C-33)} \\
p_{syy} &= -\frac{\kappa}{6}R_{rms}'^2\left(\frac{1}{\lambda_M\cos\sqrt{|\eta_R|}x + 1} - 1\right) \\
&= \frac{\kappa}{6}R_{rms}'^2\left(\frac{\lambda_M\cos\sqrt{|\eta_R|}x}{\lambda_M\cos\sqrt{|\eta_R|}x + 1}\right). \qquad \text{(C-34)}
\end{aligned}$$

Similarly, substituting (C-22) into p_d from Section 10.2.3

$$\begin{aligned}
-p_{dxx} &= \frac{2}{3}\times\frac{\rho}{8}\left(c_4^2\sinh^2\sqrt{|\eta_{\dot R}|}x\right) = \frac{\rho}{12}\frac{R_{rms}'^2}{\mathrm{R}_{\mu x}^{(eq)}}c_4^2\sinh^2\sqrt{|\eta_{\dot R}|}x \qquad \text{(C-35)} \\
p_{dyy} &= -\frac{\rho}{12}R_{rms}'^2\left(\dot\lambda_x^2\frac{\lambda_y^2}{\lambda_x^2}\right) \qquad \text{(C-36)}
\end{aligned}$$

where the last result is derived from the differentiation of $\prod \lambda_i = 1$ as in

Section 11.5. Given that $\lambda_y = \lambda_z$,

$$\lambda_x \lambda_y^2 = 1 \iff \lambda_y^2 = \frac{1}{\lambda_x} \iff \frac{\lambda_y^2}{\lambda_x^2} = \frac{1}{\lambda_x^3}. \tag{C-37}$$

Substituting (C-22), (C-10) and (C-37) into (C-36)

$$p_{dyy} = -\frac{\rho}{12} \frac{R'^2_{rms}}{\mathrm{R}_{\mu x}^{(eq)2}} \left(\frac{c_4^2 \sinh^2 \sqrt{|\eta_R|} x}{\left(\lambda_M \cos \sqrt{|\eta_R|} x + 1 \right)^3} \right). \tag{C-38}$$

The integration described by (C-30) is applied to (C-33), (C-35) and (C-38). Equation (C-34) proves difficult to integrate. It is, however, noted that

$$\frac{\lambda_M \cos \sqrt{|\eta_R|} x}{\lambda_M \cos \sqrt{|\eta_R|} x + 1}$$

is monotonically decreasing on the applicable domain $\sqrt{\eta_R} x \in [0, \frac{\pi}{2}]$ and thus a parabola is used as an approximation. Let

$$\begin{aligned} \frac{\lambda_M \cos \sqrt{\eta_R} x}{\lambda_M \cos \sqrt{\eta_R} x + 1} \approx & -\frac{8\eta_R}{\pi^2} \left(\frac{2\lambda_M}{\lambda_M + \sqrt{2}} - \frac{\lambda_M}{\lambda_M + 1} \right) x^2 + \frac{\lambda_M}{\lambda_M + 1} \\ & + \frac{2\sqrt{|\eta_R|}}{\pi} \left(\frac{4\lambda_M}{\lambda_M + \sqrt{2}} - \frac{3\lambda_M}{\lambda_M + 1} \right) x. \end{aligned} \tag{C-39}$$

Consequently

$$\begin{aligned} \int_0^{\mathrm{L}_0} \frac{p_{syy}}{\mathrm{L}_0} dx \approx & \frac{\kappa R'^2_{rms}}{6\mathrm{L}_0} \left(\frac{8\eta_R}{3\pi^2} \left(\frac{\lambda_M}{\lambda_M + 1} - \frac{2\lambda_M}{\lambda_M + \sqrt{2}} \right) \mathrm{L}_m^3 + \frac{\lambda_M}{\lambda_M + 1} \mathrm{L}_m \right. \\ & \left. + \frac{\sqrt{|\eta_R|}}{\pi} \left(\frac{4\lambda_M}{\lambda_M + \sqrt{2}} - \frac{3\lambda_M}{\lambda_M + 1} \right) \mathrm{L}_m^2 \right). \end{aligned} \tag{C-40}$$

Equations (C-33), (C-35), (C-38) and (C-40) are substituted into (C-30). Thus Equation (C-30) reduces to

$$\begin{aligned} {}^{\langle app \rangle}\sigma_{sp1}(0) = & \frac{\kappa R'^2_{rms}}{6\mathrm{L}_0} \left(\lambda_M^2 \frac{\mathrm{L}_m}{2} + \lambda_M^2 \frac{\sin 2\sqrt{|\eta_R|} \mathrm{L}_m}{4\sqrt{|\eta_R|}} + \frac{2\lambda_M}{\sqrt{|\eta_R|}} \sin \sqrt{|\eta_R|} \mathrm{L}_m \right) \\ & + \frac{\kappa R'^2_{rms}}{6\mathrm{L}_0} \left(\frac{8\eta_R}{3\pi^2} \left(\frac{\lambda_M}{\lambda_M + 1} - \frac{2\lambda_M}{\lambda_M + \sqrt{2}} \right) \mathrm{L}_m^3 \right. \\ & \left. + \frac{\sqrt{|\eta_R|}}{\pi} \left(\frac{4\lambda_M}{\lambda_M + \sqrt{2}} - \frac{3\lambda_M}{\lambda_M + 1} \right) \mathrm{L}_m^2 + \frac{\lambda_M}{\lambda_M + 1} \mathrm{L}_m \right) \end{aligned}$$

$$
\begin{aligned}
&+\frac{\rho R'^2_{rms}}{12\mathrm{L}_0}\frac{c_4^2}{\mathrm{R}_{\mu x}^{(eq)2}}\left(\frac{\sinh\left(2\sqrt{\eta_{\dot R}}\mathrm{L}_m\right)}{4\sqrt{\eta_{\dot R}}}-\frac{\mathrm{L}_m}{2}\right)\\
&-\frac{\rho}{12}R'^2_{rms}\frac{c_4^2}{\mathrm{R}_{\mu x}^{(eq)2}}\left(A(\lambda_M,\sqrt{|\eta_R|},\mathrm{L}_m)\right)\\
&-\frac{\mu}{\mathrm{L}_0}\left(c_4\sinh\sqrt{|\eta_{\dot R}|}\mathrm{L}_m\right)+\frac{4G}{\omega\mathrm{L}_0}\left(\mathrm{R}_{\mu x}^{(eq)}-\mathrm{R}_{\mu x}\mathbf{0}\right) \qquad \text{(C-41)}
\end{aligned}
$$

which represents an independent equation for determining $c_4, \mathrm{L}_m, \mathrm{R}_\mu\mathbf{0}, \eta_R, \eta_{\dot R}$ and $A(\lambda_M, \sqrt{|\eta_R|}, \mathrm{L}_m)$. The variable A, by (C-39), is given by

$$
A \approx \frac{4\eta_R}{\pi^2}\left(\frac{2\lambda_M+\lambda_M^2}{(1+\lambda_M)^2}x^2+\frac{1}{(\lambda_M+1)^2}\right)^{\frac{3}{2}}\sinh\sqrt{|\eta_{\dot R}|}x. \qquad \text{(C-42)}
$$

C-4 Solving for the initial condition parameters for $\mathrm{L}_m \leq \mathrm{L}_0$

Differentiating (C-30) with respect to time yields the stress rate equation. Further substituting the approximations $\ddot{\mathrm{R}}_{D\mu x} \approx -\omega\dot{\mathrm{R}}_{D\mu x}$ and $\dot{\mathrm{R}}_{S\mu x} = -\omega\mathrm{R}_{S\mu x}$ into the above derivative,

$$
\begin{aligned}
{}^{\langle app\rangle}\dot\sigma_{sp1}(0) &= -\frac{1}{\mathrm{L}_0}\frac{\partial}{\partial t}\int_0^{\mathrm{L}_0} p_{dxx}-p_{dyy}dx-\frac{1}{\mathrm{L}_0}\frac{\partial}{\partial t}\int_0^{\mathrm{L}_0} p_{sxx}-p_{syy}dx\\
&\quad+\frac{\omega\mu}{\mathrm{L}_0}\dot{\mathrm{R}}_{D\mu}(x)|_0^{\mathrm{L}_m}-\frac{4G}{\mathrm{L}_0}\mathrm{R}_{S\mu}(x)|_0^{\mathrm{L}_m}\\
&= -\frac{\omega\kappa R'^2_{rms}}{3\mathrm{L}_0}\left(\lambda_M^2\frac{\mathrm{L}_m}{2}+\lambda_M^2\frac{\sin 2\sqrt{|\eta_R|}\mathrm{L}_m}{4\sqrt{|\eta_R|}}\right)\\
&\quad-\frac{\omega\kappa R'^2_{rms}}{3\mathrm{L}_0}\left(\frac{2\lambda_M}{\sqrt{|\eta_R|}}\sin\sqrt{|\eta_R|}\mathrm{L}_m\right)\\
&\quad-\frac{\omega\kappa R'^2_{rms}}{3\mathrm{L}_0}\left(\frac{8\eta_R}{3\pi^2}\left(\frac{\lambda_M}{\lambda_M+1}-\frac{2\lambda_M}{\lambda_M+\sqrt{2}}\right)\mathrm{L}_m^3\right.\\
&\quad\left.+\frac{\sqrt{|\eta_R|}}{\pi}\left(\frac{4\lambda_M}{\lambda_M+\sqrt{2}}-\frac{3\lambda_M}{\lambda_M+1}\right)\mathrm{L}_m^2+\frac{\lambda_M}{\lambda_M+1}\mathrm{L}_m\right)\\
&\quad-\frac{\omega\rho R'^2_{rms}}{6}\frac{c_4^2}{\mathrm{R}_{\mu x}^{(eq)}}\left(\frac{\sinh^2\left(2\sqrt{\eta_{\dot R}}\mathrm{L}_m\right)}{4\sqrt{\eta_{\dot R}}}-\frac{\mathrm{L}_m}{2}\right)\\
&\quad+\frac{\omega\rho}{6}R'^2_{rms}\frac{c_4^2}{\mathrm{R}_{\mu x}^{(eq)2}}\left(A(\lambda_M,\sqrt{|\eta_R|},\mathrm{L}_m)\right)\\
&\quad+\frac{\omega\mu}{\mathrm{L}_0}c_4\sinh\sqrt{|\eta_{\dot R}|}\mathrm{L}_m-\frac{4G}{\mathrm{L}_0}\left(\mathrm{R}_{\mu x}^{(eq)}-\mathrm{R}_{\mu x}\mathbf{0}\right) \qquad \text{(C-43)}
\end{aligned}
$$

where $A(\lambda_M, \sqrt{|\eta_R|}, \mathrm{L}_m)$ is given by Equation (C-42). In order to fully describe the stress at time $t = 0$, it is necessary to solve all five equations. However, for the special case when the contribution of stretch rate is negligible, only three equations need to be used – (11.10), (C-13) and (C-41). The initial stress equation is truncated because of the absence of stretch rate terms. Substitute (C-32) into (C-14) to produce

$$\frac{\pi}{2}(\lambda_{spec} - 1)\mathrm{L}_0 = \mathrm{L}_m\lambda_M \iff \mathrm{L}_m = \frac{\pi}{2\lambda_M}(\lambda_{spec} - 1)\mathrm{L}_0 \tag{C-44}$$

which demonstrates that an inverse relationship exists between the maximum stretch and the length with $\lambda \neq 1$ as anticipated. Furthermore, with appropriate substitution and geometry of Figure 11.3 , it is recognised that

$$\sqrt{\eta_R}\mathrm{L}_m = \frac{\pi}{2} \iff \mathrm{L}_m = \frac{\pi}{2\sqrt{\eta_R}} \iff \sqrt{|\eta_R|} = \frac{\pi}{2\mathrm{L}_m}. \tag{C-45}$$

Substituting (C-44), (C-45) and (C-26) into Equation (C-41)

$$\begin{aligned}
{}^{\langle app\rangle}\sigma_{sp1}(0) = {} & \frac{\kappa R'^2_{rms}}{6\mathrm{L}_0}\left(\lambda_M\frac{\pi}{4}(\lambda_{spec} - 1)\mathrm{L}_0 + 2(\lambda_{spec} - 1)\mathrm{L}_0\right) \\
& \left(\frac{(\pi\lambda_{spec} - 1)\mathrm{L}_0}{3}\left(\frac{1}{\lambda_M + 1} - \frac{2}{\lambda_M + \sqrt{2}}\right)\right. \\
& + \frac{\pi(\lambda_{spec} - 1)\mathrm{L}_0}{4}\left(\frac{4}{\lambda_M + \sqrt{2}} - \frac{3}{\lambda_M + 1}\right) \\
& \left. + \frac{\pi}{2}\left(\frac{\lambda_{spec} - 1}{\lambda_M + 1}\right)\mathrm{L}_0\right) \times \frac{\kappa R'^2_{rms}}{6\mathrm{L}_0} \\
& + \frac{\rho R'^2_{rms}}{12}\frac{c_4^2}{\mathrm{R}_\mu^{(eq)2}}\left(\frac{\sinh(\pi\sqrt{|G/\mu|})}{2\pi\sqrt{|G/\mu|}} - \frac{1}{2}\right)L_0\frac{\pi(\lambda_{spec} - 1)}{2\lambda_M} \\
& - \frac{\rho}{12}R'^2_{rms}\frac{c_4^2}{\mathrm{R}_\mu^{(eq)2}}\left(A(\lambda_M, \sqrt{|\eta_R|}, \mathrm{L}_m)\right) \\
& - \frac{\mu}{\mathrm{L}_0}\left(c_4\sinh\frac{\pi}{2}\sqrt{\left|\frac{G}{\mu}\right|}\right) + \frac{4G\mathrm{R}_\mu^{(eq)}}{\omega\mathrm{L}_0}\lambda_M
\end{aligned} \tag{C-46}$$

which can be solved by the Newton-Rapheson method. It is recognised that $\sqrt{|G/\mu|}$ is negligibly small and that terms dependent on $\sinh\sqrt{|G/mu|}\pi/2x$ are negligible. The exception is

$$\frac{\sinh\pi\sqrt{|G/\mu|}}{\pi\sqrt{|G/\mu|}} \approx \lim_{x\longrightarrow 0}\frac{\sinh x}{x} = 1$$

by L'Hospital's rule. Thus, approximating $\cosh\left(-\sqrt{\eta_{\dot{R}}}\right) \approx 1$ and $\sinh\left(-\sqrt{\eta_{\dot{R}}}\right) \approx 0$, Equation (C-46) can further be approximated as

$$\begin{aligned} {}^{\langle app\rangle}\sigma_{sp1}(0) &= \frac{\kappa R'^2_{rms}}{6}\left(\lambda_M \frac{\pi}{4}(\lambda_{spec}-1) + 2(\lambda_{spec}-1)\right) \\ &\quad \frac{\kappa R'^2_{rms}}{6}\left(\frac{1/3}{\lambda_M+\sqrt{2}} + \frac{1/12}{\lambda_M+1}\right)\left(\frac{\lambda_{spec}-1}{\pi}\right) \\ &\quad + \frac{4GR^{(eq)}_{\mu}}{\omega \mathrm{L}_0}\lambda_M \end{aligned} \tag{C-47}$$

which can be solved for λ_M. The maximum stretch λ_M can be substituted in (C-44) and (C-45) to solve L_m and $\sqrt{\eta_R}$ respectively.

C-5 Solving for the initial condition parameters for $\mathrm{L}_m > \mathrm{L}_0$

For $\mathrm{L}_m > \mathrm{L}_0$, all calculations have to be performed on the domain $0 < x < \mathrm{L}_0$, $x \in \mathbb{R}$ and $\mathrm{R}_{\mu}(\mathrm{L}_0, 0) \neq \mathrm{R}^{(eq)}_{\mu}$. Equation (C-41) (ignoring stretch rate terms because $|G| \ll |\mu|$) reduces to

$$\begin{aligned} {}^{\langle app\rangle}\sigma_{sp1}(0) &= \frac{\kappa R'^2_{rms}}{6}\left(\frac{\lambda_M^2}{2} + \lambda_M^2 \frac{2\sin\sqrt{|\eta_R|}\mathrm{L}_0 \cos\sqrt{|\eta_R|}\mathrm{L}_0}{4\sqrt{|\eta_R|}\mathrm{L}_0}\right. \\ &\quad \left. + 2\lambda_M \frac{\sin\sqrt{|\eta_R|}\mathrm{L}_0}{\sqrt{|\eta_R|}\mathrm{L}_0}\right) \\ &\quad + \frac{\kappa R'^2_{rms}}{6}\left(\frac{8\eta_R}{3\pi^2}\left(\frac{\lambda_M}{\lambda_M+1} - \frac{2\lambda_M}{\lambda_M+\sqrt{2}}\right)\mathrm{L}_0^2\right. \\ &\quad \left. + \frac{\sqrt{|\eta_R|}}{\pi}\left(\frac{4\lambda_M}{\lambda_M+\sqrt{2}} - \frac{3\lambda_M}{\lambda_M+1}\right)\mathrm{L}_0 + \frac{\lambda_M}{\lambda_M+1}\right) \\ &\quad + \frac{4G}{\omega \mathrm{L}_0}\left((R_{\mu}\mathbf{0} - \mathrm{R}^{(eq)}_{\mu})\cos\sqrt{|\eta_R|}\mathrm{L}_0 + \mathrm{R}^{(eq)}_{\mu} - \mathrm{R}_{\mu}\mathbf{0}\right) \end{aligned} \tag{C-48}$$

It is recognised that for negligibly small $\sqrt{|\eta_R|}\mathrm{L}_0$, which is valid for $\mathrm{L}_m \gg \mathrm{L}_0$, $\cos\sqrt{|\eta_R|}\mathrm{L}_0 = 1$ and, consequently, Equation (C-48) reduces to

$$\begin{aligned} {}^{\langle app\rangle}\sigma_{sp1}(0) &= \frac{\kappa R'^2_{rms}}{6}\left(\frac{\lambda_M^2}{2} + \lambda_M^2 \frac{\sin\sqrt{|\eta_R|}\mathrm{L}_0}{2\sqrt{|\eta_R|}\mathrm{L}_0} + 2\lambda_M \frac{\sin\sqrt{|\eta_R|}\mathrm{L}_0}{\sqrt{|\eta_R|}\mathrm{L}_0}\right) \\ &\quad + \frac{\kappa R'^2_{rms}}{6}\left(\frac{8\eta_R \mathrm{L}_0^2}{3\pi^2}\left(\frac{\lambda_M}{\lambda_M+1} - \frac{2\lambda_M}{\lambda_M+\sqrt{2}}\right)\right. \end{aligned}$$

$$+\frac{\sqrt{|\eta_R|}\mathrm{L}_0}{\pi}\left(\frac{4\lambda_M}{\lambda_M+\sqrt{2}}-\frac{3\lambda_M}{\lambda_M+1}\right)+\frac{\lambda_M}{\lambda_M+1}\Bigg). \tag{C-49}$$

From Equation (C-17),

$$\frac{\lambda_{spec}-1}{\lambda_M}=\frac{\sin\sqrt{|\eta_R|}\mathrm{L}_0}{\sqrt{|\eta_R|}\mathrm{L}_0}. \tag{C-50}$$

Given that $\sqrt{|\eta_R|}\mathrm{L}_0$ is negligibly small, a Taylor expansion of the RHS of (C-50) can be used to produce

$$\frac{\lambda_{spec}-1}{\lambda_M}=1-\frac{\eta_R\mathrm{L}_0^2}{6}\implies\eta_R\mathrm{L}_0^2=6\frac{1+\lambda_M-\lambda_{spec}}{\lambda_M}. \tag{C-51}$$

Subsituting (C-50) and (C-51) into (C-49), Equation (C-49) reduces to

$$\begin{aligned}{}^{\langle app\rangle}\sigma_{sp1}(0) &= \frac{\kappa R'^2_{rms}}{6}\Bigg[\frac{16}{\pi^2}(1+\lambda_M-\lambda_{spec})\left(\frac{1}{\lambda_M+1}-\frac{2}{\lambda_M+\sqrt{2}}\right)\\ &\quad+\frac{\sqrt{1+\lambda_M-\lambda_{spec}}}{\pi}\left(\frac{4\sqrt{\lambda_M}}{\lambda_M+\sqrt{2}}-\frac{3\sqrt{\lambda_M}}{\lambda_M+1}\right)+\frac{\lambda_M}{\lambda_M+1}\Bigg]\\ &\quad\frac{\kappa R'^2_{rms}}{6}\left(\frac{\lambda_M^2}{2}+\frac{\lambda_M}{2}(\lambda_{spec}-1)+2(\lambda_{spec}-1)\right)\end{aligned} \tag{C-52}$$

which can be solved for λ_M by the Newton-Rapheson method. Note that, in general, $1+\lambda_M\geq\lambda_{spec}$. Furthermore $1+\lambda_M=\lambda_{spec}$ occurs at steady state when the stretch is uniformly distributed. Substituting λ_M into (C-50), one can then solve for $\sqrt{|\eta_R|}\mathrm{L}_0$ and thus $\sqrt{|\eta_R|}$.

C-6 Newton-Rapheson method for $\mathrm{L}_m\leq\mathrm{L}_0$

Applying Newton-Rapheson [131] to Equation (C-47) at $t=0$, given (3.53),

$$\begin{aligned}f(\lambda_M) &:= \frac{\kappa R'^2_{rms}}{6}\left(\lambda_M\frac{\pi}{4}(\lambda_{spec}-1)+2(\lambda_{spec}-1)\right)\\ &\quad+\frac{\kappa R'^2_{rms}}{6}\left(\frac{1/3}{\lambda_M+\sqrt{2}}+\frac{1/12}{\lambda_M+1}\right)\left(\frac{\lambda_{spec}-1}{\pi}\right)\\ &\quad+\frac{4GR^{(eq)}_{\mu x}}{\omega\mathrm{L}_0}\lambda_M-{}^{\langle app\rangle}\sigma_{sp1}(0),\end{aligned} \tag{C-53}$$

$$\begin{aligned}f'(\lambda_M) &:= -\frac{\kappa R'^2_{rms}}{6}\left(\frac{1/12}{(\lambda_M+1)^2}+\frac{1/3}{(\lambda_M+\sqrt{2})^2}\right)\left(\frac{\lambda_{spec}-1}{\pi}\right)\\ &\quad+\frac{\kappa R'^2_{rms}}{6}\frac{\pi}{4}(\lambda_{spec}-1)+\frac{4GR^{(eq)}_{\mu x}}{\omega\mathrm{L}_0}\end{aligned} \tag{C-54}$$

when one differentiates with respect to λ_M. Thus successive approximations (with $\lambda_M^{(0)} = \lambda_{spec} - 1$) give

$$\lambda_M^{(i+1)} = \lambda_M^{(i)} - \frac{f(\lambda_M^{(i)})}{f'(\lambda_M^{(i)})}.$$

C-7 Newton-Rapheson method for $\mathrm{L}_m > \mathrm{L}_0$

Applying the Newton Rapheson method to Equation (C-52)

$$\begin{aligned} f(\lambda_M) &= \frac{\kappa R_{rms}'^2}{6}\left(\frac{\lambda_M^2}{2} + \frac{\lambda_M}{2}(\lambda_{spec}-1) + 2(\lambda_{spec}-1)\right) - {}^{\langle app\rangle}\sigma_{sp1}(0) \\ &\quad + \frac{\kappa R_{rms}'^2}{6}\left[\frac{16}{\pi^2}(1+\lambda_M-\lambda_{spec})\left(\frac{1}{\lambda_M+1} - \frac{2}{\lambda_M+\sqrt{2}}\right)\right. \\ &\quad \left. + \frac{\sqrt{1+\lambda_M-\lambda_{spec}}}{\pi}\left(\frac{4\sqrt{\lambda_M}}{\lambda_M+\sqrt{2}} - \frac{3\sqrt{\lambda_M}}{\lambda_M+1}\right) + \frac{\lambda_M}{\lambda_M+1}\right], \qquad \text{(C-55)} \\ f'(\lambda_M) &= \frac{\kappa R_{rms}'^2}{6}\left(\lambda_M + \frac{\lambda_{spec}-1}{2}\right) \\ &\quad + \frac{\kappa R_{rms}'^2}{6}\left[\frac{16}{\pi^2}(\lambda_{spec}-1)\left(\frac{-1}{(\lambda_M+1)^2} + \frac{2}{(\lambda_M+\sqrt{2})^2}\right)\right] \\ &\quad - \frac{\kappa R_{rms}'^2}{6}\frac{16}{\pi^2}\left(\frac{1}{(\lambda_M^2+1)^2} - \frac{2\sqrt{2}}{(\lambda_M+\sqrt{2})^2}\right) \\ &\quad + \frac{\kappa R_{rms}'^2}{6}\left[\frac{2(1+2\lambda_M-\lambda_{spec})}{(\lambda_M+2)\sqrt{\lambda_M+\lambda_M^2-\lambda_{spec}\lambda_M}} - \frac{4\sqrt{\lambda_M+\lambda_M^2-\lambda_{spec}\lambda_M}}{(\lambda_M+\sqrt{2})^2}\right. \\ &\quad \left. - \frac{3(1+2\lambda_M-\lambda_{spec})}{2(\lambda_M+1)\sqrt{\lambda_M+\lambda_M^2-\lambda_{spec}\lambda_M}} + \frac{3\sqrt{\lambda_M+\lambda_M^2-\lambda_{spec}\lambda_M}}{(\lambda+1)^2}\right] \qquad \text{(C-56)} \end{aligned}$$

Successive approximations to λ_M are given by

$$\lambda_M^{(i+1)} = \lambda_M^{(i)} - \frac{f(\lambda_M^{(i)})}{f'(\lambda_M^{(i)})}$$

where $\lambda_M^{(0)} = \lambda_{spec} - 1$ is used as the first approximation. It should be noted that both Equation (C-53) and Equation (C-55) proved difficult to solve by the Newton-Rapheson method.

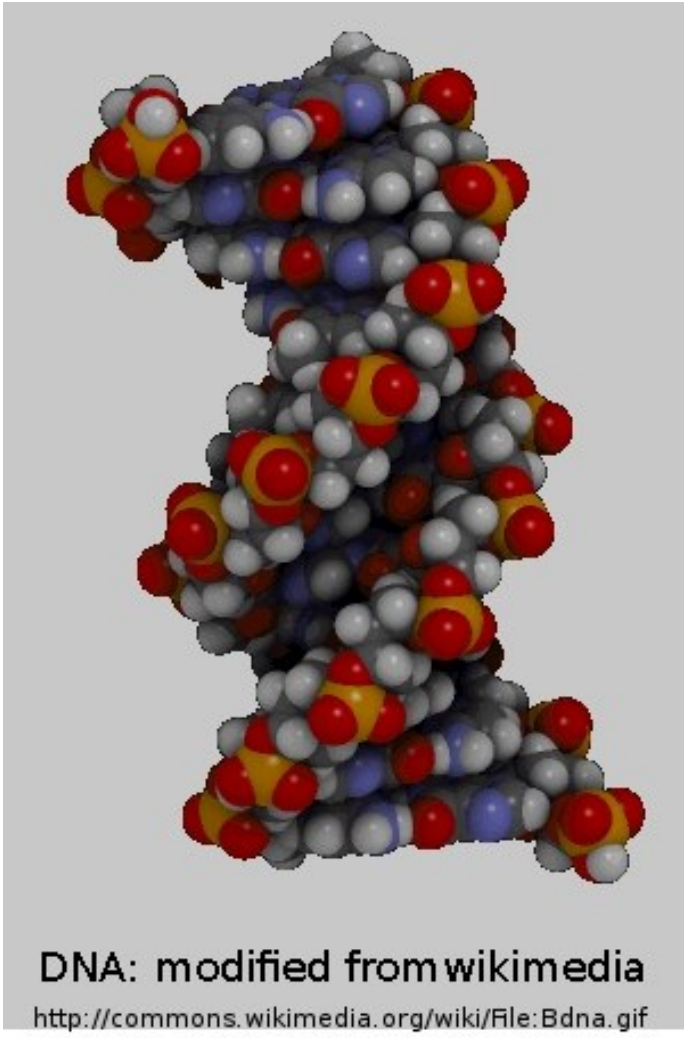

DNA: modified from wikimedia

http://commons.wikimedia.org/wiki/File:Bdna.gif